This electronic thesis or dissertation has been downloaded from the King's Research Portal at https://kclpure.kcl.ac.uk/portal/

# Brain structure, function and response to oxytocin in violent offenders with antisocial personality disorder and psychopathy

Griem, Julia

*Awarding institution:*
King's College London

**The copyright of this thesis rests with the author and no quotation from it or information derived from it may be published without proper acknowledgement.**

END USER LICENCE AGREEMENT

**Unless another licence is stated on the immediately following page** this work is licensed

under a Creative Commons Attribution-NonCommercial-NoDerivatives 4.0 International

licence. https://creativecommons.org/licenses/by-nc-nd/4.0/

You are free to copy, distribute and transmit the work

Under the following conditions:

- Attribution: You must attribute the work in the manner specified by the author (but not in any way that suggests that they endorse you or your use of the work).
- Non Commercial: You may not use this work for commercial purposes.
- No Derivative Works - You may not alter, transform, or build upon this work.

Any of these conditions can be waived if you receive permission from the author. Your fair dealings and other rights are in no way affected by the above.

**Take down policy**

If you believe that this document breaches copyright please contact librarypure@kcl.ac.uk providing details, and we will remove access to the work immediately and investigate your claim.

Download date: 27. Nov. 2023

# Brain structure, function and response to oxytocin in violent offenders with antisocial personality disorder and psychopathy

Thesis for the Degree of Doctor of Philosophy in Neuroscience

By

**Julia Griem**


Department of Forensic and Neurodevelopmental Sciences
Institute of Psychiatry, Psychology & Neuroscience
King's College London

**2023**

# Abstract

About 1% of the population is responsible for most violent crime. These individuals are typically male, have life course persistent antisocial behaviour, and meet diagnostic criteria for conduct disorder in childhood and for antisocial personality disorder (ASPD) in adulthood. Some of these individuals are additionally characterized by traits of callous unconcern in childhood and psychopathic traits in adulthood (ASPD+P). There is evidence that these individuals engage in offending behaviour from a younger age, employ more instrumental aggression, and are less responsive to punishment and treatment than individuals who have ASPD without psychopathy (ASPD-P). These two ASPD subtypes are associated with different neurocognitive and neurobiological mechanisms. It remains to be investigated whether ASPD+/-P groups also differ in terms of cortical structure or resting-state brain function. Furthermore, it has never been investigated whether potential functional brain abnormalities can be pharmacologically modulated, or 'shifted', to be more in line with typical brain function. One pharmacological agent of interest is oxytocin, a social neuropeptide. Studies in healthy individuals suggest that the intranasal administration of exogenous oxytocin can modulate processes that have been identified to be abnormal in ASPD and/or psychopathy.

The current study had two aims. First, to further investigate neurobiological underpinnings of ASPD+P and ASPD-P relative to non-offending healthy controls in terms of brain structure (cortical volume, surface area, cortical thickness) and resting-state brain function (regional cerebral blood flow, large-scale network functional connectivity, and network topology). Second, to assess the effect of intranasal oxytocin on resting-state brain function.

The study used a double-blind, placebo-controlled, randomized crossover design. Adult males with past violent convictions who met Diagnostic and Statistical Manual of Mental Disorders (5$^{th}$ edition) criteria for ASPD were recruited from South London forensic and probation services. They were

stratified into ASPD+P and ASPD-P groups according to the European threshold for psychopathy on the Psychopathy Checklist-Revised. Healthy adult non-offending males were recruited from the South London community. After self-administering the placebo and oxytocin nose sprays, all participants underwent structural magnetic resonance imaging (MRI), arterial spin labelling imaging, and resting-state functional MRI (fMRI) scans.

Individuals with ASPD+P and ASPD-P showed significant brain structure abnormalities relative to non-offenders in frontotemporal and medial parietal cortical volume, surface area, and cortical thickness, with significant differences between the ASPD subtypes. The arterial spin labelling study revealed significant reductions in frontotemporal cerebral blood flow in both antisocial groups relative to non-offenders, and significant increases in medial parietal cerebral blood flow in both antisocial groups relative to non-offenders, that was also significantly higher in ASPD+P than ASPD-P. Functional connectivity analyses of resting-state fMRI data revealed that individuals with ASPD showed significant abnormalities within several large-scale networks, including medial-temporal and salience networks relative to non-offenders. Topological analyses of resting-state fMRI data demonstrated significant differences in brain network topology in ASPD at macro-, meso-, and micro-levels in comparison to non-offenders. Intranasal oxytocin significantly attenuated resting-state brain abnormalities in the ASPD group in all three functional investigations.

These findings provided further support for differences in the neurobiological mechanisms between violent offenders with ASPD+P and ASPD-P. Moreover, they provided the first evidence that intranasal oxytocin can modulate resting-state brain function in these individuals. The results have important implications for stratification within the ASPD diagnostic group, as well as for the therapeutic potential of intranasal oxytocin.

# Table of Contents

Abstract ..... 2

Table of Contents ..... 4

Acknowledgements ..... 11

Declaration of Contributions ..... 13

Covid-19 Impact Statement ..... 14

List of Tables ..... 15

List of Figures ..... 17

List of Abbreviations ..... 19

1 General Introduction ..... 23

1.1 A developmental approach to understanding violent crime ..... 24

1.1.1 Violent crime: its extent and impact ..... 24

1.1.2 A developmental approach to understanding violence across the lifespan ..... 24

1.1.3 Conduct Disorder ..... 26

1.2 Clinical conceptualisation of antisocial personality disorder and psychopathy ..... 35

1.2.1 General features of personality disorder ..... 35

1.2.2 Antisocial Personality Disorder ..... 37

1.2.3 Psychopathy ..... 43

1.2.4 Treatment and interventions ..... 48

1.2.5 ASPD with or without psychopathy ..... 50

1.3 Neurocognitive, neurobiological, and neurochemical underpinnings of ASPD +/- P ..... 51

1.3.1 Neurocognitive and functional neurobiological underpinnings of ASPD and psychopathy ..... 51
1.3.2 Neurobiological underpinnings of ASPD and psychopathy ..... 66
1.3.3 Neurochemical underpinnings of ASPD and psychopathy ..... 75
1.4 The current project ..... 85
1.4.1 Rationale ..... 85
1.4.2 Aims ..... 86
2 General Methods ..... 87
2.1 Study design and ethical considerations ..... 87
2.2 Recruitment and participant selection ..... 88
2.3 Inclusion and exclusion criteria ..... 89
2.4 Procedure ..... 90
2.5 Psychological assessment ..... 93
2.6 Self-report questionnaires ..... 94
2.7 Neurocognitive assessment ..... 94
2.7.1 Emotion recognition and detection ..... 96
2.7.2 Reinforcement-based decision-making ..... 96
2.7.3 Temporal discounting ..... 97
2.7.4 Response inhibition ..... 97
2.7.5 Use of neurocognitive assessment data in correlation with neuroimaging findings ..... 98
2.7.6 Benefits ..... 98
2.7.7 Challenges ..... 99
2.8 Intranasal oxytocin ..... 99
2.8.1 Administration in the current study ..... 99
2.8.2 Methodological challenges in oxytocin research ..... 100

2.9 Statistical analysis overview ..... 106
2.9.1 General approach ..... 106
2.9.2 Power calculation ..... 108
3 Neuroimaging Methods ..... 110
3.1 Structural MRI ..... 110
3.1.1 Image acquisition ..... 110
3.1.2 Surface-based morphometry ..... 111
3.1.3 Pre-processing ..... 113
3.1.4 Statistical analysis ..... 115
3.1.5 Benefits ..... 119
3.1.6 Challenges ..... 119
3.2 Resting-state fMRI I: three-dimensional pseudo-continuous arterial spin labelling ..... 120
3.2.1 Regional cerebral blood flow ..... 120
3.2.2 Image acquisition ..... 121
3.2.3 Pre-processing ..... 123
3.2.4 Statistical analysis ..... 125
3.2.5 Benefits ..... 128
3.2.6 Challenges ..... 129
3.3 Resting-state fMRI II: BOLD signal imaging ..... 130
3.3.1 The BOLD signal ..... 131
3.3.2 Image acquisition ..... 133
3.3.3 Pre-processing ..... 133
3.3.4 Large-scale networks ..... 137
3.3.5 Large-scale network statistical analysis ..... 138
3.3.6 Graph theory ..... 143

3.3.7 Graph theory statistical analysis ..... 148
3.3.8 Benefits ..... 153
3.3.9 Challenges ..... 156
4 A structural MRI investigation of violent offenders with ASPD ..... 159
4.1 Introduction ..... 159
4.2 Methods ..... 163
4.2.1 Participants ..... 163
4.2.2 Procedure ..... 164
4.2.3 Image acquisition ..... 165
4.2.4 Image pre-processing ..... 165
4.2.5 Statistical analysis ..... 166
4.3 Results ..... 168
4.3.1 Demographic and clinical characteristics ..... 168
4.3.2 Global brain measures ..... 169
4.3.3 Cortical volume ..... 169
4.3.4 Cortical thickness ..... 170
4.3.5 Surface area ..... 170
4.3.6 Spatial overlap of group differences in CT and SA ..... 173
4.3.7 Contribution of CT and SA to differences in regional CV ..... 174
4.3.8 Correlation with phenotype ..... 174
4.4 Discussion ..... 176
5 An arterial spin labelling investigation to measure regional cerebral blood flow and the effect of intranasal oxytocin in violent offenders with ASPD ..... 185
5.1 Introduction ..... 185
5.2 Methods ..... 188

5.2.1 Participants ..... 188
5.2.2 Study design and procedure ..... 188
5.2.3 Image acquisition ..... 189
5.2.4 Image pre-processing ..... 190
5.2.5 Statistical analysis ..... 191
5.3 Results ..... 193
5.3.1 Demographic and clinical characteristics ..... 193
5.3.2 Global median CBF ..... 195
5.3.3 Whole-brain analysis ..... 195
5.3.4 Supplementary ROI analyses ..... 199
5.3.5 Correlation with phenotype ..... 199
5.4 Discussion ..... 201
6 A resting-state fMRI investigation into large-scale network functional connectivity and the effect of intranasal oxytocin in violent offenders with ASPD ..... 209
6.1 Introduction ..... 209
6.2 Methods ..... 215
6.2.1 Participants ..... 215
6.2.2 Study design and procedure ..... 216
6.2.3 Image acquisition ..... 217
6.2.4 Image pre-processing ..... 217
6.2.5 Statistical analysis: demographic and clinical characteristics 218
6.2.6 Statistical analysis: large-scale network analysis ..... 218
6.2.7 Statistical analysis: correlation with phenotype ..... 223
6.3 Results ..... 224
6.3.1 Demographic and clinical characteristics ..... 224

6.3.2 Large-scale network analysis ..... 225
6.3.3 Correlation with phenotype ..... 229
6.4 Discussion ..... 232
7 A resting-state fMRI investigation into network topology and the effect of intranasal oxytocin in violent offenders with ASPD ..... 239
7.1 Introduction ..... 239
7.2 Methods ..... 244
7.2.1 Participants ..... 244
7.2.2 Study design and procedure ..... 245
7.2.3 Image acquisition ..... 246
7.2.4 Image pre-processing ..... 246
7.2.5 Statistical analysis: demographic and clinical characteristics 247
7.2.6 Statistical analysis: graph theory ..... 247
7.2.7 Statistical analysis: network-based statistic ..... 251
7.2.8 Statistical analysis: correlation with phenotype ..... 252
7.3 Results ..... 253
7.3.1 Demographic and clinical characteristics ..... 253
7.3.2 Graph theory analysis ..... 254
7.3.3 Correlation with phenotype ..... 269
7.4 Discussion ..... 273
8 General Discussion ..... 282
8.1 Research problem and aims ..... 282
8.2 Summary of findings ..... 282
8.3 Emerging themes ..... 285
8.4 Limitations of the current research ..... 290
8.5 Implications and future research ..... 295

8.6 Conclusion ..... 298
Bibliography ..... 300
Appendix ..... 380
Post-hoc sensitivity analyses to measure the impact of substance use ..... 380
Supplement chapter 4: Group differences in brain structure ..... 380
Supplement chapter 5: Group differences and OT effects in rCBF .. 381
Supplement chapter 6: Group differences and OT effects in functional connectivity ..... 382
Supplement chapter 7: Group differences and OT effects in network topology ..... 382

# Acknowledgements

I would like to thank my participants. You have offered deeply personal insight into your lives and often made incredible effort to participate. I wish you all the best for your futures. Thank you also to the probation officers who worked overtime to help us recruit these participants.

I would also like to sincerely acknowledge the supervision, support, feedback, motivation, and guidance I received from my supervisors, Dr Nigel Blackwood and Prof Declan Murphy. You have continuously helped me find and see the bigger picture. Nigel, your stories always reminded me of the necessity of our work, and I do hope you now have your Sundays back; and Declan, thank you for your 'unique' feedback style and never letting me forget what I mean or why I am saying something.

Another big acknowledgement goes to Dr John Tully. Thank you for developing this project, offering great teamwork during data collection, providing guidance about the PhD process, and continuously considering my early career development through opportunities like paper authorship and conference presentations.

A massive thank you also to Dr Daniel Martins. You have taught me most of the methodological and statistical skills required for this PhD, and despite your packed schedule, you always found time to help me. I genuinely appreciated this so much. Similarly, I would like to acknowledge the data analysis support I received from Dr Charlotte Pretzsch. Thank you also for always offering your help and for giving invaluable advice about the wider PhD experience.

I would also like to acknowledge my peers, in particular Emma, Elisa, Emily, and Suzanne, and many other FANS department PhD students. Thank you for the many laughs and ranting sessions that have made this PhD more tolerable. Thank you also for sharing your various pieces of advice and experience over the years.

On a personal note, my most sincere and heartfelt gratitude is extended to my partner, and to my family and friends. Heze, thank you for always believing in me, thank you for helping me build my confidence back up when it was knocked down, thank you for supporting me to identify problems and find solutions (or to see things aren't really so problematic), thank you for your patience with me, thank you for the many delicious and nutritious meals you have cooked for me while I was engrossed in work, and thank you for your contagious laugh which never ceased to make me smile, even in the toughest moments. Natalia, mom, and dad, thank you for your continuous curiosity, your incredible and unwavering generosity, your willingness to help, your personal advice on many matters, your excellent entertainment through cat-related content, and your open home. You set the bar high, and I hope that I have made you proud. To my dear friends in England and Germany, especially Corinna and Lilla, thank you for being on this journey with me, for always having an open ear, for always being intrigued and inquisitive, and for providing much-needed respite.

*I would like to dedicate this thesis to those who have carried out and those who have suffered under acts of interpersonal violence.*

# Declaration of Contributions

The copyright of this thesis rests with the author and no quotation from it or information derived from it may be published without proper acknowledgement.

I, Julia Griem, declare that I wrote this thesis and confirm that the work in this thesis is my own. I also confirm that this thesis was evaluated by my supervisors Dr Nigel Blackwood and Prof Declan Murphy.

I am the recipient of a National Institute for Health and Care Research (NIHR) Maudsley Biomedical Research Centre (BRC) PhD studentship. The experimental studies in this thesis were partly funded by this grant, and largely funded by a Wellcome Clinical Research Training Fellowship grant awarded to Dr John Tully.

The views expressed are my own and not necessarily those of either the NIHR or the Wellcome Trust.

Dr John Tully and my supervisors conceived and designed the study protocol which included the data that I used in this thesis. Dr John Tully and I collected all the data. Together with my supervisors, I planned the analysis of the data that I used in this thesis.

Dr Charlotte Pretzsch and Dr Anke Bletsch (chapter 4), and Dr Daniel Martins and Dr Yannis Paloyelis (chapters 5-7) assisted with the data analysis. Template scripts for data pre-processing and analysis were provided by Dr Christine Ecker, Dr Daniel Martins, Dr Ottavia Dipasquale, and Dr Cathy Davies. The neurocognitive tests were kindly provided by Prof James Blair.

# Covid-19 Impact Statement

The disruption caused by the Covid-19 pandemic led a forced ending to participant recruitment and data collection in March 2020, 7 months before the official recruitment end date (September 2020). As a result, the proposed sample size of 24 participants with complete and usable data per group was not acquired. Instead, there were between 12 and 23 participants available per group across the various analyses.

As a consequence of the restricted sample size, the study had reduced statistical power. Moreover, in two of four experimental chapters, this also meant that it was not possible to further subcategorize the antisocial personality disorder (ASPD) group into a group with psychopathy and another group without psychopathy. This was an overarching aim of the study and therefore, it impacted the thesis narrative. However, the analyses could still be conducted with all individuals with ASPD in one group.

# List of Tables

Table 1.1 The general criteria for the diagnosis of a personality disorder according to the DSM-5 and the ICD-11. ..... 36
Table 1.2 The specific diagnostic criteria for ASPD according to the DSM-5. ..... 37
Table 1.3 The PCL-R items, facets, and factors. ..... 44
Table 1.4 Overview of the neurocognitive deficits in ASPD+/-P. ..... 65
Table 4.1 Demographic and clinical characteristics of participants included in the structural analysis. ..... 169
Table 4.2 Structural global brain measures. ..... 169
Table 4.3 Descriptions of clusters with significant group differences in CV, CT, and SA. ..... 171
Table 4.4 Partial Pearson coefficients for structure-phenotype correlations. ..... 176
Table 5.1 Demographic and clinical characteristics of participants included in the ASL analysis. ..... 194
Table 5.2 Global median CBF mean and standard deviation (SD). ..... 195
Table 5.3 Whole-brain clusters with significant group and interaction effects on rCBF..... 196
Table 5.4 Results from the supplementary ROI analysis of rCBF. ..... 199
Table 5.5 Partial Pearson coefficients for rCBF-phenotype correlations. 201
Table 6.1 Demographic and clinical characteristics of the participants included in the large-scale network analysis..... 224
Table 6.2 Results from the within-network functional connectivity analysis..... 226
Table 6.3 Partial Pearson coefficients for within-network functional connectivity-phenotype correlations. ..... 231
Table 7.1 Demographic and clinical characteristics of the participants included in the network topology analysis. ..... 254
Table 7.2 Meso-level nodal findings for the ROI analysis. ..... 261
Table 7.3 Meso-level nodal findings for the whole-brain analysis..... 263

Table 7.4 Dice coefficients for each large-scale network. ..... 267
Table 7.5 Details of the subnetwork at different primary t-thresholds.. 267
Table 7.6 Partial Pearson coefficients for network topology (group differences) – phenotype correlations..... 272
Table 7.7 Partial Pearson coefficients for network topology (OT responsivity) – phenotype correlations. ..... 273
Table 8.1 Summary of significant group differences across neurobiological features. ..... 284
Table 8.2 Summary of the treatment and group by treatment interaction effects across resting-state features..... 285

# List of Figures

Figure 2.1 Flowchart of the recruitment process and study procedure. .. 92
Figure 2.2 Spatiotemporal effects of intranasal oxytocin on the brain. . 100
Figure 2.3 Intranasal administration of exogenous oxytocin and production of endogenous oxytocin. ..... 102
Figure 3.1 Example of a Freesurfer cortical surface reconstruction. .... 112
Figure 3.2 Overview of the Freesurfer recon-all pipeline. ..... 115
Figure 3.3 Arterial spin labelling neuroimaging technique..... 123
Figure 3.4 BOLD signal detection in fMRI. ..... 132
Figure 3.5 Visual display of the dual regression analysis technique. .... 140
Figure 3.6 Visual representation of the graph theory metrics included in this analysis..... 146
Figure 3.7 Overview of the graph theory analysis technique. ..... 148
Figure 4.1 Significant group differences in CV, CT, and SA. ..... 172
Figure 4.2 Contribution of CT and SA to significant CV abnormalities... 173
Figure 4.3 Significant positive correlation between posterior cingulate cortex SA and reactive aggression in ASPD-P. ..... 175
Figure 5.1 Clusters with significant group differences in median rCBF in the whole-brain analysis..... 197
Figure 5.2 Cluster with a significant group by treatment interaction effect on median rCBF..... 198
Figure 5.3 Significant positive correlation between cluster 5 rCBF and emotion recognition accuracy for angry faces in ASPD+/-P. ..... 200
Figure 6.1 Large-scale network templates..... 221
Figure 6.2 Visualization of the significant group differences identified in the within-network functional connectivity analysis of candidate networks. ..... 227
Figure 6.3 Visualization of the significant group differences identified in the within-network functional connectivity analysis of non-candidate networks. ..... 228

Figure 6.4 Visualization of the cluster showing the significant group by treatment interaction effect in the within-network functional connectivity analysis..... 229
Figure 6.5 Significant negative correlation between functional connectivity in MTN and response reversal accuracy. ..... 230
Figure 7.1 Visual representation of the graph theory metrics..... 250
Figure 7.2 Significant group differences in A) global efficiency, B) local efficiency, and C) nodal efficiency (right precuneus). ..... 255
Figure 7.3 Significant treatment effects in node degree in A) the left and B) the right anterior cingulate cortex. ..... 259
Figure 7.4 Visualization of nodal metrics with large effect sizes. ..... 264
Figure 7.5 Significant interaction effects in nodal efficiency. ..... 265
Figure 7.6 Significant interaction effects in A) node degree centrality and B) betweenness centrality..... 266
Figure 7.7 Subnetwork with significantly increased edge connectivity in ASPD. ..... 268
Figure 7.8 Significant positive correlation between L mOFC BC and angry face detection speed in ASPD. ..... 270

# List of Abbreviations

| | |
|---|---|
| ADHD | Attention deficit hyperactivity disorder |
| AL | Adolescent-limited (antisocial behaviour) |
| ANOVA | Analysis of variance |
| ANCOVA | Analysis of covariance |
| ANTs | Advanced normalization tools |
| ASAP | Automatic software for ASL processing |
| ASL | Arterial spin labelling |
| ASPD | Antisocial personality disorder |
| ASPD+P | Antisocial personality disorder with psychopathy |
| ASPD-P | Antisocial personality disorder without psychopathy |
| BCT | Brain connectivity toolbox |
| BOLD | Blood oxygenation-level dependent |
| CBF | Cerebral blood flow |
| CBT | Cognitive Behavioural Therapy |
| CD | Conduct disorder |
| CT | Cortical thickness |
| CSF | Cerebrospinal fluid |
| CU | Callous-unemotional |
| CV | Cortical volume |
| Df | Degrees of freedom |
| DKA | Desikan-Killiany atlas |
| DMN | Default mode network |
| DNA | Deoxyribonucleic acid |
| DSM-5 | Diagnostic and Statistical Manual of Mental Disorders, 5$^{th}$ edition |
| eICV | Estimated intracranial volume |
| EPI | Echo planar imaging |

| | |
|---|---|
| FA | Flip angle |
| FC | Functional connectivity |
| FDR | Benjamini-Hochberg false discovery rate |
| fMRI | Functional magnetic resonance imaging |
| FOV | Field of view |
| FPN | Frontoparietal network |
| FWER | Family-wise error rate |
| g | Gram |
| GABA | Gamma aminobutyric acid |
| gICA | Group independent component analysis |
| GMV | Grey matter volume |
| GWAS | Genome-wide association studies |
| ICD-11 | International Classification of Diseases, 11$^{th}$ edition |
| IPDE | International Personality Disorder Examination |
| IQ | Intelligence quotient |
| IU | International units |
| LCP | Life-course persistent (antisocial behaviour) |
| LPE | Limited prosocial emotions |
| MAOA | Monoamine oxidase-A gene |
| ME-ICA | Multi-echo independent component analysis |
| MNI | Montreal Neurological Institute |
| ml | Millilitre |
| mm | Millimetre |
| MRI | Magnetic resonance imaging |
| ms | Millisecond |
| MTN | Medial-temporal network |
| NBS | Network-based statistic |
| NHS | National Health Service |

| | |
|---|---|
| NO | Non-offenders |
| OFC | Orbitofrontal cortex |
| OT | Intranasal oxytocin |
| OXT | Oxytocin gene |
| OXTR | Oxytocin receptor gene |
| PCL-R | Psychopathy Checklist-Revised |
| PCL-SV | Psychopathy Checklist-Revised, Short Version |
| PD | Proton density |
| PET | Positron emission tomography |
| PL | Placebo |
| PNC | Police national records |
| PTSD | Post-traumatic stress disorder |
| RDoC | Research domain criteria |
| RFT | Random field theory |
| ROI | Region of interest |
| RPQ | Reactive proactive aggression questionnaire |
| rCBF | Regional cerebral blood flow |
| rs-fMRI | Resting-state functional magnetic resonance imaging |
| SA | Surface area |
| SAL | Salience network |
| SBM | Surface-based morphometry |
| SCID-5-CV | Structured Clinical Interview according to the DSM-5, Clinical Version |
| SCID-5-PD | Structured Clinical Interview according to the DSM-5, Personality Disorder |
| sMRI | Structural magnetic resonance imaging |
| SPECT | Single-photon emission computed tomography |
| SSRT | Stop signal reaction time |
| TE | Echo time |

| | |
|---|---|
| TI | Inversion recovery |
| ToM | Theory of mind |
| TR | Repetition time |
| UK | United Kingdom |
| USA | United States of America |
| VBM | Voxel-based morphometry |
| WASI-II | Wechsler Abbreviated Scale for Intelligence, 2nd edition |
| WMV | White matter volume |
| 2D | Two dimensional |
| 3D | Three dimensional |
| 5-HTT | Serotonin transporter gene |

# 1 General Introduction

Interpersonal violence is a global public health problem. About 1% of the population is responsible for over 60% of violent crime. These individuals are typically male, have a history of life-course persistent antisocial behaviour, and meet diagnostic criteria for conduct disorder (CD) in childhood and antisocial personality disorder (ASPD) in adulthood. Adults with ASPD are a heterogeneous group. Some of these individuals additionally meet diagnostic criteria for psychopathy, offend from an earlier age, with more instrumental goals and with higher frequency and versatility. Neurocognitive and neuroimaging studies suggest that adults with ASPD (with or without additional diagnoses of psychopathy) can be distinguished. However, the extent to which the neurobiological abnormalities observed in these groups are susceptible to neurochemical modulation remains to be established. This thesis will therefore investigate brain structure, resting-state regional cerebral blood flow, resting-state functional connectivity, and resting-state network topology in male violent offenders with ASPD (with and without psychopathy). It will additionally examine the potential impact of the social neuropeptide oxytocin on brain function in these men.

This introductory chapter is split into three sections. The first section will document the extent and impact of violent crime in society and outline the developmental nature of such offending behaviours. The second section will provide an overview of the current clinical conceptualisation of personality disorders. The aetiology, psychopathology, and clinical outcomes of ASPD and psychopathy will be outlined. Current treatment interventions will be considered. The third section will review the existing literature on the neurocognitive, neurobiological, and neurochemical correlates of ASPD and psychopathy.

## 1.1 A developmental approach to understanding violent crime

### 1.1.1 Violent crime: its extent and impact

Violence may be defined as the "the intentional use of physical force or power, threatened or actual, against oneself, another person, or against a group or community, that either results in or has a high likelihood of resulting in injury, death, psychological harm, maldevelopment or deprivation" (World Health Organization & Violence and Injury Prevention Consortium, 1996). Violence is commonly categorized into interpersonal, self-directed and collective (e.g. war) subtypes (B. X. Lee, 2016). The interpersonal subtype captures most violent crime and includes the offenses of murder, attempted murder, manslaughter, grievous/actual bodily harm, common assault, robbery, and sexual violence. It is thus the most relevant to focus on in the context of ASPD and psychopathy.

Violence is a global public health problem (World Health Organization et al., 2014). It is associated with a significant psychological burden for victims, perpetrators and communities as well as considerable financial costs (Krug et al., 2002; Mikton et al., 2016). The global cost of interpersonal violence in 2021 was estimated to be $1.85 trillion, equivalent to nearly 2% of the world's gross domestic product (Institute for Economics & Peace, 2022). United Kingdom (UK) Home Office figures suggest that interpersonal violent crime costs the country £37 billion per year (Heeks et al., 2018). In England and Wales in 2021, there were 90,000 convictions for interpersonal violence and an estimated 150,000 individuals attended accident and emergency services for violence-related injuries (Ministry of Justice, 2022; Sivarajasingam et al., 2022).

### 1.1.2 A developmental approach to understanding violence across the lifespan

To reduce the prevalence and impact of violent crime, the nature of its development must be understood. The perpetration of interpersonal

violence is a form of antisocial behaviour – behaviour that goes against social norms and conventions. The recognition of age-related trends sparked an interest in understanding antisocial behaviour from a lifespan developmental perspective. For instance, irritability and interpersonal aggression (i.e. hitting, kicking, hair-pulling) are relatively normal in early childhood – in fact, 84% of pre-schoolers have temper tantrums (Wakschlag et al., 2012) and over 90% of toddlers engage in physically aggressive behaviour (Lorber et al., 2019) – but this subsides after the age of 3 in normally developing children (Nærde et al., 2014). Furthermore, the 'age-crime curve' shows that antisocial behaviour including violence and other criminal activity is disproportionately high among young males aged 15 to 29 (Mikton et al., 2016) and decreases with age thereafter (Loeber & Farrington, 2014; National Research Council et al., 1986). Therefore, developmental cohort studies have followed representative population cohorts in different countries over many years to explore the development of such behaviours (Carlisi et al., 2020; Farrington, 2019; Jennings et al., 2015; Poulton et al., 2015; Zych et al., 2021).

Drawing on consistent findings from these cohort studies, Moffitt suggested that adolescent-limited (AL) and life-course persistent (LCP) antisocial behaviours should be distinguished (Moffitt, 2018). According to the age-crime curve, most antisocial behaviour is committed by the AL subtype, but this is largely mild. Approximately half of the adolescent population will engage in offending/illegal behaviour at least once (Barberet et al., 2004; Elliott et al., 1983). Such delinquency, especially in males, is therefore common, yet transient, and hypothesized to occur due to psychosocial factors and a gap between biological and social maturity (Farrington, 2020; Moffitt, 1993). These individuals typically discontinue their antisocial behaviour and act in line with social norms by their mid-20s. The LCP antisocial behaviour group consists of the smaller proportion of individuals who engage in antisocial behaviour from childhood throughout adolescence and adulthood (Jennings et al., 2015). These individuals are exposed to

underlying biological (genetic and neurobiological) risk factors which may cause neurocognitive deficits in reward-/punishment-based learning and decision-making (Carlisi et al., 2020; Farrington, 2020; Van Goozen et al., 2022). In turn, these reduce their capacity to navigate common childhood challenges such as educational pressures, which may lead to truancy and dropout, and diminish their capability to manage and resist adolescent antisocial urges, tendencies and peer pressures (Moffitt, 1993, 2018). LCP antisocial behaviour is often more serious or violent than AL antisocial behaviour (Jennings et al., 2015).

Longitudinal cohort studies thus support the idea of a small yet significant group of individuals with LCP antisocial behaviour/offending, showing there is a clear developmental trajectory (Jolliffe, Farrington, Piquero, MacLeod, et al., 2017). Increased frequency and severity of neurobiological, cognitive, behavioural and psychosocial risk factors at an early age are prerequisites for developing LCP antisocial behaviour (Assink et al., 2015; Carlisi et al., 2020; Fairchild et al., 2013; Jolliffe, Farrington, Piquero, Loeber, et al., 2017). Those with an earlier onset and LCP antisocial behaviour are likely to have poor life outcomes (Docherty et al., 2019; Lynam et al., 2007; Moffitt, 2018; Poulton et al., 2015). Such individuals typically meet diagnostic criteria for externalising disorders including CD in childhood and ASPD in adulthood. Given that CD is the developmental precursor to ASPD, it is important to consider the clinical nature, risk factors, and neurocognitive and neurobiological correlates of CD to underpin an understanding of ASPD. This will be summarized in the next section.

### 1.1.3 Conduct Disorder

#### *1.1.3.1 Clinical profile*

CD is classified as an externalising disorder of childhood behaviour. According to the Diagnostic and Statistical Manual of Mental Disorders, 5th Edition (DSM-5; American Psychiatric Association, 2013), a diagnosis is made when two or more of fifteen behavioural abnormalities are present.

These behaviours may involve aggression against people, animals and property, arson, sexual misconduct, frequent lying or conning, and rule-breaking behaviour such as truancy, stealing, and burglary. Fundamental to all CD diagnoses is the pathological presence of antisocial behaviour including violence throughout childhood and adolescence. In the UK, about 6% of pre-school and school-aged children and adolescents meet diagnostic criteria for CD (Green et al., 2004; Kim-Cohen et al., 2005; Polanczyk et al., 2015). CD is often comorbid with other externalising pathologies such as attention deficit/hyperactivity disorder (ADHD) and early onset substance misuse, as well as depression and anxiety disorders, and reading/learning disabilities (Fairchild et al., 2019). The diagnosis of CD is a developmental precursor of ASPD as well as other psychiatric disorders in adulthood (Copeland et al., 2009), and it is predictive of increased violence in adulthood (Junewicz & Bates Billick, 2020).

The diagnostic construct conceals significant heterogeneity (Lindhiem et al., 2015). Two broad CD developmental pathways have been identified from infancy: impulsive/irritable and callous/unconcerned (Wakschlag et al., 2018). The impulsive/irritable group are characterised by abnormally frequent, persistent, and destructive temper tantrums, difficulties with emotion regulation and self-soothing, and disruptive behaviour which may be difficult to manage by adults. They also show reactive aggression, defined as an impulsive, emotionally labile response to threat and provocation (Dodge, 1991; Urben et al., 2018). The callous/unconcerned (CU) group are characterised by callousness, reduced guilt and empathy, and increased manipulativeness and exploitation of others. In addition to displays of reactive aggression, this subtype also shows proactive aggression, which is the instrumental and premeditated use of violence to achieve a goal or obtain a reward (Dodge, 1991; Fanti et al., 2009; Kohls et al., 2020). The CU subtype is captured within the DSM-5 using the CD specifier 'limited prosocial emotions' (LPE) (R. J. R. Blair, Leibenluft, et al., 2014; Pardini et al., 2010). Prevalence estimates of this LPE subgroup are

around 50% when combining child and parent reports (Colins et al., 2020). Due to their stability over time, the presence of CU traits during childhood is a significant risk factor for violence across the lifespan (Docherty et al., 2019; Frick & White, 2008; Loeber et al., 2009).

#### *1.1.3.2 Risk factors*

CD, like most mental disorders, is thought to have a complex, multifactorial aetiology. It is characterized by polygenic inheritance and genetic heterogeneity across individuals, influencing and interacting with environmental factors at any point during development. Genes operate probabilistically rather than deterministically: genes code for proteins that influence characteristics, such as neurocognitive vulnerabilities, that in turn increase the risk of CD, particularly under certain environmental conditions. Thus, genetic and environmental risk factors, and their interactions, have to be considered.

The most robust heritability estimates for CD are about 40-50% (Jaffee et al., 2005). CU traits have an even higher heritability of approximately 67% (Viding et al., 2005). A large longitudinal twin study revealed that genetic risk factors contribute to the heterogeneity of the disorder across lifespan development and to its overall stability over time (Wesseldijk et al., 2018). From a molecular perspective, candidate gene analyses have revealed suggestive differences in the gene expression for neurotransmitters such as serotonin, dopamine and oxytocin (Salvatore & Dick, 2018; Veroude et al., 2016), but these studies were under-powered, have not been robustly replicated and currently cannot predict behavioural outcomes such as antisocial behaviour (Vassos et al., 2014). Genome-wide association studies (GWAS) have explored genetic underpinnings of latent constructs associated with antisocial and externalising behaviours such as aggression and criminality (Fairchild et al., 2019; Pappa et al., 2016; Tielbeek et al., 2017, 2022). Furthermore, a recent analysis of 1.5 million people identified over 500 genetic loci associated with externalising disorders (Karlsson Linnér et al., 2021). Importantly, this study revealed numerous loci related

to neurobiological development and protein expression in the brain. Together, GWAS evidence suggests that CD and its related behaviours are polygenic, and that genetic risk is pleiotropic. Nevertheless, studies examining CD remain under-powered in comparison to those established to explore the genetic underpinnings of, for example, psychotic disorders.

Twin studies have shown that around 50% of the variance in CD is due to shared and non-shared environmental risk factors (Fairchild et al., 2019; Wesseldijk et al., 2018). Shared environmental risk factors only explain a significant amount of variance in individuals without CU traits (Viding et al., 2005). In contrast, non-shared environmental risk factors have been shown to have a moderate influence on CU traits (Sánchez de Ribera et al., 2019; Viding & McCrory, 2012). Furthermore, common prenatal and perinatal risk factors such as exposure to alcohol, nicotine, maternal anxiety, or birth complications resulting in hypoxia have been associated with an increased likelihood of developing CD, and with a higher frequency and severity associated with earlier onset and greater risk of violence (Fairchild et al., 2019). This is likely due to the impact on developing neural structures resulting in a vulnerability to conduct problems (R. J. R. Blair, Leibenluft, et al., 2014). Additionally, family and social environmental factors such as poor parenting, childhood maltreatment, poverty, community violence, and association with antisocial peers play a strong role in increasing the likelihood of developing CD (Fairchild et al., 2019).

Finally, interplay between genetic and environmental factors are critical for the development of CD and CU traits (Hyde et al., 2016; Nilsson et al., 2018). For instance, gene-environment correlations can increase risk. An individual with genetic predisposition to antisocial behaviour and CD is more likely to engage with an antisocial environment, thereby exacerbating their risk of developing LCP antisocial behaviour (Viding & McCrory, 2018). Moreover, a gene-environment interaction, which refers to a situation in which the expression of genes depends on the environment and/or the effect of the environment depends on the genotype (Dick, 2011), can also

increase risk. For example, longitudinal analyses suggest that shared environmental risk factors including negative parental discipline and a chaotic home life interact with genetic risk factors, particularly during adolescence, to increase the risk of CD (Fontaine et al., 2011). Such interactions can also be important towards the development of CU traits specifically. One study demonstrated that altered expression of a serotonin transporter gene, which is particularly involved in amygdala reactivity, is only associated with heightened risk of CU in the context of low socioeconomic status (Sadeh et al., 2010). Finally, environmental risk factors also have the potential to epigenetically modify DNA expression (Meaney, 2017). For instance, evidence has shown that increased exposure to an environmental risk factor such as maltreatment is linked with increased antisocial behaviour due to higher DNA methylation, for example in the monoamine oxidase-A (MAOA) gene (Fergusson et al., 2011; Ouellet-Morin et al., 2016). This therefore suggests a dose-dependent effect of the environment on gene expression.

In summary, the contribution of genetic and environmental risk factors towards the development of CD and CU traits, associated antisocial behaviour, and violence has been highlighted. Such risk factors, alongside dispositional risk factors such as temperament, personality traits, and even neurocognitive deficits can increase the susceptibility to further risk factors (Fairchild et al., 2019; Pardini et al., 2018).

#### *1.1.3.3 Evidence of neurocognitive and neurobiological abnormality in CD*

CD has been associated with neurocognitive and neurobiological deficits. Due to the heterogeneity of CD, and externalising disorders more widely, the extent of these deficits also varies. There is some evidence that they differ between those with CD with versus without CU traits.

On a behavioural level, deficits in emotional responsiveness such as reduced physiological reactivity to threat, poor emotion recognition and

abnormal empathic processing have been identified in children and adolescents with CD, whereby those with CU traits have more severe and/or specific deficits than those with impulsive/irritable traits only (R. J. R. Blair, Leibenluft, et al., 2014; R. J. R. Blair, White, et al., 2014; Dawel et al., 2012; De Looff et al., 2022; Fanti, Panayiotou, et al., 2016; Hartmann & Schwenck, 2020; Kohls et al., 2020; Martin-Key et al., 2017; Pasalich et al., 2014; Viding & McCrory, 2018). Deficits in reward and punishment processing, which impact reinforcement-based learning, decision-making and moral judgments, have also been identified in CD (R. J. R. Blair, White, et al., 2014; Fairchild et al., 2009; Hobson et al., 2011; Johnson et al., 2015; Kohls et al., 2020).

On a neural level, meta-analyses indicate that abnormal brain activity in several brain regions may partially explain such deficits in emotional responsiveness and reward and punishment processing in CD. These include frontotemporal cortical areas such as orbitofrontal and ventromedial prefrontal cortex, anterior cingulate cortex, anterior insula, and temporal pole, as well as subcortical regions such as the amygdala, thalamus, and striatum (Alegria et al., 2016; Noordermeer et al., 2016; Viding & McCrory, 2018). Furthermore, evidence suggests that abnormalities on the neural level may also depend on the presence of CU traits. For instance, in the amygdala, individuals with CU traits show a significant underactivation, particularly when processing fearful expressions, whereas those without CU traits show an overactivation in response to acute threat, possibly contributing to increased reactive aggression (R. J. R. Blair et al., 2018; R. J. R. Blair, Leibenluft, et al., 2014; S. W. Hawes et al., 2021; Noordermeer et al., 2016; Sethi et al., 2022; Viding et al., 2012). Similarly, only youth with significant CU traits show underactive limbic regions including the thalamus and overactive dorsal striatal regions during emotion and reward processing (Alegria et al., 2016; R. J. R. Blair, 2013b). In summary, it appears that neurocognitive impairments in the domains of emotional responsiveness and reward and

punishment processing are key features of CD. These can be linked to aberrant neurobiological mechanisms. However, the extent and specificity of impairments, alongside the neurobiological mechanisms explaining these deficits, may differ between those with and without CU traits.

In addition to the above, evidence also suggests that executive dysfunction, such deficient inhibitory control and poor problem-solving and planning is associated with CD, even after accounting for comorbid ADHD (Hobson et al., 2011; Noordermeer et al., 2016; White et al., 2014). On the neural level, meta-analytic evidence suggests that abnormal activity in the precuneus and the dorsolateral prefrontal cortex contribute to executive dysfunctions (Alegria et al., 2016; Noordermeer et al., 2016). The presence of CU traits does not seem to moderate this ability (Fanti, Kimonis, et al., 2016; White et al., 2014). Therefore, it is possible that deficits in this domain are a shared mechanism between those with CD with and without CU traits.

To further understand these abnormalities in neurocognitive performance and neural activity, other features of neurobiology have also been studied cross-sectionally in CD. This includes grey and white matter structure, and resting-state brain activity. A meta-analysis of voxel-based structural magnetic resonance imaging (sMRI) studies revealed that adolescent conduct problems are associated with reduced grey matter volumes (GMV) in frontotemporal areas important for affective and sociocognitive processes such as the superior frontal gyrus, amygdala, and insula. This meta-analysis also reported that increased CU traits were associated with less GMV reduction in the left striatum (putamen), indicating possibly distinct structural underpinnings of CD with versus without CU traits (Rogers & De Brito, 2016). Surface-based sMRI studies can assess cortical thickness and surface area in addition to GMV. Such studies (Fairchild et al., 2015; Hyatt et al., 2012; Y. Jiang et al., 2015; Oostermeijer et al., 2016; G. L. Wallace et al., 2014) have shown reduced thickness in similar areas as those showing reduced GMV, with more extreme reductions in

temporal areas associated with elevated CU traits. These studies also suggested reduced surface area, e.g., in the insula, but the evidence base is generally less coherent than for cortical thickness. Together, this suggests that grey matter structure in conduct disordered individuals is aberrant, particularly in areas that contribute to the neurocognitive deficits described above, and that the presence of CU traits may modulate the observed abnormalities.

In terms of white matter structure, diffusion tensor imaging studies assessing frontolimbic and default mode network structural connectivity have revealed somewhat inconsistent results: some studies indicated abnormalities in male CD regardless of CU traits (González-Madruga et al., 2020), while others showed that CU traits moderated or exacerbated the abnormalities in CD (Maurer et al., 2020; Puzzo et al., 2018; Sethi et al., 2018; Waller et al., 2017).

The differential neurobiological mechanisms associated with and without CU traits are also apparent when assessing resting-state brain activity. Studies measuring functional connectivity in CD have revealed aberrant connectivity in large-scale networks such as the default mode, salience, and frontoparietal networks, which was differentially impacted by CU traits (Cohn et al., 2015; F. M. Lu et al., 2017; Thijssen & Kiehl, 2017; Werhahn et al., 2021). Finally, graph theory analysis, an approach used to assess brain topology, has revealed abnormal network organization with less reliance on key hub brain regions such as the posterior cingulate cortex (Y. Jiang et al., 2016; Tillem et al., 2022). Early evidence suggests this may be driven by CU traits (Y. Jiang et al., 2021). Together, abnormal structural and functional connectivity are likely to contribute to the neurocognitive impairments and subsequently to the symptoms of CD.

In summary, there is substantial evidence of neurocognitive and neurobiological deficits cross-sectionally associated with CD. Prospective longitudinal studies exploring changes in neurobiological underpinnings of CD remain rare (Oostermeijer et al., 2016). Individuals with CU traits

(compared to those without such traits) appear to have somewhat distinct and more profound abnormalities in affective and reward-processing domains. Abnormalities in underpinning mechanisms including neural activity, structure, and connectivity may help to explain these deficits. Furthermore, these deficits can lead to reduced self-regulation and increased vulnerability to environmental risk factors such as substance misuse, which in turn may increase the overall chance of developing ASPD and psychopathic traits in adulthood (R. J. R. Blair, Leibenluft, et al., 2014; Fairchild et al., 2019; Junewicz & Bates Billick, 2020; Raine et al., 2011).

#### *1.1.3.4 Developmental trajectory of CD*

In the long-term, individuals with CD have an increased risk of poor life outcomes (Assink et al., 2015; Fairchild et al., 2019). CD is associated with unemployment, poor relationships, criminality and psychopathology later in life (Erskine et al., 2016). About 50% of individuals with CD go on to develop ASPD in adulthood and thus engage in LCP antisocial behaviour (Copeland et al., 2009; National Institute for Health and Care Excellence, 2017). A greater number of genetic risk factors, earlier age of onset, more severe neurocognitive and neurobiological abnormalities, higher severity of antisocial behaviour and violence, presence of CU traits, substance misuse, poor parenting, and school drop-out are particularly associated with the risk of developing ASPD and LCP antisocial behaviour (Assink et al., 2015; Docherty et al., 2019; Jolliffe, Farrington, Piquero, Loeber, et al., 2017; Lynam et al., 2007; Moffitt, 2018; Moore et al., 2017).

Early diagnosis and intervention in CD is thus essential for reducing the risk of later ASPD, LCP antisocial behaviour and violence (M. F. Caldwell et al., 2006; Junewicz & Bates Billick, 2020). The high prevalence of ASPD in adult prisons suggests that more investigation into the underlying causes, mechanisms, and treatments of ASPD is also required. In the long-term, better understanding of ASPD is likely to have a beneficial impact by reducing the prevalence of LCP antisocial behaviour, violent crime, and the associated high social and financial costs. Such improved understanding

may also inform novel treatment approaches. The next section will present a brief overview of personality disorders before providing detailed clinical profile of ASPD and psychopathy. A brief overview of risk factors, comorbidities and outcomes will be provided.

## 1.2 Clinical conceptualisation of antisocial personality disorder and psychopathy

### 1.2.1 General features of personality disorder

A personality disorder is a mental disorder marked by maladaptive personality traits and persistent, pervasive and problematic patterns of behaviour, cognition and inner experiences, which impair self and interpersonal functioning. *Table* 1.1 summarizes the general criteria for personality disorder in the DSM-5 (American Psychiatric Association, 2013) and the International Classification of Diseases, 11$^{th}$ Edition (ICD-11, World Health Organization, 2019). A recent meta-analysis of 46 studies across 21 countries indicated that the global prevalence of any personality disorder in the community is around 7.8% (Winsper et al., 2020). In the UK, about 4.4% of the community population meet diagnostic criteria for a personality disorder, and around 50% of these individuals have at least two personality disorders (Coid et al., 2006).

| DSM-5 | ICD-11 |
|---|---|
| An enduring pattern of inner experience and behaviour that deviates markedly from the expectations of the individual's culture (in at least two of the following areas: cognition, affectivity, interpersonal functioning, impulse control). | An enduring disturbance characterized by problems in functioning of the self and/or interpersonal dysfunction, which manifests in patterns of cognition, emotional experience and expression, and behaviours that are maladaptive, inflexible, or poorly regulated and which cannot be explained primarily by social or cultural factors. |
| The enduring pattern is inflexible and pervasive across a broad range of personal and social situations. | The disturbance manifests across a range of personal and social situations. |
| The enduring pattern leads to clinically significant distress or impairment in social, occupational, or other important areas of functioning. | The disturbance is associated with substantial distress and significant impairment in personal, social, educational, occupational, or other important areas of functioning |
| The pattern is stable and of long duration, and its onset can be traced back at least to adolescence or early adulthood. | The disturbance has persisted over an extended period (e.g., lasting two years or more) and the patterns of behaviour characterizing the disturbance are not developmentally appropriate. |
| The enduring pattern is not attributable to the physiological effects of a substance or another medical condition and is not better explained as a manifestation or consequence of another mental disorder. | The symptoms are not due to direct effects of medication or substance (incl. withdrawal effects) and are not better accounted for by another mental or medical disorder. |

Table 1.1 The general criteria for the diagnosis of a personality disorder according to the DSM-5 and the ICD-11.
*Note: These are summarized and ordered to emphasize the similarities between both manuals.*

The DSM-5 lists a total of 10 personality disorder categories in three clusters. Cluster A includes the odd and eccentric personality disorders: schizoid, schizotypal, and paranoid. Cluster B includes the dramatic and erratic personality disorders, specifically histrionic, borderline, narcissistic and antisocial. Finally, Cluster C includes the fearful and anxious personality disorders: dependent, avoidant, and obsessive-compulsive.

These categories have provided the basis for most empirical research in personality disorders. Nonetheless, the categorical approach has been criticized for its heterogeneity in symptom configurations and for assuming that a personality disorder is either present or absent, rather than fluctuating in severity (Oldham, 2015). Therefore, the ICD-11, which officially came into effect in 2022, developed a three-tier dimensional approach (mild, moderate, severe) with the option of adding up to six trait domain specifiers (negative affectivity, detachment, dissociality, disinhibition, anankastic, borderline pattern). As *Table* 1.1 shows, the general criteria for personality disorder are nevertheless similar across both classification systems. Going forward, reference to the diagnostic criteria of

the DSM-5 will be made as these were applied in the current thesis and ASPD research more broadly.

### 1.2.2 Antisocial Personality Disorder

#### *1.2.2.1 Clinical profile*

ASPD is one of the 10 types of personality disorders listed in the DSM-5, belonging to cluster B. *Table 1.2* lists the specific diagnostic criteria for ASPD, according to the DSM-5. An optimal diagnosis of ASPD involves a structured clinical interview with an experienced professional. The two main interviews used are the Structured Clinical Interview according to the DSM-5 (SCID-5-PD; First, Williams, Benjamin, & Spitzer, 2015) and the International Personality Disorder Examination (IPDE; Loranger, Janca, & Sartorius, 1997) which draws on both classification systems. Regardless of the assessment instrument used, it is important that both the general features of a personality disorder, as well as the specific criteria for ASPD are met.

| **Antisocial Personality Disorder (DSM-5)** |
|---|
| Pervasive pattern of disregard for and violation of the rights of others, occurring since the age of 15*, as indicated by three or more of the following criteria: |
| 1. Failure to conform to social norms with respect to lawful behaviours, as indicated by repeatedly performing acts that are grounds for arrest |
| 2. Consistent irresponsibility, as indicated by repeated failure to sustain consistent work behaviour or honour financial obligations |
| 3. Impulsivity or failure to plan ahead |
| 4. Irritability and aggressiveness, as indicated by repeated physical fights or assaults |
| 5. Reckless disregard for safety of self or others |
| 6. Deceitfulness, as indicated by repeated lying, use of aliases, or conning others for personal profit or pleasure |
| 7. Lack of remorse, as indicated by being indifferent to or rationalizing having hurt, mistreated, or stolen from another |
| * Meeting the diagnostic threshold for CD before the age of 15 is a prerequisite for the diagnosis of ASPD |

Table 1.2 The specific diagnostic criteria for ASPD according to the DSM-5.

In the community, ASPD has a global prevalence rate of 1.4% (Winsper et al., 2020). In Western countries, this figure is slightly higher at 2.8% (Volkert et al., 2018). In the UK, about 1% of males and 0.6% of the total community population meet diagnostic criteria for ASPD (Coid et al., 2006). Given that most prevalence estimates come from household surveys, one

may assume that these rates are likely to be an underestimate because those with more severe forms of ASPD may either not reside in the community or not participate in such studies.

In prison populations, a meta-analysis of 28 studies revealed that 47% meet the diagnostic threshold for ASPD (Fazel & Danesh, 2002). The diagnosis of ASPD is also a strong predictor of interpersonal violence (Fazel et al., 2018). Indeed, a large majority of violent offenders have or qualify for the diagnosis of ASPD (Piquero & Moffitt, 2014). One percent of the Swedish population (26% of all offenders) accounted for 63% of all violent offenses (Falk et al., 2014). The concentration of violent offenses amongst a small population of LCP offenders has also been confirmed in a meta-analysis (Martinez et al., 2017). Over 30% of the Swedish group of offenders had an official diagnosis of personality disorder, and likely even more would meet the diagnostic threshold if clinically assessed. It is therefore evident that violent crime is strongly associated with ASPD.

#### *1.2.2.2 Comorbidities*

Comorbidities are very common in ASPD. An individual with one personality disorder has a high (40-50%) chance of having another comorbid personality disorder (Coid et al., 2006; Herpertz et al., 1994). ASPD is commonly comorbid with two other Cluster B personality disorders: borderline and narcissistic (Sher et al., 2015). Comorbidities with Cluster A personality disorders, schizotypal, schizoid and paranoid have also been reported (Coid et al., 2006). An increase in the number of personality disorders reflects an increase in the general psychopathology of an individual and is associated with a higher risk of violence (Lowenstein et al., 2016). However, the number of diagnostic thresholds that are met may be overestimated due to the overlap of symptoms across disorders. Therefore, it is important to consider specific maladaptive traits and the extent to which these drive behaviour, particularly in the context of antisocial behaviour, violence and crime (Warren & South, 2009).

As ASPD is an externalising pathology, it is highly comorbid with other externalising disorders. Thus, substance and alcohol misuse disorders are the most common comorbidities of ASPD, inherently forming part of the ASPD phenotype (Blackburn et al., 2003; Compton et al., 2005). Individuals with ASPD have a 17-fold higher likelihood of drug dependence and a 8-fold higher likelihood of alcohol dependence (Trull et al., 2010). Substance and alcohol misuse may have been present since adolescence and acted as a risk factor for developing ASPD (Hodgins et al., 2018). Comorbid substance and alcohol use is also a significant driving force associated with offending and recidivism (Almeida & Moreira, 2017; Flórez et al., 2019). Similarly, there is also a high comorbidity with ADHD (Black et al., 2010).

Other mental health disorders are frequent among individuals with ASPD. Comorbidities include anxiety disorders, depressive disorders, post-traumatic stress disorder (PTSD), self-harm and suicidality (Black et al., 2010; Blackburn et al., 2003; Goodwin & Hamilton, 2003; Hodgins et al., 2010). Psychotic illnesses such as substance-induced psychoses or psychotic episodes have been associated with Cluster B personality disorders, but these are less common than other comorbid mental health illnesses (Coid et al., 2006).

There are suggestions that physical illnesses become increasingly comorbid with ASPD during older age, which may be due to the inherently unhealthy lifestyle lived during younger adulthood as well as an unwillingness to access or cooperate with treatment in older adulthood (Holzer & Vaughn, 2017).

#### *1.2.2.3 Risk factors*

A childhood diagnosis of CD and the presence of LCP antisocial behaviour are homotypic risk factors for developing ASPD. There is therefore an expected overlap in the risk factors for CD and ASPD. This section will focus on any additional risk factors for adult ASPD.

#### 1.2.2.3.1 Genetic

Behavioural genetic research suggests that stable LCP antisocial behaviour is moderately heritable, with 56% of variance explained, yet polygenic (Ferguson, 2010; Tielbeek et al., 2017). Twin studies focusing narrowly on the categorical diagnosis of ASPD, but without accounting for psychopathy, have suggested heritability estimates of 69% (Fu et al., 2002), and suggest that genetic factors are particularly important in the stability of ASPD symptoms (Wesseldijk et al., 2018). Most other research investigating genetic risk factors of ASPD are based on assessing risks for antisocial behaviour and underlying traits including aggression and impulsivity (Romero-Martínez et al., 2022). Meta-analyses have estimated heritability for these traits to be around 50-70%, broadly consistent across sex and ethnicity (Ferguson, 2010; Glenn & Raine, 2014).

The evidence base for molecular genetic risk factors for ASPD in adulthood is limited. It is important to note that no single candidate gene accounts for a significant amount of variance (Vassos et al., 2014). ASPD is thought to have a complex, multifactorial aetiology characterized by polygenic inheritance and genetic heterogeneity across individuals. As in CD, serotonergic, dopaminergic, oxytocinergic and MAOA gene alterations have been considered (Tielbeek et al., 2017, 2022). Genetic variants of other genes have also been identified in a GWAS study of individuals with ASPD (Rautiainen et al., 2016). A recent GWAS study of 1.5 million individuals with various externalizing pathologies revealed a positive correlation between polygenic risk scores of externalising disorders, including over 500 genes, and ASPD symptom counts (Karlsson Linnér et al., 2021). They also demonstrated that polygenic risk scores of externalising disorders accounted for significant proportions of variance of criminality. Together, it thus appears that genetic factors influence the risk of ASPD, but substantially more research is required, particularly to form an understanding of the key molecular genetic risk factors.

#### 1.2.2.3.2 Environmental

Meta-analytic evidence suggests that variance in LCP antisocial behaviour can be further explained by shared (11-16%) and non-shared environmental (31-43%) influences (Ferguson, 2010; Waldman et al., 2018). The impact of these non-shared environmental risk factors increases across development from CD (13%) to ASPD (57%), whereas shared environmental risk factors only play a significant role for CD in childhood (44%) (Wesseldijk et al., 2018). This suggests that the influence of peers and other external factors becomes more important than the influence of parents or family during adulthood.

As for CD, prenatal and perinatal factors including poor maternal mental health, maternal substance, alcohol and nicotine consumption, exposure to neurotoxins such as lead, maternal malnutrition, foetal maldevelopment, and birth complications have all been associated with increased risks of antisocial behaviour and violence across the lifespan, and ASPD in adulthood. Furthermore, poor parenting, childhood maltreatment, maternal rejection and neglect, social adversities, being raised in care, lower intelligence quotient (IQ), adolescent substance use, victimisation and exposure to antisocial peers also exacerbate the risk of developing ASPD (R. J. R. Blair, Leibenluft, et al., 2014; Coid et al., 2006; Glenn & Raine, 2014; Hodgins et al., 2018; Shi et al., 2012; Woehrle et al., 2022).

#### 1.2.2.3.3 Gene-environment interplay

Gene-environment correlations and interactions can also affect the risk of developing ASPD (Hodgins et al., 2018). In terms of gene-environment correlations, a recent large longitudinal cohort study revealed that inherited externalising traits in offspring can elicit environmental reactions including parent externalising behaviours, which together increases the risk for stable adult externalising disorders like ASPD in the offspring (Kretschmer et al., 2022). In terms of gene-environment interaction, an individual's genetic expression may make them more vulnerable to environmental risk

factors. For instance, one study showed that certain genetic variants were associated with increased antisocial behaviour only in those who were also exposed to perinatal maternal smoking (Ruisch et al., 2019). Furthermore, due to gene-environment interactions, an individual may be more inclined to interact with a maladaptive environment due to their genetic predispositions. For example, engaging in substance misuse with peers is more likely to occur amongst individuals with genetic predispositions to externalizing behaviours (Wesseldijk et al., 2018). In turn, this can further contribute towards the risk of developing ASPD in two ways: substance misuse is associated with the environmental risk factor of surrounding oneself with antisocial peers, reinforcing antisocial tendencies, but early-onset substance misuse has also been shown to alter adolescent brain development, reinforcing biological risk factors for ASPD (Filbey et al., 2015). Furthermore, epigenetic risk factors i.e. risk associated with environmental impacts on gene expression have also been identified in association with ASPD (Hodgins et al., 2018). For example, environmental factors such as exposure to maltreatment in childhood or dealing with significant financial stress in adulthood have been shown to alter the expression of the MAOA gene, which contributes to serotonergic dysregulation associated with increased aggression and impulsiveness in ASPD (Checknita et al., 2015; McDermott et al., 2009). As in CD, the impact of experiencing childhood maltreatment can be dose-dependent (Fergusson et al., 2011; Ouellet-Morin et al., 2016). This shows that gene-environment interplay remain important throughout the lifespan.

In summary, genetic and environmental risk factors contribute to the development and maintenance of ASPD traits throughout adulthood. Current knowledge is still limited, but it is widely recognized that interaction among risk factors is particularly important and may contribute to the heterogeneity among individuals with ASPD, including those with and without psychopathy.

### 1.2.3 Psychopathy

#### *1.2.3.1 Clinical profile*

Psychopathy is a multidimensional personality construct associated with ASPD. It is characterized by superficial charm, grandiosity, callousness, lack of empathy, conning/manipulative behaviour, affective and interpersonal disturbances, antisocial lifestyle, impulsivity, irresponsibility and high criminal versatility (Hare, 1991). There is a strong tendency to violate social norms and to have difficulty in maintaining intimate relationships. Such individuals display reactive and particularly proactive, instrumental acts of aggression (Cima & Raine, 2009).

The gold-standard and most common clinical assessment tool for psychopathy is the Hare Psychopathy Checklist-Revised (PCL-R; Hare, 1991), which is applied to clinical semi-structured interviews, such as the PCL-R interview, and collateral information. Twenty items capturing the above characteristics are constructed into two factors: 1) interpersonal-affective, and 2) social deviance. Each factor is further divided into two facets. The first factor includes the interpersonal and the affective facets, and the second factor includes the impulsive lifestyle and antisocial facets. It has been argued that the first factor is associated with traits which are more unique to psychopathy, whereas the second factor aligns with antisocial tendencies and ASPD more generally (Hare et al., 2000). *Table 1.3* shows the items, facets, and factors of the PCL-R. An individual receives a score from 0 to 40. After extensive validation of the tool, primarily in forensic and psychiatric populations, a clinical cut-off score of greater than or equal to 30 is used in North American populations to identify the categorical group (Hare et al., 2000). In Europe, a slightly lower cut-off score of greater than or equal to 25 is used to identify the categorical group (Cooke & Michie, 1999). The lower cut-off score derives from the finding that European individuals have to have higher levels of the underlying latent trait before certain psychopathic characteristics become apparent.

| Factor 1 (Interpersonal-Affective) | | Factor 2 (Social Deviance) | |
|---|---|---|---|
| **Facet 1 (Interpersonal)** | **Facet 2 (Affective)** | **Facet 3 (Lifestyle)** | **Facet 4 (Antisocial)** |
| Glibness/superficial charm | Lack of remorse or guilt | Need for stimulation/proneness to boredom | Poor behavioural controls |
| Grandiose sense of self worth | Shallow affect | Parasitic lifestyle | Early behavioural problems |
| Pathological lying | Callous/lack of empathy | Lack of realistic, long-term goals | Juvenile delinquency |
| Conning/manipulative | Failure to accept responsibility for own actions | Impulsivity | Revocation of conditional release |
| | | Irresponsibility | Criminal versatility |

Table 1.3 The PCL-R items, facets, and factors.
*Note: there are two additional items ('promiscuous sexual behaviour' and 'many short-term marital relationships'), which are part of the total PCL-R score, but which do not load onto individual facet/factor scores.*

In the community, a recent meta-analysis revealed that 1.2% of the Western population meet the PCL-R threshold for psychopathy (Sanz-García et al., 2021). A large discrepancy in the prevalence of psychopathy between community and forensic populations is evident. In the UK, about 0.6% of the community meet the diagnostic threshold for psychopathy (Coid, Yang, Ullrich, Roberts, & Hare, 2009). In contrast, within forensic populations (prison, probation and forensic mental health hospitals), the prevalence of psychopathy is 7.7% in the UK and 16% in North America (Coid, Yang, Ullrich, Roberts, Moran, et al., 2009; Kiehl & Hoffman, 2011). The prevalence estimates calculated by Coid et al. (2009) relied on the cut-off score of 30, to facilitate comparisons with North American data. If the European cut-off score of 25 was used, this prevalence would increase slightly.

#### *1.2.3.2 Comorbidities*

Most individuals with psychopathy meet diagnostic criteria for ASPD. However, less than 50% of those with ASPD additionally meet criteria for psychopathy (Baliousis et al., 2019; De Oliveira-Souza, Moll, et al., 2008; Hare, 1991). There is a highly significant positive correlation between the number of SCID-5-PD ASPD symptoms and the score on the screening

version of the PCL, the PCL-SV (Coid, Yang, Ullrich, Roberts, & Hare, 2009; DeLisi et al., 2022). A comparison of the traits associated with ASPD and psychopathy reveals an overlap, particularly between the social deviance factor of psychopathy and ASPD (Kiehl & Hoffman, 2011). With this in mind, psychopathy and ASPD could be described as comorbid syndromes. However, it is debated whether they are best considered as two separate syndromes which occur comorbidly, or if ASPD with and without psychopathy are two subtypes of ASPD (Kosson et al., 2006). Further research assessing shared and different underpinnings of ASPD and psychopathy is required to explore this.

Additionally, individuals with high psychopathy also often meet diagnostic criteria for narcissistic, schizoid and histrionic personality disorders (Coid, Yang, Ullrich, Roberts, Moran, et al., 2009), but less frequently with borderline personality disorder as compared to those with ASPD without psychopathy (Coid, Yang, Ullrich, Roberts, & Hare, 2009; Coid & Ullrich, 2010).

The research on comorbidities between psychopathy and other mental health disorders is more limited and mostly relies on forensic patients, compromising the applicability of findings for community populations (Werner et al., 2015). Findings generally indicate fewer comorbidities than in ASPD (Coid, Yang, Ullrich, Roberts, & Hare, 2009; Coid, Yang, Ullrich, Roberts, Moran, et al., 2009). Antisocial individuals with heightened psychopathy are less prone to anxiety and depression than those without or low in psychopathy (Werner et al., 2015). The comorbidity between substance and alcohol use disorders and psychopathy is higher in forensic than community populations, and has been shown to be particularly mediated by the social deviance factor of psychopathy (Coid, Yang, Ullrich, Roberts, & Hare, 2009; Werner et al., 2015). This again highlights that it is a core part of the phenotype.

#### *1.2.3.3 Risk factors*

Due to the close relationship between ASPD and psychopathy, there is an overlap in their genetic and environmental risk factors. There is further overlap between the risk factors for CU traits and psychopathy. The following will outline additional risk factors which have been associated with psychopathy.

##### 1.2.3.3.1 Genetic

In terms of behavioural genetics, CU traits, an early predictor of psychopathy, have a high genetic heritability, estimated at over 65% (Viding et al., 2005). The strength of this genetic heritability has been shown to be stable over time, particularly in males (Lynam et al., 2007; Viding & McCrory, 2012). A recent meta-analysis confirmed that genetic risk factors explained 52% of the variance in the psychopathy construct (Waldman et al., 2018). The role of genetics in psychopathy-related traits has also been assessed. For instance, variance among narcissistic and impulsive traits in the context of psychopathy has been shown to be explained to a larger extent genetically (60-75%) than environmentally (Ficks et al., 2014; Waldman et al., 2018). Despite these findings, molecular genetic research such as candidate gene studies and GWAS focusing on adult psychopathy is rare and typically underpowered (Gunter et al., 2010; Palumbo et al., 2022). A recent systematic review of 15 studies assessing molecular genetic risk factors for psychopathy as measured with the PCL-R revealed that similar genes have been implicated in psychopathy as in CD or ASPD as whole. However, they concluded that there was no consistent molecular genetic basis identified across studies (Griffiths, Jalava, Rosenberg Larsen, et al., 2022).

Therefore, although the contribution of individual genes is still largely unknown, it is clear that genetic risk factors play an important role in the development and maintenance of psychopathy, perhaps larger than for the broader ASPD and LCP antisocial behaviour constructs (Forsman et al., 2010; Kiehl & Hoffman, 2011; Werner et al., 2015). The required further

genetic research should consider controlling for the psychopathy within ASPD samples as this will allow a better breakdown of genetic contribution to each construct.

#### 1.2.3.3.2 Environmental

In line with environmental influences on CU traits in CD, a meta-analysis showed that only non-shared environmental factors explained 48% variance in adult psychopathy (Waldman et al., 2018). An earlier study suggested that affective deficits found in psychopathy are influenced by unique non-shared environmental factors which do not influence impulsive-antisocial traits (Taylor et al., 2003). A recent meta-analysis also reported that exposure to childhood abuse and neglect increased the risk for psychopathy in adulthood (De Ruiter et al., 2022). The association was stronger for the social deviance factor, which aligns with findings from another study of violent offenders that demonstrated childhood maltreatment did not predict psychopathy, but it did predict aggression (Woehrle et al., 2022). However, studies measuring the impact of childhood maltreatment are often retrospective, and it has been shown that agreement between retrospective and prospective measures is limited (Baldwin et al., 2019). To best establish the impact of early risk factors, longitudinal, prospective studies are required. Nevertheless, it becomes evident that similar to genetic risk factors, environmental risk factors are also likely to contribute to different traits of psychopathy in specific ways. There is currently limited evidence of any additional specific environmental risk factors that are specific to adult psychopathy in comparison to the broader ASPD construct.

#### 1.2.3.3.3 Gene-environment interplay

Gene-environment interplays have also been highlighted in the development of psychopathy. Similar to the development of CU traits, an unhealthy environment evoked by negative parenting style or parental psychopathic traits, as well as instable socioeconomic conditions have been

shown to exacerbate the genetic vulnerabilities towards developing psychopathic features such as interpersonal-affective deficits (Auty et al., 2015; Beaver et al., 2011; Palumbo et al., 2022; Viding & McCrory, 2018). In turn, a healthy rearing environment can protect against developing long-term psychopathic traits and antisocial behaviour (Brazil et al., 2018; Loeber et al., 2009; Salekin & Lochman, 2008; Viding & McCrory, 2018). This is particularly important in the context of intervention, as family-based and parenting therapies may have a beneficial effect in early years, and adjusting or improving environmental circumstances may improve outcomes in adulthood (Loeber et al., 2009).

In summary, the risk factor literature suggests that individuals with psychopathy suffer from a more genetically determined, biologically driven neurodevelopmental form of the disorder than those meeting criteria for the broader ASPD construct. Nevertheless, understanding the impact of the environment and its interaction with genetic predisposition is particularly important as it may offer targets for treatments and interventions.

### 1.2.4 Treatment and interventions

It is evident that the prevalence of ASPD and psychopathy in offender populations is high. A correlation between ASPD and violent offending (Sariaslan et al., 2020) and increased violent recidivism (Chang et al., 2015; Krona et al., 2016) has been shown. Recidivism rates are high: internationally, over 30% of released offenders are reconvicted within 2 years and over 50% within 5 years (Yukhnenko et al., 2019). This highlights the necessity for effective treatment, rehabilitation and prevention programmes for this population, tailored to the distinct therapeutic needs of those with and without psychopathy.

The Cochrane review of psychological and behavioural therapy approaches for ASPD concluded that there is insufficient evidence for any particular psychological intervention (Gibbon et al., 2020). A meta-analysis of 6 studies assessing treatment effects on recidivism rates in ASPD, of which

only 3 were randomized controlled trials, reported that treatment was no more successful at reducing recidivism than the control condition (Wilson, 2014). However, a meta-analysis of 19 studies assessing the effectiveness of structured psychological interventions in male violent offenders with and without personality disorders revealed a 31% reduction in violent recidivism associated with treatment (Papalia et al., 2019). Unfortunately, this meta-analysis did not assess the moderating effects of ASPD or psychopathy: the positive effect may have been driven by individuals without personality disorders. Contingency management and cognitive-behavioural therapy (CBT) showed benefits in some studies, however the evidence was inconsistent. Across different studies, these treatment benefits were mainly attributable to the positive effects of treatment on substance and alcohol misuse rates (Werner et al., 2015).

Despite these historically inconsistent findings, therapeutic approaches such as multimodal CBT, substance use relapse prevention, and interpersonal and anger management skills continue to be employed. One preliminary study assessing individuals with externalizing problems with and without psychopathy demonstrated a positive effect of cognitive remediation therapy. The therapy was designed to specifically target the cognitive-affective deficits which were empirically identified as being distinctly associated with each subtype (Baskin-Sommers, Curtin, et al., 2015). Similarly, cognitive remediation therapy focused on improving cognitive biases by modifying attention mechanisms has also shown initial positive effects in young offenders (Z. Zhao et al., 2022). Mentalization-based therapy, shown to be effective in borderline personality disorder, is currently being adapted for ASPD and focuses on the cognitive, affective, self-oriented and other-oriented mentalization deficits associated with ASPD (Bateman et al., 2013). The results of a randomized controlled trial exploring the use of mentalization-based therapy in antisocial personality disordered men without psychopathy are awaited.

Specific offender rehabilitation programmes in prisons and probation services have also had favourable outcomes. The Reasoning and Rehabilitation programme uses a CBT basis to identify and then modify dysfunctional cognitions and behaviours associated with (re-)offending. A meta-analysis reported a significant 14% reduction in recidivism, although data from randomized controlled trials is still lacking (Tong & Farrington, 2006). Finally, in the UK, the establishment of offender personality disorder pathways in prisons and across probation services has allowed increased resources to be devoted to individuals with personality disorders (Joseph & Benefield, 2010). Offending behaviour programmes are delivered alongside the Chromis approach which has been specifically developed for psychopathic offenders to increase motivation for prosocial behaviour. Although more longitudinal data is required, evidence suggests a beneficial outcome, particularly for those at high risk of violent re-offending (Skett et al., 2017), but personality factors and neurocognitive abilities affect engagement (Yeadon et al., 2021). Overall, most intervention approaches showing early promises highlight the important role of empirical neurocognitive research in informing the development of new therapy targets.

A Cochrane review of 11 trials of pharmacological or medical treatment in ASPD revealed highly inconsistent data and no therapeutic recommendations were made (Khalifa et al., 2020).

The inconsistency in evidence for effective treatments for ASPD and psychopathy may be associated with the heterogeneous nature of the disorder (Brazil et al., 2018). Treatment approaches need to take account of the differences between antisocial personality disordered individuals with or without additional diagnoses of psychopathy.

### 1.2.5 ASPD with or without psychopathy

The above has highlighted the close relationship between ASPD and psychopathy. Both are highly associated with violent crime, increased risk

of recidivism, and poor response to treatment. Nevertheless, when comparing individuals with ASPD with psychopathy (ASPD+P) and ASPD without psychopathy (ASPD-P), those with psychopathy typically have a younger age of offending onset (Kosson et al., 2006), higher risk of recidivism, especially of a violent nature (Hemphill et al., 1998; McCuish et al., 2015; Olver et al., 2011, 2013; Shepherd et al., 2018), excessive use of proactive and instrumental aggression (Azevedo et al., 2020; Flórez et al., 2019; Riser & Kosson, 2013), poorer response to treatment attempts (Mayer et al., 2018; Olver et al., 2011), and higher cost burden to society (Kiehl & Hoffman, 2011).

Given the differences in patterns of antisocial and aggressive behaviour, personality traits, and criminal offending, as well as somewhat differing genetic and environmental risk factors, between men with ASPD-P and men with ASPD+P, it is reasonable to hypothesize that the neurobiological mechanisms that initiate and maintain their aggressive behaviours differ.

## 1.3 Neurocognitive, neurobiological, and neurochemical underpinnings of ASPD +/- P

This section will start with a summary of the neurocognitive deficits of ASPD+/-P, linked with the functional neural abnormalities that might underpin these deficits. Following this, an overview of evidence for abnormal brain structure and resting-state brain function will be given. Finally, neurochemical underpinnings of ASPD+/-P will be described, with a focus on oxytocin and its potential to shift the observed neurobiological abnormalities.

### 1.3.1 Neurocognitive and functional neurobiological underpinnings of ASPD and psychopathy

Impairments in ASPD+/-P can be classified into three main domains: emotional responsiveness, reward and punishment processing, and executive function including attention. A larger proportion of research has

focused on psychopathy, and those studies assessing the ASPD construct did not always account for psychopathy. Nevertheless, it appears that among those with ASPD, psychopathic traits may impact behavioural and neural functioning across these domains to varying extents. The following will outline evidence for the behavioural and task-based functional magnetic resonance imaging (fMRI) abnormalities across these domains. To remain clinically relevant, the evidence discussed will primarily focus on findings from forensic or clinical populations.

#### *1.3.1.1 Emotional responsiveness*

Abnormalities in emotional responsiveness can be subclassified into those relating to physiological responsivity, those relating to emotion recognition, and those relating to empathic processing more broadly. Physiological responsivity reflects the reaction of the body's autonomic nervous system to emotionally arousing stimuli and thus may be considered an underlying process of emotional responsiveness (De Looff et al., 2022). Furthermore, accurate recognition and appropriate processing of others' facial emotion expressions are key skills required for intact social interaction, communication and the development of interpersonal skills and adaptive behaviour (Schönenberg et al., 2013). These factors, in turn, contribute to empathic processing (R. J. R. Blair, 2007a).

##### 1.3.1.1.1 Physiological responsivity

Reduced autonomic physiological responses, i.e., reduced startle response, heart rate, skin conductance response and pupil dilation have been shown in individuals with ASPD and psychopathy when at rest and during neurocognitive tasks such as viewing affective stimuli or anticipating threat (Anton et al., 2012; De Looff et al., 2022; Gillespie et al., 2019; Kumari et al., 2009; Loomans et al., 2015; Pfabigan et al., 2015; Raine et al., 2000). Meta-analytic evidence shows that this is particularly pronounced in violent offenders with psychopathy and high PCL-R factor 1 but not factor 2 scores, but also to a lesser extent in individuals with ASPD more broadly (De Looff et al., 2022; Kozhuharova et al., 2019; Patrick, 2015). These deficient

autonomic responses may be associated with heightened fearlessness or boldness in individuals with psychopathic tendencies (Hoppenbrouwers et al., 2016; Klingzell et al., 2016; B. Murphy et al., 2016). Furthermore, they may impact other neurocognitive processes such as attention (Hamilton & Newman, 2018a).

#### 1.3.1.1.2 Emotion recognition and processing

Facial emotion expressions enable the rapid interpersonal transmission of information and can lead to reactions in others (e.g., accurate recognition and processing of another person's fearful facial expression can serve as a distress cue to elicit aversion and inform the observer's next action). Thus, impairments in this skill may be an important neurocognitive component of ASPD and psychopathy.

On the behavioural level, two meta-analyses of studies assessing explicit emotion recognition of the six basic emotions (fear, sadness, anger, happiness, disgust and surprise) in individuals with ASPD and psychopathy, respectively, revealed similar findings (Dawel et al., 2012; A. A. Marsh & Blair, 2008). Fear, sadness, and to a smaller extent surprise and happiness recognition were consistently impaired in antisocial individuals. The recognition of fear was significantly worse than all other emotions in both meta-analyses. Furthermore, individuals with ASPD require more time to recognize unambiguous emotional expressions and are more likely to classify ambiguous faces as angry and threatening (Schönenberg et al., 2013; Schönenberg & Jusyte, 2014; Smeijers et al., 2017). The latter finding suggests the presence of a hostile attribution bias in individuals with ASPD, which may contribute to heightened reactive aggression (Dodge, 2006). Taken together, these results suggest that individuals with ASPD and psychopathy have selective perceptual impairments in emotion recognition, particularly for emotions communicating distress or threat.

On the neural level, emotion recognition and processing initially rely on a network of occipitotemporal structures including the fusiform face area for

all emotions, but subsequently different emotions are processed in different areas. For instance, fear and sadness seem to be disproportionately associated with amygdala processing, whereas disgust and anger are more related to insula processing (Fusar-Poli et al., 2009). ASPD+/-P impairments in explicit and implicit facial emotion recognition and processing have been most prominently associated with atypical functioning of the amygdala, anterior midcingulate cortex, anterior insula as well as occipitotemporal areas such as the fusiform gyrus and the cuneus (N. E. Anderson et al., 2017; R. J. R. Blair, 2007a; Contreras-Rodríguez et al., 2014; Decety et al., 2014; Deeley et al., 2006; Seara-Cardoso et al., 2022; Tully et al., 2022).

In summary, emotion recognition and processing deficits are a prominent neurocognitive feature of ASPD+/-P which have been shown to be linked with functional neural abnormalities. This atypical behaviour and brain dysfunction may be more pronounced in individuals with psychopathy, but further direct comparisons between ASPD+/-P are required. Furthermore, these deficits may partially underpin persistent aggressive behaviours and reduced empathy.

##### 1.3.1.1.3 Empathy

Empathy is a multidimensional construct involving an "affective response that stems from the apprehension or comprehension of another's emotional state or condition" (Eisenberg, Fabes, & Spinrad, 2006, p. 647). Two important dimensions in the context of ASPD+/-P are cognitive and affective empathy (Zaki & Ochsner, 2012). Cognitive empathy relates to understanding another's intentions and emotional or mental state and is related to theory of mind (ToM) and perspective-taking. Affective empathy relates to the ability to experience or resonate with another's emotions. These processes closely interact but are associated with distinct neural underpinnings (Bird & Viding, 2014; R. J. R. Blair, 2007a; Olderbak & Wilhelm, 2017).

From a behavioural perspective, reduced empathy and callousness are hallmark features of ASPD+P. In terms of cognitive empathy, a study directly comparing individuals with ASPD+/-P reported both ASPD subtypes performed normally on basic ToM tasks but were selectively impaired in one type of second-order ToM (faux pas task) (Dolan & Fullam, 2004). Furthermore, increased psychopathy has been linked with a failure in implicit, automatic but not explicit, controlled perspective-taking (Drayton et al., 2018). This suggests that perspective-taking is problematic for an individual with psychopathy when it is not explicitly required for achieving a goal. Thus, it appears as though more complex forms of behavioural cognitive empathy are impaired in ASPD+/-P, and that these may be selectively associated with ASPD+P. In terms of affective empathy, deficits in emotion recognition and processing, alongside reduced autonomic responses while witnessing others' pain or distress are key signs of impairments in this dimension, particularly in those with psychopathy (R. J. R. Blair, 2007a; Pfabigan et al., 2015). However, and surprisingly considering the phenotype, there is inconsistent evidence for behavioural impairments in affective empathy, with some (Shamay-Tsoory et al., 2010) but not all (Domes et al., 2013; Mayer et al., 2018; Newbury-Helps et al., 2017; Richell et al., 2003) findings showing a negative correlation between task performance and psychopathic traits. Such inconsistency may be related to differences in task design (Griem et al., 2022). More research is required, but to date it therefore seems that behavioural affective empathy impairments are primarily associated with emotion processing deficits, and this is primarily characteristic of ASPD+P.

There is more consistent evidence for abnormalities in the neural correlates of empathy impairments, particularly the affective dimension, in ASPD+/-P. For instance, evidence has shown that psychopathic individuals have significantly reduced neural response to imagining and viewing others' distress and pain, as well as when attributing emotional states to others, in areas including the ventromedial prefrontal cortex, orbitofrontal cortex,

anterior cingulate cortex, anterior insula, inferior parietal cortex (temporoparietal junction), amygdala, and basal ganglia (Decety et al., 2015; Decety, Chen, et al., 2013; Decety, Skelly, et al., 2013; Meffert et al., 2013). Another study revealed abnormal neural activity in these regions during implicit but not explicit affective evaluation of moral scenarios (Yoder et al., 2015), again suggesting empathy deficits may be more apparent when empathy is not directly required to achieve a goal. Unfortunately, most of these studies lacked non-offending control samples, meaning it is not clear to what extent these abnormalities are linked with criminality and antisocial behaviour as a whole. However, they were able to show distinct functional abnormalities in these regions in offenders with low versus high psychopathy (akin to offenders with ASPD-P and ASPD+P, respectively).

In summary, there is evidence for behavioural and especially functional neural abnormalities in emotional responsiveness, including physiological responsivity, emotion recognition and processing, automatic mentalising and affective empathy in individuals with ASPD+/-P. Although direct comparisons of ASPD+P vs ASPD-P are lacking, existing findings do suggest these deficits are more pronounced in individuals with high psychopathy, particularly when the functions are not directly required to achieve a goal. Key brain areas consistently associated with these deficits in ASPD+/-P include the amygdala, insula, cingulate cortex and the inferior parietal cortex (temporoparietal junction).

#### *1.3.1.2 Reward and punishment processing*

The appropriate recognition and processing of reward and punishment signals is crucial for stimulus-reinforcement learning, decision-making, and social interaction. The persistent antisocial behaviour, the high rates of reconviction and the overall poor life choices reflect serious difficulties in successfully integrating reward and punishment information in individuals with ASPD+/-P (De Brito & Hodgins, 2009; Hughes et al., 2016). Blair's Integrated Emotion Systems model of psychopathy (R. J. R. Blair, 2006,

2007a) suggested that three learning impairments are fundamental to emotional and empathic dysfunction in psychopathy (R. J. R. Blair, 2013a): an impairment in stimulus-reinforcement learning due to increased sensitivity to reward and decreased sensitivity to punishment (K. S. Blair et al., 2006); an impairment in the representation of reinforcement outcome information, i.e. the value of the outcome; and finally, an impairment in prediction error signalling, i.e. not correcting the expected reward/punishment for future actions.

The above suggests that behavioural impairments in learning and decision-making in the context of affective stimuli are fundamental to psychopathy, particularly in the context of affective reward and punishment stimuli. However, when considering reward and punishment cues beyond their affective value, there is also evidence of impairment in ASPD more broadly. A study directly comparing ASPD+/-P individuals demonstrated that both groups made poorer quality decisions despite longer periods of deliberation (De Brito et al., 2013). Both groups also did not change their behaviours in the face of changing contingencies in a response reversal task. However, findings from other studies suggest this may be different in those with higher psychopathic traits (Baliousis et al., 2019; Budhani et al., 2006; Hughes et al., 2015). Finally, in a passive avoidance learning task, De Brito and colleagues (2013) showed that both ASPD+/-P groups failed to learn from punishment cues. Together, this suggests individuals with ASPD+/-P fail to adjust their behaviour in light of a) increasing risk and b) previously rewarded behaviours being punished. It is noteworthy that the response reversal finding was only significant for the ASPD-P group (it trended towards significance in ASPD+P). This concurs with another study showing more response reversal deficits in ASPD with low as opposed to high psychopathic traits (Dolan, 2012).

On the neural level, abnormalities in the mechanisms associated with reward and punishment processing have also been detected in ASPD+/-P. When reward and punishment stimuli are associated with an affective

value, there is fMRI evidence for impaired neural processing, especially in those with high psychopathy. In line with behavioural findings, reduced amygdala activity during aversive conditioning tasks involving emotional stimuli has been shown in psychopathic offenders (Birbaumer et al., 2005). Alongside typically reduced activity in the ventromedial prefrontal and orbitofrontal cortex, it is likely that such amygdala and insula deficits contribute to the reduced response to distress cues and subsequent empathic processing impairments (R. J. R. Blair, 2007a, 2007b, 2008). Abnormal neural activity in these regions, in addition to the anterior cingulate, precuneus, and inferior parietal cortex (temporoparietal junction) have also been linked with deficits in moral reasoning in individuals with high psychopathy (Abe et al., 2018; Decety et al., 2015; Pujol et al., 2012; Yoder et al., 2015). Moral reasoning requires decision-making and is thus also related to reward and punishment processing. Overall, it is thus likely that individuals with psychopathy likely fail to appreciate the significance of affective information stimuli (De Brito et al., 2013).

The neural underpinnings of reward and punishment processing has also been assessed in the context of socioeconomic decision-making. One study directly comparing neural activity in a response reversal task in ASPD+/-P demonstrated distinct neural abnormalities associated with reward and punishment sensitivity for each subtype (Gregory et al., 2015). Specifically, in response to financial reward, ASPD+P had reduced middle and superior temporal gyrus activation whereas ASPD-P had increased activity. In response to punishment, ASPD+P had increased anterior insula and posterior cingulate activation, but ASPD-P showed decreased activation in these areas. Thus, the authors suggested differential neural sensitivities to reward and punishment information depending on the presence or absence of psychopathy in offenders with ASPD. Furthermore, a systematic review of several fMRI studies of antisocial individuals with and without psychopathy reported that antisocial behaviour as well as the social

deviance factor of psychopathy were related to increased striatal and prefrontal neural activity when anticipating reward, further supporting a hypersensitivity to reward in ASPD (Murray et al., 2018). Finally, abnormal neural response to reward expectation in the striatum has also been identified as a key mechanism underpinning reinforcement-learning deficits in individuals with ASPD and psychopathy (Geurts et al., 2016; Hosking et al., 2017; Pujara et al., 2014).

Therefore, in summary, it is apparent that both individuals with ASPD+P and ASPD-P show behavioural and neural abnormalities in reward and punishment processing. It is likely that these are more severe in individuals with ASPD+P in the context of affective value, whereas they are a shared deficit across both ASPD subtypes (linked to the shared impulsive-antisocial traits) in the context of economic value. However, even within the latter, there are likely some distinctions in the neural mechanisms underpinning these deficits. Key brain structures associated with these abnormalities are the amygdala, ventromedial and orbitofrontal prefrontal cortex, cingulate cortex, and striatum.

#### *1.3.1.3 Attention and executive function*

Executive functions are higher-order cognitive processes including the interaction between volition, planning, purposive action and effective performance required for future, goal-directed behaviour. These functions include the allocation of attentional resources, cognitive flexibility and set-shifting, response inhibition and impulse control, planning, and problem-solving. The role of behavioural and neural attention deficits has received increased consideration, particularly in the neurocognitive formulation of psychopathy, and will be discussed first. This will be followed by a summary of other evidence for impairments in ASPD+/-P in the other executive functions.

#### 1.3.1.3.1 Attention

Attention is important for perception, selection, and storage of sensory information, and the ability to select salient information while filtering out less salient information is fundamental to appropriate social behaviour (Baskin-Sommers & Brazil, 2022). Attention can be implicit (automatic) or explicit (controlled). A recent study assessing a range of neurocognitive functions in ASPD and psychopathy revealed similar behavioural attention deficits in offenders with ASPD or psychopathy (Baliousis et al., 2019). Both groups performed worse on sustained attention and visual search tasks as compared to healthy controls. This confirms earlier evidence of attention deficits in ASPD (Dolan & Park, 2002; Morgan & Lilienfeld, 2000). However, a study directly comparing offenders with ASPD with and without psychopathy suggested that the groups display differential patterns of attention deficits (Riser & Kosson, 2013). On the one hand, it has been argued that in individuals with ASPD-P, these impairments may be expressed due to a failure to ignore peripheral or distracting information, meaning that attention is not oriented to the most salient stimuli (Baskin-Sommers & Newman, 2013; Verona et al., 2012). On the other hand, in those with ASPD+P, there may be too much focus on self-benefitting goal-relevant information (possibly serving antisocial goals) which may make them less likely to attend to socially salient information such as affective cues (Tillem et al., 2021).

Indeed, the role of abnormal attention processes has been of particular interest in the context of psychopathy. Accurately attending to emotional cues is important for normal emotional responsiveness. Therefore, the Response Modulation Hypothesis of psychopathy theorizes that impairments in emotional responsiveness result from a failure to automatically attend to socially salient stimuli such as emotional cues (Hamilton & Newman, 2018a). For instance, eyes are particularly strong conveyors of emotion such as fear (Dawel et al., 2012), and eye-tracking evidence suggests that offenders with psychopathy as opposed to offenders

without psychopathy spend significantly reduced amount of time looking at their interaction partner's eyes (Gehrer et al., 2019). Furthermore, during attention tasks, physiological responsivity has been shown to be less affected by distractors (Wolf et al., 2012), and to increase when psychopathic individuals are explicitly instructed to attend to peripherally presented threatening information (Baskin-Sommers et al., 2011; Kosson et al., 2006). Considering such evidence, it is argued that socially salient information is not attended to because it is filtered out early on in the attention bottleneck, unless it is directly required for self-beneficial goal-directed behaviour (Baskin-Sommers & Brazil, 2022). In fact, the attention deficits in psychopathy have also been used to explain difficulties with reward and punishment processing, especially when multiple streams of information must be monitored simultaneously for effective learning to occur (Baskin-Sommers & Brazil, 2022; Hamilton & Newman, 2018b).

Evidence from fMRI studies has revealed possible neural correlates for the behavioural attention deficits found in individuals with ASPD+/-P. In antisocial individuals more broadly, meta-analyses revealed that impaired function of the dorsolateral prefrontal cortex, as well as reduced activity in regions of the dorsal attention network are associated with problems in directing and sustaining attention (Dugré & Potvin, 2021; Yang & Raine, 2009). In offenders with psychopathy, distinct neural correlates of the automatic attention deficits have also been identified. For instance, several studies revealed reduced brain activity during passive exposure to task stimuli, which was upregulated after receiving explicit instructions to attend to the stimuli, especially if these stimuli had an affective nature (N. E. Anderson et al., 2017, 2018; Meffert et al., 2013; Shane & Groat, 2018). This included areas such as the orbitofrontal cortex, anterior midcingulate, anterior insula, and precuneus.

In summary, differential patterns of behavioural and neural impairments in attention have been identified in ASPD+/-P. On the one hand, individuals with ASPD-P have difficulties with attention due to being overly focused on

or distracted by peripheral information. On the other hand, individuals with ASPD+P exhibit deficits in detecting and attending to socially salient information, especially when this is not directly implicated in achieving a self-beneficial goal. Similar brain regions are implicated in the latter deficits as those identified in the context of emotional responsiveness problems for individuals with ASPD+P.

#### 1.3.1.3.2 Executive function

Further executive functions include cognitive flexibility and set-shifting, planning and problem-solving, and response inhibition and impulse control. Behavioural difficulties in these functions have also been identified in ASPD+/-P.

Cognitive flexibility and set-shifting reflect the abilities to accurately shift focus between different sources of information and to adjust to situations under new rules or circumstances. Individuals with ASPD have been shown to be impaired on these functions (Baliousis et al., 2019; Dolan, 2012; Dolan & Park, 2002). Similar findings exist for planning and problem-solving abilities: significant impairments in the ability to flexibly plan solutions to problems found in individuals with ASPD do not appear to be influenced by psychopathic traits (Baliousis et al., 2019; Delfin et al., 2018; Dolan, 2012; Dolan & Park, 2002). Thus, it appears as though problems with cognitive flexibility, set-shifting, planning, and problem-solving are observed within the broad APSD construct. However, it has been suggested that individuals with psychopathy who score highly on the interpersonal facet perform better on these executive functions, which may be related to skills required for behaviours such as pathological lying and manipulation (Pera-Guardiola et al., 2016).

Finally, response inhibition and impulse control is an executive function that is closely related to self-regulation and impulsivity. Impulsivity is a key characteristic across externalising disorders including ASPD and psychopathy (Magyar et al., 2011). Neurocognitive studies show

behavioural impairments in this executive function. On motor response inhibition tasks, individuals with ASPD and subthreshold psychopathy make significantly more errors than those with above-threshold psychopathy (Dolan, 2012; W. Jiang et al., 2016). Furthermore, higher impulsive facet scores were associated with poorer impulse control, whereas higher interpersonal facet scores were associated with improved performance (Weidacker et al., 2017). Together, this indicates reduced impulse control, especially in individuals with ASPD-P. Impulsivity can also be assessed in the context of delay discounting, i.e., the preference between a smaller, more imminent or a larger, more delayed reward. Individuals with ASPD-P have been shown to prefer smaller, more imminent rewards, although the evidence is somewhat inconsistent (Turner et al., 2017; White et al., 2014). Individuals with ASPD+P have also shown similar preferences, and these appear to be more prominent when the task includes a risk of punishment (Hosking et al., 2017; Newman et al., 1992). Response inhibition and impulse control are thus likely to be modulated by sensitivity to reward/punishment information and affective cues (Verona et al., 2012). In summary, behavioural impairments in this executive function seem to be a shared underpinning of ASPD+/-P, but it may differ depending on contextual information.

Overall, ASPD-P may therefore be more affected by executive dysfunctions relating to cognitive flexibility, set-shifting, planning, and problem-solving than ASPD+P, but they have similar difficulties in response inhibition and impulse control (Baskin-Sommers, Brazil, et al., 2015). Evidence from fMRI studies has highlighted altered neural activity in brain regions including the dorsolateral, ventromedial prefrontal and orbitofrontal cortex, anterior cingulate, inferior parietal cortex (temporoparietal junction), and striatum (Dolan, 2012; Hosking et al., 2017; Pera-Guardiola et al., 2016; Rodman et al., 2016; Yang & Raine, 2009). Furthermore, altered bottom-up neural signalling between subcortical regions and the ventromedial and orbitofrontal prefrontal cortex may be more associated with executive

dysfunctions characterizing ASPD+P, whereas abnormal top-down signalling stemming from the dorsolateral prefrontal cortex may be more related to ASPD-P deficits (Contreras-Rodríguez et al., 2015; De Brito & Hodgins, 2009; Pera-Guardiola et al., 2016). Nevertheless, more research is required to disentangle the role of psychopathic traits in the neural correlates of executive dysfunction of ASPD+/-P.

#### *1.3.1.4 Limitations*

The overview above shows that research has successfully begun to outline the behavioural deficits and underpinning functional neural mechanisms of neurocognitive abilities in ASPD+/-P, albeit with some inconsistencies and uncertainties remaining. The field is plagued by several challenges and limitations (Griem et al., 2022), which likely contribute to the heterogeneity of findings (Griffiths & Jalava, 2017). For instance, inconsistent findings may be affected by the use of different measurement tools for psychopathy, and even within the gold-standard tool of the PCL-R, there may be differences in findings due to the use of different diagnostic thresholds. Results from North American studies may be more likely to find significant ASPD+/-P differences than European studies since the threshold for psychopathy is higher in North America. Findings associated with distinct facets of psychopathy also indicate that these may be more sensitive than the total score of the PCL-R. Similarly, methodological differences in the behavioural assessments may reduce the consistency of research findings. Finally, the potential impact of comorbid substance misuse on experimental findings is not always considered.

#### *1.3.1.5 Summary on neurocognitive profiles of ASPD+/-P*

The reviewed evidence suggests there are both similarities and differences in the neurocognitive profiles of ASPD with and without psychopathy (*Table 1.4*). Both subtypes appear to show difficulties with emotional responsiveness, including physiological responsivity, emotion recognition and processing, and empathy, but these seem to be more pronounced in ASPD+P. Impairments in reward and punishment processing are likely to

be common to both ASPD+P and ASPD-P in the context of economic value, however, they are more severe in ASPD+P in the context of affective or social value. Similarly, both subtypes show attention deficits, but the pattern of these impairments differ between subtypes, and the impact on behaviour is more extensive in ASPD+P. Finally, in terms of executive functioning, ASPD-P shows more widespread impairments on cognitive flexibility and set-shifting, planning and problem-solving, whereas ASPD+P more typically show difficulties with impulse control and response inhibition. In terms of the neural underpinnings, altered activity in several regions seems to contribute to behavioural difficulties. Areas that are implicated across different neurocognitive functions include parts of the prefrontal cortex, anterior cingulate, amygdala, insula, precuneus, and basal ganglia. Overall, these behavioural and neural deficits can at least partially explain some of the problematic behaviours and LCP antisocial behaviour and violence found in ASPD+/-P. They are relatively consistent with literature on CD with and without CU traits (Fairchild et al., 2019). In order to improve understanding of the neural alterations, other neurobiological features of ASPD+/-P must also be considered.

| | **ASPD+P** | **ASPD-P** |
|---|---|---|
| Emotional responsiveness | | |
| Physiological responsivity | +++ | + |
| Emotion recognition and processing | +++ | ++ |
| Empathy | +++ | + |
| Reward and punishment processing | | |
| Affective value | +++ | + |
| Economic value | ++ | ++ |
| Attention | +++ | ++ |
| Executive function | | |
| Cognitive flexibility and set-shifting | ++ | +++ |
| Planning and problem-solving | ++ | +++ |
| Impulse control and response inhibition | +++ | ++ |

Table 1.4 Overview of the neurocognitive deficits in ASPD+/-P.
*Note: + = mild impairment, ++ = moderate impairment, +++ = severe impairment.*

### 1.3.2 Neurobiological underpinnings of ASPD and psychopathy

Prior to the availability of modern neuroimaging technologies, neurocognitive deficits were compared to those found in individuals with particular (localized) lesions who showed pseudopsychopathic behavioural and personality changes. This gave early indications about the areas that might be affected (Raine et al., 2000). In recent decades, sophisticated neuroimaging methods have allowed closer investigation of the neurobiological features of LCP antisocial behaviour, ASPD and psychopathy. This includes using fMRI to investigate brain activity during neurocognitive tasks (reviewed in the above section), but also the use of sMRI to assess brain structure, as well as arterial spin labelling (ASL) to measure resting-state cerebral blood flow and fMRI to measure resting-state brain function. Improving the understanding these neurobiological mechanisms in ASPD+/-P can help to shed more light on LCP antisocial behaviour and the behavioural and personality deficits of this disorder. Extant neuroimaging literature has focused more on ASPD+P or psychopathy than on ASPD as a broad, heterogeneous construct or specifically on ASPD-P. Nevertheless, the below will review evidence for structural and resting-state neurobiological underpinnings of ASPD+P and ASPD-P, where available.

#### *1.3.2.1 Alterations in brain structure*

Structural magnetic resonance imaging (sMRI) of the brain provides a cross-sectional picture of the shape and size of the brain and its individual cortical and subcortical areas. The data is commonly analysed using two different approaches. The first approach is voxel-based morphometry (VBM) which involves the voxel-wise measurement of grey and white matter densities in the whole brain or in specific regions of interest. This results in measures of absolute and relative grey matter volume and concentration. The second approach is surface-based morphometry (SBM). This analysis applies geometric models (a triangle mesh of vertices) to the

sMRI data to identify surface boundaries between layers of the brain (pial surface and white matter surface), across cortical and subcortical regions. It results in multiple structural metrics, including cortical thickness and surface area, which multiply to produce cortical volume. Thereby, SBM provides more detail than the VBM approach. Evidence from both approaches across all three structural features will be described.

#### 1.3.2.1.1 Volume

The most commonly reported structural neurobiological marker associated with ASPD, and particularly psychopathy is reduced GMV in various frontotemporal cortical and subcortical areas (Johanson et al., 2020; Pujol et al., 2018; Raine et al., 2011). Indeed, one of the first studies assessing the structural hallmarks of ASPD demonstrated a significant reduction (11%) in prefrontal GMV, which was independent from the effects of substance misuse and psychopathy (Raine et al., 2000). Furthermore, GMV decreases in amygdala and hippocampus, and increases in inferior parietal cortex (supramarginal gyrus) have also been reported in the broad construct of ASPD (Barkataki et al., 2006; Kaya et al., 2020; Tang, Jiang, et al., 2013). A recent meta-analysis of studies of psychopathy reported widespread reductions, including in dorsolateral prefrontal and orbitofrontal cortex, cingulate cortex, superior, middle, and inferior temporal gyri, and caudate (De Brito et al., 2021). Single studies of individuals with psychopathy have also shown reduced GMV in the amygdala and hippocampus, insula, and precuneus (Contreras-Rodríguez et al., 2015; De Oliveira-Souza, Hare, et al., 2008; Ermer et al., 2012; Raine et al., 2004; Yang et al., 2009). Finally, in an attempt to account for the presence or absence of psychopathy within ASPD, a study directly comparing the structural neural architecture in ASPD+/-P revealed that ASPD+P had significantly lower GMV in the rostral prefrontal cortex, temporal pole, and insula (Gregory et al., 2012). The ASPD-P group on the other hand was not significantly different to controls. Importantly, these findings were not influenced by IQ, substance use disorders or other major psychiatric

comorbidities. These findings suggest distinct structural abnormalities that characterize ASPD+P which are not found in ASPD-P.

There have been also findings of altered white matter structure associated with ASPD and psychopathy. One study assessing individuals with ASPD found increased white matter volume (WMV) in the parietal and occipital lobes, bilaterally (Tiihonen et al., 2008). This was not accounted for by psychopathy, substance abuse, or IQ. Another study assessing ASPD without accounting for psychopathy also reported widespread increased WMV in areas including the prefrontal cortex, cingulate cortex, insula, and precuneus, and decreased WMV the middle temporal lobe and cerebellum (D. Wu et al., 2011). Finally, a study specifically assessing psychopathic individuals reported increased WMV in the corpus callosum (Raine et al., 2003). WMV consists primarily of white matter tracts and fibres. The structural integrity of white matter tracts, particularly the uncinate fasciculus connecting the ventromedial prefrontal cortex with the anterior temporal lobe has been shown to be compromised in ASPD and psychopathy (Craig et al., 2009; Johanson et al., 2020; Sundram et al., 2012; Wolf et al., 2015). Together, these findings may be due to interferences in normal pruning processes which occur during adolescence. Such interferences may be the result of early engagement in antisocial behaviour and substance misuse (Tiihonen et al., 2008). Altered white matter structure has also been associated with cognitive and neurocognitive impairments such as increased impulsivity and decreased interpersonal-affective skills in psychopathy (Vermeij et al., 2018).

In summary, reduced GMV and increased WMV appear to be a common feature of ASPD+/-P, whereby ASPD+P has more pervasive GMV reductions than ASPD-P. This is largely compatible with findings from CD with and without CU traits (B. M. Caldwell et al., 2019; Rogers & De Brito, 2016). Nevertheless, beyond the influence of methodological differences and differential measures of ASPD and psychopathy, inconsistencies in volumetric findings may be associated with a varying presence of

comorbidities, particularly substance use disorder, amongst individuals with ASPD+/-P (Griffiths & Jalava, 2017). Furthermore, volume is a product of differential, genetically determined contributions of cortical thickness and surface area (Rakic, 2007; Storsve et al., 2014; Wierenga et al., 2014). SBM may thus shed more detailed light than VBM approaches.

#### 1.3.2.1.2 Cortical thickness

Cortical thickness (CT) reflects the combined thickness of cortical layers in the area between the white matter surface and the pial surface. It is therefore one of the two grey matter measures contributing to GMV. Carlisi and colleagues investigated sMRI scans collected within the Dunedin longitudinal cohort (Carlisi et al., 2020). They found that individuals with LCP antisocial behaviour had significantly reduced mean CT compared individuals without antisocial behaviour. Although they did not assess for the diagnosis of ASPD, there is a high likelihood that the individuals with LCP antisocial behaviour do meet these criteria (Moffitt, 2018). In line with this, two studies measuring CT in ASPD revealed widespread cortical thinning in all three frontal gryi, medial prefrontal and orbitofrontal cortex, insula, precuneus, and medial and superior temporal gyrus (W. Jiang et al., 2016; Narayan et al., 2007). However, they were both subject to significant methodological limitations, meaning further research assessing CT in ASPD is required.

Substantially more research on CT has been done in psychopathy. Psychopathy is associated with reduced CT (i.e. thinning) in the insula, the orbitofrontal cortex, anterior cingulate cortex, precentral and inferior frontal gyri, the amygdala, and the temporal poles (Ermer et al., 2012; Ly et al., 2012; Schiffer et al., 2011; Yang et al., 2009, 2010).

In summary, the evidence suggests that cortical thinning, albeit in spatially different regions, is a feature of both ASPD+/-P. In ASPD+P, areas showing reduced CT overlap with areas showing reduced GMV, e.g., the orbitofrontal cortex, cingulate cortex, insula, and amygdala. In ASPD-P, prefrontal

regions seem to show both reduced CT and GMV, however other areas with reduced GMV have not been shown to have reduced CT. Altered CT might therefore be an important contribution to altered GMV, particularly in ASPD+P. Overall, these findings suggest somewhat differential profiles of CT between the groups. To date, however, there are no studies that have directly compared CT profiles in ASPD+/-P, and such investigation remains to be conducted.

#### 1.3.2.1.3 Surface area

Cortical surface area (SA) reflects the number of cortical columns found in the area between the white matter surface and the pial surface. It is the second of two grey matter measures contributing to GMV. Fewer studies have assessed differences in SA. The Dunedin longitudinal cohort study reported significantly reduced mean SA in those with LCP antisocial behaviour (Carlisi et al., 2020). In their study of the broad and heterogeneous ASPD construct, Jiang and colleagues reported increased SA in the same areas that showed decreased CT listed above, including the insula and precuneus (W. Jiang et al., 2016). This suggests that individuals with ASPD have a decreased number of horizontal cell layers but an increased number of vertical cell columns (Rakic, 2007). In individuals with ASPD+P, one study has shown that differences in SA of amygdaloid nuclei may be subject to genetic influences (Kolla et al., 2017). This strong influence of genetic factors on neurobiology is further support for the neurodevelopmental understanding of ASPD+P. Beyond this research, no further studies have measured or reported abnormal SA in ASPD+/-P, and no studies have directly compared SA between the two ASPD subtypes. In summary, this means that the commonly found reductions in GMV in psychopathy are driven by reduced CT, whereas an interplay between CT and SA can be assumed to explain the differences in GMV associated with ASPD.

#### 1.3.2.1.4 Limitations and summary

The structural neurobiological evidence base is challenged by similar limitations to the neurocognitive evidence base. Differential definitions of ASPD and psychopathy, and more specifically, different MRI data collection and analysis protocols complicate the comparison of findings across studies. Furthermore, some, but not all studies, assess the impact of substance misuse and other comorbidities, which have been associated with differential neurobiological correlates (Gómez-Coronado et al., 2018).

Despite these limitations, there is evidence of both individual and overlapping structural neurobiological underpinnings to ASPD+/-P. Key regions with structural abnormalities include prefrontal areas, cingulate cortex, insula, amygdala, and precuneus. Areas with structural abnormalities therefore overlap with areas showing altered neural signalling during cognitive tasks. Both groups showed reduced GMV, albeit in somewhat different areas. In ASPD-P, GMV decreases may be linked to SA decreases, whereas in ASPD+P and ASPD-P, decreases in CT may also contribute to GMV reductions. Furthermore, increased WMV and decreased white matter tract structural integrity seem to underpin ASPD+/-P. Overall, more research directly comparing ASPD+/-P, particularly on CT and SA, is required.

### *1.3.2.2 Alterations in resting-state brain function*

Resting-state fMRI assesses brain activity when the individual is not engaged in any particular task, i.e., they are at rest. The assessment of resting-state brain function can provide further insight into neurobiological mechanisms such as cerebral blood flow (perfusion), functional connectivity, and network topology. The below will provide an overview of evidence for alterations in cerebral blood flow, functional connectivity, and network topology in ASPD+/-P.

#### 1.3.2.2.1 Cerebral blood flow

Resting-state cerebral blood flow (CBF) is a measure of blood perfusion from cerebral capillaries into brain tissue (Detre et al., 2009). Blood carries metabolic nutrients such as oxygen and glucose, which are required for neural activity. It is thus one of the measures captured by the blood oxygenation-level dependent (BOLD) signal that is typically analysed in fMRI. To date, only a handful of studies have assessed CBF using single-photon emission computed tomography (SPECT) or positron emission tomography (PET) studies in the broad ASPD construct or in psychopathy (Goethals et al., 2005; Kolla & Houle, 2019; Kuruoglu et al., 1996; Soderstrom et al., 2000, 2002; Sutherland & Fishbein, 2017). A review of these studies revealed that ASPD and psychopathy are associated with reduced frontotemporal CBF, particularly in areas of the prefrontal cortex, the insula, and the amygdala (Kolla & Houle, 2019). This means that the regions that have been associated with abnormal task-based brain function as well as brain structure are also likely to have reduced blood flow, resulting in lower metabolism of nutrients such as glucose and more impaired neural activation patterns. However, existing studies faced limitations including poor characterisation of ASPD+/-P and imprecise neurobiological measurements. An improved neuroimaging technique for measuring CBF is ASL imaging. However, no studies so far have assessed CBF using this method in a well-characterized sample of violent offenders with ASPD+/-P. Furthermore, this method is particularly sensitive to capturing pharmacologically induced changes in brain function, and thus, it may lend itself well to studying effects of potential neurochemical treatments for ASPD+/-P (Stewart et al., 2014).

#### 1.3.2.2.2 Functional connectivity

Functional connectivity (FC) is measured by identifying temporal correlations of resting-state neural activity between individual local and/or spatially distant brain regions or within large-scale neural networks. Across disorders, alterations in FC have been associated with a breakdown in

function (Thiebaut De Schotten & Forkel, 2022), so it is important to explore FC in ASPD+/-P. Extant research has primarily assessed FC abnormalities in offenders with psychopathy, but few have also assessed those in the broad ASPD construct, regardless of the presence or severity of psychopathy. Evidence from this research suggests abnormal, typically reduced FC between specific regions, including but not limited to the ventromedial and orbitofrontal cortex, cingulate cortex, insula, amygdala, precuneus, and basal ganglia (Contreras-Rodríguez et al., 2015; Decety, Chen, et al., 2013; Hosking et al., 2017; H. Liu et al., 2014; Ly et al., 2012; Motzkin et al., 2011; Nummenmaa et al., 2021; Pujol et al., 2012; Tang, Liu, et al., 2013). Therefore, there is overlap between the areas that show altered brain structure, CBF, and task-based function with those that show abnormal resting-state FC.

Resting-state FC can also be assessed within or between large-scale networks. Large-scale networks capture multiple regions across the whole brain that are highly correlated and thus are likely to be co-activated, functionally meaningful circuits. In offenders with psychopathy, two studies have assessed large-scale network FC and found that particularly the interpersonal-affective traits were negatively associated with the FC of networks including the salience network, medial-temporal (limbic) network, default mode network, and frontoparietal network (Espinoza et al., 2018; Philippi et al., 2015). Another study that only assessed ASPD as a heterogeneous disorder also reported reduced FC in the default mode and frontoparietal network (Tang, Jiang, et al., 2013). Importantly, the regions contained within these networks are involved in attention, emotion recognition and processing, empathy, self-referential processing, and reward and punishment processing. This means that ASPD+/-P is not only characterized by neurobiological abnormalities within specific regions, but also within the networks that connect these regions. Unfortunately, there have been no studies directly comparing resting-state FC between individuals with ASPD+P and ASPD-P. Considering the variability between

these groups in neurocognitive performance and behaviour, it is likely that there are differential patterns of large-scale network connectivity between the two subtypes. This remains to be investigated.

#### 1.3.2.2.3 Network topology

Resting-state neural network topology is closely related to resting-state FC and reflects the intrinsic neural architecture of the brain (Rubinov & Sporns, 2010). It provides insight into the complex organization and efficiency of information flow throughout the brain. Understanding network topology can further help to explain abnormalities in brain function. Only three studies have assessed neural topology in offenders meeting criteria for ASPD or psychopathy (W. Jiang, Shi, Liao, et al., 2017; Tang et al., 2016; Tillem et al., 2019). Together, findings from these studies suggested abnormal network efficiency and a decreased reliance on subcortical brain regions in the flow of information across the brain. However, the individual studies produced somewhat inconsistent findings and were limited by methodological problems such as lacking control groups and poor characterisation of the sample. None of the studies to date have directly compared the neural topology of offenders with ASPD+/-P. Therefore, more research is required to improve the understanding of this neurobiological feature and its potential impact on behavioural and personality deficits associated with the disorder.

### *1.3.2.3 Summary of the neurobiological underpinnings of ASPD+/-P*

In summary, it appears that the ASPD+P phenotype is associated with more widespread neurobiological abnormalities, including typically reduced neural activity during neurocognitive performance, reduced grey matter volume and cortical thickness, and reduced functional connectivity as compared with the ASPD-P phenotype. However, ASPD-P is also characterized by neurobiological abnormalities. Key brain regions that are repeatedly associated with these phenotypes include the ventromedial and

orbitofrontal cortex, cingulate cortex, insula, amygdala, inferior parietal cortex, precuneus, and basal ganglia structures. There is a scarcity of research investigating cortical thickness and surface area, cerebral blood flow, large-scale network functional connectivity and neural topology. Furthermore, there is almost an entire lack of studies directly comparing these neurobiological markers between ASPD+/-P. Better knowledge of potential abnormalities in these features can improve the understanding of the neurobiological underpinnings of the disorder, LCP antisocial behaviour, and violence. It also increases the potential to identify mechanisms that could be treated using neurochemical agents.

### 1.3.3 Neurochemical underpinnings of ASPD and psychopathy

Neurochemical underpinnings of ASPD+/-P have been explored. This includes the assessment of abnormalities in neurotransmitter and neuropeptide synthesis and transmission. One neuropeptide with particular importance to the pathophysiology of ASPD+/-P is oxytocin. This is due to its impact on social brain processes related to antisocial behaviour, aggression, impulsivity, and empathy. Furthermore, there is suggestion from research in healthy individuals that the administration of oxytocin can shift neurobiological mechanisms that have been found to be impaired in ASPD+/-P. The following will provide an overview of the evidence base for the neurochemical alterations in ASPD+/-P. This will be followed by a more detailed review of the role of oxytocin to highlight its potential to modulate neurobiological mechanisms and thus its relevance for ASPD+/-P. It should be noted in advance that most evidence comes from studies that assessed behavioural characteristics of ASPD+/-P (e.g., aggression, impulsivity, reduced emotional responsiveness) or from studies investigating the broad and heterogenous ASPD construct.

#### *1.3.3.1 Neurotransmitters and neuropeptides*

The synthesis and transmission of neurochemicals is dependent on the expression of genes coding for proteins involved in this process. Variants

and polymorphisms in genes associated with monoamine neurotransmitters, including most prominently the MAOA, serotonin transporter (5-HTT) and various dopamine enzyme, transporter and receptor genes, have been identified as risk factors for ASPD+/-P (Cuartas Arias et al., 2011; Ficks & Waldman, 2014; Glenn, 2011; Kolla & Bortolato, 2020; Mariz et al., 2022; Sadeh et al., 2012; Sah et al., 2021; Vevera et al., 2009; Yildirim & Derksen, 2015). Evidence shows that in individuals with externalizing disorders including CD and ASPD, the MAOA and 5-HTT genes are vulnerable to the impact of environmental factors and that they can be subject to epigenetic effects via DNA methylation (Åslund et al., 2013; Burt & Klump, 2014; Byrd & Manuck, 2014; Checknita et al., 2015, 2020; Gescher et al., 2018; Nilsson et al., 2006; Nöthling et al., 2020; Reif et al., 2007; Thibodeau et al., 2015; Van Dongen et al., 2021; Van IJzendoorn et al., 2012; Waltes et al., 2016). Together, this results in abnormalities of monoamine neurotransmitter synthesis and transmission. Furthermore, genetic polymorphisms associated with other neurotransmitters including gamma aminobutyric acid (GABA) and glutamate and with neurochemical enzymes such as fatty acid amide hydrolase and tryptophan hydrolase have also been implicated (R. J. R. Blair, 2006; Cuartas Arias et al., 2011; Hoenicka et al., 2007; Kolla et al., 2021; Peng et al., 2021; Ruisch et al., 2020; Terranova et al., 2013; Wagels et al., 2021). Overall, these altered genetic processes have a direct impact on the neurochemical balance by affecting synthesis and transmission (Comai et al., 2012; Gunter et al., 2010; Holz et al., 2016; Meyer-Lindenberg et al., 2006).

An impairment in neurochemical synthesis and transmission affects brain function and contributes to neurocognitive and neurobiological deficits and maladaptive behaviours in ASPD and psychopathy. One of the most important neurotransmitters in the context of antisocial behaviour and violence is serotonin. It is related to threat and emotion processing, reactive aggression, impulsivity, and moral reasoning (Bocchio et al., 2016;

Coccaro et al., 2015; Crockett et al., 2010; Duke et al., 2013). Baseline levels of serotonin, its precursors and metabolites, as well as its transport are dysregulated in antisocial populations (Yildirim & Derksen, 2013). Studies typically show decreased serum and cerebrospinal fluid serotonin levels associated with and predictive of ASPD+/-P (Checknita et al., 2015; Kolla et al., 2015; Moul et al., 2013; Soderstrom et al., 2001, 2003; Virkkunen et al., 1995). Furthermore, PET studies have shown reduced serotonin transporter availability and receptor density in frontotemporal and subcortical limbic regions associated with ASPD, violent offending and its neurocognitive underpinnings (Da Cunha-Bang, Hjordt, Dam, et al., 2017; Da Cunha-Bang, Hjordt, Perfalk, et al., 2017; Meyer et al., 2008). These regions overlap with those showing neurobiological abnormalities, highlighting the interplay between neurochemistry and neural activity. One study reported a positive correlation between serotonin receptor availability and CU traits, yet a negative correlation with aggression after controlling for CU traits, suggesting receptor availability may distinguish between those with and without psychopathy (Van de Giessen et al., 2014).

Another important neurotransmitter in the context of ASPD+/-P is dopamine. Dopamine is crucial for reward processing, learning, and decision-making. Levels of this neurotransmitter and its precursors also seem to be dysregulated, with evidence suggesting an increase in baseline dopamine levels and metabolism, and reduced or imbalanced receptor availability in the areas of the mesocorticolimbic pathway (Buckholtz et al., 2010; Soderstrom et al., 2001; Tiihonen et al., 1995; Yildirim & Derksen, 2015). Like serotonin, a dysregulated dopaminergic system also contributes to behavioural characteristics of ASPD+/-P including impulsive aggression, novelty-seeking, and substance use. For instance, one study found that dopamine precursor activity was negatively associated with reactive aggression and positively associated with proactive aggression and PCL-R total score in individuals with ASPD (Azevedo et al., 2022). Furthermore, another study revealed a positive relationship between

dopamine levels and the social deviance traits of psychopathy that are commonly found in both ASPD+P and ASPD-P (Soderstrom et al., 2003), suggesting dopamine level abnormalities might be common to ASPD regardless of psychopathy status.

Finally, the role of hormones such as cortisol and testosterone, and neuropeptides such as oxytocin and arginine vasopressin has also been investigated. Cortisol and testosterone are adrenal and gonadal hormones, respectively, that can modulate neural activity. Cortisol is important for appropriate stress response. Some studies reported reduced baseline cortisol levels and reduced cortisol production in response to stress, particularly in individuals with interpersonal-affective traits associated with ASPD+P (Cima et al., 2008; Holi et al., 2006; Von Polier et al., 2013). This suggests a dampened hypothalamic-pituitary-adrenal axis and may result in hypoactive threat processing and more impaired reward-based decision-making (Gostisha et al., 2014; D. J. Hawes et al., 2009; Van Honk et al., 2003). It must be noted however that not all studies show a relationship between cortisol and ASPD+/-P (Feilhauer et al., 2013; Figueiredo et al., 2020), so further research is required. In terms of testosterone, some evidence revealed increased levels, especially in males with ASPD+/-P (Aromäki et al., 2002; Brooks & Reddon, 1996; Horn et al., 2014; Yildirim & Derksen, 2012a). This has been related to heightened aggression, partially explained by the modulatory effect of testosterone on serotonin and its corresponding gene expression (Yildirim & Derksen, 2012b). Cortisol and testosterone levels are also thought to interact with each other in the context of antisocial behaviour and aggression (Terburg et al., 2009).

Neuropeptides are hormones which can function as independent neurotransmitters but can also modulate, or up- and down-regulate other neurotransmitter activity and synaptic signalling in the brain. Oxytocin and arginine vasopressin are two neuropeptides with particular importance for social brain processes. They are synthesized in the hypothalamus from where they are released into the brain and body via the pituitary gland

(Meyer-Lindenberg et al., 2011). Genetically, their precursor proteins are coded for on the same chromosome, and various polymorphisms in these genes as well as their respective receptor genes have been identified in the context of social behaviours (Baribeau & Anagnostou, 2015; Ebstein et al., 2012). Oxytocin has received considerable attention in recent years. It has been studied more extensively due to its broader behavioural effects and its potential for therapeutic use in psychiatric disorders of social functioning, including ASPD.

#### *1.3.3.2 Oxytocin*

Oxytocin has many functions, ranging from its role as a neuropeptide to facilitate various social processes in male and female brains to its role as a hormone involved in lactation and childbirth in the female body (Werry et al., 2022). It is found in mammals and is increased in those species which live in more complex social structures (Anacker & Beery, 2013). In humans, evidence suggests involvement in in-group prosocial behaviour, emotion and threat processing, empathy and decision-making (Bethlehem et al., 2013; Leppanen et al., 2017, 2018; N. Marsh et al., 2021; Meyer-Lindenberg et al., 2011; Piva & Chang, 2018; Tully et al., 2018).

##### 1.3.3.2.1 Oxytocinergic system in the brain

Oxytocin is produced in the paraventricular, supraoptic and accessory nuclei of the hypothalamus and stored in the posterior pituitary gland (*Figure 2.3*). Oxytocin is released peripherally into the body via the bloodstream and centrally into several cortical and subcortical brain regions via oxytocinergic neuronal projections and diffusion from the extracellular space (Grinevich & Neumann, 2020). These brain regions have a high density of oxytocin receptors. In humans, immunohistochemical analyses suggest regions with high receptor density include the amygdala and the anterior cingulate cortex (Boccia et al., 2013). Neuroimaging and genetic analyses have confirmed this and additionally detected oxytocin-related activity in the ventromedial prefrontal and orbitofrontal cortex, insula,

hippocampus, thalamus, and basal ganglia (Bethlehem et al., 2013; Martins, Mazibuko, et al., 2020; Quintana, Rokicki, et al., 2019).

Regions with a dense population of oxytocin receptors, are implicated in social behaviours, and as described above, appear to show abnormalities in ASPD+/-P. The mechanisms behind the effect of oxytocin on behaviour in these brain regions remains to be fully understood. However, a leading theory suggests that oxytocin selectively increases the salience of information relevant for social behaviour, such as emotional cues. On a neural level, it is suggested that this occurs by oxytocin modulating the activity of excitatory and inhibitory cell firing, biasing towards the processing of socially relevant stimuli (Marlin et al., 2015; Oettl et al., 2016). On a more cognitive level, this then results in an increase in attention towards these stimuli, supporting the navigation of approach versus avoidance behaviours as well as various other social behaviours (Kemp & Guastella, 2010; Shamay-Tsoory & Abu-Akel, 2016). Although much further research is required, these processes are suggested to contribute to the allostatic feedback loops between social brain areas that project and respond to oxytocin, which ultimately shifts neurobiological function to predict future events based on past experience (Lefevre et al., 2021; Quintana, 2022; Quintana & Guastella, 2020).

The following sections will present findings associated with the oxytocinergic system that are relevant to ASPD+/-P.

##### 1.3.3.2.2 Genetic alterations of oxytocin

On the genetic level, the oxytocin gene (OXT), which codes for oxytocin's precursor, and the oxytocin receptor gene (OXTR) are two key genes involved in the synthesis and transmission of oxytocin in the brain. As with other neurochemicals discussed above, genetic variants, polymorphisms and altered allele lengths have been linked with individual differences in characteristics of ASPD+/-P. For instance, evidence suggests associations between such genetic alterations and increased CU traits, more antisocial

behaviour, severe aggression, poorer emotion recognition, increased physiological stress reactivity, and the presence of a less trusting disposition (Beitchman et al., 2012; Cecil et al., 2014; Ebstein et al., 2012; Malik et al., 2012; Nishina et al., 2015; Poore & Waldman, 2020; Rodrigues et al., 2009). It is worth noting that several of these results were only found in males but not females. The OXTR gene is also particularly vulnerable to environmental and epigenetic modulation, with evidence showing an impact of gene-environment interactions and a robust link with the experience of childhood maltreatment, OXTR methylation and development of ASPD+/-P and its hallmark features (Byrd et al., 2020; Dadds et al., 2014; Fragkaki, Cima, et al., 2019; Kraaijenvanger et al., 2019; Smearman et al., 2015; Verona et al., 2018).

Genetic polymorphisms and methylation of the OXTR gene have also been associated with structural and functional alterations in the brain, for example in the hypothalamus and the amygdala (Nishitani et al., 2021; Tost et al., 2010; Waller et al., 2016). Furthermore, increased gene expression has been shown in social brain regions, including those most impaired in ASPD+/-P (Quintana, Rokicki, et al., 2019). These findings suggest that further investigation of the oxytocinergic system in ASPD+/-P is merited.

##### 1.3.3.2.3 Endogenous levels of oxytocin

These genetic alterations affect the amount of circulating endogenous oxytocin in the brain and body. Indeed, decreased endogenous oxytocin levels in youth with CD, high CU traits and empathic deficits is a well-replicated finding (Dadds et al., 2014; Fragkaki, Verhagen, et al., 2019; Levy et al., 2015). There are fewer studies of endogenous oxytocin in adults with ASPD+/-P, with inconsistent findings. In personality disordered adults with significant aggression as well as in males convicted of homicide, cerebrospinal fluid (CSF) and plasma levels of oxytocin have been shown to be reduced (Goh et al., 2021; R. Lee et al., 2009). In contrast, increased endogenous oxytocin levels have also been reported in male forensic

inpatients with personality disorders, which positively correlated with PCL-R score and could not be accounted for by any comorbidities or psychiatric medication (Berends et al., 2022; Mitchell et al., 2013). Taken together, these findings suggest dysregulated endogenous oxytocinergic systems in ASPD.

Most of these studies measured endogenous oxytocin peripherally in the saliva or blood, and it must be considered that peripheral levels of endogenous oxytocin are a remote proxy of the central levels in the brain. One study revealed that plasma levels of oxytocin predicted CSF levels (Carson et al., 2014), and correlations between central and peripheral endogenous oxytocin levels have been shown, however this evidence is somewhat inconsistent (Lefevre et al., 2017; Martins, Gabay, et al., 2020; Valstad et al., 2017). Therefore, the above findings from peripheral biosamples should be interpreted carefully. Nevertheless, there is some rationale for an altered oxytocinergic brain system in ASPD+/-P. Another way of investigating this is by studying how brain and behaviour changes in response to exogenous oxytocin, e.g., after intranasal oxytocin administration.

#### 1.3.3.2.4 The effect of intranasal exogenous oxytocin

Neuroimaging studies have shown that intranasally administered oxytocin (OT) reaches the brain and can modulate task-based brain function, resting-state CBF, FC and topology when compared to placebo conditions, particularly in areas with a high oxytocin receptor density (Brodmann et al., 2017; Grace et al., 2018; Martins et al., 2021; Martins, Brodmann, et al., 2022; Martins, Lockwood, et al., 2022; Martins, Mazibuko, et al., 2020; Paloyelis et al., 2016; Quintana et al., 2016; Wigton et al., 2015). This includes areas identified to show neurobiological abnormalities in ASPD+/-P, such as the cingulate cortex, amygdala, and insula, as well as large-scale neural networks such as default mode and salience networks. Together, the evidence from these studies suggests that the impact of exogenous oxytocin on the brain and social behaviours is biologically meaningful,

although further understanding of the molecular processes is required (Quintana et al., 2021).

Many studies have investigated the effect of OT on a range of neurocognitive functions in both healthy and clinical populations (Peled-Avron et al., 2020). In terms of behaviours and neurobiological deficits associated with ASPD+/-P, meta-analyses have shown that OT improves emotion recognition, particularly of fear and anger (Domes et al., 2007; Evans et al., 2010; Leppanen et al., 2017; Shahrestani et al., 2013). OT has also been found to improve empathy and perspective-taking skills (Bartz et al., 2019; Hurlemann et al., 2010; Theodoridou et al., 2013). Beyond these, OT has also been shown to play a role in modulating and improving threat and reward processing and subsequent decision-making (Borland et al., 2019; Brodmann et al., 2017; Leppanen et al., 2018; Scheele et al., 2013; Sippel et al., 2021), as well as trust and learning, particularly within in-group settings (Baumgartner et al., 2008; Hurlemann et al., 2010; Kosfeld et al., 2005; Xu et al., 2019). Importantly, a meta-analysis has shown that OT also modulates neural activity in task-relevant brain regions, even when no explicit behavioural effects are found (D. Wang et al., 2017).

Together, extant research provides promising evidence that neurocognitive and neurobiological underpinnings of ASPD+/-P might be shiftable by OT. This is particularly relevant in the context of studying new pharmacological treatment approaches for ASPD+/-P. However, some studies have also shown that OT negatively impacts antisocial behaviours, including making individuals more aggressive and increasing feelings of envy, gloating and distrust (Declerck et al., 2010; Ne'eman et al., 2016; Shamay-Tsoory et al., 2009; H. Zhang et al., 2019). Across species, it has been shown that oxytocin has an important role in prosocial behaviours towards in-group, but not out-group members (Triki et al., 2022). This might explain why the studies that show a negative impact of OT typically reveal increased antisocial behaviour directed at out-group members. Therefore, it is likely

that the modulatory effect of OT on behaviour is context-dependent (Bartz et al., 2011). Assessing the effects of OT on resting-state brain function avoids the risk of context-dependent findings, since individuals are not engaging in any particular activity. This may therefore be a preferred approach to study the shiftability of neurobiological mechanisms in ASPD+/-P.

Only a small number of studies have investigated the effect of OT in clinical ASPD populations to date. Two were small, underpowered behavioural studies which did not attempt to characterise psychopathy levels (Alcorn et al., 2015; Timmermann et al., 2017). Nevertheless, Timmermann et al. (2017) suggested OT might improve emotion recognition in ASPD. Moreover, findings from the analysis of task-based fMRI data which was collected as part of this project suggested that OT increased anterior insula and anterior cingulate cortex responsivity to fearful stimuli in violent offenders with ASPD+P (Tully et al., 2022). More research studying the effects of OT on brain function is required, and the current project sought out to do this.

#### *1.3.3.3 Summary of the neurochemical underpinnings of ASPD+/-P*

In summary, the neurochemical underpinnings of ASPD+/-P are evidently complex, in part due to the heterogeneous traits associated with the disorder. Various neurochemicals including serotonin and dopamine seem to be particularly important in the context of explaining behavioural characteristics such as aggression, impulsivity, and impaired emotion and threat processing. Genetic risk factors affecting the synthesis and transmission of these neurochemicals are important, however further research is required in larger samples to replicate current findings.

It is currently not possible to create a clear distinction between ASPD with and without psychopathy on a neurochemical level. Due to the differential neurocognitive and neurobiological abnormalities associated with ASPD+/-

P, it is possible that the oxytocinergic system, and thus also the effects of OT, may also differ between the two subtypes.

## 1.4 The current project

### 1.4.1 Rationale

The reviewed evidence provides a rationale to develop the current project. Previous studies showing different underpinning neurobiological mechanisms between ASPD+/-P were important first steps towards building a model that distinguishes ASPD+P from ASPD-P on a neural level, particularly in brain areas and networks including the prefrontal cortex, cingulate cortex, amygdala, insula, precuneus, thalamus, and basal ganglia, amongst other. This builds on evidence that these phenotypes can be distinguished on a behavioural level. However, there is still a substantial lack of studies directly comparing individuals with ASPD+/-P. Furthermore, there is only limited research in certain neurobiological mechanisms including 1) cortical thickness and surface area, and how these contribute to cortical volume; 2) resting-state CBF; 3) resting-state large-scale network functional connectivity; and 4) resting-state neural network topology. It is important to study these mechanisms as they may help explain behavioural and task-based functional neural brain abnormalities in ASPD+/-P. Additionally, findings from such research can potentially provide further rationale to create distinct diagnostic subtypes of ASPD, aligning diagnostic manuals and potential treatment studies with current practice in CD. Finally, ample research in healthy individuals has shown the potential of OT to impact upon key social cognitive processes which are demonstrably abnormal in ASPD+/-P. However there have been no studies assessing whether the measures of resting-state brain function can be shifted by pharmacological agents such as oxytocin in ASPD+/-P. If this is possible, it may open new paths for treatment studies.

### 1.4.2 Aims

The current project therefore had two overarching aims. First, it aimed to directly compare measures of 1) surface-based brain structure; 2) resting-state CBF; 3) resting-state large-scale network FC; and 4) resting-state network topology between male violent offenders with ASPD with versus without psychopathy. It also sought to compare these measures within each clinical group to a male, non-offending healthy control group. Second, it aimed to investigate the effect of OT on the measures of resting-state function, to assess whether underpinning mechanisms of ASPD+/-P can be modulated.

These aims were addressed using a double-blind, placebo-controlled, randomized crossover design and a range of complementary neuroimaging techniques. Details of the project's methodologies and neuroimaging techniques are provided in the two following Methods chapters. Furthermore, four experimental chapters present the detailed rationales and distinct hypotheses for each of the four neurobiological mechanisms evaluated in this project. Finally, a Discussion chapter will review patterns of findings across these chapters and discuss the limitations and implications of this research.

# 2 General Methods

This chapter will outline the general methodology of the current project, including the study design, recruitment processes, research procedures, assessments, administration of intranasal oxytocin (OT), and the general statistical approach. The details of the neuroimaging methods are outlined in the next chapter.

## 2.1 Study design and ethical considerations

The current project had a randomised, double-blind, placebo-controlled crossover design. This means that participants received the OT and placebo (PL) nose sprays in a randomised order that was determined by the pharmacy. Researcher and participant did not know what was being administered in which session. The crossover design is the best practice for pharmaceutical challenge studies. The data was collected in a cross-sectional manner.

Ethical approval was provided by both the National Health Service (NHS) Health Research Authority (reference number 15/LO/1083) as well as the National Offender Management Services Research Committee in Her Majesty's Prison and Probation Service (reference number 2016-382). All interested individuals received a participant information sheet describing the demands of participation as well as the potential risks and benefits. Opportunities to discuss any questions or concerns were provided. Before participation, subjects provided signed informed consent.

There were several important ethical considerations. A careful evaluation of the safety of having an MRI scan was conducted with every participant. This included screening for any medical and psychological contraindications, e.g., the presence of metal in the head and body due to injuries, weapons, or operations, and claustrophobia. All participants provided details of their general practitioner, who could be contacted in case radiologists identified any unusual findings during the brain scans. The safety of the OT administration was also carefully considered during the

study design. The current study used a dose of 40 international units (IU), which is safe in humans and is not associated with any known side effects or acute, unwanted behavioural changes (MacDonald et al., 2011). Further ethical considerations included the confidentiality of the assessment data, which included deriving a PCL-R score that can be used as a risk assessment. Participants' responses and assessment scores were kept strictly confidential and not shared with probation services, unless participants gave explicit information detailing an imminent risk to their own life or someone else's life. They were informed in advance that such information would have to be shared with their clinicians and/or probation officers. If participants consented, the interviews were recorded to aid scoring evaluation. These recordings were not shared with anyone outside of the study team. To validate the history and extent of violent offending, all participants consented to review of their police national computer (PNC) offending records, which were provided by probation services. Lastly, in line with ethical standards for human research and the research ethics committee recommendations, participants received financial compensation of £75 for their time and effort. It was decided that a cash reimbursement would be most helpful for these individuals. Participation in the study did not have any impact or benefits for their community sentence with probation services or clinical care.

## 2.2 Recruitment and participant selection

The current study included males with ASPD and a history of violent offending, as well as healthy non-offending males. Participant recruitment and selection was based on purposive sampling for the offender group and a mixed opportunistic/purposive sampling approach for the control group. All participants were enrolled between September 2017 and March 2020. *Figure 2.1* provides a flowchart including the recruitment and selection process as well as the subsequent study procedure.

The violent offender group was predominantly recruited from South London National Probation Service offices and some additional participants were

recruited from the NHS South London and Maudsley Trust inpatient medium-secure forensic personality disorder services. Offender managers and clinicians identified suitable individuals based on the inclusion and exclusion criteria outlined below. They introduced the research study to potential participants and if they agreed, passed on their contact details to the research team.

The healthy non-offending (NO) control group was recruited from the local community. Advertisements for the study were placed in public buildings in the local South London community to increase the likelihood of recruiting individuals with similar sociodemographic factors. This included libraries, gyms, grocery stores and job centres. Advertisements were also placed in online job-seeking websites and research participant recruitment portals. Initially, opportunistic sampling allowed the inclusion of any participant that met the inclusion and exclusion criteria. In later stages of the recruitment process, a more purposive approach was adopted to aid the matching of sociodemographic variables. Specifically, individuals with lower levels of educational achievement were sought and selected.

## 2.3 Inclusion and exclusion criteria

Participant recruitment and selection was subject to several inclusion and exclusion criteria. The below lists A) the criteria which applied to all subjects and B) and C) any additional criteria relevant to each subject group.

A) All subjects
    a. Inclusion criteria
        i. Male sex
        ii. Aged 18 to 60 at time of consent
        iii. Ability to read and write in English
    b. Exclusion criteria
        i. Any MRI safety contraindications

ii. History of neurological disorder or head/brain injury resulting in the loss of consciousness for more than one hour
iii. IQ < 70

B) Violent offenders

a. Inclusion criteria
   i. History of violent offending that involved actual and/or threatened harm to others (minimum offense common assault, but individuals were typically convicted of actual or grievous bodily harm, armed robbery, rape, manslaughter, and/or murder)
   ii. Meet diagnostic thresholds for CD in childhood and ASPD in adulthood (this was confirmed during the psychological assessment)
   iii. Living in the community or allowance for leave from their clinical inpatient stay

b. Exclusion criteria
   i. Active substance use disorder that disturbed daily functioning
   ii. Presence of any comorbid serious mental illness including mood and psychotic disorders

C) Healthy NO participants

a. Exclusion criteria
   i. Any history of violent offending
   ii. Any current or past mental illness, personality disorder, or substance use disorder (this was confirmed during the psychological assessment)

## 2.4 Procedure

*Figure 2.1* contains a detailed flowchart of the procedures for the study. Each participant attended three research appointments. The first appointment was for the psychological assessment and the other two

appointments were for the PL and OT MRI and neuropsychology (neurocognitive) data acquisition. Where possible, the MRI and neuropsychology appointments were scheduled to start at 10:00 to maintain consistency within and between participants. The two MRI and neuropsychology appointments were scheduled at least 3 days apart to enable a wash-out period (Martins, Lockwood, et al., 2022).

Participants were asked to abstain from substance use within the 14 days before their appointments. Before the start of each MRI session, the participant completed a urine drug screening test to confirm this.

Participants self-administered 40 international units (IU) of the nose sprays (Syntocinon, Novartis, Switzerland) by inhaling one puff every 30 seconds for 5 minutes, alternating nostrils under the supervision of the researcher. The PL and OT sprays only differed in that the OT spray contained the active ingredient oxytocin. Methodological details relating to the OT administration are provided in another section of this chapter (click *here*). The exact time of the final dose administration was noted as minute 0. The imaging data used in this thesis came from a structural MRI (sMRI) scan, and two resting-state functional MRI (rs-fMRI) scans (one arterial spin labelling (ASL) scan and one blood-oxygen-level-dependent (BOLD) signal scan). The minutes between this and the start of the rs-fMRI scans was termed 'minutes since dose' and used as a covariate in the respective analyses.

The details of the neuropsychology assessments are provided below. The neuroimaging methodologies used in this project, as well as the respective pre-processing and analysis steps, are outlined in detail in *Chapter 3*.

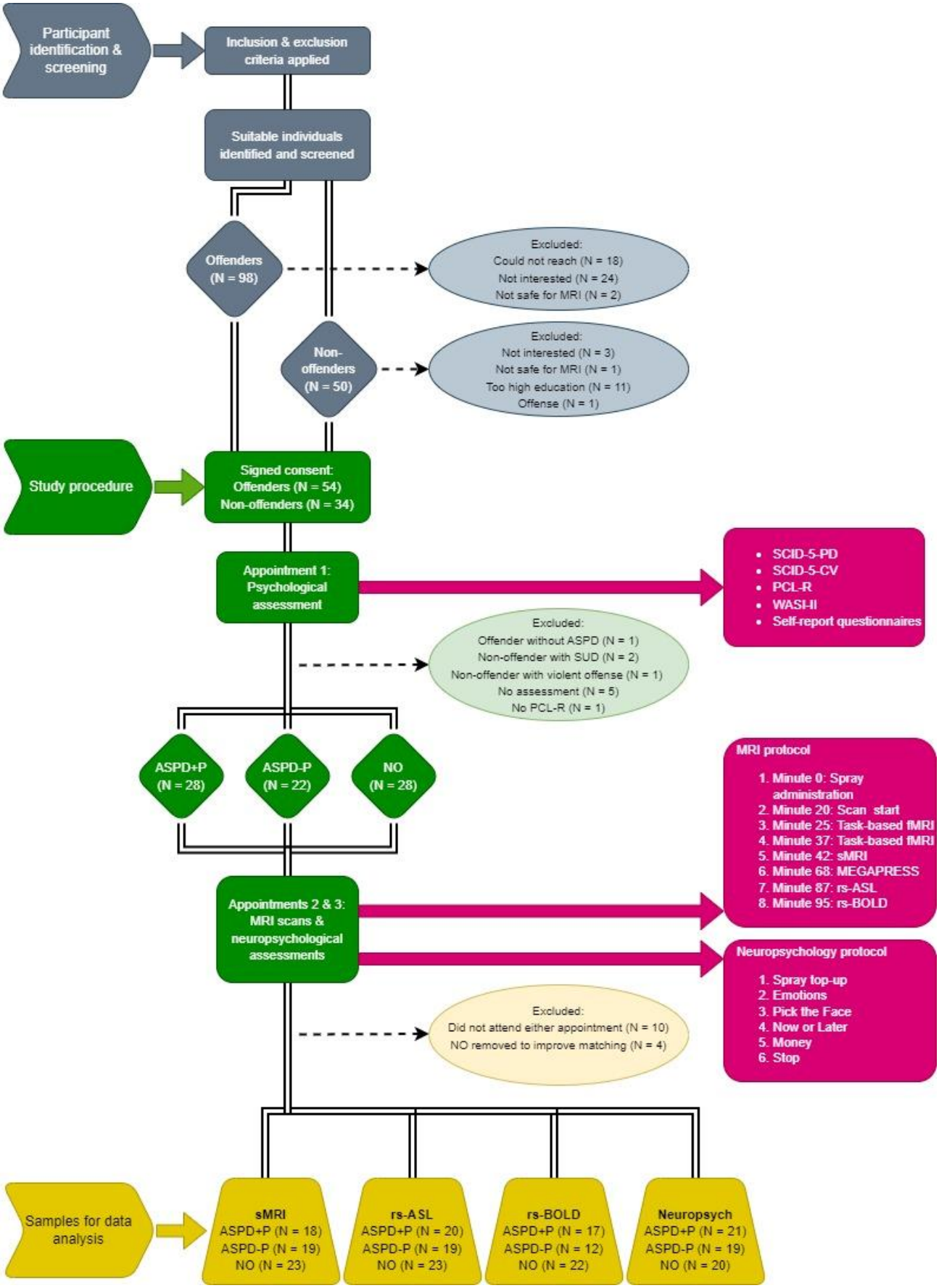


Figure 2.1 Flowchart of the recruitment process and study procedure.

*Note: The final samples for data analysis may vary slightly from what is presented in the individual results chapters, as the rs-ASL and rs-BOLD required further exclusion of some participants for the whole-brain and ROI analyses, respectively. For the neuropsychology data analysis, not all participants completed all tasks, so the numbers may also vary slightly.*

## 2.5 Psychological assessment

The psychological assessment included several interviews (*Figure 2.1*). The Structured Clinical Interview for the DSM-5, Personality Disorder (SCID-5-PD) and Clinical Version (SCID-5-CV) (First et al., 2015, 2016) were used to assess for the presence of personality disorders, depression and anxiety, severe mood disorders, psychotic disorders, substance use disorders, ADHD and PTSD. In the offender group, this was used to confirm the diagnosis of CD in childhood and ASPD in adulthood, and to ensure the absence of comorbid severe mental illness. It also captured any other comorbid personality disorders. In the NO group, this confirmed the absence of any personality disorder and mental illness.

The Psychopathy Checklist Revised (PCL-R) (Hare, 1991) was used in this study as the gold standard assessment for psychopathy. This involved completing an interview with the participants and then scoring it in line with the checklist. The PCL-R contains 20 items, outlined in *Table 1.3*, which are scored from 0-2. Thus, the total score ranges from 0-40, with a score over 25 enabling a categorical diagnosis of psychopathy. This cut-off is the European standard and was thus applied to this English sample (Cooke & Michie, 1999). To provide more detailed understanding of the total score, the items can also be summed into two factors (factor 1: interpersonal-affective features; factor 2: social deviance), or four facets (facet 1: interpersonal features; facet 2: affective deficits; facet 3: lifestyle features; facet 4: antisocial features). The PCL-R was used to determine whether a participant in the violent offender group belonged to the ASPD+P or the ASPD-P group. Thus, after the psychological assessment, the group status of every participant was finalized.

The Wechsler Abbreviated Scale for Intelligence, Second Edition (WASI-II) (Wechsler, 2011) was used to measure participants' verbal and non-verbal IQ. In most cases, the full-scale IQ based on all four subtests was used. Rarely, due to logistical constraints, the two-scale IQ score was used

instead. This also confirmed the absence of a learning disability, indicated by an IQ below 70.

## 2.6 Self-report questionnaires

During the psychological assessment, or in between appointments, participants also completed self-report questionnaires. This included the Reactive Proactive Questionnaire (RPQ) (Raine et al., 2006), which was used to measure levels of reactive and proactive aggression in the current project. It consists of 23 items exploring how often various behavioural expressions of reactive/impulsive and proactive/instrumental anger and aggression have occurred on a range from 0 (Never) to 2 (Often). Higher scores indicate increased levels of aggression. In the current study, the subscales for each type of aggression were used. They showed excellent reliability (Cronbach's alpha: reactive aggression subscale = .94, proactive aggression subscale = .95). There was no missing data on the RPQ.

The number of past violent and non-violent convictions was self-reported by participants during the PCL-R interview. This information was verified by checking the PNC records for each participant after their participation. In addition, updated PNC records were re-assessed one year after participation to check for the presence of any reconviction within one year of study participation. Reconviction within one year of study participation was used to standardize the time frame to avoid a bias in the risk of reconviction for individuals who participated earlier compared to those who participated later.

## 2.7 Neurocognitive assessment

The neurocognitive assessment was conducted after the MRI components during appointments 2 and 3. Participants thus completed the tasks once after receiving the PL nose spray and once after receiving the OT nose spray. As the sprays were initially administered before the scan, it was decided that a top-up administration from the same spray bottle would take place before the start of the neuropsychology tasks. Specifically, 10

minutes before the start of the tasks, participants self-administered another 10 puffs (40 IU) of the spray every 20 seconds into alternating nostrils. Only the data from the PL condition was used in the current thesis.

Participants completed five tasks which captured performance in emotion recognition and detection, reinforcement-based decision-making, temporal discounting, and response inhibition. They were done in the same order across participants and appointments. These tasks were adapted from those devised by Professor Blair's laboratory at Boys Town National Research Hospital in Nevada, USA. They were built and presented in E-Prime 1.0 software (Psychology Software Tools Inc., 2000). They were specifically designed to align with the Research Domain Criteria (RDoC) Framework (Insel et al., 2010). The goal of the RDoC framework is to provide a dimensional view of mental disorders which integrates multiple levels of information, from genetic via cellular and neural to behavioural, to capture the dynamic shift between function and dysfunction across populations. Measuring behavioural neurocognitive underpinnings of disorders can provide improved understanding of the brain-level systems which are affected and vice versa. It is a particularly useful framework to study the highly heterogenous and developmentally driven externalising disorders, including ASPD, aiming to improve the ability to predict poor mental outcomes and treatment response (R. J. R. Blair, White, et al., 2014). The current tasks have been used to assess neurocognitive functioning in youth with CD and CU traits (R. J. R. Blair et al., 2020; R. J. R. Blair, White, et al., 2014; Moore et al., 2019; White et al., 2014). In terms of the RDoC framework, the "Emotions" and "Pick-the-Face" games tap into the Negative Valence Systems – Acute Threat ("Fear") and the Systems for Social Processes – Social Communication; the "Pick-the-Face" game also taps into the Cognitive Systems – Attention; the "Money" game taps into the Positive Valence Systems – Reward Learning and Reward Valuation; the "Now-or-Later" game taps into the Positive Valence Systems

– Reward Valuation; and lastly, the "Stop" game taps into Cognitive Systems – Cognitive Control.

### 2.7.1 Emotion recognition and detection

There were two distinct tasks measuring emotion recognition and detection, respectively. The "Emotions" task required the recognition of an emotional expression. During this task, a participant was briefly flashed a picture of a face. A total of 240 faces were shown. There were 60 faces within each of four emotion categories: anger, sadness, fear, or happiness. These 60 faces were split into five intensity levels of 20%, 40%, 60%, 80%, or 100%, meaning that each intensity level was shown 12 times. After the face was flashed, the four emotion words were displayed on the screen and the participant was asked to label the emotion which they believe was expressed in the picture as accurately and quickly as possible. The key outcome variable was response accuracy.

The "Pick-the-Face" task required attention to detect an emotional expression. In this task, participants were asked to identify the face that is expressing an emotion in an array of otherwise neutral expressions. There were three emotion categories: anger, fear, or happiness. In each trial, the participant either saw three faces or five faces, and they were shown either for 1500 ms or 2000 ms. This resulted in four levels of difficulty within each emotion category. Each combination was shown 8 times, meaning a total of 96 faces were shown. The key outcome variable was response time.

### 2.7.2 Reinforcement-based decision-making

In the "Money" task, participants were presented with two objects and selected the object which they believed had the higher likelihood of resulting in a financial reward. Their goal was to earn as much money as possible throughout the task. The first 90 trials created the acquisition phase because the contingencies are stable, allowing an individual to learn which object is more likely to be rewarded. The contingency was 80% reward versus 20% no reward for the correct object. Then the reversal

blocks began. This meant that the other object now had an 80% likelihood of being rewarded. There were 4 reversal blocks with 20 trials each. In each block, the contingencies reversed. Therefore, individuals had to adapt their decision-making to changing contingencies. The key outcome variable was response accuracy (i.e., choosing the rewarded object) within each block.

### 2.7.3 Temporal discounting

The "Now-or-Later" task assessed temporal discounting, which reflects the preference to receive a smaller reward at an earlier time rather than a larger reward later. In this task, participants were asked to decide between receiving a varying amount of money immediately (between $0 and $10.00) or receiving a fixed amount of $10.00 after a specified waiting period (0 days/now – control items, 7 days, 30 days, 90 days, 180 days or 360 days). There were 137 items, and the choices were randomized with an equal number of items (20) for each of the 6 waiting periods. 17 items acted as control conditions to ensure individuals are paying attention. In these control conditions, the immediate reward was larger ($10.50) than the delayed reward. Across all items, participants were encouraged to select their personal preferences as if it was a real-life decision. The outcome variable was the number of times the lesser amount of money was chosen over the fixed $10.00 within each waiting period.

### 2.7.4 Response inhibition

The "Stop" task used a stop-signal reaction time design to measure an individual's ability to inhibit responses. Participants were asked to click the right mouse button if an arrow on the screen pointed to the right, and the left mouse button if the arrow pointed to the left ('click' trials: respond). On some trials, a red circle appeared, indicating that they should not click any mouse button ('stop' trials: inhibit response). There was a varied stop-signal delay, meaning that the red circle appeared at a slightly increased time of onset after a correct inhibition, and at a slightly decreased time of onset after an incorrect inhibition – it therefore fluctuated depending on performance. The key outcome variable was stop signal reaction time

(SSRT). SSRT is a latent variable as it is a function of the average response time in the 'click' trials and the average time of onset of the stop-signal (red dot) during the 'stop' trials.

### 2.7.5 Use of neurocognitive assessment data in correlation with neuroimaging findings

Performance on the neurocognitive assessment under PL condition (indicating baseline ability) was incorporated into the current thesis by correlating it with the neuroimaging results. The outcome variables, described above for each task, were partially collapsed into averages to reduce the number of correlations, and thus, the number of multiple comparisons. For the "Emotions" task, average accuracy across each intensity level was calculated for anger, sadness, and fear. For the "Pick-the-Face" game, average reaction time was calculated across each level of difficulty for anger and fear. For both tasks, happiness was not included due to ceiling effects. For the "Money" task, average accuracy across each of the acquisition and the reversal blocks was calculated. For the "Now-or-Later" task, the original outcome variable was used, indicating the preferred choice between a lower and a higher amount of money within a given waiting period. Lastly, for the "Stop" task, the SSRT outcome variable was used. All values used in the correlations were standardized against a z distribution to ease comparison across different outcome variable types.

### 2.7.6 Benefits

There were benefits associated with this neurocognitive assessment. Specifically, it included a broad range of tasks to cover several key cognitive functions which have been identified to be abnormal in ASPD and psychopathy (as described in the Introduction). Furthermore, the tasks were developed in line with the RDoC framework, meaning that results can be interpreted in the context of the RDoC domains and constructs. This also means that impairments on these tasks can potentially give theoretical insight into which brain-level systems are affected and vice versa. This was further supported by correlating neurocognitive performance with any

neurobiological abnormalities, which allowed for statistical insight into the relationship between multiple levels of functioning (behavioural and neural).

### 2.7.7 Challenges

The neurocognitive assessment was affected by some challenges. The tasks were originally designed to be used in children and youth with CD and CU traits. Therefore, they are more likely to result in ceiling effects in the adults tested in the current study. Additionally, this limitation may also mean that tasks were too simple or not sensitive enough to capture true impairments found in adults. Furthermore, the order of task completion was not counter-balanced, meaning later tasks were potentially subject to fatigue effects.

## 2.8 Intranasal oxytocin

### 2.8.1 Administration in the current study

The current study used a nose spray to deliver the exogenous oxytocin (Syntocinon, Novartis, Switzerland) to the brain. A dose of 40 IU was self-administered via ten puffs (each puff contained four IU) every 30 seconds for five minutes, alternating nostrils. This was scheduled 25 minutes before the start of the first fMRI paradigm, which was not analysed in this thesis. This timing was selected in line with spatiotemporal evaluations that showed significant effects of 40 IU of OT on the brain between 15 and 95 minutes after the final spray (Martins, Mazibuko, et al., 2020; Paloyelis et al., 2016). This includes areas relevant to the study of potential OT effects in ASPD+/-P, such as the amygdala, cingulate cortex, insula, and precuneus (see *Figure 2.2*). It should be acknowledged however that the project was originally designed to optimize the effect of OT for the task-based fMRI component, which occurred early in the MRI protocol. There has been suggestion that the effect of OT may vary across time and brain regions (Martins, Brodmann, et al., 2022; Martins, Mazibuko, et al., 2020; Paloyelis et al., 2016). The discovery of potential OT effects in the three rs-

fMRI scans of the current project might therefore be limited to the post-dose time window within which they were acquired.

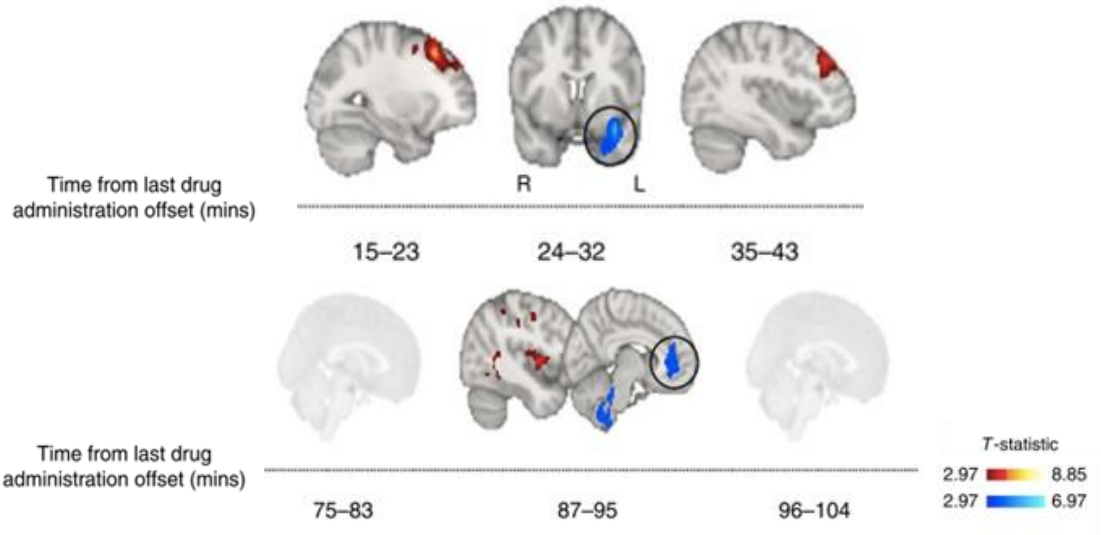


Figure 2.2 Spatiotemporal effects of intranasal oxytocin on the brain.

*Note: This figure was adapted from Figure 3 in (Martins, Mazibuko, et al., 2020)*

Intranasal administration of oxytocin has become the most common approach to studying OT effects in existing literature. The Introduction described the literature showing effects of OT on brain and behaviour. Nonetheless, there are methodological challenges that should be considered and which have led to some contention in this field of research (Leng & Ludwig, 2016). Better understanding of these challenges is pivotal for the development of oxytocin as a potential clinical treatment (Quintana et al., 2021).

### 2.8.2 Methodological challenges in oxytocin research

There are various methodological challenges that affect oxytocin research. These include the limited understanding of the neural mechanism of action of OT, the decisions over the method of administration, the optimal dosage and delivery device, and finally, concerns with statistical analysis and study design. These will be discussed in turn.

#### *2.8.2.1 Does exogenous oxytocin reach the brain?*

Oxytocin research still relies on assumptions about the neural mechanism of action, for example that exogenous oxytocin actually reaches the brain and that it can increase existing brain oxytocin levels (Quintana, 2022).

Basing research on such assumptions can challenge the interpretation of findings. However, there have been important advances towards a clearer understanding of the pathway(s) by which exogenous oxytocin can reach the brain (Quintana et al., 2021). The dominant current model suggests that intranasally administered oxytocin travels along a direct nose-to-brain pathway (*Figure 2.3*). This pathway is facilitated by the physiology and innervation of the nasal cavity (Quintana et al., 2018; Quintana, Alvares, et al., 2015). The upper posterior regions of the nasal cavity are densely packed with olfactory and trigeminal nerve endings which project from the cerebrum and the brainstem, respectively. The model posits that intranasally administered oxytocin is deposited on the nasal epithelia and then absorbed through the nasal mucosa to reach these nerve endings. The ensheathed perineural channels surrounding the nerve fibres then facilitate a direct transportation of oxytocin molecules into the brain and CSF.

This model has received support from animal and human studies. A recent study of knockout mice who could not produce endogenous oxytocin discovered extracellular oxytocin concentrations in the brain after intranasal delivery (A. S. Smith et al., 2019). Furthermore, after intranasal administration, radiolabelled oxytocin was identified in olfactory and trigeminal nerves and their trajectories, as well as in brain regions involved in social and reward processing in rodents and non-human primates (M. R. Lee et al., 2020; Yeomans et al., 2021). Importantly, these animal studies also quantified a significant increase in oxytocin levels in brain areas such as the orbitofrontal cortex, amygdala, hippocampus, and striatum, as well as the CSF, up to two hours after intranasal administration (Dal Monte et al., 2014; M. R. Lee et al., 2020; A. S. Smith et al., 2019; Yeomans et al., 2021). Therefore, these animal research findings provide support for the assumptions that exogenous oxytocin reaches the brain and increases brain oxytocin levels.

In humans, acquiring direct support for these assumptions is more difficult, largely because the methods required are too invasive. Nonetheless,

indirect evidence that OT reaches the brain comes from studies showing neural and social cognitive alterations in comparison to PL administration, even after accounting for baseline peripheral oxytocin levels (Martins et al., 2021; Martins, Mazibuko, et al., 2020; Quintana et al., 2016; Quintana, Westlye, et al., 2015, 2019). Furthermore, a rare human study provided more direct evidence by reporting that intranasally delivered oxytocin increased the concentration of oxytocin in the CSF (Striepens et al., 2013). In summary, recent findings from human studies confirm those from animal studies and support the idea that exogenous oxytocin can reach the brain and that it subsequently increases brain levels of oxytocin.

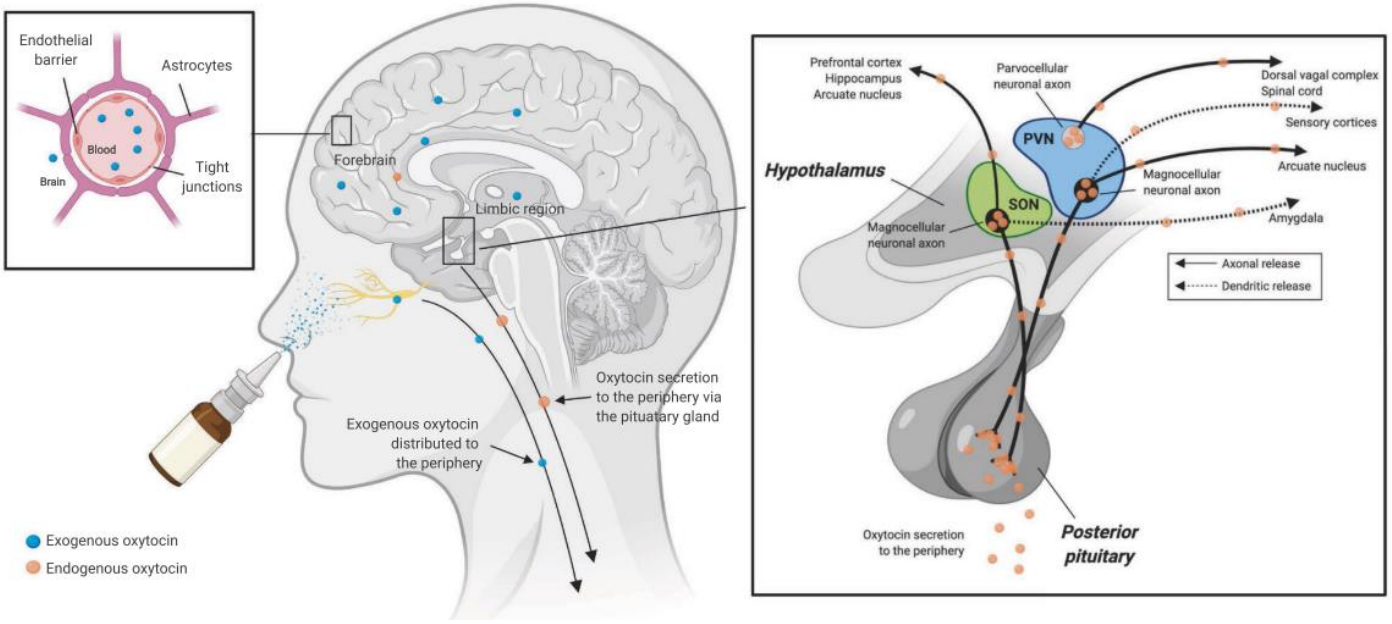


Figure 2.3 Intranasal administration of exogenous oxytocin and production of endogenous oxytocin.
*Note: This figure was copied from Figure 1 in (Quintana et al., 2021).*

### *2.8.2.2 Method of administration, optimal dosage and delivery device*

Oxytocin research in humans is marked by variable findings, and the broad range of methodological decisions regarding the method of administration as well as the optimal dosage and delivery device has been identified as an important factor contributing to this variability (Grace et al., 2018; Quintana et al., 2021; D. Wang et al., 2017; Wigton et al., 2015; Winterton et al., 2021). This is a challenge for oxytocin as a literature, but research has started to address this. For example, studies have compared the effects

of intranasal and intravenous methods of administration on human brain and behaviour. Intravenous administration requires oxytocin to reach the brain from the periphery through the systemic circulation. However due to the large molecular size of oxytocin, the blood brain barrier is thought to largely hinder this process (Leng & Ludwig, 2016; Mens et al., 1983). Thus, the results from comparative studies are mixed. On the one hand, studies revealed neural and behavioural changes only after intranasal delivery (Quintana et al., 2016; Quintana, Westlye, et al., 2015, 2019). On the other hand, two studies that used a higher dose did find that intravenous oxytocin modulated brain activity, but to a different extent than intranasal oxytocin (Martins et al., 2021; Martins, Mazibuko, et al., 2020). This suggests that, in addition to the direct nose-to-brain pathway described above, another pathway by which exogenous oxytocin reaches the brain might exist. However, the possible mechanisms of this alternative pathway remain elusive. Therefore, the intranasal method of administration is better validated and understood than the intravenous method. Additionally, intranasal administration is less invasive than intravenous administration, and thus may lend itself better to research purposes. It thus remains the favoured type of administration in human research.

Within the intranasal method of administration, there has been discussion about the optimal dosage and the most suitable delivery device. To date, human studies have typically used doses ranging from 8 IU to 48 IU (Wigton et al., 2015). Studies assessing the efficacy of various doses in modulating neural activity and behavioural outcomes have suggested a U-shaped dose-response curve: lower doses (around 8 IU), and to a slightly lesser extent higher doses (between 24-32 IU, although 40 IU has also been shown to be favourable over 32 IU) invoke the most response, whereas medium doses (between 8-24 IU) do not appear as effective (Bartz et al., 2011; Martins, Lockwood, et al., 2022; Quintana et al., 2016; Quintana, Westlye, et al., 2015; Shin et al., 2018; K. Winter et al., 2017). Notably, the studies that reported the highest efficacy after low doses opted

to use nebulisers or breath-powered delivery devices as opposed to nose sprays. These have been argued to support the delivery of oxytocin through the complex nasal anatomy and thus optimize the deposition of oxytocin available for uptake into the nose-to-brain pathway (Martins, Brodmann, et al., 2022; Martins, Mazibuko, et al., 2020; Winterton et al., 2021). In summary, recent findings reveal highest efficacy for low doses (8 IU), particularly when using nebulised or breath-powered delivery devices.

Many of these findings are recent contributions to the discussion about the optimal dosage and delivery device. Thus, when the current study was designed in 2015, there was less information about the optimal dose and device. Therefore, the most appropriate decision was to use the highest clinically safe dose (40 IU) since this had shown effects on relevant social brain regions (MacDonald et al., 2011; Paloyelis et al., 2016). Furthermore, in terms of the delivery device, the current study used a nose spray because the use of nebulisers was in its infancy. Although these decisions could now be viewed as sub-optimal, research since then has shown that a higher dose from a conventional nose spray exerts a similar effect as a lower dose from an nebuliser (Quintana, 2022). Furthermore, studies directly comparing the pharmacodynamic profiles when delivering 40 IU of oxytocin with a nose spray versus a nebuliser revealed more effects after the nose spray (Martins et al., 2021; Martins, Mazibuko, et al., 2020). In summary, the methodology employed in this study thus remains appropriate to explore the potential impact of OT on neural processing.

#### *2.8.2.3 Concerns with statistical analysis and study design*

The lack of statistical power relating to small sample sizes in most oxytocin research to date has been identified as another challenge to the oxytocin research literature (Quintana, 2020; Walum et al., 2016). On the one hand, some meta-analyses have provided promising findings by revealing robust and reproducible effects of OT on factors contributing to emotional responsiveness such as physiological responsivity to threat and facial emotion recognition, on levels of in-group trust (Leppanen et al., 2017,

2018; Shahrestani et al., 2013; Van IJzendoorn & Bakermans-Kranenburg, 2012), and on neural activity in social brain regions (Grace et al., 2018; D. Wang et al., 2017; Wigton et al., 2015) and neurocognitive impairments in clinical populations (Bakermans-Kranenburg & Van IJzendoorn, 2013; Bürkner et al., 2017). On the other hand, other meta-analytical studies revealed small or non-significant effect sizes, particularly in clinical populations with reduced power (Bürkner et al., 2017; Keech et al., 2018; Leppanen et al., 2018; Peled-Avron et al., 2020). These meta-analyses relied on individual studies with different statistical approaches and study designs. This variability in research findings may thus not only be associated to differences in the oxytocin administration methods, but also with inconsistencies in statistical analysis and study design.

In summary, various methodological challenges must be overcome in oxytocin research. As the above discussion shows, the current study relied on appropriate methodological approaches that were in line with recommendations and existing studies available at the time of study design. Importantly, these approaches also remain common to the literature to date, allowing comparability across research studies.

The below section describes the general statistical approach used in the current thesis, and the next chapter outlines the statistical methods applied to the neuroimaging data in more detail. The statistical power slightly varied across the individual experimental chapters and analyses, due to differences in the sample size. In some cases, the current results could only be considered exploratory. Such findings could nevertheless provide important results that can be used for power calculations in future research. Furthermore, in terms of study design, it has been shown that the effects of OT fluctuate with different contextual factors, such as the type of behavioural outcome, as well as individual factors, such as genetic predisposition, personality traits, traumatic life experiences, and baseline sociocognitive abilities (Bakermans-Kranenburg & Van IJzendoorn, 2013; Bartz et al., 2011; Quintana, 2022; Shamay-Tsoory & Abu-Akel, 2016;

Tops et al., 2019). The current study design controlled the possible influence of some of these factors by relying on resting-state neuroimaging techniques, which are independent from task demands and cognitive ability.

## 2.9 Statistical analysis overview

### 2.9.1 General approach

The statistical analysis in the current project was based on frequentist null hypothesis significance testing. Therefore, significance was assessed with an alpha value of $< 0.05$, and where required, this was adjusted for multiple comparisons. Furthermore, to aid the interpretation of results and provide insight into their magnitude, effect sizes were also reported for the main effects (Funder & Ozer, 2019; Lakens, 2021). Within whole-brain neuroimaging analyses, the appropriate family-wise error (FWER) corrections to mitigate against multiple comparisons was applied. Appropriate cluster-defining thresholds were also set.

For sociodemographic and clinical variables, normality was assessed using the Shapiro-Wilk test and groups were compared with analysis of variance (ANOVA) or t-tests, or their non-parametric equivalents (Kruskal-Wallis or Mann Whitney U, respectively).

The statistical analysis of functional neuroimaging data largely relied on two core approaches, and details for all analyses are provided in the next *chapter*. In summary, the first approach was a partitioned errors approach in combination with independent two-sample t-tests, one-sample t-tests, and analysis of covariance (ANCOVA). This was chosen because it is not bound by the same strict assumptions about the variance-covariance structure that apply to the repeated measures element of a simple mixed ANCOVA. It was thus decided to be more suitable for the current between-group, within-subject crossover design used to investigate group, treatment, and group by treatment interaction effects (McFarquhar et al., 2016). Where applicable, the data was prepared for partitioned errors

analysis by averaging or subtracting the PL and OT data, depending on the effect of interest. The second approach was linear mixed modelling, also to test group, treatment and group by treatment effects. This was chosen to accommodate the between- and within-subject design while allowing for potential missing data in one of the treatment conditions (D. Wallace & Green, 2002). A repeated ANCOVA approach could not accommodate this missing data. A linear mixed model approach improves the power of an analysis because incomplete data does not have to be removed on a pairwise basis (Magezi, 2015). Furthermore, it is also not bound by the same strict assumptions about the variance-covariance structure of the repeated element of the model, and it allows the hierarchical nesting of multi-level variables (Magezi, 2015). The assumptions of linear mixed models are focused on the distribution (normality and variance) of the residuals. These were tested by modelling Gaussian curves to assess normality and creating scatter plots to assess for homogeneity of variance. Importantly, it has been shown that linear mixed models are remarkably robust against violations of these assumptions (Schielzeth et al., 2020). Bootstrapping with 1000 samples was applied to confirm findings, which was particularly helpful in cases of minor assumption violations. Potentially influential outliers were assessed using Cook's distance and would have been removed if this was greater than 1, but this never occurred (Cook, 1977). Finally, it is important to note that across all functional neuroimaging analyses, the effects of OT were only interpreted to be different between groups if a significant interaction effect was demonstrated. This is the only correct approach for interpreting differential treatment effects in neuroscience research (Nieuwenhuis et al., 2011).

Any identified neurobiological abnormalities were correlated with phenotypic measures, including clinical, behavioural, and cognitive measures. Partial Pearson correlations with bootstrapping were used. Appropriate covariates were selected where required. The statistical

analysis techniques for each neuroimaging modality are provided in depth in the next chapter, and in summary in chapters 4, 5, 6, and 7 respectively.

Statistical analyses were conducted in various software, including SPSS 26 (IBM Corp, 2019), R and RStudio 2021.09.1 (R Core Team, 2021), JASP 0.15 (JASP Team, 2021), and MATLAB 2018b and 2020a (The Mathworks Inc, 2020). Furthermore, as detailed in the next chapter, the neuroimaging pre-processing and main analyses relied on analysis pipelines in Freesurfer (http://surfer.nmr.mgh.harvard.edu/), on several Matlab toolboxes including the Automatic Software for ASL Processing (Mato Abad et al., 2016), SPM12 (https://www.fil.ion.ucl.ac.uk/spm/software/spm12/), brain connectivity toolbox (Rubinov & Sporns, 2010) and network-based statistics (Zalesky et al., 2010), and finally, on commands and analysis pipelines from FSL (https://fsl.fmrib.ox.ac.uk/fsl/fslwiki).

### 2.9.2 Power calculation

As the original focus of the overarching project was on task-based functional MRI, the project was designed to achieve a power of 80% with a type I error rate of $\alpha < 0.05$, significant on a single voxel level after accounting for multiple comparisons (Desmond & Glover, 2002). According to an *a priori* power analysis, this required 24 subjects per group. Unfortunately, due to the Covid-19 pandemic, it was not possible to reach this number of subjects with complete attendance. The flowchart in *Figure 2.1* shows that for the statistical analyses of the relevant data used in this thesis, between 17 and 23 subjects per group were available. For some analyses, specified in the relevant chapters, these numbers were slightly smaller.

The completion of retrospective (post-hoc) power analyses was not recommended. Thus, comparisons with existing literature were made to indicate if adequate power was achieved. This is described in the three neuroimaging modalities in the next chapter. Based on this, the numbers of participants recruited meant that it was possible to detect medium to

large effect sizes ($f > 0.25$, $\eta^2 > 0.06$). Particularly the rs-fMRI neuroimaging data benefitted from multiple observations per condition, and linear mixed models can take advantage of this to improve the achieved power (Brysbaert & Stevens, 2018). Furthermore, in line with recommendations, effect sizes for all main effects were calculated.

# 3 Neuroimaging Methods

This chapter will outline the methodological details relating to the neuroimaging modalities and the neuroimaging data analysis. All brain images were acquired on a 3-Tesla General Electric MR750 MRI scanner using a 32-channel C-RMNova head coil. This scanner was located at the Centre for Neuroimaging Sciences, King's College London. The full scanning protocol (start of first scan to end of last scan) lasted approximately 85 minutes in length. In addition to the sMRI and the rs-fMRI (ASL and BOLD) scans used in this thesis, it also included task-based fMRI scans and a spectroscopy scan which were all acquired earlier in the protocol and used for another project. Participants were instructed to lay comfortably and completely still in the scanner. To reduce the risk of motion artefacts, their head and body was stabilized using foam padding and cushions. They were also provided with ear plugs to reduce the discomfort caused by scanner noise. Their pulse and breathing were monitored using a pulse oximeter and respiratory bellows. An emergency buzzer was provided.

## 3.1 Structural MRI

### 3.1.1 Image acquisition

As *Figure 2.1* shows, the sMRI scan was acquired during each scanning session after the completion of the fMRI tasks. It took 5 minutes, 37 seconds and was scheduled to occur around 42 minutes since dose. The sMRI consisted of a high-resolution T1-weighted anatomical Magnetization Prepared – RApid Gradient Echo (MP-RAGE) image with full head coverage. It contained 196 images, with a slice thickness of 1.2 millimetre (mm) and slice gap of 1.2 mm. The repetition time (TR) was 7.31 milliseconds (ms), and the echo time (TE) was 3.02 ms. The inversion recovery (TI) was 400 ms. The flip angle (FA) was 11° and field of view (FOV) was 270 x 270 $mm^2$. This resulted in a matrix with the size of 256 x 256 and a final voxel resolution of 1.05 x 1.05 x 1.2 $mm^3$.

If a scan was badly affected by movement, it was repeated where possible. The participant was reminded to stay extra still. Since an anatomical image was collected during each scanning session, the image from a participant's first scanning session was used in this thesis unless this was affected by more movement artefacts than the second scan, in which case the latter was used. This was determined in the first step of pre-processing, described below.

### 3.1.2 Surface-based morphometry

The cerebral cortex that contains most of the brain's grey matter has an irregular geometric topography characterized by gyri and sulci. This arises due to a dense folding mechanism required to fit the brain into the skull. Up to 70% of the cortex is contained within and alongside the sulci (Zilles et al., 1989). The cortex can therefore be described as a two-dimensional (2D) sheet that is folded to fit into a three-dimensional (3D) space.

Surface-based morphometry (SBM) relies on the principle of measuring this 2D cortical grey matter sheet by assessing the organization of vertices. Vertices represent 2D points on the surface map of a neuroanatomical structure or tissue boundary. By measuring surfaces, the complex geometrical cortical topography can be accounted for while being used advantageously for multisubject registration, resulting in more homologous cortical regions (Dale et al., 1999; Fischl et al., 1999). This is different to voxel-based morphometry (VBM) techniques, which assess 3D volume and thus cannot fully account for the complicated cortical topography (Kennedy et al., 2009). It has been argued that this might lead to less accurate registration and cortical volume calculation (Bookstein, 2001; Davatzikos, 2004; Jenkinson & Chappell, 2018c). Although estimates of cortical volume and density/thickness from each technique vary in their intrinsic calculation, they have been shown to correlate but not always overlap (Chee et al., 2011; Gerrits et al., 2016; Goto et al., 2022; Winkler et al., 2010). SBM nevertheless circumvents some of the challenges of VBM and

provides additional informative morphological features such as surface area.

The most common SBM software is Freesurfer (https://surfer.nmr.mgh.harvard.edu/) (Dale et al., 1999; Fischl et al., 1999). Freesurfer version 6.0.0 was used for this project. Freesurfer relies on an automated processing pipeline to conduct cortical surface reconstruction and produce a surface map of the brain. This involves the formation of a triangulated mesh model, i.e., a net of vertices which are connected by edges to form closed triangles (Dale et al., 1999). After several pre-processing steps described in more detail below, a single filled volume of white matter is identified for each hemisphere. This allows the detection of the white-grey matter tissue boundary, which is also called the white matter surface. The triangular mesh model is applied to the white matter surface, and then expanded to the tissue boundary between grey matter and CSF, which is also called the pial surface. Each vertex on the white matter surface has a corresponding vertex on the pial surface, encapsulating the grey matter between these surfaces. *Figure 3.1* shows an example of one individual's white matter and pial surface.

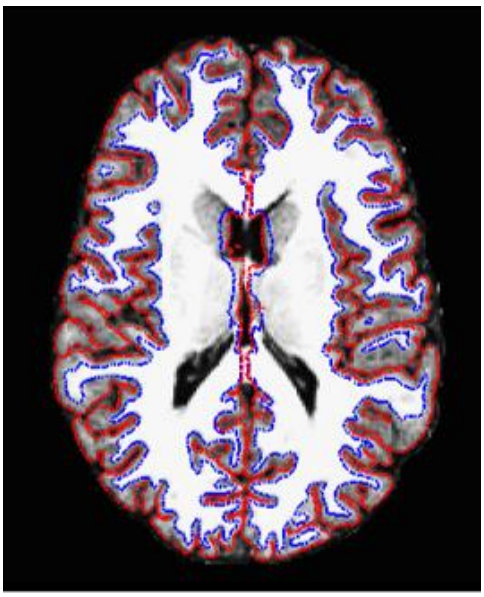

Figure 3.1 Example of a Freesurfer cortical surface reconstruction.
*Note: The blue line represents the white matter surface, and the red line represents the pial surface. The space between these surfaces represents the cortical grey matter that was subject to analysis in this research. This figure was copied from the Freesurfer training course material from April 2019 (https://surfer.nmr.mgh.harvard.edu/).*

SBM can provide a range of cortical grey matter features including cortical volume (CV), cortical thickness (CT), and surface area (SA), which were analysed in the current project. The following definitions correspond with the Freesurfer 6.0.0 procedures. CT is defined as the closest distance between a given vertex on the white matter surface and a vertex on the pial surface. This has been shown to have submillimetre accuracy, particularly when using 3T high-resolution sMRI, and can result in a measure of mean CT for a local region of interest or on a global level (Fischl & Dale, 2000). CT is related to the number and density of cells within a cortical column. SA is calculated based on an aerial pycnophylactic interpolation method and, for any given vertex, it reflects 1/3 of the sum of the area of all three faces (triangles) connected to that vertex within the closed triangulated mesh model (Winkler et al., 2012). It is related to the number of cortical columns within a particular region of interest. Lastly, CV is calculated as the real volume, i.e. the oblique truncated pyramid that connects the SA of one voxel on one surface with the closest vertex on the other surface (Winkler et al., 2018). It is a mathematically sophisticated method to calculate the product between SA and CT which accounts for complex cortical folding patterns.

### 3.1.3 Pre-processing

FSL (www.fmrib.ox.ac.uk/fsl/) image viewer 'fsleyes' 1.2.0 was used to assess image quality and identify any major MRI artefacts such as ghosting, wrap-around and signal drop-out (McCarthy, 2021). This ensured the best quality sMRI image for each participant was selected. Further quality assessment also included checking for ghosting, wrap-around and signal drop-out, as well as significant blurring, ringing, or poor contrast to noise ratio (Backhausen et al., 2016). Three individuals from the ASPD+P group were excluded from all subsequent pre-processing and analysis due to substantial motion distortion.

The Freesurfer 6.0.0 surface reconstruction and pre-processing pipeline was utilised. The full automated 'recon-all' pipeline of Freesurfer, shown in

*Figure 3.2*, was applied (Dale et al., 1999; Fischl et al., 1999). The first step involved input of the T1-weighted images and minor motion correction and alignment of the individual subject's sMRI volumes. Next, the brain was extracted through skull-stripping, which removed skull tissue from the image and resulted in a brain-only mask. An automated Talairach (affine) transformation matrix of the original image to an MNI305 (Montreal Neurological Institute) atlas was computed. This matrix was stored for subsequent steps. After volumetric and hemispheric labelling, any contrast-to-noise signal intensity variations due to magnetic radiofrequency field inhomogeneities were corrected through intensity normalisation. This improved the accuracy of tissue segmentation by ensuring that white matter had a mean intensity of 110 and grey matter was scaled proportionately below. This was followed by grey and white matter cortical tissue segmentation. Next, all images were registered to the 'fsaverage' standard space (group template) based on the inflated surfaces to ensure spatially precise, homogenous cortical surface calculations and accurate identification of cortical surface regions on the Desikan-Killiany atlas. Finally, the cortical reconstruction process involving the production of the triangulated mesh to identify white matter and pial surfaces was completed by extracting these surfaces. This pipeline produced an image that was then viewed in Freesurfer's 'freeview' image viewer to visually inspect the surface reconstruction and check for any topological defects that required manual correction.

Individual images were either accepted as they were or manually corrected and re-processed using 'recon-all' commands depending on which surface was corrected. An experienced user of the subsequent analysis provided secondary professional judgment during the correction process to ensure a high quality standard (Gudbrandsen et al., 2019).

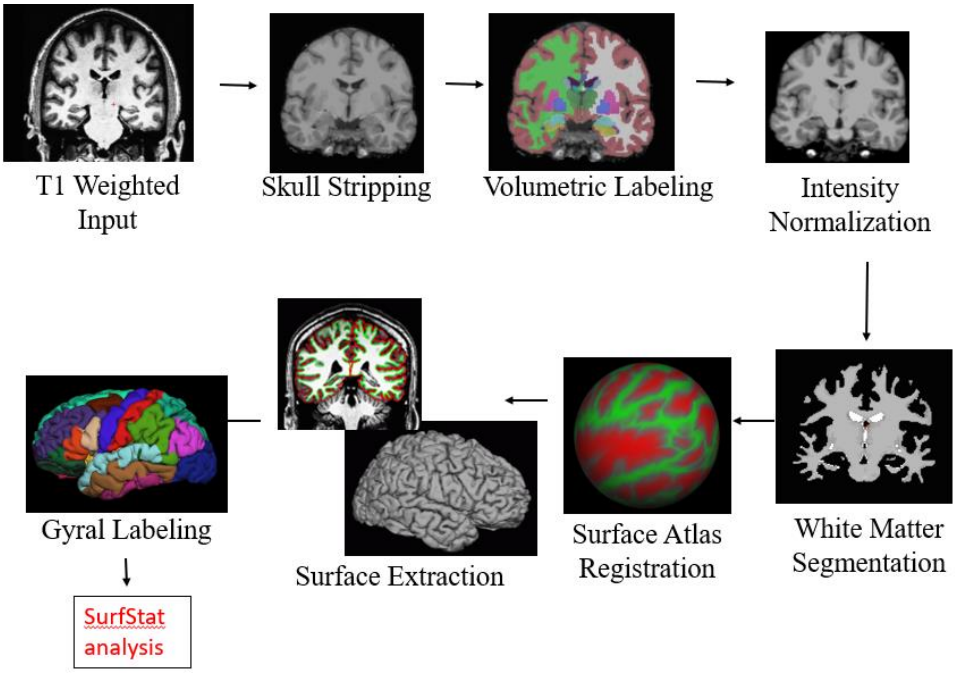


Figure 3.2 Overview of the Freesurfer recon-all pipeline.
*Note: This figure was adapted from the Freesurfer training course material from April 2019 (https://surfer.nmr.mgh.harvard.edu/).*

Once all images had an accurate surface reconstruction, they were extracted from the Freesurfer pipeline to be analysed using the SurfStat toolbox, described below. At the start of this analysis, a final pre-processing step involved spatial smoothing with a 10 mm full-width half-maximum Gaussian kernel. This helped to normalize the distribution of noise and improved statistical sensitivity for the random field theory approach embedded in SurfStat. The size of this smoothing kernel is in line with other sMRI research in the field. Furthermore, in SBM methods, the smoothing kernel can be larger than in VBM methods, since there is no risk of smoothing across gyri, as smoothing is applied to the surface map of the brain. The final cortical surface was parcellated according to the Desikan-Killiany atlas (Desikan et al., 2006). These pre-processing steps resulted in a triangulated mesh model that consisted of approximately 150,000 vertices per hemisphere, which enabled a high-resolution analysis.

### 3.1.4 Statistical analysis

The SurfStat toolbox (https://www.math.mcgill.ca/keith/surfstat/) was used for the statistical analysis of the cortical surface measures (CV, CT,

and SA) in Matlab 2020a (The Mathworks Inc, 2020). The analysis is based on the use of general linear mixed models and random field theory for non-isotropic images (Worsley et al., 1999). The SurfStat approach has been used in other studies comparing surface measures between clinical and control populations (Bletsch et al., 2018; Ecker et al., 2013; Gudbrandsen et al., 2020; Reinders et al., 2018).

#### *3.1.4.1 Calculation of cortical features*

A global brain measure extracted from the Freesurfer pipeline output was included in the model for each cortical measure to correct for any global effects. For the analysis of CV, total estimated intracranial volume (eICV) was used. For the analysis of CT, the average of the mean CT of each hemisphere was used, and for the analysis of SA, the sum of total SA in each hemisphere was used. To assess for group differences in these total brain measures, they were compared using a one-way ANCOVA, accounting for mean-centred age.

The main effect of group ($G_i$) was estimated for each surface measure using a general linear mixed model regression at each vertex i and subject j, covarying for mean-centred age ($A_i$), the respective mean-centred total brain measure ($B_i$) and adding a residual error term ($\varepsilon$).

$$Y_{ij} = \beta_0 + \beta_1 G_j + \beta_2 A_j + \beta_3 B_j + \varepsilon_{ij}$$

It is important to note that the main effect of group was a two-way contrast (t-contrast). Each ASPD group was separately compared to the NO group, and then the two ASPD groups were compared to each other.

A random field theory-based cluster-wise correction for multiple comparisons across the whole brain in non-isotropic images was applied to each model using $p < 0.05$ (two-tailed) (Worsley et al., 1999). This resulted in a binary overlay vector for each surface measure, classifying vertices in clusters that were significant after correction as 1 and vertices in non-significant clusters as 0. Any t-statistics which remained significant after

correction for multiple comparisons were visualized on the Freesurfer-produced high-resolution 'fsaverage' template.

#### *3.1.4.2 Calculation of spatial overlap between CT and SA findings*

To assess whether the two-way group differences in CT and SA were spatially independent or overlapping, a Chi-squared ($\chi^2$) test was conducted. In this case, the direction of the difference was ignored. The null hypothesis of this $\chi^2$ test was that any differences were equally distributed. To measure this, the first step was to calculate the number of vertices that had a difference in CT *only*, SA *only*, or both CT *and* SA. This calculation relied on the binary overlay vectors which indicated which vertices had a significant group difference after correction for multiple comparisons.

The second step then calculated the percentage of vertices that had a difference in CT *only* relative to all vertices with a difference, as well as the percentage of vertices that had a difference in SA *only* relative to all vertices with a difference. Third, the $\chi^2$ test was conducted to compare these percentages, where a significant result indicated that either CT or SA was uniquely driving group differences, as opposed to an overlap of both measures driving group differences.

Next, to assess whether the distribution of the vertices that had an overlapping difference in both CT *and* SA remained consistent with the idea of two spatially independent patterns, a simulation strategy using 5000 permutations of randomly generated difference patterns was applied. Each difference pattern contained random t-values, thresholded at $p < 0.05$ (two-tailed). The given distribution of overlap was then assessed in each of the 5000 permutations to derive a probability value of obtaining that percentage of overlap based on randomly varying patterns of difference. Therefore, a significant result in the simulation indicated that the

distribution of overlapping vertices was non-random and spatially independent.

#### 3.1.4.3 Contribution of CT and SA to CV

CV is the product of CT and SA. For any cluster with a significant group difference in CV, a $\chi^2$ test was used to assess whether CT or SA contributed significantly more to the CV group difference. A significant value indicated a unique contribution of one measure over the other, whereas a non-significant value indicated that differences in both measures contributed to group differences in CV.

#### 3.1.4.4 Correlations

To assess the relationship between cortical abnormalities and phenotypic variables (clinical, behavioural, and cognitive features), partial Pearson correlations with bootstrapping were conducted within each ASPD subtype. T-values from clusters with a significant ASPD+P versus NO and ASPD-P versus NO group difference after correction for multiple comparisons were extracted from the SurfStat analysis. Clinical variables included PCL-R factor and facet scores, behavioural variables included the number of violent convictions, having a reconviction within one year of study participation, and reactive and proactive aggression scores, and cognitive variables included the z-standardized averaged performance scores for each of the neurocognitive tests in the PL condition. Mean-centred age and the appropriate mean-centred total brain measure were included as covariates of no-interest for all correlations. The resulting correlations were corrected for multiple comparisons using Benjamini-Hochberg false discovery rate (FDR) in R.

#### 3.1.4.5 Power

A study indicated that to achieve a power of 0.8, with an alpha threshold of 0.05, using a 10 mm smoothing kernel and based on a two-sided hypothesis, at least 10 subjects were required per group to detect a 1 mm group difference in CT (Pardoe et al., 2013). Another study reported that

group sample sizes required to detect at least a 10% group difference ranged from 21 to 81 per group, with CV and CT measurements requiring more subjects than SA measurements (Liem et al., 2015). The larger sample size required to obtain a higher precision of estimating CT group differences may be related to the increased susceptibility of CT measurements to motion artefacts such as head tilt (Hedges et al., 2022). The current study included 18-23 participants per group. This is in line with other studies that used the same statistical approach. However, considering the above evidence, the current sample size was only powered enough to detect large effect sizes. For significant clusters, the t-statistic was visualized as an indicator of effect size.

### 3.1.5 Benefits

SBM enables disentangling of the structural neuroanatomical features that characterize a particular population. By assessing several different cortical surface features, SBM can provide more information concerning features that are subject to neurodevelopmental processes than VBM techniques (Winkler et al., 2010).

Furthermore SBM approaches circumvent the problem of partial volume effects and over- or under-estimation of cortical features associated with dense cortical folding patterns (Davatzikos, 2004; Jenkinson & Chappell, 2018c; Kennedy et al., 2009). This occurs due to the use of the surface topography to optimise registration and then measuring surface features on an inflated surface (Fischl et al., 1999). The automated Freesurfer pipeline also provides a strong advantage compared with manual tracing methods as it reduces the risk of bias. Overall, this means that SBM techniques like Freesurfer reveal more reliable measures of the tissue of interest, in this case grey matter.

### 3.1.6 Challenges

SBM techniques like Freesurfer require high quality anatomical images. For example, they require a better spatial resolution than VBM techniques.

Furthermore, due to the reliance on the identification of tissue boundaries, it is also more sensitive to poor contrast-to-noise ratio as well as other MRI artefacts (Jenkinson & Chappell, 2018c). Therefore, a stricter image quality protocol is required, which meant eliminating three ASPD+P individuals prior to analysis. The use of Freesurfer is also more computationally demanding and time-consuming (due to potential manual correction) than VBM techniques.

Furthermore, VBM may be preferred when assessing grey matter volumes, particularly in subcortical regions, since Freesurfer was not originally designed for this (Goto et al., 2022). However, it has been shown that the Freesurfer extracted volume metrics correlate with findings from VBM (Chee et al., 2011; Gerrits et al., 2016; Goto et al., 2022).

## 3.2 Resting-state fMRI I: three-dimensional pseudo-continuous arterial spin labelling

Rs-fMRI provides insight into brain function at rest. Two types of rs-fMRI that were implemented in the current project are ASL and BOLD signal imaging. This section will discuss the ASL technique, and the final section in this chapter will discuss the BOLD technique.

### 3.2.1 Regional cerebral blood flow

When a neuron is active, its metabolic demand for oxygen and nutrients such as glucose increases. These metabolites are delivered via the blood. Therefore, neural activation and blood flow are closely coupled. This is called neurovascular coupling. The haemodynamic response reflects this change in vascular activity triggered by neural activity, which can be either spontaneous (i.e., when the subject is at rest in the scanner) or task-induced. The underlying physiological component of the haemodynamic response is a change in regional cerebral blood flow (rCBF; sometimes also referred to as perfusion). Specifically, rCBF is a measure of the rate of delivery of arterial blood to the capillary tissue in a brain region. It represents the amount of blood that passes through a specific region of the

brain over a set amount of time. It is typically measured in millilitre (ml) of blood delivered per 100 gram (g) of tissue per 1 minute (Fantini et al., 2016). Importantly, rCBF therefore reflects a directly quantifiable measure of the physiological haemodynamic response to neural activation (Buxton et al., 2004).

The adult healthy brain grey matter has an average rCBF of 60-80 ml/100 g/1 min, with a normal range from 40-100 ml/100 g/1 min (Alsop et al., 2015; Vavilala et al., 2002). As this measure has been shown to be highly stable over time, any significant change over time or between a patient and healthy population can be directly indicative of abnormalities in brain functioning (Alsop et al., 2015; L. M. Parkes et al., 2004). Furthermore, it is very sensitive to pharmacological challenges and is therefore a suitable measure to studying the brain's response to such an agent (Stewart et al., 2014).

Historically, rCBF was measured using single-photon emission computed tomography (SPECT) or positron emission tomography (PET) scans. However, in more recent years, ASL imaging has provided a non-invasive imaging modality with improved signal-to-noise ratio that measures rCBF by magnetically labelling arterial blood and tracing its flow across tissue over time (Borogovac & Asllani, 2012; Detre et al., 2009).

### 3.2.2 Image acquisition

*Figure 2.1* shows that the 3D pseudo-continuous ASL scan was scheduled around 87 minutes since dose (i.e., the final spray of the OT or PL nose spray). It was the penultimate scan for each session and lasted 6 minutes and 23 seconds. Participants were instructed to remain still, stay awake, focus on a fixation cross on the screen in front of them and to let their mind wander. The 3D pseudo-continuous ASL scan acquired 60 slice partitions with a thickness and gap of 3 mm per subject. The TR and TE were 5180 ms and 1109 ms, respectively. An FA of 111° and FOV of 240 x 240 $mm^2$ was applied, and the approximate in-plane resolution was 3.6 mm. A 180°

Hanning-shaped radiofrequency inversion pulse lasting 1825 ms was applied, and after a brief delay of 2025 ms, the net magnetisation of the magnetically labelled arterial blood water was measured. The final matrix resulting from the 3D whole-brain volumes, which were read using a 3D "stack-of-spirals" Fast Spin Echo read-out, had the size 8 (interleaved spiral arms) x 518 (points per spiral). The next paragraphs describe how the ASL technique works.

This non-invasive imaging sequence relies on the magnetic response of the hydrogen nuclei found in the water molecules of cerebral blood. Pseudo-continuous radiofrequency inversion pulses are applied along the flow direction (z-axis of the magnet), which changes the magnetic state of these nuclei such that the nuclei of the blood water are 'labelled'. This occurs in the neck before the blood enters the brain. The endogenous tracer (i.e., the labelled blood water) then flows into the brain during the post-labelling delay. Then, an image is acquired, capturing the tracer by measuring the net magnetization of the brain tissue. This process is repeated immediately after, but without the application of an inversion pulse and subsequent labelling. Therefore, an adjacent control image is acquired. The labelled image is then subtracted from the control image, which creates a perfusion-weighted image that is only related to the electromagnetic signal of the label. Subtraction is an important step because it eliminates signal arising from neural tissue, which is about 100 times stronger than the signal of interest from the labelled blood water (Jenkinson & Chappell, 2018a). The current 3D pseudo-continuous ASL sequence acquired 5 label-control pairs. After each pair underwent the subtraction, the remaining 5 perfusion-weighted images were averaged to maximize tissue contrast, since this weakens over time. Four background suppression pulses were also applied to minimize the static signal from other tissue at the time of acquisition. A 3D sequence (interleaved 'stack-of-spirals' Fast Spin Echo readout) was employed, meaning that it built up information across the 3 dimensions of the brain simultaneously. This is in contrast to a 2D approach, which

sequentially collects slices through the brain, resulting in lower temporal resolution. Overall, these steps all ensured optimized signal-to-noise ratio. This acquisition approach is in line with recommendations for acquiring ASL imaging in clinical populations (Alsop et al., 2015).

*Figure 3.3* depicts the ASL process leading to the final CBF map. The ASL scan sequence also obtained a proton-density (PD)-weighted image. This quantifies the actual density, or concentration, of the endogenous tracer of rCBF, i.e. the labelled blood water. By calibrating the final perfusion-weighted image against the PD image, a CBF map containing the absolute, linear, and directly interpretable measure of rCBF in each voxel is produced. This CBF map is then used for data analysis. The T1-weighted structural scan described above was used for anatomical co-registration.

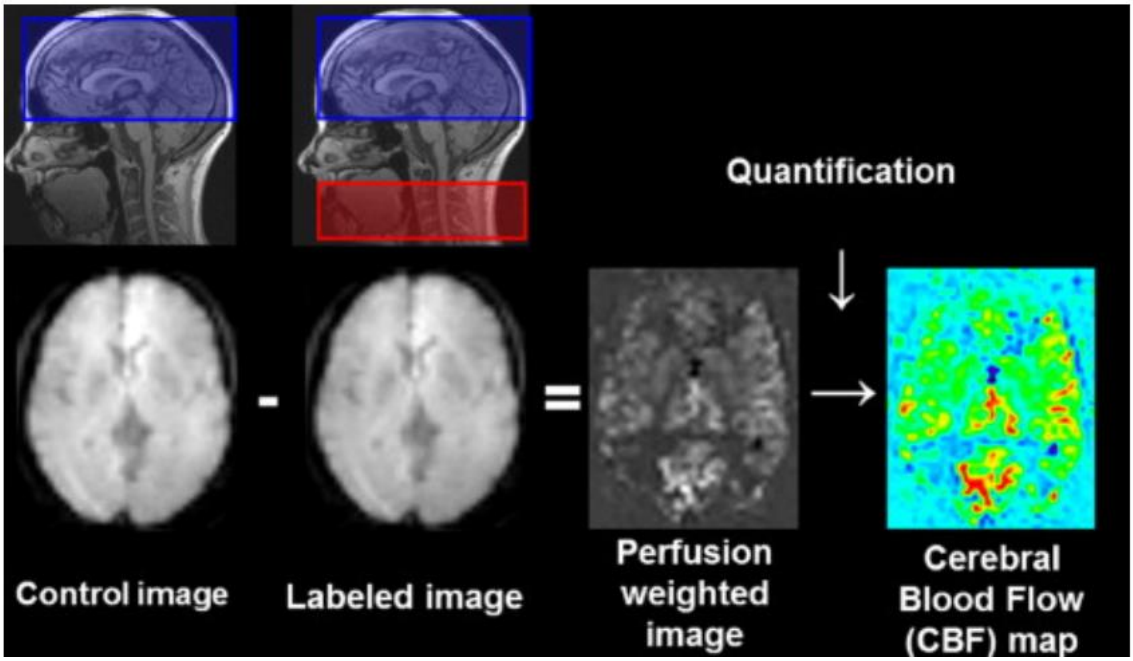


Figure 3.3 Arterial spin labelling neuroimaging technique.
*Note: this figure was copied from (Ferré et al., 2013).*

### 3.2.3 Pre-processing

Prior to any pre-processing, the quality of the final CBF map for each participant's session was inspected using FSL 'fsleyes' 1.2.0 image viewer (McCarthy, 2021). Significant blurring of the image would have indicated excessive motion artefacts that were not adequately suppressed by the ASL image acquisition parameters, but no problematic scans were identified.

Additionally, rCBF values in grey matter regions were confirmed to be between 20 and 110 ml/100 g/1 min. This indicated an accurate computation of the CBF map from the acquired MRI image, i.e., without signal drop-out (Alsop et al., 2015). No scans were excluded.

The pre-processing and normalization of the CBF maps for statistical analysis was conducted in the Automatic Software for ASL Processing (ASAP) toolbox, version 4.0 in Matlab 2018b (Mato Abad et al., 2016). This required the PD image, the CBF map and the T1 image for each participant and each session, and involved several steps: (1) the participant's PD image was co-registered to their T1 image, resulting in a transformation matrix. The origin of both images was set to the anterior commissure. This transformation matrix was applied to the participant's CBF map, transforming it to their T1 space; (2) the T1 image underwent a unified segmentation, which involved tissue segmentation and volume-to-volume registration and resulted in a binary "brain-only" mask (Ashburner & Friston, 2005); (3) this "brain-only" mask was applied to the co-registered and transformed CBF map to strip the skull and remove any extra-cerebral signal; (4) the resulting "brain-only" CBF map and the T1 image were then partial volume corrected and normalized to MNI152 space using normalization parameters obtained in the second step; (5) lastly, the CBF map was spatially smoothed using an 8mm Gaussian smoothing kernel, in line with other studies showing effects of OT on CBF.

An explicit grey matter tissue mask was applied to the final CBF map using the function 'fslstats' in FSL (www.fmrib.ox.ac.uk/fsl). The mask was derived from a standard T1-based probabilistic map of grey matter distribution by thresholding all voxels with at least 20% probability of being grey matter. This step further supports the partial volume correction by ensuring that CBF signal from white matter, which is lower, did not confound the results. It also reduces between- and within-subject variability and thus improves statistical power (Jenkinson & Chappell, 2018b). All subsequent analyses were based on this thresholded CBF map.

### 3.2.4 Statistical analysis

The analysis involved a whole-brain analysis and a supplementary region-of-interest (ROI) analysis. The following variables were mean-centred and included as covariates of no-interest in all analyses: 1) age (Bentourkia et al., 2000); 2) minutes since dose; and 3) global median CBF (shown to improve the signal-to-noise ratio by regressing out the effects of unspecific physiological variability and to improve sensitivity to within-subject change in local areas) (Jenkinson & Chappell, 2018b; Z. Wang, 2012). Median rCBF was extracted from the thresholded CBF map using the FSL command 'fslstats' and 'fslmaths' (www.fmrib.ox.ac.uk/fsl). The median values were chosen to be a more appropriate measure of central tendency because, although the normal range of rCBF is 40-100 ml/100 g/1 min, there was a skew towards the lower end of this range in the current sample (Alsop et al., 2015; Vavilala et al., 2002). The effect of group, treatment and an interaction effect on global median CBF were analysed using a two-way mixed ANCOVA in SPSS26, covarying for mean-centred age and mean-centred minutes since dose.

#### *3.2.4.1 Whole-brain analysis*

For the whole-brain analysis, only participants who attended both sessions were included. This was because missing data could not be accommodated in the whole-brain partitioned errors analysis approach that was conducted in SPM12 (https://www.fil.ion.ucl.ac.uk/spm/software/spm12/). To prepare for the partitioned errors approach analysis, the CBF maps for each participant were adjusted in two different ways: 1) an average between the CBF maps from the PL session and the OT session was produced using FSL commands 'fslmerge' and 'fslmaths', referred to as the 'average CBF map'; and 2) the CBF map from the PL session was subtracted from the CBF map from the OT session using the FSL command 'fslmaths', referred to as the 'subtracted CBF map'. Using SPM12, the main effect of group was assessed by conducting a one-way ANCOVA on the average CBF maps. The main effect of treatment was measured by conducting a one-sample t-test using

the subtracted CBF map across all participants. Finally, to assess the group by treatment interaction effect, a one-way ANCOVA of the subtracted CBF maps was conducted. For each of these analyses, a matrix containing global median CBF, age, and minutes since dose were included as covariates of no-interest.

In SPM12, an F-contrast was calculated for each described effect. The cluster-defining threshold was set to $p = 0.005$. Only clusters which survived a FWER correction for multiple comparisons on a whole-brain cluster-level inference at $\alpha = 0.05$ were interpreted. A binary mask was then created for any cluster which survived these steps. These masks were extracted from SPM12 and applied to the respective adjusted CBF maps (i.e., the average or the subtracted CBF map, depending on which effect was being assessed). With this map, the raw CBF values of each significant cluster were then extracted. Next, to break down the significant main and/or interaction effects, post-hoc pairwise comparisons or simple main effects using the Sidak correction for multiple comparisons were conducted on these values in SPSS26. This approach is in line with other work using a similar design (Martins, Leslie, et al., 2020).

#### *3.2.4.2 Supplementary ROI analysis*

For the ROI analysis, participants who only had a scan from one of two sessions could still be included because median rCBF values were extracted from the final CBF maps for each participant and each session separately.

To obtain the rCBF values for each ROI, a binary mask based on the FSL-distributed Harvard-Oxford Atlas was applied to the thresholded CBF map. The ROIs included amygdala and anterior insula, for each hemisphere. The hemispheres were treated separately as it has been shown that oxytocin may have a lateralized effect, particularly in the amygdala (Paloyelis et al., 2016). The ROI rCBF values were extracted using the FSL command 'fslstats'. For each of the four ROIs, a full factorial linear mixed model including group, treatment, and group x treatment interaction as fixed

effects and subject as a random effect was conducted in JASP. Participant age, minutes since dose, and global median CBF were mean-centred and included as covariates of no-interest. There were no significant outliers in the model. This was identified by assessing Cook's distance (all were <1). Statistical significance was assessed after bootstrapping with 1000 samples to account for potential deviation from the normal distribution. FDR correction for multiple comparisons across the four ROIs was applied. Any remaining significant main effect was followed up by pairwise comparisons, and remaining significant interaction effects were followed up by simple main effects, which were further corrected for multiple comparisons using the Holm method.

#### *3.2.4.3 Correlations*

Within the ASPD participants only, the relationship between rCBF and phenotypic variables (clinical, behavioural, and cognitive features) was assessed using partial Pearson correlation analyses. Clinical and behavioural measures included PCL-R factor and facet scores, the number of past violent convictions and the presence of a reconviction within one year of study participation, as well as scores from the reactive-proactive aggression questionnaire. Cognitive variables were the averaged, z-standardized performance scores from the neurocognitive assessments under PL condition. To assess the correlation with baseline rCBF, median rCBF values from the clusters which showed a significant main effect of group in the whole-brain analysis were used. The values from PL and OT clusters were averaged to reflect the main effect of group. To assess the correlation with the rCBF response to the OT challenge, median rCBF values from clusters which showed a significant interaction effect (if this was due to significant within-group changes in ASPD) were extracted for each participant and session, and the delta score (OT minus PL) was used. Covariates of no-interest were mean-centred global median CBF, age, and minutes since dose. Since these correlations were conducted across all ASPD participants together, the group (ASPD+P or ASPD-P) variable was

also included as a covariate to mitigate the risk of spurious (illusory) correlations caused by using the PCL-R total score as a grouping variable in the main study design. P-values were corrected for multiple comparisons using FDR.

#### *3.2.4.4 Power*

A study has evaluated the sample size required to achieve enough power to detect within-subject change or between-subject differences in rCBF on ASL scans with different types of study designs (K. Murphy et al., 2011). It revealed that a between-group crossover design requires at least 17 subjects per group to detect a 15% change (effect size) in baseline grey matter rCBF. Another study added to these findings by suggesting that to detect a 15% change in rCBF induced by a pharmacological challenge when using a 3D pseudo-continuous ASL scan, at least 7 participants are required for the within-subject comparison (Mutsaerts et al., 2015). Thus, the current study was sufficiently powered to detect at least a 15% within-subject change and between-subject difference. Other clinical and healthy studies with similar designs which have assessed the impact of OT on rCBF utilised similar sample sizes (Davies et al., 2019; Martins, Brodmann, et al., 2022; Martins, Leslie, et al., 2020; Martins, Mazibuko, et al., 2020; Paloyelis et al., 2016).

### 3.2.5 Benefits

The use of ASL imaging to measure rCBF provides a non-invasive and fully quantifiable, non-arbitrary and directly interpretable measure of neural activation using an endogenous, non-invasive tracer (Simon & Buxton, 2015; K. Zhang et al., 2018). It also provides improved spatial and temporal specificity compared with other methods of measuring perfusion such as SPECT and PET (Borogovac & Asllani, 2012). Due to its resting-state acquisition, it offers insight into the magnitude of spontaneous neural activity which can be directly interpreted and is not influenced by cognitive ability, task demand, or task-by-treatment interaction (Khalili-Mahani et al., 2017; Lv et al., 2018; Nomi & Uddin, 2015).

The current study benefitted from the use of recommended acquisition and pre-processing protocols (Alsop et al., 2015). This ensured optimized computation of rCBF. The measure of rCBF has shown excellent test-retest reliability, meaning it provides a useful and reliable tool for measuring within-subject change over time (Hodkinson et al., 2013). This is also important for pharmacological challenge studies because it means that any rCBF changes between a placebo and a non-placebo session are likely driven by the pharmacological challenge, since baseline rCBF would remain stable. In line with this, resting-state ASL imaging has been shown to be more sensitive to pharmacological challenges than resting-state BOLD imaging (Bloomfield et al., 2020; Bryant et al., 2019; Martens et al., 2021; Martins, Mazibuko, et al., 2020; Stewart et al., 2014). Lastly, rCBF has also been shown to correlate with behavioural markers of cognition and personality traits (Ma et al., 2017; Sugiura et al., 2000; Sutin et al., 2010; Weafer et al., 2015; Wei et al., 2017), providing a useful neural marker of behavioural phenotypes.

Although rCBF is closely coupled with the BOLD signal, these benefits highlight that ASL imaging may provide complementary, but novel and unique insight into functional neurobiological mechanisms of ASPD+/-P (Jann et al., 2015; Stewart et al., 2014; K. Zhang et al., 2018).

### 3.2.6 Challenges

There are some challenges associated with the ASL technique. First, the use of resting-state ASL data means it is not possible to control the individual's thought processes during image acquisition. This may introduce increased variability in the rCBF data that cannot be accounted for. Second, although ASL provides an improved measure of rCBF compared to other perfusion techniques, the measure of rCBF still inherently suffers from reduced signal-to-noise ratio (K. Zhang et al., 2018). This is due to compromises in spatial and temporal resolution. Spatial resolution is reduced by the subtraction of the labelled image from its adjacent control image, which is required to calculate blood flow. This can be enhanced by

collecting multiple pairs and then calculating the average blood flow across these. This was done in the current study. However, collecting multiple pairs increases the susceptibility to motion artefacts, which can further worsen the signal-to-noise ratio. This can be mitigated by applying background suppression during scan acquisition as well as using registration-based methods for pre-processing – both of which were also done in the current study. The use of anatomical co-registration also improves the risk of partial volume effects, which otherwise reduce spatial resolution, by providing images with higher contrasted tissue segmentation. Temporal resolution is affected by the post-labelling delay as well as the collection of multiple pairs of label-control images. The latter however is improved by the subtraction of label-control images as this removes the influence of temporal noise in the form of slow drift MRI artefacts (Jenkinson & Chappell, 2018a). The current study applied the recommendations to minimize the impact of these inherent challenges (Alsop et al., 2015).

Third, it has been argued that rCBF has considerable variation across people, with a normal range between 40 and 100 ml/100 g/1 minute. Therefore, it may be harder to detect true abnormalities in clinical populations, and adequate power as well as an appropriate healthy control group is required (Alsop et al., 2015). This was ensured in the current study.

## 3.3 Resting-state fMRI II: BOLD signal imaging

The rs-fMRI BOLD signal imaging data was analysed in two different ways: once to assess large-scale network functional connectivity, and once to assess neural topology. Both analyses were conducted in the full ASPD sample, as there was not sufficient data to split the ASPD group into those with versus without psychopathy.

### 3.3.1 The BOLD signal

The analysis of the resting-state BOLD signal is the most common rs-fMRI technique. This technique measures spontaneous low-frequency fluctuations (<0.1 Hz) in the BOLD signal over time, while the brain is not engaged in any active task and is therefore at rest. As described above, neurovascular coupling creates a haemodynamic response to the metabolic demand of a neuron. This involves a shift in rCBF, blood volume, and the metabolic rate of oxygen. Together, these changes driven by the haemodynamic response alter blood oxygenation levels (K. Zhang et al., 2018). This fluctuation in blood oxygenation levels can be captured by the MRI scanner as the BOLD signal. As *Figure 3.4* shows, the haemodynamic response leads to an influx of oxyhaemoglobin, increasing the oxyhaemoglobin/deoxyhaemoglobin ratio. In other words, paramagnetic deoxyhaemoglobin levels reduce relative to diamagnetic oxyhaemoglobin. The MRI scanner detects the change in local field potential associated with this relative reduction and re-balancing in paramagnetic deoxyhaemoglobin over time. Ultimately, this leads to an increase in the MRI signal. This is further influenced by the pulse sequence, and the echo and repetition times, which are selected *a priori*. An area with a higher oxyhaemoglobin/deoxyhaemoglobin ratio, i.e. an active area, will therefore have a higher signal intensity and appear brighter on the contrast image. Thus, an increase in the BOLD signal suggests an increase in neural activation, and vice versa.

It is important to consider that the BOLD signal reflects a combination of the physiological changes that are associated with the haemodynamic response occurring after the initial neural activity. Unlike rCBF, it is therefore only an indirect, minimally delayed proxy measure of neural activity. Nevertheless, it has been shown to be well-correlated with the local field potential, suggesting it is still likely to be a reliable indicator of neural activity (Logothetis et al., 2001).

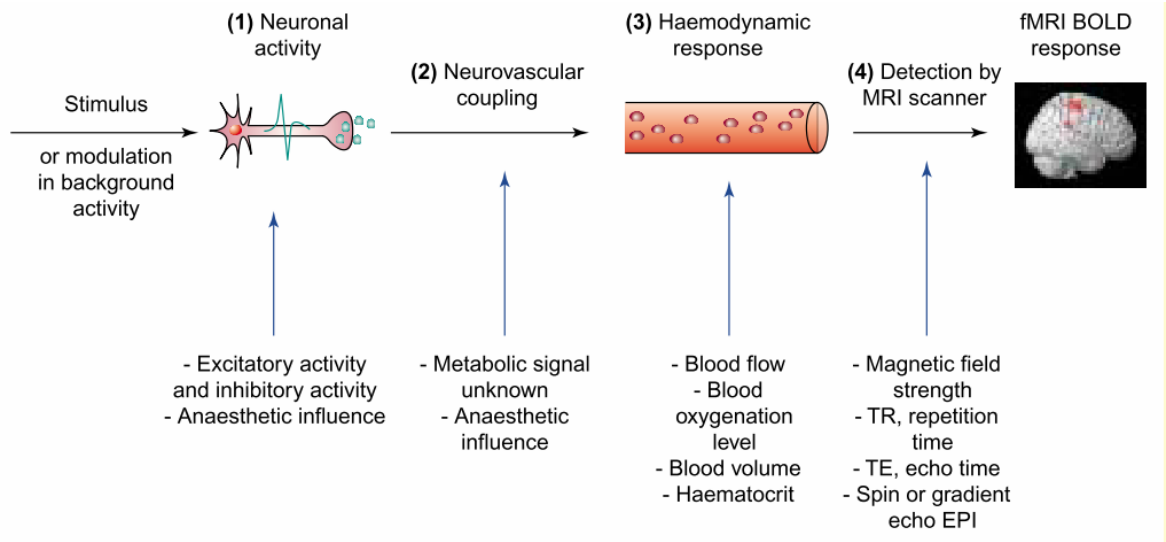


Figure 3.4 BOLD signal detection in fMRI.
*Note: Figure adapted from (Arthurs & Boniface, 2002)*

Traditionally, the rs-fMRI BOLD signal has been used to quantify functional connectivity (FC) across brain regions (Biswal et al., 1995). This involves interpreting temporal synchrony patterns in the BOLD signal (i.e., the BOLD timeseries) and relies on the assumption that a correlation between the BOLD signal of two regions of interests indicates that these regions are functionally connected at rest. Over the past 25 years, this has led to the reliable identification of several large-scale networks (Choe et al., 2015; Cole et al., 2010; De Luca et al., 2006; Mak et al., 2017). In recent years, the interpretation of the rs-fMRI BOLD signal to estimate neural network topology using a graph theory approach has also become increasingly popular (Bullmore & Sporns, 2009). More details about both approaches will be discussed below.

The rs-fMRI BOLD signal captures the intrinsic temporal dependency of brain activation patterns. Alongside the more directly quantifiable measure of brain activity that is rCBF, the use of rs-fMRI BOLD imaging thus offers an important complimentary tool to assess group differences and treatment effects on the connectivity, organization, and communication within the brain (Li et al., 2018; van den Heuvel & Hulshoff Pol, 2010).

### 3.3.2 Image acquisition

*Figure 2.1* shows that the rs-fMRI BOLD scan was acquired as the final scan within each scanning session, scheduled around 95 minutes since dose. The scan lasted 8 minutes and 10 seconds. It involved a T2*-weighted whole-brain multi-echo echo planar imaging (EPI) sequence, acquiring 192 volume per echo and 24576 images in total (32 horizontal slices top-to-bottom parallel to the anterior-posterior commissure line, slice thickness = 3 mm, slice gap = 1 mm, TR = 2500 ms, TE = 4 echoes at 12, 28, 44 and 60 ms, FA = 80°, FOV = 240 x 240 $mm^2$; matrix = 64 x 64, voxel resolution = 3.75 x 3.75 x 3 $mm^3$). Participants were instructed to remain still, stay awake, focus on a fixation cross on the screen in front of them and to let their mind wander.

The T1-weighted structural scan described above was used for anatomical co-registration.

### 3.3.3 Pre-processing

The acquisition of rs-fMRI BOLD scans is particularly susceptible to inherent physical/hardware, physiological, and motion artefacts which result in non-BOLD signal, i.e., structured noise that may distort the BOLD signal data. It is important to mitigate this prior to and during acquisition, but it is also possible to improve the impact of artefacts and thus maximize signal-to-noise ratio after acquisition. The latter requires several pre-processing steps before the cortical grey matter rs-fMRI BOLD signal can be statistically analysed. The following describes the pre-processing steps applied to the rs-fMRI BOLD and structural scans in the current project.

Using the OptiBET shell script, the T1-weighted structural image used for co-registration of the rs-fMRI BOLD image was skull-stripped and brain extracted (Lutkenhoff et al., 2014). This script relies on FSL (http://fsl.fmrib.ox.ac.uk/fsl/fslwiki/FSL/) and AFNI (http://afni.nimh.nih.gov/afni/) commands. The extracted structural images were visually examined for any abnormalities and extraction errors

using the FSL image viewer 'fsleyes' 1.2.0 (McCarthy, 2021). Next, a study-specific anatomical template across all participants was created and used as an intermediate step between within-subject co-registration and normalization to MNI space. The multivariate template construction shell script of the Advanced Normalization Tools (ANTs) module was used for this step (Avants et al., 2008). The template was visually examined for any errors using 'fsleyes' 1.2.0 brain image viewer (McCarthy, 2021). It was then co-registered to the MNI standard space, and a transformation matrix was calculated.

The T2*-weighted rs-fMRI BOLD image was formed of four echoes. Brain tissue extraction ensured only signal from brain tissue was retained. The fourth echo was removed due to poor signal-to-noise ratio associated with the non-linearity of the BOLD signal, underpinned by the saturation, or drop-out of signal intensity, over time. Furthermore, since earlier echoes have higher signal and later echoes have stronger contrast, the remaining three echoes were split using the FSL command 'fslsplit' (Kundu et al., 2017). Functional data was then optimally combined by taking a weighted average of the three echoes using an exponential T2*-weighting approach (Posse et al., 1999). The combination is "optimal" because it takes advantage of the higher signal in earlier echoes and higher sensitivity in later echoes and thus maximizes the potential of the subsequent de-noising steps.

These de-noising steps were conducted using AFNI 'afni_proc.py' tools (https://afni.nimh.nih.gov/pub/dist/doc/program_help/afni_proc.py.html) , the 'tedana' pipeline (Kundu et al., 2012, 2013; The tedana Community et al., 2021), and some FSL support functions. Conventional de-noising steps including temporal noise reduction and primary and secondary motion artefact removal were handled using 'afni_proc.py'. This involved slice timing correction and motion correction including timeseries de-spiking, volume registration and realignment. Slice timing correction ensured slices acquired later in each TR are adjusted to and temporally comparable with

slices acquired earlier in each TR. Timeseries de-spiking identified individual volumes with voxels affected by excessive movement outliers, which were scrubbed (regressed) out of the signal. Volume registration and realignment applied six rigid-body motion correction transformation parameters (three translational and three rotational parameters) to ensure volumes were spatially matched up and motion artefacts were reduced. Framewise displacement values which indicate the amount of head movement between volumes were calculated for each volume according to the realignment estimates and then averaged across each scan. Sixteen scans with an average framewise displacement value of > 0.25 mm were deemed as high movement scans and excluded from statistical analysis (L. Parkes et al., 2018; Power et al., 2014). This approach was chosen instead of scrubbing, as the number of volumes that would have required removal due to framewise displacement varied across sessions and groups, which could have introduced biases. Contrary to scrubbing, this approach has also been shown to reduce the correlation between graph theory metrics and head motion, which was desirable for the current project (Aurich et al., 2015). However, this means more data was removed, reducing the power slightly.

For additional de-noising, the 'tedana' pipeline was used to perform multi-echo independent component analysis (ME-ICA). ME-ICA uses a data-driven approach to identify any remaining structured noise resulting from various artefacts. This includes physiological noise which was not previously removed. Evidence suggests that it is the most robust method for cleaning rs-fMRI BOLD multi-echo data as it reduces the impact of non-BOLD signal noise while maintaining a good temporal signal-to-noise ratio without compromising BOLD signal (Dipasquale et al., 2017).

Next, each functional image was co-registered to the participant's structural T1 native space. This ensures that the rs-fMRI BOLD signals are localised to the correct anatomical areas within each individual and that white matter, grey matter and CSF are correctly segmented in the next step.

Using commands from the ANTs module, timeseries associated with white matter and CSF were then regressed out. This ensures that subsequent statistical analysis is only based on BOLD signal from grey matter. High-pass temporal filtering was then applied to the image using FSL commands. This filtering further de-noises the BOLD signal by removing low frequency (<0.02 Hz) signal fluctuations caused by the MRI scanner drift. The global signal was not regressed out because evidence suggests this may remove important signal fluctuations rather than simply removing noise. Furthermore, it has been shown that removing the global signal alters the connectivity structure across the brain by shifting the distribution of FC values into the negative space, i.e. producing anti-correlations (Cheng et al., 2021; Fox et al., 2009). The normalization from the individual co-registered functional images to MNI space was then conducted by applying the previously created transformation matrix to each scan. This allowed comparability of scans to each other and to the existing literature.

Lastly, in preparation for the large-scale network analysis only, the images underwent spatial smoothing with a 6-mm full-width-half-maximum Gaussian kernel using the FEAT toolbox in FSL (https://fsl.fmrib.ox.ac.uk/fsl/fslwiki/FEAT). In line with recommendations, spatial smoothing was not applied for the images used in the graph theory analysis, because graph theory uses an ROI-to-ROI (node-to-node) rather than voxel-to-voxel analysis (Alakörkkö et al., 2017). Therefore, graph theory inherently spatially smooths the BOLD signal, and further spatial smoothing would be unnecessary because it may result in the spreading of the BOLD signal across ROIs, which is not desirable.

The order of these pre-processing steps was largely consistent with that commonly used for large-scale network analyses and which has been evaluated to be most beneficial for the assessment of graph theory metrics (Gargouri et al., 2018).

### 3.3.4 Large-scale networks

In *chapter 6*, the statistical analysis of the rs-fMRI BOLD signal investigated FC within and between large-scale networks. A large-scale network is a set of multiple spatially remote and anatomically defined brain regions that have highly correlated resting-state BOLD timeseries (Biswal et al., 1995). These are stable over time (Damoiseaux et al., 2006), relevant towards active brain function and behaviour (Laird et al., 2011; Tavor et al., 2016), and abnormalities of these networks may reflect neurobiological mechanisms that underpin psychiatric disorders (Menon, 2011). Although a complete understanding of the network structure in the brain is still lacking, the presence of some large-scale networks has been reliably reproduced across studies. These include sensory networks such as the visual, auditory, and sensorimotor networks, but also cognitive and limbic networks such as the default mode network (DMN), the frontoparietal (or attention) network (FPN), the salience network (SAL), and the medial-temporal network (MTN) (Uddin et al., 2019).

Large-scale networks are typically identified by 1) using principal component analysis to determine the number of orthogonal (uncorrelated) components that should be extracted from the data to capture the maximum amount of variance; and 2) using group independent component analysis (gICA) to decompose and factorize the voxel BOLD timeseries into the previously determined number of maximally (statistically) independent components. The gICA uses the pre-processed data of individual subjects. This multivariate, linear, data-driven, model-free, exploratory approach considers the signal from all voxels simultaneously rather than analysing voxels independent of others. The components produced by gICA thus contain continuous weights for all voxels, showing which voxels are more and less strongly associated with individual components. This differs from seed-based FC analysis, which requires hypotheses to preselect brain regions of interest, resulting in binary, structurally specific masks. The gICA components are evaluated to select those reflecting noise and those that

are functionally meaningful. The functionally meaningful components can be described either in terms of a spatial map (spatial gICA), showing which brain regions show above-threshold signal and are thus associated with a network, or as a timeseries (temporal gICA), showing how the signal develops over time. Both can then be used in higher-level analyses, however spatial gICA is more common because it results in a better signal-to-noise ratio (Bijsterbosch et al., 2017) and creates group-level spatial maps that can be used in further analytic approaches such as dual regression.

### 3.3.5 Large-scale network statistical analysis

The large-scale network analysis relied on dual regression. This required group-level spatial maps which were obtained through the above approach in an independent sample of 21 healthy adult males (Dipasquale et al., 2019). The rs-fMRI data for this independent sample was acquired on the same MRI scanner with the same parameters as the data collected in the current ASPD+/-P and NO samples. Furthermore, it underwent largely similar pre-processing steps before being subjected to the principal component analysis and gICA to identify 13 functionally meaningful large-scale networks. These networks have been reliably identified in healthy and clinical populations (Damoiseaux et al., 2006; Menon, 2011; Uddin et al., 2019; Veer et al., 2010). Specifically, they reflected the (1) primary visual network, (2) sensorimotor network, (3) DMN, (4) medial visual network, (5) auditory network, (6) lateral visual network, (7) MTN, 8) cerebellum, (9) SAL, (10) task positive network, (11) ventral stream network, (12) right lateral network, and (13) thalamic network. The components were thresholded ($z \geq 3$) to visualize which voxels (and thus brain areas) were most associated with which network (*Figure 6.1*). The resulting spatial maps were used as model input for the dual regression.

Dual regression is an analytic technique implemented in FSL (https://fsl.fmrib.ox.ac.uk/fsl/fslwiki/DualRegression) which is used to obtain subject- and session-wise FC estimates for each network identified

in a gICA (Beckmann et al., 2009; Nickerson et al., 2017). Dual regression applies two multiple regression stages (displayed in *Figure 3.5*). In the first stage, the gICA components (model input), that is, the spatial maps of the 13 functionally meaningful networks, are applied to the pre-processed BOLD data from each individual subject and session (data input). This results in subject- and session-wise timeseries for each component. It is optional but recommended to normalize these timeseries to ensure that network shape and strength, rather than just network shape, are estimated in the second stage. In the second stage, these timeseries (model input) are applied to the pre-processed BOLD data for each individual subject and session (data input), resulting in subject- and session-wise spatial maps for each component, i.e., each network of interest. These maps contain beta values for every single voxel across the brain, indicating the extent to which a voxel is associated with the given spatial network. Therefore, each subject had 13 spatial network maps for each PL and OT session. The dual

regression output was then used to assess group differences and treatment effects on within- and between network connectivity.

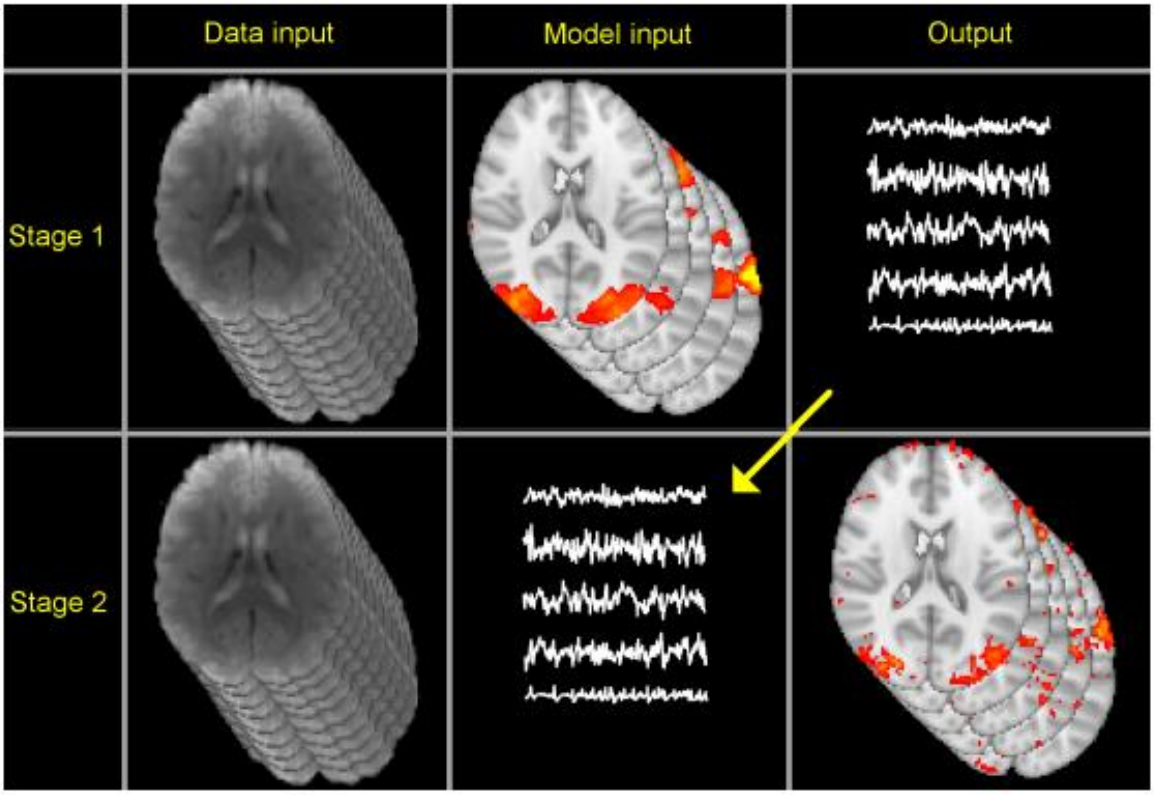


Figure 3.5 Visual display of the dual regression analysis technique.
*Note: Data input represents the pre-processed data for each individual and session and model input represents the components obtained through the independent gICA. The output of stage 1 represents the subject-specific timeseries for each component, and the output of stage 2 represents the individual spatial maps that can be used in higher-level analysis. (Image copied from Bijsterbosch et al., 2017).*

The within-network analysis relied on the 13 spatial maps, i.e., the output from stage 2 of the dual regression, whereas the between-network analysis used the 13 timeseries, i.e., the output from stage 1. A partitioned errors approach was used for both analyses. FSL commands *fslmerge* and *fslmaths* were used to prepare this. To assess the main effect of group, the respective output from each subject's PL and OT session was averaged. To assess the main effect of treatment and interaction effects, each subject's PL output was subtracted from the OT output.

#### *3.3.5.1 Within-network analysis*

The within-network analysis was then conducted in SPM12 (https://www.fil.ion.ucl.ac.uk/spm/software/spm12/). The main effect of group (ASPD vs NO) was measured using a two-sample t-test applied to

each of the 13 averaged spatial maps. The main effect of treatment was measured using a one-sample t-test applied to each of the 13 subtracted spatial maps. The interaction effect was measured with a two-sample t-test applied to each of the 13 subtracted spatial maps. Although age was not significantly different between groups, there was a broad age range in the sample, and it has been shown that age influences resting-state functional connectivity (Varangis et al., 2019). Thus, age and minutes since final dose were included as covariates of no-interest. Significant clusters were identified using a whole-brain cluster-level inference of $\alpha = .05$ and FWER correction for multiple comparisons. Only clusters surviving the cluster-defining threshold of $p < 0.001$ were interpreted (S. M. Smith et al., 2013). The two-sample t-tests required one-directional contrasts (ASPD > NO, ASPD < NO). However, since the hypotheses were two-directional, the resulting p-values were multiplied by 2 prior to interpretation. Furthermore, three networks of interest in the context of ASPD were selected *a priori* (DMN, SAL, MTN). Any findings relating to these networks were subjected to a Bonferroni correction for three multiple comparisons (adjusted $\alpha = .02$), whereas exploratory findings relating to the remaining networks were subjected to a Bonferroni correction for ten multiple comparisons (adjusted $\alpha = .005$). For any clusters with group by treatment interaction effects that survived these corrections, binary masks were created and applied to the subject- and session-wise spatial maps to extract the beta values of that cluster. Once extracted, these beta values were compared using post-hoc simple main effects with Sidak correction for multiple comparisons.

In summary, results from the within-network analysis indicate whether networks had significant group or treatment-induced differences in the shape or size of the network (i.e., which regions show significantly higher/lower correlation with the network). Due to the nature of each network map, which were thresholded for visualization but contain weights for every voxel, this can include regions anywhere across the brain, including regions not typically associated with a certain network.

#### 3.3.5.2 Correlations

As with the other neuroimaging data described previously, results from the within-network analysis were correlated with phenotypic variables of interest. Thus, within ASPD participants only, beta values from clusters with a significant group difference or a significant group by treatment interaction effect (if this was associated with significant within-group change as per the simple main effects) were correlated with clinical (PCL-R total, factor 1, and factor 2), behavioural (conviction information and aggression), and cognitive variables (averaged, z-standardized scores from the neurocognitive assessment under the PL condition). Beta values from a significant group effect were averaged across PL and OT prior to this correlation, and beta values from a significant interaction effect were subtracted. Partial Pearson correlations covarying for age and minutes since dose were used and bootstrapped 95% confidence intervals were calculated. FDR was applied to correct for multiple comparisons. Unlike the correlations conducted with structural and rCBF measures, these correlations were not conducted in each ASPD subtype separately, and did not require group as a covariate, because the main analysis consisted of a two-way analysis (ASPD vs NO). Thus, the risk of spurious (illusory) correlations with PCL-R score did not occur.

#### 3.3.5.3 Between-network analysis

The between-network analysis used the subject- and session-wise timeseries output from stage one of the dual regression, which was prepared for a partitioned errors approach as described above. The FSLNets package (https://fsl.fmrib.ox.ac.uk/fsl/fslwiki/FSLNets) was used in Matlab (S. M. Smith et al., 2013). A matrix containing the z-scores of full correlations between networks was produced. For this analysis, two networks of interest in the context of ASPD were selected *a priori* (DMN, SAL). Therefore, this between-network correlation did not require Bonferroni correction. However, the exploratory analysis assessing

between-network across all 13 networks was subjected to FDR (threshold $p < .00001$).

In summary, results from the between-subject analysis indicate the extent to which correlations between two networks differed between groups or treatment conditions. However, the nature of this analysis did not allow the extraction of any values that could be correlated with phenotype.

#### *3.3.5.4 Power*

Precise recommendations for minimum sample size in rs-fMRI FC analyses are lacking. An early study of resting-state and task-based fMRI suggested that to achieve power of 0.80, at an alpha threshold of 0.05, 12 participants would be required to detect signal changes (Desmond & Glover, 2002). Although these recommendations were also applied to resting-state data, they were primarily acquired through the analysis of task-based data. Since then, it has been recognized that samples of over 100 subjects are required to detect meaningful and non-inflated individual differences in fMRI data (Dubois & Adolphs, 2016). The sample size for the current analyses is comparable to that utilised in other studies assessing within- and between-subject FC differences in large-scale networks. Furthermore, the use of multi-echo image acquisition alongside various pre-processing steps that have been shown to be optimal for noise reduction (e.g., ME-ICA) and analytical steps (e.g., use of independent spatial network maps) is beneficial towards the statistical power in the current study (Grady et al., 2021; Lombardo et al., 2016). Nevertheless, the current sample size was rather small and thus the results should be considered to be more exploratory in nature.

### 3.3.6 Graph theory

In *chapter 7*, the statistical analysis of the rs-fMRI BOLD signal was conducted according to a graph theory approach. This is a node-based connectivity analysis that provides insight into the brain's functional topology, in other words how the flow of information (connectivity) is

structured on a local and global level. It is different to the above voxel-based connectivity analysis which mainly provides insight into the correlation of activity (FC) between brain areas and can thus illustrate the large-scale functional networks of brain.

Graph theory measures brain network characteristics by assessing nodes, or regions of interest such as anatomical elements, and edges, or structural/functional connections between these nodes. Unlike voxel-based connectivity analyses, graph theory can thus quantify the integration and segregation of information, shedding light on the complex dynamics of brain networks. It has been suggested that this is a particularly important step towards understanding the neurobiological underpinnings of behaviour (Farahani et al., 2019) and characteristics of brain networks have been shown to predict cognition (Cohen & D'Esposito, 2016; Douw et al., 2011; Welton et al., 2020). The efficiency and cost of a network can be quantitatively evaluated according to global characteristics (macro-level), local/nodal characteristics (meso-level) or edge characteristics (micro-level) (Bullmore & Sporns, 2009; Joules et al., 2015; Rubinov & Sporns, 2010; Zalesky et al., 2010). The graph theory indices used in the current project will now be described.

#### *3.3.6.1 Graph theory metrics*

*Figure 3.6* depicts the range of macro-, meso-, and micro-level network metrics that were calculated and analysed in the current study. Global efficiency reflects functional integration of information flow across the whole brain, on a macro-level. It is defined by the inverse of the average characteristic path length between all nodes in the network, whereby characteristic path length describes the smallest possible number of edges required to connect any two nodes to form a potential route for information flow (Latora & Marchiori, 2001; Rubinov & Sporns, 2010). High global efficiency suggests high integration and shorter average characteristic path length connecting all nodes of the brain.

Several meso-level network metrics were also calculated. The first was local efficiency which reflects functional segregation. Local efficiency provides insight into the extent that individual nodes are connected to neighbouring nodes (on average) and thereby reflects the extent to which the organization of the brain relies on local, segregated sub-networks (Latora & Marchiori, 2001). It is calculated as the average of all nodal efficiency values. High local efficiency suggests high functional segregation across the brain. Nodal efficiency is the second meso-level network metric that was calculated. In addition to being required to calculate local efficiency, it also offers information in its own right. It measures the inverse of the average minimum characteristic path length connecting one node with its neighbouring nodes. It is directly proportional to the clustering coefficient, which is a similar graph theory metric that measures the likelihood that two neighbouring nodes are both connected by a third neighbouring node, forming triangles (Watts & Strogatz, 1998). Due to their direct proportionality, the clustering coefficient was not calculated in this thesis. High nodal efficiency suggests a specific node is very tight-knit (integrated) with its neighbouring nodes (Rubinov & Sporns, 2010).

Finally, two further meso-level network characteristics describing the centrality, or importance, of specific nodes were calculated (Rubinov & Sporns, 2010). The first was node degree centrality. This is defined by the number of edges connected to a node, regardless of their strength. A high node degree suggests interaction with many other nodes. The second was betweenness centrality. This represents the fraction of all shortest paths that contain a certain node, meaning the most efficient information flow involves this node. In other words, it indicates how much of a hub a node is. High betweenness centrality suggests a node participates in many shortest path connections.

Lastly, micro-level edge connectivity was assessed to identify any subnetworks that significantly differed between groups or treatment

conditions. This was done using the network-based statistic method (Zalesky et al., 2010) and is described in more detail below.

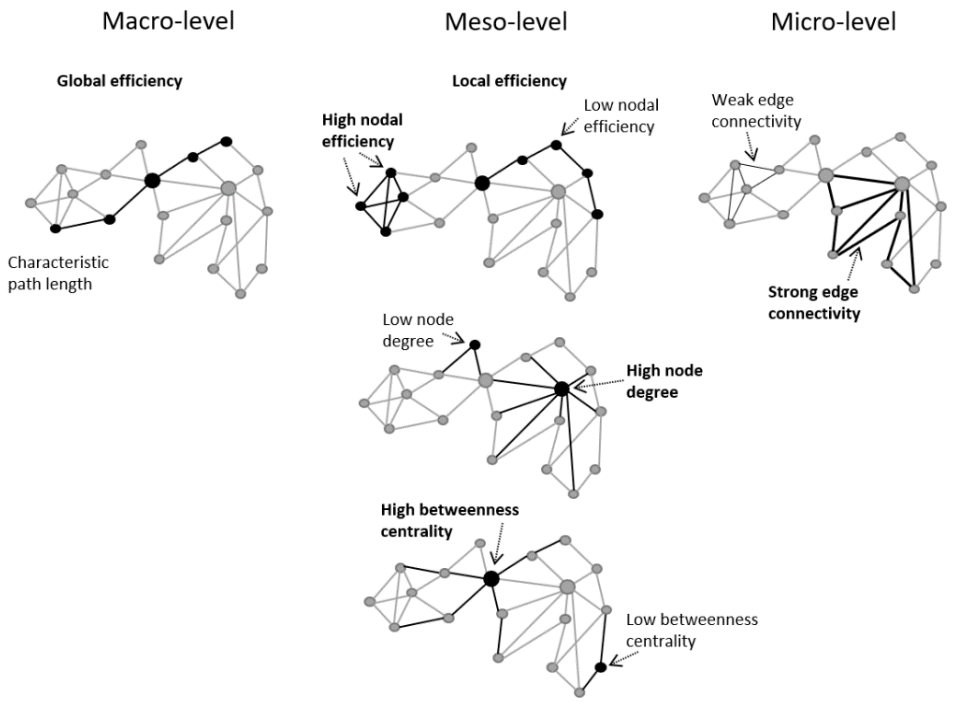


Figure 3.6 Visual representation of the graph theory metrics included in this analysis.

*Note: Due to its calculation, global efficiency is shown in the context of an example of characteristic path length. Local efficiency is shown in the context of nodal efficiency.*

### *3.3.6.2 Extraction of graph theory metrics*

Prior to running the statistical analysis, the graph theory indices of interest had to be extracted from the pre-processed rs-fMRI BOLD images. This was done using FSL commands, Matlab calculations and the Brain Connectivity Toolbox (BCT) in Matlab 2020a (Rubinov & Sporns, 2010) and the process is summarized in *Figure 3.7*. First, using FSL, the Desikan-Killiany atlas was applied to parcellate the BOLD signal timeseries of each scan into 85 individual anatomical nodes (Desikan et al., 2006). Second, using Matlab, a correlation matrix containing the full correlations between each of the 85 nodes was calculated for each scan and subsequently transformed using a Fisher Z transformation. This ensures that the correlation coefficients are normally distributed. After this step, the mean functional connectivity (FC) for each participant and each session was calculated by averaging the positive elements (correlations) in the lower triangle of each Fisher z-

transformed correlation matrix. These mean FC values were then compared between groups and treatment conditions using a linear mixed model, covarying for mean-centred age and minutes since dose. Mean FC is an indicator of total network strength (Van Den Heuvel et al., 2017). The null hypothesis assumes that there are no differences in mean FC across groups or treatment conditions, indicating that potential differences on the graph theory metrics are not due to differences in total network strength.

Third, graph theory metrics could be calculated. Using the BCT, the Z-transformed correlation matrices for each scan were concatenated into one adjacency matrix across all scans (an 85x85x89 3D matrix whereby the first two dimensions reflect the individual node-to-node correlation matrices for each subject and session and the third dimension reflects the number of combined scans). This matrix was undirected as well as weighted rather than binary, and thus contained information about the strength rather than simply the existence of connections. The adjacency matrix was thresholded across a range of network densities between 5% and 34% with a 1% interval. Network density represents the number of actual connections (edges) relative to all possible connections. This range was chosen because it has been shown that the brain generally has small worldness properties. This means it has highly clustered, densely connected areas that are typical for latticed networks but is balanced with short characteristic path lengths that are more typical for random networks (Bassett & Bullmore, 2017; Watts & Strogatz, 1998). A network density >35% is suggestive of an excessively random network structure rather than a small world network structure and would not be appropriate for subsequent analysis (Bullmore & Sporns, 2009). The area under the curve (AUC) was calculated to reflect an average of the density thresholding range (Ginestet et al., 2011). This reduced the computational demand and eliminated the necessity to correct for up to 34 multiple comparisons for each network density. Furthermore, it offered a more intuitive interpretation in subsequent data analysis because it could be assumed that

findings were not driven by individual variability in network density. Finally, the BCT (Rubinov & Sporns, 2010) was used to calculate higher level summary indices that describe different aspects of network functioning. Specifically, global, local, and nodal efficiency, node degree centrality, and betweenness centrality were calculated. The Matlab network-based statistic toolbox (Zalesky et al., 2010) was used to calculate edge connectivity.

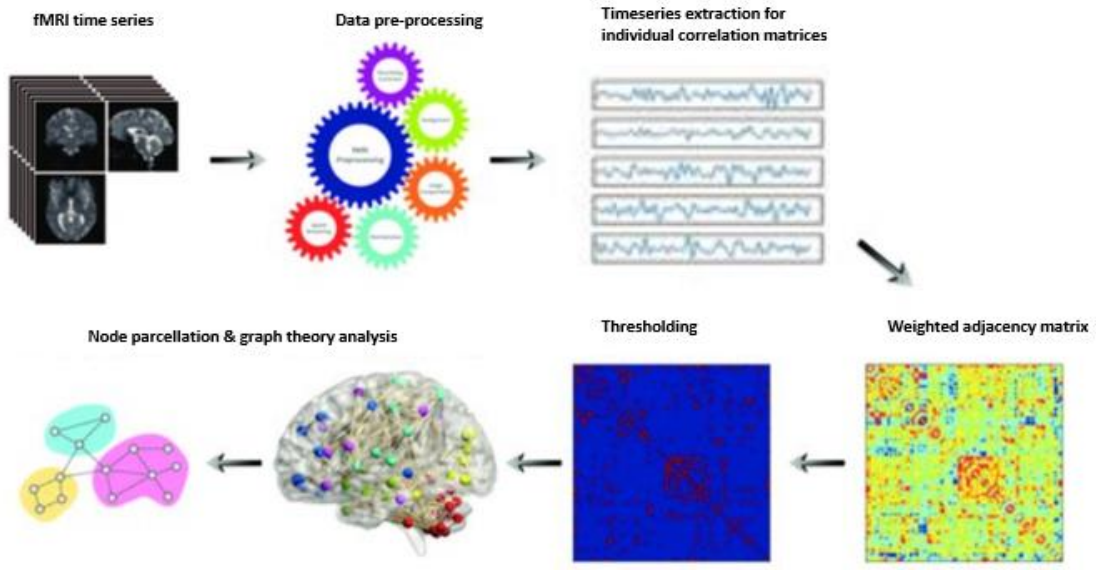


Figure 3.7 Overview of the graph theory analysis technique.
*Note: this was adapted (Farahani et al., 2019).*

## 3.3.7 Graph theory statistical analysis

### *3.3.7.1 Macro- and meso-level: topological network metrics*

Once the network metrics were extracted, a linear mixed model analysis approach which had the same format across all outcomes was taken. Fixed factors were Group, with two levels (ASPD and NO), and Treatment, also with two levels (PL and OT). Mean-centred age (network efficiency reduces with age (Achard & Bullmore, 2007)) and minutes since dose were included as covariates of no-interest. Subject was the random factor. The dependent variable was the respective network characteristic value. There were no significant outliers in the models. This was identified by assessing Cook's distance (all were <1).

Since mean FC, global, and local efficiency values were reflective of the whole brain rather than individual nodes, one linear mixed model for each

metric was run in R and did not require correction for comparisons across multiple nodes.

Meso-level network characteristics were analysed with an ROI approach, which focused on the analysis of the amygdala, anterior cingulate, and precuneus, as well as a whole-brain approach, which assessed nodes across the brain. For both approaches, linear mixed models were performed for each node. For the ROI analysis, this was done in R, and any significant main and interaction effects were corrected for six (3 ROIs x 2 hemispheres) multiple comparisons using FDR. For the whole-brain analysis that included all remaining anatomic regions not included in the ROI analysis, this was done using a loop in Matlab, and any significant main or interaction effects were corrected for 77 multiple comparisons using FDR. Partial eta-squared effect sizes were calculated for all models.

#### *3.3.7.2 Correlations*

In ASPD participants only, partial Pearson correlations with bootstrapping were used to assess the relationship between the network characteristic values and phenotypic variables (clinical, behavioural, and cognitive features). Clinical variables were the psychopathy scores (PCL-R total, factor 1 and factor 2). Behavioural variables were the number of violent convictions, the presence of a reconviction within one year of participation, and reactive and proactive aggression scores. Cognitive variables were the averaged, z-standardized scores from the neurocognitive assessment under the PL condition. Mean-centred age and minutes since dose were included as covariates of no-interest. To assess the relationship with baseline network properties, all correlation analyses were conducted using the values of brain areas that showed a significant main effect of group. Additionally, to assess the correlation with the response to the OT challenge, the OT-PL difference scores of the network properties in brain areas that showed a significant interaction effect associated with changes in ASPD participants were used. The correlations were adjusted for multiple comparisons using the FDR method. Similar to the correlations with the

within-network large-scale network connectivity findings, there was no risk of spurious (illusory) correlations with the PCL-R score, since the main analysis did not assess ASPD+/-P subtypes.

#### *3.3.7.3 Dice coefficient*

The Dice coefficient (also known as the Dice Kappa statistic) indicates the extent of spatial overlap between nodes with any meso-level (nodal efficiency, node degree, betweenness centrality) main or interaction effects, and the areas associated with large-scale networks. To calculate this, the z-thresholded 13 spatial maps ($|z| > 2$) that were used for the large-scale network analysis (*Figure 6.1*) were binarized using *fslmaths*. Similarly, binarized maps for the main effect of group, treatment, and the interaction effect were created using *fslmaths.* Specifically, the masks for the Desikan-Killiany Atlas (DKA) nodes that had a significant effect in any of the meso-level nodal metrics were merged into one overall binary image. Therefore, the Dice coefficient was then calculated for each main and interaction effect, and each of the 13 network maps using the *fslstats* toolbox.

#### *3.3.7.4 Micro-level: Network-based statistic*

The network-based statistic (NBS) is an approach used to assess edgewise connectivity between the 85 DKA nodes of the graph (Zalesky et al., 2010). It identifies subnetworks that have altered connectivity between groups or under different treatment conditions. The Matlab toolbox used to calculate NBS relies on the individual Fisher z-transformed correlation matrices as well as centre of gravity coordinates to locate the centre of each DKA region. The goal of NBS is to reduce the number of multiple comparisons and improve the analytic power by using non-parametric cluster-based thresholding. Therefore, it automatically controls the FWER, in the weak sense (i.e., guaranteeing control only when the global null hypothesis is true), after performing mass univariate analyses across all graph edges. It compares to the approach used to identify significant clusters in mass univariate testing of voxels. This means that the NBS creates topological

clusters containing graph components that comprise the contrast of interest (hypothesis), thus identifying subnetworks with significant differences between groups or conditions at a higher statistical power. These subnetworks, i.e., graph components, are identified if multiple, connected edges form suprathreshold clusters. The identification of subnetworks however means that the hypotheses cannot be interpreted on an edge level, but rather, only on the level of the subnetwork.

In the current study, a partitioned errors approach was used, so only participants with a complete PL and OT scan could be included (ASPD n = 19, NO n = 19). Using 'fslmerge' and 'fslmaths', the PL and OT correlation matrices for each individual were averaged to assess the main effect of group and subtracted to assess main effect of treatment and group by treatment interaction effect. The hypotheses to be tested across all graph edges using a general linear model were then specified in the NBS toolbox. Specifically, a two-sample t-test was used to assess group effects (average correlation matrix) and interaction effect (subtracted correlation matrix), and a one-sample t-test was used to assess treatment effects (subtracted correlation matrix). Mean-centred age (Achard & Bullmore, 2007) and minutes since dose were included as covariates of no-interest. Contrasts to assess each direction of the hypothesis were set up using design matrices in the NBS toolbox.

Once the above t-contrasts were calculated for each edge (mass univariate testing), a primary threshold was applied, identifying suprathreshold clusters containing edges above this threshold. There is no specific suggestion for selecting the optimal primary threshold and it is a user-determined parameter in the NBS. Therefore, in line with common practice, the current analysis assessed a range of primary thresholds from t = 1.5 to t = 4.0, at 0.5 intervals. Lower, more liberal thresholds may result in larger, topologically extended subnetworks, whereas higher, stricter thresholds may result in smaller, topologically focused subnetworks (Zalesky et al., 2010). Out of the above range, the final threshold chosen

for the current analysis was t = 3.0, which corresponded to an approximate alpha threshold of p ≤ .003. The selection of primary threshold does not affect subsequent FWER correction (Zalesky et al., 2010).

It is worth noting that an underlying assumption of NBS is that any suprathreshold clusters (subnetworks) which confirm the hypothesis (i.e., they reject the null hypothesis predicting no difference) occur in the form of an interconnected configuration of multiple edges rather than just single or isolated connections. In other words, a subnetwork representing a suprathreshold cluster must contain multiple edges connecting multiple nodes.

Finally, non-parametric premutation testing was used to compute the FWER-adjusted p-value of any identified suprathreshold clusters. In the current study, 5000 permutations were run. This process randomly reallocates individuals into each condition according to within- or between-subject permutation vectors (respective to the original analysis) and re-runs the above process for the specified number of permutations. For each run, the size of the largest identified subnetwork is stored, yielding an empirical null distribution for the size of the largest component. The FWER-adjusted p-value for a subnetwork of a given size is then estimated as the proportion of permutations for which the largest component was the same size or bigger (Zalesky et al., 2010). Subnetworks with a suprathreshold of t = 3.0 and an FWER-adjusted p-value of less than .05 were considered to be significant subnetworks showing the hypothesized contrast.

#### *3.3.7.5 Power*

There has been limited research proposing sample sizes required to achieve adequate statistical power in resting-state fMRI graph theory analysis. A recent review highlighted that most case-control topology studies have between 15 and 73 participants, though larger samples improve the power that graph theory analyses, which inherently rely on a high number of metrics, can offer (Helwegen et al., 2023). Moreover, a meta-analysis

demonstrated robust and replicable graph theory metrics, including those used in the current project, in studies using samples ranging from 5 to 45 individuals for within- and between-subject analyses (Welton et al., 2015). Furthermore, other research has shown that to achieve a power of 0.80 and detect medium to large effect sizes in single-site studies, sample sizes over 50 would be sufficient, although having over 100 participants would be desirable, especially to detect smaller effect sizes (Cao et al., 2019; Termenon et al., 2016). Together, this evidence suggests the current study was powered enough to detect large effect sizes. It is important to treat the current results, especially those with smaller effect sizes, as being more exploratory in nature. Effect sizes were reported to aid the interpretation of findings as well as provide useful information for future research.

### 3.3.8 Benefits

There are several benefits of the resting-state BOLD neuroimaging technique and its analysis. First, as with the resting-state ASL technique, this technique is non-invasive and does not rely on demanding task paradigms, which is particularly useful when studying a clinical population such as ASPD+/-P who may have poor engagement and attention. Furthermore, it provides insight into brain functioning independent of context, type of task, task-elicited behavioural and cognitive strategies, and performance, and it lends itself as a useful tool for studying brain shiftability by pharmacological agents independent of processes triggered by tasks (Khalili-Mahani et al., 2017; Lv et al., 2018; Nomi & Uddin, 2015). Beyond the benefits of resting-state fMRI as a technique, there were additional benefits of the acquisition, pre-processing, and analysis approaches. These will be outlined below.

In terms of acquisition and pre-processing approaches, the current project benefitted from the use of a multi-echo EPI sequence, which has been shown to optimize the sensitivity for detecting meaningful BOLD signal by allowing improved identification and subsequent removal of noise. Furthermore, it increases the power to detect signal in regions often

affected by signal drop-out in single-echo sequences (Caballero-Gaudes & Reynolds, 2017; Dipasquale et al., 2017; Kundu et al., 2017). It also has high temporal resolution, which is better than in task-based fMRI. Compared with ASL imaging, it has improved sensitivity to neural activity due to having a higher sampling rate alongside increased spatial and temporal signal-to-noise ratio (Jann et al., 2015; K. Murphy et al., 2007; K. Zhang et al., 2018). In line with acquiring multi-echo data, the project also benefitted from applying the ME-ICA pre-processing approach ('tedana' pipeline) to remove remaining artefact noise. This is more sensitive and effective than traditional methods and has been applied in large-scale network and graph theory analyses (Dipasquale et al., 2017, 2019; Openneer et al., 2020).

In terms of analysis, the large-scale network analytic approach relied on dual regression. This technique has several benefits. The first main benefit relates to the acquisition and identification of the 13 spatial network maps that were entered into the dual regression. These came from resting-state fMRI scans collected in an independent sample of healthy men, on the same scanner with almost identical scanner settings and imaging parameters (Dipasquale et al., 2019). This means the network maps likely contained the same MRI-specific artefacts and sources of noise that the data from the current study had, which is more beneficial than if relying on independent data from a different scanner. Additionally, this approach also eliminates bias that can result from producing network maps using the same individuals that are subsequently being analysed (Bijsterbosch et al., 2017). Within this independent sample, the network maps were identified using spatial gICA, which is a data-driven, multivariate approach that can reliably distinguish functionally meaningful components from noise components, and subsequently can distinguish within functionally meaningful components to identify individual, independent spatial maps (Calhoun et al., 2001). It does not rely on the pre-selection of specific seeds, meaning the network maps are not limited to the connectivity of any

particular region. Finally, the 13 network maps were spatially and functionally similar to traditionally identified networks (Uddin et al., 2019), allowing comparability of the present findings with the broader literature.

The second main benefit of the current large-scale network analysis relates to dual regression itself (Beckmann et al., 2009; Nickerson et al., 2017). Due to its reliance on group-based spatial network maps, dual regression avoids a correspondence problem which may arise when functional components are identified in individual subjects (e.g., in one subject, the default mode network is represented as one network, in another subject, it is split into two networks). Furthermore, dual regression uses multiple regression models at each stage. This means that all 13 spatial network maps (i.e., the regressors) are entered into the model simultaneously, and the best fit of each regressor is calculated while accounting for the influence of the other regressors. This is beneficial because it determines the relative contribution of individual components towards connectivity differences across groups or conditions. Finally, the use of dual regression allowed the analysis of both within- and between-network connectivity, which was a novel analysis approach that has not been employed within this population.

Graph theory analysis is also associated with unique benefits. Most importantly, and unlike voxel-based techniques such as the large-scale network analysis used in the present study, graph theory can describe the topology of complex neural network dynamics (Farahani et al., 2019). Due to its excellent test-retest reliability, it can provide concise neurobiological, quantitative summary markers that can be compared between healthy and clinical populations, and/or tested in response to pharmacological challenges (Achard & Bullmore, 2007; Alavash et al., 2018; Choe et al., 2015; Joules et al., 2015; Martins et al., 2021; Openneer et al., 2020; Welton et al., 2015). Therefore, graph theory analysis provides insight into network dynamics, or the intrinsic architecture of the brain, on multiple levels of processing. By doing so, it offers information on *how* nodes of the

brain are organized and connected, rather than simply at what strength they are connected (J. Wang et al., 2010).

### 3.3.9 Challenges

Nevertheless, there are also some challenges associated with resting-state BOLD data and its analysis. Five challenges exist with regards to the acquisition of such data. First, since the individual is at rest, there is no true control over their thought processes, which may increase the between-subject variability and obscure FC. The true functional meaning of identifying resting-state networks has also been questioned (Morcom & Fletcher, 2007). Nevertheless, the consistency in finding similar large-scale networks does point to some common fundamental truth associated with the FC of the brain at rest (Choe et al., 2015; De Luca et al., 2006; Mak et al., 2017). Second, the interpretation of the BOLD signal faces some limitations. It is only an indirect proxy measure of neural activity which has been shown to be susceptible to the influence of many artefacts (Jenkinson & Chappell, 2018a). However, advanced acquisition and pre-processing protocols, which were implemented in the current project, have been shown to result in robust removal of artefact noise. The interpretation of BOLD signal studies may also be affected by various acquisition parameters that vary across studies and sites and may therefore reduce comparability across the literature (Simon & Buxton, 2015). Furthermore, there is also some debate about whether the BOLD signal reflects only neural activity or also captures signal from other surrounding brain tissue cells (H. Lu et al., 2019). Third, the BOLD signal is less sensitive to pharmacological challenge compared to rCBF. Therefore, the use of ASL and BOLD complement each other in the current project. While ASL can inform about the magnitude of a pharmacological effect on rCBF within individual regions, BOLD can measure how the pharmacological challenge affects the connectivity and interaction between brain regions (Jann et al., 2015; Li et al., 2018; van den Heuvel & Hulshoff Pol, 2010). Fourth, the high temporal signal-to-noise ratio comes at a cost of reduced spatial resolution, although the extent of

smoothing may mitigate against this to some extent. Finally, like resting-state ASL imaging, rs-fMRI BOLD imaging also does not provide actual behavioural information. Therefore, it is only possible to indirectly infer potential behavioural consequences based on the functions of the areas or nodes that have been implicated.

In terms of the analysis, large-scale network analysis is linked with some challenges. First, the use of independently derived spatial network maps may have meant some sources of noise in the current data were not accounted for (Bijsterbosch et al., 2017). However, this risk was minimized since the independent data was acquired using the same MRI scanner with largely identical parameters. Therefore, the benefit of using independently acquired maps outweighed this challenge. Second, there are some inherent challenges associated with the use of ICA to determine distinct components (Cole et al., 2010). For example, it is possible that ICA results in different components on repeated analysis runs, despite using the same data. ICA is also dependent on the number of pre-specified components, usually determined through principal component analysis. However, these challenges affect the field as a whole, and therefore, were not specific to the current analysis. The identification of common large-scale networks, which have often been replicated, also suggests that the ICA used to identify the spatial network maps in the current study performed well. Nevertheless, related to this challenge was the third challenge, which was that the spatial maps did not include a frontoparietal network as it is typically found in other analyses. Instead, it included the task-positive network, which was only deemed to be taxonomically similar in hindsight and was thus not included as an *a priori* network of interest, despite being relevant to ASPD. This somewhat reduced the comparability to other studies. Future research should additionally aim to focus on this network. The final challenge of this large-scale network analysis was that it can only provide insight into static FC, i.e., the average connectivity across time. This foregoes the fact that the resting-state brain is dynamic and constantly

fluctuating (Hutchison et al., 2013). Future research should assess group differences and treatment effects using dynamic FC methods, to provide insight into how FC changes over time.

Similarly, graph theory analysis also faces some challenges. First, it relies on pre-defined nodes, which should have functional relevance. The current study relied on an anatomical atlas to define the nodes (Desikan-Killiany Atlas). This is the most common approach and the current study is in line with most other graph theory research; however, it has been debated whether a true functional atlas or one that combines functional and finer-grained structural information (e.g., Brainnetome Atlas, Fan et al., 2016) would be more meaningful (Shen et al., 2013). Second, graph theory metrics represent concise yet abstract, or somewhat arbitrary values. There are also no normative thresholds which indicate when a metric is considered abnormal. These factors may obscure the interpretation of network characteristics in terms of actual neural activity and functioning (De Vico Fallani et al., 2014). Finally, graph theory analysis is associated with a vast range of network metrics that provide unique, yet correlated information. Additionally, there are several paths towards calculating these metrics, which differentially account for different aspects of network topology (e.g., accounting for total network strength, density, and cost varies across studies but affects the interpretability of results). Thus, there is no consensus on the most functionally meaningful metrics or the most appropriate calculations to obtain these metrics. However it is promising that metrics including global efficiency, local efficiency, nodal efficiency (clustering coefficient), and betweenness centrality have been identified to be the most reproducible metrics (Welton et al., 2015). This finding underpinned the metrics derived in this study.

# 4 A structural MRI investigation of violent offenders with ASPD

## 4.1 Introduction

A small number of individuals account for a large proportion of violent crime (Martinez et al., 2017). These individuals are typically male, have life-course persistent (LCP) antisocial behaviour, and meet diagnostic criteria for conduct disorder (CD) in childhood and antisocial personality disorder (ASPD) in adulthood (Piquero & Moffitt, 2014). However, there is significant heterogeneity within individuals with ASPD. The majority of such individuals exhibit antisocial and impulsive behaviour, emotional lability, increased comorbidities with mood disorders and high levels of reactive aggression (Azevedo et al., 2020; Hodgins et al., 2010, 2018; Kosson et al., 2006; Moffitt, 2018). A smaller subgroup exhibit significant interpersonal and affective difficulties characterized by a lack of empathy and manipulativeness, a younger onset of offending with more violent recidivism and high levels of proactive aggression, and poorer treatment response (Azevedo et al., 2020; Hare, 1991; Mayer et al., 2018; Olver et al., 2013; Riser & Kosson, 2013). This subgroup typically meets criteria for CD with callous-unemotional traits in childhood and ASPD with psychopathy in adulthood (Frick & White, 2008; Ogloff et al., 2016). The categorical distinction between individuals with ASPD without psychopathy (ASPD-P) and individuals with ASPD with psychopathy (ASPD+P) is an attempt to reduce heterogeneity within ASPD to help to inform neurobiological understanding in the field and to refine therapeutic approaches to individuals with overlapping but distinguishable interpersonal problems.

Neuroanatomical abnormalities in social brain regions of individuals with ASPD (regardless of psychopathic traits) have previously been reported in structural magnetic resonance imaging (sMRI) studies – however, the results are conflicting. For instance, relative to control populations, some studies have revealed increased and others decreased cortical grey matter

volume (CV) in brain regions such as orbitofrontal cortex, middle frontal gyrus, posterior cingulate, insula, and inferior parietal cortex (Raine et al., 2011; Schiffer et al., 2011; Tang, Jiang, et al., 2013; Tiihonen et al., 2008). This inconsistency may be partially explained by the presence/absence of psychopathy within their ASPD samples (not all studies assessed or controlled for this). The importance of measuring psychopathy was highlighted by a recent meta-regression of eleven voxel-based morphometry (VBM) studies investigating CV in men with high psychopathy as measured with the gold-standard Psychopathy Checklist-Revised (PCL-R). The findings revealed only significant negative relationships between CV and total psychopathy score in regions including the dorsolateral prefrontal and orbitofrontal cortex, the mid-/posterior cingulate cortex, and inferior temporal gyrus (De Brito et al., 2021). Although it can only be assumed that the included individuals also largely met criteria for ASPD, these findings would suggest that ASPD+P might be distinctly associated with CV decreases in key social brain areas. Nevertheless, to gain a better understanding of the impact of psychopathy on the neuroanatomical substrates of ASPD, studies directly comparing ASPD+P, ASPD-P, and healthy non-offending (NO) control groups are required.

Only two studies have directly compared CV in offenders with ASPD+/-P (Gregory et al., 2012; Tiihonen et al., 2008). The study by Tiihonen et al. (2008) was an important first step, but it was limited by poor group characterizations. For instance, some individuals in their ASPD-P group scored above the European threshold for psychopathy on the PCL-R (Cooke & Michie, 1999), meaning that this group did not represent a true ASPD-P sample. It was also unclear if their healthy control group were non-offenders. In contrast, Gregory et al. (2012) benefitted from larger and more homogenous subgroups created by splitting male violent offenders with diagnoses of ASPD into two subgroups according to the European PCL-R threshold. They also included a non-offender (NO) healthy control group and took careful account of the potential confound of comorbid substance

misuse. Both studies reported significantly reduced CV in ASPD+P compared to controls in brain regions involved in social and emotional processing such as the anterior rostral PFC, anterior insula, temporal pole, and inferior temporal regions. However, Gregory et al. (2012) were the first to show that ASPD+P also had distinctly smaller CV relative to ASPD-P in these regions, thereby proposing differences in the neurobiological substrates of ASPD+P and ASPD-P. This study, which benefitted from a robust methodological approach to attempt to disentangle the heterogeneity of ASPD, provided a promising first step towards understanding the differential neuroanatomical underpinnings of ASPD+/-P in terms of CV.

However, CV is not a specific marker of abnormalities in brain anatomy (Winkler et al., 2018). This is because CV is the mathematical product of two other cortical features, namely cortical thickness (CT) and surface area (SA), which differentially contribute to CV (Storsve et al., 2014). Hence, variation in CV could be driven by differences in CT alone, SA alone, or a mixture of CT and SA. This is of importance because CT and SA have different cellular origins. CT is dependent on the number, size and density of cells found within cortical (vertical) columns of a particular region, whereas SA is dependent on the number and density of cortical columns (i.e., areal expansion) found within a particular region (Rakic, 2007). These two features have differential developmental origins indicated by independent genetic determinants and differing heritability estimates (Panizzon et al., 2009; Storsve et al., 2014; Wierenga et al., 2014). They are also associated with different cognitive processes (Tadayon et al., 2020). Evidence for independent contributions of CT and SA towards CV have been found in other neurodevelopmental disorders including autism, 22q11.2 deletion syndrome, and ADHD (Ecker et al., 2013; Gudbrandsen et al., 2020; Silk et al., 2016). Therefore, to better understand the neurobiological mechanisms associated with ASPD+/-P, it is essential to

assess potential abnormalities in CT and SA and to delineate their contribution to CV abnormalities.

To date, only a small number of studies have assessed CT or SA in ASPD and psychopathy, and none have directly compared these surface measures in ASPD+/-P. One study demonstrated that ASPD was associated with CT reductions in medial prefrontal regions, and that these findings were not driven by the presence of psychopathy (Narayan et al., 2007). Unfortunately, they did not correct for multiple comparisons despite taking a whole-brain approach, meaning that their conclusion that reduced CT was not associated with psychopathy in ASPD must be considered cautiously. This is particularly important because subsequent studies did reveal reduced CT in frontotemporal regions of offenders with high levels of psychopathy (Calzada-Reyes et al., 2021; Ly et al., 2012; Yang et al., 2009). Finally, only one study has assessed both CT and SA, demonstrating reduced CT and increased SA in areas including the orbitofrontal cortex, anterior cingulate cortex, insula, and precuneus in young adult offenders with ASPD relative to offenders without ASPD (W. Jiang et al., 2016). However, they did not consider the potential impact of psychopathy, and no other studies have measured SA differences in psychopathy. Overall, these prior studies provide preliminary support for the suggestion that CT and SA are abnormal in ASPD, but it is unclear how this is modulated by the presence and severity of additional psychopathic traits. Furthermore, the lack of NO control groups also limits the conclusions that can be drawn from the existing literature, since potential abnormalities beyond those associated with offending behaviour may have been missed. To overcome these limitations, a study directly comparing CT and SA in individuals with ASPD+P, ASPD-P and NO controls is required. Furthermore, the extent to which CT and SA make independent contributions to CV abnormalities, and whether this differs between ASPD+/-P, remains to be investigated.

In summary, there is evidence that CV, and potentially also CT and SA, are altered in ASPD and psychopathy. However, the findings from prior studies

are inconsistent, which may be partially explained by variations in study design, methodological techniques, and inconsistent approaches to defining psychopathy (Griffiths & Jalava, 2017). Therefore, the relationship between psychopathy and neuroanatomical variation within individuals with ASPD requires clarification. To further disentangle the neuroanatomical substrates of ASPD+/-P, more research directly comparing these ASPD subtypes to each other and to a healthy NO control group is necessary. Hence, the current study had two main aims. The first aim was to compare CV, CT, and SA in males with a history of violent offending with ASPD+P or ASPD-P relative to healthy NO controls participants – and to each other – using automated surface-based morphometry and a whole-brain analysis. It was hypothesized that there would be reduced CV and CT in both ASPD groups relative to NO, as well as in ASPD+P relative to ASPD-P. It was also hypothesized that there would be increased SA in both ASPD groups relative to NO, although the lack of previous studies meant no distinction between ASPD+/-P could be hypothesized. The second aim was to measure the extent to which differences in CT and SA contributed to differences in CV. Here it was hypothesized that there would be different patterns of SA and CT contribution towards CV abnormalities in the two ASPD groups. In addition to the two main aims, the relationship between potential neuroanatomical abnormalities and several phenotypic measures was also explored.

## 4.2 Methods

### 4.2.1 Participants

All participants were adult males aged 18-60 at the time of consent and had an IQ above 70. Offenders were recruited from South London National Probation Service offices as well as a medium secure hospital within the South London and Maudsley NHS Trust. They were selected based on having a history of violent convictions (assault, actual/grievous bodily harm, armed robbery, rape, manslaughter, murder) and a diagnosis of ASPD according to DSM-5-PD criteria (First et al., 2015). They were

excluded if they had a comorbid psychotic or mood disorder diagnosis. The offenders were allocated into the ASPD+P group if their PCL-R score was 25 or higher, and into the ASPD-P group if their PCL-R score was below 25 (Cooke & Michie, 1999). Healthy NO control participants were recruited via purposive sampling through advertising in the local community, job centres, recreational centres as well as online platforms. They were excluded if they had any current or past mental illness and/or personality disorder, or a history of offending. All participants were excluded if they had a history of neurological illness, traumatic brain injury, head injury resulting in loss of consciousness for 1 hour or longer, or any contraindications to participating in an MRI scan (e.g., having a pacemaker).

### 4.2.2 Procedure

Participants attended three appointments at the Institute of Psychiatry, Psychology and Neuroscience, King's College London. During the first appointment, a researcher qualified in administering the structured clinical DSM-5-CV, DSM-5-PD, and PCL-R interviews conducted these to assess for mental illness, personality disorders, and psychopathy (First et al., 2015, 2016; Hare, 1991). IQ was assessed using the Wechsler Abbreviated Scale of Intelligence (WASI-II) (Wechsler, 2011). Participants also completed the Reactive-Proactive Aggression questionnaire (Raine et al., 2006). During the second and third appointment, participants underwent a series of MRI scans including the structural scan and completed the neurocognitive test battery. The scanning session occurred twice to address aims of the wider study design which were not relevant to this analysis. The below will detail which structural scan was used for the current analysis.

The study was approved by London City and East Research Ethics Committee (reference: 15/LO/1083) and the National Offender Management Services Research Committee (reference: 2016-382). All participants completed signed informed consent.

### 4.2.3 Image acquisition

Participants were scanned on a General Electric MR750 3.0T MRI scanner using a 32-channel C-RMNova head coil. The high-resolution T1-weighted anatomical image was acquired with full head coverage as part of an identical series of scans conducted on the second and third appointment (SAG ADNI GO ACC MPRAGE, 196 images, slice thickness = 1.2 mm, slice gap = 1.2 mm, TR/TE = 7.31/3.02 ms, TI = 400 ms, FA = 11°, FOV = 270 x 270 $mm^2$, matrix = 256 x 256, resolution = 1.05 x 1.05 x 1.2 $mm^3$).

### 4.2.4 Image pre-processing

The anatomical image from a participant's first scanning session was used for this analysis unless this suffered from considerably more head motion artefacts than the second scan. FSLeyes brain viewer (www.fmrib.ox.ac.uk/fsl/) (McCarthy, 2021) was used to ensure an advanced quality standard for subsequent analysis, as previously established by our group (Gudbrandsen et al., 2019). Data from three participants in the ASPD+P group were excluded due to visibly obvious head motion artefacts indicated by significant blurring, ringing or poor contrast to noise ratio in both scans (Backhausen et al., 2016). Potential minor motion artefacts in the remaining data were corrected for in the automated Freesurfer pipeline (see below).

The FreeSurferv6.0.0 (https://surfer.nmr.mgh.harvard.edu/) cortical surface reconstruction software package was used to obtain measures of CV, CT, and SA. This process is based on an automated and well-validated pipeline (Dale et al., 1999; Fischl et al., 1999) detailed in the Methods chapter (*Figure 3.2*). In summary, this processing stream involves motion correction, skull stripping, automated Talairach transformation to MNI space, volume labelling, intensity normalisation, grey-white matter tissue segmentation, and surface extraction. For surface extraction, Freesurfer uses the white-matter volumes to create a triangular vertex-based cortical mesh on the white matter surface (at the boundary to the grey matter) and the pial surface (the boundary between grey matter and cerebrospinal

fluid). Spatial smoothing was done with a 10-mm full-width half-maximum Gaussian kernel. The resulting white matter and pial surface models were visually inspected to check for surface reconstruction errors and either accepted or manually corrected and reprocessed if required. The current analysis was based on the Desikan-Killiany parcellation atlas.

### 4.2.5 Statistical analysis

Demographic and clinical characteristics and global brain measures were assessed for normality using the Shapiro-Wilk test and compared across the three groups using univariate ANOVA, univariate ANCOVA or Kruskal-Wallis tests. Significant effects were followed by a Tukey post-hoc (for ANOVA), Sidak-corrected pairwise comparisons (for ANCOVA) or Mann Whitney U post-hoc tests (for Kruskal-Wallis: the alpha threshold was Bonferroni-corrected to $p \leq 0.02$ to adjust for multiple post-hoc comparisons). For comparisons between the two offender groups, t-tests or Mann Whitney U were used. Frequencies were assessed using Fisher's exact test. These tests were done in SPSS26 (IBM Corp, 2019).

Cortical surface data was analysed using the Surfstat toolbox (https://www.math.mcgill.ca/keith/surfstat/) in Matlab 2020a (The Mathworks Inc, 2020). Two-way comparisons were used to assess group effects: ASPD+P versus NO, ASPD-P versus NO, and ASPD+P versus ASPD-P. In line with previous studies using this analysis, global brain measures included as covariates were the total estimated intracranial volume (eICV) for the analysis of CV, the mean CT for the analysis of CT, and the sum SA for the analysis of SA (Ecker et al., 2013; Gudbrandsen et al., 2020). Therefore, the effect of group on CV, CT and SA was estimated using a general linear mixed model regression, accounting for mean-centred age and respective mean-centred global brain measures.

The groups did not significantly differ on age or IQ. However, age was included as a covariate given its differential impact on cortical features over time (Lemaitre et al., 2012). Random-field theory-based (RFT) cluster-

corrections for non-isotropic images at $p < 0.05$ were applied to correct for multiple comparisons (Worsley et al., 1999). T-values were displayed on the FreeSurfer high-resolution common-group template in standard space ('fsaverage'), providing an indicator of effect size.

If significant group differences were identified in both CT and SA, the potential degree of spatial overlap between these differences was investigated to explore the shared and distinct underpinning mechanisms of ASPD+/-P. Relative to the total number of vertices with significant group differences (based on the binary patterns of differences generated for each measure in the above analysis), the proportion of vertices with differences in only CT, only SA or both CT and SA was calculated. The proportion of vertices with differences in only CT versus only SA was then compared using a $\chi^2$ test. Furthermore, for vertices that had differences in both CT and SA, a simulation permutation using N = 5000 randomly generated difference patterns was conducted to assess if these vertices came from spatially independent regions. In this analysis, a significant value represented a non-random, spatially independent finding (Gudbrandsen et al., 2019, 2020). Lastly, for clusters with significant between-group differences in CV, the individual contribution of differences in CT or SA was examined using $\chi^2$ tests.

Within each ASPD group, the relationship between cortical abnormalities and relevant phenotypic variables (clinical, behavioural, and cognitive measures) was assessed with partial Pearson correlations. T-values from significant clusters were correlated with PCL-R factor and facet scores, number of violent convictions, presence of a reconviction (violent or non-violent) within one year of study participation, and reactive and proactive aggression scores. The t-values were also correlated with standardized scores from five neurocognitive paradigms measuring emotion recognition and detection, reinforcement-based decision-making, delay discounting and disinhibition (see *Methods chapter* for details). For consistency, mean-centred age and the respective mean-centred global brain measure were

included as covariates of no-interest in all correlations. Boot-strapped 95% confidence intervals were also calculated. Results were corrected for multiple comparison within each ASPD subgroup and phenotypic measure (PCL-R scores, conviction information, aggression, and each of the five neuropsychology paradigms) using false discovery rate (FDR).

## 4.3 Results

### 4.3.1 Demographic and clinical characteristics

The final sample for this study consisted of 18 ASPD+P participants, 19 ASPD-P participants and 23 NO participants. *Table 4.1* contains the details for the demographic and clinical characteristics of the three groups. Offenders with ASPD+P, ASPD-P and NO participants did not significantly differ in age and IQ. However, as expected, the three groups significantly differed on years spent in education, PCL-R total, factor and facet scores, comorbid cluster A and B personality disorders and substance use disorder, presence of positive urine drug screening tests, and total, reactive, and proactive aggression scores. Post-hoc group comparisons are shown in *Table 4.1*. A supplementary post-hoc sensitivity analysis assessed the relationship between the presence of a substance use disorder and neuroanatomical abnormalities (see *Table S1*).

| Demographic | ASPD+P | ASPD-P | NO | Main test statistic | Pairwise comparisons | | |
|---|---|---|---|---|---|---|---|
| N | 18 | 19 | 23 | | ASDP+P vs NO | ASPD-P vs NO | ASPD+P vs ASPD-P |
| Age, mean (SD) | 40.39 (9.76) | 42.32 (10.58) | 38.22 (9.63) | $F_{(2, 57)} = .884$, p = .42 | .77 | .39 | .83 |
| IQ, mean (SD) | 90.94 (11.57) | 97.63 (15.14) | 98.57 (10.69) | $F_{(2, 57)} = 2.12$, p = .13 | .14 | .97 | .30 |
| Years in education, mean (SD) | 10.06 (2.10) | 10.68 (2.00) | 13.74 (3.19) | $H_{(2)} = 19.22$, p < .001 | < .001 | .001 | .30 |
| PCL-R Total, mean (SD) | 28.91 (3.14) | 17.42 (4.17) | 3.00 (3.38) | $H_{(2)} = 51.94$, p < .001 | < .001 | < .001 | < .001 |
| PCL-R Factor 1, mean (SD) | 10.06 (3.21) | 4.86 (2.81) | 1.35 (2.01) | $H_{(2)} = 39.13$, p < .001 | < .001 | < .001 | < .001 |
| PCL-R Facet 1, mean (SD) | 4.50 (1.92) | 1.86 (1.50) | .74 (1.05) | $H_{(2)} = 30.49$, p < .001 | < .001 | < .001 | < .001 |
| PCL-R Facet 2, mean (SD) | 5.56 (1.92) | 3.00 (1.70) | .61 (1.08) | $H_{(2)} = 38.10$, p < .001 | < .001 | < .001 | < .001 |
| PCL-R Factor 2, mean (SD) | 16.22 (1.62) | 11.16 (2.80) | 1.22 (1.54) | $H_{(2)} = 49.99$, p < .001 | < .001 | < .001 | < .001 |
| PCL-R Facet 3, mean (SD) | 7.61 (1.20) | 5.37 (1.67) | 1.04 (1.22) | $H_{(2)} = 46.14$, p < .001 | < .001 | < .001 | < .001 |
| PCL-R Facet 4, mean (SD) | 8.50 (1.29) | 5.75 (2.27) | .57 (1.16) | $H_{(2)} = 46.72$, p < .001 | < .001 | < .001 | < .001 |
| Additional Cluster A, N (%) | 7 (39%) | 0 (0%) | 0 (0%) | 14.80, p < .001 † | .001 | .99 | .003 |
| Additional Cluster B, N (%) | 10 (56%) | 2 (11%) | 0 (0%) | 19.39, p < .001 † | < .001 | .20 | .005 |
| Additional Cluster C, N (%) | 0 (0%) | 2 (11%) | 0 (0%) | 2.99, p = .18 † | .99 | .20 | .49 |
| Substance Use Disorder, N (%) | 4 (22%) | 6 (32%) | 0 (0%) | 9.02, p = .007 † | .03 ◊ | .005 | .71 |
| ADHD, N (%) | 2 (11%) | 1 (5%) | 0 (0%) | 2.47, p = .19 † | .19 | .45 | .60 |
| Positive urine drug test, N (%) | 13 (72%) | 8 (42%) | 5 (22%) | $\chi^2 = 10.50$, p = .005 | .002 | .19 | .10 |
| Total Convictions, mean (SD) | 28.44 (22.84) | 20.00 (15.97) | . | U = 125.50, p = .17 | . | . | . |
| Violent Convictions, mean (SD) | 4.50 (3.17) | 3.74 (2.98) | . | U = 143.50, p = .40 | . | . | . |
| Age 1st Violent Conviction, mean (SD) | 20.12 (5.38) | 21.72 (5.21) | . | $t_{(33)} = -.90$, p = .38 | . | . | . |
| Presence of reconviction within 1 year | 3 (17%) | 3 (16%) | . | 0.005, p = .94 | . | . | . |
| Total Aggression, mean (SD) | 31.07 (9.77) | 18.67 (11.11) | 6.19 (4.25) | $F_{(2, 47)} = 37.15$, p < .001 | < .001 | < .001 | .001 |
| Reactive Aggression, mean (SD) | 16.64 (4.92) | 11.93 (5.55) | 5.67 (3.61) | $F_{(2, 47)} = 24.48$, p < .001 | < .001 | .001 | .02 |
| Proactive Aggression, mean (SD) | 14.50 (6.07) | 6.73 (6.20) | .81 (1.17) | $H_{(2)} = 31.93$, p < .001 | < .001 | < .001 | .004 |

Table 4.1 Demographic and clinical characteristics of participants included in the structural analysis.
*Note: Some participants did not complete the RPQ (final ASPD+P N = 14, ASPD-P N = 15, NO N = 21). SD = standard deviation. F-statistic = ANOVA with Tukey post-hoc, H-statistic = Kruskal Wallis with Mann Whitney U post-hoc, † Fisher's Exact test with Fisher's Exact post-hoc, $\chi^2$ = chi-squared test of independence, U-statistic = Mann Whitney U, t-statistic = t-test. ◊ pairwise comparison did not survive a Bonferroni correction for multiple comparisons (α= .05/3 = .02).*

### 4.3.2 Global brain measures

The three groups did not significantly differ on total eICV, average CT or total SA (*Table 4.2*). Therefore, no post-hoc group comparisons were required.

| Global brain measure | ASPD+P | ASPD-P | NO | Main test statistic [a] |
|---|---|---|---|---|
| Total eICV, $mm^3$, mean (SD) | 643113.41 (64337.66) | 637638.56 (58137.38) | 673678.76 (59479.60) | $F_{(2, 56)} = 1.60$, p = .21 |
| Average CT, $mm^3$, mean (SD) | 2.43 (0.09) | 2.40 (0.09) | 2.48 (0.10) | $F_{(2, 56)} = 2.26$, p = .11 |
| Total SA, $mm^2$, mean (SD) | 172390.35 (17168.09) | 171706.25 (13945.46) | 177447.68 (13945.46) | $F_{(2, 56)} = 1.02$, p = .37 |

Table 4.2 Structural global brain measures.
*Note: Means and standard deviations for each participant group. [a] This statistic was based on an ANCOVA that accounted for age. Abbreviations: SD = standard deviation, eICV = estimated intracranial volume, SA = surface area, CT = cortical thickness.*

### 4.3.3 Cortical volume

In terms of CV, *Figure 4.1* shows that, relative to NO, the offenders with ASPD+P demonstrated significant decreases in the left rostral middle and superior frontal gyri and significant increases in the left precuneus, superior parietal cortex, and cuneus. In contrast, offenders with ASPD-P showed significant decreases in the right inferior temporal gyrus and fusiform gyrus

relative to NO (see also *Table 4.3*). However, ASPD+P did not significantly differ from ASPD-P.

### 4.3.4 Cortical thickness

Relative to NO, offenders with ASPD+P or ASPD-P did not differ significantly in CT. However, as shown in *Figure 4.1*, the ASPD+P group had significantly reduced CT as compared to the ASPD-P group in the left caudal anterior and posterior cingulate cortex (see also *Table 4.3*).

### 4.3.5 Surface area

As *Figure 4.1* shows, there were significant differences in SA between all groups. Compared to NO, violent offenders with ASPD+P showed significantly decreased SA in the left rostral middle and superior frontal gyri and the orbitofrontal region as well as increased SA in the left parieto-occipital region including the precuneus, superior parietal cortex, and cuneus, and the left posterior cingulate cortex. In contrast, relative to NO, the ASPD-P group showed a small cluster of increased SA in the left posterior cingulate cortex. Finally, when comparing the two offender groups, ASPD+P individuals had significantly greater SA than ASPD-P individuals in four clusters, encompassing the bilateral middle and superior frontal gyri and orbitofrontal regions, the left insula, and the right posterior cingulate cortex and paracentral lobule (see also *Table 4.3*).

| Contrast | Cluster ID | Hemisphere | Brain region (Desikan-Killiany Atlas) | Peak vertex Talairach | | | t-value [a] | # Vertices |
|---|---|---|---|---|---|---|---|---|
| | | | | x | y | z | | |
| **Cortical Volume** | | | | | | | | |
| ASPD+P < NO | CV1 | Left | Rostral middle frontal gyrus, superior frontal gyrus | -23 | 44 | 14 | -3.73 | 1442 |
| ASPD+P > NO | CV2 | Left | Precuneus, superior parietal cortex, cuneus | -20 | -68 | 24 | 4.45 | 5722 |
| ASPD-P < NO | CV3 | Right | Inferior temporal gyrus, fusiform gyrus | 45 | -17 | -21 | -3.32 | 2033 |
| **Cortical Thickness** | | | | | | | | |
| ASPD+P < ASPD-P | CT1 | Left | Caudal anterior and posterior cingulate cortex | -3 | 8 | 25 | -3.31 | 553 |
| **Surface Area** | | | | | | | | |
| ASPD+P < NO | SA1 | Left | Rostral middle frontal gyrus, superior frontal gyrus, lateral orbital frontal cortex, inferior frontal gyrus (pars triangularis, pars orbitalis) | -24 | 48 | 12 | -5.29 | 7916 |
| ASPD+P > NO | SA2 | Left | Precuneus, superior parietal cortex, cuneus, pericalcarine cortex, lateral occipital cortex | -21 | -65 | 24 | 4.15 | 6166 |
| | SA3 | Left | Posterior cingulate cortex | -3 | -26 | 26 | 3.16 | 60 |
| ASPD-P > NO | SA4 | Left | Posterior cingulate cortex | -3 | -18 | 27 | 4.32 | 121 |
| ASPD+P > ASPD-P | SA5 | Left | Rostral and caudal middle frontal gyrus, superior frontal gyrus | -9 | 53 | 28 | 4.56 | 5667 |
| | SA6 | Left | Orbital frontal cortex, inferior frontal gyrus (pars triangularis, pars orbitalis), insula | -34 | -21 | 2 | 2.71 | 3251 |
| | SA7 | Right | Rostral middle frontal gyrus, superior frontal gyrus, inferior frontal gyrus (pars triangularis, pars orbitalis) | 19 | 41 | 29 | 3.71 | 8633 |
| | SA8 | Right | Posterior cingulate cortex, paracentral lobule | 4 | -15 | 34 | 3.09 | 1642 |

Table 4.3 Descriptions of clusters with significant group differences in CV, CT, and SA.
*Note: CV = cortical volume, CT = cortical thickness, SA = surface area. [a] This represents the largest (in magnitude) t-value within the significant cluster.*

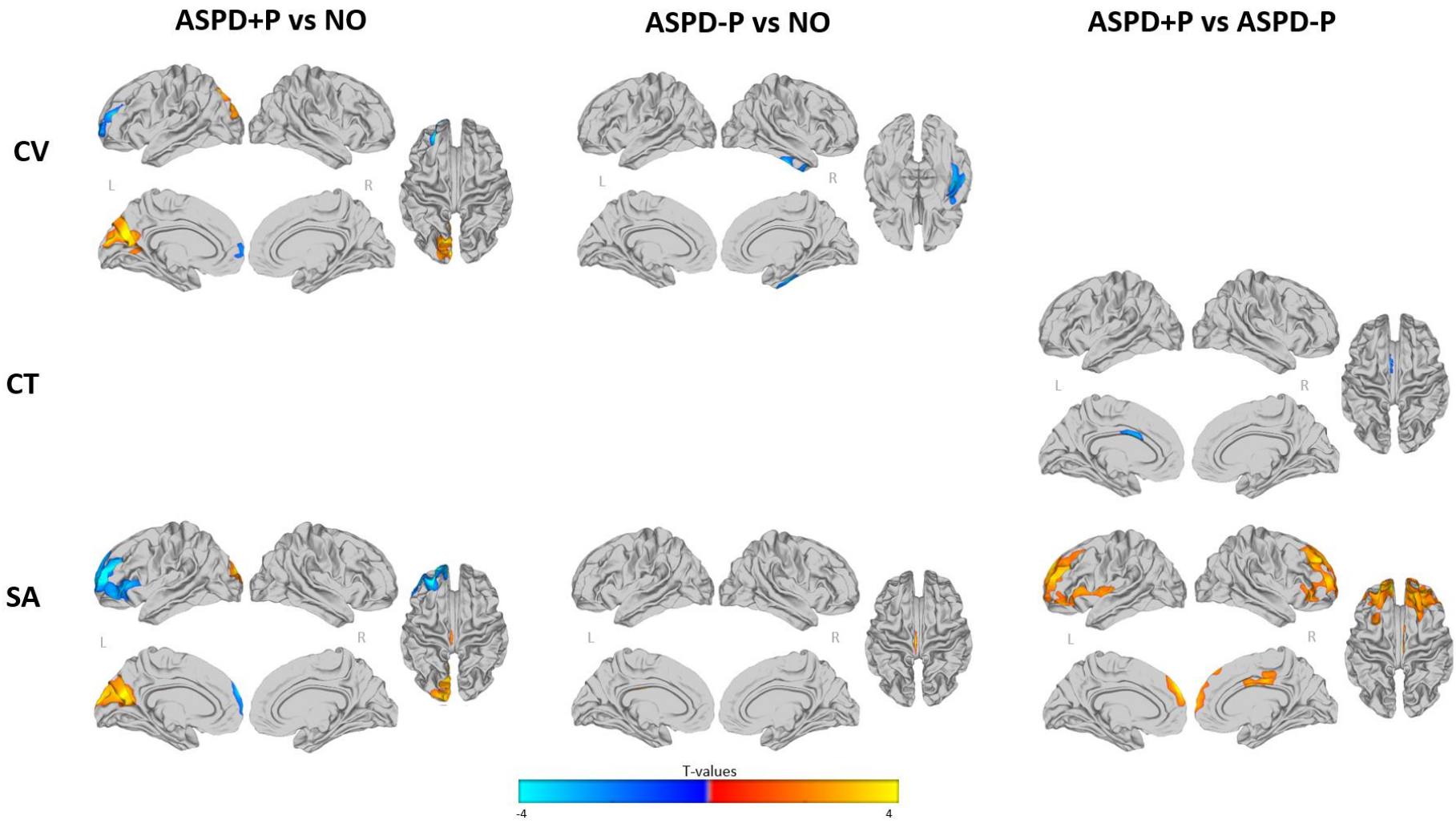


Figure 4.1 Significant group differences in CV, CT, and SA.
*Note: They depict left and right lateral and medial views of t-values which remained significant after RFT-based correction for multiple comparisons at p < 0.05. Blue clusters show decreases, with lighter blue shades representing a more significant decrease. Orange clusters show increases, with lighter orange shades representing a more significant increase. RFT = random field theory, CV = cortical volume, CT = cortical thickness, and SA = surface area.*

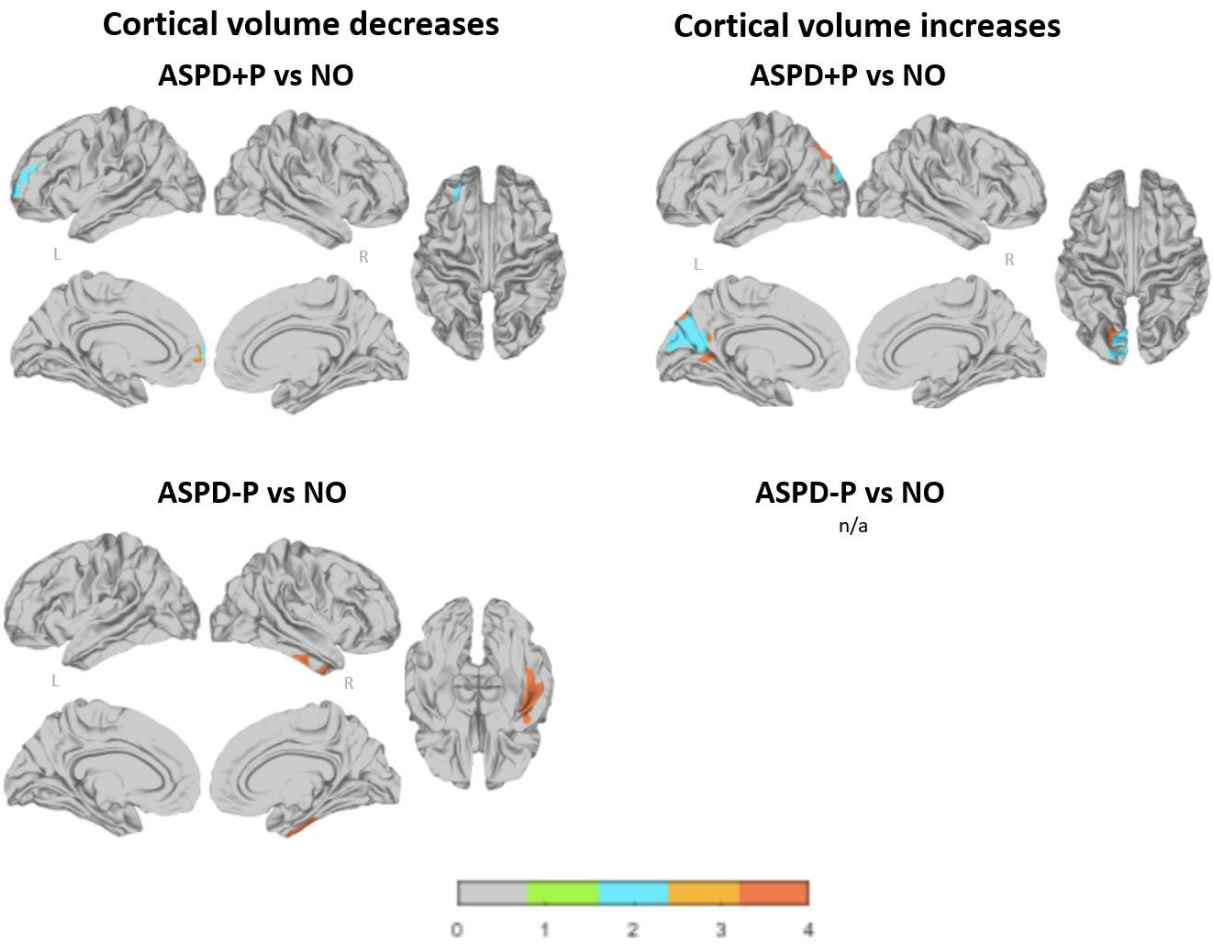


Figure 4.2 Contribution of CT and SA to significant CV abnormalities.

*Note: CV = cortical volume, CT = cortical thickness, SA = surface area; colour mapping: 0 = area with no volume difference, 1 = differences explained by CT only; 2 = differences explained by SA only; 3 = differences explained by both CT and SA; 4 = differences explained most likely by combination of sub-threshold differences in CT and SA.*

### 4.3.6 Spatial overlap of group differences in CT and SA

As noted above, the comparisons between each ASPD+/-P and NO only revealed significant differences in SA but not CT. Thus, assessing the degree of spatial overlap between CT and SA abnormalities was redundant for these group comparisons.

However, when compared to each other, ASPD+P and ASPD-P had significant differences in CT and SA in a total of 19746 vertices (*Table 4.3*). The $\chi^2$ test revealed that significantly more vertices showed a group difference in SA (97.20%, 19193 vertices) than in CT (2.80%, 553 vertices) ($\chi^2_{(df=1)} = 89.11$, $p < .001$). Furthermore, there were no vertices with differences in both SA and CT, so the simulation permutation analysis was

redundant. Abnormalities in CT and SA were thus found in different regions of the brain.

### 4.3.7 Contribution of CT and SA to differences in regional CV

The contribution of CT and SA towards differences in CV was analysed separately in positive and negative CV clusters (*Figure 4.2*). The cluster which showed significantly decreased CV in ASPD+P relative to NO was largely (89.67%) explained by group differences in SA, but not in CT ($\chi^2_{(df = 1)}$ = 89.76, p < .001). Similarly, the cluster that had increased CV in ASPD+P relative to NO was also largely (74.83%) driven by group differences in SA, but not in CT ($\chi^2_{(df= 1)}$ = 74.83, p < .001). The remaining proportions of altered CV in both clusters could not be explained by differences in either CT or SA alone and were therefore likely due to a combination of sub-threshold differences in CT and/or SA.

In contrast, the single cluster which showed significantly decreased CV in ASPD-P relative to NO could not be explained by a difference in either CT or SA alone and was therefore likely due to a combination of sub-threshold changes in CT and/or SA. There were no clusters with increased CV in ASPD-P relative to NO. There were also no significant CV differences between ASPD+P and ASPD-P, meaning the contribution analysis was redundant.

### 4.3.8 Correlation with phenotype

T-values from clusters with significant abnormalities in each ASPD subtype relative to NO were correlated with phenotypic variables (clinical, behavioural, and cognitive measures) using bootstrapped partial Pearson correlations (*Table 4.4*). The only correlation that survived FDR correction for multiple comparisons was in the ASPD-P group, between posterior cingulate SA t-values (i.e., cluster SA4, where ASPD-P had significantly increased SA relative to NO) and reactive aggression. As shown in *Figure 4.3*, as SA in the posterior cingulate increased, reactive aggression in

ASPD-P individuals also significantly increased (r = .73, FDR-corrected p-value = .02, 95% confidence intervals: .272 [lower] – .925 [upper]). *Table 4.4* contains all correlations and indicates the additional two correlations that were significant prior to, but not after, FDR correction for multiple comparisons. These correlations were not further interpreted.

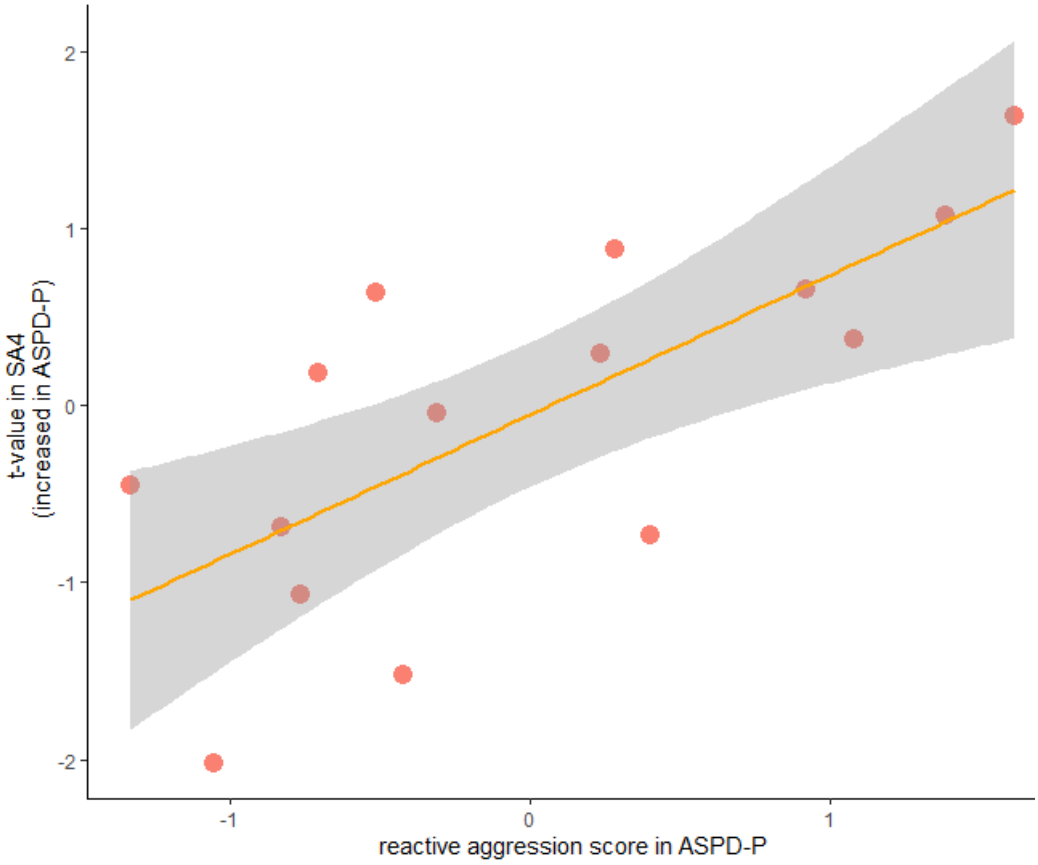


Figure 4.3 Significant positive correlation between posterior cingulate cortex SA and reactive aggression in ASPD-P.
*Note: Result from partial Pearson correlations that survived FDR correction for multiple comparisons. Reactive aggression score reflects the z-standardized residual after accounting for mean-centred age and total SA. Statistical information is provided in Table 4.4. The orange line of best fit indicates that the ASPD-P group had significantly increased SA in this cluster relative to the NO group. SA = surface area.*

| | | ASPD+P (n = 18) | | | | | ASPD-P (n = 19) | |
|---|---|---|---|---|---|---|---|---|
| | | CV1 (<) | CV2 (>) | SA1 (<) | SA2 (>) | SA3 (>) | CV3 (<) | SA4 (>) |
| PCL-R | Total | -.14 | .10 | -.02 | .01 | .26 | -.11 | .02 |
| | Factor 1 | -.14 | .13 | -.07 | .04 | .14 | .01 | .07 |
| | Factor 2 | -.22 | .29 | -.09 | .31 | .18 | -.11 | .03 |
| | Facet 1 | -.02 | -.06 | .08 | -.10 | -.07 | .06 | -.11 |
| | Facet 2 | -.22 | .31 | -.22 | .18 | .32 | -.05 | .22 |
| | Facet 3 | -.05 | .38 | .04 | .41 | -.14 | .15 | .15 |
| | Facet 4 | -.16 | -.01 | -.09 | -.03 | .40 | -.27 | -.08 |
| Conviction information | # past violent convictions | -.14 | .16 | .11 | .11 | .02 | -.30 | -.24 |
| | 1 year reconviction | .05 | .06 | .20 | .20 | .38 | .02 | -.02 |
| Aggression [a] | RPQ-Reactive | -.02 | .45 | -.05 | .47 | -.23 | -.20 | **.73 ** ** |
| | RPQ-Proactive | -.34 | .52 | -.32 | .58 * | -.12 | .03 | .59 * |
| Emotion recognition (accuracy) [b] | Angry | -.29 | -.05 | -.27 | .04 | -.18 | -.03 | -.18 |
| | Sad | -.27 | -.43 | -.12 | -.37 | .01 | .25 | -.32 |
| | Fear | .16 | -.14 | .13 | -.08 | -.35 | -.14 | -.04 |
| Emotion detection (reaction time) [b] | Angry | -.26 | .10 | -.29 | .06 | -.09 | .20 | .16 |
| | Fear | -.21 | .24 | -.24 | .21 | -.01 | -.23 | .13 |
| Reinforcement-based decision-making (accuracy) [c] | Acquisition learning | -.07 | .002 | .14 | .04 | .42 | -.07 | -.14 |
| | Response reversal | .39 | -.28 | .39 | -.15 | .36 | .24 | .18 |
| Delay discounting (# of times lesser value chosen) [c] | 7 days | .04 | -.52 | .28 | -.49 | -.21 | -.09 | -.16 |
| | 30 days | .11 | -.41 | .32 | -.37 | -.21 | -.09 | -.08 |
| | 90 days | .08 | -.42 | .27 | -.41 | -.16 | .01 | -.17 |
| | 180 days | .04 | -.51 | .19 | -.50 | -.15 | .10 | -.15 |
| | 360 days | -.14 | -.28 | .02 | -.29 | -.29 | .04 | -.06 |
| Disinhibition [c] | SSRT | .42 | -.22 | .28 | -.26 | .41 | -.13 | .32 |

Table 4.4 Partial Pearson coefficients for structure-phenotype correlations.
*Note: correlations between phenotypic characteristics and significant clusters found in the contrast between ASPD+P and NO in CV and SA, as well as in the contrast between ASPD-P and NO in CV and SA. Mean-centred age and the respective mean-centred global brain measure were included as covariates of no-interest. Bold font indicates significance after FDR correction for multiple comparisons. Note: * = uncorrected p-value < .05, ** = uncorrected p-value < .01; (<) reflects a decrease and (>) reflects an increase in the group comparison; CV = cortical volume, SA = surface area, SSRT = stop signal reaction time. Not all participants completed all study parts: [a] ASPD+P N = 14, ASPD-P N = 15, [b] ASPD+P N = 16, ASPD-P N = 18, [c] ASPD+P N = 15, ASPD-P N = 19.*

## 4.4 Discussion

To disentangle the neuroanatomical substrates of male violent offenders with ASPD+/-P, the current study had two main aims. First, to directly compare CV, CT, and SA between violent offenders with ASPD+P, ASPD-P, and healthy NO controls; and second, to assess the extent to which CT and SA independently contribute towards potential CV abnormalities. It was hypothesized that both ASPD groups would show decreased CV and CT relative to NO – with more significant reductions in ASPD+P than ASPD-P – and that both groups would show increased SA relative to NO. Findings partially supported these hypotheses. Specifically, they demonstrated that ASPD+P relative to NO had significantly decreased CV and SA in rostral prefrontal regions and significantly increased CV and SA in parieto-occipital regions. There were no significant differences in CT between ASPD+P and NO. The results also demonstrated that ASPD-P relative to NO had significantly decreased inferior temporal lobe CV and significantly increased

SA in the posterior cingulate cortex. Again, there were no differences in CT between ASPD-P and NO. Finally, when directly comparing the two ASPD groups, the analyses demonstrated that ASPD+P relative to ASPD-P had significantly decreased CT in the cingulate cortex and significantly increased SA in frontotemporal and posterior brain areas. With respect to the second aim, it was hypothesized that the two ASPD groups would show different patterns of contribution of CT and SA towards CV abnormalities. Results from this novel analysis supported the hypothesis. Specifically, in ASPD+P but not ASPD-P, abnormalities in CV were primarily driven by abnormalities in SA. In summary, for the first time, the current study demonstrated that violent offenders with ASPD+P or ASPD-P have distinct neuroanatomical profiles not only in CV, but also in CT and SA, in areas important for social cognition, and that such differences in CV are likely driven by distinct neurobiological mechanisms (as measured by CT and SA). Finally, the exploratory correlations with phenotypic measures revealed that posterior cingulate SA was positively associated with reactive aggression in ASPD-P individuals. These results will be discussed below.

The finding of CV abnormalities in ASPD+P as compared to NO aligns with existing evidence, however, it also demonstrated that ASPD+P is not only distinctly associated with CV decreases, but also CV increases. Notably, the finding of decreased rostral prefrontal CV reinforces results by Gregory et al. (2012), which is the only previous study that also directly compared CV in ASPD+/-P to NO samples using the same methodological approach as the current study (Gregory et al., 2012). Furthermore, this finding also converges with meta-analytical evidence of reduced prefrontal CV in psychopathy (De Brito et al., 2021; Deming & Koenigs, 2020; Yang & Raine, 2009). Similarly, the finding that ASPD+P demonstrated increased CV in parieto-occipital areas relative to NO partially aligns with previous results. On the one hand, it supports results from a meta-analysis of individuals with clinically significant antisocial traits including callous-unemotional traits in childhood and psychopathy in adulthood. It reported increased CV

in this region, specifically in the superior parietal cortex, which was preserved after controlling for the effect of age (Aoki et al., 2014). On the other hand, meta-analyses focusing on psychopathic samples have found reductions or no volumetric changes in this region (De Brito et al., 2021; Deming & Koenigs, 2020). These latter meta-analyses did not confirm the presence of ASPD in their psychopathic samples, meaning findings cannot be clearly compared with the current ones. Overall, it appears that reduced rostral medial and orbitofrontal CV is a consistently reported neuroanatomical associate of ASPD+P. Such reductions might contribute to abnormalities in executive function such as attention and affective decision-making (Benoit et al., 2012; Hiser & Koenigs, 2018), which are particularly characteristic of ASPD+P (see *Table 1.4*). In contrast, findings of aberrant parieto-occipital CV are more variable.

It has been argued that the variability of neuroanatomical findings within the psychopathy literature can be partially attributed to inconsistent definitions of psychopathy and control groups (Griffiths & Jalava, 2017). For instance, some studies have used low thresholds for psychopathy (e.g., PCL-R score of 20 rather than 25 (in Europe) or 30 (in North America)), thus overrepresenting individuals scoring far below the threshold in so-called forensic psychopathic samples. Other studies have used control groups that included offenders or individuals with low psychopathy scores, meaning these control groups are not representative of healthy, non-offending individuals. In contrast to this, the current study benefitted from precise group definitions. Thus, although it adds to the variability in the literature, the finding of increased parieto-occipital CV in ASPD+P should not be disregarded.

Another factor that contributes to the variability in the literature is differences in analytic techniques. To delineate the neuroanatomical mechanisms underpinning ASPD and psychopathy, this study relied on a surface-based analytic technique, as this provides insight into CT and SA in addition to CV. The present findings demonstrated that, in ASPD+P relative

to NO, the abnormalities in CV corresponded with abnormalities in SA. In other words, rostral prefrontal regions which had reduced CV also showed reduced SA, whereas parieto-occipital regions which had increased CV also showed increased SA. There were no significant abnormalities in CT when compared to NO. It was therefore not surprising that the contribution analysis revealed that aberrant CV in the ASPD+P group was primarily driven by aberrant SA, but not CT. Overall, this represented the first study to compare CT and SA between offenders with ASPD+P and NO controls, revealing SA but not CT abnormalities in individuals with ASPD+P.

In addition to revealing cortical surface abnormalities in ASPD+P, the current findings also demonstrated abnormalities in ASPD-P, albeit in different brain regions and less widespread. This indicates that psychopathy does differentially impact the neuroanatomical substrates of ASPD. Relative to NO, ASPD-P was marked by reduced inferior temporal lobe CV. This aligns with findings from existing studies of ASPD that also showed volume reductions; however, these studies could not disentangle the impact of psychopathy on their findings. For instance, some studies were limited by a lack of capturing psychopathy (Barkataki et al., 2006; Kaya et al., 2020; Raine et al., 2011). Another study of violent offenders only measured psychopathic traits continuously and reported strong negative correlations between CV and the PCL-R social deviance factor only (Hofhansel et al., 2020). The social deviance factor captures antisocial-impulsive traits and behaviours that are typically found in individuals with ASPD regardless of additional psychopathy. Thus, it could be argued that Hofhansel et al.'s findings showed that CV reductions were not driven by the interpersonal-affective traits typically associated with additional psychopathy. The current study clarified existing literature by disentangling the categorical impact of psychopathy in ASPD and revealing that decreased inferior temporal lobe CV in individuals with ASPD cannot be attributed to the presence of psychopathy. Nevertheless, it must be acknowledged that several previous studies reported volume loss in the inferior temporal and fusiform gyrus in

ASPD+P but not ASPD-P individuals (De Brito et al., 2021; Gregory et al., 2012; Tiihonen et al., 2008). This directly contradicts the current findings and means that further investigation into the role of psychopathic traits on CV abnormalities in this region is required.

Beyond CV, the current study also compared CT and SA between ASPD-P and NO groups for the first time. There were no significant group differences in CT. Moreover, only a small cluster in the posterior cingulate cortex had increased SA. It was therefore not surprising that there were no clear, above-threshold contributions of either cortical feature to explain the reduced inferior temporal lobe CV. Instead, it is likely that sub-threshold differences in both CT and SA were driving the CV reductions found in the ASPD-P group. The only other study that has assessed SA in individuals with ASPD also reported increased SA relative to controls, albeit in more widespread frontotemporal and parietal brain regions and not in the posterior cingulate cortex (W. Jiang et al., 2016). However, they did not measure the impact of psychopathic traits. Considering the present finding that ASPD+P had widespread SA increases, it is possible that Jiang et al.'s finding was related to the presence of more severe psychopathic traits in their sample as compared to the current ASPD-P sample. This means that they may have overestimated SA abnormalities. Together, this indicates that further exploration of potential SA abnormalities in ASPD-P individuals is required.

In the current study, this small cluster of increased posterior cingulate cortex SA also significantly positively correlated with self-reported reactive aggression in ASPD-P. High reactive aggression is a key feature of ASPD-P (Azevedo et al., 2020), and the current ASPD-P group also scored significantly higher than the NO group. This represents the first time that a surface-based structural abnormality has been associated with aggression in adults with ASPD. However, it has been previously reported that structural abnormalities, including increased CT in the posterior cingulate cortex, are correlated with increased reactive aggression in youth with CD

(Y. Jiang et al., 2022; Yang et al., 2017). The posterior cingulate cortex is an important communication hub that is linked to many regions of the brain (Leech & Sharp, 2014). It is possible that structural abnormalities disrupt this communication, which in turn contributes to mechanisms involved in reactive aggression such as impulsivity (J. Zhao et al., 2017). However, considering the limited statistical power due to the small sample size for the correlation analyses, further investigations with larger sample sizes should be conducted to establish a clearer picture the relationship between CT and SA abnormalities and aggression in individuals with ASPD.

Overall, the current results so far indicate that ASPD+P and ASPD-P have different patterns of cortical surface abnormalities relative to NO. More support for this conclusion was found in the direct comparisons between ASPD+P and ASPD-P. These novel analyses could address whether the ASPD subtypes truly differed from each other, or whether, as the above has shown, they simply have differing neuroanatomical profiles relative to the healthy NO control population. The findings suggested that the two groups differed from each other in terms of CT and SA, but not in CV. Specifically, when compared to ASPD-P, ASPD+P had significantly reduced CT in the cingulate cortex and significantly increased SA in several prefrontal and posterior regions. The finding of reduced cingulate cortex CT confirms the limited previous evidence of cortical thinning in this and other frontotemporal brain areas in adults with psychopathy and youth with CD and callous-unemotional traits (Calzada-Reyes et al., 2021; Ly et al., 2012; G. L. Wallace et al., 2014; Yang et al., 2009). Together, this evidence implies that ASPD+P but not ASPD-P is characterized by CT reductions. However, this conclusion is tentative since the cluster was relatively small and findings were not replicated when comparing ASPD+P to the NO group. In terms of SA, the finding of widespread SA increases in ASPD+P relative to ASPD-P confirms the suggestion that the presence of psychopathy in ASPD is distinctly related to aberrant SA.

The current findings therefore suggest a series of cortical surface abnormalities that are distinctly associated with ASPD+P. Particularly the novel findings of significantly different patterns of SA and CT abnormalities relative to ASPD-P and NO are important since it is known that these two neuroanatomical features have unique genetic determinants and subsequent neurodevelopmental trajectories (Panizzon et al., 2009; Wierenga et al., 2014). For instance, it has been shown that SA has higher heritability estimates than CT, especially near the parietal regions identified in the current study such as the precuneus (Eyler et al., 2012; Patel et al., 2018), and that SA is more stable over time (Lemaitre et al., 2012; Storsve et al., 2014). Genetic analyses have shown that psychopathy and callous-unemotional traits are particularly heritable (Viding et al., 2005). Although distinct genes have not been identified and most candidate gene and genome-wide association studies are underpowered (Griffiths, Jalava, Larsen, et al., 2022; Gunter et al., 2010), the current finding could provide impetus to investigate whether genetic markers for SA are implicated in the genetic risk for ASPD+P. Furthermore, early trauma and significant life adversities are common in individuals with ASPD and psychopathy (DeLisi et al., 2019), and it has been shown that the development of SA but not CT is vulnerable to the impact of such adversities (Hodel et al., 2015). Thus, both genetic and environmental risk factors might modulate neurodevelopmental processes associated with SA. Longitudinal studies will help disentangle these developmental trajectories further. One such study, the longitudinal Dunedin birth cohort study following individuals with LCP versus adolescence-limited antisocial behaviour showed SA but not CT abnormalities in those with LCP antisocial behaviour (Carlisi et al., 2020). This supports the notion that particularly aberrant surface structure is associated with the development of LCP antisocial behaviour. However, the role of psychopathic traits was not clear in this study. Future research using longitudinal designs to measure the contribution of SA and CT towards CV in youth with conduct disorder with and without callous-unemotional traits and adults with ASPD with versus without psychopathy is needed. In

summary, the current findings provide support that neuroanatomical underpinnings of ASPD+P and ASPD-P are different, and that these may have differential neurodevelopmental origins.

Some limitations of the current study should be considered when interpreting the results. First, ASPD is a disorder that is associated with several other comorbidities, particularly substance use disorders (Coid et al., 2006; Coid, Yang, Ullrich, Roberts, & Hare, 2009; Trull et al., 2010). Although these were measured in the current sample, they were not added to the model as covariates. This was chosen to avoid overcorrecting and removing important variance since these features are inherently already captured in the core ASPD phenotype. It is nonetheless possible that the comorbidities impacted the neuroanatomical profiles found within ASPD+/-P. However, a sensitivity analysis showed that the presence of a lifetime substance use disorder did not significantly predict neuroanatomical findings in either ASPD subtype. Second, the current study was focused on males only. Although ASPD and psychopathy are more common in males, and males make up the majority of violent offenders within the prison system (Fazel & Danesh, 2002), the current findings cannot be extrapolated to females with ASPD+/-P. Finally, there were some limitations with respect to the statistical power of the study. For instance, it is possible that the study was not adequately powered to detect CV differences between ASPD+P and ASPD-P. Moreover, some of the significant clusters had a small number of vertices and may not be found to have significance if a stricter RFT-based correction (e.g. $p < .01$) was applied.

In conclusion, the current study was the first study to compare CV, CT, and SA between violent offenders with ASPD+P or ASPD-P relative to healthy NO controls and to each other. It demonstrated that the two ASPD subtypes have distinct neuroanatomical profiles compared to NO but also compared to each other. Thereby, it helped to clarify the role that psychopathy plays in the context of the neurobiological underpinnings of ASPD and suggests that ASPD+P and ASPD-P form more biologically homogenous subtypes of

the heterogenous ASPD construct. This study was also the first time that the contribution of SA and CT towards CV was assessed in this population. SA, but not CT, explained aberrant CV in ASPD+P only, suggesting distinct neurodevelopmental mechanisms between the two ASPD subtypes. Overall, this study added neurobiological evidence to the behavioural evidence (such as those related to offending and aggression) that ASPD+P and ASPD-P should be distinguished. These findings have implications for future research, which should routinely assess neuroanatomical features beyond CV while also focusing on comparing ASPD+P and ASPD-P according to a consistent definition of psychopathy. They also have important clinical implications. Specifically, diagnostic approaches and treatment trials should clearly differentiate between the two ASPD subtypes to move towards a more personalized medicine approach and identify better treatment options.

# 5 An arterial spin labelling investigation to measure regional cerebral blood flow and the effect of intranasal oxytocin in violent offenders with ASPD

## 5.1 Introduction

Individuals with antisocial personality disorder with or without psychopathy (ASPD+/-P) have functional neural abnormalities in limbic and paralimbic frontotemporal brain regions when compared to healthy non-offending individuals. For instance, meta-analyses have reported aberrant neural responsivity in brain areas such as the orbitofrontal cortex, anterior cingulate cortex, amygdala, and insula during resting-state as well as during neurocognitive tasks (Deming & Koenigs, 2020; Dugré et al., 2020; Dugré & Potvin, 2021). Furthermore, there are functional brain differences between ASPD+P and ASPD-P when these groups are directly compared to each other. Specifically, ASPD+P is marked by abnormal frontotemporal activity during emotion and reward processing relative to ASPD-P (Gregory et al., 2015; Tully et al., 2022). These latter findings were important first steps because they suggest that there may be different underpinning functional mechanisms associated with each subtype of ASPD. However, these two studies measured task-related brain activity according to the blood-oxygen-level-dependent (BOLD) contrast, which is only an indirect proxy measure of neural activity. Thus, it remains unknown whether there are differences between ASPD+P and ASPD-P in resting-state activity, and whether such differences are also found when using more direct measures of neural activity such as regional cerebral blood flow. Furthermore, it has also not been assessed whether such differences between ASPD+/-P can be modified, for example by pharmacological agents. Arterial spin labelling (ASL), a neuroimaging technique designed to measure rCBF and the impact

of potential treatments, can be used to address these gaps in the evidence base.

Regional cerebral blood flow (rCBF) refers to the perfusion of blood and its metabolic nutrients including oxygen and glucose from cerebral capillaries into brain tissue. It provides direct physiological quantification of spontaneous or task-related neural activity. It does not suffer from the same limitations as the BOLD contrast, which can only measure neural activity indirectly as a complex interaction between rCBF, blood volume and oxygen metabolism (Simon & Buxton, 2015; Stewart et al., 2014). ASL offers an endogenous, non-invasive measure of rCBF with improved spatial resolution and excellent test-retest reliability (Borogovac & Asllani, 2012; Hodkinson et al., 2013). Furthermore, ASL imaging is particularly sensitive to detect the effects of pharmacological challenges on the brain (Bloomfield et al., 2020; Bryant et al., 2019; Martens et al., 2021; Stewart et al., 2014), with observable dose-dependent changes in rCBF (Martins, Brodmann, et al., 2022). ASL is thus a useful tool to investigate if resting-state rCBF is abnormal in ASPD+/-P.

Only a small number of studies have measured rCBF in individuals with ASPD or psychopathy. They all used resting-state single photon emission computed tomography (SPECT) or task-based positron emission tomography (PET) imaging. These studies demonstrated decreased rCBF in frontotemporal cortical and subcortical brain regions in adults with ASPD or psychopathy (Goethals et al., 2005; Kolla & Houle, 2019; Kuruoglu et al., 1996; Soderstrom et al., 2000, 2002; Sutherland & Fishbein, 2017). However, these prior studies were limited by the inclusion of heterogenous clinical samples, use of large regions of interest, and reliance on visual judgement of perfusion data. To date, no study in ASPD+/-P has used ASL to assess rCBF abnormalities, related this to the clinical phenotype, and/or investigated if these putative differences can be modified by potential treatment agents.

One such agent is oxytocin, a neuropeptide central to the regulation of complex social behaviours, that has a heightened receptor distribution in areas implicated in ASPD, including the insula and amygdala (Boccia et al., 2013; Quintana, Rokicki, et al., 2019). The only existing study using intranasal oxytocin (OT) as an experimental probe in adults with ASPD demonstrated that it increased BOLD activity in the anterior insula and anterior cingulate cortex of violent offenders with ASPD+P but not ASPD-P when they were implicitly engaged in processing others' fearful faces (Tully et al., 2022). However, as noted above, the BOLD signal is a proxy measure of brain activity, and it is unknown if OT can modulate direct measures such as rCBF in ASPD+/-P. In healthy individuals, ASL studies have demonstrated that OT altered rCBF in subcortical and cortical brain regions that contribute to sociocognitive processes which have been identified to be impaired in ASPD+/-P. This includes reports that OT decreased rCBF in the amygdala and increased it in the anterior insula and basal ganglia structures such as the globus pallidus and striatum (Martins, Mazibuko, et al., 2020; Paloyelis et al., 2016). It remains to be investigated whether OT can alter rCBF in ASPD+/-P, and whether this also differs between ASPD+P and ASPD-P. If so, this may have implications for developing treatments for ASPD+/-P. However, nobody has assessed this.

Hence, the current study represents the first double-blind, placebo-controlled, randomised crossover study in male violent offenders with ASPD+P and ASPD-P and healthy non-offenders to examine the impact of OT on resting-state rCBF using ASL imaging. It was hypothesized that (1) both ASPD groups would show reduced frontotemporal rCBF compared to non-offenders (NO), and (2) that there would be further reductions in ASPD+P relative to ASPD-P. Furthermore, considering the finding that OT increased BOLD activity in ASPD+P only (Tully et al., 2022), it was hypothesized that (3) OT would increase rCBF in frontotemporal regions (particularly anterior insula) in ASPD+P but not ASPD-P. Finally, this study also sought to explore the relationship between potential rCBF

abnormalities, rCBF responsivity to OT, and phenotypic characteristics of ASPD+/-P. As this was exploratory, no distinct hypotheses were made.

## 5.2 Methods

### 5.2.1 Participants

This study included 39 male violent offenders with a diagnosis of ASPD and 23 male NO participants. All participants were aged between 18 and 60 years old at the time of study enrolment and had an IQ above 70. Offenders with convictions for assault, actual/grievous bodily harm, armed robbery, rape, manslaughter, and/or murder were recruited from South London national probation services and medium secure forensic inpatient services. The diagnosis of ASPD was confirmed using the SCID-5-PD (First et al., 2015). Offenders with a comorbid mood or psychotic disorder were excluded. According to the European clinical cut-off for psychopathy on the PCL-R, violent offenders were categorized as ASPD+P if they scored ≥25 (n = 20) or ASPD-P if they scored <25 (n = 19) (Cooke & Michie, 1999; Hare, 1991). The NO participants were recruited from the general population in the local community through public and online advertising via purposive sampling. They were excluded if they had a history of offending or a current or past mental illness, substance use disorder, or personality disorder. The presence of neurological trauma, illness, or magnetic resonance imaging (MRI) safety contraindications (e.g., claustrophobia) was grounds for exclusion across all participants.

The study was approved by London City and East Research Ethics Committee and the Health Research Authority (reference: 15/LO/1083), as well as the National Offender Management Services Research Committee (reference: 2016-382). All participants completed signed informed consent.

### 5.2.2 Study design and procedure

This study had a double-blind, placebo-controlled, randomised crossover design. Participants attended an assessment appointment during which clinical (SCID-5-CV) (First et al., 2016), personality (SCID-5-PD, PCL-R)

and IQ (WASI-II) (Wechsler, 2011) assessments were conducted. Participants completed the Reactive-Proactive Aggression Questionnaire (RPQ) (Raine et al., 2006). During two further appointments scheduled on average 16 days apart, structural and ASL scans, as well as neurocognitive testing were conducted. Participants completed urine drug screening tests to assess for recent substance use on each of these two appointments. The participant was randomly and blindly allocated 40 IU of OT (Syntocinon, Novartis, Switzerland) or a placebo nose spray (PL; same ingredients but without the oxytocin), receiving the other spray on their second appointment. They self-administered the spray by inhaling one puff every 30 seconds through alternating nostrils, for 5 minutes. The researcher supervised this process to ensure correct administration. The oxytocin dose was selected in line with safety standards and previous studies measuring effects of OT on rCBF (MacDonald et al., 2011; Martins, Brodmann, et al., 2022; Martins, Mazibuko, et al., 2020; Paloyelis et al., 2016). The ASL scans (06:23 minutes) were acquired on average at 84 (±9) minutes and 85 (±12) minutes after administration of PL and OT, respectively. This time delay is referred to as the variable 'minutes since dose'.

### 5.2.3 Image acquisition

A General Electric MR750 3Tesla MRI scanner and 32-channel C-RMNova head coil was used for this study. A 3-dimensional pseudo-continuous ASL scan was acquired during each session (60 slice partitions with thickness and gap = 3 mm, TE = 1109 ms, TR = 5180 ms, FA = 111°, FOV = 240 x 240 $mm^2$, matrix = 518 x 8, in-plane resolution = 3.6 mm). During acquisition, participants were instructed to remain still, stay awake and focus on a fixation cross. This scanning sequence acquires a proton density (PD) image as well as a labelled and a control perfusion-weighted image. The labelled perfusion-weighted image is based on a measurement of the magnetically labelled arterial blood water which functions as an endogenous tracer. It is created by applying a 180° Hanning-shaped radiofrequency inversion pulse (1825 ms) and, after a brief delay (2025

ms), measuring the net magnetisation of brain tissue. Net magnetization reduces after applying the inversion pulse, leading to a decrease in MRI signal and image intensity. The control image is acquired in a similar manner however without applying the inversion pulse. The control image is then subtracted from the labelled image. The current sequence acquired 5 control-label pairs and averaged these to improve signal-to-noise ratio. The image resulting from the control-label subtraction is calibrated against the PD image to create the final cerebral blood flow (CBF) map, which is a linear representation of rCBF in each voxel (see *Figure 3.3*). These steps are in line with recent recommendations for acquiring ASL (Alsop et al., 2015).

A 3D high-resolution T1-weighted whole-brain anatomical image was also acquired during each scanning protocol (SAG ADNI GO ACC MPRAGE, 196 slices with thickness and gap = 1.2 mm, TE = 3.02 ms, TR = 7.31 ms, TI = 400 ms, FA = 11°, FOV = 270 x 270 $mm^2$, matrix = 256 x 256, voxel resolution = 1.05 x 1.05 x 1.2 $mm^3$). The current analysis used the same scan that was used in the structural analysis for each participant.

### 5.2.4 Image pre-processing

A preliminary quality check of the CBF maps for both scans of each participant was conducted using FSLeyes (McCarthy, 2021). Regional CBF values were confirmed to be between 20 and 110 ml/100 g/1 min, indicating accurate computation of the CBF maps from the MRI signal (Alsop et al., 2015). Scans were also assessed for excessive movement indicated by significant blurring. Pre-processing was conducted in the Automatic Software for ASL Processing (ASAP) toolbox, version 4.0 in Matlab 2018b (Mato Abad et al., 2016). For each scan, pre-processing steps included (1) co-registration of the PD image to the participant's T1 anatomical image; (2) application of the co-registration transformation matrix to the participant's CBF map to normalize the CBF image into the space of the T1 image; (3) skull-stripping, segmentation and removal of extra-cerebral signal from the normalized CBF map; (4) partial volume correction and normalization of the CBF map to MNI152 space; and (5) spatial smoothing

of the CBF map with an 8mm Gaussian kernel. Finally, an explicit grey matter tissue probability mask to threshold and retain all CBF map voxels with at least 20% probability of being grey matter was applied.

### 5.2.5 Statistical analysis

Demographic and clinical characteristics were compared using SPSS26 (IBM Corp, 2019). Analyses included ANOVA and Chi-squared ($\chi^2$) tests, or their non-parametric equivalent (Kruskal-Wallis, Fisher's exact) in case the assumption of normality (Shapiro-Wilk test) was not met. Bonferroni-corrected pairwise comparisons were conducted to interpret a significant main effect. Global median CBF was compared across groups and treatment type using a two-way mixed ANCOVA, covarying for mean-centred age and mean-centred minutes since dose.

An exploratory whole-brain analysis was conducted in SPM12 (www.fil.ion.ucl.ac.uk/spm/software/spm12). The following analyses were based on a partitioned errors approach rather than a simple mixed ANCOVA analysis of covariance to avoid violating common assumptions of repeated measures design (McFarquhar et al., 2016). The data was prepared for this approach to ensure appropriate assessment for each main effect (group and treatment) and their interaction effect. To analyse the main effect of group, an average of the treatment conditions (the PL and OT CBF maps) for each individual was created. A one-way ANOVA was then used to compare the three groups. To test the main effect of treatment, the PL CBF map was subtracted from the OT CBF map for each participant and analysed using a one-sample t-test. Finally, to assess the group by treatment interaction effect, the subtracted images for each participant were compared across the three groups using a one-way ANOVA. Global median CBF, age, and minutes since dose were included as covariates of no-interest. An F-contrast was calculated for each main and interaction effect. A whole-brain cluster-level inference at $\alpha = 0.05$ using family-wise error correction for multiple comparisons was applied. Only clusters which survived the cluster-defining threshold of $p = 0.005$ were interpreted. This

is in line with other studies using similar designs (Martins, Leslie, et al., 2020). For any significant group, treatment or group by treatment interaction effect, a binary mask of the significant cluster(s) was created within SPM. These masks were then used to extract raw CBF values within these significant clusters. To interpret F-contrasts in significant clusters, these raw values were compared using post-hoc pairwise comparisons or simple main effects tests with the Sidak correction for multiple comparisons in SPSS26.

A supplementary ROI analysis focused on the amygdala and anterior insula. These regions were selected *a priori* since prior studies assessing ASPD+/-P have consistently demonstrated abnormal neural functioning in these regions (Deming & Koenigs, 2020; Dugré et al., 2020; Dugré & Potvin, 2021), with differences between the two subtypes also identified (R. J. R. Blair, 2010; Fanti et al., 2019; Gregory et al., 2015; White et al., 2016). Moreover, prior studies have shown effects of OT on rCBF in these areas in healthy individuals (Martins, Brodmann, et al., 2022; Martins, Mazibuko, et al., 2020; Paloyelis et al., 2016). A binary mask based on the FSL-distributed Harvard-Oxford Atlas was applied to extract median rCBF in the ROIs. To assess group and treatment effects a linear mixed model (with bootstrapping, 1000 samples) including group, treatment and group by treatment as fixed effects and subject as the random effect was run in JASP (JASP Team, 2021). Global median CBF, age, and minutes since dose were all mean-centred and included as covariates of no-interest. The main effects were corrected for multiple comparisons using false discovery rate (FDR). For any main or interaction effect that remained significant after correction, Holm-corrected pairwise comparisons and simple main effects were used to further dissect these effects.

Partial Pearson correlations (SPSS26) were used to assess the relationship between rCBF and phenotypic features (clinical, behavioural, and cognitive measures) across all individuals with ASPD+/-P. Specifically, for correlations with baseline group differences in rCBF, raw rCBF values from

clusters with significant group differences were extracted and averaged over treatment conditions. Moreover, to assess the correlation with differential responsivity to OT, raw rCBF values from clusters with a significant group by treatment interaction effect (if simple main effects revealed significant change within the ASPD group) were extracted. A delta score (OT rCBF minus PL rCBF) was then calculated and used in the correlations. Clinical and behavioural features included the PCL-R factor and facet scores, the number of previous violent convictions and the presence of a reconviction (violent or non-violent) within one year of study participation, and the RPQ questionnaire reactive and proactive aggression scores. Cognitive variables included standardized scores from five neurocognitive paradigms measuring emotion recognition and detection, reinforcement-based decision-making, delay discounting, and disinhibition (see *Methods chapter* for details). Global median CBF, age, and minutes since dose were included as covariates of no-interest. These analyses were only conducted within ASPD participants since the phenotypic variables were not of interest or relevance in the NO group. Moreover, they were conducted across all ASPD participants as one group. However, by design, the two ASPD subgroups differed on average for PCL-R scores. Thus, to avoid spurious (illusory) correlations between CBF group differences and PCL-R scores, group was added as a further covariate in these correlations. Boot-strapped 95% confidence intervals were also calculated. Results were FDR-corrected for multiple comparisons within each phenotype cluster (PCL-R scores, conviction information, aggression, and each of the five neuropsychology paradigms).

## 5.3 Results

### 5.3.1 Demographic and clinical characteristics

*Table 5.1* shows the demographic and clinical characteristics of the three participant groups. They did not differ on age or IQ. However, relative to NO, they differed in years of education, PCL-R total, factor, and facet scores, presence of a comorbid personality disorder and substance use

disorder, presence of a positive urine drug screening test, as well as total, reactive, and proactive aggression scores. The post-hoc group comparisons are shown in *Table 5.1*. The two ASPD groups did not significantly differ in comorbid lifetime substance use disorder or positive urine drug screening tests. To maximize power and to avoid over-correcting for phenotypic variance inherent to ASPD, the presence of a positive urine drug screening test was not included as a covariate in the main analysis. Instead, supplementary post-hoc sensitivity analyses using linear regression assessed whether this predicted the main findings (see Table S2). Drug use on the day was preferred over the presence of a substance use disorder because it is more appropriate in the context of conducting a pharmacological challenge and because its measure via the urine sample is more objective.

| **Demographic** | **ASPD+P** | **ASPD-P** | **NO** | **Main test statistic** | **Pairwise comparisons** | | |
|---|---|---|---|---|---|---|---|
| **N** | **20** | **19** | **23** | | **ASDP+P vs NO** | **ASPD-P vs NO** | **ASPD+P vs ASPD-P** |
| Age, mean (SD) | 39.35 (9.52) | 42.32 (10.58) | 38.22 (9.63) | $F_{(2, 59)} = 0.93$, p = .40 | . | . | . |
| IQ, mean (SD) | 92.47 (12.14) | 97.63 (15.14) | 98.57 (10.69) | $F_{(2, 58)} = 1.34$, p = .27 | . | . | . |
| Years in education, mean (SD) | 9.90 (1.71) | 10.68 (2.00) | 13.74 (3.19) | $H_{(2)} = 21.44$, p < .001 | p < .001 | p = .001 | p = .25 |
| PCL-R Total, mean (SD) | 28.40 (3.16) | 17.37 (4.14) | 3.00 (3.38) | $H_{(2)} = 53.84$, p < .001 | p < .001 | p < .001 | p < .001 |
| PCL-R Factor 1, mean (SD) | 9.55 (3.15) | 4.86 (2.81) | 1.35 (2.01) | $H_{(2)} = 39.89$, p < .001 | p < .001 | p < .001 | p < .001 |
| PCL-R Facet 1, mean (SD) | 4.35 (1.79) | 1.86 (1.50) | 0.74 (1.05) | $H_{(2)} = 32.83$, p < .001 | p < .001 | p < .008 | p < .001 |
| PCL-R Facet 2, mean (SD) | 5.20 (1.99) | 3.00 (1.70) | 0.61(1.08) | $H_{(2)} = 37.30$, p < .001 | p < .001 | p < .001 | p < .003 |
| PCL-R Factor 2, mean (SD) | 16.20 (1.57) | 11.16 (2.79) | 1.22 (1.54) | $H_{(2)} = 51.57$, p < .001 | p < .001 | p < .001 | p < .001 |
| PCL-R Facet 3, mean (SD) | 7.65 (1.27) | 5.37 (1.67) | 1.04 (1.22) | $H_{(2)} = 47.70$, p < .001 | p < .001 | p < .001 | p < .001 |
| PCL-R Facet 4, mean (SD) | 8.45 (1.28) | 5.75 (2.27) | 0.57 (1.16) | $H_{(2)} = 47.98$, p < .001 | p < .001 | p < .001 | p < .001 |
| Cluster A, N (%) | 6 (30%) | 0 (0%) | 0 (0%) | 10.99, p = .001 † | p = .006 | p = 1.00 | p = .02 |
| Cluster B, not ASPD, N (%) | 11 (55%) | 2 (11%) | 0 (0%) | 20.12, p < .001 † | p < .001 | p = .20 | p = .006 |
| Cluster C, N (%) | 1 (5%) | 2 (11%) | 0 (0%) | 2.34, p = .19 † | p = .47 | p = .20 | p = .61 |
| Substance Use Disorder, N (%) | 4 (20%) | 6 (32%) | 0 (0%) | 8.79, p = .007 † | p = .04 ◊ | p = .005 | p = .48 |
| ADHD, N (%) | 2 (10%) | 1 (5%) | 0 (0%) | 2.23, p = .29 † | p = .21 | p = .45 | p = 1.00 |
| Positive urine drug test PL, N (%) | 13 (68%) | 6 (33%) | 5 (22%) | $\chi2 = 9.92$, p = .007 | p = .002 | p = .001 | p = .03 ◊ |
| Positive urine drug test OT, N (%) | 15 (75%) | 8 (42%) | 6 (26%) | $\chi2 = 10.52$, p = .005 | p = .001 | p = .27 | p = .04 ◊ |
| Total Convictions, mean (SD) | 28.15 (23.31) | 20.00 (15.97) | . | U = 144.00, p = .20 | . | . | . |
| Violent Convictions, mean (SD) | 4.10 (3.04) | 3.74 (2.98) | . | U = 174.00, p = .65 | . | . | . |
| Age 1st Violent Conviction, mean (SD) | 19.95 (5.13) | 21.74 (5.21) | . | U = 131.50, p = .23 | . | . | . |
| Presence of reconviction within 1 year | 3 (15%) | 3 (16%) | . | 0.005, p = .95 † | . | . | . |
| Total Aggression, mean (SD) | 30.53 (9.64) | 18.67 (11.11) | 6.19 (4.25) | $F_{(2, 48)} = 37.09$, p < .001 | p < .001 | p = .002 | p = .01 |
| Reactive Aggression, mean (SD) | 16.47 (4.73) | 11.93 (5.55) | 5.67 (3.61) | $F_{(2, 48)} = 25.15$, p < .001 | p < .001 | p = .001 | p = .03 ◊ |
| Proactive Aggression, mean (SD) | 14.07 (6.09) | 6.73 (6.20) | 0.81 (1.17) | $F_{(2, 48)} = 34.05$, p < .001 | p < .001 | p = .006 | p = .008 |

Table 5.1 Demographic and clinical characteristics of participants included in the ASL analysis.
*Note: The whole-brain analysis included a subsample of participants (final ASPD+P N = 17, ASPD-P N = 14, NO N = 22) as some did not attend both sessions and thus had missing scans. Demographic group differences remained similar even after excluding the participants with missing scans. Some participants did not complete the RPQ (final ASPD+P N = 15, ASPD-P N = 15, NO N = 21). SD = standard deviation, PL = placebo, OT = oxytocin. F-statistic = ANOVA with Tukey post-hoc, H-statistic = Kruskal Wallis with Mann Whitney U post hoc, † Fisher's Exact test with Fisher's Exact post-hoc, $\chi^2$ = chi-squared test of independence with chi-squared test of independence as post hoc, U-statistic = Mann Whitney U. ◊ pairwise comparison did not survive a Bonferroni correction for multiple comparisons (α= .05/3 = .02).*

### 5.3.2 Global median CBF

There was no significant main effect of group ($F_{(2, 48)}$ = 0.53, p = .59, $\eta_p^2$ = .02), treatment ($F_{(1, 48)}$ = 1.23, p = .27, $\eta_p^2$ = .03), or group by treatment interaction effect ($F_{(2, 48)}$ = 1.93, p = .16, $\eta_p^2$ = .07) on global median CBF (*Table 5.2*).

| Global Median CBF | ASPD+P | ASPD-P | NO | Main effect of group | Main effect of treatment | Group x treatment |
|---|---|---|---|---|---|---|
| PL, mean (SD) | 47.59 (9.53) | 46.07 (11.06) | 44.77 (7.02) | $F_{(2, 48)}$ = 0.53, p = .59 | $F_{(1, 48)}$ = 1.23, p = .27 | $F_{(2, 48)}$ = 1.93, p = .16 |
| OT, mean (SD) | 46.35 (7.93) | 41.50 (7.74) | 46.36 (8.45) | | | |

Table 5.2 Global median CBF mean and standard deviation (SD).
*Note: PL = placebo, OT = oxytocin, CBF = cerebral blood flow.*

### 5.3.3 Whole-brain analysis

The whole-brain analysis revealed a significant main effect of group in five clusters (described in *Table 5.3* and visualized in *Figure 5.1A-E*). These spanned the right frontal, temporal, and parietal areas. The post-hoc pairwise comparisons with Sidak correction for multiple comparisons showed that both ASPD+P and ASPD-P had reduced rCBF relative to NO in four of these clusters. By contrast, in the fifth cluster, both ASPD groups had increased rCBF relative to NO, and ASPD+P had further increased rCBF compared to the ASPD-P. There were no significant main effects of treatment. However, a significant group by treatment interaction effect was found in one cluster spanning the left globus pallidus, putamen and caudate (*Table 5.3*, *Figure 5.2*). Simple main effects tests revealed that this was driven by a significant decrease in rCBF after OT in ASPD-P only.

| Cluster description | Cluster-wise analysis: Hemisphere | K | $P_{FWE}$ | F | Peak coordinates: x | y | z | Estimated Marginal Means (SE): ASPD+P | ASPD-P | NO | Pairwise Comparisons: Sidak-corrected p-values: ASPD+P vs NO | ASPD-P vs NO | ASPD+P vs ASPD-P |
|---|---|---|---|---|---|---|---|---|---|---|---|---|---|
| **Main effect of group (F-contrast)** | | | | | | | | | | | | | |
| Cluster 1: Medial superior frontal gyrus | Right | 410 | < .001 | 18.12 | 18 | 34 | 40 | 39.74 (0.91) | 38.68 (1.03) | 44.70 (0.81) | p = .001 | p < .001 | p = .83 |
| Cluster 2: Anterior cingulate cortex | Right | 218 | .007 | 10.77 | 6 | 36 | 16 | 57.55 (0.75) | 58.48 (0.85) | 62.77 (0.66) | p < .001 | p = .001 | p = .80 |
| Cluster 3: Pars orbitalis, orbitofrontal cortex | Right | 163 | .04 | 10.32 | 46 | 40 | -12 | 58.22 (1.07) | 59.66 (1.22) | 65.53 (0.95) | p < .001 | p = .002 | p = .77 |
| Cluster 4: Rolandic operculum, pre- and postcentral gyrus, superior temporal gyrus | Right | 490 | < .001 | 13.26 | 58 | -4 | 12 | 49.77 (1.66) | 51.75 (1.88) | 57.75 (1.47) | p = .002 | p = .05 | p = .82 |
| Cluster 5: Posterior (isthmus) cingulate cortex, precuneus, hippocampus | Right | 270 | .001 | 9.90 | 22 | -42 | 8 | 35.14 (0.71) | 32.31 (0.81) | 29.49 (0.63) | p < .001 | p = .03 | p = .04 |
| **Group x treatment interaction effect (F-contrast)** | | | | | | | | | | | | **PL vs OT:** | |
| | | | | | | | | | | | **ASPD+P** | **ASDP-P** | **NO** |
| Globus pallidus, putamen, caudate | Left | 258 | .02 | 9.32 | -22 | 2 | -6 | PL: 43.57 (1.78) OT: 45.57 (1.78) | PL: 46.33 (2.05) OT: 40.62 (2.05) | PL: 43.99 (1.62) OT: 43.80 (1.62) | p = .20 | p = .002 | p = .89 |

Table 5.3 Whole-brain clusters with significant group and interaction effects on rCBF.
*Note: main effects were measured with F-contrasts. Clusters labelled according to Automated Anatomical Labelling (AAL3) atlas built into SPM12 and confirmed by mapping MNI peak coordinates to Talairach space in BioImage Suite (https://bioimagesuiteweb.github.io/bisweb-manual/tools/mni2tal.html). SE = standard error. PL = placebo scan, OT = oxytocin scan.*

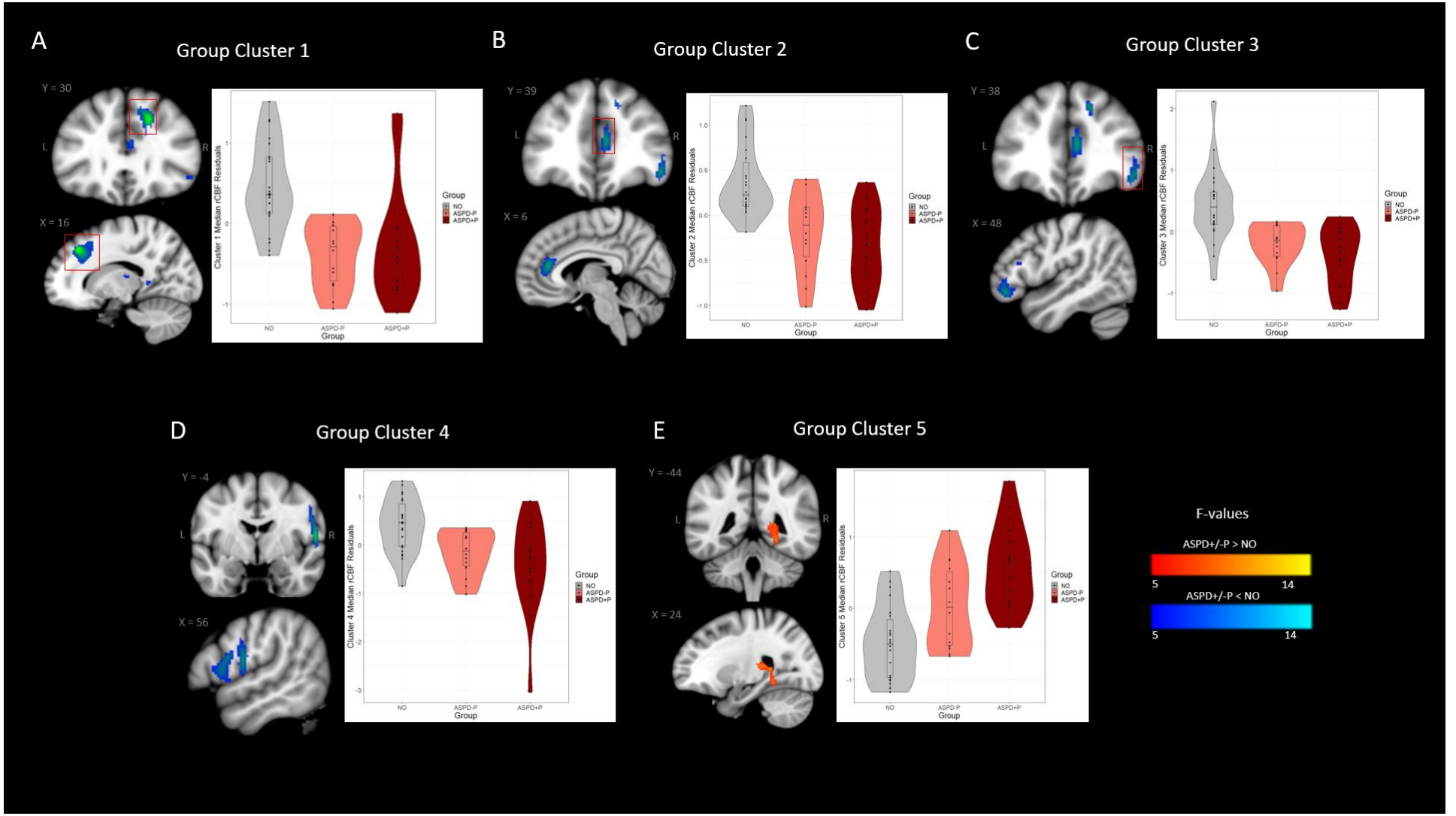


Figure 5.1 Clusters with significant group differences in median rCBF in the whole-brain analysis.

*Note: The violin plots (with box plots inside) show the marginal mean and individual datapoints (z-standardized residuals) to depict spread of the data. For cluster D), the main effect of group and pairwise comparisons remained significant after removing the ASPD+P outlier (z-standardized residual < -3.0), so this was kept in the analysis to increase power. Blue shaded clusters indicate reductions, red shaded cluster indicates increase. A red box indicates the cluster of interest for a particular effect in case other clusters are also visible in that slice. rCBF = regional cerebral blood flow.*

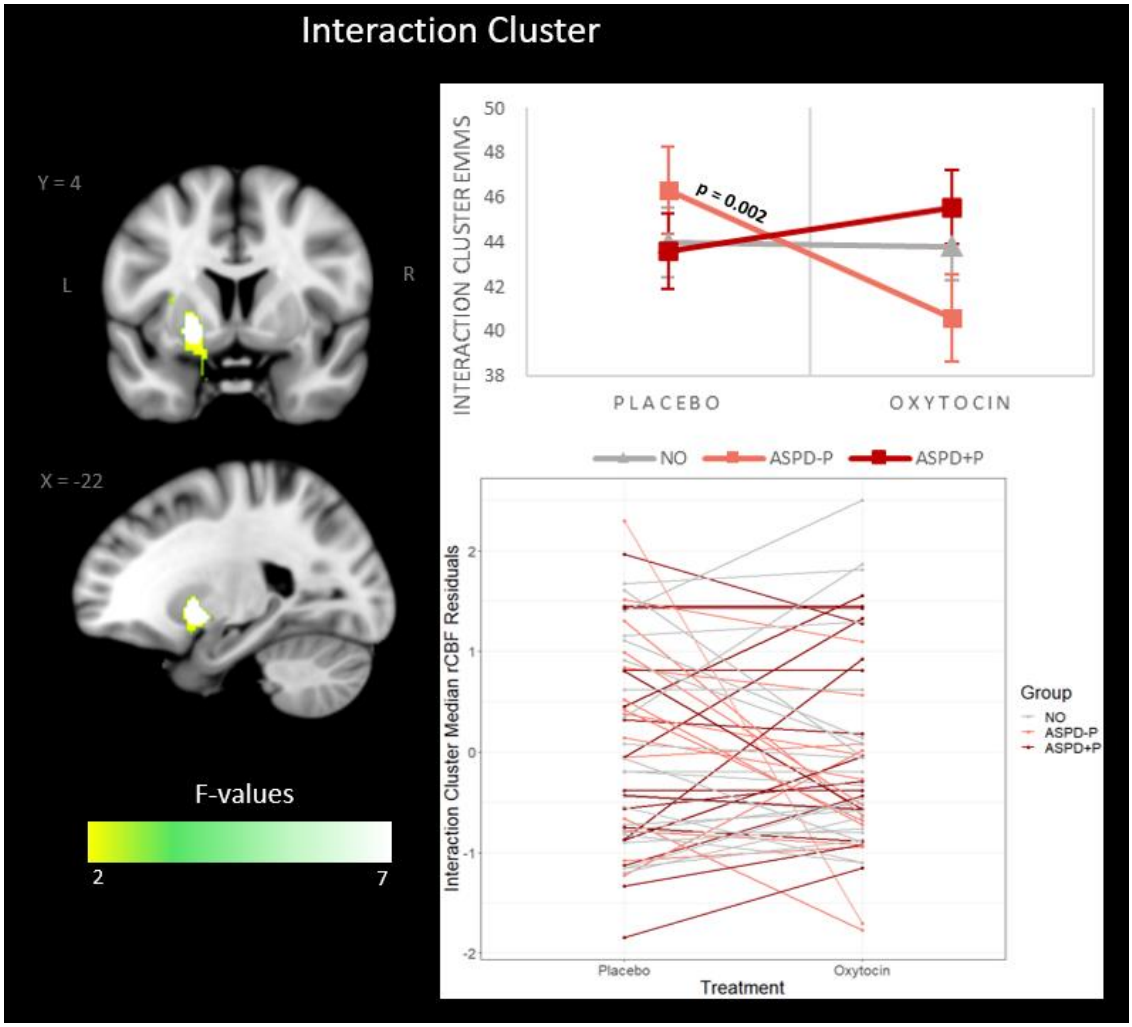


Figure 5.2 Cluster with a significant group by treatment interaction effect on median rCBF.
*Notes: The top line plot shows the estimated marginal means (EMMs) that reflect the average rCBF for each group under each treatment condition, after accounting for the effect of global median CBF, age, and minutes since dose. The bottom spaghetti plot shows individual participants' responsivity to OT. rCBF = regional cerebral blood flow, OT = oxytocin.*

### 5.3.4 Supplementary ROI analyses

The boot-strapped linear mixed models revealed no significant group, treatment, or group by treatment interaction effect on rCBF in the amygdala or the anterior insula after FDR correction for multiple comparisons (*Table 5.4*). The main effect of treatment in the left insula was trending towards significance before FDR correction for multiple comparisons (p = .05). The covariate of no-interest global median CBF had a significant effect on all areas (all F ≥ 445.70, all FDR-corrected p < .001, all $\eta_p^2$ ≥ .82), and the covariate of no-interest age had a significant effect on right and left amygdala (both F ≥ 8.54, both FDR-corrected p = .08, both $\eta_p^2$ ≥ .13).

| Main effect | Test statistic | FDR-corrected p | Effect size ($\eta_p^2$) |
|---|---|---|---|
| **Right amygdala** | | | |
| Group | $F_{(2, 53.33)} = 0.87$ | .55 | .03 |
| Treatment | $F_{(1, 50.14)} = 0.07$ | .81 | .001 |
| Group x treatment | $F_{(2, 50.60)} = 0.83$ | .80 | .03 |
| **Left amygdala** | | | |
| Group | $F_{(2, 53.74)} = 0.21$ | .81 | .008 |
| Treatment | $F_{(1, 49.22)} = 0.63$ | .61 | .01 |
| Group x treatment | $F_{(2, 49.71)} = 2.11$ | .52 | .08 |
| **Right insula** | | | |
| Group | $F_{(2, 57.29)} = 1.14$ | .55 | .04 |
| Treatment | $F_{(1, 50.75)} = 1.16$ | .61 | .02 |
| Group x treatment | $F_{(2, 51.22)} = 0.02$ | .98 | <.001 |
| **Left insula** | | | |
| Group | $F_{(2, 57.56)} = 1.11$ | .55 | .04 |
| Treatment | $F_{(1, 52.83)} = 4.48$ | .20 * | .08 |
| Group x treatment | $F_{(2, 53.33)} = 0.52$ | .80 | .02 |

Table 5.4 Results from the supplementary ROI analysis of rCBF.
*Note: Results from all variables of interest in the linear mixed models measuring rCBF in the right and left amygdala and anterior insula are shown. Results from the covariates of no-interest are not listed for the sake of brevity (see text). * uncorrected p = .05. rCBF = regional cerebral blood flow.*

### 5.3.5 Correlation with phenotype

The correlations between rCBF in the five significant group clusters and the phenotypic variables (clinical, behavioural, and cognitive measures) within the ASPD participants revealed four significant correlations, but only one remained significant after applying FDR correction for multiple comparisons. Specifically, the accuracy of recognizing angry faces correlated significantly positively with rCBF in cluster 5 (r = .617, FDR-corrected p-value = .02, 95% confidence intervals = .224 [lower] – .841 [upper]). Hence, as *Figure 5.3* shows, higher rCBF in the cluster spanning the posterior cingulate, precuneus and hippocampus was associated with

more accurate recognition of angry expressions. There were no significant correlations between the rCBF responsivity to OT and phenotype. *Table 5.5* indicates the r-values of all correlations.

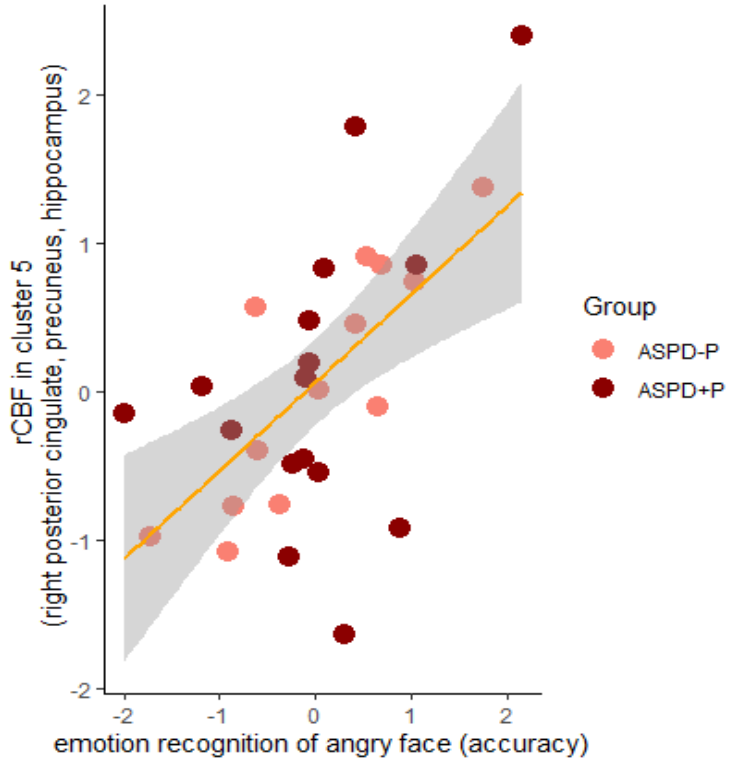


Figure 5.3 Significant positive correlation between cluster 5 rCBF and emotion recognition accuracy for angry faces in ASPD+/-P.
*Note: The rCBF values were first extracted from cluster 5, which showed a significant main effect of group, and were then averaged over treatment. The orange line indicates that rCBF in cluster 5 was significantly increased in both ASPD groups relative to NO in this analysis. rCBF = regional cerebral blood flow.*

| | | Group effect | | | | | Interaction effect |
|---|---|---|---|---|---|---|---|
| | | Cluster 1 | Cluster 2 | Cluster 3 | Cluster 4 | Cluster 5 | |
| PCL-R | Total | -.173 | -.346 | -.026 | -.111 | .109 | .165 |
| | Factor 1 | -.059 | -.252 | .015 | -.010 | .160 | .273 |
| | Factor 2 | -.008 | -.133 | -.060 | -.096 | -.200 | -.004 |
| | Facet 1 | -.053 | -.211 | .091 | -.122 | .315 | .328 |
| | Facet 2 | -.046 | -.210 | -.065 | .104 | -.045 | .156 |
| | Facet 3 | -.070 | -.016 | -.135 | -.101 | -.035 | .099 |
| | Facet 4 | .081 | -.220 | .014 | -.091 | -.221 | -.060 |
| Conviction information | # past violent convictions | -.022 | .028 | .291 | -.058 | .027 | .015 |
| | 1 year reconviction | .432 * | -.224 | .155 | -.499 ** | .065 | .334 |
| Aggression [a] | RPQ-Reactive | .104 | -.018 | -.026 | .212 | -.256 | .110 |
| | RPQ-Proactive | .152 | -.180 | .094 | .425 * | -.075 | .370 |
| Emotion recognition (accuracy) [b] | Angry | -.280 | -.297 | -.043 | -.210 | **.617 ** ** | -.105 |
| | Sad | -.111 | -.009 | .027 | .055 | -.105 | .105 |
| | Fear | -.253 | -.268 | -.223 | -.237 | .155 | -.007 |
| Emotion detection (reaction time) [c] | Angry | -.248 | .108 | -.162 | .077 | <.001 | -.104 |
| | Fear | -.207 | .061 | -.086 | .069 | .006 | -.179 |
| Reinforcement-based decision-making (accuracy) [b] | Acquisition learning | .201 | .061 | .073 | .185 | -.135 | -.007 |
| | Response reversal | .231 | -.126 | .146 | .225 | -.094 | -.058 |
| Delay discounting (# of times lesser value chosen) [b] | 7 days | -.158 | -.067 | -.107 | -.155 | .075 | -.081 |
| | 30 days | -.098 | .036 | .020 | -.136 | .045 | -.055 |
| | 90 days | -.041 | .140 | .032 | -.106 | -.110 | .045 |
| | 180 days | -.048 | .133 | .062 | -.044 | -.124 | .054 |
| | 360 days | -.094 | .117 | .029 | <.001 | -.055 | .073 |
| Disinhibition [b] | SSRT | -.009 | .061 | -.001 | .012 | -.089 | -.076 |

Table 5.5 Partial Pearson coefficients for rCBF-phenotype correlations.
*Note: These are the r-values from the partial Pearson correlations between rCBF in clusters with a significant group difference and phenotypic variables, as well as those from correlations between differential rCBF responsivity to OT (from the interaction cluster) and phenotypic measures within the ASPD participants (N = 25). Group, age, global median CBF, and minutes since dose were included as covariates of no-interest. Note: * = uncorrected p <.05, ** = uncorrected p < .01. Bold font means the p-value survived the FDR correction for multiple comparisons. Not all participants completed all study parts: [a] N = 20, [b] N = 23, [c] N = 24. SSRT = stop signal reaction time. rCBF = regional cerebral blood flow. RPQ = reactive-proactive aggression questionnaire.*

## 5.4 Discussion

The current study aimed to assess differences in resting-state rCBF between male violent offenders with ASPD+P, ASPD-P, and healthy NO individuals, and to investigate the effect of OT on rCBF in these groups. It was hypothesized that 1) both ASPD groups would show significantly reduced frontotemporal rCBF relative to NO; 2) that the ASPD+P group would show further decreases relative to ASPD-P; and 3) that OT would increase frontotemporal rCBF (particularly anterior insula) in ASPD+P but not ASPD-P. Results from the whole-brain analysis partially supported these hypotheses. Specifically, with respect to the first hypothesis, the findings indeed demonstrated that both ASPD groups showed reduced rCBF in several frontotemporal and parietal cortical regions relative to NO. These regions spanned the medial superior frontal cortex, orbitofrontal cortex, and anterior cingulate cortex as well as Rolandic operculum, superior temporal gyrus, and inferior pre- and post-central gyri. With respect to the

second hypothesis, there were no differences between the two ASPD subtypes in these clusters. However, in another cluster covering parts of the right posterior cingulate cortex, precuneus, and hippocampus, the analysis revealed significantly increased rCBF in both ASPD subtypes relative to NO, which was significantly more pronounced in ASPD+P relative to ASPD-P. With respect to the third hypothesis, a group by treatment interaction effect revealed that OT significantly reduced rCBF in the left subcortical structures including globus pallidus, putamen and caudate in ASPD-P only. Taken together, these findings suggest shared and different resting-state abnormalities in rCBF between ASPD+P and ASPD-P. Finally, the exploratory correlations between rCBF abnormalities, OT responsivity, and phenotypic characteristics revealed a positive relationship between rCBF in the medial parietal region and accuracy in recognition of angry faces. These results will be discussed.

The current findings build on previous SPECT and PET imaging studies which also revealed reduced frontotemporal perfusion in ASPD and psychopathy (Goethals et al., 2005; Kolla & Houle, 2019; Kuruoglu et al., 1996; Soderstrom et al., 2000, 2002; Sutherland & Fishbein, 2017). However, the novel use of ASL, which is more spatially precise, non-invasive, and low demand, has given a clearer understanding of the profiles of rCBF in this phenotype. For example, while prior studies often focused on large regions of interest (e.g., frontal lobe), the current findings demonstrated rCBF reductions in specific, functionally meaningful brain regions (e.g., orbitofrontal cortex, superior frontal gyrus, anterior cingulate cortex). Furthermore, the use of an automated processing pipeline to analyse the ASL data offered a more reliable approach compared to previous work that relied on visual judgment of perfusion data. These improvements have provided the opportunity to build on existing research and to discover novel evidence that ASPD+P and ASPD-P can be distinguished. Together, the current findings thus confirm that although ASPD+/-P share some differences from controls, there is also variation in

the functional neurobiological underpinnings of clinical subgroups within ASPD.

In terms of the shared mechanisms, the findings revealed that both ASPD subtypes showed reduced rCBF mainly spanning frontotemporal regions. This is in agreement with previous task-based fMRI studies of individuals with ASPD and psychopathy that reported reduced BOLD activity in similar areas (orbitofrontal, superior frontal gyrus, anterior cingulate cortex and superior temporal gyrus), which in turn has been associated with deficient fear and threat processing, empathic processing, reinforcement-based learning (Birbaumer et al., 2005; R. J. R. Blair, 2010; Decety, Chen, et al., 2013; Decety, Skelly, et al., 2013; Dugré et al., 2020; Gregory et al., 2015). Considering that rCBF is one of the physiological variables contributing to the proxy measure of brain activity that is the BOLD signal, it is possible that reductions in rCBF may partly explain the reduced neural responsivity in these regions. That is, if there is reduced perfusion, there is reduced delivery of oxygen and other nutrients, which impacts brain function and behaviour. However, it must be acknowledged that the current study measured resting-state rCBF. Therefore, the impact of altered rCBF on potential behavioural impairments remains to be investigated. Future research could employ task-based ASL imaging to explore whether this profile of reduced frontotemporal rCBF is shared across both ASPD subtypes beyond the resting-state.

Beyond these shared neurobiological underpinnings, significantly increased rCBF was observed in ASPD+P relative to ASPD-P and NO in the medial parietal region of the brain (i.e., posterior cingulate and precuneus). This adds to findings, including those from *chapter 4*, that ASPD+P is not only marked by different structural and task-based functional, but also resting-state rCBF neurobiological mechanisms when directly compared to ASPD-P (Gregory et al., 2012, 2015; Tully et al., 2022). Previous studies have demonstrated increased cortical volume and surface area, and increased resting-state and task-based BOLD activity in this medial parietal region

specifically within the ASPD+P phenotype (Deming & Koenigs, 2020; Gregory et al., 2015). This medial parietal region acts as an information integration hub with an important contribution towards self-referential processing, first-person perspective-taking, and representing of subjective value, particularly in relation to rewards and prediction error signalling after omission of an expected reward (Cavanna & Trimble, 2006; Kable & Glimcher, 2007; X. Liu et al., 2011). Moreover, the posterior cingulate has been associated with the perception of faces and emotional stimuli, which may explain the positive correlation between recognition of angry faces and rCBF in this cluster (J. B. Freeman et al., 2015; Maddock, 1999; Y. Wang et al., 2020). The medial parietal region is also a central component of the default-mode network (DMN). Activity in this network typically reduces during task engagement, but it has been shown that the DMN does not appropriately deactivate during task engagement in psychopathic offenders (S. M. Freeman et al., 2015). Moreover, Freeman and colleagues (2015) showed that this failure to deactivate was due to an overactive medial parietal region. They also reported that the overactive medial parietal region could be specifically attributed to high PCL-R factor 1 scores in the psychopathic offenders. Together, this evidence suggests that abnormalities in the medial parietal region play a distinctive role in the manifestation of ASPD+P, differentiating it from ASPD-P.

Another finding that revealed differences between ASPD+P and ASPD-P related to the effect of OT. A group by treatment interaction effect revealed that in ASPD-P but not ASPD+P, OT significantly reduced rCBF in the left globus pallidus and dorsal striatum (putamen and caudate) when compared to PL. The globus pallidus and dorsal striatum have a particularly high density of oxytocin receptors which makes these regions, at least theoretically, particularly sensitive to effects of exogenous oxytocin (Quintana, Rokicki, et al., 2019). The dorsal striatum has been linked to reinforcement-based learning and deciding on an appropriate action to achieve a goal (Balleine et al., 2007). A previous behavioural study directly

comparing violent offenders with ASPD+/-P found that only ASPD-P individuals were significantly impaired relative to NOs on this ability (De Brito et al., 2013). Furthermore, in youth with conduct disorder, a large cohort study revealed dorsal striatum abnormalities during reinforcement-based learning in those without CU traits (the ASPD-P precursor) compared to those with CU traits (the ASPD+P precursor) (S. W. Hawes et al., 2021). Another study in adult offenders found that the impulsive-antisocial traits in ASPD-P contributed to aberrant striatal functional connectivity (Korponay et al., 2017b). Together, these findings suggest that abnormal dorsal striatal activity and deficient reinforcement-based learning is associated with ASPD-P. Given the modulatory effect of OT on dorsal striatum rCBF in the current ASPD-P group and findings from studies showing a beneficial effect of OT on reinforcement-based learning in other populations (Kruppa et al., 2019; Martins, Lockwood, et al., 2022; Zhuang et al., 2021), future studies investigating whether OT might impact reinforcement-based learning and decision-making in ASPD-P are required. It must be noted that the lack of a significant correlation between reinforcement-based decision-making and OT responsivity rCBF in this cluster in the current study was likely due to low statistical power and potentially also because of methodological limitations of the task itself.

The supplementary ROI analysis in the current study did not reveal group or treatment effects on amygdala or anterior insula rCBF – suggesting no differences in either resting-state rCBF or responsivity to pharmacological challenge with a neuropeptide that is particularly implicated in social behaviour. These findings were unexpected because they contradict the results from the only previous study showing OT modulated anterior insula BOLD activity in ASPD+P (Tully et al., 2022). Moreover, the lack of group differences in amygdala rCBF was unexpected given the pivotal role this structure has previously been reported to display in impaired emotion and threat processing, empathy and decision-making in ASPD+/-P and CD+/-CU (R. J. R. Blair, 2010; Fanti et al., 2019; White et al., 2016). One

explanation for the current finding could be that this study focused on amygdala rCBF at rest and not during a task. However, studies measuring resting-state BOLD signal in ASPD+/-P have revealed reduced functional connectivity and centrality of the amygdala and anterior insula within relevant networks (Dugré & Potvin, 2021; Espinoza et al., 2019; Ly et al., 2012; Siep et al., 2019; Tillem et al., 2019; Yoder et al., 2015). This means that the amygdala and anterior insula have weaker and fewer functional connections with other brain areas, suggesting tasks which typically utilize these brain regions may not recruit them as effectively in individuals with ASPD+/-P. Therefore, considering the current findings that rCBF was not abnormal in these regions, it remains to be investigated what other factors might be contributing to the aberrant BOLD signals shown in other studies. For instance, it is possible that the inconsistency in evidence relating to amygdala impairments might be associated with variable accounting of comorbid mental health problems or substance use. With this in mind however, it must be noted that the central role of functional impairments in the amygdala, particularly in psychopathy, has recently become more disputed (Deming et al., 2022). Hence, the current findings may also contribute to this recent development in the literature.

With respect to the lack of a treatment effect on the amygdala and anterior insula, it is important to consider some methodological aspects of this study. For instance, it has been shown that the effect of OT on rCBF is most noticeable globally 39-51 minutes after OT administration, and after 24-32 minutes in the amygdala (Martins, Mazibuko, et al., 2020; Paloyelis et al., 2016). However, with regards to the anterior insula, rCBF increases have been reported up to 95 minutes post OT administration (Martins, Mazibuko, et al., 2020). In the current study, the ASL scan took place on average 85 minutes after administration. This was due to procedural limitations as the MRI protocol involved other scans prior to the ASL scan. Therefore, it is possible that the time window to detect effects of OT on the amygdala – if indeed they existed – was simply missed. Alternatively, the lack of

treatment effects in the amygdala and the anterior insula could be associated with low statistical power. Given the previously suggested contribution of amygdala and anterior insula abnormalities to ASPD+/-P as well as their important role in the oxytocinergic system, future research could assess the effect of OT on amygdala and anterior insula rCBF in ASPD+/-P at earlier time points and at different doses.

There were some limitations of the current study. First, as noted above, the post-dose time delay (ca. 85 minutes on average) was on the upper end of what has previously been investigated in studies looking at the effect of OT on rCBF (Martins, Mazibuko, et al., 2020; Paloyelis et al., 2016). Although Martins and colleagues (2020) did show effects of OT up to 95 minutes post-dose, including in the insula, it is possible that the effect of OT in the current study was underestimated. Also as mentioned above, this might particularly be the case for brain areas like the amygdala, where the effect of OT was so far only identified much earlier (Martins, Mazibuko, et al., 2020). Second, although the current sample size was adequately powered to detect between-group differences in rCBF in a crossover design (K. Murphy et al., 2011), it was too small to reasonably detect correlations between significant rCBF clusters and phenotypic features. For such brain-behaviour correlations, it has been suggested that at least 1000 subjects would be required (Marek et al., 2022). This means the correlations must be interpreted very cautiously. Finally, main analyses did not covary for the presence of a lifetime substance use disorder or the having a positive urine drug test because substance use is an inherent component of the clinical phenotype of ASPD (Trull et al., 2010), and accounting for it may remove important variance. The sensitivity analyses did reveal however that recent drug use was negatively related to rCBF in clusters 1 and 3. It is worth noting that previous studies which accounted for substance use or psychotropic medication use showed that this did not explain rCBF reductions found in ASPD (Soderstrom et al., 2000, 2002; Sutherland & Fishbein, 2017).

In conclusion, this first study using ASL to measure rCBF discovered novel evidence that ASPD+/-P have both shared and different resting-state functional neurobiological mechanisms. This adds support to the notion of stratifying ASPD into more biologically homogenous subgroups (i.e., those with and without psychopathy). Furthermore, it provided the first evidence that OT differentially modulates rCBF in ASPD-P individuals. This lends support to the further exploration of OT as a potential therapeutic agent using more personalised medicine approaches. That is, the results suggest that treatment approaches need to target the features of each subtype differently.

# 6 A resting-state fMRI investigation into large-scale network functional connectivity and the effect of intranasal oxytocin in violent offenders with ASPD

## 6.1 Introduction

Antisocial personality disorder (ASPD) remains difficult to treat. This is partially because a comprehensive understanding of the underpinning neurobiological mechanisms is not yet available. As described in earlier chapters, existing research in ASPD populations has begun to demonstrate abnormalities in brain structure, resting-state regional cerebral blood flow (rCBF), and functional connectivity (FC). FC reflects the pattern of complex temporal correlations of spontaneous neural activation between anatomically defined and spatially remote brain regions. FC is typically explored using resting-state functional magnetic resonance imaging (rs-fMRI) when the brain is not engaged in any externally specified activity. While resting-state FC is closely coupled with individuals' active brain function (Tavor et al., 2016; Thiebaut De Schotten & Forkel, 2022), this task-free approach enables the exploration of neurobiological mechanisms which are not constrained by task selection, demand, performance, or strategy (Bressler & Menon, 2010; Lv et al., 2018). As such, resting-state FC has been used to offer insight into intrinsic functional networks, that is, the dynamic systems of communication and interaction between individual brain areas. Differences in FC are likely to be important in understanding the anomalous neurobiological mechanisms that underpin interpersonal and behavioural impairments associated with ASPD.

Previous studies have identified aberrant FC of individual brain regions (seeds) associated with sociocognitive impairments (e.g., emotion processing, moral reasoning, learning) in individuals with ASPD and

psychopathy. For instance, there is evidence that offenders with high levels of psychopathy compared to offenders with low levels and non-offenders have reduced FC of the ventromedial/orbitofrontal prefrontal cortex, anterior cingulate, insula, medial parietal cortex (i.e., posterior cingulate, precuneus), amygdala, striatum, and thalamus (Contreras-Rodríguez et al., 2015; Decety, Chen, et al., 2013; Hosking et al., 2017; Ly et al., 2012; Motzkin et al., 2011; Nummenmaa et al., 2021; Pujol et al., 2012). Similar findings have been shown in offenders with ASPD compared to healthy non-offending comparison subjects (H. Liu et al., 2014; Tang, Liu, et al., 2013), as well as in a recent meta-analysis of individuals with antisocial behaviour (Dugré & Potvin, 2021). These findings are further supported by evidence of reduced white matter structural connectivity between frontotemporal and frontoparietal cortical and subcortical regions in ASPD and psychopathy (Craig et al., 2009; W. Jiang, Shi, Liu, et al., 2017; Motzkin et al., 2011; Sethi et al., 2015). Taken together, these prior studies were a valuable first step, suggesting that the communication between individual brain regions that are important for sociocognitive functioning is abnormal in ASPD and psychopathy.

However, the complexity of sociocognitive functioning requires multiple rather than individual brain regions to communicate with each other (Thiebaut De Schotten & Forkel, 2022). Seed-based FC studies may lead to the overestimation of dysfunction in one area relative to the rest of the brain, and potential FC abnormalities of other brain regions or larger networks may be missed (Cole et al., 2010). Therefore, another approach to understanding FC abnormalities in psychiatric disorders involves the analysis of FC across the whole brain, by assessing the connectivity of large-scale intrinsic functional networks. Large-scale networks reflect a collection of brain areas that have highly correlated FC, typically identified through independent component analysis of the timeseries of individual voxels (Biswal et al., 1995). They have functional relevance (Laird et al., 2011) and are typically stable over time (Damoiseaux et al., 2006).

Commonly identified networks include the default mode network (DMN), the frontoparietal network (FPN; otherwise known as the attention and executive control network), the salience network (SAL; otherwise known as the cingulo-opercular network) and the medial-temporal network (MTN; otherwise known as the subcortical/limbic network) (Menon, 2011; Uddin et al., 2019). The DMN is involved in self-referential processes and internally oriented attention. It is typically less active during externally oriented attention and goal-directed behaviour (Harrison et al., 2008; Mak et al., 2017). In contrast, the FPN is usually more active during active task engagement and executive functioning (Uddin et al., 2019). The SAL is involved in the detection of salient, behaviourally relevant information, and it is also important for empathic processing (Engen & Singer, 2013; Uddin et al., 2019). It has been suggested that the SAL has an important function in mediating the dynamics between the DMN and the FPN (Zhou et al., 2018). Finally, the MTN typically encompasses limbic/paralimbic structures such as the amygdala- hippocampus formation and the entorhinal and parahippocampal cortices (Dipasquale et al., 2019; Veer et al., 2010), thus including areas which are thought to be dysfunctional in ASPD and psychopathy (Deming & Koenigs, 2020; Dugré & Potvin, 2021).

Dysfunction within and between these networks has previously been reported in ASPD and psychopathy. For example, a study of a group of offenders with ASPD compared to healthy non-offenders revealed reduced FC in the DMN and FPN (Tang, Jiang, et al., 2013). Furthermore, research in offenders revealed that FC in the DMN, FPN, and SAL correlates negatively with PCL-R total psychopathy and factor 1 scores (interpersonal-affective traits), but positively with factor 2 scores (impulsive-antisocial traits) (Philippi et al., 2015). Another study using a large sample of offenders with varying degrees of psychopathic traits further highlighted the relationship with factor 1 scores, as only these were associated with abnormal FC in several large-scale networks, including the DMN, FPN, SAL, and MTN (Espinoza et al., 2018). Importantly, these three studies all

revealed aberrant FC both within *and* between the stated networks. Moreover, the large-scale networks that were shown to be abnormal in these three studies encompass regions identified to have abnormal FC in the seed-based analyses. Together, this prior work suggests that the dynamics of functional communication across the brain is altered in ASPD and psychopathy (Espinoza et al., 2019; Hamilton et al., 2015; Pu et al., 2017).

However, these studies have important limitations. The sample studied by Tang et al. (Tang, Jiang, et al., 2013) was a young adult sample aged 18-22, meaning that the brain regions studied had not reached full maturity, particularly the frontal regions. They also did not capture psychopathic traits within their ASPD sample, nor the extent of violent offending. In turn, the two studies using samples of psychopathic offenders (Espinoza et al., 2018; Philippi et al., 2015) did not specify the presence/absence of ASPD in their sample, limiting the potential generalization of findings. Furthermore, all three of these prior studies either selected multiple seed regions typically associated with the large-scale networks *a priori* (Philippi et al., 2015) or they correlated activity between pairs of regions and attributed these to large-sale networks *a posteriori* (Espinoza et al., 2018; Tang, Jiang, et al., 2013). Thus, none of the studies assessed FC of a network as a whole. They also used their own data to identify the temporal correlations that were analysed, rather than using externally sourced imaging data. Such an approach has the potential to introduce bias (Bijsterbosch et al., 2017), including, for example, finding temporal correlation structures that are inherent to that particular clinical sample but which are not reflective of a non-clinical, non-offending population. This potential bias likely limits the replicability and comparability of the findings. Dual regression could be used to explore these issues (D. V. Smith et al., 2014), and will be used for the first time in ASPD in this study. It produces a 'version' of each network for each subject by applying the spatial network maps (i.e., the components identified through group independent

component analysis) to individual data in a whole-brain voxel-wise analysis. Higher-level within-network analyses can then assess whether the 'versions' of these networks differ, for instance revealing that a brain area is correlated with the component and thus *within* the network in one group but not another. It is thus more likely to capture inter-individual variability than the approaches used in previous studies. Additionally, dual regression can also be used to analyse *between*-network connectivity, which has also not previously been examined using this approach in ASPD or psychopathy.

A thorough understanding of within- and between-network connectivity abnormalities as a potential neurobiological mechanism underpinning ASPD and psychopathy is also important because of the potential functional implications. Two recent meta-analyses of conduct disorder, ASPD, and psychopathy highlighted that areas with task-based functional impairments largely map onto these large-scale networks (Deming & Koenigs, 2020; Dugré & Potvin, 2021). Large-scale network FC abnormalities might thus relate to behavioural factors such as aggression, or cognitive deficits including impaired emotion processing, reinforcement-based decision-making, delay discounting, and disinhibition. Indeed, studies have revealed that characteristic features of ASPD and psychopathy such as reactive and proactive aggression appear to be related to FC in offenders and others prone to violence (Kolla et al., 2018; Romero-Martínez et al., 2019; Siep et al., 2019; Werhahn et al., 2021). However, the relationship between large-scale network FC abnormalities and behavioural and cognitive factors in ASPD and psychopathy has not yet been studied. This will be addressed in the current study for the first time.

Importantly, no study to date has explored whether the observed FC abnormalities in ASPD and psychopathy can be modulated by pharmacological challenges. This is important because if abnormalities in FC can be 'shifted' by pharmacological agents, these could subsequently be investigated for their potential to treat functional and behavioural difficulties. One such agent is oxytocin. Oxytocin is a neuropeptide which

has been studied in the context of disorders characterized by sociocognitive impairments, including ASPD and psychopathy (Timmermann et al., 2017; Tully et al., 2022). It modulates rCBF and brain activity in limbic and paralimbic frontotemporal, medial parietal and subcortical regions which are known to be implicated in ASPD and psychopathy, and which have heightened oxytocin receptor density (Boccia et al., 2013; Grace et al., 2018; Martins, Brodmann, et al., 2022; Martins, Mazibuko, et al., 2020; Quintana, Rokicki, et al., 2019; Tully et al., 2018, 2022). In healthy individuals (mostly males), meta-analyses have suggested that intranasally administered oxytocin (OT) also modulates brain FC, typically diminishing FC of medial parietal regions such as the posterior cingulate and precuneus (areas associated with the DMN) and enhancing FC between the amygdala and the medial prefrontal cortex (areas associated with the MTN and SAL) (Bethlehem et al., 2013; Grace et al., 2018; X. Jiang et al., 2021; Kumar et al., 2020; S. H. Seeley et al., 2018; H. Wu et al., 2020). In line with this, large-scale network analyses show that OT alters within- and between-network FC, reducing DMN activity while enhancing SAL activity (Brodmann et al., 2017; Xin et al., 2021). The effect of OT on the MTN has not been assessed, but considering this network contains structures that show enhanced FC in response to OT (e.g., amygdala) (Bethlehem et al., 2013), it is possible that wider connectivity across this network could also be increased. Therefore, it is apparent that OT shifts the dynamics of functional communication across the brain (X. Jiang et al., 2021; Q. Wu et al., 2022). No study to date has examined the impact of OT on FC in ASPD and psychopathy.

The current study addressed limitations of previous research by including a carefully characterized sample of offenders across adulthood and using a novel data analytic approach (dual regression). It aimed to assess FC within and between large-scale networks in male violent offenders with ASPD and varying degrees of psychopathy, relative to healthy non-offending controls. Furthermore, it had the novel aim to investigate whether OT could modulate

FC, testing the 'shiftability' of any observed abnormalities in the ASPD group. Last, this study sought to explore the relationship between large-scale network FC and its responsivity to OT with several phenotypic characteristics of ASPD. Based on the prior research described above, it was hypothesized that the ASPD group would show abnormal *within-network* FC of the DMN (possibly increased), the SAL (possibly decreased), and the MTN (possibly decreased); and abnormal *between-network* FC of the DMN and the SAL. Furthermore, it was hypothesized that OT would modulate FC differences both within and between these networks, possibly enhancing potential SAL hypoconnectivity in the ASPD group. There was no specific hypothesis for the correlation between FC and phenotypic measures, as this investigation was exploratory in nature.

## 6.2 Methods

### 6.2.1 Participants

This study included 19 male violent offenders with a diagnosis of ASPD and 19 male non-offending (NO) healthy control participants. For the current analysis, violent offenders were not categorized into ASPD+/-P groups because the final sample sizes were too small. However, according to the PCL-R Interview (Hare, 1991), 12 violent offenders scored above the European cut-off of 25 (Cooke & Michie, 1999). Across both groups, participants were included if they were aged between 18 and 60 at time of consent, had an IQ above 70 (as per WASI-II (Wechsler, 2011)), did not suffer from any current or past neurological illness/trauma, and if it was safe for them to undergo an MRI scan. Offenders were recruited from South London medium secure clinical forensic services and National Probation Services. They were selected based on having a history of violent offending, with convictions including assault, actual/grievous bodily harm, armed robbery, rape, manslaughter, or murder. Offenders were excluded if they had a comorbid mood or psychotic disorder. Healthy NO control participants were recruited through purposive sampling from the general community via advertisements placed online and in public spaces in the local area. They

were eligible for inclusion if they did not have any history of offending and did not currently or historically meet the criteria for mental illness or personality disorder.

The study was approved by London City and East Research Ethics Committee and the Health Research Authority (reference: 15/LO/1083), as well as the National Offender Management Services Research Committee (reference: 2016-382). All participants completed signed informed consent.

### 6.2.2 Study design and procedure

This study used a double-blind, placebo-controlled, randomized crossover design. All participants attended an assessment day where diagnostic interviews and IQ testing were completed. The SCID-5-PD (First et al., 2015) and the SCID-5-CV (First et al., 2016) were used to confirm the ASPD diagnosis and to assess for any other comorbidities. The PCL-R interview was conducted to measure the severity of psychopathic traits. Participants also completed the reactive-proactive aggression questionnaire (RPQ) (Raine et al., 2006). Participants attended two further days where an identical protocol of MRI sequences including the resting-state fMRI scan and neurocognitive testing were completed. These were scheduled on average 16 days apart. On each day, participants completed a urine drug screening test to check for recent substance use. Participants were randomly - and blindly - allocated to receive an OT (Syntocinon, Novartis, Switzerland) or placebo dose (PL; same ingredients but without oxytocin). They received the alternative on the second day. Each OT dose contained 40 IU, and was self-administered via a nose spray, inhaling one puff every 30 seconds in alternating nostrils. This process was supervised by the researcher. The selected dose was in line with other studies testing the effect of OT on brain activity and behaviour and corresponds with safety standards (MacDonald et al., 2011; Martins et al., 2021; Martins, Brodmann, et al., 2022; Paloyelis et al., 2016). The resting-state fMRI scan (08:10 minutes) was acquired 92 (±9 minutes) and 90 (±14 minutes) after

the final PL and OT dosing puff, respectively. This time delay is referred to as the variable 'minutes since dose' in the subsequent analyses.

### 6.2.3 Image acquisition

The resting-state fMRI scan was acquired on a General Electric MR750 3Tesla MRI scanner with a 32-channel C-RMNova head coil. A T2*-weighted whole-brain multi-echo echo planar imaging (EPI) sequence with 192 volume per echo and 24576 images in total was acquired during each scanning session (32 horizontal slices top-to-bottom parallel to the anterior-posterior commissure line, slice thickness = 3 mm, slice gap = 1 mm, TR = 2500 ms, TE = 4 echoes at 12, 28, 44 and 60 ms, FA = 80°, FOV = 240 x 240 $mm^2$; matrix = 64 x 64, voxel resolution = 3.75 x 3.75 x 3 $mm^3$). Participants were instructed to remain still, stay awake, focus on a fixation cross and to let their mind wander. A high-resolution T1-weigthed structural image was also acquired and used for anatomical co-registration (196 image, slice thickness = 1.2 mm, slice gap = 1.2 mm, TR = 7.32 ms, TE = 3.02 ms, TI = 400 ms, FA = 11°, FOV = 270 x 270 $mm^2$, matrix = 256 x 256, voxel resolution = 1.05 x 1.05 x 1.2 $mm^3$). The same scan was used for co-registration as was analysed in *chapter 4*.

### 6.2.4 Image pre-processing

The resting-state fMRI data was pre-processed for this analysis and the graph theory analysis simultaneously. Details and justifications of the fMRI pre-processing steps are provided in the *Methods chapter*. In summary, these steps included: (1) skull-stripping and brain extraction of structural image to prepare a study-specific anatomical template; (2) calculation of a transformation matrix of this template to MNI152 standard space; (3) brain tissue extraction from the resting-state fMRI image; (4) splitting of the first three echoes and removal of the fourth echo in preparation for subsequent denoising by optimally combining the data using a weighted average approach; (5) slice timing correction; (6) motion correction including timeseries de-spiking, and volume registration and realignment by applying six rigid-body transformation parameters (images with a framewise

displacement value larger than 0.25 mm were excluded); (7) further noise artefact removal using multi-echo independent component analysis; 8) co-registration of the final denoised resting-state fMRI image to T1 native space in preparation for tissue segmentation; (9) removal of timeseries associated with signal from white matter and cerebrospinal fluid; (10) high-pass temporal filtering to remove low signal frequencies (<0.02 Hz); (11) normalization of the co-registered resting-state fMRI images to MNI152 space by application of the previously calculated transformation matrix from step (2); (12) spatial smoothing with a 6-mm full-width-half-maximum Gaussian kernel. The global signal was not regressed out as this may have adverse effects on the data, including the production of anti-correlations (Cheng et al., 2021; Fox et al., 2009).

### 6.2.5 Statistical analysis: demographic and clinical characteristics

The demographic and clinical characteristics of the ASPD and NO groups were compared using SPSS26 (IBM Corp, 2019). Two-sample independent t-tests (or Mann Whitney U in case of violation of assumptions) were used to compare age, IQ, years in education, PCL-R and RPQ scores. The groups did not significantly differ in age or IQ. Chi-squared ($\chi^2$) tests (or Fisher exact test in case of violation of assumptions) were used to assess differences in the frequency of positive urine drug screening tests on the days of the MRI assessments. Due to the study design, the frequency of comorbid disorders and conviction information were not subject to group comparisons because they were not present in the NO group.

### 6.2.6 Statistical analysis: large-scale network analysis

Due to the nature of this analysis, only participants who completed both PL and OT sessions could be included. The final pre-processed and smoothed images were prepared for FSL dual regression to analyse within- and between- large-scale network FC (Beckmann et al., 2009; Nickerson et al., 2017). *Figure 3.5* in the Methods chapter contains the overview of the dual regression analysis process. Stage 1 of dual regression identified the unique

timeseries for each subject and each treatment session by applying 13 spatial regressors to the pre-processed input data. The spatial regressors, i.e., the template whole-brain thresholded spatial maps of 13 large-scale networks, were previously identified as functionally relevant components in a group independent component analysis of resting-state fMRI data conducted in the MELODIC toolbox in FSL (https://fsl.fmrib.ox.ac.uk/fsl/fslwiki/MELODIC). This data came from an independent healthy adult male sample (n = 21), collected in the same MRI scanner with largely similar parameters and pre-processed using similar steps as the current study (Dipasquale et al., 2019). The identified networks have repeatedly been described and referred to in other large-scale network research (Damoiseaux et al., 2006; Menon, 2011; Uddin et al., 2019; Veer et al., 2010). They include the (1) primary visual network, (2) sensorimotor network, (3) DMN, (4) medial visual network, (5) auditory network, (6) lateral visual network, (7) MTN, 8) cerebellum, (9) SAL, (10) task positive network, (11) ventral stream network, (12) right lateral network, and (13) thalamic network. *Figure 6.1* provides a visualization of these networks, with FC values for each voxel thresholded at $|z| \geq 3$ to help show which brain regions typically have higher functional connectivity with each other, weighted by the group independent component analysis to contribute more to the network. Note that these 13 spatial network maps do not include one that fits the brain areas traditionally included in the FPN. This was only noted in hindsight. Stage 2 of the dual regression then applied the unique timeseries of each of these 13 networks, generated in the first stage, to the individual pre-processed input data to produce subject- and session-specific 4D spatial maps. Importantly, its reliance on multiple regression allowed the calculation of the weighted connectivity of one network with voxels across the entire brain while accounting for the connectivity of all other networks.

The within-network analysis used the spatial maps generated in stage 2 of the dual regression. It assessed FC across the whole brain, i.e., without

being spatially bound to the thresholded network maps. Thus, it identified group or treatment differences in the network shape and size, that is, the extent to which any given brain area (cluster) was functionally connected with the rest of the network. To do this, the spatial maps generated in stage 2 were prepared for a partitioned errors approach analysis. An average spatial map for each of the 13 networks (averaging PL and OT) for each subject was used to assess the main effect of group, using a two-sample t-test in SPM12 (https://www.fil.ion.ucl.ac.uk/spm/); a subtracted spatial map (OT minus PL) was used to assess the main effect of treatment, using a one-sample t-test; and the subtracted spatial map was also used to assess the group by treatment interaction effect, using a two-sample t-test. For the main effect of group and the interaction effect, t-contrasts assessing NO > ASPD and NO < ASPD were specified. For the main effect of treatment, only one t-contrast was required to interpret the one-sample t-test. Minutes since dose and age were included as covariates of no-interest in all analyses.

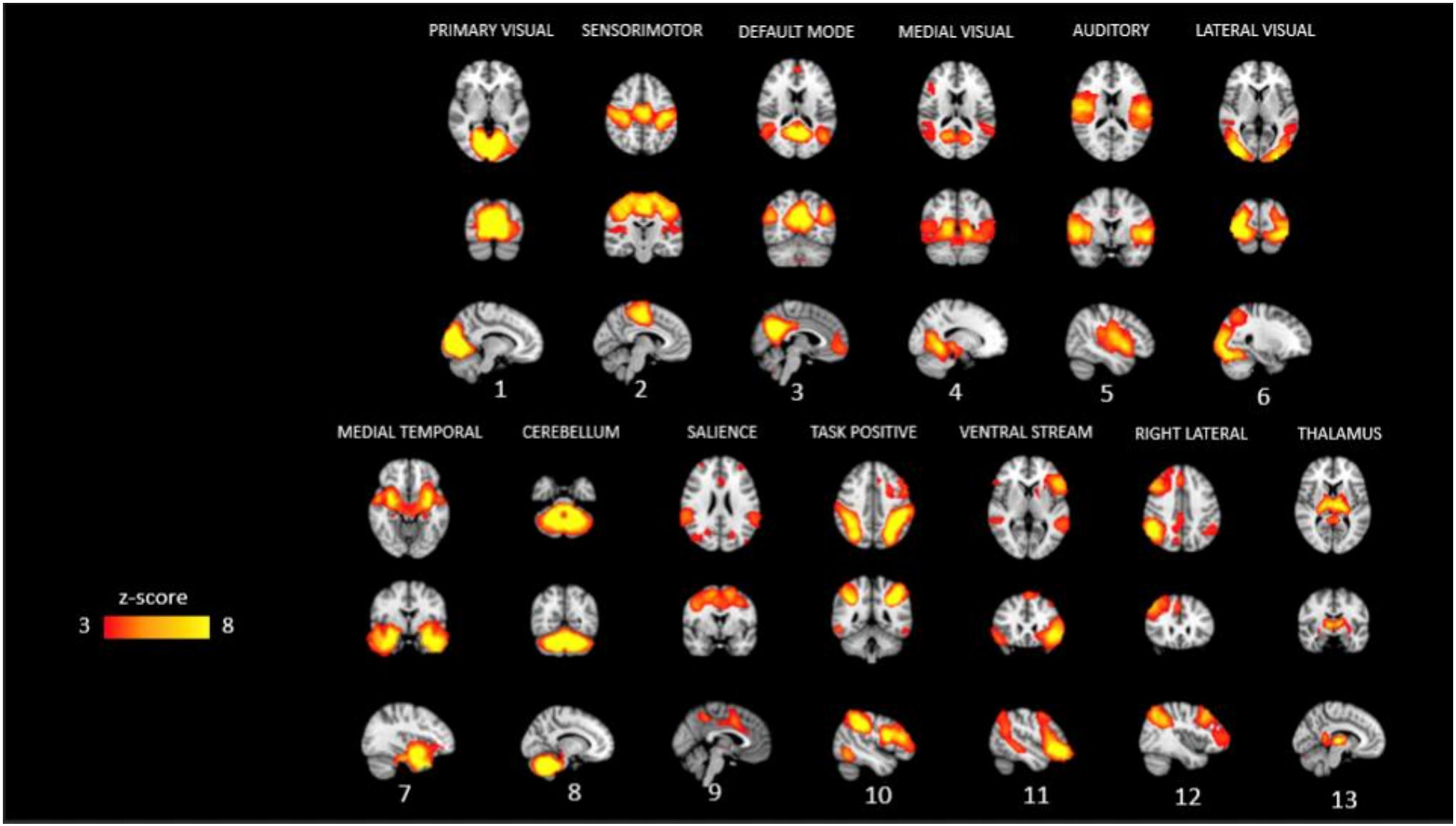


Figure 6.1 Large-scale network templates.

*Note: These were identified through group independent component analysis in an independent sample of healthy individuals' resting-state fMRI data. This figure is copied from (Dipasquale et al. (2019).*

A whole-brain cluster-level inference at α = .05 using family-wise error correction for multiple comparisons was applied. In line with the convention for BOLD resting-state fMRI (S. M. Smith et al., 2013), only clusters which survived the cluster-defining threshold of p = .001 were interpreted. For any significant cluster, the resulting one-tailed p-values were then multiplied by 2 to create two-tailed p-values for interpretation. Furthermore, to correct for multiple comparisons across the networks, Bonferroni corrections were applied. For p-values relating to the three networks selected as candidates of interest *a priori* (DMN, MTN, SAL), the adjusted alpha threshold was p = .02. For p-values relating to the remaining ten networks included in the exploratory whole-brain analysis, the adjusted alpha threshold was p = .005. For any cluster with a significant effect, the individual beta-values (parameter estimates, i.e., the correlation coefficients) which represent the FC of the respective large-scale network with this significant cluster were extracted by applying a binary mask of the significant cluster onto the subject- and session-specific spatial maps generated in stage 2 of the dual regression. To interpret significant interaction effects, the extracted beta values were compared using post-hoc simple main effects with the Sidak correction for multiple comparisons.

The between-network analysis assessed the correlation between any two functional networks. This utilized the timeseries created in stage 1 of the dual regression and was thus spatially bound to the thresholded network maps. The FSLNets package (https://fsl.fmrib.ox.ac.uk/fsl/fslwiki/FSLNets) was used in Matlab (S. M. Smith et al., 2013). The timeseries for each subject and each session were prepared for analysis in a similar manner as above. To assess the main effect of group, the PL and OT timeseries were averaged for each subject. To assess the main effect of treatment and the interaction effect, the timeseries for OT and PL were subtracted from each other for each subject. Age and minutes since dose were included as covariates of no-interest. FSLNets produced z-scores representing the full correlations between each of the networks. The correlation between the

two networks selected as candidates of interest *a priori* (DMN, SAL) was followed by an exploratory analysis, which assessed the correlation between all 13 networks. The exploratory analysis was corrected for family wise error within FSLNets and false discovery rate (FDR) was applied (threshold $p < .00001$).

### 6.2.7 Statistical analysis: correlation with phenotype

Partial Pearson correlations were conducted to assess the relationship between within-network FC abnormalities and responsivity to OT with phenotypic variables (clinical, behavioural, and cognitive characteristics). This was conducted in the ASPD participants only. The extracted beta values from clusters with a significant main effect of group or interaction effect (if simple main effects revealed a significant within-group change for ASPD) were used. The clinical variables included the PCL-R total, factor, and facet scores. The behavioural phenotyping variables included conviction information and aggression (RPQ) scores. The cognitive variables included standardized scores from the five neurocognitive assessments described in detail in the *Methods chapter*. These focused on emotion recognition and detection, reinforcement-based decision-making, delay discounting, and disinhibition.

For correlations with findings from a significant main effect of group, extracted beta values from the respective PL and OT data were averaged. For correlations with findings from a significant interaction effect, the extracted values were subtracted (OT minus PL). This was done to ensure compatibility with the main analysis. Age and minutes since dose were included as covariates of no-interest. FDR was applied to correct for multiple comparisons within each analysis and across each phenotypic cluster and bootstrapped 95% confidence intervals were also calculated.

## 6.3 Results

### 6.3.1 Demographic and clinical characteristics

*Table 6.1* shows the demographic and clinical characteristics of the sample. By nature of the design, the groups were similar in age and IQ. However, as expected, the groups significantly differed on years in education, PCL-R total, factor and facet scores, and total, reactive, and proactive aggression scores. In this analysis, the two groups did not significantly differ on the presence of a positive urine screening test during either session. Nevertheless, a supplementary post-hoc sensitivity analysis assessed whether having a positive urine drug screening test on the day of either scan predicted any significant findings from the main analysis (see Table S3). Information on comorbid disorders and conviction history for the ASPD group is also shown in *Table 6.1*.

| **Demographic**<br>**N** | **ASPD**<br>**19** | **NO**<br>**19** | **Main test statistic** |
|---|---|---|---|
| Age, mean (SD) | 42.47 (10.05) | 37.42 (10.02) | U = 125.50, p = .11 |
| IQ, mean (SD) | 95.28 (14.49) | 99.42 (10.95) | U = 147.00, p = .47 |
| Years in education, mean (SD) | 10.32 (1.83) | 14.16 (3.32) | U = 47.00, p < .001 |
| +P, N (%) | 12 (63%) | 0 (0%) | . |
| PCL-R Total, mean (SD) | 24.55 (6.94) | 2.84 (3.11) | U = 1.00, p < .001 |
| PCL-R Factor 1, mean (SD) | 8.02 (3.40) | 1.16 (1.71) | U = 25.00, p < .001 |
| PCL-R Facet 1, mean (SD) | 3.70 (2.15) | .74 (.99) | U = 41.50, p < .001 |
| PCL-R Facet 2, mean (SD) | 4.32 (2.24) | .47 (.84) | U = 29.00, p < .001 |
| PCL-R Factor 2, mean (SD) | 14.11 (3.23) | 1.21 (1.51) | U = 0.00, p < .001 |
| PCL-R Facet 3, mean (SD) | 6.42 (1.84) | 1.11 (1.29) | U = 5.00, p < .001 |
| PCL-R Facet 4, mean (SD) | 7.63 (1.95) | .53 (1.22) | U = 2.00, p < .001 |
| Cluster A, N (%) | 3 (16%) | 0 (0%) | . |
| Cluster B, not ASPD, N (%) | 5 (26%) | 0 (0%) | . |
| Cluster C, N (%) | 3 (16%) | 0 (0%) | . |
| Substance Use Disorder, N (%) | 4 (21%) | 0 (0%) | . |
| ADHD, N (%) | 2 (11%) | 0 (0%) | . |
| Positive urine drug test PL, N (%) | 10 (52%) | 5 (26%) | $\chi^2$ = 2.75, p = .18 |
| Positive urine drug test OT, N (%) | 11 (69%) | 5 (26%) | $\chi^2$ = 3.89, p = .10 |
| Total Convictions, mean (SD) | 27.53 (24.12) | . | . |
| Violent Convictions, mean (SD) | 3.84 (2.81) | . | . |
| Age 1st Violent Conviction, mean (SD) | 20.11 (5.68) | . | . |
| Presence of reconviction | 2 (11%) | . | . |
| Total Aggression, mean (SD) | 24.94 (11.23) | 6.65 (4.37) | U = 21.00, p < .001 |
| Reactive Aggression, mean (SD) | 14.31 (5.38) | 5.94 (3.82) | t(31) = -5.18, p < .001 |
| Proactive Aggression, mean (SD) | 10.63 (6.38) | .71 (1.21) | U = 14.00, p < .001 |

Table 6.1 Demographic and clinical characteristics of the participants included in the large-scale network analysis.

*Note: Some participants did not complete the RPQ (final ASPD N = 16, NO N = 17). SD = standard deviation, PL = placebo, OT = oxytocin, +P = individuals with ASPD and a PCL-R score above the cut-off of 25, U-statistic = Mann Whitney U, $\chi^2$ = chi-squared test of independence, t-statistic = t-test. RPQ = reactive-proactive aggression questionnaire.*

### 6.3.2 Large-scale network analysis

#### *6.3.2.1 Within-network analysis*

*Table 6.2* summarizes the significant findings identified in the within-network analysis. Amongst the candidate networks, significant main effects of group were identified in the MTN and SAL, indicating these networks have a different shape within each group (*Figure 6.2*). In the ASPD group, the MTN demonstrated decreased FC in the right superior frontal gyrus, as well as increased FC in the bilateral orbitofrontal cortex (OFC), midcingulate cortex, anterior insula, caudate and putamen (note that the midcingulate cortex finding was approaching significance after Bonferroni correction for multiple comparisons). Furthermore, the SAL demonstrated decreased FC in the right superior and middle temporal gyrus. There were no significant main effects of treatment or interaction effects in the candidate networks.

The exploratory analysis revealed several significant main effects of group within other networks (*Table 6.2*, *Figure 6.3*). In the ASPD group, the lateral visual network demonstrated decreased FC in the bilateral medial superior frontal gyrus and anterior midcingulate cortex. The primary visual network exhibited decreased FC in the right angular gyrus, superior and middle temporal gyrus and supramarginal gyrus, and the thalamic network demonstrated increased FC in the thalamus (latter findings not significant after correction for multiple comparisons). No significant main effect of treatment was found. However, there was a significant group by treatment interaction effect within the thalamic network (approaching significance after correction for multiple comparisons). Simple main effects revealed that under PL, the middle and inferior temporal gyrus of ASPD group exhibited significantly higher FC than the NO group. OT administration significantly decreased FC in the ASPD group, while also significantly increasing FC in the NO group, abolishing group differences (*Figure 6.4*).

| | Cluster name | Hemi. | Cluster description | X | Y | Z | k | $P_{FWE\text{-}corr}$ One-tailed | $P_{FWE\text{-}corr}$ Two-tailed |
|---|---|---|---|---|---|---|---|---|---|
| **Candidate networks** | | | | | | | | | |
| *Main effect of group* | | | | | | | | | |
| ASPD < NO | | | | | | | | | |
| Medial-temporal network | AprClus1 | RH | Superior frontal gyrus | 26 | 64 | 8 | 330 | .004 | .008 |
| Salience network | AprClus2 | RH | Superior and middle temporal gyrus | 60 | -42 | 6 | 297 | .004 | .008 |
| ASPD > NO | | | | | | | | | |
| | AprClus3 | RH | OFC, anterior insula, caudate, putamen | 26 | 30 | -4 | 1527 | <.0001 | <.0002 |
| Medial-temporal network | AprClus4 | LH | OFC, anterior insula, caudate, putamen | -26 | 26 | -4 | 676 | <.0001 | <.0002 |
| | AprClus5 | Both | Midcingulate | 6 | -12 | 28 | 261 | .013 | .026 † |
| **Whole-brain analysis** | | | | | | | | | |
| *Main effect of group* | | | | | | | | | |
| ASPD < NO | | | | | | | | | |
| Primary visual network | ExpClus1 | RH | Angular gyrus, superior and middle temporal gyrus, supramarginal gyrus | 50 | -52 | 24 | 222 | .019 | .038 ◊ |
| Lateral visual network | ExpClus2 | Both | Medial superior frontal gyrus, anterior midcingulate | 0 | 46 | 28 | 619 | <.0001 | <.0002 |
| ASPD > NO | | | | | | | | | |
| Thalamic network | ExpClus3 | LH | Thalamus | -18 | -24 | 14 | 301 | .007 | .014 ◊ |
| *Interaction effect* | | | | | | | | | |
| Thalamic network | ExpInteractClus1 | RH | Middle and inferior temporal gyrus | 56 | -34 | -18 | 307 | .003 | .006 † |

Table 6.2 Results from the within-network functional connectivity analysis.

*Note: The top part of the table shows the results from the candidate networks selected a priori, and the lower part of the table shows the results from the exploratory analysis. All clusters survived the cluster-defining threshold of p = .001. The original one-tailed and adjusted two-tailed group or interaction effect significance values for all clusters are shown in the table. Due to the novelty of this analysis, and in line with other studies (Nomi & Uddin, 2015; Uddin et al., 2013), all significant findings were interpreted, even if the Bonferroni-corrected two-tailed p-values did not survive the Bonferroni correction for multiple comparisons. For transparency, those p-values which did not survive this correction are marked: ◊ Corrected two-tailed p-value not significant, † Corrected two-tailed p-value is approaching significance. Those without a symbol survived Bonferroni correction. RH = right hemisphere, LH = left hemisphere, OFC = orbitofrontal cortex. Clusters labelled according to Automated Anatomical Labelling (AAL3) atlas built into SPM12 and confirmed by mapping MNI peak coordinates to Talairach space and Brodmann areas in BioImage Suite (https://bioimagesuiteweb.github.io/bisweb-manual/tools/mni2tal.html).*

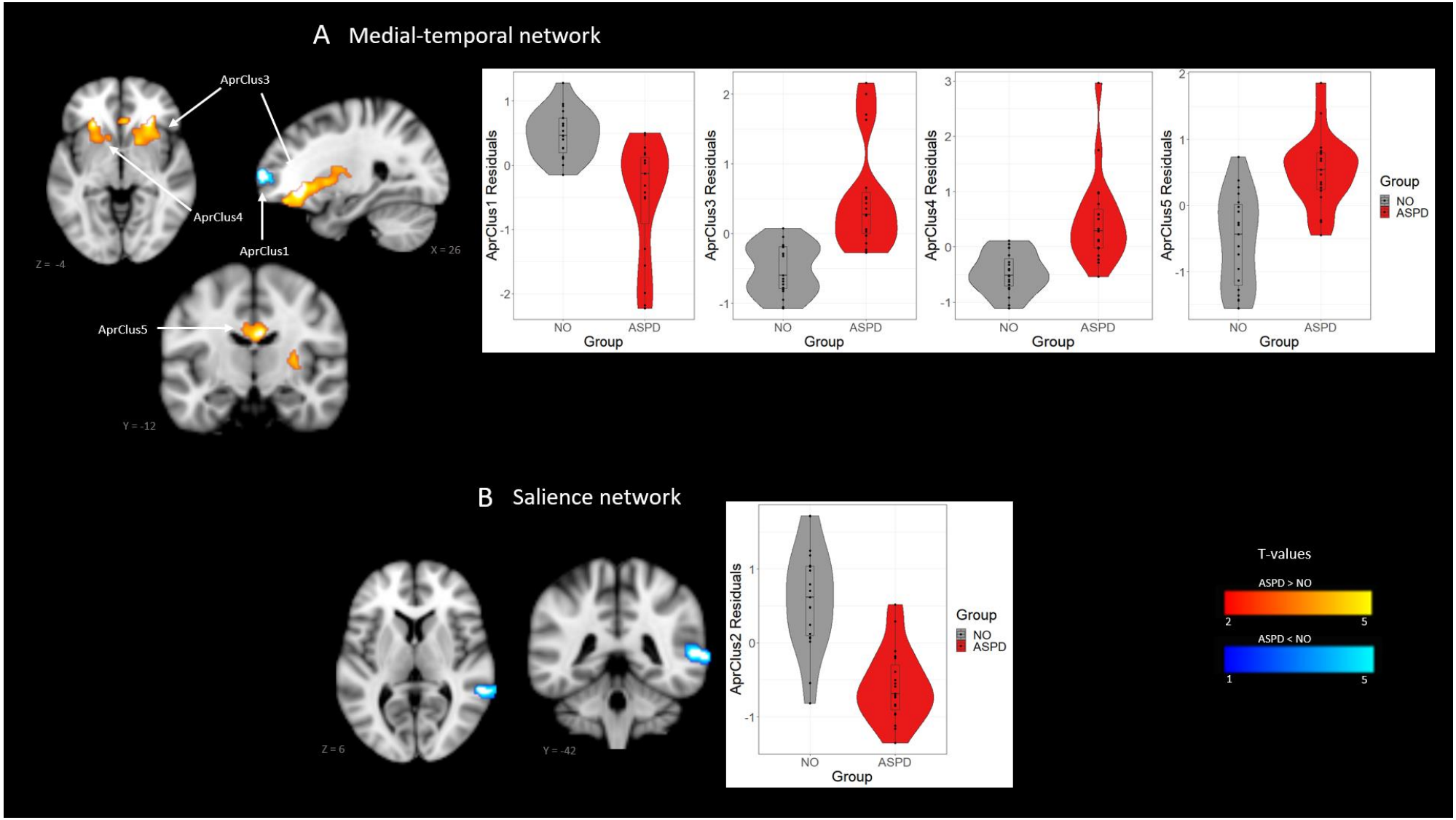


Figure 6.2 Visualization of the significant group differences identified in the within-network functional connectivity analysis of candidate networks.

*Note: The violin plots (with box plots inside) show the EMM and individual points (residuals) to see the spread of data. Note: EMMs = estimated marginal means.*

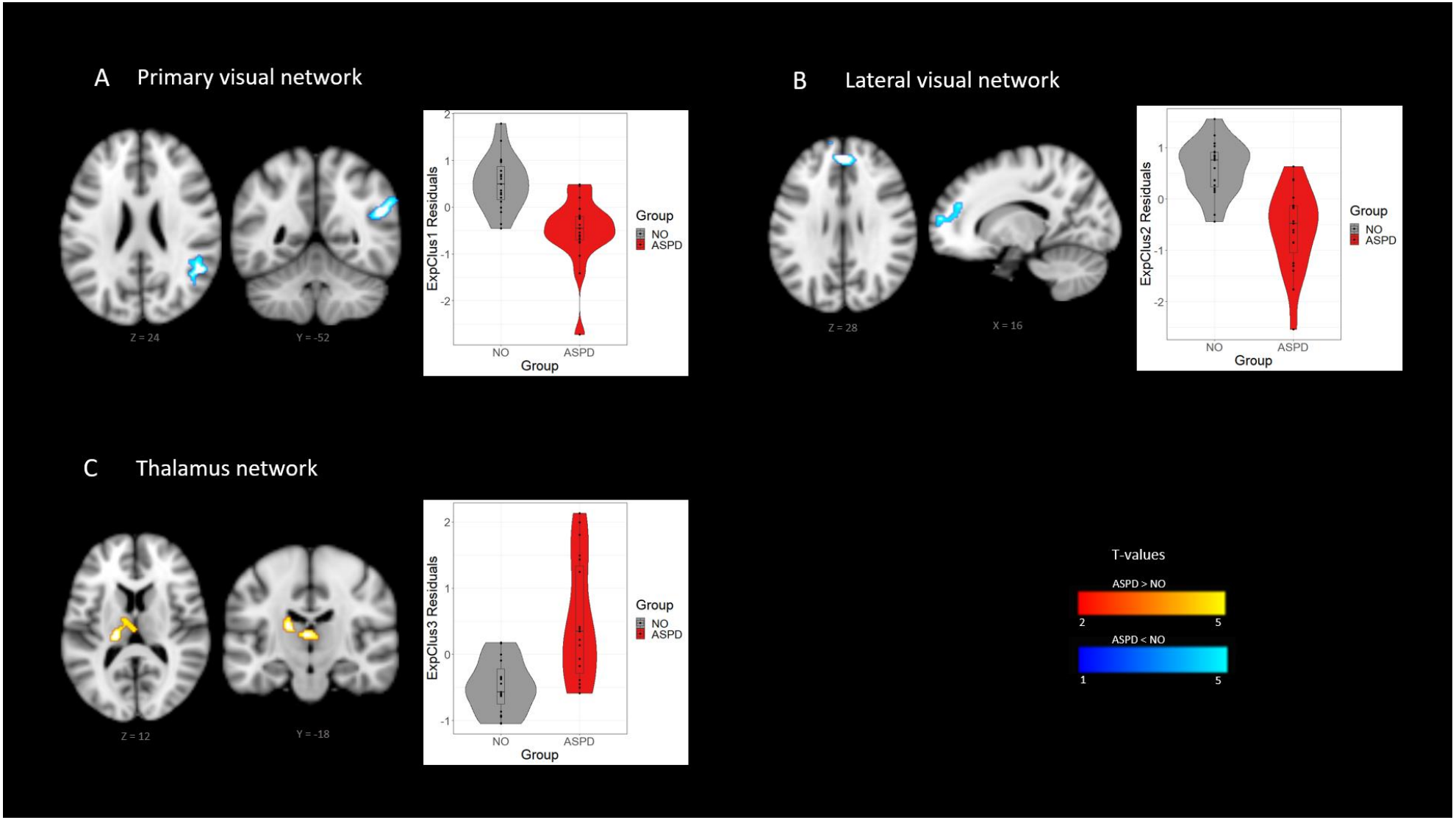


Figure 6.3 Visualization of the significant group differences identified in the within-network functional connectivity analysis of non-candidate networks.
*Note: The violin plots (with box plots inside) show the EMM and individual points (residuals) to see the spread of data. Note: EMMs = estimated marginal means.*

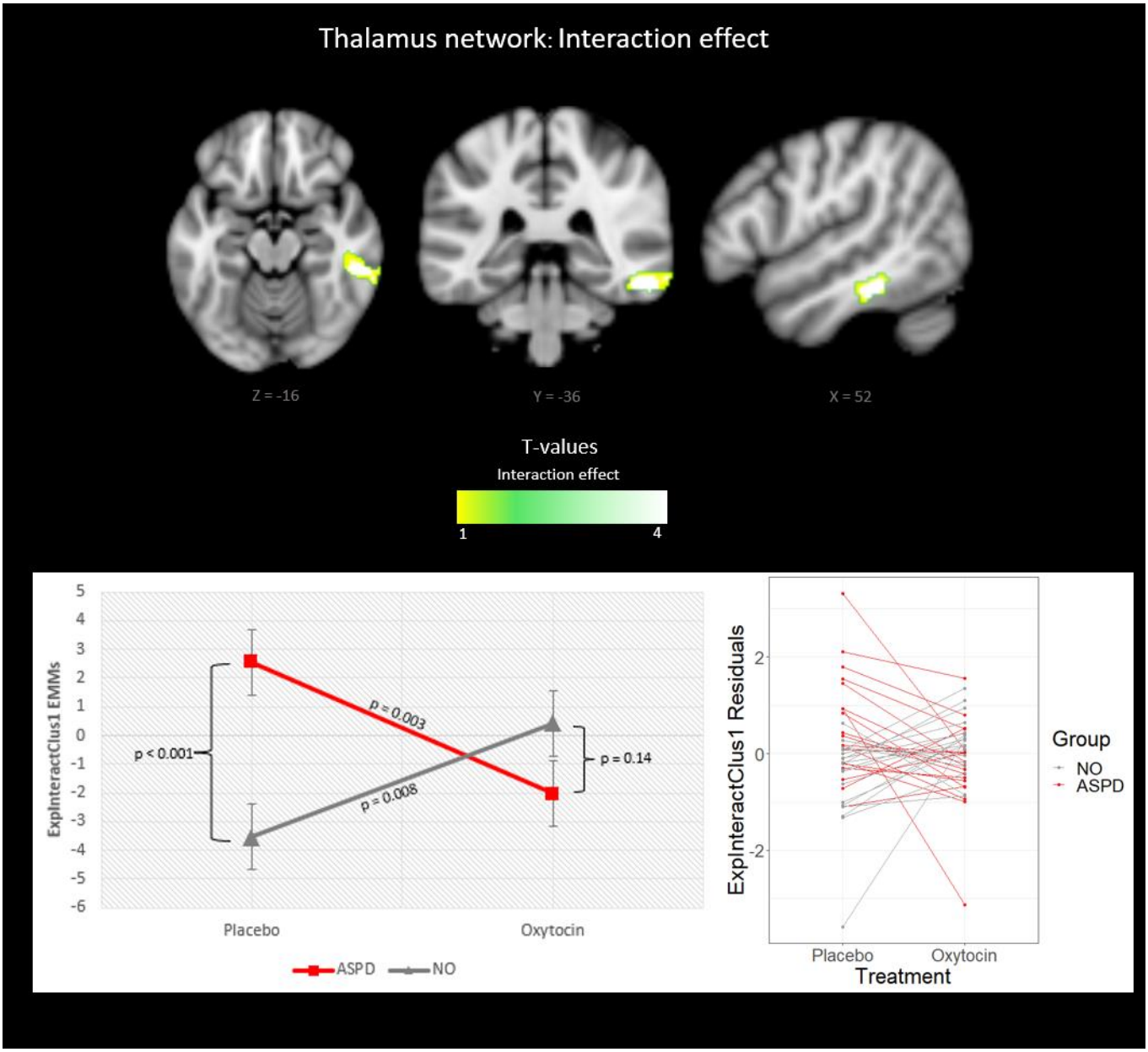


Figure 6.4 Visualization of the cluster showing the significant group by treatment interaction effect in the within-network functional connectivity analysis.

*Note: The line plot shows the EMMs and provide the Sidak-corrected p-values associated with the simple main effects, and the Spaghetti plot shows the individual responses to the OT challenge (standardized residuals accounting for covariates of no-interest). EMMs = estimated marginal means.*

#### *6.3.2.2 Between-network analysis*

The analyses assessing the full correlations between the candidate networks selected *a priori*, as well as the exploratory analysis assessing full correlations between all networks did not reveal any significant findings.

### 6.3.3 Correlation with phenotype

Within the ASPD participants only, two correlations survived the FDR correction for multiple comparisons (*Table 6.3*). There was a significant

negative relationship between accurate response reversal in the reinforcement-based decision-making task and FC in AprClus3 (right OFC, anterior insula, putamen and caudate; r = .724, FDR-corrected p = .04, 95% confidence intervals = -.885 – -.425) and AprClus4 (left OFC, anterior insula, putamen and caudate; r = -.669, FDR-corrected p = .05, 95% confidence intervals = -.867 – -.320). *Figure 6.5* therefore shows that as FC in the MTN decreased, the ability to accurately adapt decision-making improved. There were additional correlations which showed significance prior to FDR correction for multiple comparisons, as shown in *Table 6.3*, however these were not interpreted.

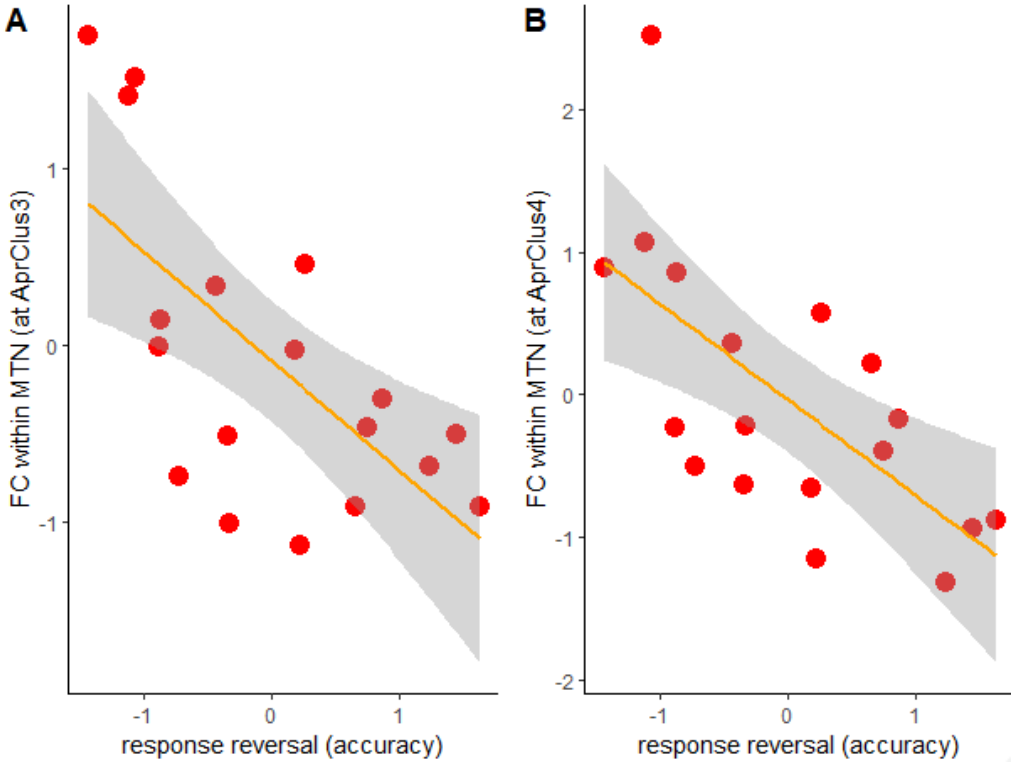


Figure 6.5 Significant negative correlation between functional connectivity in MTN and response reversal accuracy.
*Note: Correlations in ASPD subjects only. Panel A shows FC of MTN within AprClus3, which is the right OFC, anterior insula, caudate, and putamen, and panel B shows FC of MTN within AprClus4, which is the left OFC, anterior insula, caudate, and putamen. Orange lines indicate that the ASPD group had significantly higher FC than the NO group within this network cluster. MTN = medial temporal network, FC = functional connectivity, OFC = orbitofrontal cortex.*

| | | Candidate networks | | | | | Exploratory networks | | | |
|---|---|---|---|---|---|---|---|---|---|---|
| | | **AprClus1** | **AprClus2** | **AprClus3** | **AprClus4** | **AprClus5** | **ExpClus1** | **ExpClus2** | **ExpClus3** | **ExpIntract Clus1** |
| PCL-R | Total | .048 | -.147 | .141 | .402 | -.159 | .041 | -.113 | .099 | .200 |
| | Factor 1 | .026 | .093 | .035 | .221 | -.240 | .052 | -.113 | -.084 | .337 |
| | Factor 2 | .002 | -.344 | .307 | .485* | -.070 | .063 | -.174 | .246 | .158 |
| | Facet 1 | -.024 | .153 | -.075 | .245 | -.201 | .032 | -.049 | -.021 | .040 |
| | Facet 2 | .064 | .022 | .123 | .155 | -.226 | .060 | -.145 | -.122 | .552 * |
| | Facet 3 | -.045 | -.243 | .184 | .387 | -.159 | .288 | -.168 | .296 | -.082 |
| | Facet 4 | .086 | -.301 | .283 | .356 | .026 | -.163 | -.127 | .123 | .324 |
| Conviction information | # past violent convictions | -.032 | -.107 | .337 | .411 | .191 | -.067 | -.012 | -.088 | -.003 |
| | 1 year reconviction | .323 | -.334 | -.271 | -.251 | -.292 | .071 | .425 | -.443 | .160 |
| Aggression [a] | RPQ-Reactive | .128 | .366 | .221 | .201 | -.140 | -.046 | -.621 * | .538 * | .341 |
| | RPQ-Proactive | -.121 | .542 * | .123 | .329 | -.131 | -.126 | -.657 ** | .108 | .302 |
| Emotion recognition (accuracy) [b] | Angry | .055 | -.035 | .209 | .118 | .115 | .199 | -.024 | -.387 | -.108 |
| | Sad | .005 | -.234 | .004 | .328 | -.346 | .232 | .303 | .196 | -.003 |
| | Fear | .275 | .043 | .386 | .452 | .273 | -.058 | -.169 | .472 | -.243 |
| Emotion detection (reaction time) [b] | Angry | -.137 | -.192 | -.233 | -.082 | .012 | .069 | .397 | -.153 | -.387 |
| | Fear | .195 | -.259 | -.235 | -.017 | -.061 | .135 | .482 | -.223 | -.329 |
| Reinforcement-based decision-making (accuracy) [b] | Acquisition learning | .001 | .154 | -.217 | -.410 | -.122 | -.318 | .176 | -.293 | .001 |
| | Response reversal | .274 | .126 | **-.724 ** ** | **-.669 ** ** | -.167 | .223 | .167 | -.274 | .129 |
| Delay discounting (# of times lesser value chosen) [b] | 7 days | .186 | -.296 | -.099 | -.109 | -.018 | -.148 | .418 | .340 | -.197 |
| | 30 days | .305 | -.276 | -.122 | -.126 | -.032 | -.128 | .367 | .444 | -.111 |
| | 90 days | .016 | -.320 | -.017 | .028 | .067 | -.349 | .353 | .459 | -.215 |
| | 180 days | -.098 | -.297 | .112 | .126 | .108 | -.448 | .334 | .406 | -.219 |
| | 360 days | -.054 | -.281 | .121 | .091 | .105 | -.467 | .372 | .397 | -.235 |
| Disinhibition [b] | SSRT | .041 | .038 | .290 | .201 | -.090 | .192 | -.196 | .017 | -.003 |

Table 6.3 Partial Pearson coefficients for within-network functional connectivity-phenotype correlations.

*Note: correlations between the FC beta values and phenotypic variables. The correlations for FC in clusters with significant main effects of group, the average beta value extracted from the PL and OT scan was used. For correlations with the FC interaction effect, the OT minus PL delta score was used. Bold font indicates the p-value survived FDR correction for multiple comparisons. * uncorrected p ≤ .05, ** uncorrected p ≤ .01. Not all participants completed all components: [a] N = 16, [b] N = 18. SSRT = stop signal reaction time. RPQ = reactive-proactive aggression questionnaire.*

## 6.4 Discussion

This study investigated large-scale network FC and, for the first time, compared the effect of OT on FC in violent offenders with ASPD relative to a healthy NO control group. It was hypothesized that the ASPD group would show aberrant within-network and between-network FC when compared to the NO group, with an *a priori* focus on the DMN, SAL, and MTN. It was also predicted that OT would modulate FC in different ways across the two groups. The results revealed two key findings, partially supporting these hypotheses. First, the ASPD group showed aberrant FC within several large-scale networks, including the SAL, the MTN, the thalamic network and two visual networks. Not all effects survived correction for multiple comparisons. Second, there was a distinct effect of OT on FC of the thalamic network, significantly decreasing it in the ASPD and significantly increasing it in the NO group, such that significant group differences were abolished. Finally, the exploratory correlations between FC and phenotypic characteristics of ASPD revealed an inverse relationship between MTN connectivity and learning accuracy in a reinforcement-based decision-making task. These findings will be discussed below.

Violent offenders with ASPD showed FC differences relative to NO. For instance, they demonstrated significantly decreased FC within the SAL, specifically in the right posterior superior and middle temporal gyrus. This supports existing evidence showing that offenders with significant antisocial behaviour, ASPD, and psychopathy have differences in resting-state and task-based activity in the SAL - and in individual areas within this network (Deming & Koenigs, 2020; Espinoza et al., 2018; Hamilton et al., 2015; W. Jiang et al., 2021; Philippi et al., 2015). It was also demonstrated that the lateral visual network had reduced connectivity in individuals with ASPD, particularly in the bilateral anterior midcingulate, which is also an area that is typically associated with the SAL (Uddin et al., 2019). Taken together, such abnormalities may have implications relevant for the neurocognitive and behavioural dysfunctions experienced by individuals with ASPD and

psychopathy. For instance, the SAL is critical for detecting emotionally and socially salient information (W. W. Seeley et al., 2007; Uddin et al., 2019). Moreover, the right posterior superior and middle temporal gyrus region is involved in social cognition such as face perception and theory of mind (Deen et al., 2015). Hypoconnectivity in this network might hence contribute to difficulties associated with identifying and attending to such behaviourally relevant information (N. E. Anderson et al., 2018; Schönenberg et al., 2013; Yoder et al., 2015). The lack of significance of the negative correlations between SAL hypoconnectivity and facial emotion detection in the current study were likely due to methodological limitations, and significantly larger sample sizes would ideally be required to power such analyses (Marek et al., 2022). In summary, these findings suggest that individuals with ASPD have reduced resting-state FC in regions important for social cognition.

A further finding that demonstrated FC differences in ASPD relative to NO was within the MTN. Individuals with ASPD showed MTN FC decreases in the right superior frontal gyrus, and MTN FC increases in the bilateral OFC, midcingulate cortex, anterior insula, and dorsal striatum (i.e., caudate and putamen). This aligns with evidence from previous analyses, which also suggested that ASPD and psychopathy are characterized by aberrant FC between medial-temporal subcortical and frontotemporal cortical structures (Contreras-Rodríguez et al., 2015; Decety, Chen, et al., 2013; Hosking et al., 2017; H. Liu et al., 2014; Ly et al., 2012; Motzkin et al., 2011; Philippi et al., 2015; Pujol et al., 2012). However, this prior research typically suggested hypoconnectivity, whereas the current results predominantly indicated hyperconnectivity in the ASPD group. It is possible that different methodological approaches contributed to this divergence in findings. For instance, although all studies assessed offenders, the samples were heterogeneous with respect to the presence of ASPD and/or the severity of PCL-R factor/facet scores. Most, but not all, prior studies focused on high psychopathy samples (i.e., with high PCL-R factor 1 scores). It is likely that

such sample heterogeneity contributes to discrepancy across study findings. This notion is supported by one of the previous large-scale network analyses (Philippi et al., 2015), which showed that PCL-R factor 2 scores, which more closely align with the behavioural ASPD symptoms, were associated with increased FC of anterior insula and midcingulate networks, whereas factor 1 scores were associated with decreased FC in these areas. Similarly, seed-based FC analyses have also reported positive associations between factor 2 but not factor 1 scores and frontostriatal connectivity in offender populations (Korponay et al., 2017a, 2017b). Finally, in the current study, the positive correlation between MTN hyperconnectivity and PCL-R factor 2 score but not factor 1 score was significant (albeit only before correction for multiple comparisons). Together, this might suggest that hyperconnectivity is attributed to the antisocial-impulsive (factor 2) behavioural features of ASPD and psychopathy. However, to improve the understanding of whether - and - how specific traits are truly linked with unique connectivity profiles, and to reduce the discrepancy in research findings, it is important that future research assesses FC in more biologically homogenous subgroups, e.g., those with ASPD with psychopathy versus those without psychopathy (chapters 4-5; De Brito et al., 2013; Gregory et al., 2012; Sethi et al., 2015; Tully et al., 2022).

This study used methodological (pre-processing) approaches which may also contribute to the discrepancy in findings for subcortical-frontotemporal connectivity (Shirer et al., 2015). The current study was the first to use multi-echo independent component analysis to denoise the data (Kundu et al., 2017), which has been shown to be more effective than other approaches (Dipasquale et al., 2017). Furthermore, previous studies analysed FC abnormalities within temporal correlation structures that were identified in their own data, whereas the current study assessed FC abnormalities with respect to externally-sourced network maps, which may be less biased (Bijsterbosch et al., 2017). Finally, this was the first study

to use a dual regression analysis approach (Beckmann et al., 2009; Nickerson et al., 2017). As noted above, dual regression assesses individuals' FC by applying group-level spatial maps onto individual data while controlling for the influence of all other networks and variability by using multiple regression. This is contrary to other large-scale network analyses that simply compare FC abnormalities of networks without controlling for their influence on each other. Furthermore, dual regression measures FC within an entire network across the whole brain, rather than just the FC of pre-selected nodes associated with a network. Thus, dual regression is better than traditional seed-based or large-scale network analyses at detecting meaningful inter-individual variability (Smith et al., 2014). However, the novel methodological approach that was used may also contribute to the divergence in MTN connectivity findings. Future research should seek to compare results using different analysis approaches. Nevertheless, the current state of the evidence base converges in suggesting the presence of FC abnormalities within MTN areas.

Abnormal MTN connectivity is expected to have implications for dysfunction experienced by individuals with ASPD and psychopathy. Indeed, another finding of the current study was the significant inverse association between MTN connectivity, specifically in the bilateral OFC, anterior insula, and dorsal striatum, and the ability to accurately reverse responses under changing reward contingencies (i.e., reinforcement-based learning). As MTN FC decreased, the response accuracy improved. Previous studies have highlighted that difficulties with reinforcement-based learning are characteristic of this population (e.g., Budhani et al., 2006; De Brito et al., 2013; Gregory et al., 2015). Furthermore, such response reversal difficulties have been associated with functional anomalies within and between the same areas (Budhani et al., 2007). The current findings thus further suggest that resting-state MTN abnormalities relate to differences in social cognitive functioning in ASPD, though future research should seek to verify these findings in much larger sample sizes.

Although abnormalities in MTN FC were not modulated by OT, the current results demonstrated that other FC differences can be shifted by OT. Specifically, it was discovered, for the first time, that OT significantly modulated thalamic network FC differences. The ASPD group showed hyperconnectivity within this network, specifically in the thalamus itself, as well as in the middle and inferior temporal gyrus. However, within the temporal regions, OT administration significantly decreased this hyperconnectivity, abolishing significant group differences with the NO group. Together, these results suggest that FC abnormalities in the thalamic network of offenders with ASPD, which are independent of task and context, can be 'shifted' towards NO. In individuals with ASPD and psychopathy, aberrant thalamic activity and FC has been associated with reduced threat response and impaired moral processing (Kumari et al., 2009; Nummenmaa et al., 2021; Yoder et al., 2015). The thalamus has increased oxytocin receptor binding and higher expression of the oxytocin receptor gene than most other brain regions (Boccia et al., 2013; Quintana, Rokicki, et al., 2019). However, in the current study, the effect of OT on thalamic network connectivity was strongest in the right middle and inferior temporal gyri. This could mean that OT has an indirect effect on thalamic network connectivity by mediating activity in areas involved in theory of mind and social cognition or behaviour (Wigton et al., 2015). However, further research investigating the mechanisms of OT action on the brain is required (Quintana et al., 2021). It also remains to be understood whether - and how - FC responsivity to OT relates to clinical and behavioural outcomes.

Several limitations of the current study should also be discussed. First, due to the smaller number of subjects with complete datasets, this analysis could not differentiate between individuals with ASPD with versus without psychopathy. Post-hoc correlations between FC abnormalities in the ASPD group and PCL-R scores revealed two relationships with factor 2 and facet 2 scores, though these were not significant after correction for multiple

comparisons. A second limitation of this study was that the externally sourced network maps that were employed in this study did not include a map that fits the traditional FPN. However, the task positive network included areas typically encompassed in the FPN, and no within- or between-network differences were detected in ASPD in this network. Nevertheless, considering the other large-scale network analyses have revealed abnormalities in the FPN (Espinoza et al., 2018; Philippi et al., 2015; Tang, Jiang, et al., 2013), future research utilizing a more traditional template of the FPN is required to assess this more thoroughly. Third, due to the analysis of resting-state FC, the findings from this study cannot provide direct insight into the neurobiological underpinnings of specific behaviours. However, the significant post-hoc correlation between abnormal MTN connectivity and reinforcement-based learning does suggest some possible association between these resting-state findings and neurocognitive performance. Furthermore, since this paradigm is task-free by nature, there is no control over individuals' behaviour while in the scanner. Thus, it is possible that the current findings reflect differences in brain responses towards the instructions to focus on the fixation cross and let the mind wander (Cole et al., 2010). Future research could use fMRI that integrates resting- and task-state by relying on methods that are low-demand and experimentally controlled across studies but which still evoke task-free, self-generated neural activity (Finn, 2021). A final methodological limitation of this study relates to the length of time between the OT administration and the acquisition of the rs-fMRI scan. The rs-fMRI scan was scheduled to occur 75 minutes after OT administration, however in reality, the average time since administration was 90 minutes. This is towards the end of the temporal profile of OT pharmacological action (Paloyelis et al., 2016). Hence the amount of OT in the brain may already have been decreasing, and potential effects of OT which occur earlier in the window of pharmacological action may have been missed. However, a previous study showed effects of OT on whole-brain large-scale networks in scans acquired 75 minutes after OT administration (Brodmann et al.,

2017), and another study assessing the impact of OT on regional cerebral blood flow revealed significant effects up to 95 minutes post-dose (Martins, Brodmann, et al., 2022). Together, these findings thus suggest that a single dose of 40 IU of OT may have effects on brain function as late as 90-100 minutes after administration. Nevertheless, future research should assess how OT affects FC in ASPD and psychopathy at different time windows.

In conclusion, taken together, these results provide further insight into the underpinning neurobiological mechanisms of ASPD and show that violent offenders with ASPD and varying severity of psychopathy have abnormal resting-state FC across several networks. These were partly related to differences in cognitive functions reported to be abnormal in ASPD and were partly modifiable through OT.

# 7 A resting-state fMRI investigation into network topology and the effect of intranasal oxytocin in violent offenders with ASPD

## 7.1 Introduction

As discussed in earlier chapters, brain structure, regional cerebral blood flow (rCBF), and resting-state functional connectivity (FC) are abnormal in forensic populations of violent offenders with ASPD and varying degrees of psychopathy. Resting-state FC reflects the temporal correlations of spontaneous neural activation patterns between spatially distinct brain regions. In this disorder, it has typically been examined by means of seed-based and large-scale network analyses. As detailed in *chapter 6*, this research has revealed reduced FC between subcortical (e.g., amygdala, striatum) and cortical regions (e.g., anterior cingulate, ventromedial prefrontal cortex, precuneus), and unusual activation patterns within the default mode (DMN), salience, medial-temporal, and frontoparietal large-scale networks (Contreras-Rodríguez et al., 2015; Espinoza et al., 2018; H. Liu et al., 2014; Ly et al., 2012; Motzkin et al., 2011; Nummenmaa et al., 2021; Pujol et al., 2012; Tang, Jiang, et al., 2013; Tang, Liu, et al., 2013). Such abnormalities have been linked to clinical, behavioural, and/or cognitive features, such as psychopathic traits, aggression, criminality, empathic processing and decision-making (Decety, Chen, et al., 2013; Hosking et al., 2017; Kolla et al., 2018; Philippi et al., 2015; Siep et al., 2019; Werhahn et al., 2021).

These studies were important first steps, providing converging evidence that impaired resting-state FC is a neurobiological mechanism correlated with aspects of the clinical phenotype in those with ASPD and psychopathy. However, traditional FC analytic methods cannot offer insight into network topology, or the organization of brain networks. Understanding network topology is important because it tells us about the intrinsic architecture of

the brain in terms of the complex integration and segregation of information processing (Bullmore & Sporns, 2009; Farahani et al., 2019; Rubinov & Sporns, 2010). Graph theory analysis has evolved as a powerful tool for examining functional network topology.

As detailed previously in the *Methods chapter*, graph theory analysis produces a network model of the brain, comprising nodes (brain areas) and edges (the connection between brain areas) (Bullmore & Sporns, 2009; Rubinov & Sporns, 2010; Zalesky et al., 2010). This network model is characterized by a range of topological properties, which can be evaluated with metrics that give insight into multiple levels of processing (Bassett & Bullmore, 2017; Cohen & D'Esposito, 2016; Joules et al., 2015; Sporns, 2013). At the macro-level, the global efficiency metric is used to reflect the functional *integration* of the brain, that is, the capacity for parallel information processing across the whole brain. At the meso-level, four metrics are typically determined. The local efficiency metric is used to determine the functional *segregation* of the brain, that is, the average capacity for information processing within individual brain regions. The nodal efficiency metric is used to determine the information processing capacity of an individual node. The centrality metrics of node degree and betweenness centrality are used to determine (respectively) the connectivity and importance of individual nodes for communication across the network. At the micro-level, the edge connectivity metric is used to determine the strength of connections between nodes. *Figure 7.1* shows a visual depiction of these topological network properties. It is critical to understand if - and how - these topological network properties deviate from the norm in ASPD to reveal the neurobiological substrates of connectivity differences in ASPD and potential markers of therapeutic targets for pharmacological treatments (Buckholtz & Meyer-Lindenberg, 2012; He & Evans, 2010; Khalili-Mahani et al., 2017).

To date, only three studies have used graph theory analysis to study network topology in adult antisocial offender populations, and all suggested

aberrant topology in the disorder. Two studies were conducted in groups of delinquent young men with and without ASPD (W. Jiang, Shi, Liao, et al., 2017; Tang et al., 2016); and one in a large group of incarcerated men characterised by their psychopathy scores (Tillem et al., 2019). All three studies converge on the finding that subcortical structures have reduced centrality in this population, suggesting that these nodes are less of a communication hub in those with ASPD as compared to controls. However, Jiang et al. (2017) examined individual subcortical areas only if these were explicitly included within previously identified networks, and Tang et al. (2016) and Tillem et al. (2019) examined the centrality of subcortical structures collectively. Therefore, it remains to be investigated which individual subcortical areas might contribute to this general reduction in centrality. One subcortical region of particular interest in this case is the amygdala given that it has frequently been shown to have reduced structural and functional connectivity in ASPD and psychopathy (Contreras-Rodríguez et al., 2015; Dugré & Potvin, 2021; Motzkin et al., 2011).

Concerning other topological metrics, the findings from these three past graph theory studies were less clear. In the two studies comparing delinquent young males with versus without ASPD, one revealed significant increases in global and local efficiency in ASPD, suggesting abnormally high functional integration and segregation (Tang et al., 2016), whereas the other showed reduced global and local efficiency (W. Jiang, Shi, Liao, et al., 2017). Furthermore, Tang et al. (2016) found increases in edge connectivity in ASPD, showing that the precuneus, a core hub of the default mode network, had abnormally high connectivity with nodes associated with other networks. In contrast, Jiang et al. (2017) found decreased edge connectivity between parietal and frontal nodes. These studies were important first steps showing aberrant macro-, meso-, and micro-level topology in ASPD, but further clarification of the discrepancy in findings is required. Methodological differences may have contributed to the differences in findings. For instance, Jiang et al. (2017) applied spatial

smoothing during pre-processing, even though this is not recommended for graph theory analysis because it distorts the model metrics (Alakörkkö et al., 2017). Additionally, both studies also had significant methodological limitations. First, neither study employed a non-offending control group, so it is unclear how findings relate to offending behaviours. Second, they both used only young adult samples, aged 18-22, meaning findings may be more reflective of late adolescence, when brain and personality development may not yet be complete, rather than adulthood. Finally, neither study phenotyped their participants in terms of psychopathy, even though its presence has been associated with specific mechanisms in ASPD (De Brito et al., 2013; Gregory et al., 2012, 2015).

The third study improved on the latter two limitations (Tillem et al., 2019). Their large incarcerated male sample represented an adult sample, with an average age of 33, characterized using the PCL-R. Results showed that, after accounting for the presence of a substance use disorder, increasing severity of psychopathy was associated with significantly increased efficiency, or functional integration, within the frontoparietal (i.e., dorsal attention) network. Furthermore, there were no significant alterations in the topology of the default mode and salience networks. Therefore, their results, when taken in combination with those by Tang et al. (2016), suggest that the brain networks of antisocial offender populations are characterized by significantly increased functional integration. However, the extent of abnormal functional segregation and differences in edge connectivity remain unclear, and the efficiency of specific nodes has yet to be studied. Thus, in summary, further investigation is required to disentangle the brain topology of individuals with ASPD.

Abnormal topological metrics may serve as useful targets which could potentially be used to help develop new treatments for the disorder. However, no study to date has assessed whether topological properties of neural networks in ASPD could be shifted by a potential treatment. One pharmacological agent of interest is intranasal oxytocin (OT) – a

neuropeptide that impacts on social behaviours and empathy. Previous work has shown that OT can shift FC in the brain (Brodmann et al., 2017; Grace et al., 2018; X. Jiang et al., 2021; S. H. Seeley et al., 2018; Xin et al., 2021; Z. Zhao et al., 2019). Furthermore, two graph theory studies in healthy individuals revealed that OT modulates meso-level network topology, including topological features which appear abnormal in ASPD (Martins et al., 2021; Zheng et al., 2021). For example, Zheng et al. (2021) revealed that OT increased the connectivity of subcortical structures including the amygdala, increasing the number of edges with frontal regions. Their results also indicated that OT reduced network segregation as measured by a close correlate of the local efficiency metric. Furthermore, Martins et al. (2021) also showed that exogenous oxytocin shifts the centrality and efficiency of individual nodes associated with medial-temporal, salience, and default mode networks, such as the amygdala, anterior cingulate cortex, and precuneus. The impact of OT on these nodes is likely to be more profound due to their relatively high oxytocin receptor density (Quintana, Rokicki, et al., 2019). Overall, there is emerging evidence from studies of healthy individuals that OT modulates network topology properties that may be abnormal in ASPD and psychopathy. This, however, remains to be directly investigated.

This study therefore sought to explore five key aspects of brain topology in ASPD, using a carefully phenotyped sample of adult males with a history of violent offending and a non-offender control group. First, to seek to confirm the reduced centrality of individual subcortical nodes identified in extant studies. Second, to resolve outstanding contradictions in global efficiency, local efficiency, and edge connectivity in the disorder. Third, for the first time, to explore the impact of the social neuropeptide oxytocin on network topology in ASPD. Fourth, to explore how aberrant network topology might contribute to FC in networks shown to be impaired in ASPD (see *Chapter 6*) by evaluating the spatial overlap between nodal findings and large-scale networks. Finally, as recommended by Tillem et al. (2019), to explore

correlations between potential topological abnormalities and phenotypic characteristics in the ASPD group. For the meso-level metrics, an initial ROI analysis focused on the amygdala, anterior cingulate, and precuneus as probes of the medial-temporal, salience, and default mode networks. These are regions that have previously been demonstrated to have abnormal FC in ASPD as well as higher oxytocin receptor density (Kumar et al., 2020). Furthermore, examination of the macro- and micro-level metrics, as well as additional exploration of meso-level metrics, was conducted on a whole-brain basis. It was hypothesized that the ASPD group would show decreased centrality of subcortical nodes, increased global and local efficiency, as well as altered nodal efficiency and edge connectivity. Furthermore, it was hypothesized that OT would 'shift' these abnormalities and attenuate differences between the ASPD and the non-offending control groups. There were no distinct hypotheses for the fourth and fifth aspects of this investigation as these were exploratory.

## 7.2 Methods

### 7.2.1 Participants

This study included 29 male violent offenders with a diagnosis of ASPD and 22 male non-offending (NO) healthy control participants. The PCL-R score was collected, but for this analysis, violent offenders were not categorized into ASPD+/-P groups because the final sample sizes were too small (for information only, N = 17 scored above European threshold of 25). Across both groups, participants were eligible for inclusion if they were aged between 18 and 60, had an IQ above 70, did not suffer any past or current neurological illness/trauma, and if it was safe for them to undergo an MRI scan. Offenders were recruited from South London NHS medium secure forensic clinical services and National Probation Services. They were selected based on having a history of violent offending, with convictions including assault, actual/grievous bodily harm, armed robbery, rape, manslaughter, or murder. Offenders with a current or past diagnosis of mood or psychotic disorder were excluded. Healthy NO control participants

were recruited through purposive sampling from the general community. Individuals expressed their interest in participating by responding to advertisements placed online and in public spaces in the local area. They were excluded if they had any history of offending, or a current or past mental illness or personality disorder.

The study was approved by London City and East Research Ethics Committee and the Health Research Authority (reference: 15/LO/1083), as well as the National Offender Management Services Research Committee (reference: 2016-382). All participants completed signed informed consent.

### 7.2.2 Study design and procedure

This study used a double-blind, placebo-controlled, randomized crossover design. All participants attended an assessment day where diagnostic interviews were conducted. This included the PCL-R (Hare, 1991), the SCID-5-PD (First et al., 2015) to confirm the diagnosis of ASPD and to assess for any comorbid personality disorders, as well as the SCID-5-CV (First et al., 2016) to assess for any other comorbid mental disorders. IQ testing (WASI-II) (Wechsler, 2011) and completion of the reactive-proactive aggression questionnaire (RPQ) (Raine et al., 2006) was also done during the assessment day. Participants attended two further days where an identical protocol of MRI sequences and neurocognitive testing were completed. These were scheduled on average 16 days apart. On each day, participants completed a urine drug screening test to check for recent substance use. Participants were randomly and blindly allocated to receive the OT (Syntocinon, Novartis, Switzerland) or placebo dose (PL; same ingredients but without oxytocin). They received the alternative on the second day. Each dose contained 40 IU, and was self-administered via a nose spray, inhaling one puff every 30 seconds in alternating nostrils. This process was supervised by the researcher. The selected dose is in line with other studies testing the effect of OT on brain activity and behaviour and corresponds with safety standards (MacDonald et al., 2011; Martins et al., 2021; Martins, Brodmann, et al., 2022; Paloyelis et al., 2016). The resting-

state fMRI scan (08:10 minutes) was the final scan in the MRI protocol. It was acquired 92 (±9 minutes) and 90 (±14 minutes) after the final PL and OT dose, respectively. This time delay will be considered as the variable 'minutes since dose' in the subsequent analyses.

### 7.2.3 Image acquisition

The resting-state fMRI scan was acquired on a General Electric MR750 3Tesla MRI scanner with a 32-channel C-RMNova head coil. A T2*-weighted whole-brain multi-echo echo planar imaging (EPI) sequence with 192 volumes per echo and 24576 images in total was acquired during each scanning session (32 horizontal slices top-to-bottom parallel to the anterior-posterior commissure line, slice thickness = 3 mm, slice gap = 1 mm, TR = 2500 ms, TE = 4 echoes at 12, 28, 44 and 60 ms, FA = 80°, FOV = 240 x 240 $mm^2$; matrix = 64 x 64, voxel resolution = 3.75 x 3.75 x 3 $mm^3$). Participants were instructed to remain still, stay awake, focus on a fixation cross on the screen in front of them and to let their mind wander. The same high-resolution T1-weigthed structural image which was acquired and used for analysis in *chapter 4* was here used for anatomical co-registration (196 image, slice thickness = 1.2 mm, slice gap = 1.2 mm, TR = 7.32 ms, TE = 3.02 ms, TI = 400 ms, FA = 11°, FOV = 270 x 270 $mm^2$, matrix = 256 x 256, voxel resolution = 1.05 x 1.05 x 1.2 $mm^3$).

### 7.2.4 Image pre-processing

The pre-processing of the resting-state fMRI data was conducted in an order that has been recommended for graph theory analysis (Gargouri et al., 2018). Details and justifications are provided in the *Methods chapter*. In summary, these steps included: (1) skull-stripping and brain extraction of the structural image to prepare a study-specific anatomical template; (2) calculation of a transformation matrix of this template to MNI152 standard space; (3) brain tissue extraction from the resting-state fMRI image; (4) splitting of the first three echoes and removal of the fourth echo in preparation for subsequent denoising by optimally combining the data using a weighted average approach; (5) slice timing correction; (6) motion

correction including timeseries de-spiking, and volume registration and realignment by applying six rigid-body transformation parameters (images with a framewise displacement value larger than 0.25 mm were excluded); (7) further noise artefact removal using multi-echo independent component analysis; 8) co-registration of the final denoised resting-state fMRI image to T1 native space in preparation for tissue segmentation; (9) removal of timeseries associated with signal from white matter and cerebrospinal fluid; (10) high-pass temporal filtering to remove low signal frequencies (<0.02 Hz); (11) normalization of the co-registered resting-state fMRI images to MNI152 space by application of the previously calculated transformation matrix from step (2). The global signal was not regressed out as this may have adverse effects for graph theory analysis, including the production of anti-correlations (Cheng et al., 2021; Fox et al., 2009). Furthermore, spatial smoothing should not be performed for graph theory analysis (Alakörkkö et al., 2017). Thus, the images used for this analysis were not exposed to the final step of smoothing that was applied in Chapter 6.

### 7.2.5 Statistical analysis: demographic and clinical characteristics

The demographic and clinical characteristics were compared between groups using SPSS26 (IBM Corp, 2019). Independent t-tests (or Mann Whitney U if normality assumption violated) were used to assess differences in age, IQ, years in education, PCL-R and RPQ scores. The groups did not significantly differ in age or IQ. Chi-squared ($X^2$) tests (or Fisher exact test in case of violation of assumptions) were used to assess differences in the frequency of positive urine drug screening tests. Due to the exclusion criteria, the frequency of comorbid disorders and conviction information were not subject to group comparisons because they were not present in the NO group.

### 7.2.6 Statistical analysis: graph theory

This analysis relied on linear mixed modelling, which means that participants with missing data due to non-attendance of one session could

still be included since this approach is appropriate for repeated designs even if data is missing (Magezi, 2015). The final pre-processed (unsmoothed) images for each participant and each session were prepared for graph theory analysis. This involved parcellating the timeseries of each final scan into an 85 x 85 correlation matrix according to the Desikan-Killiany atlas (DKA, Desikan et al., 2006). The 85 regions of this atlas correspond to cortical and subcortical regions but exclude cerebellar regions. Each region was considered as a node in the graph theory analysis. The connection between each node (the correlation between each area) was considered as an edge. The correlation matrices were then Fisher z-transformed. The average of the positive elements in the lower triangle of each Fisher z-transformed correlation matrix for each individual and each session was calculated to assess group, treatment, and interaction effects for mean functional connectivity (FC) using a linear mixed model. Mean FC is an indicator of total network strength (Van Den Heuvel et al., 2017).

The Brain Connectivity Toolbox (BCT) (Rubinov & Sporns, 2010) was then implemented in Matlab 2017a (The Mathworks Inc, 2020) for the next steps. First, correlation matrices of each participant and each session were concatenated into one weighted, undirected adjacency matrix. Second, to reduce the likelihood of findings being associated with a specific network density, and in line with recommendations linked to the small-world organization of the brain (Bassett & Bullmore, 2017; Watts & Strogatz, 1998), the adjacency matrix was then thresholded across a range of network densities between 5% and 34%, at a 1% interval. This ensured that graph theory metrics were not driven by variability in the density of individual networks. Finally, BCT was used to calculate the area under the curve (average) of the thresholded network densities of the following higher level summary graph theory metrics, also visualized in *Figure 7.1*.

- **Macro-level: Global efficiency**: This is a measure of functional integration across the whole brain. It is defined by the inverse of the average characteristic path length between all nodes in the

network. The characteristic path length describes the smallest possible number of edges required to connect any two nodes to form a potential route along which information can flow (Achard & Bullmore, 2007; Latora & Marchiori, 2001; Rubinov & Sporns, 2010).

- **Meso-level: Local efficiency**: This is a measure of functional segregation. It reflects the average of all nodal efficiency values across the whole brain and thus indicates the extent to which local areas form sub-networks.
- **Meso-level: Nodal efficiency**: This reflects functional integration of each node. It is defined by the inverse of the average minimum characteristic path length connecting one node with its neighbouring nodes (Latora & Marchiori, 2001).
- **Meso-level: Node degree centrality**: This is a simple measure of centrality of an individual node. It is defined by the number of edges connected to a node (Rubinov & Sporns, 2010).
- **Meso-level: Betweenness centrality**: This is a more complex measure of centrality, or importance, of a particular node. It is defined by the proportion of shortest paths that flow through a particular node, providing information on how much of a communication hub a node is (i.e., "hubness").
- **Micro-level: Edge connectivity**: This reflects the strength of edges that connect individual nodes (Zalesky et al., 2010). This was calculated with the network-based statistic, outlined below.

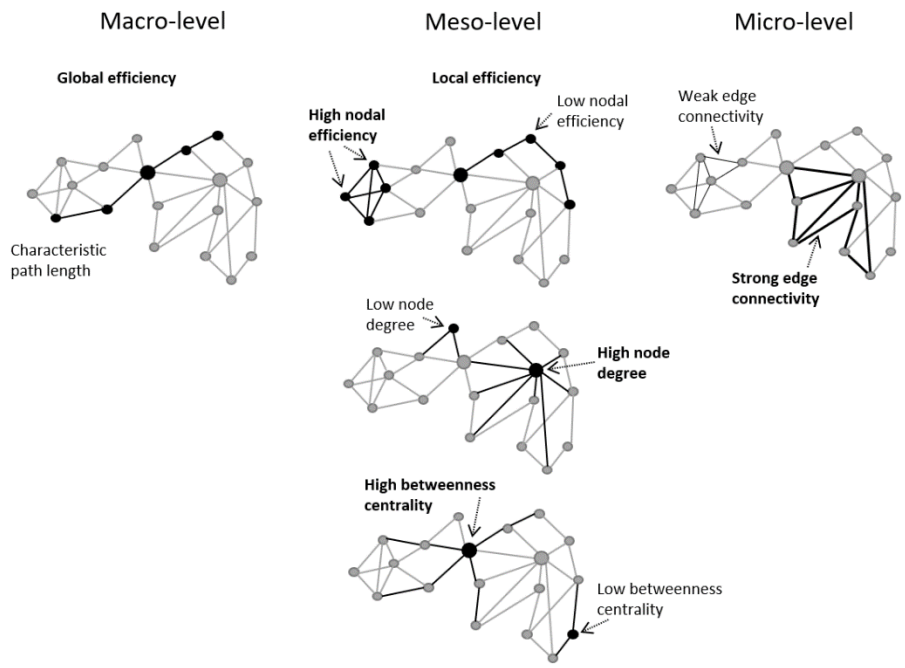


Figure 7.1 Visual representation of the graph theory metrics.
*Note: due to its calculation, global efficiency is shown in the context of an example of characteristic path length. Local efficiency is shown in the context of nodal efficiency.*

These summary graph theory metrics were extracted for each DKA node, in each participant and each session. Linear mixed modelling was then applied to calculate the main effect of group, treatment, and group by treatment interaction effects on mean FC, global efficiency, and all nodal metrics. Linear mixed modelling allowed the inclusion of participants who were only able to attend one session, since they can be used for repeated analysis even if individual data points are missing. Across all models, the fixed factors were group (ASPD and NO), treatment (PL and OT), and their interaction. The random factor was subject. Mean-centred age and mean-centred minutes since dose were included as covariates of no-interest. The dependent variable was the respective graph theory metric value. For global efficiency, only one model was required. For the meso-level metrics, a model for each node was calculated. To remain consistent with the large-scale network FC analysis in the previous chapter, and with previous evidence that these regions and networks have impaired connectivity in ASPD, the ROI analysis focused on the amygdala, anterior cingulate cortex, and precuneus as probes of the medial-temporal, salience, and default mode networks, respectively. Values were extracted for these regions in each hemisphere. The DKA separates the anterior cingulate into rostral and

caudal regions, meaning values for the anterior cingulate cortex consisted of an average between rostral and caudal nodes. For the ROI analysis, a false discovery rate (FDR) correction for six multiple comparisons was applied (left and right hemisphere treated separately). An exploratory whole-brain analysis across the remaining 77 DKA nodes was conducted thereafter. An FDR correction for 77 multiple comparisons was applied. Partial eta-squared effect sizes were calculated for all analyses. Significant findings prior to FDR correction were also reported but not interpreted.

The Dice coefficient was calculated to measure the extent of spatial overlap between DKA areas with a significant nodal meso-level group, treatment, or interaction effect and the 13 large-scale networks described in chapter 6 (*Figure 6.1*). This exploratory approach indicates which large-scale networks the meso-level findings map onto.

### 7.2.7 Statistical analysis: network-based statistic

To investigate micro-level edge connectivity, the network-based statistic (NBS) toolbox in Matlab 2017a was used (Zalesky et al., 2010). NBS automatically controls the family-wise error rate (FWER) by treating all edges in the graph as one family. Therefore, the statistics are conducted on the level of the graph component, as opposed to the individual connections between nodes, reducing the number of multiple comparisons. This improves the power of the analysis and is thus comparable to the cluster-based approaches applied in mass univariate testing of voxels. Overall, a significant result represents the extraction of a topologically meaningful subnetwork (or multiple subnetworks) that is (are) significantly different between conditions. As this method is designed to function on the connectome level, it cannot inform us about individual node-to-node connections. However, it provides insight into potential functional differences in network organization.

For this analysis, a partitioned errors approach was applied. This means that the connectivity matrices from each participant's PL and OT session

were averaged to assess the main effect of group and subtracted from each other to assess the main effect of treatment and the interaction effect. Therefore, only participants who attended both scan sessions were included in this part of the analysis (n = 19 in each group, see *Table 6.1* for details on these subjects). The main effect of group was calculated using a two-sample t-test on the averaged correlation matrix. The main effect of treatment was calculated using a one-sample t-test on the subtracted correlation matrix. The interaction effect was calculated using a two-sample t-test on the subtracted correlation matrix. In all analyses, mean-centred age and mean-centred minutes since dose were included as covariates of no-interest. In line with another recent study assessing the impact of OT on network topology (Martins et al., 2021) , and considering that the selection of thresholds is arbitrary, a series of primary suprathreshold values ranging from t = 1.5 to t = 4.0, with 0.5 intervals, was applied (Zalesky et al., 2010). The FWER-adjusted p-value for any graph component above the primary threshold was then calculated using 5000 non-parametric permutations and deemed significant if the p-value was less than 0.05.

### 7.2.8 Statistical analysis: correlation with phenotype

Partial Pearson correlations were conducted to assess if network topology was correlated with phenotypic variables (clinical, behavioural, and cognitive measures). Any macro- and meso-level graph metrics which had a significant main effect of group were used to assess the relationship with topological abnormalities. Furthermore, macro- and meso-level metrics that showed a significant interaction effect (if simple main effects showed a significant within-group change for ASPD) were also of interest to assess whether there were specific correlations with the responsivity to the OT challenge. The clinical variables included the PCL-R total, factor, and facet scores. The behavioural variables included conviction information and aggression (RPQ) scores. Lastly, the cognitive variables included standardized scores from the five neurocognitive tasks described in detail

in the *Methods chapter*. These focused on emotion recognition and detection, reinforcement-based decision-making, delay discounting, and disinhibition.

As in the previous chapters, correlations with findings that showed a significant main effect of group used an average between the PL and OT scan. Correlations with findings that showed a significant interaction effect used the delta score (OT minus PL).

All correlations with phenotypic variables were only conducted within the ASPD participants. Mean-centred age and mean-centred minutes since dose were included as covariates of no-interest. FDR was applied to correct for multiple comparisons within each analysis and across each phenotypic cluster and 95% confidence intervals were also calculated.

## 7.3 Results

### 7.3.1 Demographic and clinical characteristics

*Table 7.1* provides the means (standard deviations) and frequencies (percentages) of the demographic and clinical characteristics for each group. The test statistics are also provided, where required. The ASPD and NO groups did not significantly differ on age or IQ. The ASPD group, as expected, had significantly less years in education than the NO group; and scored significantly higher on PCL-R total, factor, and facet scores, as well as on total, reactive, and proactive aggression scores. Furthermore, the ASPD group had a significantly higher rate of positive urine drug screening tests on the days of both the PL and the OT scans. Supplementary post-hoc sensitivity analyses assessed the impact of the presence of a positive drug test on topological findings (see Table S4). No statistical comparisons were required for the rate of comorbid disorders or the conviction information, since the NO group did not have any mental or personality disorders and no history of offending.

| Demographic<br>N | ASPD<br>29 | NO<br>22 | Main test statistic |
|---|---|---|---|
| Age, mean (SD) | 42.00 (9.86) | 37.73 (9.56) | U = 245.00, p = .16 |
| IQ, mean (SD) | 94.04 (13.69) | 98.95 (10.77) | t(48) = 1.38, p = .17 |
| Years in education, mean (SD) | 9.97 (1.76) | 13.77 (3.27) | U = 81.00, p < .001 |
| +P, N (%) | 17 (59%) | 0 (0%) | . |
| PCL-R Total, mean (SD) | 24.18 (6.52) | 2.64 (2.97) | U = 1.00, p < .001 |
| PCL-R Factor 1, mean (SD) | 7.80 (3.78) | 1.09 (1.63) | U = 33.50, p < .001 |
| PCL-R Facet 1, mean (SD) | 3.39 (2.17) | 0.64 (0.95) | U = 87.00, p < .001 |
| PCL-R Facet 2, mean (SD) | 4.41 (2.03) | 0.46 (0.80) | U = 34.00, p < .001 |
| PCL-R Factor 2, mean (SD) | 14.24 (3.30) | 1.09 (1.44) | U = 0.00, p < .001 |
| PCL-R Facet 3, mean (SD) | 6.69 (1.67) | 1.00 (1.23) | U = 5.50, p < .001 |
| PCL-R Facet 4, mean (SD) | 7.46 (2.25) | 0.50 (1.14) | U = 5.00, p < .001 |
| Cluster A, N (%) | 5 (17%) | 0 (0%) | . |
| Cluster B, not ASPD, N (%) | 10 (35%) | 0 (0%) | . |
| Cluster C, N (%) | 3 (10%) | 0 (0%) | . |
| Substance Use Disorder, N (%) | 6 (21%) | 0 (0%) | . |
| ADHD, N (%) | 3 (10%) | 0 (0%) | . |
| Positive urine drug test PL, N (%) | 15 (52%) | 5 (23%) | χ2 = 4.88, p = .03 |
| Positive urine drug test OT, N (%) | 18 (62%) | 6 (27%) | χ2 = 6.08, p = .01 |
| Total Convictions, mean (SD) | 25.72 (21.60) | 0 (0.00) | . |
| Violent Convictions, mean (SD) | 4.45 (3.19) | 0 (0.00) | . |
| Age 1st Violent Conviction, mean (SD) | 20.43 (4.94) | . | . |
| Presence of reconviction | 5 (17%) | . | . |
| Total Aggression, mean (SD) | 26.67 (11.69) | 6.35 (4.30) | t(42) = -7.36, p < .001 |
| Reactive Aggression, mean (SD) | 14.83 (5.65) | 5.90 (3.54) | t(42) = -6.14, p < .001 |
| Proactive Aggression, mean (SD) | 11.83 (6.96) | 0.75 (1.16) | U = 23.00, p < .001 |

Table 7.1 Demographic and clinical characteristics of the participants included in the network topology analysis. *Note: The NBS analysis included a subsample of participants (ASPD N = 19, NO N = 19) as some did not attend both sessions. These are the same individuals analysed in Chapter 6, see Table 6.1 for an overview of their characteristics. The characteristics were largely similar except that the two subsample groups did not significantly differ on the presence of positive urine drug screening tests during either session. In the current analysis, some participants did not complete the RPQ (final ASPD N = 24, NO N = 20). +P = above-threshold PCL-R score SD = standard deviation, PL = placebo, OT = oxytocin, U-statistic = Mann Whitney U, $\chi^2$ = chi-squared test of independence, t-statistic = t-test.*

## 7.3.2 Graph theory analysis

### *7.3.2.1 Mean functional connectivity*

The linear mixed model revealed a significant main effect of group on mean FC ($F_{(1, 42.86)} = 4.62$, $p = .04$, $\eta_p^2 = .10$), whereby the ASPD group had significantly higher mean FC than the NO group. The main effect of treatment ($F_{(1, 35.26)} = 0.01$, $p = .92$, $\eta_p^2 < .01$) and the interaction effect ($F_{(1, 36.29)} = 0.73$, $p = .40$, $\eta_p^2 = .02$) were not significant. The covariates of no-interest were also not significant (age: $F_{(1, 42.75)} = 3.85$, $p = .06$, $\eta_p^2 = .08$; minutes since dose: $F_{(1, 78.12)} = 0.20$, $p = .66$, $\eta_p^2 < .01$).

### *7.3.2.2 Macro-level: global efficiency*

The linear mixed model revealed a significant main effect of group on global efficiency ($F_{(1, 41.64)} = 7.27$, $p = .01$, $\eta_p^2 = .15$), whereby the ASPD group had significantly higher global efficiency values than the NO group (*Figure 7.2A*). The main effect of treatment ($F_{(1, 34.07)} = 0.05$, $p = .82$, $\eta_p^2 < .01$)

and the group by treatment interaction effect ($F_{(1, 35.09)}$ = 0.28, p = .60, $\eta_p^2$ < .01) were not significant. The covariates of no-interest also did not have significant effects (age: $F_{(1, 41.52)}$ = 3.79, p = .06, $\eta_p^2$ = .08; minutes since dose: $F_{(1, 77.82)}$ = 1.26, p = .27, $\eta_p^2$ = .02).

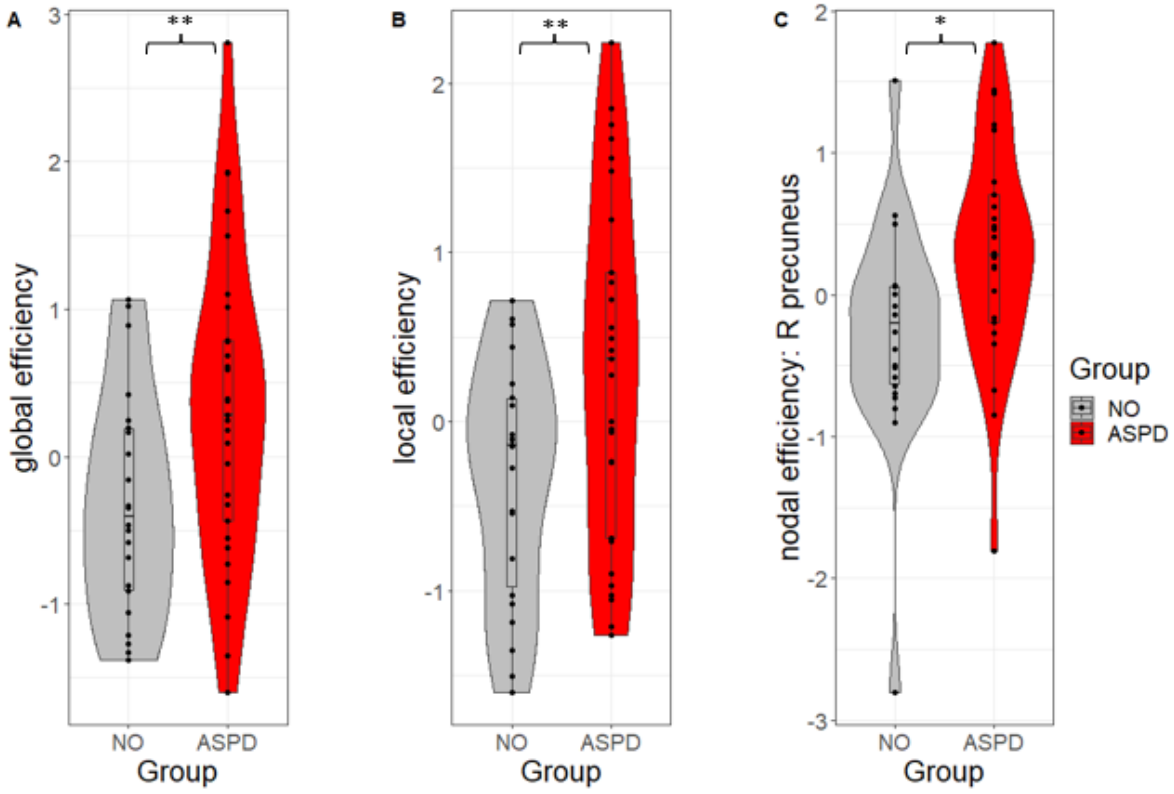


Figure 7.2 Significant group differences in A) global efficiency, B) local efficiency, and C) nodal efficiency (right precuneus).
*Note: The violin plots (with box plots to show the marginal mean and individual points showing spread of data) show the residuals after accounting for the effect of age and minutes since dose. * = (corrected) p-value < 0.05, ** = (corrected) p-value < 0.01. R = right hemisphere*

### *7.3.2.3 Meso-level: local and nodal metrics*

*Table 7.2* (ROI analysis) and *Table 7.3* (whole-brain analysis) provide the summary of all statistical findings for the nodal meso-level analyses (nodal efficiency, node degree, and betweenness centrality).

#### 7.3.2.3.1 Local efficiency

The linear mixed model revealed a significant main effect of group on local efficiency ($F_{(1, 41.12)}$ = 8.37, p = .006, $\eta_p^2$ = .17). Individuals with ASPD had significantly higher local efficiency than NO individuals (*Figure 7.2B*). The main effect of treatment ($F_{(1, 35.68)}$ = .11, p = .75, $\eta_p^2$ = .003) and the group

by treatment interaction effect ($F_{(1, 36.71)}$ = 2.53, p = .12, $\eta_p^2$ = .06) were not significant. The covariates of no-interest also did not have significant effects (age: $F_{(1, 40.84)}$ = 3.49, p = .07, $\eta_p^2$ = .08; minutes since dose: $F_{(1, 82.95)}$ = 2.69, p = .11, $\eta_p^2$ = .03).

#### 7.3.2.3.2 Nodal efficiency

The ROI analysis revealed a main effect of group in the right precuneus that survived FDR correction for multiple comparisons (*Table 7.2*). The ASPD group had higher nodal efficiency than the NO group (*Figure 7.2C*). Furthermore, prior to FDR correction for multiple comparisons (*Table 7.2*), there was a significant main effect of group in the left precuneus (ASPD > NO, uncorrected p = .05), and a significant group by treatment interaction effect in the left anterior cingulate cortex (uncorrected p = .02, but simple main effects not significant). The remaining effects were not significant.

In the whole-brain analysis, no effects survived FDR correction for multiple comparisons. However, as *Table 7.3* shows, there were several significant effects prior to this correction. These are reported but were not interpreted. *Figure 7.4* visualizes those with large effects sizes ($\eta_p^2 \geq .14$). A main effect of group was found bilaterally in the lateral orbitofrontal cortex, entorhinal cortex, parahippocampal gyrus, paracentral lobule, globus pallidus, caudate, and nucleus accumbens, in the left temporal pole, superior temporal gyrus, and lingual gyrus, and in the right middle temporal gyrus and cuneus. In all regions, the ASPD group had higher nodal efficiency than the NO group. There was also a main effect of treatment in the left precentral gyrus, postcentral gyrus, supramarginal gyrus, and right caudal middle frontal gyrus, whereby OT significantly reduced nodal efficiency compared to PL. Lastly, significant group by treatment interaction effects were found bilaterally in the medial and lateral orbitofrontal cortex, precentral gyrus, supramarginal gyrus, caudate, putamen, and nucleus accumbens, in the left temporal pole and globus pallidus, and in the right entorhinal cortex. The interaction effect in the left precentral and supramarginal gyrus was disordinal, meaning the significant treatment

effects in these areas should be interpreted with caution. *Figure 7.5* shows the significant simple main effects of the interaction effects with large effect sizes ($\eta_p^2 \geq .14$), displaying estimated marginal means from each group under each treatment condition. In all nodes, the ASPD group had significantly higher nodal efficiency than the NO group under PL. This was attenuated after OT administration, which significantly modulated nodal efficiency in either the ASPD group (left temporal pole, bilateral supramarginal gyrus) or the NO group (left medial orbitofrontal cortex (OFC), left nucleus accumbens, and left caudate). There were no significant group differences in any area under OT. *Figure 7.5* also depicts these interaction effects in the form of spaghetti plots, which demonstrate the individual responses to the OT challenge in each participant. Most ASPD participants responded to OT administration with a reduction in nodal efficiency, however for some regions, there are a few ASPD individuals who respond with an increase. This highlights the potential individual differences in the effects of OT.

#### 7.3.2.3.3 Node degree

The ROI analysis revealed a significant main effect of group in the left amygdala (ASPD > NO, uncorrected p = .03), but this did not survive FDR correction for multiple comparisons. There were no other significant group differences in the ROI analysis (*Table 7.2*). However, the ROI analysis did reveal a significant main effect of treatment in the left and right anterior cingulate cortex which survived FDR correction for multiple comparisons (*Table 7.2*). OT significantly reduced node degree compared to PL in both ROIs (*Figure 7.3A-B*). Further treatment or interaction effects were not significant.

In the whole-brain analysis (*Table 7.3*), no effects survived FDR correction for multiple comparisons, however there were several effects that were significant before this correction. These are reported but they were not further interpreted. *Figure 7.4* shows those effects with large effect sizes ($\eta_p^2 \geq .14$). A main effect of group showing ASPD had significantly higher

node degree than NO was detected bilaterally in the nucleus accumbens, in the left temporal pole, entorhinal cortex, and globus pallidus, and in the right caudate. Additionally, the ASPD group had significantly lower node degree of the bilateral posterior cingulate cortex than the NO group. A main effect of treatment was found in the bilateral globus pallidus and the left medial orbitofrontal cortex, where OT increased node degree, and in the bilateral transverse temporal gyrus and the right posterior cingulate cortex and pars opercularis, where OT decreased node degree. Lastly, group by treatment interaction effects were also found bilaterally in the posterior cingulate cortex and nucleus accumbens, in the left temporal pole, entorhinal cortex and globus pallidus, and in the right caudate (*Table 7.3*). Figure *7.6A* shows the simple main effects of the interaction effects with effect sizes of $\eta_p^2 \geq .14$. In this case, the only significant simple main effect was that the ASPD group had a significantly higher node degree under PL in the left nucleus accumbens, as was already revealed by the main effect of group. The spaghetti plot for the same interaction effect also shown in *Figure 7.6A* might explain why the simple main effects for within-group differences between PL and OT were not significant. Some individuals responded with an increase in node degree, whereas others responded with a decrease.

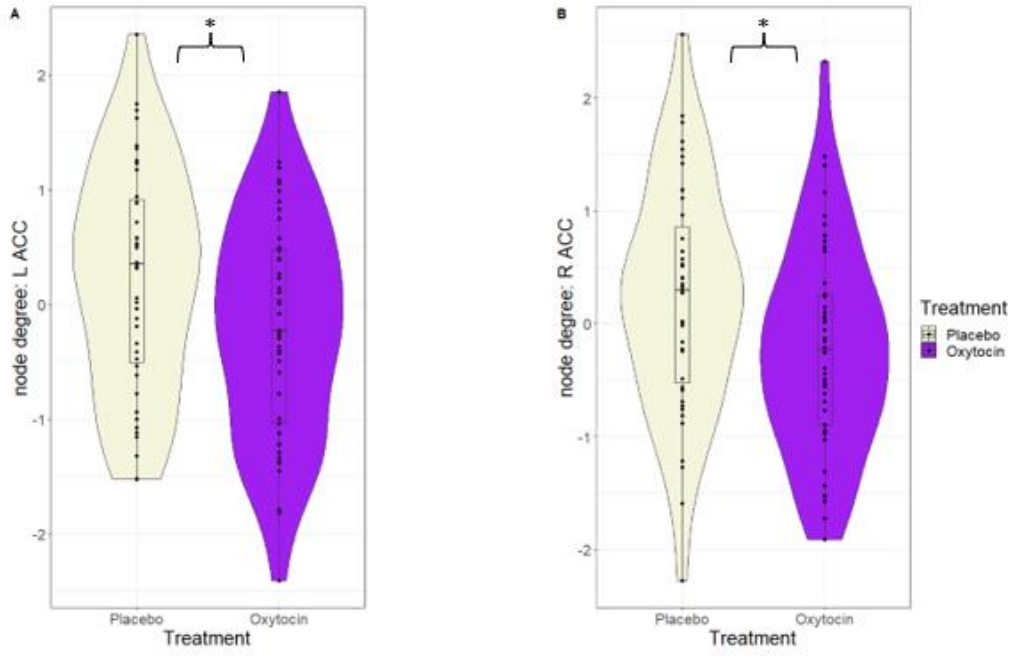


Figure 7.3 Significant treatment effects in node degree in A) the left and B) the right anterior cingulate cortex. *Note: The violin plots (with box plots to show the marginal mean and individual points showing spread of data) show the residuals after accounting for the effect of age and minutes since dose. * = corrected p-value < 0.05, R = right hemisphere, L = left hemisphere, ACC = anterior cingulate cortex.*

#### 7.3.2.3.4 Betweenness centrality

In the ROI analysis, no effects survived FDR correction for multiple comparisons (*Table 7.2*). However, before this, there was a significant group by treatment interaction effect in the left anterior cingulate cortex (uncorrected p = .02). Simple main effects revealed that under PL, the ASPD group had significantly higher betweenness centrality than the NO group (p = .03), but a significant effect of OT in the ASPD group only (p = .03) attenuated this group difference. The remaining effects were not significant.

The whole-brain analysis revealed a group by treatment interaction effect in the right cuneus that remained significant after FDR correction for multiple comparisons ($F_{(1, 40.7)}$ = 22.52, FDR-corrected p = .002, $\eta_p^2$ = .36). Under PL, the NO group had a mean betweenness centrality of 34.8 (standard error (SE) = 4.81) and the ASPD group had a mean of 45.5 (SE = 4.50). After OT, this increased in the NO group to 42.4 (SE = 4.91), whereas it decreased in the ASPD group to 25.7 (SE = 4.27). Simple main

effects revealed a significant difference between groups after OT ($p = .04$), which was driven by a significant reduction in the ASPD group ($p < .001$) (*Figure 7.4*, *Figure 7.6B*).

Several other nodes in the whole-brain analysis also showed main effects that were significant prior to FDR correction for multiple comparisons (*Table 7.3*), which are reported but not further interpreted. *Figure 7.4* shows those effects with large effect sizes ($\eta_p^2 \geq .14$). The left medial orbitofrontal cortex and parahippocampal gyrus, and the right globus pallidus showed significant main effects of group, whereby betweenness centrality was significantly lower in the ASPD group than the NO group in both areas. Additionally, the ASPD group had significantly higher betweenness centrality than the NO group in the left pars orbitalis and the right postcentral gyrus. A main effect of treatment was found in the left globus pallidus and the right entorhinal cortex, where OT significantly increased betweenness centrality compared to PL, and in the right superior frontal gyrus and cuneus, where OT significantly decreased betweenness centrality compared to PL. Significant group by treatment interaction effects were found bilaterally in the lateral orbitofrontal cortex, ventral diencephalon, in the left transverse temporal gyrus and supramarginal gyrus, and the right rostral middle frontal gyrus. *Figure 7.6B* demonstrates the simple main effects for those interaction effects with an effect size of $\eta_p^2 \geq .14$. This only revealed a significant oxytocinergic modulation of betweenness centrality in the right lateral OFC of the NO group. The spaghetti plots in *Figure 7.6B* support this finding by indicating that there was typically more modulation of betweenness centrality in the NO individuals than the ASPD individuals.

| ROI | PL mean (SD) | | OT mean (SD) | | Main effect of group | | | Main effect of treatment | | | Interaction effect | | |
|---|---|---|---|---|---|---|---|---|---|---|---|---|---|
| | ASPD | NO | ASPD | NO | $F_{(df1, df2)}$ | FDR-corrected p-value | Effect size $\eta_p^2$ | $F_{(df1, df2)}$ | FDR-corrected p-value | Effect size $\eta_p^2$ | $F_{(df1, df2)}$ | FDR-corrected p-value | Effect size $\eta_p^2$ |
| **Nodal efficiency** | | | | | | | | | | | | | |
| L Amygdala | 0.130 (0.041) | 0.111 (0.043) | 0.125 (0.040) | 0.118 (0.047) | $F_{(1, 43.89)} = 1.49$ | .26 | .03 | $F_{(1, 40.84)} = 0.11$ | .87 | .003 | $F_{(1, 41.77)} = 0.50$ | .72 | .01 |
| R Amygdala | 0.139 (0.046) | 0.120 (0.033) | 0.122 (0.039) | 0.121 (0.041) | $F_{(1, 44.03)} = 1.32$ | .26 | .03 | $F_{(1, 38.59)} = 0.71$ | .87 | .02 | $F_{(1, 39.64)} = 1.41$ | .48 | .03 |
| L A. Cingulate | 0.139 (0.035) | 0.109 (0.022) | 0.122 (0.048) | 0.125 (0.033) | $F_{(1, 46.95)} = 2.20$ | .26 | .04 | $F_{(1, 43.97)} = 0.03$ | .87 | <.001 | $F_{(1, 44.90)} = 5.70$ | .12 * | .11 |
| R A. Cingulate | 0.129 (0.034) | 0.106 (0.029) | 0.119 (0.049) | 0.117 (0.027) | $F_{(1, 45.63)} = 1.42$ | .26 | .03 | $F_{(1, 44.00)} = 0.06$ | .87 | .01 | $F_{(1, 44.83)} = 2.23$ | .42 | .05 |
| L Precuneus | 0.152 (0.027) | 0.141 (0.024) | 0.154 (0.027) | 0.142 (0.028) | $F_{(1, 44.29)} = 3.94$ | .15 * | .08 | $F_{(1, 38.96)} = 0.26$ | .87 | .006 | $F_{(1, 40.01)} = 0.17$ | .72 | .004 |
| R Precuneus | 0.149 (0.031) | 0.136 (0.025) | 0.150 (0.028) | 0.132 (0.026) | **$F_{(1, 43.08)} = 8.12$** | **.04** | **.16** | $F_{(1, 42.94)} = 0.04$ | .87 | <.001 | $F_{(1, 43.65)} = 0.13$ | .72 | .003 |
| **Node degree** | | | | | | | | | | | | | |
| L Amygdala | 5.65 (1.91) | 4.42 (1.54) | 5.36 (1.66) | 4.54 (1.70) | $F_{(1, 34.62)} = 5.30$ | .18 * | .13 | $F_{(1, 32.28)} = 0.001$ | .97 | <.001 | $F_{(1, 33.14)} = 0.28$ | .87 | .008 |
| R Amygdala | 5.46 (1.82) | 4.75 (1.54) | 5.63 (1.78) | 5.06 (1.74) | $F_{(1, 38.54)} = 1.20$ | .51 | .05 | $F_{(1, 36.68)} = 0.84$ | .72 | .02 | $F_{(1, 37.52)} = 0.02$ | .87 | <.001 |
| L A. Cingulate | 4.72 (1.41) | 4.39 (1.32) | 3.95 (1.36) | 3.94 (1.31) | $F_{(1, 45.74)} = 0.04$ | .87 | <.001 | **$F_{(1, 41.37)} = 7.13$** | **.03** | **.15** | $F_{(1, 42.38)} = 0.34$ | .87 | .008 |
| R A. Cingulate | 4.48 (1.66) | 4.24 (1.30) | 3.61 (1.39) | 3.88 (1.45) | $F_{(1, 44.92)} = 0.08$ | .87 | .002 | **$F_{(1, 38.16)} = 9.77$** | **.02** | **.20** | $F_{(1, 39.23)} = 0.46$ | .87 | .01 |
| L Precuneus | 4.71 (1.58) | 4.78 (1.31) | 4.86 (1.62) | 4.88 (1.77) | $F_{(1, 48.10)} = 0.03$ | .87 | <.001 | $F_{(1, 43.39)} = 0.11$ | .96 | .003 | $F_{(1, 44.42)} = 0.07$ | .87 | .002 |
| R Precuneus | 5.22 (1.71) | 4.64 (1.45) | 5.02 (1.55) | 4.73 (1.95) | $F_{(1, 47.55)} = 0.54$ | .87 | .01 | $F_{(1, 42.70)} = 0.07$ | .96 | .002 | $F_{(1, 43.73)} = 0.50$ | .87 | .01 |
| **Betweenness Centrality** | | | | | | | | | | | | | |
| L Amygdala | 57.12 (42.69) | 33.04 (22.36) | 33.46 (17.30) | 37.27 (17.30) | $F_{(1, 43.46)} = 2.06$ | .85 | .05 | $F_{(1, 43.78)} = 2.65$ | .39 | .06 | $F_{(1, 44.45)} = 5.74$ | .12 * | .11 |
| R Amygdala | 41.43 (31.00) | 39.50 (31.21) | 42.96 (30.23) | 50.12 (35.36) | $F_{(1, 46.66)} = 0.44$ | .85 | .009 | $F_{(1, 43.37)} = 1.28$ | .52 | .03 | $F_{(1, 44.31)} = 0.58$ | .74 | .01 |
| L A. Cingulate | 32.53 (16.18) | 32.32 (14.40) | 28.88 (18.16) | 28.17 (16.01) | $F_{(1, 49.30)} = 0.03$ | .85 | <.001 | $F_{(1, 43.65)} = 2.33$ | .39 | .05 | $F_{(1, 44.70)} = 2.33$ | .89 | <.001 |
| R A. Cingulate | 30.13 (16.43) | 29.71 (12.44) | 28.12 (17.68) | 30.83 (14.41) | $F_{(1, 45.84)} = 0.08$ | .85 | .002 | $F_{(1, 39.75)} = 0.19$ | .67 | .002 | $F_{(1, 40.81)} = 0.33$ | .74 | .008 |
| L Precuneus | 34.27 (22.53) | 32.34 (28.94) | 28.49 (14.01) | 30.39 (15.97) | $F_{(1, 43.55)} = 0.18$ | .85 | .004 | $F_{(1, 42.67)} = 0.64$ | .56 | .01 | $F_{(1, 43.44)} = 0.24$ | .74 | .006 |
| R Precuneus | 36.70 (22.32) | 30.09 (16.89) | 33.04 (17.57) | 38.67 (22.80) | $F_{(1, 41.06)} = 0.08$ | .85 | .002 | $F_{(1, 39.45)} = 0.52$ | .56 | .01 | $F_{(1,40.28)} = 2.42$ | .39 | .06 |

Table 7.2 Meso-level nodal findings for the ROI analysis.

*Note: This shows the means (standard deviations) of the respective meso-level metrics for each of the ROIs. All statistical results obtained with linear mixed modelling for the variables of interest are shown. The effects of the covariates of no-interest were not significant in any model and are thus not listed for the sake of brevity. * significant prior to correction for multiple comparisons (p<0.05). L = left hemisphere, R = right hemisphere, SD = standard deviations, df = degrees of freedom.*

| | $F_{(df1, df2)}$ | Uncorrected p-value | FDR-corrected p-value | Effect size $\eta_p^2$ |
|---|---|---|---|---|
| **Nodal efficiency** | | | | |
| *Main effect of group (ASPD > NO)* | | | | |
| Left nucleus accumbens ◊ | F(1, 43.61) = 11.79 | .001 | .07 | **.21** |
| Right caudate | F(1, 45.51) = 10.14 | .003 | .07 | **.18** |
| Right nucleus accumbens | F(1, 45.60) = 10.29 | .002 | .07 | **.18** |
| Right globus pallidus | F(1, 45.32) = 8.43 | .006 | .10 | **.16** |
| Left caudate ◊ | F(1, 43.78) = 8.15 | .007 | .10 | **.16** |
| Left entorhinal cortex | F(1, 47.01) = 7.47 | .009 | .10 | **.14** |
| Left temporal pole ◊ | F(1, 43.50) = 7.22 | .01 | .10 | **.14** |
| Right lateral OFC | F(1, 45.07) = 7.13 | .01 | .10 | **.14** |
| Left globus pallidus ◊ | F(1, 38.63) = 5.57 | .02 | .13 | .13 |
| Right middle temporal gyrus | F(1, 44.46) = 5.88 | .02 | .13 | .12 |
| Right paracentral lobule | F(1, 48.17) = 6.52 | .01 | .12 | .12 |
| Left lingual gyrus | F(1, 43.25) = 5.57 | .02 | .13 | .11 |
| Left parahippocampal gyrus | F(1, 42.53) = 5.47 | .02 | .13 | .11 |
| Right cuneus | F(1, 48.56) = 5.48 | .02 | .13 | .10 |
| Left superior temporal gyrus | F(1, 40.20) = 4.37 | .04 | .18 | .10 |
| Left lateral OFC ◊ | F(1, 44.81) = 4.31 | .04 | .18 | .09 |
| Left paracentral lobule | F(1, 48.55) = 4.61 | .04 | .18 | .09 |
| Right entorhinal cortex ◊ | F(1, 46.68) = 4.11 | .05 | .18 | .08 |
| Right parahippocampal gyrus | F(1, 47.25) = 4.15 | .05 | .18 | .08 |
| *Main effect of treatment (OT < PL)* | | | | |
| Left postcentral gyrus | F(1, 38.82) = 8.45 | .006 | .46 | **.18** |
| Left supramarginal gyrus † | F(1, 33.54) = 4.33 | .05 | .67 | .11 |
| Right caudal middle frontal gyrus | F(1, 38.56) = 4.85 | .03 | .67 | .11 |
| Left precentral gyrus † | F(1, 42.46) = 4.43 | .04 | .67 | .09 |
| *Interaction effect* | | | | |
| Left medial OFC | F(1, 41.77) = 11.16 | .002 | .11 | **.21** |
| Left supramarginal gyrus | F(1, 34.38) = 9.10 | .005 | .11 | **.21** |
| Left temporal pole | F(1, 42.86) = 8.61 | .005 | .11 | **.17** |
| Left nucleus accumbens | F(1, 43.90) = 8.41 | .006 | .11 | **.16** |
| Right supramarginal gyrus | F(1, 39.28) = 6.75 | .01 | .12 | **.15** |
| Left caudate | F(1, 42.37) = 7.42 | .009 | .12 | **.15** |
| Left putamen | F(1, 37.86) = 6.32 | .02 | .12 | **.14** |
| Right entorhinal cortex | F(1, 44.05) = 6.90 | .01 | .12 | **.14** |
| Left precentral gyrus | F(1, 43.46) = 6.72 | .01 | .12 | .13 |
| Right caudate | F(1, 44.77) = 5.90 | .02 | .12 | .12 |
| Right nucleus accumbens | F(1, 45.93) = 6.20 | .02 | .12 | .12 |
| Left globus pallidus | F(1, 36.12) = 4.88 | .03 | .17 | .12 |
| Right medial OFC | F(1, 42.81) = 6.00 | .02 | .12 | .12 |
| Right precentral gyrus | F(1, 42.56) = 5.76 | .02 | .12 | .12 |
| Left lateral OFC | F(1, 44.21) = 5.48 | .02 | .13 | .11 |
| Right putamen | F(1, 39.38) = 4.51 | .04 | .18 | .10 |
| Right lateral OFC | F(1, 45.74) = 4.72 | .04 | .17 | .09 |
| **Node degree** | | | | |
| *Main effect of group (ASPD > NO)* | | | | |
| Left nucleus accumbens ◊ | F(1, 44.40) = 10.19 | .003 | .20 | **.19** |
| Left entorhinal cortex ◊ | F(1, 41.60) = 7.42 | .009 | .36 | **.15** |
| Left globus pallidus ◊ | F(1, 39.46) = 5.23 | .03 | .42 | .12 |
| Right nucleus accumbens ◊ | F(1, 45.41) = 5.03 | .03 | .42 | .10 |
| Right caudate ◊ | F(1, 46.95) = 4.28 | .04 | .42 | .08 |
| Left temporal pole [a] ◊ | F(1, 83.00) = 4.56 | .04 | .42 | .05 |
| *Main effect of group (ASPD < NO)* | | | | |
| Left posterior cingulate cortex ◊ | F(1, 38.89) = 4.44 | .04 | .42 | .10 |
| Right posterior cingulate cortex ◊ | F(1, 42.72) = 4.66 | .04 | .42 | .10 |
| *Main effect of treatment (OT > PL)* | | | | |
| Left medial OFC | F(1, 40.80) = 7.00 | .01 | .47 | **.15** |
| Left globus pallidus ◊ | F(1, 35.99) = 5.61 | .02 | .47 | .13 |
| Right globus pallidus [a] | F(1, 83.00) = 4.33 | .04 | .47 | .05 |
| *Main effect of treatment (OT < PL)* | | | | |
| Left transverse temporal gyrus | F(1, 39.10) = 6.61 | .01 | .47 | **.14** |
| Right pars opercularis | F(1, 41.35) = 4.65 | .04 | .47 | .10 |
| Right transverse temporal gyrus | F(1, 41.82) = 4.84 | .03 | .47 | .10 |
| Right posterior cingulate cortex ◊ | F(1, 41.80) = 4.38 | .04 | .47 | .09 |
| *Interaction effect* | | | | |
| Left nucleus accumbens | F(1, 44.40) = 10.19 | .003 | .20 | **.19** |
| Left entorhinal cortex | F(1, 41.60) = 7.42 | .009 | .36 | **.15** |

| | | | | |
|---|---|---|---|---|
| Left globus pallidus | F(1, 39.47) = 5.23 | .03 | .42 | .12 |
| Right nucleus accumbens | F(1, 45.41) = 5.03 | .03 | .42 | .10 |
| Right posterior cingulate cortex | F(1, 42.72) = 4.66 | .04 | .42 | .10 |
| Left posterior cingulate cortex | F(1, 38.89) = 4.44 | .04 | .42 | .10 |
| Right caudate | F(1, 46.95) = 4.28 | .04 | .42 | .08 |
| Left temporal pole [a] | F(1, 83.00) = 4.57 | .04 | .42 | .05 |
| **Betweenness Centrality** | | | | |
| *Main effect of group (ASPD > NO)* | | | | |
| Right postcentral gyrus | F(1, 40.91) = 4.87 | .03 | .57 | .11 |
| Left pars orbitalis [a] | F(1, 83.00) = 5.51 | .02 | .55 | .06 |
| *Main effect of group (ASPD < NO)* | | | | |
| Left parahippocampal gyrus | F(1, 31.60) = 7.70 | .009 | .35 | **.20** |
| Left medial OFC | F(1, 48.50) = 10.41 | .002 | .17 | **.18** |
| Right globus pallidus [a] | F(1, 83.00) = 4.50 | .04 | .57 | .05 |
| *Main effect of treatment (OT > PL)* | | | | |
| Right entorhinal cortex | F(1, 45.30) = 7.74 | .008 | .58 | **.15** |
| Left globus pallidus [a] | F(1, 83.00) = 4.57 | .04 | .58 | .05 |
| *Main effect of treatment (OT < PL)* | | | | |
| Right cuneus | F(1, 39.69) = 4.60 | .04 | .58 | .10 |
| Right superior frontal gyrus | F(1, 42.49) = 4.59 | .04 | .58 | .10 |
| *Interaction effect* | | | | |
| Right lateral OFC | F(1, 45.10) = 8.24 | .006 | .16 | **.15** |
| Left transverse temporal gyrus | F(1, 42.20) = 6.81 | .01 | .23 | **.14** |
| Left lateral OFC | F(1, 44.66) = 6.39 | .02 | .23 | .13 |
| Right ventral diencephalon | F(1, 45.04) = 5.00 | .03 | .33 | .10 |
| Left supramarginal gyrus [a] | F(1, 83.00) = 7.85 | .006 | .16 | .09 |
| Right rostral middle frontal gyrus | F(1, 44.83) = 4.43 | .04 | .39 | .09 |
| Left ventral diencephalon [a] | F(1, 83.00) = 5.45 | .02 | .28 | .06 |

Table 7.3 Meso-level nodal findings for the whole-brain analysis.

*Note: All listed main effects of group, treatment and interaction effect were significant before FDR correction for multiple comparisons only, but those with large effect sizes are presented in bold font ($\eta_p^2 \geq .14$). Within each effect, findings are listed in descending order of effect size. [a] These results stem from models with singular fits. Thus, these results should be interpreted with caution. [◇] This region also had a significant interaction effect, but this was ordinal, meaning the main effect can be interpreted. [†] This region also had a significant interaction effect, but this was disordinal, meaning the main effect must be interpreted with caution. OFC = orbitofrontal cortex, OT = oxytocin, PL = placebo, df = degrees of freedom.*

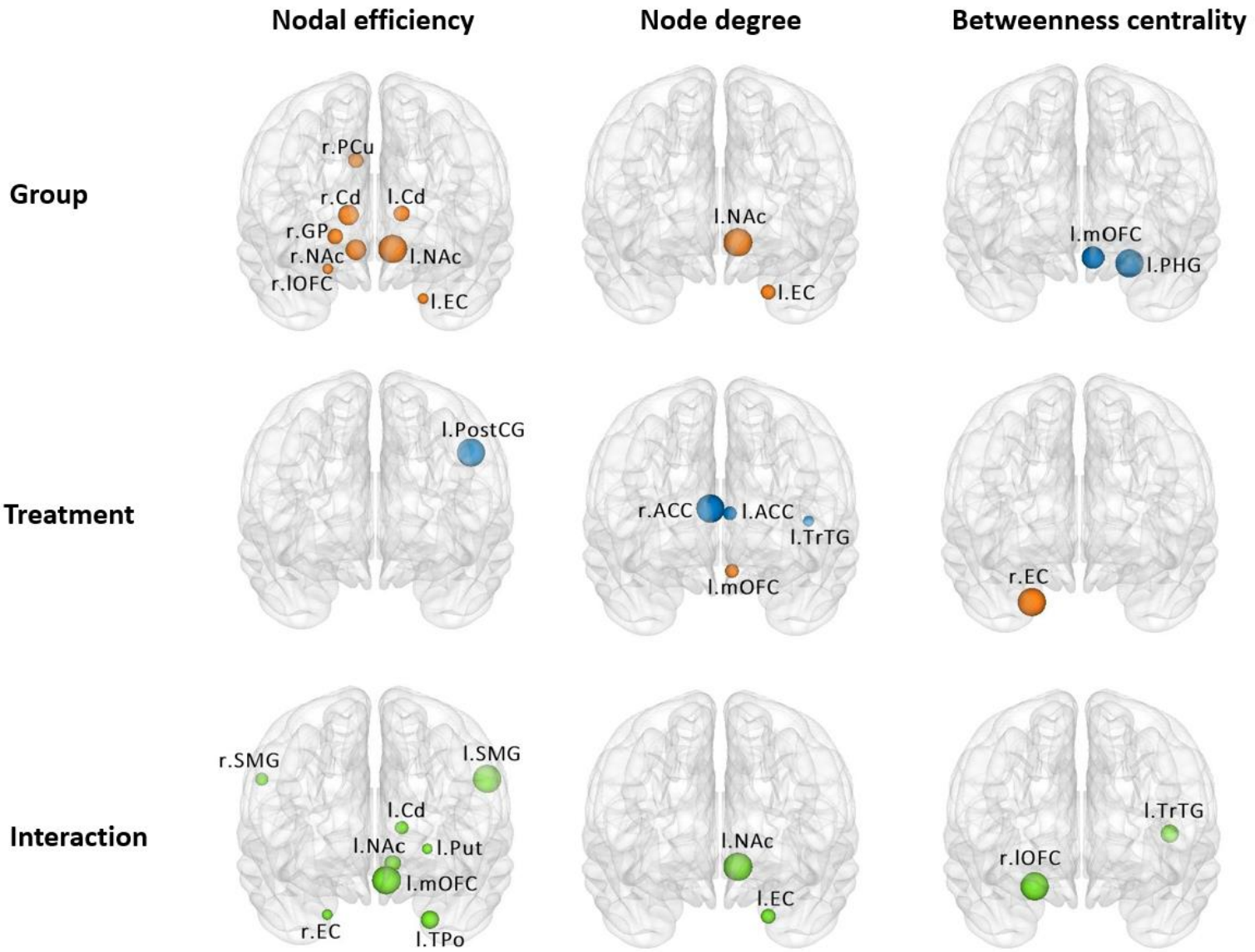


Figure 7.4 Visualization of nodal metrics with large effect sizes.

*Note: This figure shows significant findings from the ROI analysis which survived FDR correction for multiple comparisons, as well as any ROI or exploratory whole-brain analysis findings only significant before correction but with a large effect size ($\eta_p^2 \geq .14$). Colour mapping: Orange = increase in ASPD group relative to NO, blue = decrease in ASPD group relative to NO, green = interaction effect. r. = right hemisphere, l. = left hemisphere, l/mOFC = lateral/medial orbitofrontal cortex, ACC = anterior cingulate cortex, TPo = temporal pole, EC = entorhinal cortex, PHG = parahippocampal gyrus, TrTG = transverse temporal gyrus, PCu = precuneus, SMG = supramarginal gyrus, PostCG = postcentral gyrus, Cd = caudate, GP = globus pallidus, NAc = nucleus accumbens, Put = putamen*

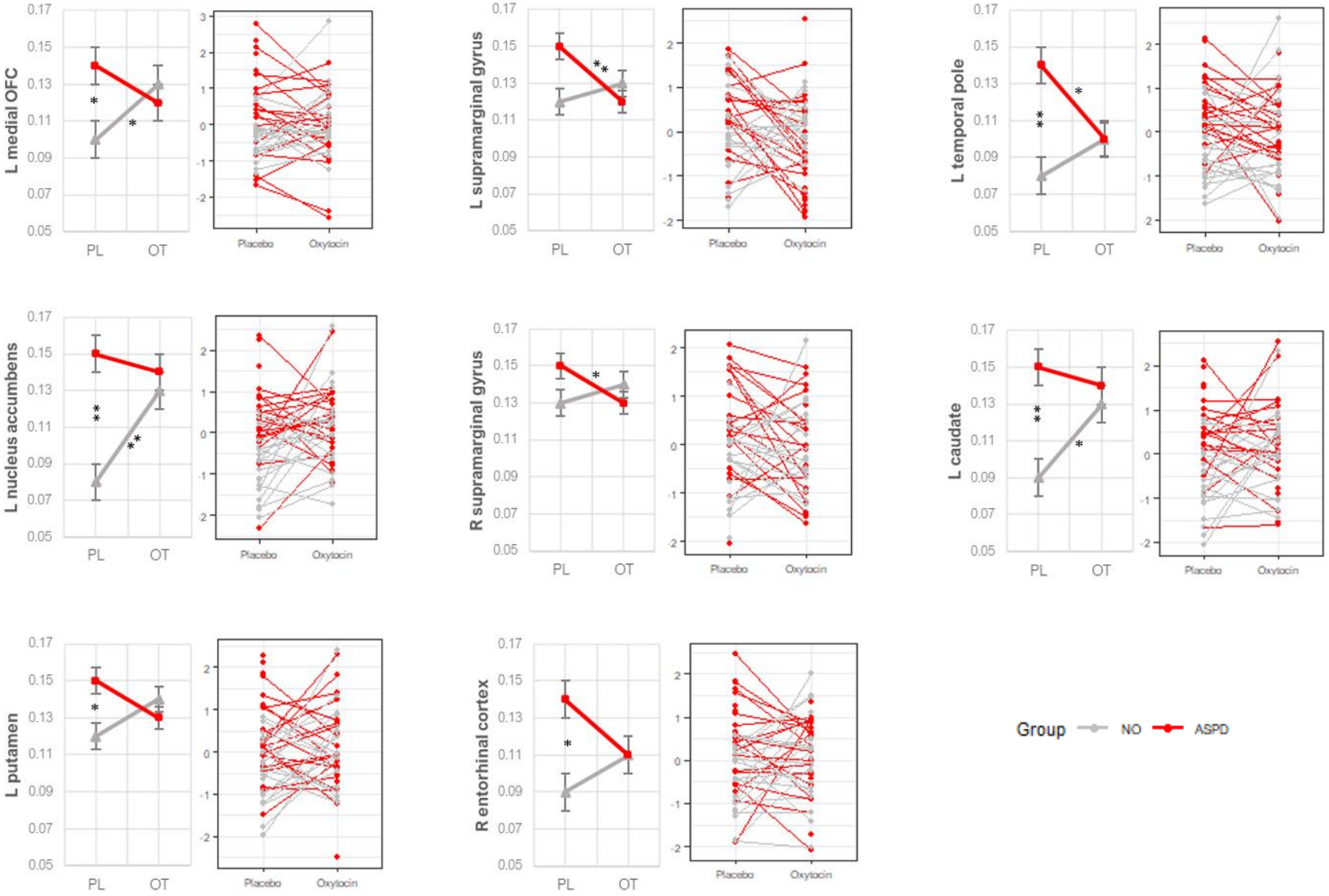


Figure 7.5 Significant interaction effects in nodal efficiency.

*Note: These effects were significant prior to FDR correction for multiple comparisons and had large effect sizes ($\eta_p^2 \geq .14$). The left line plots display the estimated marginal means (the error bars are the standard error) after accounting for the covariates of non-interest. The right spaghetti plots display the residuals of each metric for each subject under each condition after accounting for the covariates. Significant simple main effects (with FDR correction) are indicated: * p < .05, ** p < .01. L = left hemisphere, R = right hemisphere, PL = placebo, OT = oxytocin. OFC = orbitofrontal cortex.*

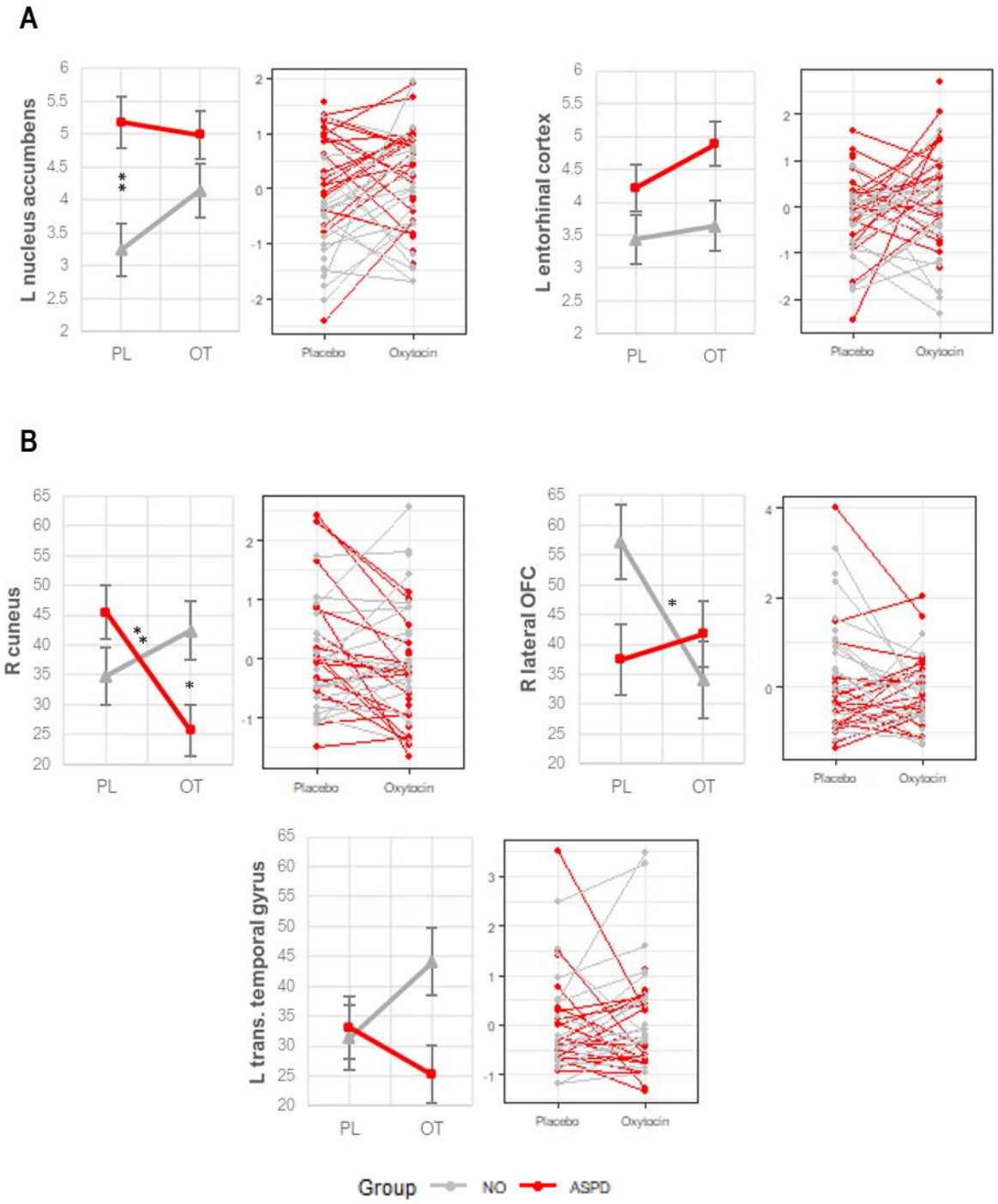


Figure 7.6 Significant interaction effects in A) node degree centrality and B) betweenness centrality.
*Note: Only the effect on betweenness centrality in the right cuneus survived FDR correction for multiple comparisons. The remaining findings were significant prior to this correction and had large effect sizes ($\eta_p^2 \geq .14$). The left line plots display the estimated marginal means (the error bars are the standard error) after accounting for the covariates of non-interest. The right spaghetti plots display the residuals of each metric for each subject under each condition after accounting for the covariates. Significant simple main effects (with FDR correction) are indicated: * p < .05, ** p < .01. L = left hemisphere, R = right hemisphere, PL = placebo, OT = oxytocin. OFC = orbitofrontal cortex. Trans. = transverse.*

### 7.3.2.4 Dice coefficient

The Dice coefficient was calculated to indicate the extent of spatial overlap between the meso-level graph theory metrics and the large-scale networks assessed in *chapter 6* (Dipasquale et al., 2019). As this was exploratory, all nodes that showed a meso-level group, treatment or interaction effect, even if they were only significant before correction for multiple comparisons, were included. Results revealed that group effects overlapped with the DMN to the largest extent (followed by the medial-temporal network), treatment effects overlapped with the salience network to the largest extent, and interaction effects with the thalamic network to the largest extent (*Table 7.4*).

| LSN | 1 | 2 | 3 | 4 | 5 | 6 | 7 | 8 | 9 | 10 | 11 | 12 | 13 |
|---|---|---|---|---|---|---|---|---|---|---|---|---|---|
| **Group** | .049 | .079 | **.174** | .081 | .078 | .009 | .132 | .000 | .100 | .105 | .078 | .057 | .063 |
| **Treatment** | .016 | .085 | .034 | .007 | .104 | .000 | .018 | .000 | **.120** | .011 | .071 | .092 | .036 |
| **Interaction** | .012 | .077 | .037 | .056 | .105 | .000 | .103 | .000 | .101 | .009 | .044 | .088 | **.132** |

Table 7.4 Dice coefficients for each large-scale network.
*Note: these indicate the extent of spatial overlap (correlation) between each effect type, merged across nodal metrics, and the 13 large-scale networks (LSN) that were included in chapter 6 (Dipasquale et al., 2019). 1 = primary visual network, 2 = sensorimotor network, 3 = default mode network, 4 = medial visual network, 5 = auditory network, 6 = lateral visual network, 7 = medial-temporal network, 8 = cerebellum, 9 = salience network, 10 = task positive network, 11 = ventral stream network, 12 = right lateral, 13 = thalamic network.*

### 7.3.2.5 Micro-level: edge connectivity

The NBS analysis revealed one subnetwork with significantly increased edge connectivity in the ASPD group compared with the NO group (FWER-corrected p = .03). This subnetwork was identified at a primary threshold of t = 3.0 (p ≤ .003) and was in primarily subcortical, but also temporal, and prefrontal social brain regions including the amygdala and anterior cingulate (*Table 7.5*, *Figure 7.7*). It is important that with this analysis approach, no individual edge abnormalities can be interpreted; rather, it is simply the entire subnetwork that had significantly increased connectivity in ASPD compared to the NO group (Zalesky et al., 2010).

| Primary threshold | Nodes (#) | Edges (#) | FWER-corrected p-value |
|---|---|---|---|
| 2.7 | 55 | 28 | .04 |
| **3.0** | **31** | **21** | **.03** |
| 3.3 | 11 | 10 | .05 |

Table 7.5 Details of the subnetwork at different primary t-thresholds.
*Note: For the sake of transparency, this table indicates the number of nodes and edges revealed at a threshold of t = 2.7, 3.0, and 3.3, however as in previous NBS analyses in ASPD populations, only the threshold of 3.0 was interpreted (hence this is marked in bold font). NBS = network-based statistic. FWER = family-wise error rate.*

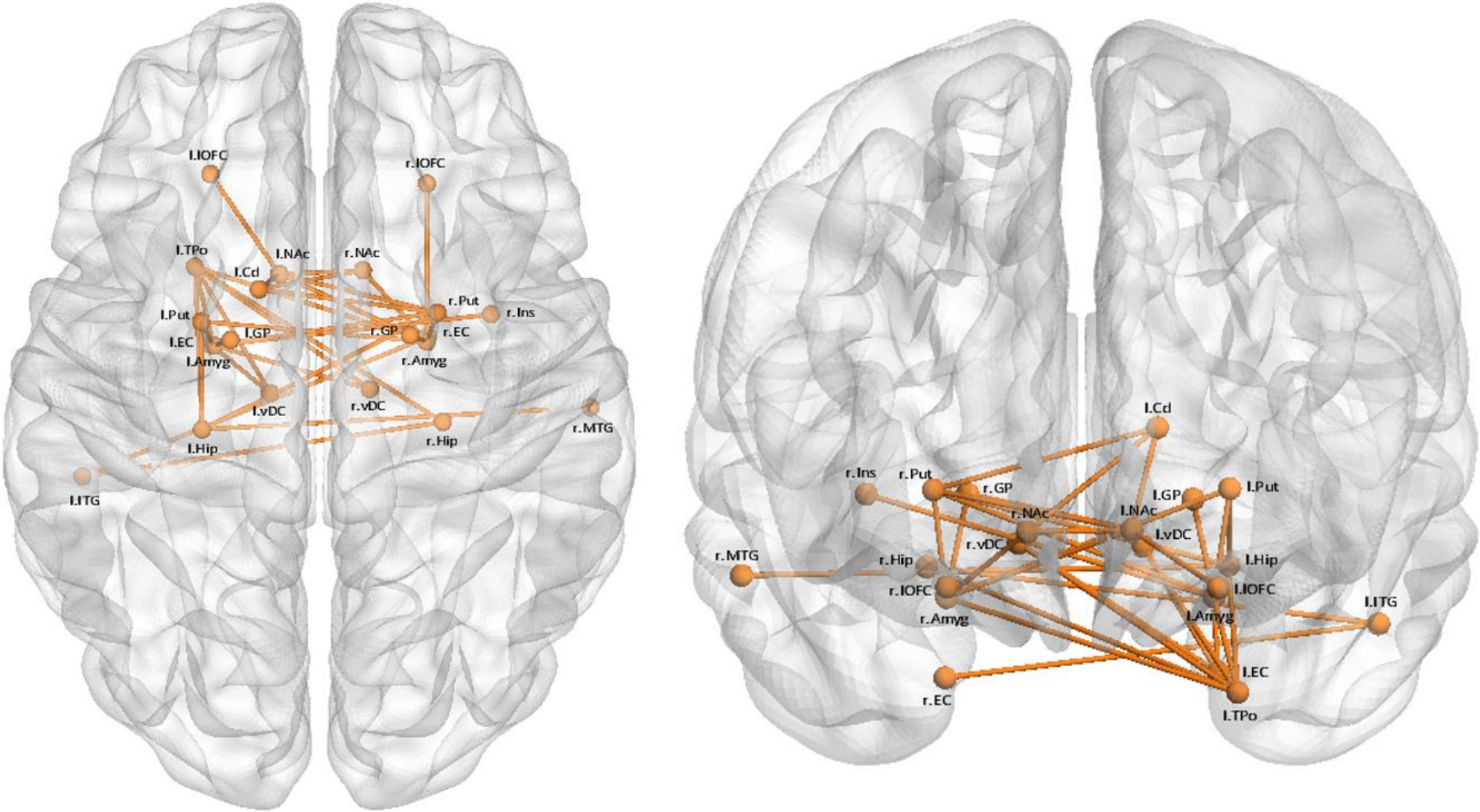


Figure 7.7 Subnetwork with significantly increased edge connectivity in ASPD.

*Note: this is at the primary threshold of t = 3.0. l. = left hemisphere, r. = right hemisphere, lOFC = lateral orbitofrontal cortex, TPo = temporal pole, EC = entorhinal cortex, MTG/ITG = medial/inferior temporal gyrus, Ins = insula, Amyg = amygdala, Hip = hippocampus, NAc = nucleus accumbens, Cd = caudate, Put = putamen, GP = globus pallidus, vDC = ventral*

### 7.3.3 Correlation with phenotype

*Table 7.6* shows the correlations between macro- and meso-level network properties and phenotypic features (clinical, behavioural, and cognitive measures) within the ASPD participants. It only included those metrics which revealed a significant main effect of group after FDR correction for multiple comparisons, or those with a large effect size ($\eta_p^2 \geq .14$, as indicated in *Table 7.2* and *Table 7.3*) which did not survive the FDR correction. Across all correlations, only one survived the FDR correction for multiple comparisons. This revealed that there was a significant positive correlation between betweenness centrality in the left medial OFC and the speed of detecting angry faces (r = .737, FDR-corrected p-value = .006, 95% confidence intervals = .289 [lower] – .925 [upper]). Thus, as betweenness centrality increased, the reaction time to correctly detect an angry face also increased (*Figure 7.8*). There were several other correlations which were only significant prior to FDR correction for multiple comparisons, and which for completeness are indicated in the table; however, given that they did not survive correction for multiple comparisons these were not interpreted. Similarly, *Table 7.7* contains the correlations between the graph theory metrics that had a significant group by treatment interaction effect and the phenotypic variables. No correlations survived the FDR correction for multiple comparisons, and those which were significant prior to this correction were not interpreted.

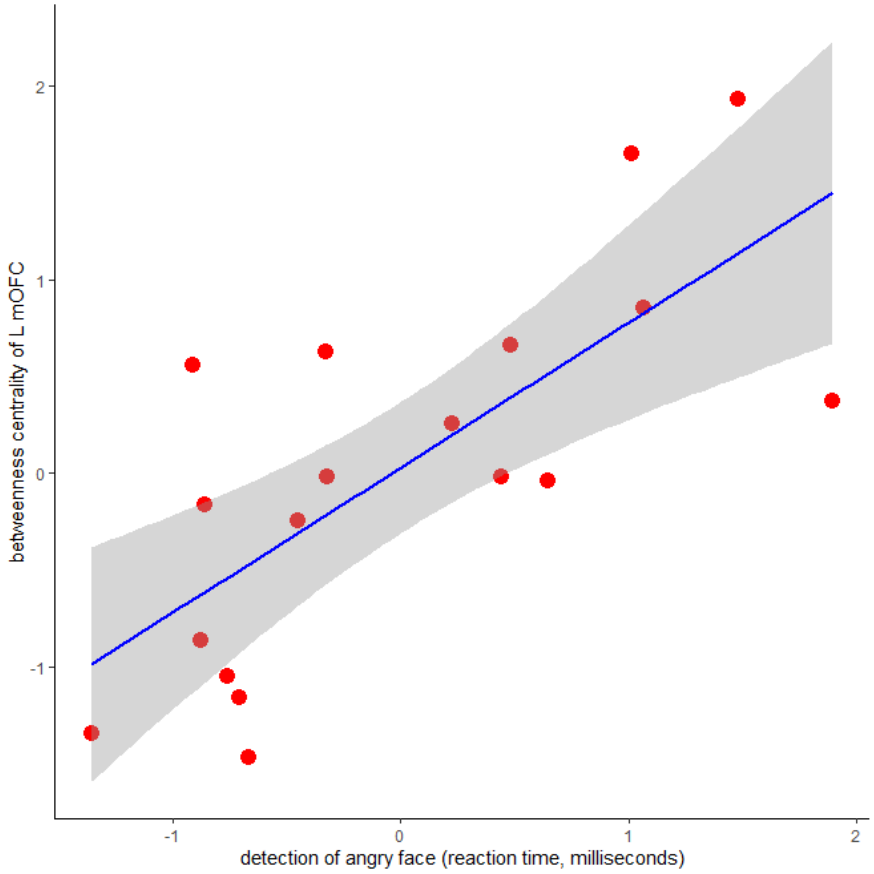


Figure 7.8 Significant positive correlation between L mOFC BC and angry face detection speed in ASPD.
*Note: The statistical result is shown in Table 7.6. Blue line indicates the fact that the ASPD group had significantly lower betweenness centrality in this region relative to the NO group. BC = betweenness centrality, L mOFC = left medial orbitofrontal cortex.*

| | | GEFF | LocEFF | NEFF | | | | | | | | |
|---|---|---|---|---|---|---|---|---|---|---|---|---|
| | | | | R lOFC | L TPo | L EC | R PCu | R Cd | L Cd | R NAc | L NAc | R GP |
| PCL-R | Total | .132 | .088 | -.488 * | .082 | -.250 | .011 | -.389 | -.344 | -.465 | -.485 * | -.096 |
| | Factor 1 | .070 | -.025 | -.489 * | .075 | -.251 | -.107 | -.533 * | -.519 * | -.627 ** | -.585 * | -.231 |
| | Factor 2 | .104 | .180 | -.296 | .079 | -.214 | .034 | -.115 | -.046 | -.186 | -.242 | .023 |
| | Facet 1 | .124 | -.120 | -.612 ** | .103 | -.084 | -.109 | -.573 * | -.594 * | -.672 ** | -.639 ** | -.195 |
| | Facet 2 | .009 | .062 | -.283 | .035 | -.345 | -.084 | -.392 | -.350 | -.461 | -.420 | -.215 |
| | Facet 3 | -.068 | -.037 | -.329 | -.025 | -.107 | -.173 | -.034 | .028 | -.153 | -.159 | -.062 |
| | Facet 4 | .248 | .317 | -.184 | .131 | -.257 | .190 | -.148 | -.101 | -.163 | -.245 | .082 |
| Conviction information | # past violent convictions | .150 | .138 | .175 | .174 | -.085 | .276 | -.093 | -.138 | -.139 | -.011 | -.024 |
| | 1 year reconviction | -.434 | -.497 * | -.267 | -.255 | -.653 ** | -.584 * | -.414 | -.328 | -.285 | -.248 | -.472 |
| Aggression [a] | RPQ-Reactive | .353 | .182 | .124 | .491 | .135 | -.104 | .057 | .028 | -.221 | -.152 | -.002 |
| | RPQ-Proactive | .194 | -.035 | -.039 | .667 ** | .093 | -.193 | -.299 | -.330 | -.509 | -.453 | -.228 |
| Emotion recognition (accuracy) [b] | Angry | .199 | .226 | .071 | .120 | .376 | .155 | -.019 | -.083 | .091 | .087 | .145 |
| | Sad | -.101 | -.034 | -.343 | -.085 | -.218 | .038 | -.312 | -.225 | -.379 | -.371 | .006 |
| | Fear | .529 * | .442 | -.139 | .186 | .305 | .404 | .126 | .113 | .059 | .052 | .312 |
| Emotion detection (reaction time) [b] | Angry | -.323 | -.330 | -.203 | -.628 ** | -.286 | .063 | -.144 | -.130 | -.043 | .021 | -.216 |
| | Fear | -.318 | -.336 | -.306 | -.563 * | -.503 * | .028 | -.316 | -.259 | -.229 | -.154 | -.385 |
| Reinforcement-based decision-making (accuracy) [b] | Acquisition learning | -.049 | -.259 | .293 | .167 | -.018 | -.144 | -.210 | -.314 | -.197 | -.143 | -.177 |
| | Response reversal | -.356 | -.465 | -.049 | -.296 | -.638 ** | -.540 * | -.155 | -.068 | -.177 | -.120 | -.472 |
| Delay discounting (# of times lesser value chosen) [b] | 7 days | .347 | .211 | -.231 | -.214 | -.011 | .164 | .078 | .062 | .059 | -.049 | .382 |
| | 30 days | .226 | .145 | -.121 | -.171 | -.167 | .066 | .185 | .224 | .143 | .062 | .294 |
| | 90 days | .121 | .035 | -.122 | -.170 | -.170 | .129 | .154 | .180 | .151 | .053 | .254 |
| | 180 days | .049 | .008 | .024 | -.072 | -.114 | .189 | .159 | .184 | .205 | .120 | .244 |
| | 360 days | .054 | .018 | .071 | -.088 | -.078 | .223 | .176 | .187 | .224 | .152 | .247 |
| Disinhibition [b] | SSRT | -.128 | .053 | .442 | .492 | .113 | -.111 | .345 | .386 | .261 | .303 | .036 |

| | | ND | | BC | |
|---|---|---|---|---|---|
| | | L EC | L NAc | L mOFC | L PHG |
| PCL-R | Total | -.432 | -.356 | .042 | .296 |
| | Factor 1 | -.250 | -.394 | .132 | .347 |
| | Factor 2 | -.453 | -.145 | -.132 | .286 |
| | Facet 1 | -.165 | -.386 | .263 | .359 |
| | Facet 2 | -.274 | -.321 | -.008 | .267 |
| | Facet 3 | -.366 | .102 | .119 | .426 |
| | Facet 4 | -.433 | -.318 | -.323 | .056 |
| Conviction information | # past violent convictions | -.155 | .034 | .280 | .213 |
| | 1 year reconviction | -.443 | -.089 | .105 | -.180 |
| Aggression [a] | RPQ-Reactive | -.118 | .136 | -.495 | .049 |
| | RPQ-Proactive | -.005 | .030 | -.166 | .310 |
| Emotion recognition (accuracy) [b] | Angry | .141 | -.162 | -.068 | .349 |
| | Sad | .113 | -.604 * | .076 | .169 |
| | Fear | -.171 | -.200 | -.388 | -.141 |
| Emotion detection (reaction time) [b] | Angry | -.276 | .091 | **.737 ** ** | -.178 |
| | Fear | -.433 | -.178 | .550 * | -.181 |

Cont. on next page

| | | | | | |
|---|---|---|---|---|---|
| Reinforcement-based decision-making (accuracy) [b] | Acquisition learning | .334 | -.080 | -.131 | -.302 |
| | Response reversal | -.384 | .165 | .268 | -.266 |
| Delay discounting (# of times lesser value chosen) [b] | 7 days | -.097 | -.485 | -.343 | -.334 |
| | 30 days | -.217 | -.267 | -.356 | -.492 |
| | 90 days | -.170 | -.103 | -.160 | -.526 * |
| | 180 days | -.019 | -.018 | -.142 | -.621 * |
| | 360 days | .047 | -.039 | -.188 | -.658 ** |
| Disinhibition [b] | SSRT | .188 | .461 | .032 | .342 |

Table 7.6 Partial Pearson coefficients for network topology (group differences) – phenotype correlations.

*Note: Only group differences with large effect sizes ($\eta_p^2 \geq .14$) were included. The average metrics between PL and OT sessions were used. Hence only ASPD participants who completed both sessions were included (N = 19). Bold font indicates the p-value survived FDR correction for multiple comparisons. Uncorrected p: * $p \leq .05$, ** $p \leq .01$. OT = oxytocin, PL = placebo, SSRT = stop signal reaction time, GEFF = global efficiency, LocEFF = local efficiency, NEFF = nodal efficiency, ND = node degree, BC = betweenness centrality, lOFC / mOFC = lateral/medial orbitofrontal cortex, TPo = temporal pole, EC = entorhinal cortex, PCu = precuneus, Cd = caudate, NAc = nucleus accumbens, GP = globus pallidus, PHG = parahippocampal gyrus. Not all participants completed all components: [a] N = 16, [b] N = 18.*

| | | NEFF | | | BC |
|---|---|---|---|---|---|
| | | R TPo | R SMG | L SMG | R Cu |
| PCL-R | Total | .172 | -.091 | .052 | .134 |
| | Factor 1 | -.030 | -.240 | -.145 | -.046 |
| | Factor 2 | .375 | -.006 | .201 | .237 |
| | Facet 1 | -.128 | -.065 | -.118 | .196 |
| | Facet 2 | .065 | -.373 | -.153 | -.266 |
| | Facet 3 | .429 | .196 | .216 | .469 |
| | Facet 4 | .202 | -.171 | .107 | -.084 |
| Conviction information | # past violent convictions | -.103 | .285 | .144 | .117 |
| | 1 year reconviction | -.169 | -.026 | .103 | -.309 |
| Aggression [a] | RPQ-Reactive | .338 | .133 | .214 | .268 |
| | RPQ-Proactive | .265 | .063 | .284 | .315 |
| Emotion recognition (accuracy) [b] | Angry | -.028 | .504 * | .240 | .296 |
| | Sad | -.287 | -.339 | -.088 | .059 |
| | Fear | .132 | .308 | .293 | .251 |
| Emotion detection (reaction time) [b] | Angry | -.006 | .171 | -.063 | -.054 |
| | Fear | .099 | .240 | .322 | -.093 |
| Reinforcement-based decision-making (accuracy) [b] | Acquisition learning | -.506 * | .083 | -.083 | -.117 |
| | Response reversal | .237 | .056 | .140 | -.296 |
| Delay discounting (# of times lesser value chosen) [b] | 7 days | -.395 | -.034 | -.346 | .054 |
| | 30 days | -.224 | -.102 | -.258 | -.070 |
| | 90 days | -.294 | -.251 | -.398 | -.097 |
| | 180 days | -.374 | -.347 | -.654 | -.193 |
| | 360 days | -.441 | -.345 | -.458 | -.234 |
| Disinhibition [b] | SSRT | .410 | .196 | .323 | .319 |

Table 7.7 Partial Pearson coefficients for network topology (OT responsivity) – phenotype correlations.
*Note: Only interaction effects with large effect sizes ($\eta_p^2 \geq .14$) were included. The OT-PL delta scores were used, therefore only ASPD participants who completed both sessions were included here (N = 19). Uncorrected p: * p ≤ .05, ** p ≤ .01. OT = oxytocin, PL = placebo, SSRT = stop signal reaction time, NEFF = nodal efficiency, BC = betweenness centrality, TPo = temporal pole, SMG = supramarginal gyrus, Cu = Cuneus. Not all participants completed all components: [a] N = 16, [b] N = 18.*

## 7.4 Discussion

This study explored five aspects of brain network topology across multiple levels of processing in male violent offenders with ASPD and varying degrees of psychopathy relative to non-offending control individuals. These aspects related to investigating group differences in the global, local, and nodal efficiency, centrality, and edge connectivity, as well as treatment effects of OT on network topology. Possible relationships with phenotypic measures were also explored. Significant findings that survived correction for multiple comparisons will be considered primarily and discussed below.

The first aspect concerned the centrality of subcortical nodes. The three previous graph theory studies of ASPD revealed reduced centrality in subcortical regions (W. Jiang, Shi, Liao, et al., 2017; Tang et al., 2016; Tillem et al., 2019). However, the current study did not reveal significant group differences in either centrality metric in any node, including the amygdala. It is worth noting that previous studies assessed the centrality

of subcortical nodes collectively, whereas here, it was assessed individually. Therefore, fewer corrections for multiple comparisons were required in previous studies, meaning they may have been more likely to detect significance. One study in particular also benefitted from a substantially larger sample size than the current study, meaning they were better powered to detect potential differences (Tillem et al., 2019).

The second aspect which was explored in the present study addressed the contradictory findings for global and local efficiency, as well as edge connectivity. Two of the three past studies reported increases in global and local efficiency (Tang et al., 2016; Tillem et al., 2019). The current results supported this finding by demonstrating that the ASPD group had significantly higher global and local efficiency than the NO group. However, prior evidence that individuals with ASPD have abnormalities in edge connectivity was less clear. The results of the current study showed one largely subcortical subnetwork with significantly increased edge connectivity in the ASPD group relative to NO. Taken together with previous findings (Tang et al., 2016; Tillem et al., 2019), this suggests that aberrant intrinsic architecture across macro-, meso-, and micro-levels of neural processing is a neurobiological associate of ASPD and psychopathy. These abnormalities exist when compared to non-offending controls and when including individuals with ages ranging across adulthood. They will be discussed in turn.

Increased global efficiency suggests that, when at rest, the brains of individuals with ASPD have higher functional integration. This may imply that that the brain is intrinsically organized in a more effective way. However, global efficiency is related to the average characteristic path length, which is the smallest number of edges required to connect any two nodes that form a route along which information can flow. (Achard & Bullmore, 2007; Latora & Marchiori, 2001; Rubinov & Sporns, 2010). Therefore, higher global efficiency in ASPD suggests that fewer edges are used to form information processing routes, meaning that individuals in this

group might have reduced communication between brain areas that should be communicating. In other words, there may be shortcuts in the topology of individuals with ASPD, which make the brain topologically more efficient, but at a potential functional cost.

Furthermore, the finding of increased meso-level local efficiency suggests higher functional segregation in individuals with ASPD. Local efficiency is the average of all nodal efficiency values. This means that, on average, there is more efficient communication of individual brain regions with their immediate neighbours, forming modules. However, considering the finding of increased global efficiency, this may not be functionally meaningful since information processed in one module might not be adequately shared with other modules of the brain. Future research should assess the modularity metric, which provides an objective measure of the grouping of individual brain regions, to provide more insight into this. Taken together, the current findings contribute to the wider evidence base that neurodevelopmental and neuropsychiatric disorders, including externalizing disorders such as conduct disorder and ADHD, are characterized by abnormalities in functional integration and segregation (Y. Jiang et al., 2021; Openneer et al., 2020; Tillem et al., 2022).

Related to the finding of increased local efficiency was the finding of increased nodal efficiency of the right precuneus in ASPD relative to NO. This is a novel topological finding since this was not assessed in previous studies. However, it corresponds with previous work that identified structural (*chapter 4*) and functional abnormalities in the precuneus in ASPD and particularly, in psychopathy (Deming & Koenigs, 2020; Dugré & Potvin, 2021; Gregory et al., 2015). The precuneus is involved in a range of functions, including self-referential processing and subjective valuation of reward (Cavanna & Trimble, 2006; Kable & Glimcher, 2007; X. Liu et al., 2011). Abnormalities in this region may contribute to deficits in these functions. Furthermore, it is intriguing that this node showed increased efficiency since it is a key node of the DMN and an important communication

hub of the brain. This means, at least in the brains of healthy individuals, it likely already has increased efficiency when compared to other nodes. Importantly, the current results did not show aberrant centrality metrics for the precuneus in individuals with ASPD, suggesting it maintains its hub status in this group. However, increased nodal efficiency of the precuneus suggests that it is more strongly connected to its neighbouring nodes and thus has a higher ability to propagate information with them (J. Wang et al., 2010). It could be speculated that this might be a compensation mechanism for increased functional segregation. Together with evidence from other research, it is possible that increased dysfunction of the precuneus is thus a key underpinning mechanism in ASPD and psychopathy.

Last, with regards to edge connectivity, the current results revealed one subnetwork with significantly increased edge connectivity in the ASPD group. This network involved several bilateral subcortical nodes (basal ganglia, amygdala, hippocampus), cortical temporal nodes (temporal pole, entorhinal cortex, temporal gyri, insula), as well as the lateral OFC. Tang et al. (2016) also found one subnetwork with increased connectivity in ASPD, although they included a larger range of nodes, whereas the current finding suggests a relatively spatially focused subnetwork with only few long-distance connections. The subcortical, limbic and paralimbic brain areas included in this network have been previously reported as being dysfunctional in ASPD and psychopathy (Baskin-Sommers et al., 2016; Deming & Koenigs, 2020; Dugré & Potvin, 2021; Gregory et al., 2012, 2015; Juárez et al., 2013). The connectivity between individual nodes cannot be interpreted with the NBS, since this treats the entire subnetwork as one component. Thus, it is inappropriate to discuss individual edges of the subnetwork. Nevertheless, it is worth noting that other research, particularly seed-based FC analyses, have revealed FC abnormalities, albeit typically reductions, of similar nodes within ASPD and psychopathy (Contreras-Rodríguez et al., 2015; Hosking et al., 2017; Korponay et al.,

2017a; H. Liu et al., 2014; Ly et al., 2012). Furthermore, it has been suggested that increased micro-level edge connectivity may represent a compensatory mechanism for structural deficits (Iraji et al., 2016). This could be true considering ASPD and psychopathy have previously been linked to reduced white matter connectivity between amygdala and medial prefrontal regions (Motzkin et al., 2011), which were both included in the subnetwork. In summary, the findings relating to the second aspect of network topology that was explored in the present study support the notion that individuals with ASPD have abnormalities across multiple levels of processing.

The third aspect of this study related to the novel exploration of OT effects on network topology in ASPD and assessed whether aberrant metrics could be 'shifted' by a potential drug treatment. Results revealed that OT significantly reduced node degree centrality in the bilateral anterior cingulate cortex in both groups (treatment effect), whereas in the right cuneus, OT significantly decreased betweenness centrality in the ASPD group only (interaction effect). These two findings were thus in line with previous work showing that OT only shifts meso-level, but not macro- or micro-level properties (Martins et al., 2021). The anterior cingulate cortex has above-average expression of oxytocin receptors (Boccia et al., 2013; Quintana, Rokicki, et al., 2019) so it is likely to be somewhat more responsive to OT than other brain regions. This possibly explains the similar effect OT had in both groups. In contrast, the finding of OT-induced reductions in betweenness centrality of the cuneus in the ASPD group only was more surprising - because the cuneus is not typically associated with OT effects and has a lower than average number of OT receptors (Boccia et al., 2013; Quintana, Rokicki, et al., 2019). Despite this, Martins et al. (2021) also found significant effects of OT on the nodal efficiency of the cuneus in healthy individuals. It is possible that effects of OT on the cuneus are downstream, or secondary, effects arising from neural input from other areas that respond to OT more directly. Moreover, the interpretation of the

interaction effect showed that there were no significant group differences in the cuneal betweenness centrality in the placebo condition, suggesting that this is not a baseline impairment of ASPD. Instead, the groups significantly differed in the OT condition, since OT significantly reduced cuneal betweenness centrality in individuals with ASPD only. This suggests significant group differences in the neural responsivity to OT, which may be an indication of impaired allostatic (homeostatic) processes (Quintana & Guastella, 2020). Overall, further research should attempt to understand the potential functional (behavioural) implications of the findings that OT shifted anterior cingulate and cuneal topology, and whether this could have a positive impact on functional abnormalities in ASPD.

The fourth aspect of the study concerned the spatial overlap between meso-level topological findings and large-scale networks. Analysis revealed that group effects mapped mostly onto the DMN. A common finding in ASPD and psychopathy is abnormal FC in the DMN (Espinoza et al., 2018; Philippi et al., 2015; Tang, Jiang, et al., 2013). The DMN includes areas such as the precuneus, posterior cingulate cortex, and parahippocampal and middle temporal gyri (Uddin et al., 2019), which all showed significant group differences between ASPD and NO (albeit most only prior to correction for multiple comparisons). It is therefore possible that significant topological differences in the DMN help to explain aberrant large-scale network FC. In contrast, treatment effects mostly mapped onto the salience network. This is in line with previous research that has revealed OT modulation of FC of this network or areas within it (Brodmann et al., 2017; X. Jiang et al., 2021; P. Liu et al., 2022; Xin et al., 2021). It is likely that effects of OT on the salience network help to explain the behavioural effects that other studies have revealed after OT administration, especially those requiring external attention to socially salient stimuli (Yao et al., 2018). Finally, the interaction effects in the nodal metrics mapped mostly onto the thalamic network. The thalamic network incorporates the thalamus, basal ganglia structures, and posterior cingulate regions, amongst others (*Figure 6.1*). This corresponds

with the finding in the previous *chapter*, which also showed an interaction effect in the within-network FC of thalamic network. In both cases, under placebo, the ASPD group demonstrated increases in the graph theory metric or within-network FC (respectively), which were largely attenuated by the differential effects of OT on each of the groups. Together, these findings suggest that ASPD is characterized by resting-state functional abnormalities in subcortical midbrain structures, which respond to an OT challenge. Future research should assess thalamic functioning and OT responsivity in the context of behaviours which recruit structures within the thalamic network.

The fifth and final aspect of network topology in ASPD related to potential correlations between topological abnormalities and phenotypic data. Exploratory analyses revealed that increased betweenness centrality in the left medial OFC was associated with slower detection of angry faces. The correlation finding itself was significant after correction for multiple comparisons, however, it must be noted that betweenness centrality in the left medial OFC was only significantly higher in the ASPD group relative to the NO group prior to correction for multiple comparisons. Although cautious interpretation is therefore required, this exploratory finding might suggest that as the abnormality in left medial OFC betweenness centrality reduces, ASPD individuals are slower to detect angry faces. Indeed, previous evidence suggests that ASPD is characterized by significantly faster speed to detect angry faces (Timmermann et al., 2017), which may contribute to the hostile attribution bias (Schönenberg & Jusyte, 2014). It may be possible that reduced reliance on the medial OFC, which is an important area for emotion processing and decision-making that incorporates social cues, is an underpinning of this cognitive dysfunction (R. J. R. Blair, 2004). Other correlations did not survive correction for multiple comparisons. Nevertheless, the current findings provide rationale for future research to take a more targeted approach to understand the

relationship between network topology and clinical, behavioural, and cognitive measures.

Several limitations must be considered when interpreting the above findings. First, due to a lower number of participants undergoing this final part of the MRI protocol, the sample size was smaller. This meant it was not possible to conduct group comparisons between those with ASPD with and without psychopathy. There were no significant correlations that survived correction for multiple comparisons between the topological metrics that had significant group differences and psychopathy scores, suggesting that – at least statistically speaking – the current findings are a shared mechanism found in those with and without psychopathy. Nonetheless, there were some correlations between psychopathy scores and nodes with topological abnormalities that were only significant before correction for multiple comparisons. Furthermore, the only graph theory study in psychopathy revealed that network topology was increasingly abnormal with higher psychopathy scores, revealing a more continuous relationship (Tillem et al., 2019). Together, this highlights that further research is required to disentangle how the presence of significant psychopathy affects network topology in individuals with ASPD. The small sample size also meant that the study had low statistical power, and it has recently been highlighted that brain topology analyses should utilise large samples (>65 per group) due to the number of metrics this approach relies on (Helwegen et al., 2023). Future research should hence aim to replicate the current findings in a large sample. A second limitation relates to the timing of the OT administration, which was relatively late within the suggested timeframe for OT action (Martins, Mazibuko, et al., 2020; Paloyelis et al., 2016). Thus, it is possible that some effects of OT on network topology in areas such as the amygdala were missed. The third limitation relates to the presence of substance misuse in the ASPD group. A significant proportion of the ASPD group tested positive on urine drug screening tests on the days of MRI acquisition. This reflects the typical

comorbidity found in this patient group (Blackburn et al., 2003; Compton et al., 2005; Trull et al., 2010), therefore the current results reflect a realistic clinical sample that is representative of the core ASPD phenotype. Nevertheless, in the post-hoc sensitivity analyses, when adding a binary variable of no-interest reflecting the presence of a positive urine drug screening test into the linear mixed models, the above findings remained significant. The effect of a positive drug test was not significant. Thus, it is likely that the current findings were not driven to a significant extent by substance misuse. Finally, the current study did not measure metrics required to assess for topological network organization such as small worldness and modularity (Bassett & Bullmore, 2017; Latora & Marchiori, 2001; Watts & Strogatz, 1998). These reflect more normalized metrics and would thus improve comparability across studies.

In conclusion, the current results extended existing evidence by revealing that male violent offenders with ASPD have significant differences in macro-, meso-, and micro-level network topology. This supports wider findings that ASPD is associated with abnormal FC. Furthermore, it provides further evidence that OT can shift network topology, potentially revealing a therapeutic target for individuals with ASPD.

# 8 General Discussion

## 8.1 Research problem and aims

There is still limited understanding of the neurobiological mechanisms underpinning ASPD. However, only a small number of studies to date have sought to compare the ASPD+P and ASPD-P subtypes within the disorder. Failing to account for neurobiological differences between these subgroups may impede treatment development.

The current research had two overarching aims. The first was to provide further insight into neurobiological mechanisms by directly comparing male violent offenders with ASPD+P, ASPD-P, and healthy non-offenders on a range of neurobiological features, including different morphological measures of cortical structure, resting-state regional cerebral blood flow (rCBF), resting-state functional connectivity (FC), and resting-state network topology. The second aim was to investigate the effects of intranasal oxytocin (OT) on measures of resting-state function to assess whether neurobiological mechanisms can be modulated. An overview of the findings pertaining to these aims will be given below.

## 8.2 Summary of findings

This research project used a double-blind, placebo-controlled, randomized crossover design to evaluate group and treatment effects across the features listed above. *Table 8.1* provides a summary of the significant group effects, and *Table 8.2* shows the findings relating to significant treatment and group by treatment interaction effects. In this concluding discussion chapter, themes across the results will be highlighted, limitations discussed, and clinical implications identified.

In terms of group effects, ASPD+P and ASPD-P demonstrated different neurobiological abnormalities relative to each other. Specifically, they had distinct profiles of abnormalities in cortical structure (cortical thickness and surface area) and resting-state rCBF. This builds on existing evidence that

these subtypes show different structural (cortical volume) and task-based functional neurobiological, cognitive, and behavioural features (Azevedo et al., 2020; De Brito et al., 2013; Flórez et al., 2019; Gregory et al., 2012, 2015; Hemphill et al., 1998; Kosson et al., 2006; McCuish et al., 2015; Olver et al., 2011, 2013; Riser & Kosson, 2013; Shepherd et al., 2018). Moreover, individuals with ASPD+/-P were also found to have aberrant brain structure and function when compared to healthy non-offenders. This included abnormalities across all features that were studied: cortical structure (cortical volume, cortical thickness, and surface), resting-state rCBF, resting-state FC, and resting-state network topology. Taken together, these findings were demonstrated in brain regions that have commonly been linked to ASPD+/-P in previous research, including areas of the prefrontal cortex (e.g., ventromedial prefrontal and orbitofrontal cortex, middle frontal gyrus, and superior frontal gyrus), anterior and posterior cingulate cortex, insula, precuneus, and subcortical structures (thalamus, basal ganglia, and striatum).

| Group effect | | | |
|---|---|---|---|
| | **ASPD+P vs NO** | **ASPD-P vs NO** | **ASPD+P vs ASPD-P** |
| **Cortical structure** | Decreased CV and SA in rostral middle and superior frontal gyrus, with SA findings extending into lateral OFC and inferior frontal gyrus. | Decreased CV in inferior temporal gyrus and fusiform gyrus. | Decreased CT in anterior and posterior cingulate cortex. |
| | Increased CV and SA in precuneus, superior parietal cortex, and cuneus, with SA findings extending into posterior cingulate, pericalcarine cortex, and lateral occipital cortex. | Increased SA in posterior cingulate. | Increased SA in rostral middle and superior frontal gyrus, OFC, inferior frontal gyrus, insula, posterior cingulate, and paracentral lobule |
| | Differences in SA largely explained differences in CV. | Combination of subthreshold differences in CT and SA may explain differences in CV. | |
| **Resting-state rCBF** | Decreased rCBF in medial superior frontal gyrus, inferior frontal gyrus, OFC, anterior cingulate cortex, pre-/post-central gyrus, Rolandic operculum, superior temporal gyrus | Decreased rCBF in medial superior frontal gyrus, inferior frontal gyrus, OFC, anterior cingulate cortex, pre-/post-central gyrus, Rolandic operculum, superior temporal gyrus | |
| | Increased rCBF in posterior cingulate cortex, precuneus, and hippocampus | Increased rCBF in posterior cingulate cortex, precuneus, and hippocampus | Increased rCBF in posterior cingulate cortex, precuneus, and hippocampus |
| **ASPD+/-P vs NO** | | | |
| **Resting-state FC** | Decreased FC within salience network (at superior and middle temporal gyrus), medial-temporal network (at superior frontal gyrus), primary visual network (at angular gyrus, superior and middle temporal gyrus, supramarginal gyrus) and lateral visual network (at medial superior frontal gyrus, anterior midcingulate)<br><br>Increased FC in medial-temporal network (at OFC, midcingulate, anterior insula, caudate, putamen) and thalamic network (at thalamus) | | n/a |
| **Resting-state network topology** | Increased global, local, and nodal (precuneus) efficiency, and increased edge connectivity in one cortical-subcortical network (incl basal ganglia, striatum, amygdala, hippocampus, entorhinal cortex, temporal pole, inferior and middle temporal gyrus, insula, and OFC) | | n/a |

Table 8.1 Summary of significant group differences across neurobiological features.
*Note: The cortical structure and resting-state rCBF analyses compared ASPD+P, ASPD-P, and NO groups. The resting-state FC and resting-state network topology analyses only compared all ASPD and NO groups. Hence, for the latter, no direct ASPD+P vs ASPD-P comparisons were available. rCBF = regional cerebral blood flow, FC = functional connectivity, CV = cortical volume, SA = surface area, CT = cortical thickness, OFC = orbitofrontal cortex.*

In terms of effects of OT, the current results were the first to demonstrate that the resting-state brain function in violent offenders with ASPD+/-P is responsive to a pharmacological challenge, both in similar and different ways to non-offenders. More importantly, it was reported that this response partly differed between those with ASPD with versus without psychopathy (in resting-state rCBF), which adds to the suggestion that these subtypes are characterized by differential neurobiological mechanisms. Finally, the results also revealed that specific neurobiological abnormalities in violent offenders with ASPD may be attenuated after the administration of OT. In other words, abnormalities that existed at baseline (placebo) were no longer present in the OT condition.

| | Treatment effect | Group x Treatment Interaction |
|---|---|---|
| **Resting-state rCBF** | Ns | OT decreased rCBF in globus pallidus and striatum in ASPD-P, but did not modulate it in ASPD+P or NO |
| **Resting-state FC** | Ns | OT decreased FC of thalamic network (at middle and inferior temporal gyrus) in ASPD and increased it in NO |
| **Resting-state network topology** | Decreased node degree centrality of anterior cingulate cortex | OT decreased betweenness centrality of the cuneus in ASPD but not in NO |

Table 8.2 Summary of the treatment and group by treatment interaction effects across resting-state features. *Note: There were no main effects of treatment in resting-state rCBF or resting-state FC. Only the resting-state analysis compared ASPD+P, ASPD-P, and NO in the interaction effect. rCBF = regional cerebral blood flow, FC = functional connectivity, Ns = not significant.*

## 8.3 Emerging themes

Four main themes emerge in considering the detailed findings of the four experimental results chapters. The first two relate to the presence of shared and discrete abnormalities in brain structure and function between the groups; the third relates to the absence of significant amygdala abnormalities; and the fourth relates to the differential effects of OT.

With respect to the first theme, the results revealed that violent offenders with ASPD show increases in several morphological features (cortical volume and surface area) and functional measures (i.e., resting-state rCBF and nodal efficiency) in the posterior medial cortex region. Where this could be distinguished, findings demonstrated that this was largely characteristic

of individuals with ASPD+P, suggesting potential neurobiological differences between ASPD+P and ASPD-P. This supports findings from a recent meta-analysis in individuals with high levels of psychopathy, as well as from a study directly comparing neural activity between ASPD+P to ASPD-P during reward and punishment processing, which both also revealed abnormally increased neural activity in this region in ASPD+P individuals (Deming & Koenigs, 2020; Gregory et al., 2015). The posterior medial cortex region includes the posterior cingulate cortex and precuneus, which together have been implicated in the default mode network and form an important communication hub (Fransson & Marrelec, 2008; Hagmann et al., 2008; Uddin et al., 2019). In healthy individuals, it contributes to important aspects of social cognition, including self-referential processing, moral reasoning, attention, and reward evaluation (Brewer et al., 2013; Bzdok et al., 2012, 2015; Cavanna & Trimble, 2006; Kable & Glimcher, 2007; Leech & Sharp, 2014; X. Liu et al., 2011; Pearson et al., 2011). Individuals with psychopathy are typically marked by neural and behavioural impairments in these functions, and it is possible that structural and functional abnormalities such as those found in the current study contribute to these abnormalities. Moreover, there is some support that these abnormalities have a neurodevelopmental origin. Studies of boys with CD with versus without CU traits reported that CD with CU traits was associated with increased posterior medial cortex grey matter volume and density (De Brito et al., 2009), as well as increased activity during reward processing (S. W. Hawes et al., 2021). This suggests there is some developmental continuity, which may be one of the many factors contributing to the development of life-course persistent (LCP) antisocial behaviour (Moffitt, 2018). Taken together, it appears that structural and functional abnormalities in the posterior medial cortex are neurobiological correlates of ASPD, and particularly those with ASPD+P rather than ASPD-P.

The second theme that emerges from the current data are decreases in size, rCBF, and functional connectivity in various frontotemporal regions. These reductions were characteristic of ASPD regardless of psychopathy, suggesting potentially shared abnormalities – albeit in the structural analysis, there were some differences in the distinct spatial location and severity of the decreases between the two ASPD subtypes. As discussed in the individual chapters, these findings aligned with previous research that revealed decreased frontotemporal cortical volume to be characteristic of ASPD+P and to a lesser extent also ASPD-P (De Brito et al., 2021; Gregory et al., 2012; Hofhansel et al., 2020; Raine et al., 2000, 2011), reduced frontotemporal perfusion to be associated with ASPD (Kolla & Houle, 2019), and diminished functional connectivity within networks encompassing frontotemporal cortical and subcortical structures to be linked with ASPD and psychopathy (Espinoza et al., 2018; Philippi et al., 2015; Tang, Jiang, et al., 2013). Moreover, these findings are consistent with evidence from youth with CD, as well as individuals with antisocial behaviour and externalizing disorders more broadly (B. M. Caldwell et al., 2019; Carlisi et al., 2020; Dugré & Potvin, 2021; Rogers & De Brito, 2016; Thijssen & Kiehl, 2017). This overlap might indicate a developmental continuity of the neurobiological correlates of ASPD+/-P, which may contribute to the LCP antisocial behavioural problems (Moffitt, 2018). However, the aetiology and specificity of such frontotemporal abnormalities remain to be established. A recent meta-analysis showed that reduced frontotemporal volume is a shared feature that can be found across most mental illnesses (McCutcheon et al., 2023). In this context, the current approach to investigate how SA and CT contribute to group differences in volume was an important first step towards increasing the specific understanding of what contributes to frontotemporal reductions in ASPD+/-P. Further research to disentangle the factors that contribute to decreases in frontotemporal structure, but also function, and whether this differs between ASPD+/-P, must be implemented. It also remains to be ascertained whether – and how – the

structural reductions in frontotemporal areas are linked to the reductions in neural function in these regions.

The third theme that can be identified from this dataset is the relative lack of functional abnormalities in the amygdala. The only finding that included the amygdala was the micro-level network topology analysis assessing edge connectivity, which revealed that the amygdala is part of the largely subcortical neural network that showed increased edge connectivity in ASPD relative to NO (*chapter 7*). This was somewhat surprising because previous research has often linked amygdalar structural and functional abnormalities with ASPD and especially with psychopathy (N. E. Anderson et al., 2017; Contreras-Rodríguez et al., 2014; Decety et al., 2015; Decety, Chen, et al., 2013; Decety, Skelly, et al., 2013; S. W. Hawes et al., 2021; Meffert et al., 2013; Noordermeer et al., 2016; Sethi et al., 2022). Moreover, various aetiological theories of psychopathy have included amygdala dysfunction as a core feature of psychopathy (R. J. R. Blair, 2008; Kiehl, 2006; Lykken, 1957; Moul et al., 2012; Patrick, 1994). However, a recent meta-analysis of studies assessing the neurobiological correlates of psychopathy found that many studies report null findings, and those studies that do report amygdala abnormalities use ROI analyses and are typically lower in power and utilise community samples (Deming et al., 2022). Similarly, a meta-analysis of children with conduct problems and varying severity of CU traits also did not show significant functional impairments in the amygdala (Alegria et al., 2016). While the current findings could be a result of limited statistical power (type II error; although null findings also reported in the ROI analyses), they do align with these meta-analytical findings and together, they challenge the centrality of the amygdala for the development of psychopathy across the lifespan. It is possible that a shift away from the amygdala-centric view of ASPD and psychopathy is underway. Future research should use large samples (>1000 individuals (Marek et al., 2022)) and appropriate analyses and designs to further evaluate the role of the amygdala. This could be achieved

by relying on shared data from large-scale collaborations such as the Enhancing NeuroImaging Genetics through Meta-Analysis (ENIGMA) for Antisocial Behaviours consortium (https://enigma.ini.usc.edu/ongoing/enigma-antisocial-behavior/) or the FemNAT-CD consortium (Freitag et al., 2018). Moreover, there is a general move away from studying individual brain structures and towards studying brain networks (Thiebaut De Schotten & Forkel, 2022). It is conceivable that amygdala dysfunction, particularly in its functional connectivity and communication with other brain regions (as shown in the micro-level network topology findings, *chapter 7*), may continue to be identified as important, albeit as part of a network rather than on its own.

The final theme that emerges across the findings in the current project was an effect of OT on all measures of resting-state brain function, even with a relatively long time period since OT administration. Therefore, for the first time, it was shown that resting-state brain function in areas important for social cognition can be modulated, or 'shifted', using a pharmacological challenge in violent offenders with ASPD. Specifically, OT decreased previously heightened function in subcortical structures (basal ganglia, striatum), in the middle and inferior temporal gyrus, the cuneus, and in the anterior cingulate cortex. These findings add to existing evidence that OT also modulates task-based brain activity in the anterior cingulate cortex and anterior insula in these individuals, specifically in those with ASPD+P (Tully et al., 2022). Across these studies, the effects of OT in ASPD+/-P largely differed from those found in the NO individuals. The precise neural mechanisms of action of OT remain to be fully understood. The recent discovery of a neurochemical ligand to the human oxytocin receptor will aid in increasing this understanding (Beard et al., 2018). However, as described in the Introduction *chapter*, a leading theory of the role of oxytocin in the brain suggests that it selectively and dynamically modulates the activity of excitatory and inhibitory cell firing, relying on allostatic (i.e., homeostatic) feedback processes to support selection of and attention

towards socially salient stimuli that are important for learning, adapting/responding to, and interacting with the changing environment (Lefevre et al., 2021; Marlin et al., 2015; Oettl et al., 2016; Quintana & Guastella, 2020; Shamay-Tsoory & Abu-Akel, 2016). Considering evidence that oxytocin levels, at least when measured in the plasma, are dysregulated in individuals with phenotypic characteristics of ASPD (Berends et al., 2022; Goh et al., 2021; R. Lee et al., 2009; Mitchell et al., 2013), it could by hypothesized that the allostatic processes responding to endogenous oxytocin also do not function in the same way as in healthy individuals. Similarly, the neural responsivity to exogenous OT also likely differs, underpinning the observed group differences in OT effects. Underlying mechanistic differences in the allostatic responsivity of neurons to OT within ASPD individuals might also help to explain why OT effects were found in areas such as the cuneus, which is not typically associated with a high oxytocin receptor density (Boccia et al., 2013; Quintana, Rokicki, et al., 2019) but may show (unusually) modulated activity as a downstream consequence of abnormal neural responsivity to OT elsewhere. With this in mind, it is important to note that OT also showed differential effects on the neural activity of individuals with ASPD+P versus ASPD-P. Thus, it is likely that the neural responsivity to exogenous OT also differs between these two subtypes, providing further support for the notion that ASPD+P and ASPD-P are marked by differential neurobiological mechanisms. This highlights the importance of stratifying ASPD subtypes for studies assessing mechanisms and treatment response. Taken together, these findings provide important first steps towards investigating the treatment potential that OT might have for ASPD. However, to truly evaluate and understand the potential therapeutic utility of OT in ASPD, it is crucial that the mechanisms of its action are better understood.

## 8.4 Limitations of the current research

There were three overarching limitations to the current research project: 1) relatively low sample size and subsequently reduced statistical power;

2) the presence of substance use within the participants; 3) minor methodological challenges related to the OT administration and the neurocognitive tasks that were used for the exploratory correlation analyses.

In terms of the sample size, there was some variability across the individual results chapters. Chapter 4, which assessed brain structure, benefitted from the largest sample size across groups (ASPD+/-P N = 37) whereas chapter 6, which assessed large-scale network functional connectivity, had a significantly smaller sample size (ASPD+/-P N = 19). This variability in group size emerged for different reasons, including participant difficulties (not attending both placebo and oxytocin sessions), protocol timing (scans towards the end of the long MRI protocol were sometimes not conducted because of a lack of time or participant discomfort) and data analysis (excluding raw data due to too much motion). Furthermore, due to the Covid-19 pandemic, the recruitment period for this project was drastically shortened, meaning that the original goal of recruiting up to 24 participants per ASPD subtype was impossible. It must therefore be acknowledged that the current experiments were likely to be underpowered, and only large effect sizes could be detected. However, the current sample sizes are comparable to much existing research in the fields of ASPD and intranasal oxytocin, and they were largely in line with recommendations for the individual analytic approaches (as detailed in the *Methods chapter*). Nevertheless, it has been recently suggested that in order to detect true effects with sufficient statistical power, neuroimaging studies must include over 1000 individuals (Marek et al., 2022). The current data can contribute to the efforts of large-scale consortiums (e.g., ENIGMA for Antisocial Behaviour), which is the only feasible approach for collecting such large sample sizes. However, a current limitation of the large-scale approaches is that they often lack detailed and comparable phenotypic characterisation of the sample(s), which is a strength of the current participant groups. It will be important to assess whether the neurobiological and neurocognitive

differences identified between the ASPD subtypes can also be replicated in much larger meta-analytic samples, but this is only possible if the large-scale efforts also improve and standardize their approach and guidelines for phenotypic characterisation (Griem et al., 2022). Another impact of the small sample size in the current study was on the analysis of the resting-state functional connectivity and network topology data. Specifically, due to a fewer number of individuals undergoing the rs-fMRI BOLD scan, these analyses could not compare individuals with ASPD+P versus ASPD-P. This affected the ability to fulfil one of the two project aims. In summary, the current project suffers from low statistical power, however, considering its novelty and careful phenotypic characterization, it has provided important preliminary findings that can be exploited in future larger-scale efforts.

The second limitation of the current project relates to the presence of significant comorbid lifetime substance use disorders within the offenders with ASPD+/-P (up to 32%, as per the SCID-5-CV; note the presence of a lifetime substance use disorder was an exclusion criteria for NO participants, and for ASPD individuals, it was an exclusion criteria if it actively disturbed their daily functioning), as well as the presence of active 'recreational' substance use that was revealed in participants by the urine drug testing that captured drug use in the past 14 days (up to 75% in the ASPD participants: mainly cannabis, cocaine, opioids; up to 42% in the NO participants: mainly cannabis). While participants were asked to abstain from substance use in the two weeks before participating in the study, this was clearly not always adhered to. If participants' urine drug tests revealed recent substance use, information about when the most recent use occurred was verbally collected on an individual basis. Due to the difficulty of recruiting these participants, only participants who attended an MRI with their function manifestly impaired by substances were turned away from the relevant scanning session.

However, the main analyses did not include substance use or the presence of a positive urine drug test as a covariate. Substance use is a very common

behaviour found in individuals with ASPD+/-P and it is an inherent part of the disorder phenotype (Blackburn et al., 2003; Compton et al., 2005; Trull et al., 2010). This inclusive approach is in line with other research in LCP offenders (Carlisi et al., 2020). Moreover, the use of cannabis is also becoming more popular in Western countries including the UK (United Nations Office on Drugs and Crime, 2021). This means healthy NO control populations are also likely to engage in recreational cannabis use more frequently, especially those who were recruited to match the demographic and intellectual characteristics of the ASPD sample (e.g., lower education/income, lower IQ) (Jeffers et al., 2021). It must therefore be acknowledged that it is possible that some of the current findings could be attributed to the impact of substance use on neurobiological structure and function. Hence, post-hoc sensitivity analyses that assessed the relationship between the presence of a lifetime substance use disorder (for brain structure) or the presence of a positive urine drug screening test on the day of scanning (for brain function) were conducted. They revealed no significant relationship between lifetime substance use disorder and brain structure, or between the presence of a positive urine drug test and neural topology. However, the presence of a positive urine drug test was associated with median rCBF in clusters 1 and 3, as well as with FC in the medial temporal network (see Table S2 and Table S3). Developmental and longitudinal studies will be required to explore the neurobiological correlates of substance use independent of antisocial personality disorder. These can support the identification of causal mechanisms while also delineating the possible additive risk of various parts of the antisocial phenotype (e.g., Blair, 2020).

Finally, the last limitation involves a set of minor methodological challenges that were faced in this project. The current study used an OT dose of 40 IU. At the time of study design, this was chosen because it was in line with other studies that showed OT effects on resting-state brain function (Paloyelis et al., 2016) and had been deemed to be safe (MacDonald et al.,

2011). However, since then, it has been reported that lower doses of OT may have stronger effects on brain function. It has also been demonstrated that the dose-response relationship differs across and within brain regions (Martins, Brodmann, et al., 2022). For instance, rCBF of the individual nuclei of the amygdala show different profiles of responsivity to low versus high OT doses (Martins, Brodmann, et al., 2022). Equally, the time between OT administration and measurement of effect was rather late within the time window that has previously been demonstrated to show significant effects on resting-state rCBF, FC, and network topology (Brodmann et al., 2017; Martins et al., 2021; Martins, Mazibuko, et al., 2020; Paloyelis et al., 2016). The effects of OT on brain areas that only occur closer to the time of administration may have been missed. Nevertheless, the current project has provided crucial first steps to show that the resting-state brain function of violent offenders with ASPD and varying levels of psychopathy responds to OT administration. However, future research should consider recent developments in the wider field of OT research, and for example, investigate the effect of a lower dose of OT earlier in the time window.

Another methodological challenge that was faced in this project related to the neurocognitive assessment. The tasks utilised aligned with the Research Domain Criteria framework (Insel et al., 2010), meaning that they offered common behavioural outcome measures that can be correlated with neurological functioning. This was beneficial since in the current project, they were used in the exploratory correlations with findings of neurobiological abnormalities. Furthermore, they have been implemented to demonstrate neurocognitive impairments in adolescents with CD+/-CU traits (R. J. R. Blair et al., 2020; R. J. R. Blair, White, et al., 2014; Moore et al., 2019; White et al., 2014). However, due to their intended use in youth populations, it is possible that they were too easy for the adult participants in this study, leading to ceiling effects. This might explain why the exploratory correlations did not reveal many significant findings across the four experimental chapters. It is also possible that the tasks measured

behaviours that were too complex to delineate such precise neurobiological underpinnings. Future research should utilize tasks that have been used to demonstrate significant neurocognitive impairments in adults with ASPD and psychopathy.

## 8.5 Implications and future research

The individual findings, as well as the themes that emerge across these findings, have several important implications for future research and clinical practice. In terms of research implications, the first one is that the findings provide evidence that ASPD can be stratified into two more biologically homogenous subtypes (ASPD+P and ASPD-P), at least in terms of cortical structure and rCBF. This is further supported by the differential response to OT challenge. Future research studies may find it beneficial to apply such stratification, as it may lead to a more precise identification of neural correlates of behaviour. Delineating more homogenous neurobiological and cognitive phenotypes of antisocial behaviours has been identified as one of the most crucial improvements in the research approach to this population (Brazil et al., 2018).

A second implication for research practice comes from the fact that this was the first study to demonstrate that resting-state neurobiological mechanisms in ASPD and psychopathy could be modulated by a pharmacological challenge, in some cases attenuating significant baseline group differences. The impact of these modulations could be explored in future behavioural research studies that use larger samples and more appropriate neurocognitive measures than the current study. Moreover, it was also shown that there are some differences in the neural responsivity to such challenges within each ASPD subtype. This may provide important rationale and guidance for future research that plans to measure the impact of other pharmacological agents, for example probing the serotonergic system in the context of interpersonal aggression. Finally, findings that OT modulated resting-state functional connectivity and network topology ca.

90 minutes after administration (in both offenders and non-offenders) has implications for the wider field of OT research. Specifically, it supports findings from a study showing OT effects on rCBF up to 95 minutes after administration (Martins, Mazibuko, et al., 2020). Together, these findings suggest that a dose of 40 IU of OT may have a longer effect on brain function than initially expected based on earlier research (Paloyelis et al., 2016). However, it is possible that OT effects that are only evident earlier in the time window were missed in the current study. With this in mind, it is important that future research examines the spatiotemporal profile of OT responsivity within individuals with ASPD, to assess whether the responsivity differs in different parts of the brain across different times. This will also help to determine the therapeutic potential.

The current findings also have implications for clinical practice. First, the findings of different neurobiological underpinnings of ASPD+/-P add important biological evidence to the existing behavioural evidence that the diagnosis for ASPD should be stratified according to the presence or absence of psychopathy (Azevedo et al., 2020; De Brito et al., 2013; Flórez et al., 2019; Gregory et al., 2012, 2015; Hemphill et al., 1998; Kosson et al., 2006; McCuish et al., 2015; Olver et al., 2011, 2013; Riser & Kosson, 2013; Shepherd et al., 2018). Together, this evidence suggests that psychopathy is not merely a more severe form of ASPD, but that it has some underlying differences in the mechanisms that drives it. The diagnostic criteria for ASPD should therefore have the option to specify whether an individual shows additional, above-threshold characteristics of psychopathy. This already exists for the DSM-5 diagnosis of CD (i.e., the optional categorisation specifying the presence of 'limited prosocial emotions') (Pardini et al., 2010). Creating such a diagnostic category would thus further support the notion that CD+/-CU traits is the developmental precursor of ASPD+/-P, which in itself may have important implications for identifying early intervention targets. A psychopathy specifier based on fearlessness and boldness traits also already exists in the DSM-5 Section

III Alternative Model for Personality Disorders (First et al., 2015). This section presents emerging measures and models to help clinicians to evaluate their patients in alternative ways. The inclusion of the psychopathy specifier has been considered to be an important improvement of the ASPD diagnosis relative to previous iterations of the diagnosis, however due to its base in character and temperament, it has limitations with regards to its validity and is not often utilized in clinical practice (J. L. Anderson & Kelley, 2022; Fuller et al., 2022). It is possible that the current and recent neurobiological and behavioural evidence that is based on the difference between ASPD +/-P according to the PCL-R threshold will benefit the approach to evaluating the evidence base for the utility and validity of adding a psychopathy subtype to the diagnosis of ASPD in the main personality disorder section of the DSM.

The evidence for differential responsivity to OT also has important implications for clinical practice, in particular for the approach to treating ASPD+/-P. With respect to identifying the 'true' treatment potential of OT specifically, it is important that future research establishes whether pharmacologically induced shifts in brain function are linked to improvements in behavioural features of the disorder (Quintana, 2022; Yeomans et al., 2021). Furthermore, the effects of longer-term or chronic rather than acute OT dosing need to be established in ASPD+/-P. Meta-analytic evidence has indicated the safety of long-term OT use (Cai et al., 2018), though possible adversities such as increased anxiety need to be better understood (J. Winter et al., 2021). Beyond this, the current findings suggest that individuals with ASPD+P may respond differently to treatment than individuals with ASPD-P. The importance and potential of adapting treatment approaches to more homogenous subtypes of ASPD has been shown by a trial that successfully used cognitive remediation therapy to target and improve attention deficits found specifically in individuals with ASPD+P (Baskin-Sommers, Curtin, et al., 2015).

In summary, the current findings have clear implications for the design of future research studies as well as for clinical practice. To further improve the understanding of the neurobiological and behavioural mechanisms associated with ASPD and psychopathy, and to subsequently develop more personalised medicine approaches, it is crucial that ASPD+P and ASPD-P are treated as distinct, more biologically homogenous subtypes of ASPD.

## 8.6 Conclusion

In conclusion, the findings from this project demonstrated that male violent offenders with a diagnosis of ASPD with or without significant psychopathy have neurobiological abnormalities when compared to non-offenders. There was novel evidence that some of these neurobiological abnormalities were shared between both ASPD subtypes, but more importantly, there was also evidence that some neurobiological abnormalities differed between the ASPD subtypes. This has important implications for future research and clinical practice, suggesting that such stratification into more homogenous subtypes is not only found on a behavioural level, but also in various neurobiological mechanisms. These findings align with reports of neurobiological abnormalities in children with CD with or without CU traits, suggesting there is some degree of neurodevelopmental continuity. This may contribute to the development of LCP antisocial behaviour and violence. Moreover, the current project also provided novel evidence for the modulatory effects of OT. This creates a promising rationale for new research that aims to evaluate the therapeutic potential of OT in ASPD. With improvements in the understanding of the neurobiological underpinnings as well possible normalizing mechanisms, there is increased hope that new treatment options will become available. This is crucial to improve the health and well-being of individuals suffering from ASPD and psychopathy, which are debilitating conditions. Moreover, this is essential to reduce the high amount of violent crime that is committed by such individuals, which comes at an immense emotional and financial cost to human society. The current work therefore provided an important

contribution towards improving the understanding of factors contributing to one of the world’s major global public health problems: interpersonal violence.

# Bibliography


Abe, N., Greene, J. D., & Kiehl, K. A. (2018). Reduced engagement of the anterior cingulate cortex in the dishonest decision-making of incarcerated psychopaths. *Social Cognitive and Affective Neuroscience*, *13*(8), 797–807. https://doi.org/10.1093/SCAN/NSY050

Achard, S., & Bullmore, E. (2007). Efficiency and Cost of Economical Brain Functional Networks. *PLoS Computational Biology*, *3*(2), 174–183. https://doi.org/10.1371/JOURNAL.PCBI.0030017

Alakörkkö, T., Saarimäki, H., Glerean, E., Saramäki, J., & Korhonen, O. (2017). Effects of spatial smoothing on functional brain networks. *European Journal of Neuroscience*, *46*(9), 2471–2480. https://doi.org/10.1111/EJN.13717

Alavash, M., Lim, S. J., Thiel, C., Sehm, B., Deserno, L., & Obleser, J. (2018). Dopaminergic modulation of hemodynamic signal variability and the functional connectome during cognitive performance. *NeuroImage*, *172*(5), 341–356. https://doi.org/10.1016/J.NEUROIMAGE.2018.01.048

Alcorn, J. L., Rathnayaka, N., Swann, A. C., Moeller, F. G., & Lane, S. D. (2015). Effects of Intranasal Oxytocin on Aggressive Responding in Antisocial Personality Disorder. *The Psychological Record*, *65*(4), 691–703. https://doi.org/10.1007/s40732-015-0139-y

Alegria, A. A., Radua, J., & Rubia, K. (2016). Meta-analysis of fMRI studies of disruptive behavior disorders. *American Journal of Psychiatry*, *173*(11), 1119–1130. https://doi.org/10.1176/appi.ajp.2016.15081089

Almeida, F., & Moreira, D. (2017). Crime, re-offence, and substance abuse of patients with severe mental disorder. *Integrative Molecular Medicine*, *4*(2), 1–6. https://doi.org/10.15761/IMM.1000281

Alsop, D. C., Detre, J. A., Golay, X., Günther, M., Hendrikse, J., Hernandez-Garcia, L., Lu, H., Macintosh, B. J., Parkes, L. M., Smits, M., Van Osch, M. J. P., Wang, D. J. J., Wong, E. C., & Zaharchuk, G. (2015). Recommended implementation of arterial spin-labeled perfusion MRI for clinical applications: A consensus of the ISMRM perfusion study group and the European consortium for ASL in dementia. *Magnetic Resonance in Medicine*, *73*(1), 102–116. https://doi.org/10.1002/MRM.25197

American Psychiatric Association. (2013). *Diagnostic and Statistical Manual of Mental Disorders, 5th edition* (5th ed.). American Psychiatric Association. https://doi.org/10.1176/appi.books.9780890425596

Anacker, A. M. J., & Beery, A. K. (2013). Life in groups: the roles of oxytocin in mammalian sociality. *Frontiers in Behavioral Neuroscience*, *7*(185), 1–10. https://doi.org/10.3389/FNBEH.2013.00185

Anderson, J. L., & Kelley, S. E. (2022). Antisocial Personality Disorder and Psychopathy: The AMPD in Review. *Personality Disorders: Theory, Research, and Treatment*, *13*(4), 397–401. https://doi.org/10.1037/per0000525

Anderson, N. E., Maurer, J. M., Steele, V. R., & Kiehl, K. A. (2018). Psychopathic traits associated with abnormal hemodynamic activity in salience and default mode networks during auditory oddball task. *Cognitive, Affective and Behavioral Neuroscience*, *18*(3), 564–580. https://doi.org/10.3758/S13415-018-0588-2/TABLES/8

Anderson, N. E., Steele, V. R., Maurer, J. M., Rao, V., Koenigs, M. R., Decety, J., Kosson, D. S., Calhoun, V. D., & Kiehl, K. A. (2017). Differentiating emotional processing and attention in psychopathy with functional neuroimaging. *Cognitive, Affective and Behavioral Neuroscience*, *17*(3), 491–515. https://doi.org/10.3758/S13415-016-0493-5

Anton, M. E., Baskin-Sommers, A. R., Vitale, J. E., Curtin, J. J., & Newman, J. P. (2012). Differential effects of psychopathy and antisocial personality disorder symptoms on cognitive and fear processing in female offenders. *Cognitive, Affective and Behavioral Neuroscience*, *12*(4), 761–776. https://doi.org/10.3758/S13415-012-0114-X/FIGURES/2

Aoki, Y., Inokuchi, R., Nakao, T., & Yamasue, H. (2014). Neural bases of antisocial behavior: A voxel-based meta-analysis. *Social Cognitive and Affective Neuroscience*, *9*(8), 1223–1231. https://doi.org/10.1093/scan/nst104

Aromäki, A. S., Lindman, R. E., & Eriksson, C. J. P. (2002). Testosterone, sexuality and antisocial personality in rapists and child molesters: a pilot study. *Psychiatry Research*, *110*(3), 239–247. https://doi.org/10.1016/S0165-1781(02)00109-9

Arthurs, O. J., & Boniface, S. (2002). How well do we understand the neural origins of the fMRI BOLD signal? *Trends in Neurosciences*, *25*(1), 27–31. https://doi.org/10.1016/S0166-2236(02)02138-0

Ashburner, J., & Friston, K. J. (2005). Unified segmentation. *NeuroImage*, *26*(3), 839–851. https://doi.org/10.1016/j.neuroimage.2005.02.018

Åslund, C., Comasco, E., Nordquist, N., Leppert, J., Oreland, L., & Nilsson, K. W. (2013). Self-Reported Family Socioeconomic Status, the 5-HTTLPR Genotype, and Delinquent Behavior in a Community-Based Adolescent Population. *Aggressive Behavior*, *39*(1), 52–63. https://doi.org/10.1002/AB.21451

Assink, M., Van der Put, C. E., Hoeve, M., De Vries, S. L. A., Stams, G. J. J. M., & Oort, F. J. (2015). Risk factors for persistent delinquent behavior among juveniles: A meta-analytic review. *Clinical Psychology Review*, *42*(12), 47–61. https://doi.org/10.1016/j.cpr.2015.08.002

Aurich, N. K., Filho, J. O. A., Da Silva, A. M. M., & Franco, A. R. (2015). Evaluating the reliability of different preprocessing steps to estimate graph theoretical measures in resting state fMRI data. *Frontiers in Neuroscience*, *9*(48), 1–10. https://doi.org/10.3389/FNINS.2015.00048

Auty, K. M., Farrington, D. P., & Coid, J. (2015). Intergenerational transmission of psychopathy and mediation via psychosocial risk factors. *British Journal of Psychiatry*, *206*(1), 26–31. https://doi.org/10.1192/bjp.bp.114.151050

Avants, B., Duda, J. T., Kim, J., Zhang, H., Pluta, J., Gee, J. C., & Whyte, J. (2008). Multivariate Analysis of Structural and Diffusion Imaging in Traumatic Brain Injury. *Academic Radiology*, *15*(11), 1360–1375. https://doi.org/10.1016/J.ACRA.2008.07.007

Azevedo, J., Carvalho, C., Serrão, M. P., Coelho, R., Vieira-Coelho, M. A., & Figueiredo-Braga, M. (2022). Association between S-COMT activity and impulsive and premeditated aggression in a population of violent offenders: preliminary results of a cross sectional study. *F1000 Research*, *11*(24), 1–14. https://doi.org/10.12688/f1000research.75318.1

Azevedo, J., Vieira-Coelho, M., Castelo-Branco, M., Coelho, R., & Figueiredo-Braga, M. (2020). Impulsive and premeditated aggression in male offenders with antisocial personality disorder. *PLoS ONE*, *15*(3), e0229876. https://doi.org/10.1371/JOURNAL.PONE.0229876

Backhausen, L. L., Herting, M. M., Buse, J., Roessner, V., Smolka, M. N., & Vetter, N. C. (2016). Quality control of structural MRI images applied using FreeSurfer-a hands-on workflow to rate motion artifacts. *Frontiers in Neuroscience*, *10*(558), 1–2. https://doi.org/10.3389/FNINS.2016.00558/BIBTEX

Bakermans-Kranenburg, M. J., & Van IJzendoorn, M. H. (2013). Sniffing around oxytocin: review and meta-analyses of trials in healthy and clinical groups with implications for pharmacotherapy. *Translational Psychiatry*, *3*(5), 1–14. https://doi.org/10.1038/TP.2013.34

Baldwin, J. R., Reuben, A., Newbury, J. B., & Danese, A. (2019). Agreement between prospective and retrospective measures of childhood maltreatment: A systematic review and meta-analysis. *JAMA Psychiatry*, *76*(6), 584–593. https://doi.org/10.1001/jamapsychiatry.2019.0097

Baliousis, M., Duggan, C., McCarthy, L., Huband, N., & Völlm, B. (2019).

Executive function, attention, and memory deficits in antisocial personality disorder and psychopathy. *Psychiatry Research*, *278*, 151–161. https://doi.org/10.1016/j.psychres.2019.05.046

Balleine, B. W., Delgado, M. R., & Hikosaka, O. (2007). The Role of the Dorsal Striatum in Reward and Decision-Making. *The Journal of Neuroscience*, *27*(31), 8161. https://doi.org/10.1523/JNEUROSCI.1554-07.2007

Barberet, R., Bowling, B., Junger-Tas, J., Rechea-Alberola, C., van Kesteren, J., & Zurawan, A. (2004). *Self-reported juvenile delinquency in England and Wales, The Netherlands and Spain*. European Institute for Crime Prevention and Control (United Nations).

Baribeau, D. A., & Anagnostou, E. (2015). Oxytocin and vasopressin: Linking pituitary neuropeptides and their receptors to social neurocircuits. *Frontiers in Neuroscience*, *9*(335), 1–21. https://doi.org/10.3389/FNINS.2015.00335/BIBTEX

Barkataki, I., Kumari, V., Das, M., Taylor, P., & Sharma, T. (2006). Volumetric structural brain abnormalities in men with schizophrenia or antisocial personality disorder. *Behavioural Brain Research*, *169*(2), 239–247. https://doi.org/10.1016/j.bbr.2006.01.009

Bartz, J. A., Nitschke, J. P., Krol, S. A., & Tellier, P. P. (2019). Oxytocin Selectively Improves Empathic Accuracy: A Replication in Men and Novel Insights in Women. *Biological Psychiatry: Cognitive Neuroscience and Neuroimaging*, *4*(12), 1042–1048. https://doi.org/10.1016/J.BPSC.2019.01.014

Bartz, J. A., Zaki, J., Bolger, N., & Ochsner, K. N. (2011). Social effects of oxytocin in humans: Context and person matter. *Trends in Cognitive Sciences*, *15*(7), 301–309. https://doi.org/10.1016/j.tics.2011.05.002

Baskin-Sommers, A. R., & Brazil, I. A. (2022). The importance of an exaggerated attention bottleneck for understanding psychopathy. *Trends in Cognitive Sciences*, *26*(4), 325–336. https://doi.org/10.1016/J.TICS.2022.01.001

Baskin-Sommers, A. R., Brazil, I. A., Ryan, J., Kohlenberg, N. J., Neumann, C. S., & Newman, J. P. (2015). Mapping the association of global executive functioning onto diverse measures of psychopathic traits. *Personality Disorders*, *6*(4), 336–346. https://doi.org/10.1037/PER0000125

Baskin-Sommers, A. R., Curtin, J. J., & Newman, J. P. (2011). Specifying the attentional selection that moderates the fearlessness of psychopathic offenders. *Psychological Science*, *22*(2), 226–234. https://doi.org/10.1177/0956797610396227

Baskin-Sommers, A. R., Curtin, J. J., & Newman, J. P. (2015). Altering the

cognitive-affective dysfunctions of psychopathic and externalizing offender subtypes with cognitive remediation. *Clinical Psychological Science*, *3*(1), 45–57. https://doi.org/10.1177/2167702614560744

Baskin-Sommers, A. R., Neumann, C. S., Cope, L. M., & Kiehl, K. A. (2016). Latent-variable modeling of brain gray-matter volume and psychopathy in incarcerated offenders. *Journal of Abnormal Psychology*, *125*(6), 811–817. https://doi.org/10.1037/abn0000175

Baskin-Sommers, A. R., & Newman, J. P. (2013). Differentiating the cognition-emotion interactions that characterize psychopathy versus externalizing disorders. In M. Robinson, E. Harmon-Jones, & E. Watkins (Eds.), *Cognition and Emotion* (pp. 501–520). Guilford Press. https://doi.org/10.1017/CBO9781107415324.004

Bassett, D. S., & Bullmore, E. T. (2017). Small-World Brain Networks Revisited. *Neuroscientist*, *23*(5), 499–516. https://doi.org/10.1177/1073858416667720

Bateman, A., Bolton, R., & Fonagy, P. (2013). Antisocial Personality Disorder: A Mentalizing Framework. *Focus*, *11*(2), 178–186. https://doi.org/10.1176/appi.focus.11.2.178

Baumgartner, T., Heinrichs, M., Vonlanthen, A., Fischbacher, U., & Fehr, E. (2008). Oxytocin Shapes the Neural Circuitry of Trust and Trust Adaptation in Humans. *Neuron*, *58*(4), 639–650. https://doi.org/10.1016/J.NEURON.2008.04.009

Beard, R., Singh, N., Grundschober, C., Gee, A. D., & Tate, E. W. (2018). High-yielding 18 F radiosynthesis of a novel oxytocin receptor tracer, a probe for nose-to-brain oxytocin uptake in vivo. *Chemical Communications*, *54*(58), 8120–8123. https://doi.org/10.1039/C8CC01400K

Beaver, K. M., Barnes, J. C., May, J. S., & Schwartz, J. A. (2011). Psychopathic Personality Traits, Genetic Risk, and Gene-Environment Correlations. *Criminal Justice and Behavior*, *38*(9), 896–912. https://doi.org/10.1177/0093854811411153

Beckmann, C. F., Mackay, C. E., Filippini, N., & Smith, S. M. (2009). Group comparison of resting-state FMRI data using multi-subject ICA and dual regression. *NeuroImage*, *47*, S148. https://doi.org/10.1016/S1053-8119(09)71511-3

Beitchman, J. H., Zai, C. C., Muir, K., Berall, L., Nowrouzi, B., Choi, E., & Kennedy, J. L. (2012). Childhood aggression, callous-unemotional traits and oxytocin genes. *European Child & Adolescent Psychiatry*, *21*(3), 125–132. https://doi.org/10.1007/S00787-012-0240-6

Benoit, R. G., Gilbert, S. J., Frith, C. D., & Burgess, P. W. (2012). Rostral Prefrontal Cortex and the Focus of Attention in Prospective Memory.

*Cerebral Cortex*, *22*(8), 1876–1886. https://doi.org/10.1093/CERCOR/BHR264

Bentourkia, M., Bol, A., Ivanoiu, A., Labar, D., Sibomana, M., Coppens, A., Michel, C., Cosnard, G., & De Volder, A. G. (2000). Comparison of regional cerebral blood flow and glucose metabolism in the normal brain: effect of aging. *Journal of the Neurological Sciences*, *181*(1–2), 19–28. https://doi.org/10.1016/S0022-510X(00)00396-8

Berends, Y. R., Tulen, J. H. M., Wierdsma, A. I., Van Pelt, J., Feldman, R., Zagoory-Sharon, O., De Rijke, Y. B., Kushner, S. A., & Van Marle, H. J. C. (2022). Oxytocin and vasopressin in male forensic psychiatric patients with personality disorders and healthy controls. *The Journal of Forensic Psychiatry & Psychology*, *33*(1), 130–151. https://doi.org/10.1080/14789949.2021.1985158

Bethlehem, R. A. I., van Honk, J., Auyeung, B., & Baron-Cohen, S. (2013). Oxytocin, brain physiology, and functional connectivity: A review of intranasal oxytocin fMRI studies. *Psychoneuroendocrinology*, *38*(7), 962–974. https://doi.org/10.1016/j.psyneuen.2012.10.011

Bijsterbosch, J., Smith, S., & Beckmann, C. F. (2017). Voxel-based Connectivity Analyses. In M. Jenkinson & M. Chappell (Eds.), *Introduction to Resting State fMRI Functional Connectivity* (pp. 51–80). Oxford University Press.

Birbaumer, N., Veit, R., Lotze, M., Erb, M., Hermann, C., Grodd, W., & Flor, H. (2005). Deficient fear conditioning in psychopathy: A functional magnetic resonance imaging study. *Archives of General Psychiatry*, *62*(7), 799–805. https://doi.org/10.1001/archpsyc.62.7.799

Bird, G., & Viding, E. (2014). The self to other model of empathy: Providing a new framework for understanding empathy impairments in psychopathy, autism, and alexithymia. *Neuroscience and Biobehavioral Reviews*, *47*, 520–532. https://doi.org/10.1016/j.neubiorev.2014.09.021

Biswal, B., Zerrin Yetkin, F., Haughton, V. M., & Hyde, J. S. (1995). Functional connectivity in the motor cortex of resting human brain using echo-planar MRI. *Magnetic Resonance in Medicine*, *34*(4), 537–541. https://doi.org/10.1002/mrm.1910340409

Black, D. W., Gunter, T., Loveless, P., Allen, J., & Sieleni, B. (2010). Antisocial personality disorder in incarcerated offenders: Psychiatric comorbidity and quality of life. *Annals of Clinical Psychiatry*, *22*(2), 113–120.

Blackburn, R., Logan, C., Donnelly, J., & Renwick, S. (2003). Personality disorders, psychopathy and other mental disorders: co-morbidity among patients at English and Scottish high-security hospitals.

*Journal of Forensic Psychiatry & Psychology*, *14*(1), 111–137. https://doi.org/10.1080/1478994031000077925

Blair, K. S., Morton, J., Leonard, A., & Blair, R. J. R. (2006). Impaired decision-making on the basis of both reward and punishment information in individuals with psychopathy. *Personality and Individual Differences*, *41*(1), 155–165. https://doi.org/10.1016/j.paid.2005.11.031

Blair, R. J. R. (2004). The roles of orbital frontal cortex in the modulation of antisocial behavior. *Brain and Cognition*, *55*(1), 198–208. https://doi.org/10.1016/S0278-2626(03)00276-8

Blair, R. J. R. (2006). The emergence of psychopathy: Implications for the neuropsychological approach to developmental disorders. *Cognition*, *101*(2), 414–442. https://doi.org/10.1016/j.cognition.2006.04.005

Blair, R. J. R. (2007a). Empathic dysfunction in psychopathic individuals. In T. F. D. Farrow & P. W. R. Woodruff (Eds.), *Empathy in Mental Illness* (pp. 3–16). Cambridge University Press. https://doi.org/10.1017/CBO9780511543753.002

Blair, R. J. R. (2007b). The amygdala and ventromedial prefrontal cortex in morality and psychopathy. *Trends in Cognitive Sciences*, *11*(9), 387–392. https://doi.org/10.1016/j.tics.2007.07.003

Blair, R. J. R. (2008). The amygdala and ventromedial prefrontal cortex: functional contributions and dysfunction in psychopathy. *Philosophical Transactions of the Royal Society B: Biological Sciences*, *363*(1503), 2557–2565. https://doi.org/10.1098/rstb.2008.0027

Blair, R. J. R. (2010). Neuroimaging of Psychopathy and Antisocial Behavior: A Targeted Review. *Current Psychiatry Reports*, *12*(1), 76–82. https://doi.org/10.1007/s11920-009-0086-x

Blair, R. J. R. (2013a). Psychopathy: cognitive and neural dysfunction. *Dialogues in Clinical Neuroscience*, *15*(2), 181–190. https://doi.org/10.31887/dcns.2013.15.2/rblair

Blair, R. J. R. (2013b). The neurobiology of psychopathic traits in youths. *Nature Reviews Neuroscience*, *14*(11), 786–799. https://doi.org/10.1038/nrn3577

Blair, R. J. R. (2020). Modeling the Comorbidity of Cannabis Abuse and Conduct Disorder/Conduct Problems from a Cognitive Neuroscience Perspective. *Journal of Dual Diagnosis*, *16*(1), 3–21. https://doi.org/10.1080/15504263.2019.1668099

Blair, R. J. R., Bashford-Largo, J., Zhang, R., Lukoff, J., Elowsky, J. S., Leibenluft, E., Hwang, S., Dobbertin, M., & Blair, K. S. (2020). Temporal Discounting Impulsivity and Its Association with Conduct Disorder and Irritability. *Journal of Child and Adolescent*

*Psychopharmacology*, *30*(9), 542–548. https://doi.org/10.1089/CAP.2020.0001

Blair, R. J. R., Leibenluft, E., & Pine, D. S. (2014). Conduct Disorder and Callous-Unemotional Traits in Youth. *New England Journal of Medicine*, *371*, 2207–2216. https://doi.org/10.1056/NEJMra1315612

Blair, R. J. R., Veroude, K., & Buitelaar, J. K. (2018). Neuro-cognitive system dysfunction and symptom sets: A review of fMRI studies in youth with conduct problems. *Neuroscience and Biobehavioral Reviews*, *91*, 69–90. https://doi.org/10.1016/j.neubiorev.2016.10.022

Blair, R. J. R., White, S. F., Meffert, H., & Hwang, S. (2014). Disruptive Behaviour Disorders: Taking an RDoC(ish) Approach. *Current Topics in Behavioural Neurosciences*, *16*, 319–336. https://doi.org/10.1007/7854

Bletsch, A., Mann, C., Andrews, D. S., Daly, E., Tan, G. M. Y., Murphy, D. G. M., & Ecker, C. (2018). Down syndrome is accompanied by significantly reduced cortical grey–white matter tissue contrast. *Human Brain Mapping*, *39*(10), 4043–4054. https://doi.org/10.1002/hbm.24230

Bloomfield, M. A. P., Green, S. F., Hindocha, C., Yamamori, Y., Yim, J. L. L., Jones, A. P. M., Walker, H. R., Tokarczuk, P., Statton, B., Howes, O. D., Curran, H. V., & Freeman, T. P. (2020). The effects of acute cannabidiol on cerebral blood flow and its relationship to memory: An arterial spin labelling magnetic resonance imaging study. *Journal of Psychopharmacology*, *34*(9), 981–989. https://doi.org/10.1177/0269881120936419

Bocchio, M., McHugh, S. B., Bannerman, D. M., Sharp, T., & Capogna, M. (2016). Serotonin, Amygdala and Fear: Assembling the Puzzle. *Frontiers in Neural Circuits*, *10*(24), 1–15. https://doi.org/10.3389/FNCIR.2016.00024

Boccia, M. L., Petrusz, P., Suzuki, K., Marson, L., & Pedersen, C. A. (2013). Immunohistochemical localization of oxytocin receptors in human brain. *Neuroscience*, *253*, 155–164. https://doi.org/10.1016/J.NEUROSCIENCE.2013.08.048

Bookstein, F. L. (2001). "Voxel-Based Morphometry" Should Not Be Used with Imperfectly Registered Images. *NeuroImage*, *14*(6), 1454–1462. https://doi.org/10.1006/NIMG.2001.0770

Borland, J. M., Rilling, J. K., Frantz, K. J., & Albers, H. E. (2019). Sex-dependent regulation of social reward by oxytocin: an inverted U hypothesis. *Neuropsychopharmacology*, *44*(1), 97–110. https://doi.org/10.1038/s41386-018-0129-2

Borogovac, A., & Asllani, I. (2012). Arterial Spin Labeling (ASL) fMRI: Advantages, Theoretical Constrains and Experimental Challenges in Neuroscience. *International Journal of Biomedical Imaging*, *2012*(818456), 1–13. https://doi.org/10.1155/2012/818456

Brazil, I. A., van Dongen, J. D. M., Maes, J. H. R., Mars, R. B., & Baskin-Sommers, A. R. (2018). Classification and treatment of antisocial individuals: From behavior to biocognition. *Neuroscience and Biobehavioral Reviews*, *91*, 259–277. https://doi.org/10.1016/j.neubiorev.2016.10.010

Bressler, S. L., & Menon, V. (2010). Large-scale brain networks in cognition: emerging methods and principles. *Trends in Cognitive Sciences*, *14*(6), 277–290. https://doi.org/10.1016/J.TICS.2010.04.004

Brewer, J. A., Garrison, K. A., & Whitfield-Gabrieli, S. (2013). What about the "self" is processed in the posterior cingulate cortex? *Frontiers in Human Neuroscience*, *7*(647), 1–7. https://doi.org/10.3389/fnhum.2013.00647

Brodmann, K., Gruber, O., & Goya-Maldonado, R. (2017). Intranasal Oxytocin Selectively Modulates Large-Scale Brain Networks in Humans. *Brain Connectivity*, *7*(7), 454–463. https://doi.org/10.1089/brain.2017.0528

Brooks, J. H., & Reddon, J. R. (1996). Serum testosterone in violent and nonviolent young offenders. *Journal of Clinical Psychology*, *52*(4), 475–483. https://doi.org/10.1002/(sici)1097-4679(199607)52:4<475::aid-jclp14>3.0.co;2-d

Bryant, J. E., Frölich, M., Tran, S., Reid, M. A., Lahti, A. C., & Kraguljac, N. V. (2019). Ketamine induced changes in regional cerebral blood flow, interregional connectivity patterns, and glutamate metabolism. *Journal of Psychiatric Research*, *117*, 108–115. https://doi.org/10.1016/j.jpsychires.2019.07.008

Brysbaert, M., & Stevens, M. (2018). Power analysis and effect size in mixed effects models: A tutorial. *Journal of Cognition*, *1*(9), 1–20. https://doi.org/10.5334/JOC.10/METRICS/

Buckholtz, J. W., & Meyer-Lindenberg, A. (2012). Psychopathology and the Human Connectome: Toward a Transdiagnostic Model of Risk For Mental Illness. *Neuron*, *74*(6), 990–1004. https://doi.org/10.1016/J.NEURON.2012.06.002

Buckholtz, J. W., Treadway, M. T., Cowan, R. L., Woodward, N. D., Benning, S. D., Li, R., Ansari, M. S., Baldwin, R. M., Schwartzman, A. N., Shelby, E. S., Smith, C. E., Cole, D., Kessler, R. M., & Zald, D. H. (2010). Mesolimbic dopamine reward system hypersensitivity in individuals with psychopathic traits. *Nature Neuroscience*, *13*(4), 419–

421. https://doi.org/10.1038/NN.2510

Budhani, S., Marsh, A. A., Pine, D. S., & Blair, R. J. R. (2007). Neural correlates of response reversal: Considering acquisition. *NeuroImage*, *34*(4), 1754–1765. https://doi.org/10.1016/J.NEUROIMAGE.2006.08.060

Budhani, S., Richell, R. A., & Blair, R. J. R. (2006). Impaired reversal but intact acquisition: Probabilistic response reversal deficits in adult individuals with psychopathy. *Journal of Abnormal Psychology*, *115*(3), 552–558. https://doi.org/10.1037/0021-843X.115.3.552

Bullmore, E., & Sporns, O. (2009). Complex brain networks: graph theoretical analysis of structural and functional systems. *Nature Reviews Neuroscience*, *10*(3), 186–198. https://doi.org/10.1038/nrn2575

Bürkner, P. C., Williams, D. R., Simmons, T. C., & Woolley, J. D. (2017). Intranasal Oxytocin May Improve High-Level Social Cognition in Schizophrenia, But Not Social Cognition or Neurocognition in General: A Multilevel Bayesian Meta-analysis. *Schizophrenia Bulletin*, *43*(6), 1291–1303. https://doi.org/10.1093/SCHBUL/SBX053

Burt, S. A., & Klump, K. L. (2014). Prosocial peer affiliation suppresses genetic influences on non-aggressive antisocial behaviors during childhood. *Psychological Medicine*, *44*(4), 821–830. https://doi.org/10.1017/S0033291713000974

Buxton, R. B., Uludağ, K., Dubowitz, D. J., & Liu, T. T. (2004). Modeling the hemodynamic response to brain activation. *NeuroImage*, *23*(SUPPL. 1), S220–S233. https://doi.org/10.1016/J.NEUROIMAGE.2004.07.013

Byrd, A. L., & Manuck, S. B. (2014). MAOA, childhood maltreatment, and antisocial behavior: meta-analysis of a gene-environment interaction. *Biological Psychiatry*, *75*(1), 9–17. https://doi.org/10.1016/J.BIOPSYCH.2013.05.004

Byrd, A. L., Tung, I., Manuck, S. D., Vine, V., Horner, M., Hipwell, A. E., & Stepp, S. D. (2020). An interaction between early threat exposure and the oxytocin receptor in females: Disorder-specific versus general risk for psychopathology and social–emotional mediators. *Development and Psychopathology*, *33*(4), 1248–1263. https://doi.org/10.1017/s0954579420000462

Bzdok, D., Heeger, A., Langner, R., Laird, A. R., Fox, P. T., Palomero-Gallagher, N., Vogt, B. A., Zilles, K., & Eickhoff, S. B. (2015). Subspecialization in the human posterior medial cortex. *NeuroImage*, *106*, 55–71. https://doi.org/10.1016/J.NEUROIMAGE.2014.11.009

Bzdok, D., Schilbach, L., Vogeley, K., Schneider, K., Laird, A. R., Langner,

R., & Eickhoff, S. B. (2012). Parsing the neural correlates of moral cognition: ALE meta-analysis on morality, theory of mind, and empathy. *Brain Structure & Function*, *217*(4), 783. https://doi.org/10.1007/S00429-012-0380-Y

Caballero-Gaudes, C., & Reynolds, R. C. (2017). Methods for cleaning the BOLD fMRI signal. *NeuroImage*, *154*, 128–149. https://doi.org/10.1016/J.NEUROIMAGE.2016.12.018

Cai, Q., Feng, L., & Yap, K. Z. (2018). Systematic review and meta-analysis of reported adverse events of long-term intranasal oxytocin treatment for autism spectrum disorder. *Psychiatry and Clinical Neurosciences*, *72*(3), 140–151. https://doi.org/10.1111/pcn.12627

Caldwell, B. M., Anderson, N. E., Harenski, K. A., Sitney, M. H., Caldwell, M. F., Van Rybroek, G. J., & Kiehl, K. A. (2019). The structural brain correlates of callous-unemotional traits in incarcerated male adolescents. *NeuroImage: Clinical*, *22*, 1–10. https://doi.org/10.1016/j.nicl.2019.101703

Caldwell, M. F., Skeem, J., Salekin, R. T., & Van Rybroek, G. (2006). Treatment Response of Adolescent Offenders With Psychopathy Features. *Criminal Justice and Behavior*, *33*(5), 571–596. https://doi.org/10.1177/0093854806288176

Calhoun, V. D., Adali, T., Pearlson, G. D., & Pekar, J. J. (2001). A method for making group inferences from functional MRI data using independent component analysis. *Human Brain Mapping*, *14*(3), 140–151. https://doi.org/10.1002/HBM.1048

Calzada-Reyes, A., Alvarez-Amador, A., Galán-Garcia, L., & Valdés-Sosa, M. (2021). Electroencephalographic and morphometric abnormalities in psychopath offenders. *Behavioral Sciences & the Law*, *39*(5), 597–610. https://doi.org/10.1002/BSL.2548

Cao, H., McEwen, S. C., Forsyth, J. K., Gee, D. G., Bearden, C. E., Addington, J., Goodyear, B., Cadenhead, K. S., Mirzakhanian, H., Cornblatt, B. A., Carrión, R. E., Mathalon, D. H., McGlashan, T. H., Perkins, D. O., Belger, A., Seidman, L. J., Thermenos, H., Tsuang, M. T., Van Erp, T. G. M., … Cannon, T. D. (2019). Toward Leveraging Human Connectomic Data in Large Consortia: Generalizability of fMRI-Based Brain Graphs Across Sites, Sessions, and Paradigms. *Cerebral Cortex*, *29*(3), 1263–1279. https://doi.org/10.1093/CERCOR/BHY032

Carlisi, C. O., Moffitt, T. E., Knodt, A. R., Harrington, H., Ireland, D., Melzer, T. R., Poulton, R., Ramrakha, S., Caspi, A., Hariri, A. R., & Viding, E. (2020). Associations between life-course-persistent antisocial behaviour and brain structure in a population-representative longitudinal birth cohort. *The Lancet Psychiatry*, *7*(3), 245–253. https://doi.org/10.1016/S2215-0366(20)30002-X

Carson, D. S., Berquist, S. W., Trujillo, T. H., Garner, J. P., Hannah, S. L., Hyde, S. A., Sumiyoshi, R. D., Jackson, L. P., Moss, J. K., Strehlow, M. C., Cheshier, S. H., Partap, S., Hardan, A. Y., & Parker, K. J. (2014). Cerebrospinal fluid and plasma oxytocin concentrations are positively correlated and negatively predict anxiety in children. *Molecular Psychiatry*, *20*(9), 1085–1090. https://doi.org/10.1038/mp.2014.132

Cavanna, A. E., & Trimble, M. R. (2006). The precuneus: a review of its functional anatomy and behavioural correlates. *Brain*, *129*(3), 564–583. https://doi.org/10.1093/BRAIN/AWL004

Cecil, C. A. M., Lysenko, L. J., Jaffee, S. R., Pingault, J. B., Smith, R. G., Relton, C. L., Woodward, G., McArdle, W., Mill, J., & Barker, E. D. (2014). Environmental risk, Oxytocin Receptor Gene (OXTR) methylation and youth callous-unemotional traits: a 13-year longitudinal study. *Molecular Psychiatry*, *19*(10), 1071–1077. https://doi.org/10.1038/mp.2014.95

Chang, Z., Larsson, H., Lichtenstein, P., & Fazel, S. (2015). Psychiatric disorders and violent reoffending: A national cohort study of convicted prisoners in Sweden. *The Lancet Psychiatry*, *2*(10), 891–900. https://doi.org/10.1016/S2215-0366(15)00234-5

Checknita, D. R., Bendre, M., Ekström, T. J., Comasco, E., Tiihonen, J., Hodgins, S., & Nilsson, K. W. (2020). Monoamine oxidase A genotype and methylation moderate the association of maltreatment and aggressive behaviour. *Behavioural Brain Research*, *382*(112476), 1–13. https://doi.org/10.1016/J.BBR.2020.112476

Checknita, D. R., Maussion, G., Labonté, B., Comai, S., Tremblay, R. E., Vitaro, F., Turecki, N., Bertazzo, A., Gobbi, G., Côté, G., & Turecki, G. (2015). Monoamine oxidase A gene promoter methylation and transcriptional downregulation in an offender population with antisocial personality disorder. *British Journal of Psychiatry*, *206*(3), 216–222. https://doi.org/10.1192/bjp.bp.114.144964

Chee, M. W. L., Zheng, H., Goh, J. O. S., Park, D., & Sutton, B. P. (2011). Brain Structure in Young and Old East Asians and Westerners: Comparisons of Structural Volume and Cortical Thickness. *Journal of Cognitive Neuroscience*, *23*(5), 1065–1079. https://doi.org/10.1162/JOCN.2010.21513

Cheng, Y., Chou, J., Martínez, R. M., Fan, Y.-T., & Chen, C. (2021). Psychopathic traits mediate guilt-related anterior midcingulate activity under authority pressure. *Scientific Reports*, *11*(14856), 1–11. https://doi.org/10.1038/s41598-021-94372-5

Choe, A. S., Jones, C. K., Joel, S. E., Muschelli, J., Belegu, V., Caffo, B. S., Lindquist, M. A., Van Zijl, P. C. M., & Pekar, J. J. (2015).

Reproducibility and Temporal Structure in Weekly Resting-State fMRI over a Period of 3.5 Years. *PLoS ONE*, *10*(10), e0140134. https://doi.org/10.1371/journal.pone.0140134

Cima, M., & Raine, A. (2009). Distinct characteristics of psychopathy relate to different subtypes of aggression. *Personality and Individual Differences*, *47*(8), 835–840. https://doi.org/10.1016/j.paid.2009.06.031

Cima, M., Smeets, T., & Jelicic, M. (2008). Self-reported trauma, cortisol levels, and aggression in psychopathic and non-psychopathic prison inmates. *Biological Psychology*, *78*(1), 75–86. https://doi.org/10.1016/J.BIOPSYCHO.2007.12.011

Coccaro, E. F., Fanning, J. R., Phan, K. L., & Lee, R. (2015). Serotonin and impulsive aggression. *CNS Spectrums*, *20*(3), 295–302. https://doi.org/10.1017/S1092852915000310

Cohen, J. R., & D'Esposito, M. (2016). The segregation and integration of distinct brain networks and their relationship to cognition. *Journal of Neuroscience*, *36*(48), 12083–12094. https://doi.org/10.1523/JNEUROSCI.2965-15.2016

Cohn, M. D., Pape, L. E., Schmaal, L., van den Brink, W., van Wingen, G., Vermeiren, R. R. J. M., Doreleijers, T. A. H., Veltman, D. J., & Popma, A. (2015). Differential relations between juvenile psychopathic traits and resting state network connectivity. *Human Brain Mapping*, *36*(6), 2396–2405. https://doi.org/10.1002/HBM.22779

Coid, J., & Ullrich, S. (2010). Antisocial personality disorder is on a continuum with psychopathy. *Comprehensive Psychiatry*, *51*(4), 426–433. https://doi.org/10.1016/j.comppsych.2009.09.006

Coid, J., Yang, M., Tyrer, P., Roberts, A., & Ullrich, S. (2006). Prevalence and correlates of personality disorder in Great Britain. *British Journal of Psychiatry*, *188*, 423–431. https://doi.org/10.1192/bjp.188.5.423

Coid, J., Yang, M., Ullrich, S., Roberts, A., & Hare, R. D. (2009). Prevalence and correlates of psychopathic traits in the household population of Great Britain. *International Journal of Law and Psychiatry*, *32*(2), 65–73. https://doi.org/10.1016/j.ijlp.2009.01.002

Coid, J., Yang, M., Ullrich, S., Roberts, A., Moran, P., Bebbington, P., Brugha, T., Jenkins, R., Farrell, M., Lewis, G., Singleton, N., & Hare, R. D. (2009). Psychopathy among prisoners in England and Wales. *International Journal of Law and Psychiatry*, *32*(3), 134–141. https://doi.org/10.1016/j.ijlp.2009.02.008

Cole, D. M., Smith, S. M., & Beckmann, C. F. (2010). Advances and pitfalls in the analysis and interpretation of resting-state fMRI data. *Frontiers in Systems Neuroscience*, *4*(8), 1–15.

https://doi.org/10.3389/fnsys.2010.00008

Colins, O. F., Van Damme, L., Hendriks, A. M., & Georgiou, G. (2020). The DSM-5 with Limited Prosocial Emotions Specifier for Conduct Disorder: a Systematic Literature Review. *Journal of Psychopathology and Behavioral Assessment*, *42*(2), 248–258. https://doi.org/10.1007/s10862-020-09799-3

Comai, S., Tau, M., & Gobbi, G. (2012). The psychopharmacology of aggressive behavior: A translational approach: Part 1: Neurobiology. *Journal of Clinical Psychopharmacology*, *32*(1), 83–94. https://doi.org/10.1097/JCP.0b013e31823f8770

Compton, W., Conway, K. P., Stinson, F. S., Colliver, J. D., & Grant, B. F. (2005). Prevalence, Correlates, and Comorbidity of DSM-IV Antisocial Personality Syndromes and Alcohol and Specific Drug Use Disorders in the United States. *Journal of Clinical Psychiatry*, *66*, 667–685. https://doi.org/10.4088/JCP.v66n0602

Contreras-Rodríguez, O., Pujol, J., Batalla, I., Harrison, B. J., Bosque, J., Ibern-Regàs, I., Hernández-Ribas, R., Soriano-Mas, C., Deus, J., López-Solà, M., Pifarré, J., Menchón, J. M., & Cardoner, N. (2014). Disrupted neural processing of emotional faces in psychopathy. *Social Cognitive and Affective Neuroscience*, *9*(4), 505–512. https://doi.org/10.1093/SCAN/NST014

Contreras-Rodríguez, O., Pujol, J., Batalla, I., Harrison, B. J., Soriano-Mas, C., Deus, J., López-Solà, M., Macià, D., Pera-Guardiola, V., Hernández-Ribas, R., Pifarré, J., Menchón, J. M., & Cardoner, N. (2015). Functional connectivity bias in the prefrontal cortex of psychopaths. *Biological Psychiatry*, *78*(9), 647–655. https://doi.org/10.1016/j.biopsych.2014.03.007

Cook, R. D. (1977). Detection of Influential Observations in Linear Regression. *Technometrics*, *19*(1), 15–18. https://doi.org/10.2307/1268249

Cooke, D. J., & Michie, C. (1999). Psychopathy across cultures: North America and Scotland compared. *Journal of Abnormal Psychology*, *108*(1), 58–68. https://doi.org/10.1037/0021-843X.108.1.58

Copeland, W. E., Shanahan, L., Costello, E. J., & Angold, A. (2009). Childhood and adolescent psychiatric disorders as predictors of young adult disorders. *Archives of General Psychiatry*, *66*(7), 764–772. https://doi.org/10.1001/archgenpsychiatry.2009.85

Craig, M. C., Catani, M., Deeley, Q., Latham, R., Daly, E., Kanaan, R., Picchioni, M., McGuire, P. K., Fahy, T., & Murphy, D. G. M. (2009). Altered connections on the road to psychopathy. *Molecular Psychiatry*, *14*(10), 946–953. https://doi.org/10.1038/mp.2009.40

Crockett, M. J., Clark, L., Hauser, M. D., & Robbins, T. W. (2010). Serotonin selectively influences moral judgment and behavior through effects on harm aversion. *Proceedings of the National Academy of Sciences of the United States of America*, *107*(40), 17433–17438. https://doi.org/10.1073/pnas.1009396107

Cuartas Arias, J. M., Palacio Acosta, C. A., Garcia Valencia, J., Montoya, G. J., Arango Viana, J. C., Campo Nieto, O., Flórez, A. F., Camarena Medellin, B. E., Rojas Montoya, W., Lopez Jaramillo, C. A., Gutierrez Achury, J., Cruz Fuentes, C., Bedoya Berrio, G., & Ruiz-Linares, A. (2011). Exploring epistasis in candidate genes for antisocial personality disorder. *Psychiatric Genetics*, *21*(3), 115–124. https://doi.org/10.1097/YPG.0b013e3283437175

Da Cunha-Bang, S., Hjordt, L. V., Dam, V. H., Stenbæk, D. S., Sestoft, D., & Knudsen, G. M. (2017). Anterior cingulate serotonin 1B receptor binding is associated with emotional response inhibition. *Journal of Psychiatric Research*, *92*, 199–204. https://doi.org/10.1016/J.JPSYCHIRES.2017.05.003

Da Cunha-Bang, S., Hjordt, L. V., Perfalk, E., Beliveau, V., Bock, C., Lehel, S., Thomsen, C., Sestoft, D., Svarer, C., & Knudsen, G. M. (2017). Serotonin 1B Receptor Binding Is Associated With Trait Anger and Level of Psychopathy in Violent Offenders. *Biological Psychiatry*, *82*(4), 267–274. https://doi.org/10.1016/J.BIOPSYCH.2016.02.030

Dadds, M. R., Moul, C., Cauchi, A., Dobson-Stone, C., Hawes, D. J., Brennan, J., & Ebstein, R. E. (2014). Methylation of the oxytocin receptor gene and oxytocin blood levels in the development of psychopathy. *Development and Psychopathology*, *26*(1), 33–40. https://doi.org/10.1017/S0954579413000497

Dal Monte, O., Noble, P. L., Turchi, J., Cummins, A., & Averbeck, B. B. (2014). CSF and Blood Oxytocin Concentration Changes following Intranasal Delivery in Macaque. *PLoS ONE*, *9*(8), e103677. https://doi.org/10.1371/JOURNAL.PONE.0103677

Dale, A. M., Fischl, B., & Sereno, M. I. (1999). Cortical Surface-Based Analysis, I. Segmentation and surface reconstruction. *NeuroImage*, *9*(2), 179–194. https://doi.org/10.1006/nimg.1998.0395

Damoiseaux, J. S., Rombouts, S. A. R. B., Barkhof, F., Scheltens, P., Stam, C. J., Smith, S. M., & Beckmann, C. F. (2006). Consistent resting-state networks across healthy subjects. *Proceedings of the National Academy of Sciences of the United States of America*, *103*(37), 13848–13853. https://doi.org/10.1073/pnas.0601417103

Davatzikos, C. (2004). Why voxel-based morphometric analysis should be used with great caution when characterizing group differences. *NeuroImage*, *23*(1), 17–20.

https://doi.org/10.1016/J.NEUROIMAGE.2004.05.010

Davies, C., Paloyelis, Y., Rutigliano, G., Cappucciati, M., De Micheli, A., Ramella-Cravaro, V., Provenzani, U., Antoniades, M., Modinos, G., Oliver, D., Stahl, D., Murguia, S., Zelaya, F., Allen, P., Shergill, S., Morrison, P., Williams, S., Taylor, D., McGuire, P., & Fusar-Poli, P. (2019). Oxytocin modulates hippocampal perfusion in people at clinical high risk for psychosis. *Neuropsychopharmacology*, *44*(7), 1300–1309. https://doi.org/10.1038/s41386-018-0311-6

Dawel, A., O'Kearney, R., McKone, E., & Palermo, R. (2012). Not just fear and sadness: Meta-analytic evidence of pervasive emotion recognition deficits for facial and vocal expressions in psychopathy. *Neuroscience and Biobehavioral Reviews*, *36*(10), 2288–2304. https://doi.org/10.1016/j.neubiorev.2012.08.006

De Brito, S. A., & Hodgins, S. (2009). Executive functions of persistent violent offenders : A critical review of the literature. In S. Hodgins, E. Viding, & A. Plodowski (Eds.), *The neurobiological basis of violence: Science and rehabilitation* (pp. 167–218). Oxford University Press.

De Brito, S. A., McDonald, D., Camilleri, J. A., & Rogers, J. C. (2021). Cortical and subcortical gray matter volume in psychopathy: a voxel-wise meta-analysis. *Journal of Abnormal Psychology*, *130*(6), 627–640. https://doi.org/https://doi.org/10.1037/abn0000698

De Brito, S. A., Mechelli, A., Wilke, M., Laurens, K. R., Jones, A. P., Barker, G. J., Hodgins, S., & Viding, E. (2009). Size matters: Increased grey matter in boys with conduct problems and callous–unemotional traits. *Brain*, *132*(4), 843–852. https://doi.org/10.1093/BRAIN/AWP011

De Brito, S. A., Viding, E., Kumari, V., Blackwood, N., & Hodgins, S. (2013). Cool and Hot Executive Function Impairments in Violent Offenders with Antisocial Personality Disorder with and without Psychopathy. *PLoS ONE*, *8*(6), e65566. https://doi.org/10.1371/journal.pone.0065566

De Looff, P. C., Cornet, L. J. M., De Kogel, C. H., Fernández-Castilla, B., Embregts, P. J. C. M., Didden, R., & Nijman, H. L. I. (2022). Heart rate and skin conductance associations with physical aggression, psychopathy, antisocial personality disorder and conduct disorder: An updated meta-analysis. *Neuroscience & Biobehavioral Reviews*, *132*(May 2021), 553–582. https://doi.org/10.1016/j.neubiorev.2021.11.003

De Luca, M., Beckmann, C. F., De Stefano, N., Matthews, P. M., & Smith, S. M. (2006). fMRI resting state networks define distinct modes of long-distance interactions in the human brain. *NeuroImage*, *29*(4), 1359–1367. https://doi.org/10.1016/J.NEUROIMAGE.2005.08.035

De Oliveira-Souza, R., Hare, R. D., Bramati, I. E., Garrido, G. J., Azevedo Ignácio, F., Tovar-Moll, F., & Moll, J. (2008). Psychopathy as a disorder of the moral brain: Fronto-temporo-limbic grey matter reductions demonstrated by voxel-based morphometry. *NeuroImage*, *40*(3), 1202–1213. https://doi.org/10.1016/j.neuroimage.2007.12.054

De Oliveira-Souza, R., Moll, J., Ignacio, F. A., & Hare, R. D. (2008). Psychopathy in a civil psychiatric outpatient sample. *Criminal Justice and Behavior*, *35*(4), 427–437. https://doi.org/10.1177/0093854807310853

De Ruiter, C., Burghart, M., De Silva, R., Griesbeck Garcia, S., Mian, U., Walshe, E., & Zouharova, V. (2022). A meta-analysis of childhood maltreatment in relation to psychopathic traits. *PLoS ONE*, *17*(8), e0272704. https://doi.org/10.1371/JOURNAL.PONE.0272704

De Vico Fallani, F., Richiardi, J., Chavez, M., & Achard, S. (2014). Graph analysis of functional brain networks: practical issues in translational neuroscience. *Philosophical Transactions of the Royal Society B: Biological Sciences*, *369*(1653), 1–17. https://doi.org/10.1098/RSTB.2013.0521

Decety, J., Chen, C., Harenski, C., & Kiehl, K. A. (2013). An fMRI study of affective perspective taking in individuals with psychopathy: Imagining another in pain does not evoke empathy. *Frontiers in Human Neuroscience*, *7*(489), 1–12. https://doi.org/10.3389/FNHUM.2013.00489/BIBTEX

Decety, J., Chen, C., Harenski, C. L., & Kiehl, K. A. (2015). Socioemotional processing of morally-laden behavior and their consequences on others in forensic psychopaths. *Human Brain Mapping*, *36*(6), 2015–2026. https://doi.org/10.1002/HBM.22752

Decety, J., Skelly, L. R., & Kiehl, K. A. (2013). Brain response to empathy-eliciting scenarios involving pain in incarcerated individuals with psychopathy. *JAMA Psychiatry*, *70*(6), 638–645. https://doi.org/10.1001/jamapsychiatry.2013.27

Decety, J., Skelly, L. R., Yoder, K. J., & Kiehl, K. A. (2014). Neural processing of dynamic emotional facial expressions in psychopaths. *Social Neuroscience*, *9*(1), 36–49. https://doi.org/10.1080/17470919.2013.866905

Declerck, C. H., Boone, C., & Kiyonari, T. (2010). Oxytocin and cooperation under conditions of uncertainty: The modulating role of incentives and social information. *Hormones and Behavior*, *57*(3), 368–374. https://doi.org/10.1016/J.YHBEH.2010.01.006

Deeley, Q., Daly, E., Surguladze, S., Tunstall, N., Mezey, G., Beer, D., Ambikapathy, A., Robertson, D., Giampietro, V., Brammer, M. J.,

Clarke, A., Dowsett, J., Fahy, T., Phillips, M. L., & Murphy, D. G. M. (2006). Facial emotion processing in criminal psychopathy: Preliminary functional magnetic resonance imaging study. *The British Journal of Psychiatry*, *189*(6), 533–539. https://doi.org/10.1192/BJP.BP.106.021410

Deen, B., Koldewyn, K., Kanwisher, N., & Saxe, R. (2015). Functional Organization of Social Perception and Cognition in the Superior Temporal Sulcus. *Cerebral Cortex*, *25*(11), 4596–4609. https://doi.org/10.1093/CERCOR/BHV111

Delfin, C., Andiné, P., Hofvander, B., Billstedt, E., & Wallinius, M. (2018). Examining Associations Between Psychopathic Traits and Executive Functions in Incarcerated Violent Offenders. *Frontiers in Psychiatry*, *9*, 310. https://doi.org/10.3389/fpsyt.2018.00310

DeLisi, M., Drury, A. J., & Elbert, M. J. (2019). The etiology of antisocial personality disorder: The differential roles of adverse childhood experiences and childhood psychopathology. *Comprehensive Psychiatry*, *92*, 1–6. https://doi.org/10.1016/J.COMPPSYCH.2019.04.001

DeLisi, M., Peters, D. J., Hochstetler, A., Butler, H. D., & Vaughn, M. G. (2022). Psychopathy among condemned capital murderers. *Psychiatry & Behavioral Science*, *00*, 1–10. https://doi.org/10.1111/1556-4029.15188

Deming, P., Heilicher, M., & Koenigs, M. (2022). How reliable are amygdala findings in psychopathy? A systematic review of MRI studies. *Neuroscience and Biobehavioral Reviews*, *142*(104875), 1–18. https://doi.org/10.1016/j.neubiorev.2022.104875

Deming, P., & Koenigs, M. (2020). Functional neural correlates of psychopathy: a meta-analysis of MRI data. *Translational Psychiatry*, *10*(133), 1–8. https://doi.org/10.1038/s41398-020-0816-8

Desikan, R. S., Ségonne, F., Fischl, B., Quinn, B. T., Dickerson, B. C., Blacker, D., Buckner, R. L., Dale, A. M., Maguire, R. P., Hyman, B. T., Albert, M. S., & Killiany, R. J. (2006). An automated labeling system for subdividing the human cerebral cortex on MRI scans into gyral based regions of interest. *NeuroImage*, *31*(3), 968–980. https://doi.org/10.1016/J.NEUROIMAGE.2006.01.021

Desmond, J. E., & Glover, G. H. (2002). Estimating sample size in functional MRI (fMRI) neuroimaging studies: Statistical power analyses. *Journal of Neuroscience Methods*, *118*(2), 115–128. https://doi.org/10.1016/S0165-0270(02)00121-8

Detre, J. A., Wang, J., Wang, Z., & Rao, H. (2009). Arterial spin-labeled perfusion MRI in basic and clinical neuroscience. *Current Opinion in Neurology*, *22*(4), 348–355.

https://doi.org/10.1097/WCO.0b013e32832d9505

Dick, D. M. (2011). Gene-Environment Interaction in Psychological Traits and Disorders. *Annual Review of Clinical Psychology*, *7*, 383–409. https://doi.org/10.1146/annurev-clinpsy-032210-104518

Dipasquale, O., Selvaggi, P., Veronese, M., Gabay, A. S., Turkheimer, F., & Mehta, M. A. (2019). Receptor-Enriched Analysis of functional connectivity by targets (REACT): A novel, multimodal analytical approach informed by PET to study the pharmacodynamic response of the brain under MDMA. *Neuroimage*, *195*, 252. https://doi.org/10.1016/J.NEUROIMAGE.2019.04.007

Dipasquale, O., Sethi, A., Lagan, M. M., Baglio, F., Baselli, G., Kundu, P., Harrison, N. A., & Cercignani, M. (2017). Comparing resting state fMRI de-noising approaches using multi-and single-echo acquisitions. *PLoS ONE*, *12*(3), 1–25. https://doi.org/10.1371/journal.pone.0173289

Docherty, M., Beardslee, J., Byrd, A. L., Yang, V. J. H., & Pardini, D. (2019). Developmental Trajectories of Interpersonal Callousness From Childhood to Adolescence as Predictors of Antisocial Behavior and Psychopathic Features in Young Adulthood. *Journal of Abnormal Psychology*, *128*(7), 700–709. https://doi.org/10.1037/abn0000449

Dodge, K. A. (1991). The structure and function of reactive and proactive aggression. *The Development and Treatment of Childhood Aggression*, *16*(5), 201–218. https://doi.org/10.1111/j.14676494.2009.00610.x

Dodge, K. A. (2006). Translational science in action: Hostile attributional style and the development of aggressive behavior problems. *Development and Psychopathology*, *18*(3), 791–814. https://doi.org/10.1017/S0954579406060391

Dolan, M. C. (2012). The neuropsychology of prefrontal function in antisocial personality disordered offenders with varying degrees of psychopathy. *Psychological Medicine*, *42*(8), 1715–1725. https://doi.org/10.1017/S0033291711002686

Dolan, M. C., & Fullam, R. (2004). Theory of mind and mentalizing ability in antisocial personality disorders with and without psychopathy. *Psychological Medicine*, *34*(6), 1093–1102. https://doi.org/10.1017/S0033291704002028

Dolan, M. C., & Park, I. (2002). The neuropsychology of antisocial personality disorder. *Psychological Medicine*, *32*(3), 417–427. https://doi.org/10.1017/S0033291702005378

Domes, G., Heinrichs, M., Michel, A., Berger, C., & Herpertz, S. C. (2007). Oxytocin Improves “Mind-Reading” in Humans. *Biological Psychiatry*,

*61*(6), 731–733. https://doi.org/10.1016/j.biopsych.2006.07.015

Domes, G., Hollerbach, P., Vohs, K., Mokros, A., & Habermeyer, E. (2013). Emotional empathy and psychopathy in offenders: An experimental study. *Journal of Personality Disorders*, *27*(1), 67–84. https://doi.org/10.1521/pedi.2013.27.1.67

Douw, L., Schoonheim, M. M., Landi, D., van der Meer, M. L., Geurts, J. J. G., Reijneveld, J. C., Klein, M., & Stam, C. J. (2011). Cognition is related to resting-state small-world network topology: an magnetoencephalographic study. *Neuroscience*, *175*, 169–177. https://doi.org/10.1016/J.NEUROSCIENCE.2010.11.039

Drayton, L. A., Santos, L. R., & Baskin-Sommers, A. R. (2018). Psychopaths fail to automatically take the perspective of others. *Proceedings of the National Academy of Sciences of the United States of America*, *115*(13), 3302–3307. https://doi.org/10.1073/pnas.1721903115

Dubois, J., & Adolphs, R. (2016). Building a Science of Individual Differences from fMRI. *Trends in Cognitive Sciences*, *20*(6), 425–443. https://doi.org/10.1016/J.TICS.2016.03.014

Dugré, J. R., & Potvin, S. (2021). Impaired attentional and socio-affective networks in subjects with antisocial behaviors: a meta-analysis of resting-state functional connectivity studies. *Psychological Medicine*, *51*(8), 1249–1259. https://doi.org/10.1017/S0033291721001525

Dugré, J. R., Radua, J., Carignan-Allard, M., Dumais, A., Rubia, K., & Potvin, S. (2020). Neurofunctional abnormalities in antisocial spectrum: A meta-analysis of fMRI studies on Five distinct neurocognitive research domains. *Neuroscience and Biobehavioral Reviews*, *119*, 168–183. https://doi.org/10.1016/j.neubiorev.2020.09.013

Duke, A. A., Bègue, L., Bell, R., & Eisenlohr-Moul, T. (2013). Revisiting the serotonin-aggression relation in humans: A meta-analysis. *Psychological Bulletin*, *139*(5), 1148–1172. https://doi.org/10.1037/a0031544

Ebstein, R. P., Knafo, A., Mankuta, D., Chew, S. H., & Lai, P. S. (2012). The contributions of oxytocin and vasopressin pathway genes to human behavior. *Hormones and Behavior*, *61*(3), 359–379. https://doi.org/10.1016/J.YHBEH.2011.12.014

Ecker, C., Ginestet, C., Feng, Y., Johnston, P., Lombardo, M. V., Lai, M. C., Suckling, J., Palaniyappan, L., Daly, E., Murphy, C. M., Williams, S. C., Bullmore, E. T., Baron-Cohen, S., Brammer, M., & Murphy, D. G. M. (2013). Brain surface anatomy in adults with autism: The relationship between surface area, cortical thickness, and autistic symptoms. *Archives of General Psychiatry*, *70*(1), 59–70.

https://doi.org/10.1001/jamapsychiatry.2013.265

Eisenberg, N., Fabes, R. A., & Spinrad, T. L. (2006). Relation of emotion-related regulation to children's social competence: A longitudinal study. In W. Damon, R. M. Lerner, & N. Eisenberg (Eds.), *Handbook of child psychology: Vol. 3 Social, emotional, and personality development* (pp. 646–718). Wiley.

Elliott, D. S., Ageton, S. S., Huizinga, D., Knowles, B. A., & Canter, R. J. (1983). *The prevalence and incidence of delinquent behavior: 1976-1980. National estimates of delinquent behavior by sex, race, social class, an other selected variables.* https://www.ojp.gov/ncjrs/virtual-library/abstracts/prevalence-and-incidence-delinquent-behavior-1976-1980-national

Engen, H. G., & Singer, T. (2013). Empathy circuits. *Current Opinion in Neurobiology*, *23*(2), 275–282. https://doi.org/10.1016/J.CONB.2012.11.003

Ermer, E., Cope, L. M., Nyalakanti, P. K., Calhoun, V. D., & Kiehl, K. A. (2012). Aberrant paralimbic gray matter in criminal psychopathy. *Journal of Abnormal Psychology*, *121*(3), 649–658. https://doi.org/10.1037/a0026371

Erskine, H. E., Norman, R. E., Ferrari, A. J., Chan, G. C. K., Copeland, W. E., Whiteford, H. A., & Scott, J. G. (2016). Long-Term Outcomes of Attention-Deficit/Hyperactivity Disorder and Conduct Disorder: A Systematic Review and Meta-Analysis. *Journal of the American Academy of Child and Adolescent Psychiatry*, *55*(10), 841–850. https://doi.org/10.1016/j.jaac.2016.06.016

Espinoza, F. A., Anderson, N. E., Vergara, V. M., Harenski, C. L., Decety, J., Rachakonda, S., Damaraju, E., Koenigs, M., Kosson, D. S., Harenski, K., Calhoun, V. D., & Kiehl, K. A. (2019). Resting-state fMRI dynamic functional network connectivity and associations with psychopathy traits. *NeuroImage: Clinical*, *24*(101970), 1–9. https://doi.org/10.1016/j.nicl.2019.101970

Espinoza, F. A., Vergara, V. M., Reyes, D., Anderson, N. E., Harenski, C. L., Decety, J., Rachakonda, S., Damaraju, E., Rashid, B., Miller, R. L., Koenigs, M., Kosson, D. S., Harenski, K., Kiehl, K. A., & Calhoun, V. D. (2018). Aberrant functional network connectivity in psychopathy from a large (N = 985) forensic sample. *Human Brain Mapping*, *39*(6), 2624–2634. https://doi.org/10.1002/HBM.24028

Evans, S., Shergill, S. S., & Averbeck, B. B. (2010). Oxytocin Decreases Aversion to Angry Faces in an Associative Learning Task. *Neuropsychopharmacology*, *35*(13), 2502–2509. https://doi.org/10.1038/npp.2010.110

Eyler, L. T., Chen, C. H., Panizzon, M. S., Fennema-Notestine, C., Neale,

M. C., Jak, A., Jernigan, T. L., Fischl, B., Franz, C. E., Lyons, M. J., Grant, M., Prom-Wormley, E., Seidman, L. J., Tsuang, M. T., Fiecas, M. J. A., Dale, A. M., & Kremen, W. S. (2012). A comparison of heritability maps of cortical surface area and thickness and the influence of adjustment for whole brain measures: A magnetic resonance imaging twin study. *Twin Research and Human Genetics*, *15*(3), 304–314. https://doi.org/10.1017/thg.2012.3

Fairchild, G., Hawes, D. J., Frick, P. J., Copeland, W. E., Odgers, C. L., Franke, B., Freitag, C. M., & De Brito, S. A. (2019). Conduct disorder. *Nature Reviews Disease Primers*, *5*(43), 1–25. https://doi.org/10.1038/s41572-019-0095-y

Fairchild, G., Toschi, N., Hagan, C. C., Goodyer, I. M., Calder, A. J., & Passamonti, L. (2015). Cortical thickness, surface area, and folding alterations in male youths with conduct disorder and varying levels of callous–unemotional traits. *NeuroImage: Clinical*, *8*, 253–260. https://doi.org/10.1016/j.nicl.2015.04.018

Fairchild, G., Van Goozen, S. H. M., Calder, A. J., & Goodyer, I. M. (2013). Research Review: Evaluating and reformulating the developmental taxonomic theory of antisocial behaviour. *Journal of Child Psychology and Psychiatry*, *54*(9), 924–940. https://doi.org/10.1111/jcpp.12102

Fairchild, G., van Goozen, S. H. M., Stollery, S. J., Aitken, M. R. F., Savage, J., Moore, S. C., & Goodyer, I. M. (2009). Decision Making and Executive Function in Male Adolescents with Early-Onset or Adolescence-Onset Conduct Disorder and Control Subjects. *Biological Psychiatry*, *66*(2), 162–168. https://doi.org/10.1016/j.biopsych.2009.02.024

Falk, Ö., Wallinius, M., Lundström, S., Frisell, T., Anckarsäter, H., & Kerekes, N. (2014). The 1 % of the population accountable for 63 % of all violent crime convictions. *Social Psychiatry and Psychiatric Epidemiology*, *49*, 559–571. https://doi.org/10.1007/s00127-013-0783-y

Fan, L., Li, H., Zhuo, J., Zhang, Y., Wang, J., Chen, L., Yang, Z., Chu, C., Xie, S., Laird, A. R., Fox, P. T., Eickhoff, S. B., Yu, C., & Jiang, T. (2016). The Human Brainnetome Atlas: A New Brain Atlas Based on Connectional Architecture. *Cerebral Cortex*, *26*(8), 3508–3526. https://doi.org/10.1093/CERCOR/BHW157

Fanti, K. A., Frick, P. J., & Georgiou, S. (2009). Linking callous-unemotional traits to instrumental and non-instrumental forms of aggression. *Journal of Psychopathology and Behavioral Assessment*, *31*(4), 285–298. https://doi.org/10.1007/s10862-008-9111-3

Fanti, K. A., Kimonis, E. R., Hadjicharalambous, M.-Z., & Steinberg, L.

(2016). Do neurocognitive deficits in decision making differentiate conduct disorder subtypes? *European Child & Adolescent Psychiatry*, *25*(9), 989–996. https://doi.org/10.1007/s00787-016-0822-9

Fanti, K. A., Konikou, K., Cohn, M., Popma, A., & Brazil, I. A. (2019). Amygdala functioning during threat acquisition and extinction differentiates antisocial subtypes. *Journal of Neuropsychology*. https://doi.org/10.1111/jnp.12183

Fanti, K. A., Panayiotou, G., Lazarou, C., Michael, R., & Georgiou, G. (2016). The better of two evils? Evidence that children exhibiting continuous conduct problems high or low on callous-unemotional traits score on opposite directions on physiological and behavioral measures of fear. *Development and Psychopathology*, *28*(1), 185–198. https://doi.org/10.1017/S0954579415000371

Fantini, S., Sassaroli, A., Tgavalekos, K. T., & Kornbluth, J. (2016). Cerebral blood flow and autoregulation: current measurement techniques and prospects for noninvasive optical methods. *Neurophotonics*, *3*(3), 031411. https://doi.org/10.1117/1.NPH.3.3.031411

Farahani, F. V., Karwowski, W., & Lighthall, N. R. (2019). Application of graph theory for identifying connectivity patterns in human brain networks: A systematic review. *Frontiers in Neuroscience*, *13*(585), 1–27. https://doi.org/10.3389/FNINS.2019.00585/BIBTEX

Farrington, D. P. (2019). The development of violence from age 8 to 61. *Aggressive Behavior*, *45*(4), 365–376. https://doi.org/10.1002/ab.21831

Farrington, D. P. (2020). The Integrated Cognitive Antisocial Potential (ICAP) Theory: Past, Present, and Future. *Journal of Developmental and Life-Course Criminology*, *6*, 172–187. https://doi.org/10.1007/s40865-019-00112-9

Fazel, S., & Danesh, J. (2002). Serious mental disorder in 23000 prisoners: A systematic review of 62 surveys. *The Lancet*, *359*(9306), 545–550. https://doi.org/10.1016/S0140-6736(02)07740-1

Fazel, S., Smith, E. N., Chang, Z., & Geddes, J. R. (2018). Risk factors for interpersonal violence: an umbrella review of meta-analyses. *The British Journal of Psychiatry*, *213*, 609–614. https://doi.org/10.1192/bjp.2018.145

Feilhauer, J., Cima, M., Korebrits, A., & Nicolson, N. A. (2013). Salivary cortisol and psychopathy dimensions in detained antisocial adolescents. *Psychoneuroendocrinology*, *38*(9), 1586–1595. https://doi.org/10.1016/J.PSYNEUEN.2013.01.005

Ferguson, C. J. (2010). Genetic Contributions to Antisocial Personality and

Behavior: A Meta-Analytic Review From an Evolutionary Perspective. *The Journal of Social Psychology*, *150*(2), 160–180. https://doi.org/10.1080/00224540903366503

Fergusson, D. M., Boden, J. M., Horwood, L. J., Miller, A. L., & Kennedy, M. A. (2011). MAOA, abuse exposure and antisocial behaviour: 30-Year longitudinal study. *British Journal of Psychiatry*, *198*(6), 457–463. https://doi.org/10.1192/bjp.bp.110.086991

Ferré, J. C., Bannier, E., Raoult, H., Mineur, G., Carsin-Nicol, B., & Gauvrit, J. Y. (2013). Arterial spin labeling (ASL) perfusion: Techniques and clinical use. *Diagnostic and Interventional Imaging*, *94*(12), 1211–1223. https://doi.org/10.1016/j.diii.2013.06.010

Ficks, C. A., Dong, L., & Waldman, I. D. (2014). Sex Differences in the Etiology of Psychopathic Traits in Youth. *Journal of Abnormal Psychology*, *123*(2), 406–411. https://doi.org/10.1037/a0036457

Ficks, C. A., & Waldman, I. D. (2014). Candidate genes for aggression and antisocial behavior: a meta-analysis of association studies of the 5HTTLPR and MAOA-uVNTR. *Behavior Genetics*, *44*(5), 427–444. https://doi.org/10.1007/S10519-014-9661-Y/TABLES/7

Figueiredo, P., Ramião, E., Azeredo, A., Moreira, D., Barroso, R., & Barbosa, F. (2020). Relation between basal cortisol and reactivity cortisol with externalizing problems: A systematic review. *Physiology & Behavior*, *225*(113088), 1–12. https://doi.org/10.1016/J.PHYSBEH.2020.113088

Filbey, F. M., McQueeny, T., DeWitt, S. J., & Mishra, V. (2015). Preliminary findings demonstrating latent effects of early adolescent marijuana use onset on cortical architecture. *Developmental Cognitive Neuroscience*, *16*, 16–22. https://doi.org/10.1016/j.dcn.2015.10.001

Finn, E. S. (2021). Is it time to put rest to rest? *Trends in Cognitive Sciences*, *25*(12), 1021–1032. https://doi.org/10.1016/J.TICS.2021.09.005

First, M. B., Williams, J. B. W., Benjamin, L. S., & Spitzer, R. L. (2015). *User's Guide for the SCID-5-PD (Structured Clinical Interview for DSM-5 Personality Disorder)*. American Psychiatric Association.

First, M. B., Williams, J. B. W., Karg, R. S., & Spitzer, R. L. (2016). *User's Guide to Structured Clinical Interview for DSM-5 Disorders, Clinical Version*. American Psychiatric Association.

Fischl, B., & Dale, A. M. (2000). Measuring the thickness of the human cerebral cortex from magnetic resonance images. *Proceedings of the National Academy of Sciences*, *97*(20), 11050–11055. https://doi.org/10.1073/pnas.200033797

Fischl, B., Sereno, M. I., & Dale, A. M. (1999). Cortical Surface-Based

Analysis, II: Inflation, flattening, and a surface-based coordinate system. *NeuroImage*, *9*(2), 195–207. https://doi.org/10.1006/nimg.1998.0396

Flórez, G., Ferrer, V., García, L. S., Crespo, M. R., Pérez, M., & Saiz, P. A. (2019). Personality disorders, addictions and psychopathy as predictors of criminal behaviour in a prison sample. *Revista Española de Sanidad Penitenciaria*, *21*(2), 62–79. https://doi.org/10.4321/s1575-06202019000200002

Fontaine, N. M. G., McCrory, E. J., Boivin, M., Moffitt, T. E., & Viding, E. (2011). Predictors and Outcomes of Joint Trajectories of Callous-Unemotional Traits and Conduct Problems in Childhood. *Journal of Abnormal Psychology*, *120*(3), 730–742. https://doi.org/10.1037/a0022620

Forsman, M., Lichtenstein, P., Andershed, H., & Larsson, H. (2010). A longitudinal twin study of the direction of effects between psychopathic personality and antisocial behaviour. *Journal of Child Psychology and Psychiatry*, *51*(1), 39–47. https://doi.org/10.1111/j.1469-7610.2009.02141.x

Fox, M. D., Zhang, D., Snyder, A. Z., & Raichle, M. E. (2009). The global signal and observed anticorrelated resting state brain networks. *Journal of Neurophysiology*, *101*(6), 3270–3283. https://doi.org/10.1152/jn.90777.2008

Fragkaki, I., Cima, M., Verhagen, M., Maciejewski, D. F., Boks, M. P., van Lier, P. A. C., Koot, H. M., Branje, S. J. T., & Meeus, W. H. J. (2019). Oxytocin Receptor Gene (OXTR) and Deviant Peer Affiliation: A Gene–Environment Interaction in Adolescent Antisocial Behavior. *Journal of Youth and Adolescence*, *48*(1), 86–101. https://doi.org/10.1007/S10964-018-0939-X/TABLES/6

Fragkaki, I., Verhagen, M., van Herwaarden, A. E., & Cima, M. (2019). Daily oxytocin patterns in relation to psychopathy and childhood trauma in residential youth. *Psychoneuroendocrinology*, *102*, 105–113. https://doi.org/10.1016/J.PSYNEUEN.2018.11.040

Fransson, P., & Marrelec, G. (2008). The precuneus/posterior cingulate cortex plays a pivotal role in the default mode network: Evidence from a partial correlation network analysis. *NeuroImage*, *42*(3), 1178–1184. https://doi.org/10.1016/J.NEUROIMAGE.2008.05.059

Freeman, J. B., Ma, Y., Barth, M., Young, S. G., Han, S., & Ambady, N. (2015). The Neural Basis of Contextual Influences on Face Categorization. *Cerebral Cortex*, *25*(2), 415–422. https://doi.org/10.1093/CERCOR/BHT238

Freeman, S. M., Clewett, D. V., Bennett, C. M., Kiehl, K. A., Gazzaniga, M. S., & Miller, M. B. (2015). The posteromedial region of the default

mode network shows attenuated task-induced deactivation in psychopathic prisoners. *Neuropsychology*, *29*(3), 493–500. https://doi.org/10.1037/NEU0000118

Freitag, C. M., Konrad, K., Stadler, C., De Brito, S. A., Popma, A., Herpertz, S. C., Herpertz-Dahlmann, B., Neumann, I., Kieser, M., Chiocchetti, A. G., Schwenck, C., & Fairchild, G. (2018). Conduct disorder in adolescent females: current state of research and study design of the FemNAT-CD consortium. *European Child & Adolescent Psychiatry*, *27*(9), 1077–1093. https://doi.org/10.1007/S00787-018-1172-6

Frick, P. J., & White, S. F. (2008). Research Review: The importance of callous-unemotional traits for developmental models of aggressive and antisocial behavior. *Journal of Child Psychology and Psychiatry*, *49*(4), 359–375. https://doi.org/10.1111/J.1469-7610.2007.01862.X

Fu, Q., Heath, A. C., Bucholz, K. K., Nelson, E., Goldberg, J., Lyons, M. J., True, W. R., Jacob, T., Tsuang, M. T., & Eisen, S. A. (2002). Shared Genetic Risk of Major Depression, Alcohol Dependence, and Marijuana Dependence. *Archives of General Psychiatry*, *59*(12), 1125–1132. https://doi.org/10.1001/archpsyc.59.12.1125

Fuller, E. K., Gatner, D. T., & Douglas, K. S. (2022). Concurrent, Convergent, and Discriminant Validity of the DSM-5 Section III Psychopathy Specifier. *Assessment*, *0*(0), 1–21. https://doi.org/10.1177/10731911221124344

Funder, D. C., & Ozer, D. J. (2019). Evaluating Effect Size in Psychological Research: Sense and Nonsense: *Advances in Methods and Practices in Psychological Science*, *2*(2), 156–168. https://doi.org/10.1177/2515245919847202

Fusar-Poli, P., Placentino, A., Carletti, F., Landi, P., Allen, P., Surguladze, S., Benedetti, F., Abbamonte, M., Gasparotti, R., Barale, F., Perez, J., McGuire, P., & Politi, P. (2009). Functional atlas of emotional faces processing: a voxel-based meta-analysis of 105 functional magnetic resonance imaging studies. *Journal of Psychiatry & Neuroscience*, *34*(6), 418–450.

Gargouri, F., Kallel, F., Delphine, S., Hamida, A. Ben, Lehéricy, S., & Valabregue, R. (2018). The influence of preprocessing steps on graph theory measures derived from resting state fMRI. *Frontiers in Computational Neuroscience*, *12*(8), 1–9. https://doi.org/10.3389/fncom.2018.00008

Gehrer, N. A., Scheeff, J., Jusyte, A., & Schönenberg, M. (2019). Impaired attention toward the eyes in psychopathic offenders: Evidence from an eye tracking study. *Behaviour Research and Therapy*, *118*, 121–129. https://doi.org/10.1016/j.brat.2019.04.009

Gerrits, N. J. H. M., Van Loenhoud, A. C., Van den Berg, S. F., Berendse, H. W., Foncke, E. M. J., Klein, M., Stoffers, D., Van der Werf, Y. D., & Van den Heuvel, O. A. (2016). Cortical Thickness, Surface Area and Subcortical Volume Differentially Contribute to Cognitive Heterogeneity in Parkinson's Disease. *PloS ONE*, *11*(2), e0148852. https://doi.org/10.1371/JOURNAL.PONE.0148852

Gescher, D. M., Kahl, K. G., Hillemacher, T., Frieling, H., Kuhn, J., & Frodl, T. (2018). Epigenetics in Personality Disorders: Today's Insights. *Frontiers in Psychiatry*, *9*(579), 1–20. https://doi.org/10.3389/FPSYT.2018.00579/BIBTEX

Geurts, D. E. M., von Borries, K., Volman, I., Bulten, B. H., Cools, R., & Verkes, R. J. (2016). Neural connectivity during reward expectation dissociates psychopathic criminals from non-criminal individuals with high impulsive/antisocial psychopathic traits. *Social Cognitive and Affective Neuroscience*, *11*(8), 1326–1334. https://doi.org/10.1093/SCAN/NSW040

Gibbon, S., Khalifa, N. R., Cheung, N. H. Y., Völlm, B. A., & McCarthy, L. (2020). Psychological interventions for antisocial personality disorder (Review). *Cochrane Database of Systematic Reviews*, *9*, 1–207. https://doi.org/10.1002/14651858.CD007668.pub3

Gillespie, S. M., Rotshtein, P., Chapman, H., Brown, E., Beech, A. R., & Mitchell, I. J. (2019). Pupil reactivity to emotional faces among convicted violent offenders: The role of psychopathic traits. *Journal of Abnormal Psychology*, *128*(6), 622–632. https://doi.org/10.1037/abn0000445

Ginestet, C. E., Nichols, T. E., Bullmore, E. T., & Simmons, A. (2011). Brain Network Analysis: Separating Cost from Topology Using Cost-Integration. *PLOS ONE*, *6*(7), e21570. https://doi.org/10.1371/JOURNAL.PONE.0021570

Glenn, A. L. (2011). The other allele: Exploring the long allele of the serotonin transporter gene as a potential risk factor for psychopathy: A review of the parallels in findings. *Neuroscience & Biobehavioral Reviews*, *35*(3), 612–620. https://doi.org/10.1016/J.NEUBIOREV.2010.07.005

Glenn, A. L., & Raine, A. (2014). Neurocriminology: Implications for the punishment, prediction and prevention of criminal behaviour. *Nature Reviews Neuroscience*, *15*(1), 54–63. https://doi.org/10.1038/nrn3640

Goethals, I., Audenaert, K., Jacobs, F., Eynde, F. Van Den, Bernagie, K., Kolindou, A., Vervaet, M., Dierckx, R., & Heeringen, C. Van. (2005). Brain perfusion SPECT in impulsivity-related personality disorders. *Behavioural Brain Research*, *157*(1), 187–192.

https://doi.org/10.1016/j.bbr.2004.06.022

Goh, K. K., Lu, M. L., & Jou, S. (2021). Childhood Trauma and Aggression in Persons Convicted for Homicide: An Exploratory Study Examines the Role of Plasma Oxytocin. *Frontiers in Psychiatry*, *12*(719282), 1–11. https://doi.org/10.3389/FPSYT.2021.719282

Gómez-Coronado, N., Sethi, R., Bortolasci, C. C., Arancini, L., Berk, M., & Dodd, S. (2018). A review of the neurobiological underpinning of comorbid substance use and mood disorders. *Journal of Affective Disorders*, *241*(12), 388–401. https://doi.org/10.1016/j.jad.2018.08.041

González-Madruga, K., Rogers, J. C., Toschi, N., Riccelli, R., Smaragdi, A., Puzzo, I., Clanton, R., Andersson, J., Baumann, S., Kohls, G., Raschle, N., Fehlbaum, L., Menks, W., Stadler, C., Konrad, K., Freitag, C. M., De Brito, S. A., Sonuga-Barke, E., & Fairchild, G. (2020). White matter microstructure of the extended limbic system in male and female youth with conduct disorder. *Psychological Medicine*, *50*, 58–67. https://doi.org/10.1017/S0033291718003951

Goodwin, R. D., & Hamilton, S. P. (2003). Lifetime comorbidity of antisocial personality disorder and anxiety disorders among adults in the community. *Psychiatry Research*, *117*(2), 159–166. https://doi.org/10.1016/S0165-1781(02)00320-7

Gostisha, A. J., Vitacco, M. J., Dismukes, A. R., Brieman, C., Merz, J., & Shirtcliff, E. A. (2014). Beyond physiological hypoarousal: the role of life stress and callous-unemotional traits in incarcerated adolescent males. *Hormones and Behavior*, *65*(5), 469–479. https://doi.org/10.1016/J.YHBEH.2014.03.016

Goto, M., Abe, O., Hagiwara, A., Fujita, S., Kamagata, K., Hori, M., Aoki, S., Osada, T., Konishi, S., Masutani, Y., Sakamoto, H., Sakano, Y., Kyogoku, S., & Daida, H. (2022). Advantages of Using Both Voxel- and Surface-based Morphometry in Cortical Morphology Analysis: A Review of Various Applications. *Magnetic Resonance in Medical Sciences*, *21*(1), 41–57. https://doi.org/10.2463/MRMS.REV.2021-0096

Grace, S. A., Rossell, S. L., Heinrichs, M., Kordsachia, C., & Labuschagne, I. (2018). Oxytocin and brain activity in humans: A systematic review and coordinate-based meta-analysis of functional MRI studies. *Psychoneuroendocrinology*, *96*, 6–24. https://doi.org/10.1016/J.PSYNEUEN.2018.05.031

Grady, C. L., Rieck, J. R., Nichol, D., Rodrigue, K. M., & Kennedy, K. M. (2021). Influence of sample size and analytic approach on stability and interpretation of brain-behavior correlations in task-related fMRI data. *Human Brain Mapping*, *42*(1), 204–219.

https://doi.org/10.1002/HBM.25217

Green, H., Mcginnity, Á., Meltzer, H., Ford, T., & Goodman, R. (2004). Mental health of children and young people in Great Britain, 2004: Summary report. In *Office for National Statistics*. http://content.digital.nhs.uk/catalogue/PUB06116/ment-heal-chil-youn-peop-gb-2004-rep2.pdf

Gregory, S., Blair, R. J. R., Ffytche, D., Simmons, A., Kumari, V., Hodgins, S., & Blackwood, N. (2015). Punishment and psychopathy: a case-control functional MRI investigation of reinforcement learning in violent antisocial personality disordered men. *The Lancet Psychiatry*, *2*(2), 153–160. https://doi.org/10.1016/S2215-0366(14)00071-6

Gregory, S., Ffytche, D., Simmons, A., Kumari, V., Howard, M., Hodgins, S., & Blackwood, N. (2012). The antisocial brain: Psychopathy matters. A structural MRI investigation of antisocial male violent offenders. *Archives of General Psychiatry*, *69*(9), 962–972. https://doi.org/10.1001/archgenpsychiatry.2012.222

Griem, J., Kolla, N. J., & Tully, J. (2022). Key challenges in neurocognitive assessment of individuals with antisocial personality disorder and psychopathy. *Frontiers in Behavioral Neuroscience*, *16*(1007121), 1–6. https://doi.org/10.3389/FNBEH.2022.1007121

Griffiths, S. Y., Jalava, J., Rosenberg Larsen, R., & Alcott, B. E. (2022). Genetic correlates of PCL-R psychopathy: A systematic review. *Aggression and Violent Behavior*, *66*(101765), 1–12. https://doi.org/10.1016/j.avb.2022.101765

Griffiths, S. Y., & Jalava, J. V. (2017). A comprehensive neuroimaging review of PCL-R defined psychopathy. *Aggression and Violent Behavior*, *36*, 60–75. https://doi.org/10.1016/j.avb.2017.07.002

Griffiths, S. Y., Jalava, J. V., Larsen, R. R., & Alcott, B. E. (2022). Genetic correlates of PCL-R psychopathy: a systematic review. *Aggression and Violent Behavior*, 127248. https://doi.org/10.1016/j.avb.2022.101765

Grinevich, V., & Neumann, I. D. (2020). Brain oxytocin: how puzzle stones from animal studies translate into psychiatry. *Molecular Psychiatry*, *26*(1), 265–279. https://doi.org/10.1038/s41380-020-0802-9

Gudbrandsen, M., Daly, E., Murphy, C. M., Blackmore, C. E., Rogdaki, M., Mann, C., Bletsch, A., Kushan, L., Bearden, C. E., Murphy, D. G. M., Craig, M. C., & Ecker, C. (2020). Brain morphometry in 22q11.2 deletion syndrome: an exploration of differences in cortical thickness, surface area, and their contribution to cortical volume. *Scientific Reports*, *10*(18845), 1–12. https://doi.org/10.1038/s41598-020-75811-1

Gudbrandsen, M., Daly, E., Murphy, C. M., Wichers, R. H., Stoencheva, V., Perry, E., Andrews, D., Blackmore, C. E., Rogdaki, M., Kushan, L., Bearden, C. E., Murphy, D. G. M., Craig, M. C., & Ecker, C. (2019). The Neuroanatomy of Autism Spectrum Disorder Symptomatology in 22q11.2 Deletion Syndrome. *Cerebral Cortex*, *29*(8), 3655–3665. https://doi.org/10.1093/CERCOR/BHY239

Gunter, T. D., Vaughn, M. G., & Philibert, R. A. (2010). Behavioral genetics in antisocial spectrum disorders and psychopathy: A review of the recent literature. *Behavioral Sciences & the Law*, *28*(2), 148–173. https://doi.org/10.1002/bsl

Hagmann, P., Cammoun, L., Gigandet, X., Meuli, R., Honey, C. J., Van Wedeen, J., & Sporns, O. (2008). Mapping the Structural Core of Human Cerebral Cortex. *PLoS Biology*, *6*(7), e159. https://doi.org/10.1371/JOURNAL.PBIO.0060159

Hamilton, R. K. B., & Newman, J. P. (2018a). The response modulation hypothesis: formulation, development, and implications for psychopathy. In C. J. Patrick (Ed.), *Handbook of Psychopathy* (pp. 80–93). Guilford Press.

Hamilton, R. K. B., & Newman, J. P. (2018b). Information processing capacity in psychopathy: Effects of anomalous attention. *Personality Disorders: Theory, Research, and Treatment*, *9*(2), 182–187. https://doi.org/10.1037/PER0000223

Hamilton, R. K. B., Racer, K. H., & Newman, J. P. (2015). Impaired integration in psychopathy: A unified theory of psychopathic dysfunction. *Psychological Review*, *122*(4), 770–791. https://doi.org/10.1037/a0039703

Hare, R. D. (1991). *Manual for the Hare Psychopathy Checklist-Revised* (2nd ed.). Guilford. https://doi.org/10.1007/978-0-387-79948-3_837

Hare, R. D., Clark, D., Grann, M., & Thornton, D. (2000). Psychopathy and the predictive validity of the PCL-R: An international perspective. *Behavioral Sciences & the Law*, *18*(5), 623–645. https://doi.org/10.1002/1099-0798(200010)18:5<623::AID-BSL409>3.0.CO;2-W

Harrison, B. J., Pujol, J., López-Solà, M., Hernández-Ribas, R., Deus, J., Ortiz, H., Soriano-Mas, C., Yücel, M., Pantelis, C., & Cardoner, N. (2008). Consistency and functional specialization in the default mode brain network. *Proceedings of the National Academy of Sciences of the United States of America*, *105*(28), 9781–9786. https://doi.org/10.1073/PNAS.0711791105/SUPPL_FILE/0711791105SI.PDF

Hartmann, D., & Schwenck, C. (2020). Emotion Processing in Children with Conduct Problems and Callous-Unemotional Traits: An

Investigation of Speed, Accuracy, and Attention. *Child Psychiatry and Human Development*, *51*(5), 721–733. https://doi.org/10.1007/s10578-020-00976-9

Hawes, D. J., Brennan, J., & Dadds, M. R. (2009). Cortisol, callous-unemotional traits, and pathways to antisocial behavior. *Current Opinion in Psychiatry*, *22*(4), 357–362. https://doi.org/10.1097/YCO.0b013e32832bfa6d

Hawes, S. W., Waller, R., Byrd, A. L., Bjork, J. M., Dick, A. S., Sutherland, M. T., Riedel, M. C., Tobia, M. J., Thomson, N., Laird, A. R., & Gonzalez, R. (2021). Reward Processing in Children With Disruptive Behavior Disorders and Callous-Unemotional Traits in the ABCD Study. *The American Journal of Psychiatry*, *178*(4), 333–342. https://doi.org/10.1176/appi.ajp.2020.19101092

He, Y., & Evans, A. C. (2010). Graph theoretical modeling of brain connectivity. *Current Opinion in Neurology*, *23*(4), 341–350. https://doi.org/10.1097/WCO.0b013e32833aa567

Hedges, E. P., Dimitrov, M., Zahid, U., Brito Vega, B., Si, S., Dickson, H., McGuire, P., Williams, S., Barker, G. J., & Kempton, M. J. (2022). Reliability of structural MRI measurements: The effects of scan session, head tilt, inter-scan interval, acquisition sequence, FreeSurfer version and processing stream. *NeuroImage*, *246*, 118751. https://doi.org/10.1016/J.NEUROIMAGE.2021.118751

Heeks, M., Reed, S., Tafsiri, M., & Prince, S. (2018). *The economic and social costs of crime*. https://www.gov.uk/government/publications/the-economic-and-social-costs-of-crime

Helwegen, K., Libedinsky, I., & Heuvel, M. P. van den. (2023). Statistical power in network neuroscience. *Trends in Cognitive Sciences*, *0*(0), 1–20. https://doi.org/10.1016/J.TICS.2022.12.011

Hemphill, J. F., Hare, R. D., & Wong, S. (1998). Psychopathy and recidivism: A review. *Legal and Criminological Psychology*, *3*(1), 139–170. https://doi.org/10.1111/J.2044-8333.1998.TB00355.X

Herpertz, S. C., Steinmeyer, E. M., & Saß, H. (1994). "Patterns of comorbidity" among DSM-III-R and ICD-10 personality disorders as observed with a new inventory for the assessment of personality disorders. *European Archives of Psychiatry and Clinical Neuroscience*, *244*(3), 161–169. https://doi.org/10.1007/BF02191892

Hiser, J., & Koenigs, M. (2018). The Multifaceted Role of the Ventromedial Prefrontal Cortex in Emotion, Decision Making, Social Cognition, and Psychopathology. *Biological Psychiatry*, *83*(8), 638–647. https://doi.org/10.1016/J.BIOPSYCH.2017.10.030

Hobson, C. W., Scott, S., & Rubia, K. (2011). Investigation of cool and hot executive function in ODD/CD independently of ADHD. *Journal of Child Psychology and Psychiatry*, *52*(10), 1035–1043. https://doi.org/10.1111/j.1469-7610.2011.02454.x

Hodel, A. S., Hunt, R. H., Cowell, R. A., Van den Heuvel, S. E., Gunnar, M. R., & Thomas, K. M. (2015). Duration of early adversity and structural brain development in post-institutionalized adolescents. *NeuroImage*, *105*, 112–119. https://doi.org/10.1016/J.NEUROIMAGE.2014.10.020

Hodgins, S., Checknita, D. R., Lindner, P., Schiffer, B., & De Brito, S. A. (2018). Antisocial personality disorder. In A. R. Beech, A. J. Carter, R. E. Mann, & P. Rotshtein (Eds.), *The Wiley Blackwell Handbook of Forensic Neuroscience, I and II*. John Wiley & Sons, Ltd. https://doi.org/10.1007/s00278-019-0357-x

Hodgins, S., De Brito, S. A., Chhabra, P., & Gilles, C. (2010). Anxiety Disorders Among Offenders With Antisocial Personality Disorders: A Distinct Subtype? *Canadian Journal of Psychiatry*, *55*(12), 784–791. https://doi.org/10.1177/070674371005501206

Hodkinson, D. J., Krause, K., Khawaja, N., Renton, T. F., Huggins, J. P., Vennart, W., Thacker, M. A., Mehta, M. A., Zelaya, F. O., Williams, S. C. R., & Howard, M. A. (2013). Quantifying the test–retest reliability of cerebral blood flow measurements in a clinical model of on-going post-surgical pain: A study using pseudo-continuous arterial spin labelling. *NeuroImage: Clinical*, *3*, 301–310. https://doi.org/10.1016/j.nicl.2013.09.004

Hoenicka, J., Ponce, G., Jiménez-Arriero, M. A., Ampuero, I., Rodríguez-Jiménez, R., Rubio, G., Aragüés, M., Ramos, J. A., & Palomo, T. (2007). Association in alcoholic patients between Psychopathic Traits and the additive effect of allelic forms of theCNR1 andFAAH endocannabinoid genes, and the 3′ Region of theDRD2 Gene. *Neurotoxicity Research*, *11*(1), 51–59. https://doi.org/10.1007/BF03033482

Hofhansel, L., Weidler, C., Votinov, M., Clemens, B., Raine, A., & Habel, U. (2020). Morphology of the criminal brain: gray matter reductions are linked to antisocial behavior in offenders. *Brain Structure & Function*, *225*, 2017–2028. https://doi.org/10.1007/s00429-020-02106-6

Holi, M., Auvinen-Lintunen, L., Lindberg, N., Tani, P., & Virkkunen, M. (2006). Inverse correlation between severity of psychopathic traits and serum cortisol levels in young adult violent male offenders. *Psychopathology*, *39*(2), 102–104. https://doi.org/10.1159/000091021

Holz, N., Boecker, R., Buchmann, A. F., Blomeyer, D., Baumeister, S., Hohmann, S., Jennen-Steinmetz, C., Wolf, I., Rietschel, M., Witt, S. H., Plichta, M. M., Meyer-Lindenberg, A., Schmidt, M. H., Esser, G., Banaschewski, T., Brandeis, D., & Laucht, M. (2016). Evidence for a Sex-Dependent MAOA× Childhood Stress Interaction in the Neural Circuitry of Aggression. *Cerebral Cortex*, *26*(3), 904–914. https://doi.org/10.1093/CERCOR/BHU249

Holzer, K. J., & Vaughn, M. G. (2017). Antisocial Personality Disorder in Older Adults: A Critical Review. *Journal of Geriatric Psychiatry and Neurology*, *30*(6), 291–302. https://doi.org/10.1177/0891988717732155

Hoppenbrouwers, S. S., Bulten, B. H., & Brazil, I. A. (2016). Parsing fear: A reassessment of the evidence for fear deficits in psychopathy. *Psychological Bulletin*, *142*(6), 573–600. https://doi.org/10.1037/bul0000040

Horn, M., Potvin, S., Allaire, J. F., Cot^é, G., Gobbi, G., Benkirane, K., Vachon, J., & Dumais, A. (2014). Male inmate profiles and their biological correlates. *Canadian Journal of Psychiatry*, *59*(8), 441–449. https://doi.org/10.1177/070674371405900807

Hosking, J. G., Kastman, E. K., Dorfman, H. M., Samanez-Larkin, G. R., Baskin-Sommers, A. R., Kiehl, K. A., Newman, J. P., & Buckholtz, J. W. (2017). Disrupted Prefrontal Regulation of Striatal Subjective Value Signals in Psychopathy. *Neuron*, *95*(1), 221-231.e4. https://doi.org/10.1016/j.neuron.2017.06.030

Hughes, M. A., Dolan, M. C., & Stout, J. C. (2016). Decision-making in Psychopathy. *Psychiatry, Psychology and Law*, *23*(4), 521–537. https://doi.org/10.1080/13218719.2015.1081228

Hughes, M. A., Dolan, M. C., Trueblood, J. S., & Stout, J. C. (2015). Psychopathic Personality Traits and Iowa Gambling Task Performance in Incarcerated Offenders. *Psychiatry, Psychology and Law*, *22*(1), 134–144. https://doi.org/10.1080/13218719.2014.919689

Hurlemann, R., Patin, A., Onur, O. A., Cohen, M. X., Baumgartner, T., Metzler, S., Dziobek, I., Gallinat, J., Wagner, M., Maier, W., & Kendrick, K. M. (2010). Oxytocin Enhances Amygdala-Dependent, Socially Reinforced Learning and Emotional Empathy in Humans. *Journal of Neuroscience*, *30*(14), 4999–5007. https://doi.org/10.1523/JNEUROSCI.5538-09.2010

Hutchison, R. M., Womelsdorf, T., Allen, E. A., Bandettini, P. A., Calhoun, V. D., Corbetta, M., Della Penna, S., Duyn, J. H., Glover, G. H., Gonzalez-Castillo, J., Handwerker, D. A., Keilholz, S., Kiviniemi, V., Leopold, D. A., De Pasquale, F., Sporns, O., Walter, M., & Chang, C. (2013). Dynamic functional connectivity: Promise, issues, and

interpretations. *NeuroImage*, *80*, 360–378. https://doi.org/10.1016/J.NEUROIMAGE.2013.05.079

Hyatt, C. J., Haney-Caron, E., & Stevens, M. C. (2012). Cortical thickness and folding deficits in conduct-disordered adolescents. *Biological Psychiatry*, *72*(3), 207–214. https://doi.org/10.1016/j.biopsych.2011.11.017

Hyde, L. W., Waller, R., Trentacosta, C. J., Shaw, D. S., Neiderhiser, J. M., Ganiban, J. M., Reiss, D., & Leve, L. D. (2016). Heritable and nonheritable pathways to early callous-unemotional behaviors. *American Journal of Psychiatry*, *173*(9), 903–910. https://doi.org/10.1176/appi.ajp.2016.15111381

IBM Corp. (2019). *IBM SPSS Statistics for Windows, Version 26.0*. IBM Corp.

Insel, T., Cuthbert, B., Garvey, M., Heinssen, R., Pine, D. S., Quinn, K., Sanislow, C., Wang, P., & National Institute of Mental Health. (2010). Research Domain Criteria (RDoC): Toward a new classification framework for research on mental disorders. *American Journal of Psychiatry*, *167*(7), 748–751. https://doi.org/10.1176/appi.ajp.2010.09091379

Institute for Economics & Peace. (2022). *Global Peace Index 2022: Measuring peace in a complex world*. http://visionofhumanity.org/resources

Iraji, A., Chen, H., Wiseman, N., Welch, R. D., O'Neil, B. J., Haacke, E. M., Liu, T., & Kou, Z. (2016). Compensation through functional hyperconnectivity: A longitudinal connectome assessment of mild traumatic brain injury. *Neural Plasticity*, *2016*(4072402), 1–13. https://doi.org/10.1155/2016/4072402

Jaffee, S. R., Caspi, A., Moffitt, T. E., Dodge, K. A., Rutter, M., Taylor, A., & Tully, L. A. (2005). Nature x nurture: Genetic vulnerabilities interact with physical maltreatment to promote conduct problems. *Development and Psychopathology*, *17*(1), 67–84. https://doi.org/10.1017/S0954579405050042

Jann, K., Gee, D. G., Kilroy, E., Schwab, S., Smith, R. X., Cannon, T. D., & Wang, D. J. J. (2015). Functional connectivity in BOLD and CBF data: Similarity and reliability of resting brain networks. *NeuroImage*, *106*, 111–122. https://doi.org/10.1016/J.NEUROIMAGE.2014.11.028

JASP Team. (2021). *JASP* (0.16). https://jasp-stats.org/

Jeffers, A. M., Glantz, S., Byers, A., & Keyhani, S. (2021). Sociodemographic Characteristics Associated With and Prevalence and Frequency of Cannabis Use Among Adults in the US. *JAMA Network Open*, *4*(11), 1–16.

https://doi.org/10.1001/JAMANETWORKOPEN.2021.36571

Jenkinson, M., & Chappell, M. (2018a). MRI Modalities for Neuroimaging. In *Introduction to Neuroimaging Analysis* (pp. 23–83). Oxford University Press.

Jenkinson, M., & Chappell, M. (2018b). Overview of MRI analysis. In *Introduction to Neuroimaging Analysis* (pp. 85–143). Oxford University Press.

Jenkinson, M., & Chappell, M. (2018c). Surface-based analysis. In *Introduction to Neuroimaging Analysis* (pp. 223–234). Oxford University Press.

Jennings, W. G., Loeber, R., Pardini, D. A., Piquero, A. R., & Farrington, D. P. (2015). *Offending from Childhood to Young Adulthood: Recent Results from the Pittsburgh Youth Study*. Springer. https://doi.org/10.1007/978-3-319-25966-6

Jiang, W., Li, G., Liu, H., Shi, F., Wang, T., Shen, C., Shen, H., Lee, S.-W., Hu, D., Wang, W., & Shen, D. (2016). Reduced cortical thickness and increased surface area in antisocial personality disorder. *Neuroscience*, *337*, 143–152. https://doi.org/10.1016/J.NEUROSCIENCE.2016.08.052

Jiang, W., Shi, F., Liao, J., Liu, H., Wang, T., Shen, C., Shen, H., Hu, D., Wang, W., & Shen, D. (2017). Disrupted functional connectome in antisocial personality disorder. *Brain Imaging and Behavior*, *11*(4), 1071–1084. https://doi.org/10.1007/s11682-016-9572-z

Jiang, W., Shi, F., Liu, H., Li, G., Ding, Z., Shen, H., Shen, C., Lee, S. W., Hu, D., Wang, W., & Shen, D. (2017). Reduced White Matter Integrity in Antisocial Personality Disorder: A Diffusion Tensor Imaging Study. *Scientific Reports*, *7*(43002), 1–11. https://doi.org/10.1038/SREP43002

Jiang, W., Zhang, H., Zeng, L. L., Shen, H., Qin, J., Thung, K. H., Yap, P. T., Liu, H., Hu, D., Wang, W., & Shen, D. (2021). Dynamic neural circuit disruptions associated with antisocial behaviors. *Human Brain Mapping*, *42*(2), 329–344. https://doi.org/10.1002/HBM.25225

Jiang, X., Ma, X., Geng, Y., Zhao, Z., Zhou, F., Zhao, W., Yao, S., Yang, S., Zhao, Z., Becker, B., & Kendrick, K. M. (2021). Intrinsic, dynamic and effective connectivity among large-scale brain networks modulated by oxytocin. *NeuroImage*, *227*(117668), 1–13. https://doi.org/10.1016/J.NEUROIMAGE.2020.117668

Jiang, Y., Gao, Y., Dong, D., Sun, X., Situ, W., & Yao, S. (2021). Impaired global efficiency in boys with conduct disorder and high callous unemotional traits. *Journal of Psychiatric Research*, *138*, 560–568. https://doi.org/10.1016/J.JPSYCHIRES.2021.04.041

Jiang, Y., Gao, Y., Dong, D., Sun, X., Situ, W., & Yao, S. (2022). Brain Anatomy in Boys with Conduct Disorder: Differences Among Aggression Subtypes. *Child Psychiatry & Human Development*, *6*, 1–11. https://doi.org/10.1007/S10578-022-01360-5

Jiang, Y., Guo, X., Zhang, J., Gao, Y., Wang, X., Situ, W., Yi, J., Zhang, X., Zhu, X., Yao, S., & Huang, B. (2015). Abnormalities of cortical structures in adolescent-onset conduct disorder. *Psychological Medicine*, *45*, 3467–3479. https://doi.org/10.1017/S0033291715001361

Jiang, Y., Liu, W., Ming, Q., Gao, Y., Ma, R., Zhang, X., Situ, W., Wang, X., Yao, S., & Huang, B. (2016). Disrupted Topological Patterns of Large-Scale Network in Conduct Disorder. *Scientific Reports*, *6*(37053), 1–10. https://doi.org/10.1038/SREP37053

Johanson, M., Vaurio, O., Tiihonen, J., & Lähteenvuo, M. (2020). A Systematic Literature Review of Neuroimaging of Psychopathic Traits. *Frontiers in Psychiatry*, *10*(1027), 1–20. https://doi.org/10.3389/fpsyt.2019.01027

Johnson, V. A., Kemp, A. H., Heard, R., Lennings, C. J., & Hickie, I. B. (2015). Childhood- versus Adolescent-Onset Antisocial Youth with Conduct Disorder: Psychiatric Illness, Neuropsychological and Psychosocial Function. *PLoS ONE*, *10*(4), e0121627. https://doi.org/10.1371/journal.pone.0121627

Jolliffe, D., Farrington, D. P., Piquero, A. R., Loeber, R., & Hill, K. G. (2017). Systematic review of early risk factors for life-course-persistent, adolescence-limited, and late-onset offenders in prospective longitudinal studies. *Aggression and Violent Behavior*, *33*, 15–23. https://doi.org/10.1016/j.avb.2017.01.009

Jolliffe, D., Farrington, D. P., Piquero, A. R., MacLeod, J. F., & Van de Weijer, S. (2017). Prevalence of life-course-persistent, adolescence-limited, and late-onset offenders: A systematic review of prospective longitudinal studies. *Aggression and Violent Behavior*, *33*, 4–14. https://doi.org/10.1016/j.avb.2017.01.002

Joseph, N., & Benefield, N. (2010). The development of an offender personality disorder strategy. *Mental Health Review Journal*, *15*(4), 10–15. https://doi.org/10.5042/mhrj.2010.0731

Joules, R., Doyle, O. M., Schwarz, A. J., O'Daly, O. G., Brammer, M., Williams, S. C., & Mehta, M. A. (2015). Ketamine induces a robust whole-brain connectivity pattern that can be differentially modulated by drugs of different mechanism and clinical profile. *Psychopharmacology*, *232*(21–22), 4205–4218. https://doi.org/10.1007/S00213-015-3951-9

Juárez, M., Kiehl, K. A., & Calhoun, V. D. (2013). Intrinsic limbic and

paralimbic networks are associated with criminal psychopathy. *Human Brain Mapping*, *34*(8), 1921–1930. https://doi.org/10.1002/HBM.22037

Junewicz, A., & Bates Billick, S. (2020). Conduct Disorder: Biology and Developmental Trajectories. *Psychiatric Quarterly*, *91*, 77–90. https://doi.org/10.1007/s11126-019-09678-5

Kable, J. W., & Glimcher, P. W. (2007). The neural correlates of subjective value during intertemporal choice. *Nature Neuroscience*, *10*(12), 1625–1633. https://doi.org/10.1038/nn2007

Karlsson Linnér, R., Mallard, T. T., Barr, P. B., Sanchez-Roige, S., Madole, J. W., Driver, M. N., Poore, H. E., De Vlaming, R., Grotzinger, A. D., Tielbeek, J. J., Johnson, E. C., Liu, M., Rosenthal, S. B., Ideker, T., Zhou, H., Kember, R. L., Pasman, J. A., Verweij, K. J. H., Liu, D. J., … Dick, D. M. (2021). Multivariate analysis of 1.5 million people identifies genetic associations with traits related to self-regulation and addiction. *Nature Neuroscience*, *24*(10), 1367–1376. https://doi.org/10.1038/s41593-021-00908-3

Kaya, S., Yildirim, H., & Atmaca, M. (2020). Reduced hippocampus and amygdala volumes in antisocial personality disorder. *Journal of Clinical Neuroscience*, *75*, 199–203. https://doi.org/10.1016/j.jocn.2020.01.048

Keech, B., Crowe, S., & Hocking, D. R. (2018). Intranasal oxytocin, social cognition and neurodevelopmental disorders: A meta-analysis. *Psychoneuroendocrinology*, *87*, 9–19. https://doi.org/10.1016/J.PSYNEUEN.2017.09.022

Kemp, A. H., & Guastella, A. J. (2010). Oxytocin: Prosocial Behavior, Social Salience, or Approach-Related Behavior? *Biological Psychiatry*, *67*(6), 33–34. https://doi.org/10.1016/J.BIOPSYCH.2009.11.019

Kennedy, K. M., Erickson, K. I., Rodrigue, K. M., Voss, M. W., Colcombe, S. J., Kramer, A. F., Acker, J. D., & Raz, N. (2009). Age-related differences in regional brain volumes: a comparison of optimized voxel-based morphometry to manual volumetry. *Neurobiology of Aging*, *30*(10), 1657–1676. https://doi.org/10.1016/J.NEUROBIOLAGING.2007.12.020

Khalifa, N. R., Gibbon, S., Völlm, B. A., Cheung, N. H. Y., & McCarthy, L. (2020). Pharmacological interventions for antisocial personality disorder (Review). *Cochrane Database of Systematic Reviews*, *9*, 1–108. https://doi.org/10.1002/14651858.CD007667.pub3

Khalili-Mahani, N., Rombouts, S. A. R. B., van Osch, M. J. P., Duff, E. P., Carbonell, F., Nickerson, L. D., Becerra, L., Dahan, A., Evans, A. C., Soucy, J. P., Wise, R., Zijdenbos, A. P., & van Gerven, J. M. (2017). Biomarkers, designs, and interpretations of resting-state fMRI in

translational pharmacological research: A review of state-of-the-Art, challenges, and opportunities for studying brain chemistry. *Human Brain Mapping*, *38*(4), 2276–2325. https://doi.org/10.1002/HBM.23516

Kiehl, K. A. (2006). A cognitive neuroscience perspective on psychopathy: Evidence for paralimbic system dysfunction. *Psychiatry Research*, *142*(2), 107–128. https://doi.org/10.1016/j.psychres.2005.09.013

Kiehl, K. A., & Hoffman, M. B. (2011). The criminal psychopath: history, neuroscience, treatment and economics. *Jurimetrics*, *51*, 355–397.

Kim-Cohen, J., Arseneault, L., Caspi, A., Polo Tomás, M., Taylor, A., & Moffitt, T. E. (2005). Validity of DSM-IV Conduct Disorder in 4½-5-Year-Old Children: A Longitudinal Epidemiological Study. *American Journal of Psychiatry*, *162*(6), 1108–1117. https://doi.org/10.1176/appi.ajp.162.6.1108

Klingzell, I., Fanti, K. A., Colins, O. F., Frogner, L., Andershed, A. K., & Andershed, H. (2016). Early Childhood Trajectories of Conduct Problems and Callous-Unemotional Traits: The Role of Fearlessness and Psychopathic Personality Dimensions. *Child Psychiatry and Human Development*, *47*(2), 236–247. https://doi.org/10.1007/s10578-015-0560-0

Kohls, G., Baumann, S., Gundlach, M., Scharke, W., Bernhard, A., Martinelli, A., Ackermann, K., Kersten, L., Prätzlich, M., Oldenhof, H., Jansen, L., Van den Boogaard, L., Smaragdi, A., Gonzalez-Madruga, K., Cornwell, H., Rogers, J. C., Pauli, R., Clanton, R., Baker, R., … Konrad, K. (2020). Investigating Sex Differences in Emotion Recognition, Learning, and Regulation Among Youths With Conduct Disorder. *Journal of the American Academy of Child and Adolescent Psychiatry*, *59*(2), 263–273. https://doi.org/10.1016/j.jaac.2019.04.003

Kolla, N. J., Boileau, I., Karas, K., Watts, J. J., Rusjan, P., Houle, S., & Mizrahi, R. (2021). Lower amygdala fatty acid amide hydrolase in violent offenders with antisocial personality disorder: an [11C]CURB positron emission tomography study. *Translational Psychiatry*, *11*(57), 1–11. https://doi.org/10.1038/s41398-020-01144-2

Kolla, N. J., & Bortolato, M. (2020). The role of monoamine oxidase A in the neurobiology of aggressive, antisocial, and violent behavior: A tale of mice and men. *Progress in Neurobiology*, *194*(101875), 1–24. https://doi.org/10.1016/J.PNEUROBIO.2020.101875

Kolla, N. J., Dunlop, K., Meyer, J. H., & Downar, J. (2018). Corticostriatal Connectivity in Antisocial Personality Disorder by MAO-A Genotype and Its Relationship to Aggressive Behavior. *The International Journal of Neuropsychopharmacology*, *21*(8), 725–733.

https://doi.org/10.1093/IJNP/PYY035

Kolla, N. J., & Houle, S. (2019). Single-Photon Emission Computed Tomography and Positron Emission Tomography Studies of Antisocial Personality Disorder and Aggression: a Targeted Review. *Current Psychiatry Reports*, *21*(24), 1–11. https://doi.org/10.1007/s11920-019-1011-6

Kolla, N. J., Matthews, B., Wilson, A. A., Houle, S., Michael Bagby, R., Links, P., Simpson, A. I., Hussain, A., & Meyer, J. H. (2015). Lower Monoamine Oxidase-A Total Distribution Volume in Impulsive and Violent Male Offenders with Antisocial Personality Disorder and High Psychopathic Traits: An 11C Harmine Positron Emission Tomography Study. *Neuropsychopharmacology*, *40*(11), 2596–2603. https://doi.org/10.1038/npp.2015.106

Kolla, N. J., Patel, R., Meyer, J. H., & Chakravarty, M. M. (2017). Association of monoamine oxidase-A genetic variants and amygdala morphology in violent offenders with antisocial personality disorder and high psychopathic traits. *Scientific Reports*, *7*(9607), 1–13. https://doi.org/10.1038/s41598-017-08351-w

Korponay, C., Pujara, M., Deming, P., Philippi, C., Decety, J., Kosson, D. S., Kiehl, K. A., & Koenigs, M. (2017a). Impulsive-Antisocial Dimension of Psychopathy Linked to Enlargement and Abnormal Functional Connectivity of the Striatum. *Biological Psychiatry: Cognitive Neuroscience and Neuroimaging*, *2*(2), 149–157. https://doi.org/10.1016/J.BPSC.2016.07.004

Korponay, C., Pujara, M., Deming, P., Philippi, C., Decety, J., Kosson, D. S., Kiehl, K. A., & Koenigs, M. (2017b). Impulsive-antisocial psychopathic traits linked to increased volume and functional connectivity within prefrontal cortex. *Social Cognitive and Affective Neuroscience*, *12*(7), 1169–1178. https://doi.org/10.1093/scan/nsx042

Kosfeld, M., Heinrichs, M., Zak, P. J., Fischbacher, U., & Fehr, E. (2005). Oxytocin increases trust in humans. *Nature*, *435*(7042), 673–676. https://doi.org/10.1038/nature03701

Kosson, D. S., Lorenz, A. R., & Newman, J. P. (2006). Effects of comorbid psychopathy on criminal offending and emotion processing in male offenders with antisocial personality disorder. *Journal of Abnormal Psychology*, *115*(4), 798–806. https://doi.org/10.1037/0021-843X.115.4.798

Kozhuharova, P., Dickson, H., Tully, J., & Blackwood, N. (2019). Impaired processing of threat in psychopathy: A systematic review and meta-analysis of factorial data in male offender populations. *PLos ONE*, *14*(10), e0224455. https://doi.org/10.1371/journal.pone.0224455

Kraaijenvanger, E. J., He, Y., Spencer, H., Smith, A. K., Bos, P. A., & Boks, M. P. M. (2019). Epigenetic variability in the human oxytocin receptor (OXTR) gene: A possible pathway from early life experiences to psychopathologies. *Neuroscience & Biobehavioral Reviews*, *96*, 127–142. https://doi.org/10.1016/j.neubiorev.2018.11.016

Kretschmer, T., Vrijen, C., Nolte, I. M., Wertz, J., & Hartman, C. A. (2022). Gene-environment interplay in externalizing behavior from childhood through adulthood. *The Journal of Child Psychology and Psychiatry*, *63*(10), 1206–1213. https://doi.org/10.1111/JCPP.13652

Krona, H., Nyman, M., Andreasson, H., Vicencio, N., Anckarsäter, H., Wallinius, M., Nilsson, T., & Hofvander, B. (2016). Mentally disordered offenders in Sweden: differentiating recidivists from non-recidivists in a 10-year follow-up study. *Nordic Journal of Psychiatry*, *71*(2), 102–109. https://doi.org/10.1080/08039488.2016.1236400

Krug, E. G., Mercy, J. A., Dahlberg, L. L., & Zwi, A. B. (2002). The world report on violence and health. *The Lancet*, *360*, 1083–1088. https://doi.org/10.1016/S0140-6736(02)11133-0

Kruppa, J. A., Gossen, A., Oberwelland Weiß, E., Kohls, G., Großheinrich, N., Cholemkery, H., Freitag, C. M., Karges, W., Wölfle, E., Sinzig, J., Fink, G. R., Herpertz-Dahlmann, B., Konrad, K., & Schulte-Rüther, M. (2019). Neural modulation of social reinforcement learning by intranasal oxytocin in male adults with high-functioning autism spectrum disorder: a randomized trial. *Neuropsychopharmacology*, *44*(4), 749–756. https://doi.org/10.1038/S41386-018-0258-7

Kumar, J., Iwabuchi, S. J., Völlm, B. A., & Palaniyappan, L. (2020). Oxytocin modulates the effective connectivity between the precuneus and the dorsolateral prefrontal cortex. *European Archives of Psychiatry and Clinical Neuroscience*, *270*(5), 567–576. https://doi.org/10.1007/S00406-019-00989-Z/FIGURES/4

Kumari, V., Das, M., Taylor, P. J., Barkataki, I., Andrew, C., Sumich, A., Williams, S. C. R., & ffytche, D. H. (2009). Neural and behavioural responses to threat in men with a history of serious violence and schizophrenia or antisocial personality disorder. *Schizophrenia Research*, *110*(1–3), 47–58. https://doi.org/10.1016/j.schres.2009.01.009

Kundu, P., Brenowitz, N. D., Voon, V., Worbe, Y., Vértes, P. E., Inati, S. J., Saad, Z. S., Bandettini, P. A., & Bullmore, E. T. (2013). Integrated strategy for improving functional connectivity mapping using multiecho fMRI. *Proceedings of the National Academy of Sciences of the United States of America*, *110*(40), 16187–16192. https://doi.org/10.1073/pnas.1301725110

Kundu, P., Inati, S. J., Evans, J. W., Luh, W. M., & Bandettini, P. A.

(2012). Differentiating BOLD and non-BOLD signals in fMRI time series using multi-echo EPI. *NeuroImage*, *60*(3), 1759–1770. https://doi.org/10.1016/J.NEUROIMAGE.2011.12.028

Kundu, P., Voon, V., Balchandani, P., Lombardo, M. V., Poser, B. A., & Bandettini, P. A. (2017). Multi-echo fMRI: A review of applications in fMRI denoising and analysis of BOLD signals. *NeuroImage*, *154*(1), 59–80. https://doi.org/10.1016/J.NEUROIMAGE.2017.03.033

Kuruoglu, A. C., Arikan, Z., Vural, G., Karatas, M., Arac, M., & Isik, E. (1996). Single Photon Emission Computerised Tomography in Chronic Alcoholism: Antisocial Personality Disorder may be associated with decreased frontal perfusion. *British Journal of Psychiatry*, *169*, 348–354.

Laird, A. R., Fox, P. M., Eickhoff, S. B., Turner, J. A., Ray, K. L., Mckay, D. R., Glahn, D. C., Beckmann, C. F., Smith, S. M., & Fox, P. T. (2011). Behavioral Interpretations of Intrinsic Connectivity Networks. *Journal of Cognitive Neuroscience*, *23*(12), 4022–4037. https://doi.org/10.1162/JOCN_A_00077

Lakens, D. (2021). The Practical Alternative to the p Value Is the Correctly Used p Value. *Perspectives on Psychological Science : A Journal of the Association for Psychological Science*, *16*(3), 639–648. https://doi.org/10.1177/1745691620958012

Latora, V., & Marchiori, M. (2001). Efficient Behavior of Small-World Networks. *Physical Review Letters*, *87*(19), 1–4. https://doi.org/10.1103/PhysRevLett.87.198701

Lee, B. X. (2016). Causes and cures IX: Consequences of violence. *Aggression and Violent Behavior*, *30*, 110–114. https://doi.org/10.1016/j.avb.2016.06.013

Lee, M. R., Shnitko, T. A., Blue, S. W., Kaucher, A. V., Winchell, A. J., Erikson, D. W., Grant, K. A., & Leggio, L. (2020). Labeled oxytocin administered via the intranasal route reaches the brain in rhesus macaques. *Nature Communications*, *11*(1), 1–10. https://doi.org/10.1038/s41467-020-15942-1

Lee, R., Ferris, C., Van de Kar, L. D., & Coccaro, E. F. (2009). Cerebrospinal fluid oxytocin, life history of aggression, and personality disorder. *Psychoneuroendocrinology*, *34*(10), 1567–1573. https://doi.org/10.1016/j.psyneuen.2009.06.002

Leech, R., & Sharp, D. J. (2014). The role of the posterior cingulate cortex in cognition and disease. *Brain*, *137*(1), 12–32. https://doi.org/10.1093/BRAIN/AWT162

Lefevre, A., Benusiglio, D., Tang, Y., Krabichler, Q., Charlet, A., & Grinevich, V. (2021). Oxytocinergic Feedback Circuitries: An

Anatomical Basis for Neuromodulation of Social Behaviors. *Frontiers in Neural Circuits*, *15*(668234), 1–7. https://doi.org/10.3389/fncir.2021.688234

Lefevre, A., Mottolese, R., Dirheimer, M., Mottolese, C., Duhamel, J. R., & Sirigu, A. (2017). A comparison of methods to measure central and peripheral oxytocin concentrations in human and non-human primates. *Scientific Reports 2017 7:1*, *7*(1), 1–10. https://doi.org/10.1038/s41598-017-17674-7

Lemaitre, H., Goldman, A. L., Sambataro, F., Verchinski, B. A., Meyer-Lindenberg, A., Weinberger, D. R., & Mattay, V. S. (2012). Normal age-related brain morphometric changes: Nonuniformity across cortical thickness, surface area and gray matter volume? *Neurobiology of Aging*, *33*(3), 617.e1-617.e9. https://doi.org/10.1016/j.neurobiolaging.2010.07.013

Leng, G., & Ludwig, M. (2016). Intranasal Oxytocin: Myths and Delusions. *Biological Psychiatry*, *79*(3), 243–250. https://doi.org/10.1016/j.biopsych.2015.05.003

Leppanen, J., Ng, K. W., Kim, Y.-R., Tchanturia, K., & Treasure, J. (2018). Meta-analytic review of the effects of a single dose of intranasal oxytocin on threat processing in humans. *Journal of Affective Disorders*, *225*, 167–179. https://doi.org/10.1016/j.jad.2017.08.041

Leppanen, J., Ng, K. W., Tchanturia, K., & Treasure, J. (2017). Meta-analysis of the effects of intranasal oxytocin on interpretation and expression of emotions. *Neuroscience & Biobehavioral Reviews*, *78*, 125–144. https://doi.org/10.1016/j.neubiorev.2017.04.010

Levy, T., Bloch, Y., Bar-Maisels, M., Gat-Yablonski, G., Djalovski, A., Borodkin, K., & Apter, A. (2015). Salivary oxytocin in adolescents with conduct problems and callous-unemotional traits. *European Child & Adolescent Psychiatry*, *24*(12), 1543–1551. https://doi.org/10.1007/S00787-015-0765-6/TABLES/4

Li, Z., Vidorreta, M., Katchmar, N., Alsop, D. C., Wolf, D. H., & Detre, J. A. (2018). Effects of resting state condition on reliability, trait specificity, and network connectivity of brain function measured with arterial spin labeled perfusion MRI. *NeuroImage*, *173*, 165–175. https://doi.org/10.1016/J.NEUROIMAGE.2018.02.028

Liem, F., Mérillat, S., Bezzola, L., Hirsiger, S., Philipp, M., Madhyastha, T., & Jäncke, L. (2015). Reliability and statistical power analysis of cortical and subcortical FreeSurfer metrics in a large sample of healthy elderly. *NeuroImage*, *108*, 95–109. https://doi.org/10.1016/J.NEUROIMAGE.2014.12.035

Lindhiem, O., Bennett, C. B., Hipwell, A. E., & Pardini, D. A. (2015). Beyond Symptom Counts for Diagnosing Oppositional Defiant Disorder

and Conduct Disorder? *Journal of Abnormal Child Psychology*, *43*(7), 1379–1387. https://doi.org/10.1007/s10802-015-0007-x

Liu, H., Liao, J., Jiang, W., & Wang, W. (2014). Changes in low-frequency fluctuations in patients with antisocial personality disorder revealed by resting-state functional MRI. *PloS ONE*, *9*(3), e89790. https://doi.org/10.1371/JOURNAL.PONE.0089790

Liu, P., Lin, T., Feifel, D., & Ebner, N. C. (2022). Intranasal Oxytocin Modulates the Salience Network in Aging. *NeuroImage*, *253*(119045), 1–12. https://doi.org/10.1016/j.neuroimage.2022.119045

Liu, X., Hairston, J., Schrier, M., & Fan, J. (2011). Common and distinct networks underlying reward valence and processing stages: A meta-analysis of functional neuroimaging studies. *Neuroscience & Biobehavioral Reviews*, *35*(5), 1219–1236. https://doi.org/10.1016/J.NEUBIOREV.2010.12.012

Loeber, R., Burke, J. D., & Pardini, D. A. (2009). Development and Etiology of Disruptive and Delinquent Behavior. *Annual Review of Clinical Psychology*, *5*(1), 291–310. https://doi.org/10.1146/annurev.clinpsy.032408.153631

Loeber, R., & Farrington, D. P. (2014). Age-Crime Curve. In G. Bruinsma & D. Weisbund (Eds.), *Encyclopedia of Criminology and Criminal Justice* (pp. 12–18). Springer New York. https://doi.org/10.1007/978-1-4614-5690-2_474

Logothetis, N. K., Pauls, J., Augath, M., Trinath, T., & Oeltermann, A. (2001). Neurophysiological investigation of the basis of the fMRI signal. *Nature*, *412*(6843), 150–157. https://doi.org/10.1038/35084005

Lombardo, M. V., Auyeung, B., Holt, R. J., Waldman, J., Ruigrok, A. N. V., Mooney, N., Bullmore, E. T., Baron-Cohen, S., & Kundu, P. (2016). Improving effect size estimation and statistical power with multi-echo fMRI and its impact on understanding the neural systems supporting mentalizing. *NeuroImage*, *142*(1), 55. https://doi.org/10.1016/J.NEUROIMAGE.2016.07.022

Loomans, M. M., Tulen, J. H. M., & van Marle, H. J. C. (2015). The startle paradigm in a forensic psychiatric setting: Elucidating psychopathy. *Criminal Behaviour and Mental Health*, *25*(1), 42–53. https://doi.org/10.1002/cbm.1906

Loranger, A. W., Janca, A., & Sartorius, N. (1997). *Assessment and diagnosis of personality disorders: the ICD-10 international personality disorder examination (IPDE)*. Cambridge University Press.

Lorber, M. F., Del Vecchio, T., Slep, A. M. S., & Scholer, S. J. (2019). Normative Trends in Physically Aggressive Behavior: Age-Aggression

Curves from 6 to 24 Months. *Journal of Pediatrics*, *206*, 197–203. https://doi.org/10.1016/j.jpeds.2018.10.025

Lowenstein, J., Purvis, C., & Rose, K. (2016). A systematic review on the relationship between antisocial, borderline and narcissistic personality disorder diagnostic traits and risk of violence to others in a clinical and forensic sample. *Borderline Personality Disorder and Emotion Dysregulation*, *3*(14), 1–12. https://doi.org/10.1186/s40479-016-0046-0

Lu, F. M., Zhou, J. S., Wang, X. P., Xiang, Y. T., & Yuan, Z. (2017). Short- and long-range functional connectivity density alterations in adolescents with pure conduct disorder at resting-state. *Neuroscience*, *351*, 96–107. https://doi.org/10.1016/j.neuroscience.2017.03.040

Lu, H., Jaime, S., & Yang, Y. (2019). Origins of the Resting-State Functional MRI Signal: Potential Limitations of the "Neurocentric" Model. *Frontiers in Neuroscience*, *13*(1136), 1–8. https://doi.org/10.3389/fnins.2019.01136

Lutkenhoff, E. S., Rosenberg, M., Chiang, J., Zhang, K., Pickard, J. D., Owen, A. M., & Monti, M. M. (2014). Optimized brain extraction for pathological brains (optiBET). *PloS ONE*, *9*(12), e115551. https://doi.org/10.1371/journal.pone.0115551

Lv, H., Wang, Z., Tong, E., Williams, L. M., Zaharchuk, G., Zeineh, M., Goldstein-Piekarski, A. N., Ball, T. M., Liao, C., & Wintermark, M. (2018). Resting-State Functional MRI: Everything That Nonexperts Have Always Wanted to Know. *American Journal of Neuroradiology*, *39*(8), 1390–1399. https://doi.org/10.3174/AJNR.A5527

Ly, M., Motzkin, J. C., Philippi, C. L., Kirk, G. R., Newman, J. P., Kiehl, K. A., & Koenigs, M. (2012). Cortical thinning in psychopathy. *American Journal of Psychiatry*, *169*(7), 743–749. https://doi.org/10.1176/appi.ajp.2012.11111627

Lykken, D. T. (1957). A study of anxiety in the sociopathic personality. *Journal of Abnormal and Social Psychology*, *55*(1), 6–10. https://doi.org/10.1037/h0047232

Lynam, D. R., Caspi, A., Moffitt, T. E., Loeber, R., & Stouthamer-Loeber, M. (2007). Longitudinal Evidence that Psychopathy Scores in Early Adolescence Predict Adult Psychopathy. *Journal of Abnormal Psychology*, *116*(1), 155–165. https://doi.org/10.1037/0021-843X.116.1.155

Ma, H. R., Pan, P. L., Sheng, L. Q., Dai, Z. Y., Wang, G. Di, Luo, R., Chen, J. H., Xiao, P. R., Zhong, J. G., & Shi, H. C. (2017). Aberrant pattern of regional cerebral blood flow in Alzheimer's disease: a voxel-wise meta-analysis of arterial spin labeling MR imaging studies. *Oncotarget*, *8*(54), 93196–93208.

https://doi.org/10.18632/ONCOTARGET.21475

MacDonald, E., Dadds, M. R., Brennan, J. L., Williams, K., Levy, F., & Cauchi, A. J. (2011). A review of safety, side-effects and subjective reactions to intranasal oxytocin in human research. *Psychoneuroendocrinology*, *36*(8), 1114–1126. https://doi.org/10.1016/J.PSYNEUEN.2011.02.015

Maddock, R. J. (1999). The retrosplenial cortex and emotion: new insights from functional neuroimaging of the human brain. *Trends in Neurosciences*, *22*(7), 310–316. https://doi.org/10.1016/S0166-2236(98)01374-5

Magezi, D. A. (2015). Linear mixed-effects models for within-participant psychology experiments: An introductory tutorial and free, graphical user interface (LMMgui). *Frontiers in Psychology*, *6*(2), 1–7. https://doi.org/10.3389/FPSYG.2015.00002/BIBTEX

Magyar, M. S., Edens, J. F., Lilienfeld, S. O., Douglas, K. S., & Poythress, N. G. (2011). Examining the relationship among substance abuse, negative emotionality and impulsivity across subtypes of antisocial and psychopathic substance abusers. *Journal of Criminal Justice*, *39*(3), 232–237. https://doi.org/10.1016/j.jcrimjus.2011.02.013

Mak, L. E., Minuzzi, L., MacQueen, G., Hall, G., Kennedy, S. H., & Milev, R. (2017). The Default Mode Network in Healthy Individuals: A Systematic Review and Meta-Analysis. *Brain Connectivity*, *7*(1), 25–33. https://doi.org/10.1089/brain.2016.0438

Malik, A. I., Zai, C. C., Abu, Z., Nowrouzi, B., & Beitchman, J. H. (2012). The role of oxytocin and oxytocin receptor gene variants in childhood-onset aggression. *Genes, Brain, and Behavior*, *11*(5), 545–551. https://doi.org/10.1111/J.1601-183X.2012.00776.X

Marek, S., Tervo-Clemmens, B., Calabro, F. J., Montez, D. F., Kay, B. P., Hatoum, A. S., Donohue, M. R., Foran, W., Miller, R. L., Hendrickson, T. J., Malone, S. M., Kandala, S., Feczko, E., Miranda-Dominguez, O., Graham, A. M., Earl, E. A., Perrone, A. J., Cordova, M., Doyle, O., … Dosenbach, N. U. F. (2022). Reproducible brain-wide association studies require thousands of individuals. *Nature*, *605*(7902), 654–660. https://doi.org/10.1038/s41586-022-04492-9

Mariz, C., Cruz, O. S., & Moreira, D. (2022). The influence of environmental and genetic factors on the development of psychopathy: A systematic review. *Aggression and Violent Behavior*, *62*(101715), 1–17. https://doi.org/10.1016/J.AVB.2021.101715

Marlin, B. J., Mitre, M., D'Amour, J. A., Chao, M. V., & Froemke, R. C. (2015). Oxytocin enables maternal behaviour by balancing cortical inhibition. *Nature*, *520*(7548), 499–504. https://doi.org/10.1038/nature14402

Marsh, A. A., & Blair, R. J. R. (2008). Deficits in facial affect recognition among antisocial populations: a meta-analysis. *Neuroscience and Biobehavioral Reviews*, *32*(3), 454–465. https://doi.org/10.1016/j.neubiorev.2007.08.003

Marsh, N., Marsh, A. A., Lee, M. R., & Hurlemann, R. (2021). Oxytocin and the Neurobiology of Prosocial Behavior. *The Neuroscientist*, *27*(6), 604–619. https://doi.org/10.1177/1073858420960111

Martens, M. A. G., McConnell, F. K., Filippini, N., Mackay, C. E., Harrison, P. J., & Tunbridge, E. M. (2021). Dopaminergic modulation of regional cerebral blood flow: An arterial spin labelling study of genetic and pharmacological manipulation of COMT activity. *NeuroImage*, *234*, 117999. https://doi.org/10.1016/j.neuroimage.2021.117999

Martin-Key, N., Brown, T., & Fairchild, G. (2017). Empathic Accuracy in Male Adolescents with Conduct Disorder and Higher versus Lower Levels of Callous-Unemotional Traits. *Journal of Abnormal Child Psychology*, *45*(7), 1385–1397. https://doi.org/10.1007/s10802-016-0243-8

Martinez, N. N., Lee, Y. J., Eck, J. E., & O, S. (2017). Ravenous wolves revisited: A systematic review of offending concentration. *Crime Science*, *6*(10), 1–16. https://doi.org/10.1186/s40163-017-0072-2

Martins, D., Brodmann, K., Veronese, M., Dipasquale, O., Mazibuko, N., Schuschnig, U., Zelaya, F., Fotopoulou, A., & Paloyelis, Y. (2022). "Less is more": a dose-response account of intranasal oxytocin pharmacodynamics in the human brain. *Progress in Neurobiology*, *211*(102239), 1–17. https://doi.org/10.1016/j.pneurobio.2022.102239

Martins, D., Dipasquale, O., & Paloyelis, Y. (2021). Oxytocin modulates local topography of human functional connectome in healthy men at rest. *Communications Biology*, *4*(68), 1–14. https://doi.org/10.1038/s42003-020-01610-z

Martins, D., Gabay, A., Mehta, M. A., & Paloyelis, Y. (2020). Are single peripheral measurements of baseline oxytocin in saliva and plasma reliable biomarkers of the physiology of the oxytocin system in humans? *BioRxiv*, 1–35. https://doi.org/10.1101/2020.07.14.202622

Martins, D., Leslie, M., Rodan, S., Zelaya, F., Treasure, J., & Paloyelis, Y. (2020). Investigating resting brain perfusion abnormalities and disease target-engagement by intranasal oxytocin in women with bulimia nervosa and binge-eating disorder and healthy controls. *Translational Psychiatry*, *10*(180), 1–13. https://doi.org/10.1038/s41398-020-00871-w

Martins, D., Lockwood, P., Cutler, J., Moran, R., & Paloyelis, Y. (2022). Oxytocin modulates neurocomputational mechanisms underlying

prosocial reinforcement learning. *Progress in Neurobiology*, *213*(102253), 1–15. https://doi.org/10.1101/2021.05.26.445739

Martins, D., Mazibuko, N., Zelaya, F., Vasilakopoulou, S., Loveridge, J., Oates, A., Maltezos, S., Mehta, M., Wastling, S., Howard, M., McAlonan, G. M., Murphy, D., Williams, S. C. R., Fotopoulou, A., Schuschnig, U., & Paloyelis, Y. (2020). Effects of route of administration on oxytocin-induced changes in regional cerebral blood flow in humans. *Nature Communications*, *11*(1160), 1–16. https://doi.org/10.1038/s41467-020-14845-5

Mato Abad, V., García-Polo, P., O'Daly, O., Hernández-Tamames, J. A., & Zelaya, F. (2016). ASAP (Automatic Software for ASL Processing): A toolbox for processing Arterial Spin Labeling images. *Magnetic Resonance Imaging*, *34*(3), 334–344. https://doi.org/10.1016/j.mri.2015.11.002

Maurer, J. M., Paul, S., Anderson, N. E., Nyalakanti, P. K., & Kiehl, K. A. (2020). Youth with elevated psychopathic traits exhibit structural integrity deficits in the uncinate fasciculus. *NeuroImage: Clinical*, *26*(102236), 1–8. https://doi.org/10.1016/j.nicl.2020.102236

Mayer, S. V., Jusyte, A., Klimecki-Lenz, O. M., & Schönenberg, M. (2018). Empathy and altruistic behavior in antisocial violent offenders with psychopathic traits. *Psychiatry Research*, *269*, 625–632. https://doi.org/10.1016/j.psychres.2018.08.035

McCarthy, P. (2021). *FSLeyes* (1.2.0). Wellcome Centre for Integrative Neuroimaging, University of Oxford. https://doi.org/10.5281/zenodo.5504114

McCuish, E. C., Corrado, R. R., Hart, S. D., & DeLisi, M. (2015). The role of symptoms of psychopathy in persistent violence over the criminal career into full adulthood. *Journal of Criminal Justice*, *43*(4), 345–356. https://doi.org/10.1016/j.jcrimjus.2015.04.008

McCutcheon, R. A., Pillinger, T., Guo, X., Rogdaki, M., Welby, G., Vano, L., Cummings, C., Ann-Heron, T., Brugger, S., Davies, D., Ghanem, M., Efthimiou, O., Cipriani, A., & Howes, O. D. (2023). Shared and separate patterns in brain morphometry across transdiagnostic dimensions. *Nature Mental Health*, *1*, 55–65. https://doi.org/10.1038/s44220-022-00010-y

McDermott, R., Tingley, D., Cowden, J., Frazzetto, G., & Johnson, D. D. P. (2009). Monoamine oxidase A gene (MAOA) predicts behavioral aggression following provocation. *Proceedings of the National Academy of Sciences of the United States of America*, *106*(7), 2118–2123. https://doi.org/10.1073/pnas.0808376106

McFarquhar, M., McKie, S., Emsley, R., Suckling, J., Elliott, R., & Williams, S. (2016). Multivariate and repeated measures (MRM): A new toolbox

for dependent and multimodal group-level neuroimaging data. *NeuroImage*, *132*, 373–389. https://doi.org/10.1016/J.NEUROIMAGE.2016.02.053

Meaney, M. J. (2017). Epigenetics and the Biology of Gene × Environment Interactions. In P. Tolan & B. Leventhal (Eds.), *Gene-Environment Transactions in Developmental Psychopathology. Advances in Development and Psychopathology: Brain Research Foundation Symposium Series, vol 2.* (2nd ed., pp. 59–94). Springer. https://doi.org/10.1007/978-3-319-49227-8_4

Meffert, H., Gazzola, V., Den Boer, J. A., Bartels, A. A. J., & Keysers, C. (2013). Reduced spontaneous but relatively normal deliberate vicarious representations in psychopathy. *Brain*, *136*, 2550–2562. https://doi.org/10.1093/brain/awt190

Menon, V. (2011). Large-scale brain networks and psychopathology: a unifying triple network model. *Trends in Cognitive Sciences*, *15*(10), 483–506. https://doi.org/10.1016/J.TICS.2011.08.003

Mens, W. B. J., Witter, A., & Van Wimersma Greidanus, T. B. (1983). Penetration of neurohypophyseal hormones from plasma into cerebrospinal fluid (CSF): half-times of disappearance of these neuropeptides from CSF. *Brain Research*, *262*(1), 143–149. https://doi.org/10.1016/0006-8993(83)90478-X

Meyer-Lindenberg, A., Buckholtz, J. W., Kolachana, B., Hariri, A. R., Pezawas, L., Blasi, G., Wabnitz, A., Honea, R., Verchinski, B., Callicott, J. H., Egan, M., Mattay, V., & Weinberger, D. R. (2006). Neural mechanisms of genetic risk for impulsivity and violence in humans. *Proceedings of the National Academy of Sciences*, *103*(16), 6269–6274. https://doi.org/10.1073/PNAS.0511311103

Meyer-Lindenberg, A., Domes, G., Kirsch, P., & Heinrichs, M. (2011). Oxytocin and vasopressin in the human brain: social neuropeptides for translational medicine. *Nature Reviews Neuroscience*, *12*(9), 524–538. https://doi.org/10.1038/nrn3044

Meyer, J. H., Wilson, A. A., Rusjan, P., Clark, M., Houle, S., Woodside, S., Arrowood, J., Martin, K., & Colleton, M. (2008). Serotonin2A receptor binding potential in people with aggressive and violent behaviour. *Journal of Psychiatry and Neuroscience*, *33*(6), 499–508.

Mikton, C. R., Butchart, A., Dahlberg, L. L., & Krug, E. G. (2016). Global Status Report on Violence Prevention 2014. *American Journal of Preventive Medicine*, *50*(5), 652–659. https://doi.org/10.1016/j.amepre.2015.10.007

Ministry of Justice. (2022). *Criminal justice system statistics quarterly: December 2021 - GOV.UK*. Criminal Justice Statistics Quarterly. https://www.gov.uk/government/statistics/criminal-justice-system-

statistics-quarterly-december-2021

Mitchell, I. J., Smid, W., Troelstra, J., Wever, E., Ziegler, T. E., & Beech, A. R. (2013). Psychopathic characteristics are related to high basal urinary oxytocin levels in male forensic patients. *Journal of Forensic Psychiatry & Psychology*, *24*(3), 309–318. https://doi.org/10.1080/14789949.2013.773455

Moffitt, T. E. (1993). Adolescence-Limited and Life-Course-Persistent Antisocial Behavior: A Developmental Taxonomy. *Psychological Review*, *100*(4), 674–701. https://doi.org/https://doi.org/10.1037/0033-295X.100.4.674

Moffitt, T. E. (2018). Male antisocial behaviour in adolescence and beyond. *Nature Human Behaviour*, *2*, 177–186. https://doi.org/10.1038/s41562-018-0309-4

Moore, A. A., Rappaport, L. M., Blair, R. J. R., Pine, D. S., Leibenluft, E., Brotman, M. A., Hettema, J. M., & Roberson-Nay, R. (2019). Genetic underpinnings of callous-unemotional traits and emotion recognition in children, adolescents, and emerging adults. *Journal of Child Psychology and Psychiatry*, *60*(6), 638–645. https://doi.org/10.1111/jcpp.13018

Moore, A. A., Silberg, J. L., Roberson-Nay, R., & Mezuk, B. (2017). Life course persistent and adolescence limited conduct disorder in a nationally representative US sample: prevalence, predictors, and outcomes. *Social Psychiatry and Psychiatric Epidemiology*, *52*(4), 435–443. https://doi.org/10.1007/s00127-017-1337-5

Morcom, A. M., & Fletcher, P. C. (2007). Does the brain have a baseline? Why we should be resisting a rest. *NeuroImage*, *37*(4), 1073–1082. https://doi.org/10.1016/J.NEUROIMAGE.2006.09.013

Morgan, A. B., & Lilienfeld, S. O. (2000). A meta-analytic review of the relation between antisocial behavior and neuropsychological measures of executive function. *Clinical Psychology Review*, *20*(1), 113–136.

Motzkin, J. C., Newman, J. P., Kiehl, K. A., & Koenigs, M. (2011). Reduced Prefrontal Connectivity in Psychopathy. *Journal of Neuroscience*, *31*(48), 17348–17357. https://doi.org/10.1523/JNEUROSCI.4215-11.2011

Moul, C., Dobson-Stone, C., Brennan, J., Hawes, D., & Dadds, M. (2013). An exploration of the serotonin system in antisocial boys with high levels of callous-unemotional traits. *PloS One*, *8*(2), e56619. https://doi.org/10.1371/JOURNAL.PONE.0056619

Moul, C., Killcross, S., & Dadds, M. R. (2012). A Model of Differential Amygdala Activation in Psychopathy. *Psychological Review*, *119*(4), 789–806. https://doi.org/10.1037/a0029342

Murphy, B., Lilienfeld, S., Skeem, J., & Edens, J. F. (2016). Are fearless dominance traits superfluous in operationalizing psychopathy? Incremental validity and sex differences. *Psychological Assessment*, *28*(12), 1597–1607. https://doi.org/10.1037/pas0000288

Murphy, K., Bodurka, J., & Bandettini, P. A. (2007). How long to scan? The relationship between fMRI temporal signal to noise ratio and necessary scan duration. *NeuroImage*, *34*(2), 565–574. https://doi.org/10.1016/J.NEUROIMAGE.2006.09.032

Murphy, K., Harris, A. D., Diukova, A., Evans, C. J., Lythgoe, D. J., Zelaya, F., & Wise, R. G. (2011). Pulsed arterial spin labeling perfusion imaging at 3 T: estimating the number of subjects required in common designs of clinical trials. *Magnetic Resonance Imaging*, *29*(10), 1382–1389. https://doi.org/10.1016/j.mri.2011.02.030

Murray, L., Waller, R., & Hyde, L. W. (2018). A systematic review examining the link between psychopathic personality traits, antisocial behavior, and neural reactivity during reward and loss processing. *Personality Disorders*, *9*(6), 497–509. https://doi.org/10.1037/per0000308

Mutsaerts, H. J. M. M., Steketee, R. M. E., Heijtel, D. F. R., Kuijer, J. P. A., van Osch, M. J. P., Majoie, C. B. L. M., Smits, M., & Nederveen, A. J. (2015). Reproducibility of pharmacological ASL using sequences from different vendors: implications for multicenter drug studies. *Magnetic Resonance Materials in Physics, Biology and Medicine*, *28*(5), 427–436. https://doi.org/10.1007/S10334-014-0480-1/FIGURES/4

Nærde, A., Ogden, T., Janson, H., & Zachrisson, H. D. (2014). Normative development of physical aggression from 8 to 26 months. *Developmental Psychology*, *50*(6), 1710–1720. https://doi.org/10.1037/a0036324

Narayan, V. M., Narr, K. L., Kumari, V., Woods, R. P., Thompson, P. M., Toga, A. W., & Sharma, T. (2007). Regional Cortical Thinning in Subjects With Violent Antisocial Personality Disorder or Schizophrenia. *American Journal of Psychiatry*, *164*(9), 1418–1427.

National Institute for Health and Care Excellence. (2017). *Antisocial behaviour and conduct disorders in children and young people: recognition, intervention and management*. The British Psychological Society.

National Research Council, Division of Behavioral and Social Sciences and Education, Commission on Behavioral and Social Sciences and Education, Panel on Research on Criminal Careers, Committee on Research on Law Enforcement and the Administration of Justice, Blumstein, A., Cohen, J., Roth, J. A., & Visher, C. A. (1986). *Criminal careers and "career criminals": Volume 1*. The National Academies

Press. https://doi.org/10.17226/922

Ne'eman, R., Perach-Barzilay, N., Fischer-Shofty, M., Atias, A., & Shamay-Tsoory, S. G. (2016). Intranasal administration of oxytocin increases human aggressive behavior. *Hormones and Behavior*, *80*, 125–131. https://doi.org/10.1016/J.YHBEH.2016.01.015

Newbury-Helps, J., Feigenbaum, J., & Fonagy, P. (2017). Offenders with antisocial personality disorder display more impairments in mentalizing. *Journal of Personality Disorders*, *31*(2), 232–255. https://doi.org/10.1521/pedi_2016_30_246

Newman, J. P., Kosson, D. S., & Patterson, C. M. (1992). Delay of Gratification in Psychopathic and Nonpsychopathic Offenders. *Journal of Abnormal Psychology*, *101*(4), 630–636. https://doi.org/10.1037/0021-843X.101.4.630

Nickerson, L. D., Smith, S. M., Öngür, D., & Beckmann, C. F. (2017). Using dual regression to investigate network shape and amplitude in functional connectivity analyses. *Frontiers in Neuroscience*, *11*(115), 1–18. https://doi.org/10.3389/FNINS.2017.00115/BIBTEX

Nieuwenhuis, S., Forstmann, B. U., & Wagenmakers, E. J. (2011). Erroneous analyses of interactions in neuroscience: a problem of significance. *Nature Neuroscience*, *14*(9), 1105–1107. https://doi.org/10.1038/nn.2886

Nilsson, K. W., Åslund, C., Comasco, E., & Oreland, L. (2018). Gene–environment interaction of monoamine oxidase A in relation to antisocial behaviour: current and future directions. *Journal of Neural Transmission*, *125*(11), 1601–1626. https://doi.org/10.1007/s00702-018-1892-2

Nilsson, K. W., Sjöberg, R. L., Damberg, M., Leppert, J., Öhrvik, J., Alm, P. O., Lindström, L., & Oreland, L. (2006). Role of monoamine oxidase A genotype and psychosocial factors in male adolescent criminal activity. *Biological Psychiatry*, *59*(2), 121–127. https://doi.org/10.1016/J.BIOPSYCH.2005.06.024

Nishina, K., Takagishi, H., Inoue-Murayama, M., Takahashi, H., & Yamagishi, T. (2015). Polymorphism of the Oxytocin Receptor Gene Modulates Behavioral and Attitudinal Trust among Men but Not Women. *PloS One*, *10*(10), e0137089. https://doi.org/10.1371/JOURNAL.PONE.0137089

Nishitani, S., Fujisawa, T. X., Hiraoka, D., Makita, K., Takiguchi, S., Hamamura, S., Yao, A., Shimada, K., Smith, A. K., & Tomoda, A. (2021). A multi-modal MRI analysis of brain structure and function in relation to OXT methylation in maltreated children and adolescents. *Translational Psychiatry*, *11*(589), 1–9. https://doi.org/10.1038/s41398-021-01714-y

Nomi, J. S., & Uddin, L. Q. (2015). Developmental changes in large-scale network connectivity in autism. *NeuroImage: Clinical*, *7*, 732–741. https://doi.org/10.1016/J.NICL.2015.02.024

Noordermeer, S. D. S., Luman, M., & Oosterlaan, J. (2016). A Systematic Review and Meta-analysis of Neuroimaging in Oppositional Defiant Disorder (ODD) and Conduct Disorder (CD) Taking Attention-Deficit Hyperactivity Disorder (ADHD) Into Account. *Neuropsychology Review*, *26*(1), 44–72. https://doi.org/10.1007/s11065-015-9315-8

Nöthling, J., Malan-Müller, S., Abrahams, N., Hemmings, S. M. J., & Seedat, S. (2020). Epigenetic alterations associated with childhood trauma and adult mental health outcomes: A systematic review. *The World Journal of Biological Psychiatry*, *21*(7), 493–512. https://doi.org/10.1080/15622975.2019.1583369

Nummenmaa, L., Lukkarinen, L., Sun, L., Vesa, P., Seppala, K., Karjalainen, T., Karlsson, H. K., Hudson, M., Venetjoki, N., Salomaa, M., Rautio, P., Hirvonen, J., Lauerma, H., & Tiihonen, J. (2021). Brain Basis of Psychopathy in Criminal Offenders and General Population. *Cerebral Cortex*, *31*(9), 4104–4114. https://doi.org/10.1093/cercor/bhab072

Oettl, L. L., Ravi, N., Schneider, M., Scheller, M. F., Schneider, P., Mitre, M., Da Silva Gouveia, M., Froemke, R. C., Chao, M. V., Young, W. S., Meyer-Lindenberg, A., Grinevich, V., Shusterman, R., & Kelsch, W. (2016). Oxytocin Enhances Social Recognition by Modulating Cortical Control of Early Olfactory Processing. *Neuron*, *90*(3), 609–621. https://doi.org/10.1016/J.NEURON.2016.03.033

Ogloff, J. R. P., Campbell, R. E., & Shepherd, S. M. (2016). Disentangling Psychopathy from Antisocial Personality Disorder: An Australian Analysis. *Journal of Forensic Psychology Practice*, *16*(3), 198–215. https://doi.org/10.1080/15228932.2016.1177281

Olderbak, S., & Wilhelm, O. (2017). Emotion Perception and Empathy: An Individual Differences Test of Relations. *Emotion*, *17*(7), 1092–1106. https://doi.org/10.1037/emo0000308

Oldham, J. M. (2015). The alternative DSM-5 model for personality disorders. *World Psychiatry*, *14*(2), 234–236. https://doi.org/10.1002/wps.20232

Olver, M. E., Lewis, K., & Wong, S. C. P. (2013). Risk Reduction Treatment of High-Risk Psychopathic Offenders: The Relationship of Psychopathy and Treatment Change to Violent Recidivism. *Personality Disorders: Theory, Research, and Treatment*, *4*(2), 160–167. https://doi.org/10.1037/a0029769

Olver, M. E., Stockdale, K. C., & Wormith, J. S. (2011). A meta-analysis of predictors of offender treatment attrition and its relationship to

recidivism. *Journal of Consulting and Clinical Psychology*, *79*(1), 6–21. https://doi.org/10.1037/a0022200

Oostermeijer, S., Whittle, S., Suo, C., Allen, N. B., Simmons, J. G., Vijayakumar, N., Van de Ven, P., Jansen, L., Yücel, M., & Popma, A. (2016). Trajectories of adolescent conduct problems in relation to cortical thickness development: a longitudinal MRI study. *Translational Psychiatry*, *6*, e841. https://doi.org/10.1038/tp.2016.111

Openneer, T. J. C., Marsman, J. B. C., van der Meer, D., Forde, N. J., Akkermans, S. E. A., Naaijen, J., Buitelaar, J. K., Dietrich, A., & Hoekstra, P. J. (2020). A graph theory study of resting-state functional connectivity in children with Tourette syndrome. *Cortex*, *126*, 63–72. https://doi.org/10.1016/J.CORTEX.2020.01.006

Ouellet-Morin, I., Côté, S. M., Vitaro, F., Hébert, M., Carbonneau, R., Lacourse, É., Turecki, G., & Tremblay, R. E. (2016). Effects of the MAOA gene and levels of exposure to violence on antisocial outcomes. *British Journal of Psychiatry*, *208*(1), 42–48. https://doi.org/10.1192/bjp.bp.114.162081

Paloyelis, Y., Doyle, O. M., Zelaya, F. O., Maltezos, S., Williams, S. C., Fotopoulou, A., & Howard, M. A. (2016). A spatiotemporal profile of in vivo cerebral blood flow changes following intranasal oxytocin in humans. *Biological Psychiatry*, *79*(8), 693–705. https://doi.org/10.1016/j.biopsych.2014.10.005

Palumbo, S., Mariotti, V., Vellucci, S., Antonelli, K., Anderson, N. E., Harenski, C., Pietrini, P., Kiehl, K. A., & Pellegrini, S. (2022). HTR1B genotype and psychopathy: Main effect and interaction with paternal maltreatment. *Psychoneuroendocrinology*, *144*(105861), 1–9. https://doi.org/10.1016/j.psyneuen.2022.105861

Panizzon, M. S., Fennema-Notestine, C., Eyler, L. T., Jernigan, T. L., Prom-Wormley, E., Neale, M., Jacobson, K., Lyons, M. J., Grant, M. D., Franz, C. E., Xian, H., Tsuang, M., Fischl, B., Seidman, L., Dale, A., & Kremen, W. S. (2009). Distinct Genetic Influences on Cortical Surface Area and Cortical Thickness. *Cerebral Cortex*, *19*, 2728–2735. https://doi.org/10.1093/cercor/bhp026

Papalia, N., Spivak, B., Daffern, M., & Ogloff, J. R. P. (2019). A meta-analytic review of the efficacy of psychological treatments for violent offenders in correctional and forensic mental health settings. *Clinical Psychology: Science and Practice*, *26*(2), 1–28. https://doi.org/10.1111/cpsp.12282

Pappa, I., St Pourcain, B., Benke, K., Cavadino, A., Hakulinen, C., Nivard, M. G., Nolte, I. M., Tiesler, C. M. T., Bakermans-Kranenburg, M. J., Davies, G. E., Evans, D. M., Geoffroy, M.-C., Grallert, H., Groen-

Blokhuis, M. M., Hudziak, J. J., Kemp, J. P., Keltikangas-Järvinen, L., McMahon, G., Mileva-Seitz, V. R., … Tiemeier, H. (2016). A genome-wide approach to children's aggressive behavior: The EAGLE consortium. *American Journal of Medical Genetics Part B*, *171B*(5), 562–572. https://doi.org/10.1002/ajmg.b.32333

Pardini, D. A., Byrd, A. L., Hawes, S. W., & Docherty, M. (2018). Unique Dispositional Precursors to Early-Onset Conduct Problems and Criminal Offending in Adulthood. *Journal of the American Academy of Child and Adolescent Psychiatry*, *57*(8), 583–592. https://doi.org/10.1016/j.jaac.2018.04.013

Pardini, D. A., Frick, P. J., & Moffitt, T. E. (2010). Building an Evidence Base for DSM-5 Conceptualizations of Oppositional Defiant Disorder and Conduct Disorder: Introduction to the Special Section. *Journal of Abnormal Psychology*, *119*(4), 683–688. https://doi.org/10.1037/a0021441

Pardoe, H. R., Abbott, D. F., Jackson, G. D., & The Alzheimer's Disease Neuroimaging Initiative. (2013). Sample size estimates for well-powered cross-sectional cortical thickness studies. *Human Brain Mapping*, *34*(11), 3000–3009. https://doi.org/10.1002/HBM.22120

Parkes, L., Fulcher, B., Yücel, M., & Fornito, A. (2018). An evaluation of the efficacy, reliability, and sensitivity of motion correction strategies for resting-state functional MRI. *NeuroImage*, *171*, 415–436. https://doi.org/10.1016/J.NEUROIMAGE.2017.12.073

Parkes, L. M., Rashid, W., Chard, D. T., & Tofts, P. S. (2004). Normal cerebral perfusion measurements using arterial spin labeling: Reproducibility, stability, and age and gender effects. *Magnetic Resonance in Medicine*, *51*(4), 736–743. https://doi.org/10.1002/MRM.20023

Pasalich, D. S., Dadds, M. R., & Hawes, D. J. (2014). Cognitive and affective empathy in children with conduct problems: Additive and interactive effects of callous-unemotional traits and autism spectrum disorders symptoms. *Psychiatry Research*, *219*(3), 625–630. https://doi.org/10.1016/j.psychres.2014.06.025

Patel, S., Patel, R., Park, M. T. M., Masellis, M., Knight, J., & Chakravarty, M. M. (2018). Heritability estimates of cortical anatomy: The influence and reliability of different estimation strategies. *NeuroImage*, *178*, 78–91. https://doi.org/10.1016/j.neuroimage.2018.05.014

Patrick, C. J. (1994). Emotion and psychopathy: startling new insights. *Psychophysiology*, *31*(4), 319–330. https://doi.org/10.1111/j.1469-8986.1994.tb02440.x

Patrick, C. J. (2015). Physiological correlates of psychopathy, antisocial personality disorder, habitual aggression, and violence. *Current Topics*

*in Behavioural Neurosciences*, *21*, 197–227. https://doi.org/10.1007/7854

Pearson, J. M., Heilbronner, S. R., Barack, D. L., Hayden, B. Y., & Platt, M. L. (2011). Posterior cingulate cortex: adapting behavior to a changing world. *Trends in Cognitive Sciences*, *15*(4), 143–151. https://doi.org/10.1016/J.TICS.2011.02.002

Peled-Avron, L., Abu-Akel, A., & Shamay-Tsoory, S. G. (2020). Exogenous effects of oxytocin in five psychiatric disorders: a systematic review, meta-analyses and a personalized approach through the lens of the social salience hypothesis. *Neuroscience and Biobehavioral Reviews*, *114*, 70–95. https://doi.org/10.1016/J.NEUBIOREV.2020.04.023

Peng, S. X., Wang, Y. Y., Zhang, M., Zang, Y. Y., Wu, D., Pei, J., Li, Y., Dai, J., Guo, X., Luo, X., Zhang, N., Yang, J. J., Zhang, C., Gao, X., Liu, N., & Shi, Y. S. (2021). SNP rs10420324 in the AMPA receptor auxiliary subunit TARP γ-8 regulates the susceptibility to antisocial personality disorder. *Scientific Reports*, *11*(11997), 1–15. https://doi.org/10.1038/S41598-021-91415-9

Pera-Guardiola, V., Batalla, I., Bosque, J., Kosson, D., Pifarré, J., Hernández-Ribas, R., Goldberg, X., Contreras-Rodríguez, O., Menchón, J. M., Soriano-Mas, C., & Cardoner, N. (2016). Modulatory effects of psychopathy on Wisconsin Card Sorting Test performance in male offenders with Antisocial Personality Disorder. *Psychiatry Research*, *235*, 43–48. https://doi.org/10.1016/j.psychres.2015.12.003

Pfabigan, D. M., Seidel, E. M., Wucherer, A. M., Keckeis, K., Derntl, B., & Lamm, C. (2015). Affective empathy differs in male violent offenders with high- and low-trait psychopathy. *Journal of Personality Disorders*, *29*(1), 42–61. https://doi.org/10.1521/pedi_2014_28_145

Philippi, C. L., Pujara, M. S., Motzkin, J. C., Newman, J., Kiehl, K. A., & Koenigs, M. (2015). Altered resting-state functional connectivity in cortical networks in psychopathy. *The Journal of Neuroscience*, *35*(15), 6068–6078. https://doi.org/10.1523/JNEUROSCI.5010-14.2015

Piquero, A. R., & Moffitt, T. E. (2014). Moffitt's Developmental Taxonomy of Antisocial Behaviour. In G. Bruinsma & D. Weisburd (Eds.), *Encyclopedia of Criminology and Criminal Justice* (pp. 3121–3127). Springer. https://doi.org/10.1007/978-1-4614-5690-2_506

Piva, M., & Chang, S. W. C. (2018). An integrated framework for the role of oxytocin in multistage social decision-making. *American Journal of Primatology*, *80*(10), 1–12. https://doi.org/10.1002/AJP.22735

Polanczyk, G. V., Salum, G. A., Sugaya, L. S., Caye, A., & Rohde, L. A.

(2015). A meta-analysis of the worldwide prevalence of mental disorders in children and adolescents. *Journal of Child Psychology and Psychiatry*, *56*(3), 345–365. https://doi.org/10.1111/jcpp.12381

Poore, H. E., & Waldman, I. D. (2020). The Association of Oxytocin Receptor Gene (OXTR) Polymorphisms Antisocial Behavior: A Meta-analysis. *Behavior Genetics*, *50*(3), 161–173. https://doi.org/10.1007/s10519-020-09996-6

Posse, S., Wiese, S., Gembris, D., Mathiak, K., Kessler, C., Grosse-Ruyken, M.-L., Elghahwagi, B., Richards, T., Dager, S. R., & Kiselev, V. G. (1999). Enhancement of BOLD-Contrast Sensitivity by Single-Shot Multi-Echo Functional MR Imaging. *Magnetic Resonance in Medicine*, *42*, 87–97. https://doi.org/10.1002/(SICI)1522-2594(199907)42:1

Poulton, R., Moffitt, T. E., & Silva, P. A. (2015). The Dunedin Multidisciplinary Health and Development Study: overview of the first 40 years, with an eye to the future. *Social Psychiatry and Psychiatric Epidemiology*, *50*, 679–693. https://doi.org/10.1007/s00127-015-1048-8

Power, J. D., Mitra, A., Laumann, T. O., Snyder, A. Z., Schlaggar, B. L., & Petersen, S. E. (2014). Methods to detect, characterize, and remove motion artifact in resting state fMRI. *NeuroImage*, *84*, 320–341. https://doi.org/10.1016/J.NEUROIMAGE.2013.08.048

Psychology Software Tools Inc. (2000). *E-Prime 1.0*.

Pu, W., Luo, Q., Jiang, Y., Gao, Y., Ming, Q., & Yao, S. (2017). Alterations of Brain Functional Architecture Associated with Psychopathic Traits in Male Adolescents with Conduct Disorder. *Scientific Reports*, *7*(11349), 1–11. https://doi.org/10.1038/s41598-017-11775-z

Pujara, M., Motzkin, J. C., Newman, J. P., Kiehl, K. A., & Koenigs, M. (2014). Neural correlates of reward and loss sensitivity in psychopathy. *Social Cognitive and Affective Neuroscience*, *9*(6), 794–801. https://doi.org/10.1093/SCAN/NST054

Pujol, J., Batalla, I., Contreras-Rodríguez, O., Harrison, B. J., Pera-Guardiola, V., Hernández-Ribas, R., Real, E., Bosa, L., Soriano-Mas, C., Deus, J., López-Solà, M., Pifarré, J., Menchón, J. M., & Cardoner, N. (2012). Breakdown in the brain network subserving moral judgment in criminal psychopathy. *Social Cognitive and Affective Neuroscience*, *7*(8), 917–923. https://doi.org/10.1093/SCAN/NSR075

Pujol, J., Harrison, B. J., Contreras-Rodríguez, O., & Cardoner, N. (2018). The contribution of brain imaging to the understanding of psychopathy. *Psychological Medicine*, *49*(1), 20–31. https://doi.org/10.1017/S0033291718002507

Puzzo, I., Seunarine, K., Sully, K., Darekar, A., Clark, C., Sonuga-Barke, E. J. S., & Fairchild, G. (2018). Altered White-Matter Microstructure in Conduct Disorder Is Specifically Associated with Elevated Callous-Unemotional Traits. *Journal of Abnormal Child Psychology*, *46*(7), 1451–1466. https://doi.org/10.1007/s10802-017-0375-5

Quintana, D. S. (2020). Most oxytocin administration studies are statistically underpowered to reliably detect (or reject) a wide range of effect sizes. *Comprehensive Psychoneuroendocrinology*, *4*(100014), 1–4. https://doi.org/10.1016/J.CPNEC.2020.100014

Quintana, D. S. (2022). Towards better hypothesis tests in oxytocin research: Evaluating the validity of auxiliary assumptions. *Psychoneuroendocrinology*, *137*(105642), 1–11. https://doi.org/10.1016/J.PSYNEUEN.2021.105642

Quintana, D. S., Alvares, G. A., Hickie, I. B., & Guastella, A. J. (2015). Do delivery routes of intranasally administered oxytocin account for observed effects on social cognition and behavior? A two-level model. *Neuroscience and Biobehavioral Reviews*, *49*, 182–192. https://doi.org/10.1016/j.neubiorev.2014.12.011

Quintana, D. S., & Guastella, A. J. (2020). An Allostatic Theory of Oxytocin. *Trends in Cognitive Sciences*, *24*(7), 515–528. https://doi.org/10.1016/j.tics.2020.03.008

Quintana, D. S., Lischke, A., Grace, S., Scheele, D., Ma, Y., & Becker, B. (2021). Advances in the field of intranasal oxytocin research: lessons learned and future directions for clinical research. *Molecular Psychiatry*, *26*(1), 80–91. https://doi.org/10.1038/s41380-020-00864-7

Quintana, D. S., Rokicki, J., van der Meer, D., Alnæs, D., Kaufmann, T., Córdova-Palomera, A., Dieset, I., Andreassen, O. A., & Westlye, L. T. (2019). Oxytocin pathway gene networks in the human brain. *Nature Communications*, *10*(1), 1–12. https://doi.org/10.1038/s41467-019-08503-8

Quintana, D. S., Smerud, K. T., Andreassen, O. A., & Djupesland, P. G. (2018). Evidence for intranasal oxytocin delivery to the brain: recent advances and future perspectives. *Therapeutic Delivery*, *9*(7), 515–525. https://doi.org/10.4155/TDE-2018-0002

Quintana, D. S., Westlye, L. T., Alnæs, D., Kaufmann, T., Mahmoud, R. A., Smerud, K. T., Djupesland, P. G., & Andreassen, O. A. (2019). Low-dose intranasal oxytocin delivered with Breath Powered device modulates pupil diameter and amygdala activity: a randomized controlled pupillometry and fMRI study. *Neuropsychopharmacology*, *44*(2), 306–313. https://doi.org/10.1038/S41386-018-0241-3

Quintana, D. S., Westlye, L. T., Alnæs, D., Rustan, Ø. G., Kaufmann, T.,

Smerud, K. T., Mahmoud, R. A., Djupesland, P. G., & Andreassen, O. A. (2016). Low dose intranasal oxytocin delivered with Breath Powered device dampens amygdala response to emotional stimuli: A peripheral effect-controlled within-subjects randomized dose-response fMRI trial. *Psychoneuroendocrinology*, *69*, 180–188. https://doi.org/10.1016/j.psyneuen.2016.04.010

Quintana, D. S., Westlye, L. T., Rustan, O. G., Tesli, N., Poppy, C. L., Smevik, H., Tesli, M., Røine, M., Mahmoud, R. A., Smerud, K. T., Djupesland, P. G., & Andreassen, O. A. (2015). Low-dose oxytocin delivered intranasally with Breath Powered device affects social-cognitive behavior: a randomized four-way crossover trial with nasal cavity dimension assessment. *Translational Psychiatry*, *5*(7), 1–9. https://doi.org/10.1038/TP.2015.93

R Core Team. (2021). *R: A language and environment for statistical computing*. R Foundation for Statistical Computing. https://www.r-project.org/

Raine, A., Dodge, K. A., Loeber, R., Gatzke-Kopp, L., Lynam, D., Reynolds, C., Stouthamer-Loeber, M., & Liu, J. (2006). The Reactive–Proactive Aggression Questionnaire: Differential Correlates of Reactive and Proactive Aggression in Adolescent Boys. *Aggressive Behavior*, *32*(2), 159–171. https://doi.org/10.1002/AB.20115

Raine, A., Ishikawa, S. S., Arce, E., Lencz, T., Knuth, K. H., Bihrle, S., LaCasse, L., & Colletti, P. (2004). Hippocampal structural asymmetry in unsuccessful psychopaths. *Biological Psychiatry*, *55*(2), 185–191. https://doi.org/10.1016/S0006-3223(03)00727-3

Raine, A., Lencz, T., Bihrle, S., LaCasse, L., & Colletti, P. (2000). Reduced prefrontal gray matter volume and reduced autonomic activity in antisocial personality disorder. *Archives of General Psychiatry*, *57*(2), 119–127. https://doi.org/10.1001/archpsyc.57.2.119

Raine, A., Lencz, T., Taylor, K., Hellige, J. B., Bihrle, S., Lacasse, L., Lee, M., Ishikawa, S., & Colletti, P. (2003). Corpus Callosum Abnormalities in Psychopathic Antisocial Individuals. *Archives of General Psychiatry*, *60*(11), 1134–1142. https://doi.org/10.1001/archpsyc.60.11.1134

Raine, A., Yang, Y., Narr, K. L., & Toga, A. W. (2011). Sex differences in orbitofrontal gray as a partial explanation for sex differences in antisocial personality. *Molecular Psychiatry*, *16*, 227–236. https://doi.org/10.1038/mp.2009.136

Rakic, P. (2007). The radial edifice of cortical architecture: from neuronal silhouettes to genetic engineering. *Brain Research Reviews*, *55*(2), 204–219. https://doi.org/10.1016/j.brainresrev.2007.02.010

Rautiainen, M. R., Paunio, T., Repo-Tiihonen, E., Virkkunen, M., Ollila, H. M., Sulkava, S., Jolanki, O., Palotie, A., & Tiihonen, J. (2016).

Genome-wide association study of antisocial personality disorder. *Translational Psychiatry*, *6*(9), e883. https://doi.org/10.1038/tp.2016.155

Reif, A., Rösler, M., Freitag, C. M., Schneider, M., Eujen, A., Kissling, C., Wenzler, D., Jacob, C. P., Retz-Junginger, P., Thome, J., Lesch, K. P., & Retz, W. (2007). Nature and Nurture Predispose to Violent Behavior: Serotonergic Genes and Adverse Childhood Environment. *Neuropsychopharmacology*, *32*(11), 2375–2383. https://doi.org/10.1038/sj.npp.1301359

Reinders, A. A. T. S., Chalavi, S., Schlumpf, Y. R., Vissia, E. M., Nijenhuis, E. R. S., Jäncke, L., Veltman, D. J., & Ecker, C. (2018). Neurodevelopmental origins of abnormal cortical morphology in dissociative identity disorder. *Acta Psychiatrica Scandinavica*, *137*(2), 157–170. https://doi.org/10.1111/acps.12839

Richell, R. A., Mitchell, D. G. V., Newman, C., Leonard, A., Baron-Cohen, S., & Blair, R. J. R. (2003). Theory of mind and psychopathy: can psychopathic individuals read the 'language of the eyes'? *Neuropsychologia*, *41*(5), 523–526. https://doi.org/10.1016/S0028-3932(02)00175-6

Riser, R. E., & Kosson, D. S. (2013). Criminal behavior and cognitive processing in male offenders with antisocial personality disorder with and without comorbid psychopathy. *Personality Disorders: Theory, Research, and Treatment*, *4*(4), 332–340. https://doi.org/10.1037/a0033303

Rodman, A. M., Kastman, E. K., Dorfman, H. M., Baskin-Sommers, A. R., Kiehl, K. A., Newman, J. P., & Buckholtz, J. W. (2016). Selective Mapping of Psychopathy and Externalizing to Dissociable Circuits for Inhibitory Self-Control. *Clinical Psychological Science*, *4*(3), 559–571. https://doi.org/10.1177/2167702616631495

Rodrigues, S. M., Saslow, L. R., Garcia, N., John, O. P., & Keltner, D. (2009). Oxytocin receptor genetic variation relates to empathy and stress reactivity in humans. *Proceedings of the National Academy of Sciences*, *106*(50), 21437–21441. https://doi.org/10.1073/PNAS.0909579106

Rogers, J. C., & De Brito, S. A. (2016). Cortical and subcortical gray matter volume in youths with conduct problems: a meta-analysis. *JAMA Psychiatry*, *73*(1), 64–72. https://doi.org/10.1001/jamapsychiatry.2015.2423

Romero-Martínez, Á., González, M., Lila, M., Gracia, E., Martí-Bonmatí, L., Alberich-Bayarri, Á., Maldonado-Puig, R., Ten-Esteve, A., & Moya-Albiol, L. (2019). The Brain Resting-State Functional Connectivity Underlying Violence Proneness: Is It a Reliable Marker for

Neurocriminology? A Systematic Review. *Behavioral Sciences*, *9*(1), 1–19. https://doi.org/10.3390/BS9010011

Romero-Martínez, Á., Sarrate-Costa, C., & Moya-Albiol, L. (2022). Reactive vs proactive aggression: A differential psychobiological profile? Conclusions derived from a systematic review. *Neuroscience & Biobehavioral Reviews*, *136*(104626), 1–28. https://doi.org/10.1016/J.NEUBIOREV.2022.104626

Rubinov, M., & Sporns, O. (2010). Complex network measures of brain connectivity: Uses and interpretations. *NeuroImage*, *52*(3), 1059–1069. https://doi.org/10.1016/J.NEUROIMAGE.2009.10.003

Ruisch, I. H., Dietrich, A., Glennon, J. C., Buitelaar, J. K., & Hoekstra, P. J. (2019). Interplay between genome-wide implicated genetic variants and environmental factors related to childhood antisocial behavior in the UK ALSPAC cohort. *European Archives of Psychiatry and Clinical Neuroscience*, *269*(6), 741–752. https://doi.org/10.1007/S00406-018-0964-5/TABLES/4

Ruisch, I. H., Dietrich, A., Klein, M., Faraone, S. V., Oosterlaan, J., Buitelaar, J. K., & Hoekstra, P. J. (2020). Aggression based genome-wide, glutamatergic, dopaminergic and neuroendocrine polygenic risk scores predict callous-unemotional traits. *Neuropsychopharmacology*, *45*(5), 761–769. https://doi.org/10.1038/s41386-020-0608-0

Sadeh, N., Javdani, S., Jackson, J. J., Reynolds, E. K., Potenza, M. N., Gelernter, J., Lejuez, C. W., & Verona, E. (2010). Serotonin transporter gene associations with psychopathic traits in youth vary as a function of socioeconomic resources. *Journal of Abnormal Psychology*, *119*(3), 604–609. https://doi.org/10.1037/a0019709

Sadeh, N., Javdani, S., & Verona, E. (2012). Analysis of Monoaminergic Genes, Childhood Abuse, and Dimensions of Psychopathy. *Journal of Abnormal Psychology*, *122*(1), 167–179. https://doi.org/10.1037/a0029866

Sah, I., Yukseloglu, E. H., Kocabasoglu, N., Bayoglu, B., Cirakoglu, E., & Cengiz, M. (2021). The effects of 5-HTTLPR/rs25531 serotonin transporter gene polymorphisms on antisocial personality disorder among criminals in a sample of the Turkish population. *Molecular Biology Reports*, *48*(1), 77–84. https://doi.org/10.1007/S11033-021-06137-Y/TABLES/4

Salekin, R. T., & Lochman, J. E. (2008). Child and Adolescent Psychopathy: The search for protective factors. *Criminal Justice and Behavior*, *35*(2), 159–172. https://doi.org/10.1177/0093854807311330

Salvatore, J. E., & Dick, D. M. (2018). Genetic influences on conduct disorder. *Neuroscience and Biobehavioral Reviews*, *91*, 91–101.

https://doi.org/10.1016/j.neubiorev.2016.06.034

Sánchez de Ribera, O., Kavish, N., Katz, I. M., & Boutwell, B. B. (2019). Untangling Intelligence, Psychopathy, Antisocial Personality Disorder, and Conduct Problems: A Meta-analytic Review. *European Journal of Personality*, *33*(5), 529–564. https://doi.org/10.1002/per.2207

Sanz-García, A., Gesteira, C., Sanz, J., & García-Vera, M. P. (2021). Prevalence of Psychopathy in the General Adult Population: A Systematic Review and Meta-Analysis. *Frontiers in Psychology*, *12*(661044), 1–14. https://doi.org/10.3389/FPSYG.2021.661044/BIBTEX

Sariaslan, A., Arseneault, L., Larsson, H., Lichtenstein, P., & Fazel, S. (2020). Risk of Subjection to Violence and Perpetration of Violence in Persons with Psychiatric Disorders in Sweden. *JAMA Psychiatry*, *77*(4), 359–367. https://doi.org/10.1001/jamapsychiatry.2019.4275

Scheele, D., Wille, A., Kendrick, K. M., Stoffel-Wagner, B., Becker, B., Güntürkün, O., Maier, W., & Hurlemann, R. (2013). Oxytocin enhances brain reward system responses in men viewing the face of their female partner. *Proceedings of the National Academy of Sciences of the United States of America*, *110*(50), 20308–20313. https://doi.org/10.1073/PNAS.1314190110/-/DCSUPPLEMENTAL

Schielzeth, H., Dingemanse, N. J., Nakagawa, S., Westneat, D. F., Allegue, H., Teplitsky, C., Réale, D., Dochtermann, N. A., Garamszegi, L. Z., & Araya-Ajoy, Y. G. (2020). Robustness of linear mixed-effects models to violations of distributional assumptions. *Methods in Ecology and Evolution*, *11*(9), 1141–1152. https://doi.org/10.1111/2041-210X.13434

Schiffer, B., Müller, B. W., Scherbaum, N., Hodgins, S., Forsting, M., Wiltfang, J., Gizewski, E. R., & Leygraf, N. (2011). Disentangling structural brain alterations associated with violent behavior from those associated with substance use disorders. *Archives of General Psychiatry*, *68*(10), 1039–1049. https://doi.org/10.1001/archgenpsychiatry.2011.61

Schönenberg, M., & Jusyte, A. (2014). Investigation of the hostile attribution bias toward ambiguous facial cues in antisocial violent offenders. *European Archives of Psychiatry and Clinical Neuroscience*, *264*(1), 61–69. https://doi.org/10.1007/s00406-013-0440-1

Schönenberg, M., Louis, K., Mayer, S., & Jusyte, A. (2013). Impaired identification of threat-related social information in male delinquents with antisocial personality disorder. *Journal of Personality Disorders*, *27*(4), 496–505. https://doi.org/10.1521/pedi_2013_27_100

Seara-Cardoso, A., Vasconcelos, M., Sampaio, A., & Neumann, C. S. (2022). Neural correlates of psychopathy: a comprehensive review. In

*Psychopathy and Criminal Behavior: Current Trends and Challenges* (pp. 43–73). Academic Press. https://doi.org/10.1016/B978-0-12-811419-3.00019-4

Seeley, S. H., Chou, Y., & O'Connor, M.-F. (2018). Intranasal oxytocin and OXTR genotype effects on resting state functional connectivity: A systematic review. *Neuroscience & Biobehavioral Reviews*, *95*, 17–32. https://doi.org/10.1016/J.NEUBIOREV.2018.09.011

Seeley, W. W., Menon, V., Schatzberg, A. F., Keller, J., Glover, G. H., Kenna, H., Reiss, A. L., & Greicius, M. D. (2007). Dissociable intrinsic connectivity networks for salience processing and executive control. *Journal of Neuroscience*, *27*(9), 2349–2356. https://doi.org/10.1523/JNEUROSCI.5587-06.2007

Sethi, A., Gregory, S., Dell'Acqua, F., Periche Thomas, E., Simmons, A., Murphy, D. G. M., Hodgins, S., Blackwood, N. J., & Craig, M. C. (2015). Emotional detachment in psychopathy: Involvement of dorsal default-mode connections. *Cortex*, *62*, 11–19. https://doi.org/10.1016/j.cortex.2014.07.018

Sethi, A., O'Brien, S., Blair, R. J. R., Viding, E., Mehta, M., Ecker, C., Blackwood, N., Doolan, M., Catani, M., Scott, S., Murphy, D. G. M., & Craig, M. C. (2022). Selective amygdala hypoactivity to fear in boys with persistent conduct problems after parent training. *Biological Psychiatry*, *0*(0), 1–7. https://doi.org/10.1016/j.biopsych.2022.09.031

Sethi, A., Sarkar, S., Dell'Acqua, F., Viding, E., Catani, M., Murphy, D. G. M., & Craig, M. C. (2018). Anatomy of the dorsal default-mode network in conduct disorder: Association with callous-unemotional traits. *Developmental Cognitive Neuroscience*, *30*, 87–92. https://doi.org/10.1016/j.dcn.2018.01.004

Shahrestani, S., Kemp, A. H., & Guastella, A. J. (2013). The Impact of a Single Administration of Intranasal Oxytocin on the Recognition of Basic Emotions in Humans: A Meta-Analysis. *Neuropsychopharmacology*, *38*(10), 1929–1936. https://doi.org/10.1038/npp.2013.86

Shamay-Tsoory, S. G., & Abu-Akel, A. (2016). The Social Salience Hypothesis of Oxytocin. *Biological Psychiatry*, *79*(3), 194–202. https://doi.org/10.1016/j.biopsych.2015.07.020

Shamay-Tsoory, S. G., Fischer, M., Dvash, J., Harari, H., Perach-Bloom, N., & Levkovitz, Y. (2009). Intranasal Administration of Oxytocin Increases Envy and Schadenfreude (Gloating). *Biological Psychiatry*, *66*(9), 864–870. https://doi.org/10.1016/J.BIOPSYCH.2009.06.009

Shamay-Tsoory, S. G., Harari, H., Aharon-Peretz, J., & Levkovitz, Y. (2010). The role of the orbitofrontal cortex in affective theory of mind

deficits in criminal offenders with psychopathic tendencies. *Cortex*, *46*(5), 668–677. https://doi.org/10.1016/j.cortex.2009.04.008

Shane, M. S., & Groat, L. L. (2018). Capacity for upregulation of emotional processing in psychopathy: all you have to do is ask. *Social Cognitive and Affective Neuroscience*, *13*(11), 1163–1176. https://doi.org/10.1093/SCAN/NSY088

Shen, X., Tokoglu, F., Papademetris, X., & Constable, R. T. (2013). Groupwise whole-brain parcellation from resting-state fMRI data for network node identification. *NeuroImage*, *82*, 403–415. https://doi.org/10.1016/J.NEUROIMAGE.2013.05.081

Shepherd, S. M., Campbell, R. E., & Ogloff, J. R. P. (2018). Psychopathy, Antisocial Personality Disorder, and Reconviction in an Australian Sample of Forensic Patients. *International Journal of Offender Therapy and Comparative Criminology*, *62*(3), 609–628. https://doi.org/10.1177/0306624X16653193

Sher, L., Siever, L. J., Goodman, M., McNamara, M., Hazlett, E. A., Koenigsberg, H. W., & New, A. S. (2015). Gender differences in the clinical characteristics and psychiatric comorbidity in patients with antisocial personality disorder. *Psychiatry Research*, *229*(3), 685–689. https://doi.org/10.1016/j.psychres.2015.08.022

Shi, Z., Bureau, J.-F., Easterbrooks, M. A., Zhao, X., & Lyons-Ruth, K. (2012). Childhood maltreatment and prospectively observed quality of early care as predictors of antisocial personality disorder features. *Infant Mental Health Journal*, *33*(1), 55–69. https://doi.org/10.1002/IMHJ.20295

Shin, N. Y., Park, H. Y., Jung, W. H., & Kwon, J. S. (2018). Effects of Intranasal Oxytocin on Emotion Recognition in Korean Male: A Dose-Response Study. *Psychiatry Investigation*, *15*(7), 710–716. https://doi.org/10.30773/PI.2018.02.19

Shirer, W. R., Jiang, H., Price, C. M., Ng, B., & Greicius, M. D. (2015). Optimization of rs-fMRI Pre-processing for Enhanced Signal-Noise Separation, Test-Retest Reliability, and Group Discrimination. *NeuroImage*, *117*, 67–79. https://doi.org/10.1016/J.NEUROIMAGE.2015.05.015

Siep, N., Tonnaer, F., Van de Ven, V., Arntz, A., Raine, A., & Cima, M. (2019). Anger provocation increases limbic and decreases medial prefrontal cortex connectivity with the left amygdala in reactive aggressive violent offenders. *Brain Imaging and Behavior*, *13*(5), 1311–1323. https://doi.org/10.1007/s11682-018-9945-6

Silk, T. J., Beare, R., Malpas, C., Adamson, C., Vilgis, V., Vance, A., & Bellgrove, M. A. (2016). Cortical morphometry in attention deficit/hyperactivity disorder: Contribution of thickness and surface

area to volume. *Cortex*, *82*, 1–10. https://doi.org/10.1016/j.cortex.2016.05.012

Simon, A. B., & Buxton, R. B. (2015). Understanding the dynamic relationship between cerebral blood flow and the BOLD signal: Implications for quantitative functional MRI. *NeuroImage*, *116*, 158–167. https://doi.org/10.1016/j.neuroimage.2015.03.080

Sippel, L. M., Flanagan, J. C., Holtzheimer, P. E., Moran-Santa-Maria, M. M., Brady, K. T., & Joseph, J. E. (2021). Effects of intranasal oxytocin on threat- and reward-related functional connectivity in men and women with and without childhood abuse-related PTSD. *Psychiatry Research: Neuroimaging*, *317*(111368), 1–9. https://doi.org/10.1016/J.PSCYCHRESNS.2021.111368

Sivarajasingam, V., Guan, B., Page, N., & Moore, S. (2022). *Violence in England and Wales in 2021: An accident and emergency perspective*. Cardiff University.

Skett, S., Goode, I., & Barton, S. (2017). A joint NHS and NOMS offender personality disorder pathway strategy: A perspective from 5 years of operation. *Criminal Behaviour and Mental Health*, *27*, 214–221. https://doi.org/10.1002/cbm

Smearman, E. L., Winiarski, D. A., Brennan, P. A., Najman, J., & Johnson, K. C. (2015). Social stress and the oxytocin receptor gene interact to predict antisocial behavior in an at-risk cohort. *Development and Psychopathology*, *27*(1), 309–318. https://doi.org/10.1017/S0954579414000649

Smeijers, D., Rinck, M., Bulten, E., Van den Heuvel, T., Verkes, R.-J., Heuvel, T. van den, & Verkes, R.-J. (2017). Generalized hostile interpretation bias regarding facial expressions: Characteristic of pathological aggressive behavior. *Aggressive Behavior*, *43*(4), 386–397. https://doi.org/10.1002/AB.21697

Smith, A. S., Korgan, A. C., & Young, W. S. (2019). Oxytocin delivered nasally or intraperitoneally reaches the brain and plasma of normal and oxytocin knockout mice. *Pharmacological Research*, *146*(104324), 1–7. https://doi.org/10.1016/J.PHRS.2019.104324

Smith, S. M., Beckmann, C. F., Andersson, J., Auerbach, E. J., Bijsterbosch, J., Douaud, G., Duff, E., Feinberg, D. A., Griffanti, L., Harms, M. P., Kelly, M., Laumann, T., Miller, K. L., Moeller, S., Petersen, S., Power, J., Salimi-Khorshidi, G., Snyder, A. Z., Vu, A. T., … Glasser, M. F. (2013). Resting-state fMRI in the Human Connectome Project. *NeuroImage*, *80*, 144–168. https://doi.org/10.1016/J.NEUROIMAGE.2013.05.039

Smith, D. V., Utevsky, A. V., Bland, A. R., Clement, N., Clithero, J. A., Harsch, A. E. W., McKell Carter, R., & Huettel, S. A. (2014).

Characterizing individual differences in functional connectivity using dual-regression and seed-based approaches. *NeuroImage*, *95*, 1–12. https://doi.org/10.1016/J.NEUROIMAGE.2014.03.042

Soderstrom, H., Blennow, K., Manhem, A., & Forsman, A. (2001). CSF studies in violent offenders: I. 5-HIAA as a negative and HVA as a positive predictor of psychopathy. *Journal of Neural Transmission*, *108*(7), 869–878. https://doi.org/10.1007/S007020170036

Soderstrom, H., Blennow, K., Sjodin, A. K., & Forsman, A. (2003). New evidence for an association between the CSF HVA:5-HIAA ratio and psychopathic traits. *Journal of Neurology Neurosurgery and Psychiatry*, *74*(7), 918–921. https://doi.org/10.1136/JNNP.74.7.918

Soderstrom, H., Hultin, L., Tullberg, M., Wikkelso, C., Ekholm, S., & Forsman, A. (2002). Reduced frontotemporal perfusion in psychopathic personality. *Psychiatry Research - Neuroimaging*, *114*(2), 81–94. https://doi.org/10.1016/S0925-4927(02)00006-9

Soderstrom, H., Tullberg, M., Wikkelsö, C., Ekholm, S., & Forsman, A. (2000). Reduced regional cerebral blood flow in non-psychotic violent offenders. *Psychiatry Research - Neuroimaging*, *98*(1), 29–41. https://doi.org/10.1016/S0925-4927(99)00049-9

Sporns, O. (2013). Network attributes for segregation and integration in the human brain. *Current Opinion in Neurobiology*, *23*(2), 162–171. https://doi.org/10.1016/j.conb.2012.11.015

Stewart, S. B., Koller, J. M., Campbell, M. C., & Black, K. J. (2014). Arterial spin labeling versus BOLD in direct challenge and drug-task interaction pharmacological fMRI. *PeerJ*, *2*(e687), 1–14. https://doi.org/10.7717/peerj.687

Storsve, A. B., Fjell, A. M., Tamnes, C. K., Westlye, L. T., Overbye, K., Aasland, H. W., & Walhovd, K. B. (2014). Differential Longitudinal Changes in Cortical Thickness, Surface Area and Volume across the Adult Life Span: Regions of Accelerating and Decelerating Change. *The Journal of Neuroscience*, *34*(25), 8488–8498. https://doi.org/10.1523/JNEUROSCI.0391-14.2014

Striepens, N., Kendrick, K. M., Hanking, V., Landgraf, R., Wüllner, U., Maier, W., & Hurlemann, R. (2013). Elevated cerebrospinal fluid and blood concentrations of oxytocin following its intranasal administration in humans. *Scientific Reports*, *3*(1), 1–5. https://doi.org/10.1038/srep03440

Sugiura, M., Kawashima, R., Nakagawa, M., Okada, K., Sato, T., Goto, R., Sato, K., Ono, S., Schormann, T., Zilles, K., & Fukuda, H. (2000). Correlation between Human Personality and Neural Activity in Cerebral Cortex. *NeuroImage*, *11*(5), 541–546. https://doi.org/10.1006/NIMG.2000.0564

Sundram, F., Deeley, Q., Sarkar, S., Daly, E., Latham, R., Craig, M., Raczek, M., Fahy, T., Picchioni, M., UK AIMS Network, Barker, G. J., & Murphy, D. G. M. (2012). White matter microstructural abnormalities in the frontal lobe of adults with antisocial personality disorder. *Cortex*, *48*(2), 216–229. https://doi.org/10.1016/j.cortex.2011.06.005

Sutherland, M. T., & Fishbein, D. H. (2017). Higher trait psychopathy is associated with increased risky decision-making and less coincident insula and striatal activity. *Frontiers in Behavioral Neuroscience*, *11*(245), 1–12. https://doi.org/10.3389/fnbeh.2017.00245

Sutin, A. R., Beason-Held, L. L., Dotson, V. M., Resnick, S. M., & Costa, P. T. (2010). The neural correlates of Neuroticism differ by sex prospectively mediate depressive symptoms among older women. *Journal of Affective Disorders*, *127*(1–3), 241–247. https://doi.org/10.1016/J.JAD.2010.06.004

Tadayon, E., Pascual-Leone, A., & Santarnecchi, E. (2020). Differential Contribution of Cortical Thickness, Surface Area, and Gyrification to Fluid and Crystallized Intelligence. *Cerebral Cortex*, *30*(1), 215–225. https://doi.org/10.1093/CERCOR/BHZ082

Tang, Y., Jiang, W., Liao, J., Wang, W., & Luo, A. (2013). Identifying Individuals with Antisocial Personality Disorder Using Resting-State fMRI. *PLoS ONE*, *8*(4), e60652. https://doi.org/10.1371/journal.pone.0060652

Tang, Y., Liu, W., Chen, J., Liao, J., Hu, D., & Wang, W. (2013). Altered spontaneous activity in antisocial personality disorder revealed by regional homogeneity. *NeuroReport*, *24*(11), 590–595. https://doi.org/10.1097/WNR.0b013e3283627993

Tang, Y., Long, J., Wang, W., Liao, J., Xie, H., Zhao, G., & Zhang, H. (2016). Aberrant functional brain connectome in people with antisocial personality disorder. *Scientific Reports*, *6*(26209), 1–12. https://doi.org/10.1038/SREP26209

Tavor, I., Parker Jones, O., Mars, R. B., Smith, S. M., Behrens, T. E., & Jbabdi, S. (2016). Task-free MRI predicts individual differences in brain activity during task performance. *Science*, *352*(6282), 216–220. https://doi.org/10.1126/SCIENCE.AAD8127/SUPPL_FILE/AAD8127S7.GIF

Taylor, J., Loney, B. R., Bobadilla, L., Iacono, W. G., & McGue, M. (2003). Genetic and Environmental Influences on Psychopathy Trait Dimensions in a Community Sample of Male Twins. *Journal of Abnormal Child Psychology*, *31*(6), 633–645. https://doi.org/10.1023/A:1026262207449

Terburg, D., Morgan, B., & van Honk, J. (2009). The testosterone-cortisol

ratio: A hormonal marker for proneness to social aggression. *International Journal of Law and Psychiatry*, *32*(4), 216–223. https://doi.org/10.1016/J.IJLP.2009.04.008

Termenon, M., Jaillard, A., Delon-Martin, C., & Achard, S. (2016). Reliability of graph analysis of resting state fMRI using test-retest dataset from the Human Connectome Project. *NeuroImage*, *142*, 172–187. https://doi.org/10.1016/J.NEUROIMAGE.2016.05.062

Terranova, C., Tucci, M., Sartore, D., Cavarzeran, F., Di Pietra, L., Barzon, L., Palù, G., & Ferrara, S. D. (2013). GABA receptors, alcohol dependence and criminal behavior. *Journal of Forensic Sciences*, *58*(5), 1227–1232. https://doi.org/10.1111/1556-4029.12201

The Mathworks Inc. (2020). *MATLAB* (9.8.0.1323502 (R2020a)). The Mathworks Inc.

The tedana Community, Ahmed, Z., Bandettini, P. A., Bottenhorn, K. L., Caballero-Gaudes, C., Dowdle, L. T., DuPre, E., Gonzalez-Castillo, J., Handwerker, D., Heunis, S., Kundu, P., Laird, A. R., Markello, R., Markiewicz, C. J., Maullin-Sapey, T., Moia, S., Salo, T., Staden, I., Teves, J., … Whitaker, K. (2021). *ME-ICA/tedana: 0.0.11*. https://doi.org/10.5281/ZENODO.5541689

Theodoridou, A., Rowe, A. C., & Mohr, C. (2013). Men perform comparably to women in a perspective taking task after administration of intranasal oxytocin but not after placebo. *Frontiers in Human Neuroscience*, *7*(197), 1–11. https://doi.org/10.3389/FNHUM.2013.00197

Thibodeau, E. L., Cicchetti, D., & Rogosch, F. A. (2015). Child maltreatment, impulsivity, and antisocial behavior in African American children: Moderation effects from a cumulative dopaminergic gene index. *Development and Psychopathology*, *27*(4), 1621–1636. https://doi.org/10.1017/S095457941500098X

Thiebaut De Schotten, M., & Forkel, S. J. (2022). The emergent properties of the connected brain. *Science*, *378*, 505–510. https://doi.org/10.1126/science.abq2591

Thijssen, S., & Kiehl, K. A. (2017). Functional connectivity in incarcerated male adolescents with psychopathic traits. *Psychiatry Research: Neuroimaging*, *265*, 35–44. https://doi.org/10.1016/J.PSCYCHRESNS.2017.05.005

Tielbeek, J. J., Johansson, A., Polderman, T. J. C., Rautiainen, M.-R., Jansen, P., Taylor, M., Tong, X., Lu, Q., Burt, A. S., Tiemeier, H., Viding, E., Plomin, R., Martin, N. G., Heath, A. C., Madden, P. A. F., Montgomery, G., Beaver, K. M., Waldman, I., Gelernter, J., … Posthuma, D. (2017). Genome-wide association studies of a broad spectrum of antisocial behavior. *JAMA Psychiatry*, *74*(12), 1242–1250.

https://doi.org/10.1001/jamapsychiatry.2017.3069

Tielbeek, J. J., Uffelmann, E., Williams, B. S., Colodro-Conde, L., Gagnon, É., Mallard, T. T., Levitt, B. E., Jansen, P. R., Johansson, A., Sallis, H. M., Pistis, G., Saunders, G. R. B., Allegrini, A. G., Rimfeld, K., Konte, B., Klein, M., Hartmann, A. M., Salvatore, J. E., Nolte, I. M., … Posthuma, D. (2022). Uncovering the genetic architecture of broad antisocial behavior through a genome-wide association study meta-analysis. *Molecular Psychiatry*, *27*(11), 4453–4463. https://doi.org/10.1038/S41380-022-01793-3

Tiihonen, J., Kuikka, J., Bergström, K., Hakola, P., Karhu, J., Ryynänen, O. P., & Föhr, J. (1995). Altered striatal dopamine re-uptake site densities in habitually violent and non-violent alcoholics. *Nature Medicine*, *1*(7), 654–657. https://doi.org/10.1038/nm0795-654

Tiihonen, J., Rossi, R., Laakso, M. P., Hodgins, S., Testa, C., Perez, J., Repo-Tiihonen, E., Vaurio, O., Soininen, H., Aronen, H. J., Könönen, M., Thompson, P. M., & Frisoni, G. B. (2008). Brain anatomy of persistent violent offenders: More rather than less. *Psychiatry Research: Neuroimaging*, *163*(3), 201–212. https://doi.org/10.1016/j.pscychresns.2007.08.012

Tillem, S., Conley, M. I., & Baskin-Sommers, A. R. (2022). Conduct disorder symptomatology is associated with an altered functional connectome in a large national youth sample. *Development and Psychopathology*, *34*(4), 1573–1584. https://doi.org/10.1017/S0954579421000237

Tillem, S., Harenski, K., Harenski, C., Decety, J., Kosson, D., Kiehl, K. A., & Baskin-Sommers, A. R. (2019). Psychopathy is associated with shifts in the organization of neural networks in a large incarcerated male sample. *NeuroImage: Clinical*, *24*(102083), 1–12. https://doi.org/10.1016/j.nicl.2019.102083

Tillem, S., Weinstein, H., & Baskin-Sommers, A. R. (2021). Psychopathy is associated with an exaggerated attention bottleneck: EEG and behavioral evidence from a dual-task paradigm. *Cognitive, Affective and Behavioral Neuroscience*. https://doi.org/10.3758/s13415-021-00891-z

Timmermann, M., Jeung, H., Schmitt, R., Boll, S., Freitag, C. M., Bertsch, K., & Herpertz, S. C. (2017). Oxytocin improves facial emotion recognition in young adults with antisocial personality disorder. *Psychoneuroendocrinology*, *85*(11), 158–164. https://doi.org/10.1016/j.psyneuen.2017.07.483

Tong, L. S. J., & Farrington, D. P. (2006). How effective is the "Reasoning and Rehabilitation" programme in reducing reoffending? A meta-analysis of evaluations in four countries. *Psychology, Crime & Law*,

*12*(1), 3–24. https://doi.org/10.1080/10683160512331316253

Tops, S., Habel, U., & Radke, S. (2019). Genetic and epigenetic regulatory mechanisms of the oxytocin receptor gene (OXTR) and the (clinical) implications for social behavior. *Hormones and Behavior*, *108*, 84–93. https://doi.org/10.1016/J.YHBEH.2018.03.002

Tost, H., Kolachana, B., Hakimi, S., Lemaitre, H., Verchinski, B. A., Mattay, V. S., Weinberger, D. R., & Meyer-Lindenberg, A. (2010). A common allele in the oxytocin receptor gene (OXTR) impacts prosocial temperament and human hypothalamic-limbic structure and function. *Proceedings of the National Academy of Sciences of the United States of America*, *107*(31), 13936–13941. https://doi.org/10.1073/PNAS.1003296107/-/DCSUPPLEMENTAL

Triki, Z., Daughters, K., & De Dreu, C. K. W. (2022). Oxytocin has 'tend-and-defend' functionality in group conflict across social vertebrates. *Philosophical Transactions of the Royal Society B*, *377*(1851). https://doi.org/10.1098/RSTB.2021.0137

Trull, T. J., Jahng, S., Tomko, R. L., Wood, P. K., & Sher, K. J. (2010). Revised NESARC personality disorder diagnoses: Gender, prevalence, and comorbidity with substance dependence disorders. *Journal of Personality Disorders*, *24*(4), 412–426. https://doi.org/10.1521/pedi.2010.24.4.412

Tully, J., Gabay, A. S., Brown, D., Murphy, D. G. M., & Blackwood, N. (2018). The effect of intranasal oxytocin on neural response to facial emotions in healthy adults as measured by functional MRI: A systematic review. *Psychiatry Research: Neuroimaging*, *272*, 17–29. https://doi.org/10.1016/j.pscychresns.2017.11.017

Tully, J., Sethi, A., Griem, J., Paloyelis, Y., Craig, M., Williams, S., Murphy, D. G. M., Blair, R. J. R., & Blackwood, N. (2022). Oxytocin normalises the implicit processing of fearful faces in psychopathy: a randomised crossover study using fMRI. *ResearchSquare*, 1–17. https://doi.org/10.21203/rs.3.rs-1885292/v1

Turner, D., Sebastian, A., & Tüscher, O. (2017). Impulsivity and Cluster B Personality Disorders. *Current Psychiatry Reports*, *19*(3). https://doi.org/10.1007/s11920-017-0768-8

Uddin, L. Q., Supekar, K., Lynch, C. J., Khouzam, A., Phillips, J., Feinstein, C., Ryali, S., & Menon, V. (2013). Salience network-based classification and prediction of symptom severity in children with autism. *JAMA Psychiatry*, *70*(8), 869–879. https://doi.org/10.1001/JAMAPSYCHIATRY.2013.104

Uddin, L. Q., Yeo, B. T. T., & Spreng, R. N. (2019). Towards a universal taxonomy of macro-scale functional human brain networks. *Brain Topography*, *32*(6), 926–942. https://doi.org/10.1007/S10548-019-

00744-6

United Nations Office on Drugs and Crime. (2021). *World Drug Report 2021*. https://www.unodc.org/unodc/en/data-and-analysis/wdr2021.html

Urben, S., Habersaat, S., Pihet, S., Suter, M., De Ridder, J., & Stéphan, P. (2018). Specific Contributions of Age of Onset, Callous-Unemotional Traits and Impulsivity to Reactive and Proactive Aggression in Youths with Conduct Disorders. *Psychiatric Quarterly*, *89*(1), 1–10. https://doi.org/10.1007/s11126-017-9506-y

Valstad, M., Alvares, G. A., Egknud, M., Matziorinis, A. M., Andreassen, O. A., Westlye, L. T., & Quintana, D. S. (2017). The correlation between central and peripheral oxytocin concentrations: A systematic review and meta-analysis. *Neuroscience & Biobehavioral Reviews*, *78*, 117–124. https://doi.org/10.1016/J.NEUBIOREV.2017.04.017

Van de Giessen, E., Rosell, D. R., Thompson, J. L., Xu, X., Girgis, R. R., Ehrlich, Y., Slifstein, M., Abi-Dargham, A., & Siever, L. J. (2014). Serotonin transporter availability in impulsive aggressive personality disordered patients: A PET study with [11C]DASB. *Journal of Psychiatric Research*, *58*, 147–154. https://doi.org/10.1016/J.JPSYCHIRES.2014.07.025

Van Den Heuvel, M. P., De Lange, S. C., Zalesky, A., Seguin, C., Yeo, B. T. T., & Schmidt, R. (2017). Proportional thresholding in resting-state fMRI functional connectivity networks and consequences for patient-control connectome studies: Issues and recommendations. *NeuroImage*, *152*, 437–449. https://doi.org/10.1016/J.NEUROIMAGE.2017.02.005

van den Heuvel, M. P., & Hulshoff Pol, H. E. (2010). Exploring the brain network: A review on resting-state fMRI functional connectivity. *European Neuropsychopharmacology*, *20*(8), 519–534. https://doi.org/10.1016/J.EURONEURO.2010.03.008

Van Dongen, J., Hagenbeek, F. A., Suderman, M., Roetman, P. J., Sugden, K., Chiocchetti, A. G., Ismail, K., Mulder, R. H., Hafferty, J. D., Adams, M. J., Walker, R. M., Morris, S. W., Lahti, J., Küpers, L. K., Escaramis, G., Alemany, S., Jan Bonder, M., Meijer, M., Ip, H. F., … Boomsma, D. I. (2021). DNA methylation signatures of aggression and closely related constructs: A meta-analysis of epigenome-wide studies across the lifespan. *Molecular Psychiatry*, *26*(1), 2148–2162. https://doi.org/10.1038/s41380-020-00987-x

Van Goozen, S. H. M., Langley, K., & Hobson, C. W. (2022). Childhood Antisocial Behavior: A Neurodevelopmental Problem. *Annual Review of Psychology*, *73*, 353–377. https://doi.org/10.1146/ANNUREV-PSYCH-052621-045243

Van Honk, J., Schutter, D. J. L. G., Hermans, E. J., & Putman, P. (2003). Low cortisol levels and the balance between punishment sensitivity and reward dependency. *NeuroReport*, *14*(15), 1993–1996. https://doi.org/10.1097/00001756-200310270-00023

Van IJzendoorn, M. H., & Bakermans-Kranenburg, M. J. (2012). A sniff of trust: meta-analysis of the effects of intranasal oxytocin administration on face recognition, trust to in-group, and trust to out-group. *Psychoneuroendocrinology*, *37*(3), 438–443. https://doi.org/10.1016/J.PSYNEUEN.2011.07.008

Van IJzendoorn, M. H., Belsky, J., & Bakermans-Kranenburg, M. J. (2012). Serotonin transporter genotype 5HTTLPR as a marker of differential susceptibility? A meta-analysis of child and adolescent gene-by-environment studies. *Translational Psychiatry*, *2*(8), 1–6. https://doi.org/10.1038/TP.2012.73

Varangis, E., Habeck, C. G., Razlighi, Q. R., & Stern, Y. (2019). The Effect of Aging on Resting State Connectivity of Predefined Networks in the Brain. *Frontiers in Aging Neuroscience*, *11*, 234. https://doi.org/10.3389/FNAGI.2019.00234/BIBTEX

Vassos, E., Collier, D. A., & Fazel, S. (2014). Systematic meta-analyses and field synopsis of genetic association studies of violence and aggression. *Molecular Psychiatry*, *19*(4), 471–477. https://doi.org/10.1038/mp.2013.31

Vavilala, M. S., Lee, L. A., & Lam, A. M. (2002). Cerebral blood flow and vascular physiology. *Anesthesiology Clinics of North America*, *20*(2), 247–264. https://doi.org/10.1016/S0889-8537(01)00012-8

Veer, I. M., Beckmann, C. F., Van Tol, M.-J., Ferrarini, L., Milles, J., Veltman, D. J., Aleman, A., Van Buchem, M. A., Van der Wee, N. J., & Rombouts, S. A. R. B. (2010). Whole brain resting-state analysis reveals decreased functional connectivity in major depression. *Frontiers in Systems Neuroscience*, *4*(41), 1–10. https://doi.org/10.3389/FNSYS.2010.00041/BIBTEX

Vermeij, A., Kempes, M. M., Cima, M. J., Mars, R. B., & Brazil, I. A. (2018). Affective traits of psychopathy are linked to white-matter abnormalities in impulsive male offenders. *Neuropsychology*, *32*(6), 735–745. https://doi.org/10.1037/neu0000448

Verona, E., Murphy, B., & Bresin, K. (2018). Oxytocin-related single-nucleotide polymorphisms, family environment, and psychopathic traits. *Personality Disorders*, *9*(6), 584–589. https://doi.org/10.1037/PER0000290

Verona, E., Sprague, J., & Sadeh, N. (2012). Inhibitory control and negative emotional processing in psychopathy and antisocial personality disorder. *Journal of Abnormal Psychology*, *121*(2), 498–

510. https://doi.org/10.1037/a0025308

Veroude, K., Zhang-James, Y., Fernàndez-Castillo, N., Bakker, M. J., Cormand, B., & Faraone, S. V. (2016). Genetics of aggressive behavior: An overview. *American Journal of Medical Genetics Part B*, *171B*(1), 3–43. https://doi.org/10.1002/ajmg.b.32364

Vevera, J., Stopkova, R., Bes, M., Albrecht, T., Papezova, H., Zukov, I., Raboch, J., & Stopka, P. (2009). COMT polymorphisms in impulsively violent offenders with antisocial personality disorder. *Neuroendocrinology Letters*, *30*(6), 753–756. www.nel.edu

Viding, E., Blair, R. J. R., Moffitt, T. E., & Plomin, R. (2005). Evidence for substantial genetic risk for psychopathy in 7-years-olds. *Journal of Child Psychology and Psychiatry*, *46*(6), 592–597. https://doi.org/10.1111/j.1469-7610.2004.00393.x

Viding, E., & McCrory, E. J. (2012). Genetic and neurocognitive contributions to the development of psychopathy. *Development and Psychopathology*, *24*(3), 969–983. https://doi.org/10.1017/S095457941200048X

Viding, E., & McCrory, E. J. (2018). Understanding the development of psychopathy: progress and challenges. *Psychological Medicine*, *48*(4), 566–577. https://doi.org/10.1017/S0033291717002847

Viding, E., Sebastian, C. L., Dadds, M. R., Lockwood, P. L., Cecil, C. A. M., De Brito, S. A., & McCrory, E. J. (2012). Amygdala response to preattentive masked fear in children with conduct problems: The role of callous-unemotional traits. *American Journal of Psychiatry*, *169*(10), 1109–1116. https://doi.org/10.1176/appi.ajp.2012.12020191

Virkkunen, M., Goldman, D., Nielsen, D. A., & Linnoila, M. (1995). Low brain serotonin turnover rate (low CSF 5-HIAA) and impulsive violence. *Journal of Psychiatry and Neuroscience*, *20*(4), 271. /pmc/articles/PMC1188701/?report=abstract

Volkert, J., Gablonski, T.-C., & Rabung, S. (2018). Prevalence of personality disorders in the general adult population in Western countries: systematic review and meta-analysis. *The British Journal of Psychiatry*, *213*, 709–715. https://doi.org/10.1192/bjp.2018.202

Von Polier, G. G., Herpertz-Dahlmann, B., Konrad, K., Wiesler, K., Rieke, J., Heinzel-Gutenbrunner, M., Bachmann, C. J., & Vloet, T. D. (2013). Reduced cortisol in boys with early-onset conduct disorder and callous-unemotional traits. *BioMed Research International*, *2013*(349530), 1–9. https://doi.org/10.1155/2013/349530

Wagels, L., Habel, U., Raine, A., & Clemens, B. (2021). Neuroimaging, hormonal and genetic biomarkers for pathological aggression —

success or failure? *Current Opinion in Behavioral Sciences*, *43*, 101–110. https://doi.org/10.1016/J.COBEHA.2021.08.007

Wakschlag, L. S., Choi, S. W., Carter, A. S., Hullsiek, H., Burns, J., McCarthy, K., Leibenluft, E., & Briggs-Gowan, M. J. (2012). Defining the developmental parameters of temper loss in early childhood: implications for developmental psychopathology. *Journal of Child Psychology and Psychiatry*, *53*(11), 1099–1108. https://doi.org/10.1111/j.1469-7610.2012.02595.x

Wakschlag, L. S., Perlman, S. B., Blair, R. J. R., Leibenluft, E., Briggs-Gowan, M. J., & Pine, D. S. (2018). The Neurodevelopmental Basis of Early Childhood Disruptive Behavior: Irritable and Callous Phenotypes as Exemplars. *American Journal of Psychiatry*, *175*, 114–130. https://doi.org/10.1176/appi.ajp.2017.17010045

Waldman, I. D., Rhee, S., LoParo, D., & Park, Y. (2018). Genetic and environmental influences on psychopathy and antisocial behavior. In C. J. Patrick (Ed.), *Handbook of Psychopathy* (pp. 335–353). Guilford Press.

Wallace, D., & Green, S. B. (2002). Analysis of repeated measures designs with linear mixed models. In D. S. Moskowitz & S. L. Herschberger (Eds.), *Modeling intraindividual variability with repeated measures data: Methods and applications* (pp. 103–134). Lawrence Erlbaum Associates Publishers.

Wallace, G. L., White, S. F., Robustelli, B., Sinclair, S., Hwang, S., Martin, A., & Blair, R. J. R. (2014). Cortical and subcortical abnormalities in youths with conduct disorder and elevated callous-unemotional traits. *Journal of the American Academy of Child and Adolescent Psychiatry*, *53*(4), 456–465. https://doi.org/10.1016/j.jaac.2013.12.008

Waller, R., Corral-Frías, N. S., Vannucci, B., Bogdan, R., Knodt, A. R., Hariri, A. R., & Hyde, L. W. (2016). An oxytocin receptor polymorphism predicts amygdala reactivity and antisocial behavior in men. *Social Cognitive and Affective Neuroscience*, *11*(8), 1218–1226. https://doi.org/10.1093/SCAN/NSW042

Waller, R., Dotterer, H. L., Murray, L., Maxwell, A. M., & Hyde, L. W. (2017). White-matter tract abnormalities and antisocial behavior: A systematic review of diffusion tensor imaging studies across development. *NeuroImage: Clinical*, *14*, 201–215. https://doi.org/10.1016/j.nicl.2017.01.014

Waltes, R., Chiocchetti, A. G., & Freitag, C. M. (2016). The neurobiological basis of human aggression: A review on genetic and epigenetic mechanisms. *American Journal of Medical Genetics Part B: Neuropsychiatric Genetics*, *171*(5), 650–675. https://doi.org/10.1002/AJMG.B.32388

Walum, H., Waldman, I. D., & Young, L. J. (2016). Statistical and Methodological Considerations for the Interpretation of Intranasal Oxytocin Studies. *Biological Psychiatry*, *79*(3), 251–257. https://doi.org/10.1016/J.BIOPSYCH.2015.06.016

Wang, D., Yan, X., Li, M., & Ma, Y. (2017). Neural substrates underlying the effects of oxytocin: a quantitative meta-analysis of pharmaco-imaging studies. *Social Cognitive and Affective Neuroscience*, *12*(10), 1565–1573. https://doi.org/10.1093/SCAN/NSX085

Wang, J., Zuo, X., & He, Y. (2010). Graph-based network analysis of resting-state functional MRI. *Frontiers in Systems Neuroscience*, *4*(16), 1–14. https://doi.org/10.3389/FNSYS.2010.00016/BIBTEX

Wang, Y., Metoki, A., Smith, D. V., Medaglia, J. D., Zang, Y., Benear, S., Popal, H., Lin, Y., & Olson, I. R. (2020). Multimodal mapping of the face connectome. *Nature Human Behaviour*, *4*(4), 397–411. https://doi.org/10.1038/s41562-019-0811-3

Wang, Z. (2012). Improving cerebral blood flow quantification for arterial spin labeled perfusion MRI by removing residual motion artifacts and global signal fluctuations. *Magnetic Resonance Imaging*, *30*(10), 1409–1415. https://doi.org/10.1016/J.MRI.2012.05.004

Warren, J. I., & South, S. C. (2009). A symptom level examination of the relationship between Cluster B personality disorders and patterns of criminality and violence in women. *International Journal of Law and Psychiatry*, *32*(1), 10–17. https://doi.org/10.1016/j.ijlp.2008.11.005

Watts, D. J., & Strogatz, S. H. (1998). Collective dynamics of 'small-world' networks. *Nature*, *393*(6684), 440–442. https://doi.org/10.1038/30918

Weafer, J., Dzemidzic, M., Eiler, W., Oberlin, B. G., Wang, Y., & Kareken, D. A. (2015). Associations between regional brain physiology and trait impulsivity, motor inhibition, and impaired control over drinking. *Psychiatry Research*, *233*(2), 81–87. https://doi.org/10.1016/J.PSCYCHRESNS.2015.04.010

Wechsler, D. (2011). *Wechlser Abbreviated Scale of Intelligence, Second Edition (WASI-II)*. NCS Pearson. https://doi.org/10.1177/0734282912467756

Wei, S. M., Eisenberg, D. P., Nabel, K. G., Kohn, P. D., Shane Kippenhan, J., Dickinson, D., Kolachana, B., & Berman, K. F. (2017). Brain-Derived Neurotrophic Factor Val66Met Polymorphism Affects the Relationship Between an Anxiety-Related Personality Trait and Resting Regional Cerebral Blood Flow. *Cerebral Cortex*, *27*(3), 2175–2182. https://doi.org/10.1093/CERCOR/BHW072

Weidacker, K., Snowden, R. J., Boy, F., & Johnston, S. J. (2017).

Response inhibition in the parametric Go/No-Go task in psychopathic offenders. *Psychiatry Research*, *250*, 256–263. https://doi.org/10.1016/j.psychres.2017.01.083

Welton, T., Constantinescu, C. S., Auer, D. P., & Dineen, R. A. (2020). Graph Theoretic Analysis of Brain Connectomics in Multiple Sclerosis: Reliability and Relationship with Cognition. *Brain Connectivity*, *10*(2), 95–104. https://doi.org/10.1089/brain.2019.0717

Welton, T., Kent, D. A., Auer, D. P., & Dineen, R. A. (2015). Reproducibility of Graph-Theoretic Brain Network Metrics: A Systematic Review. *Brain Connectivity*, *5*(4), 193–202. https://doi.org/10.1089/brain.2014.0313

Werhahn, J. E., Mohl, S., Willinger, D., Smigielski, L., Roth, A., Hofstetter, C., Stämpfli, P., Naaijen, J., Mulder, L. M., Glennon, J. C., Hoekstra, P. J., Dietrich, A., Kleine Deters, R., Aggensteiner, P. M., Holz, N. E., Baumeister, S., Banaschewski, T., Saam, M. C., Schulze, U. M. E., … Brandeis, D. (2021). Aggression subtypes relate to distinct resting state functional connectivity in children and adolescents with disruptive behavior. *European Child & Adolescent Psychiatry*, *30*(8), 1237–1249. https://doi.org/10.1007/S00787-020-01601-9

Werner, K. B., Few, L. R., & Bucholz, K. K. (2015). Epidemiology, Comorbidity, and Behavioral Genetics of Antisocial Personality Disorder and Psychopathy. *Psychiatric Annals*, *45*(4), 195–199. https://doi.org/10.3928/00485713-20150401-08

Werry, E. L., Reekie, T. A., & Kassiou, M. (2022). *Oxytocin*. Springer Nature.

Wesseldijk, L. W., Bartels, M., Vink, J. M., Van Beijsterveldt, C. E. M., Ligthart, L., Boomsma, D. I., & Middeldorp, C. M. (2018). Genetic and environmental influences on conduct and antisocial personality problems in childhood, adolescence, and adulthood. *European Child & Adolescent Psychiatry*, *27*(9), 1123–1132. https://doi.org/10.1007/s00787-017-1014-y

White, S. F., Clanton, R., Brislin, S. J., Meffert, H., Hwang, S., Sinclair, S., & Blair, R. J. R. (2014). Temporal Discounting and Conduct Disorder in Adolescents. *Journal of Personality Disorders*, *28*(1), 5–18. https://doi.org/10.1521/pedi.2014.28.1.5

White, S. F., Van Tieghem, M., Brislin, S. J., Sypher, I., Sinclair, S., Pine, D. S., Hwang, S., & Blair, R. J. R. (2016). Neural correlates of the propensity for retaliatory behavior in youths with disruptive behavior disorders. *American Journal of Psychiatry*, *173*(3), 282–290. https://doi.org/10.1176/appi.ajp.2015.15020250

Wierenga, L. M., Langen, M., Oranje, B., & Durston, S. (2014). Unique developmental trajectories of cortical thickness and surface area.

*NeuroImage*, *87*, 120–126. https://doi.org/10.1016/j.neuroimage.2013.11.010

Wigton, R., Radua, J., Allen, P., Averbeck, B., Meyer-Lindenberg, A., McGuire, P., Sukhi, S., & Fusar-Poli, P. (2015). Neurophysiological effects of acute oxytocin administration: systematic review and meta-analysis of placebo-controlled imaging studies. *Journal of Psychiatry and Neuroscience*, *40*(1), E1–E22. https://doi.org/10.1503/JPN.130289

Wilson, H. A. (2014). Can Antisocial Personality Disorder Be Treated? A Meta-Analysis Examining the Effectiveness of Treatment in Reducing Recidivism for Individuals Diagnosed with ASPD. *International Journal of Forensic Mental Health*, *13*(1), 36–46. https://doi.org/10.1080/14999013.2014.890682

Winkler, A. M., Greve, D. N., Bjuland, K. J., Nichols, T. E., Sabuncu, M. R., Håberg, A. K., Skranes, J., & Rimol, L. M. (2018). Joint Analysis of Cortical Area and Thickness as a Replacement for the Analysis of the Volume of the Cerebral Cortex. *Cerebral Cortex*, *28*(2), 738–749. https://doi.org/10.1093/CERCOR/BHX308

Winkler, A. M., Kochunov, P., Blangero, J., Almasy, L., Zilles, K., Fox, P. T., Duggirala, R., & Glahn, D. C. (2010). Cortical thickness or grey matter volume? The importance of selecting the phenotype for imaging genetics studies. *NeuroImage*, *53*(3), 1135–1146. https://doi.org/10.1016/j.neuroimage.2009.12.028

Winkler, A. M., Sabuncu, M. R., Yeo, B. T. T., Fischl, B., Greve, D. N., Kochunov, P., Nichols, T. E., Blangero, J., & Glahn, D. C. (2012). Measuring and comparing brain cortical surface area and other areal quantities. *NeuroImage*, *61*(4), 1428–1443. https://doi.org/10.1016/j.neuroimage.2012.03.026

Winsper, C., Bilgin, A., Thompson, A., Marwaha, S., Chanen, A. M., Singh, S. P., Wang, A., & Furtado, V. (2020). The prevalence of personality disorders in the community: a global systematic review and meta-analysis. *The British Journal of Psychiatry*, *216*, 69–78. https://doi.org/10.1192/bjp.2019.166

Winter, J., Meyer, M., Berger, I., Royer, M., Bianchi, M., Kuffner, K., Peters, S., Stang, S., Langgartner, D., Hartmann, F., Schmidtner, A. K., Reber, S. O., Bosch, O. J., Bludau, A., Slattery, D. A., van den Burg, E. H., Jurek, B., & Neumann, I. D. (2021). Chronic oxytocin-driven alternative splicing of Crfr2α induces anxiety. *Molecular Psychiatry*, *5*, 1–14. https://doi.org/10.1038/s41380-021-01141-x

Winter, K., Spengler, S., Bermpohl, F., Singer, T., & Kanske, P. (2017). Social cognition in aggressive offenders: Impaired empathy, but intact theory of mind. *Scientific Reports*, *7*(1), 1–11.

https://doi.org/10.1038/s41598-017-00745-0

Winterton, A., Westlye, L. T., Steen, N. E., Andreassen, O. A., & Quintana, D. S. (2021). Improving the precision of intranasal oxytocin research. *Nature Human Behaviour*, *5*(1), 9–18. https://doi.org/10.1038/s41562-020-00996-4

Woehrle, L., Retz-Junginger, P., Retz, W., & Barra, S. (2022). The Maltreatment-Aggression Link among Prosecuted Males: What about Psychopathy? *International Journal of Environmental Research and Public Health*, *19*(15), 1–15. https://doi.org/10.3390/IJERPH19159584

Wolf, R. C., Carpenter, R. W., Warren, C. M., Zeier, J. D., Baskin-Sommers, A. R., & Newman, J. P. (2012). Reduced Susceptibility to the Attentional Blink in Psychopathic Offenders: Implications for the Attention Bottleneck Hypothesis. *Neuropsychology*, *26*(1), 102–109. https://doi.org/10.1037/A0026000

Wolf, R. C., Pujara, M. S., Motzkin, J. C., Newman, J. P., Kiehl, K. A., Decety, J., Kosson, D. S., & Koenigs, M. (2015). Interpersonal traits of psychopathy linked to reduced integrity of the uncinate fasciculus. *Human Brain Mapping*, *36*(10), 4202–4209. https://doi.org/10.1002/hbm.22911

World Health Organization. (2019). *International statistical classification of diseases and related health problems (11th ed.)*. https://icd.who.int/

World Health Organization, United Nations Office on Drugs and Crime, & United Nations Development Program. (2014). *Global Status Report on Violence Prevention 2014*. https://www.who.int/publications/i/item/9789241564793

World Health Organization, & Violence and Injury Prevention Consortium. (1996). *Violence: a public health priority. WHO Global Consultation on Violence and Health. (WHO/EHA/SPI. POA.2.)*. World Health Organization.

Worsley, K. J., Andermann, M., Koulis, T., MacDonald, D., & Evans, A. C. (1999). Detecting changes in nonisotropic images. *Human Brain Mapping*, *8*(2–3), 98–101. https://doi.org/10.1002/(sici)1097-0193(1999)8:2/3<98::aid-hbm5>3.0.co;2-f

Wu, D., Zhao, Y., Liao, J., Yin, H., & Wang, W. (2011). White matter abnormalities in young males with antisocial personality disorder: Evidence from voxel-based morphometry-diffeomorphic anatomical registration using exponentiated lie algebra analysis. *Neural Regeneration Research*, *6*(25), 1965–1970. https://doi.org/10.3969/j.issn.1673-5374.2011.25.008

Wu, H., Feng, C., Lu, X., Liu, X., & Liu, Q. (2020). Oxytocin effects on the resting-state mentalizing brain network. *Brain Imaging and Behavior*, *14*(6), 2530–2541. https://doi.org/10.1007/S11682-019-00205-5/FIGURES/5

Wu, Q., Huang, Q., Liu, C., & Wu, H. (2022). Oxytocin modulates social brain network correlations in resting and task state. *Cerebral Cortex*, *32*(15), 1–14. https://doi.org/10.1093/cercor/bhac295

Xin, F., Zhou, F., Zhou, X., Ma, X., Geng, Y., Zhao, W., Yao, S., Dong, D., Biswal, B. B., Kendrick, K. M., & Becker, B. (2021). Oxytocin Modulates the Intrinsic Dynamics Between Attention-Related Large-Scale Networks. *Cerebral Cortex*, *31*(3), 1848–1860. https://doi.org/10.1093/CERCOR/BHY295

Xu, L., Becker, B., & Kendrick, K. M. (2019). Oxytocin facilitates social learning by promoting conformity to trusted individuals. *Frontiers in Neuroscience*, *13*(56), 1–10. https://doi.org/10.3389/fnins.2019.00056

Yang, Y., Joshi, S. H., Jahanshad, N., Thompson, P. M., & Baker, L. A. (2017). Neural correlates of proactive and reactive aggression in adolescent twins. *Aggressive Behavior*, *43*(3), 230–240. https://doi.org/10.1002/AB.21683

Yang, Y., & Raine, A. (2009). Prefrontal structural and functional brain imaging findings in antisocial, violent, and psychopathic individuals: A meta-analysis. *Psychiatry Research: Neuroimaging*, *174*(2), 81–88. https://doi.org/10.1016/j.pscychresns.2009.03.012

Yang, Y., Raine, A., Colletti, P., Toga, A. W., & Narr, K. L. (2009). Abnormal temporal and prefrontal cortical gray matter thinning in psychopaths. *Molecular Psychiatry*, *14*(6), 561–562. https://doi.org/10.1038/mp.2009.12

Yang, Y., Raine, A., Colletti, P., Toga, A. W., & Narr, K. L. (2010). Morphological Alterations in the Prefrontal Cortex and the Amygdala in Unsuccessful Psychopaths. *Journal of Abnormal Psychology*, *119*(3), 546–554. https://doi.org/10.1037/a0019611

Yao, S., Becker, B., Zhao, W., Zhao, Z., Kou, J., Ma, X., Geng, Y., Ren, P., & Kendrick, K. M. (2018). Oxytocin Modulates Attention Switching Between Interoceptive Signals and External Social Cues. *Neuropsychopharmacology*, *43*(2), 294–301. https://doi.org/10.1038/NPP.2017.189

Yeadon, E., Shaw, J., & Egan, V. (2021). The Offender Personality Disorder Pathway: An exploration of the differences between offenders accessing a prison pathway service and a non-accessing population. *The Journal of Forensic Psychiatry & Psychology*, *32*(2), 213–225. https://doi.org/10.1080/14789949.2020.1850843

Yeomans, D. C., Hanson, L. R., Carson, D. S., Tunstall, B. J., Lee, M. R., Tzabazis, A. Z., Jacobs, D., & Frey, W. H. (2021). Nasal oxytocin for the treatment of psychiatric disorders and pain: achieving meaningful brain concentrations. *Translational Psychiatry*, *11*(388), 1–10. https://doi.org/10.1038/s41398-021-01511-7

Yildirim, B. O., & Derksen, J. J. L. (2012a). A review on the relationship between testosterone and the interpersonal/affective facet of psychopathy. *Psychiatry Research*, *197*(3), 181–198. https://doi.org/10.1016/J.PSYCHRES.2011.08.016

Yildirim, B. O., & Derksen, J. J. L. (2012b). A review on the relationship between testosterone and life-course persistent antisocial behavior. *Psychiatry Research*, *200*(2), 984–1010. https://doi.org/10.1016/J.PSYCHRES.2012.07.044

Yildirim, B. O., & Derksen, J. J. L. (2013). Systematic review, structural analysis, and new theoretical perspectives on the role of serotonin and associated genes in the etiology of psychopathy and sociopathy. *Neuroscience and Biobehavioral Reviews*, *37*(7), 1254–1296. https://doi.org/10.1016/J.NEUBIOREV.2013.04.009

Yildirim, B. O., & Derksen, J. J. L. (2015). Mesocorticolimbic dopamine functioning in primary psychopathy: A source of within-group heterogeneity. *Psychiatry Research*, *229*(3), 633–677. https://doi.org/10.1016/J.PSYCHRES.2015.07.005

Yoder, K. J., Harenski, C., Kiehl, K. A., & Decety, J. (2015). Neural networks underlying implicit and explicit moral evaluations in psychopathy. *Translational Psychiatry*, *5*(e625), 1–8. https://doi.org/10.1038/tp.2015.117

Yukhnenko, D., Sridhar, S., & Fazel, S. (2019). A systematic review of criminal recidivism rates worldwide: 3-year update. *Wellcome Open Research*, *4*(28), 1–22. https://doi.org/10.12688/wellcomeopenres.14970.1

Zaki, J., & Ochsner, K. N. (2012). The neuroscience of empathy: progress, pitfalls and promise. *Nature Neuroscience*, *15*(5), 675–680. https://doi.org/10.1038/nn.3085

Zalesky, A., Fornito, A., & Bullmore, E. T. (2010). Network-based statistic: Identifying differences in brain networks. *NeuroImage*, *53*(4), 1197–1207. https://doi.org/10.1016/J.NEUROIMAGE.2010.06.041

Zhang, H., Gross, J., De Dreu, C. K. W., & Ma, Y. (2019). Oxytocin promotes coordinated out-group attack during intergroup conflict in humans. *ELife*, *8*(40698), 1–19. https://doi.org/10.7554/ELIFE.40698

Zhang, K., Huang, D., & Shah, N. J. (2018). Comparison of Resting-State

Brain Activation Detected by BOLD, Blood Volume and Blood Flow. *Frontiers in Human Neuroscience*, *12*, 443. https://doi.org/10.3389/fnhum.2018.00443

Zhao, J., Tomasi, D., Wiers, C. E., Shokri-Kojori, E., Demiral, Ş. B., Zhang, Y., Volkow, N. D., & Wang, G.-J. (2017). Correlation between Traits of Emotion-Based Impulsivity and Intrinsic Default-Mode Network Activity. *Neural Plasticity*, *2017*(9297621), 1–9. https://doi.org/10.1155/2017/9297621

Zhao, Z., Ma, X., Geng, Y., Zhao, W., Zhou, F., Wang, J., Markett, S., Biswal, B. B., Ma, Y., Kendrick, K. M., & Becker, B. (2019). Oxytocin differentially modulates specific dorsal and ventral striatal functional connections with frontal and cerebellar regions. *NeuroImage*, *184*, 781–789. https://doi.org/10.1016/J.NEUROIMAGE.2018.09.067

Zhao, Z., Yu, X., Ren, Z., Zhang, L., & Li, X. (2022). The remediating effect of Attention Bias Modification on aggression in young offenders with antisocial tendency: A randomized controlled trial. *Journal of Behavior Therapy and Experimental Psychiatry*, *75*(101711), 1–10. https://doi.org/10.1016/J.JBTEP.2021.101711

Zheng, S., Punia, D., Wu, H., & Liu, Q. (2021). Graph Theoretic Analysis Reveals Intranasal Oxytocin Induced Network Changes Over Frontal Regions. *Neuroscience*, *459*, 153–165. https://doi.org/10.1016/J.NEUROSCIENCE.2021.01.018

Zhou, Y., Friston, K. J., Zeidman, P., Chen, J., Li, S., & Razi, A. (2018). The Hierarchical Organization of the Default, Dorsal Attention and Salience Networks in Adolescents and Young Adults. *Cerebral Cortex*, *28*(2), 726–737. https://doi.org/10.1093/CERCOR/BHX307

Zhuang, Q., Zhu, S., Yang, X., Zhou, X., Xu, X., Chen, Z., Lan, C., Zhao, W., Becker, B., Yao, S., & Kendrick, K. M. (2021). Oxytocin-induced facilitation of learning in a probabilistic task is associated with reduced feedback- and error-related negativity potentials. *Journal of Psychopharmacology*, *35*(1), 40–49. https://doi.org/10.1177/0269881120972347

Zilles, K., Armstrong, E., Moser, K. H., Schleicher, A., & Stephan, H. (1989). Gyrification in the Cerebral Cortex of Primates. *Brain, Behavior and Evolution*, *34*(1), 143–150. https://doi.org/10.1159/000116500

Zych, I., Farrington, D. P., Ribeaud, D., & Eisner, M. P. (2021). Childhood Explanatory Factors for Adolescent Offending: a Cross-national Comparison Based on Official Records in London, Pittsburgh, and Zurich. *Journal of Developmental and Life-Course Criminology*, *7*, 308–330. https://doi.org/10.1007/s40865-021-00167-7

# Appendix

## Post-hoc sensitivity analyses to measure the impact of substance use

### Supplement chapter 4: Group differences in brain structure

The post-hoc sensitivity analyses for this chapter relied on measuring the impact of having a lifetime substance use disorder. This was chosen because acute drug use (as measured through the urine drug test) is unlikely to affect brain structure whereas a lifetime substance use disorder is more likely to impact brain structure. As shown in *Table 4.1*, the two ASPD groups each had a significantly higher frequency for the presence of a lifetime substance use disorder, since such a diagnosis was an exclusion criteria for the NO group. However, the frequency of lifetime substance use disorders did not differ between the two ASPD groups. Therefore, for each cluster that showed a significant two-way (ASPD+P vs NO, ASPD-P vs NO) group difference in cortical volume, surface area, or cortical thickness, a linear regression analysis was conducted. Specifically, in each regression analysis, the presence of a lifetime substance use disorder (binary), age (mean-centred), and the respective global brain measure (mean-centred) were the predictor variables, and the t-values from the significant clusters were the outcome variables. The participants included in each regression analysis corresponded with those for the respective groups involved in the original comparison (so for clusters stemming from ASPD+P vs NO comparisons, all ASPD+P and NO participants were included in the regression analysis). Since the two ASPD groups did not have significantly different frequencies in lifetime substance use disorders, no post-hoc sensitivity tests were needed for the cortical thickness and surface area clusters where they showed significant structural differences. The results of the individual regression analyses are shown in Table S1. The presence of a lifetime substance use disorder did not significantly predict the t-values in any cluster.

| | Main model | Beta-values | | |
|---|---|---|---|---|
| | | Age | Global | SUD |
| **ASPD+P vs NO** | | | | |
| CV1 | $F_{(3, 37)} = 18.11$, $p < .001$ | .001 | < .001 ** | -.14 |
| CV2 | $F_{(3, 37)} = 13.78$, $p < .001$ | .004 | < .001 ** | .21 |
| SA1 | $F_{(3, 37)} = 21.81$, $p < .001$ | < .001 | < .001 ** | -.04 |
| SA2 | $F_{(3, 37)} = 14.24$, $p < .001$ | .001 | < .001 ** | .08 |
| SA3 | $F_{(3, 37)} = 1.84$, $p = .16$ | -.002 | < .001 | .07 |
| **ASPD-P vs NO** | | | | |
| CV3 | $F_{(3, 38)} = 3.64$, $p = .02$ | -.004 | < .001 * | -.10 |
| SA4 | $F_{(3, 38)} = .57$, $p = .64$ | -.001 | < .001 | .04 |

Table S1. Effect of lifetime substance use disorder on structural group differences.
*Note: * = Bonferroni-corrected p-value < .01, ** = Bonferroni-corrected p-value < .001; SUD = lifetime substance use disorder. CV = cortical volume, SA = surface area.*

## Supplement chapter 5: Group differences and OT effects in rCBF

For the post-hoc sensitivity analyses to measure the effect of substance misuse on resting-state brain rCBF, the presence of a positive urine drug test from the day of the MRI scan was used. This was chosen over lifetime substance use disorder due to its objectivity as well as the fact that acute drug use might affect brain function on the day. The same approach was used as above. The predictor variables were the presence of a positive urine drug test (binary), age (mean-centred), minutes since OT dose (mean-centred), global median CBF (mean-centred). The outcome variables were the raw median rCBF values for each cluster that showed a significant group or interaction effect. Specifically, for clusters with a group effect, the average median rCBF values between OT and PL scans was used, and for the interaction effect, the difference score between OT and PL scans was used. As the main analysis for this data relied on a three-way group test, all participants were included in these regression analyses. The results of the individual regression analyses are shown in Table S2. The presence of a positive urine drug test had a significant negative relationship with rCBF in clusters 1 and 3.

| | Main model | Beta-values | | | |
|---|---|---|---|---|---|
| | | Age | Minutes | Global | Positive drug test |
| **Group effect** | | | | | |
| Cluster 1 | $F_{(4, 48)} = 26.65$, $p < .001$ | -.05 | .02 | .84 ** | -3.79 * |
| Cluster 2 | $F_{(4, 48)} = 110.39$, $p < .001$ | .12 | -.001 | 1.55 ** | -2.34 |
| Cluster 3 | $F_{(4, 48)} = 49.94$, $p < .001$ | .04 | .06 | 1.45 ** | -4.13 * |
| Cluster 4 | $F_{(4, 48)} = 27.34$, $p < .001$ | -.07 | -.06 | 1.52 ** | -2.66 |
| Cluster 5 | $F_{(4, 48)} = 20.32$, $p < 001$ | .06 | -.10 | .63 ** | .68 |
| **Interaction effect** | | | | | |
| Interaction cluster | $F_{(4, 48)} = 27.99$, $p < .001$ | -.03 | .004 | .62 ** | .63 |

Table S2. Effect of acute drug use on rCBF group differences and interaction effects
*Note: * = Bonferroni-corrected p-value < .01, ** = Bonferroni-corrected p-value < .001; rCBF = regional cerebral blood flow.*

## Supplement chapter 6: Group differences and OT effects in functional connectivity

The same approach as the post-hoc sensitivity analyses for rCBF was used here. The presence of a positive urine drug test (binary), age (mean-centred), and minutes since OT dose (mean-centred) were used as predictor variables. The extracted functional connectivity values from clusters showing a significant within-network group difference were used as the outcome variable in the regression. Table S3 shows the results of the regression. The functional connectivity in AprClus1 and AprClus5 was significantly negatively related to the presence of a positive urine test.

| | Main model | Beta-values | | |
|---|---|---|---|---|
| | | Age | Minutes | Positive drug test |
| **Group effect** | | | | |
| AprClus1 | $F_{(3, 34)} = 3.61$, $p = .02$ | .11 | -.40 | -14.71 * |
| AprClus2 | $F_{(3, 34)} = .25$, $p = .86$ | .004 | -.08 | -2.46 |
| AprClus3 | $F_{(3, 34)} = 2.27$, $p = .10$ | -.13 | -.06 | 2.39 |
| AprClus4 | $F_{(3, 34)} = 2.86$, $p = .05$ | -.08 | -.05 | 2.19 |
| AprClus5 | $F_{(3, 34)} = 3.25$, $p = .03$ | -.03 | -.007 | 2.47 * |
| ExpClus1 | $F_{(3, 34)} = .32$, $p = .81$ | -.02 | -.08 | -.83 |
| ExpClus2 | $F_{(3, 34)} = 2.96$, $p = .05$ | .30 | -.03 | -7.16 |
| ExpClus3 | $F_{(3, 34)} = 1.59$, $p = .21$ | -.05 | .10 | 5.04 |
| **Interaction effect** | | | | |
| ExpInteractClus1 | $F_{(3, 34)} = 5.01$, $p = .006$ | -.22 | -.15 | -5.89 |

Table S3. Effect of acute drug use on functional connectivity group differences and interaction effects.
*Note: * = Bonferroni-corrected p-value < .01.*

## Supplement chapter 7: Group differences and OT effects in network topology

For the post-hoc sensitivity analyses, the binary variable for the presence of a positive urine drug test was added into the original linear mixed models as an additional fixed factor for those models which originally revealed significant group, treatment, or interaction effects. Age (mean-centred) and minutes since OT dose (mean-centred) remained fixed factors of no-

interest, and subject remained the random factor. Most effects remained significant, including all of those that were interpreted in the chapter. The below Table S4 shows only those effects where the significance of a main or interaction effect changed after including the binary positive drug test variable.

| Graph theory metric | Group | Treatment | Interaction | Age | Minutes | Positive drug test |
|---|---|---|---|---|---|---|
| Mean FC | $F_{(1, 41.45)} = 3.19$, $p = .08$ | $F_{(1, 34.32)} = .02$, $p = .90$ | $F_{(1, 36.20)} = .73$, $p = .40$ | $F_{(1, 41.64)} = 3.92$, $p = .05$ | $F_{(1, 80.45)} = .33$, $p = .57$ | $F_{(1, 45.00)} = .92$, $p = .32$ |
| NEFF L ACC | $F_{(1, 44.93)} = 2.38$, $p = .13$ | $F_{(1, 43.75)} = .03$, $p = .86$ | $F_{(1, 44.62)} = 5.68$, $p = .02^{\dagger}$ | $F_{(1, 45.48)} = .09$, $p = .77$ | $F_{(1, 76.33)} = 3.40$, $p = .07$ | $F_{(1, 47.04)} = .22$, $p = .64$ |
| NEFF R Prec | $F_{(1, 40.23)} = 5.99$, $p = .02^{\dagger}$ | $F_{(1, 42.49)} = .04$, $p = .85$ | $F_{(1, 43.15)} = .14$, $p = .71$ | $F_{(1, 40.90)} = 2.06$, $p = .16$ | $F_{(1, 63.75)} = 1.41$, $p = .24$ | $F_{(1, 41.86)} = 1.33$, $p = .26$ |
| NEFF L Prec | $F_{(1, 41.68)} = 2.2$, $p = .14$ | $F_{(1, 38.52)} = .22$, $p = .64$ | $F_{(1, 39.46)} = .15$, $p = .70$ | $F_{(1, 42.12)} = 1.68$, $p = .20$ | $F_{(1, 80.40)} = .36$, $p = .54$ | $F_{(1, 44.23)} = 2.47$, $p = .12$ |
| ND L Amyg | $F_{(1, 33.24)} = 2.85$, $p = .10$ | $F_{(1, 33.49)} = .002$, $p = .97$ | $F_{(1, 34.27)} = .27$, $p = .61$ | $F_{(1, 33.83)} = .02$, $p = .89$ | $F_{(1, 66.32)} = .52$, $p = .47$ | $F_{(1, 35.09)} = 5.48$, $p = .03^{\dagger}$ |
| BC L Amyg | $F_{(1, 82)} = 2.8$, $p = .10$ | $F_{(1, 82)} = 2.63$, $p = .11$ | $F_{(1, 82)} = 5.79$, $p = .02^{\dagger}$ | $F_{(1, 82)} = .90$, $p = .35$ | $F_{(1, 82)} = .11$, $p = .75$ | $F_{(1, 82)} = 1.09$, $p = .30$ |
| NEFF L GP | $F_{(1, 38.13)} = 3.33$, $p = .08$ | $F_{(1, 36.52)} = .02$, $p = .87$ | $F_{(1, 37.40)} = 4.86$, $p = .04^{\circ}$ | $F_{(38.66)} = .009$, $p = .93$ | $F_{(1, 75.78)} = 4.43$, $p = .04$ | $F_{(1, 40.35)} = 2.61$, $p = .11$ |
| NEFF R Mid Temp | $F_{(1, 42.33)} = 3.33$, $p = .08$ | $F_{(1, 42.81)} = 1.50$, $p = .23$ | $F_{(1, 43.59)} = .17$, $p = .69$ | $F_{(1, 42.96)} = 1.29$, $p = .26$ | $F_{(1, 70.60)} = .07$, $p = .80$ | $F_{(1, 44.21)} = 4.52$, $p = .04$ |
| NEFF L Parahip | $F_{(1,40.87)} = 2.85$, $p = .10$ | $F_{(1, 41.36)} = .43$, $p = .51$ | $F_{(1, 42.15)} = .64$, $p = .43$ | $F_{(1, 41.49)} = 13.09$, $p < .001$ | $F_{(1, 69.81)} = .11$, $p = .74$ | $F_{(1, 42.75)} = 6.11$, $p = .01$ |
| NEFF L Sup Temp | $F_{(1, 38.73)} = 3.08$, $p = .08$ | $F_{(1, 33.96)} = .38$, $p = .54$ | $F_{(1, 34.88)} = .20$, $p = .65$ | $F_{(1, 39.05)} = .05$, $p = .83$ | $F_{(1, 82.00)} = .16$, $p = .70$ | $F_{(1, 41.75)} = .76$, $p = .39$ |
| NEFF L Lat OFC | $F_{(1, 42.89)} = 3.68$, $p = .06$ | $F_{(1, 43.47)} = 74$, $p = .39$ | $F_{(1, 44.16)} = 5.40$, $p = .02^{\circ}$ | $F_{(1, 43.51)} = .71$, $p = .41$ | $F_{(1, 70.81)} = .41$, $p = .52$ | $F_{(1, 44.75)} = .04$, $p = .85$ |
| NEFF R EC | $F_{(1, 44.99)} = 2.83$, $p = .10$ | $F_{(1, 43.33)} < .001$, $p = .99$ | $F_{(1, 44.23)} = 6.80$, $p = .01^{\circ}$ | $F_{(1, 45.52)} = 1.39$, $p = .24$ | $F_{(1, 77.57)} = .10$, $p = .75$ | $F_{(1, 47.20)} = .86$, $p = .36$ |
| NEFF R Parahip | $F_{(1, 45.45)} = 2.42$, $p = .13$ | $F_{(1, 44.53)} = .69$, $p = .41$ | $F_{(1, 45.39)} = 1.16$, $p = .29$ | $F_{(1, 46.01)} = 5.27$, $p = .03$ | $F_{(1, 75.80)} = 1.33$, $p = .25$ | $F_{(1, 47.51)} = 2.19$, $p = .14$ |
| ND L NAcc | $F_{(1, 42.42)} = 8.49$, $p = .006^{\circ}$ | $F_{(1, 41.42)} = 1.10$, $p = .30$ | $F_{(1, 42.29)} = 2.44$, $p = .13$ | $F_{(1, 42.99)} = .77$, $p = .39$ | $F_{(1, 75.13)} = 1.07$, $p = .30$ | $F_{(1, 44.53)} = .013$, $p = .72$ |
| ND L EC | $F_{(1, 82)} = 4.69$, $p = .03^{\circ}$ | $F_{(1, 82)} = 1.49$, $p = .23$ | $F_{(1, 82)} = .47$, $p = .49$ | $F_{(1, 82)} = 2.96$, $p = .09$ | $F_{(1, 82)} = 1.20$, $p = .28$ | $F_{(1, 82)} = 3.42$, $p = .07$ |
| ND L GP | $F_{(1, 38.21)} = 3.78$, $p = .06$ | $F_{(1, 36.52)} = 5.62$, $p = .03^{\circ}$ | $F_{(1, 37.41)} = .92$, $p = .34$ | $F_{(1, 38.74)} = .14$, $p = .71$ | $F_{(1, 76.07)} = 1.48$, $p = .23$ | $F_{(1, 40.45)} = .69$, $p = .41$ |
| ND R NAcc | $F_{(1, 43.70)} = 5.27$, $p = .03^{\circ}$ | $F_{(1, 39.10)} = .69$, $p = .41$ | $F_{(1, 40.05)} = 1.93$, $p = .17$ | $F_{(1, 44.03)} = 1.44$, $p = .24$ | $F_{(1, 81.98)} = .03$, $p = .86$ | $F_{(1, 46.61)} = .31$, $p = .58$ |
| ND L TP | $F_{(1, 82)} = 2.96$, $p = .09$ | $F_{(1, 82)} = .08$, $p = .78$ | $F_{(1, 82)} = .63$, $p = .43$ | $F_{(1, 82)} = 1.31$, $p = .26$ | $F_{(1, 82)} = .75$, $p = .39$ | $F_{(1, 82)} = 1.60$, $p = .21$ |
| ND L PCC | $F_{(1, 36.43)} = 4.13$, $p = .05^{\circ}$ | $F_{(1, 38.11)} = 2.61$, $p = .11$ | $F_{(1, 38.81)} = .22$, $p = .64$ | $F_{(1, 37.08)} = .47$, $p = .50$ | $F_{(1, 62.96)} = 2.68$, $p = .10$ | $F_{(1, 38.13)} = .01$, $p = .92$ |
| ND R PCC | $F_{(1, 40.80)} = 4.04$, $p = .05^{\circ}$ | $F_{(1, 41.81)} = 4.40$, $p = .04^{\circ}$ | $F_{(1, 42.56)} = .13$, $p = .73$ | $F_{(1, 41.44)} = .14$, $p = .71$ | $F_{(1, 68.11)} = 5.87$, $p = .02$ | $F_{(1, 42.61)} = .02$, $p = .88$ |
| BC R Postcent | $F_{(1, 39.34)} = 3.64$, $p = .06$ | $F_{(1, 28.07)} = 3.24$, $p = .08$ | $F_{(1, 38.95)} = .03$, $p = .87$ | $F_{(1, 39.89)} = .003$, $p = .10$ | $F_{(1, 75.01)} = .02$, $p = .90$ | $F_{(1, 41.51)} = .41$, $p = .78$ |
| BC R GP | $F_{(1, 82)} = 3.77$, $p = .06$ | $F_{(1, 82)} = .80$, $p = .37$ | $F_{(1, 82)} = .78$, $p = .38$ | $F_{(1, 82)} = .80$, $p = .37$ | $F_{(1, 82)} = .10$, $p = .75$ | $F_{(1, 82)} = .11$, $p = .74$ |

Table S4. Network topology metrics that were no longer significant after including binary drug use variable
*Note: ˆsince this was a metric from the ROI analysis, an FDR correction was applied to these p-values, and the p-value was no longer significant after FDR correction. ° This effect was originally significant and remained significant after inclusion of the binary drug use variable but is shown here because another effect in the same model lost significance. FC = functional connectivity, NEFF = nodal efficiency, ND = node degree, BC = betweenness centrality, L = left hemisphere, R = right hemisphere, ACC = anterior cingulate cortex, Prec = precuneus, Amyg = amygdala, GP = globus pallidus, Mid Temp = middle temporal gyrus, Parahip = parahippocampal gyrus, Sup Temp = superior temporal gyrus, Lat OFC = lateral orbitofrontal cortex, EC = entorhinal cortex, NAcc = nucleus accumbens, TP = temporal pole, PCC = posterior cingulate cortex, Postcen = postcentral gyrus.*